RED BLOOD CELLS AT THE MOUNT OF TRUTH: HIGHLIGHTS OF THE 22ND MEETING OF THE EUROPEAN RED CELL RESEARCH SOCIETY

EDITED BY: Anna Bogdanova and Lars Kaestner
PUBLISHED IN: Frontiers in Physiology

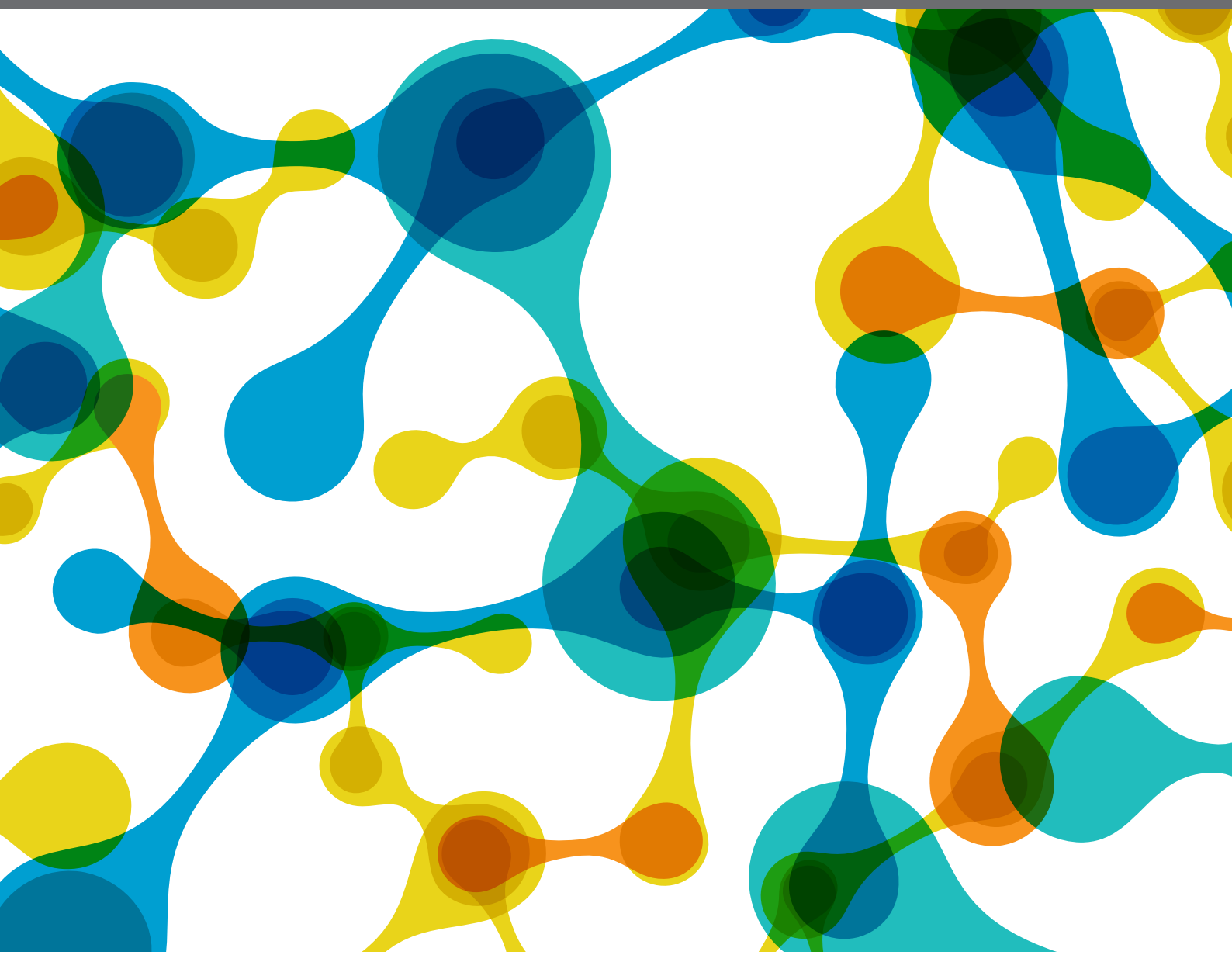

frontiers Research Topics

frontiers

ISSN 1664-8714
ISBN 978-2-88966-351-4
DOI 10.3389/978-2-88966-351-4

About Frontiers

Frontiers is more than just an open-access publisher of scholarly articles: it is a pioneering approach to the world of academia, radically improving the way scholarly research is managed. The grand vision of Frontiers is a world where all people have an equal opportunity to seek, share and generate knowledge. Frontiers provides immediate and permanent online open access to all its publications, but this alone is not enough to realize our grand goals.

Frontiers Journal Series

The Frontiers Journal Series is a multi-tier and interdisciplinary set of open-access, online journals, promising a paradigm shift from the current review, selection and dissemination processes in academic publishing. All Frontiers journals are driven by researchers for researchers; therefore, they constitute a service to the scholarly community. At the same time, the Frontiers Journal Series operates on a revolutionary invention, the tiered publishing system, initially addressing specific communities of scholars, and gradually climbing up to broader public understanding, thus serving the interests of the lay society, too.

Dedication to Quality

Each Frontiers article is a landmark of the highest quality, thanks to genuinely collaborative interactions between authors and review editors, who include some of the world's best academicians. Research must be certified by peers before entering a stream of knowledge that may eventually reach the public - and shape society; therefore, Frontiers only applies the most rigorous and unbiased reviews.
Frontiers revolutionizes research publishing by freely delivering the most outstanding research, evaluated with no bias from both the academic and social point of view. By applying the most advanced information technologies, Frontiers is catapulting scholarly publishing into a new generation.

What are Frontiers Research Topics?

Frontiers Research Topics are very popular trademarks of the Frontiers Journals Series: they are collections of at least ten articles, all centered on a particular subject. With their unique mix of varied contributions from Original Research to Review Articles, Frontiers Research Topics unify the most influential researchers, the latest key findings and historical advances in a hot research area! Find out more on how to host your own Frontiers Research Topic or contribute to one as an author by contacting the Frontiers Editorial Office: researchtopics@frontiersin.org

RED BLOOD CELLS AT THE MOUNT OF TRUTH: HIGHLIGHTS OF THE 22ND MEETING OF THE EUROPEAN RED CELL RESEARCH SOCIETY

Topic Editors:
Anna Bogdanova, University of Zurich, Switzerland
Lars Kaestner, Saarland University, Germany

Citation: Bogdanova, A., Kaestner, L., eds. (2021). Red Blood Cells at the Mount of Truth: Highlights of the 22nd Meeting of the European Red Cell Research Society. Lausanne: Frontiers Media SA. doi: 10.3389/978-2-88966-351-4

Table of Contents

frontiers in Physiology

EDITORIAL
published: 19 November 2020
doi: 10.3389/fphys.2020.607456

Editorial: Red Blood Cells at the Mount of Truth: Highlights of the 22nd Meeting of the European Red Cell Research Society

Anna Bogdanova[1]* *and Lars Kaestner*[2,3]

[1] *Red Blood Cell Research Group, Institute of Veterinary Physiology, Vetsuisse Faculty and the Zurich Center for Integrative Human Physiology (ZIHP), University of Zurich, Zurich, Switzerland,* [2] *Theoretical Medicine and Biosciences, Saarland University, Homburg, Germany,* [3] *Experimental Physics, Saarland University, Saarbrücken, Germany*

Keywords: red blood cells, anemia, technology development, adaptation, modeling

Editorial on the Research Topic

Red Blood Cells at the Mount of Truth: Highlights of the 22nd Meeting of the European Red Cell Research Society

This topic is a result, and in memory of the 22nd meeting of European Red Cell Society (ERCS) in March 2019. The meeting venue, the Stefano Franscini Congress Center Monte Verità (Mount of Truth) at Ascona in Switzerland, is famous amongst creative and artistic people for over a century. The magic of the Monte Verità inspired, and its Bauhaus architecture provided shelter to theosophists, reformers, anarchists, communists, psychoanalysts, writers, poets, artists, dancers, emigrants of both world wars (Bollmann, 2019), and to approximately 100 "ERCS family members" from all over the world **Figure 1**. Traditionally, the ERCS meetings create a lively and informal platform bringing together the scientists studying red blood cells (RBCs), practicing hematologists, and those that develop new tools to study RBCs and diagnose blood diseases (Bogdanova et al., 2020). Looking at the problems from various perspectives, finding common interdisciplinary language, brain-storming, are the features of ERCS meetings since 1976. Each of the articles of this collection is based on a meeting's presentation.

Adaptation of healthy humans to environmental challenges such as high altitude and endurance sport is mirrored by the changes in RBCs. Such adaptations include broad metabolic remodeling that occurs in elite cyclists (San-Millán et al.). Less extreme, modest physical exercises induces adaptive processes that impact RBC rheology and may be used to improve quality of life of patients with sickle cell disease (SCD) (Nader et al.). Further adaptations, including those to high altitude, result in production of subsets of RBCs that differ from the ones produced on a regular basis (Bogdanova, Kaestner et al.).

A systemic approach was used to analyze the processes in the organism that are associated with stimulation of erythropoiesis by hypoxia or ischemia or by administration of recombinant erythropoietin (Epo) (Suresh et al.). Recent studies revealed a number of tissues apart of erythroid precursor cells in the bone marrow that express Epo receptors and respond to an increase in Epo turning this cytokine to a regulator of adipogenesis, osteogenesis, brain and heart development (Suresh et al.). Further cross-talk was shown between megakaryocytes, and erythroid lineage that rely on glutamatergic signaling via N-methyl D-aspartate receptors to differentiate, proliferate and survive in the bone marrow (Kalev-Zylinska et al.). Better understanding of this receptor-mediated signaling pathway may help in treatment of leukemia and other forms of cancer that require glutamatergic stimulation to support high proliferative activity (Kalev-Zylinska et al.). Recent developments of our understanding of the role of hepcidin in regulation of iron uptake and, hence,

OPEN ACCESS

Edited and reviewed by:
Eitan Fibach,
Hadassah Medical Center, Israel

***Correspondence:**
Anna Bogdanova
annab@access.uzh.ch

Specialty section:
This article was submitted to Red Blood Cell Physiology, a section of the journal Frontiers in Physiology

Received: *17 September 2020*
Accepted: *28 September 2020*
Published: *19 November 2020*

Citation:
Bogdanova A and Kaestner L (2020) Editorial: Red Blood Cells at the Mount of Truth: Highlights of the 22nd Meeting of the European Red Cell Research Society. Front. Physiol. 11:607456. doi: 10.3389/fphys.2020.607456

FIGURE 1 | After the sessions: View to the Lake Maggiore from Monte Verita in March 2019.

erythropoietic activity and progression of anemia is reviewed by Pagani et al. along with therapeutic strategies based on modulation of hepcidin levels in the organism. Summarized by Salinas Cisneros and Thein, recent advances in therapeutic options for the most wide-spread hereditary anemia, SCD are discussed. They range from gene editing and bone marrow transplantation to an increasing number of drugs for symptomatic treatment of the disease. Furthermore, specially designed physical exercises are suggested by Nadir et al. as a complementary treatment that may help to improve condition of SCD patients.

From the physicist's point of view, the RBC can be regarded as a concentrated solution of hemoglobin and other minor components of the cytosol surrounded by plasma membrane (Svetina). A review article of Svetina shows how recently discovered mechano-sensitive Piezo1 ion channels contribute to the feedback between cell volume and its shape. The article gives an overview of development of theoretical models describing RBC shape and volume changes and introduces the problems that still have to be resolved to understand the mechanisms in control of RBC reversible and irreversible shape transitions, that define RBC rheology and functionality, but also describe cell-to-cell differences in shape, density, and deformability. Causes of intercellular heterogeneity for RBCs are discussed in detail in a review article of Bogdanova, Kaestner et al.. Those include the cell age, and the changes in micro- and macro-environment of erythroid precursors as well as of circulating RBCs. Cloos et al. have visualized the cross-talk between the lipid domains and proteins in the course of vesiculation of stored RBCs. The role of ATP depletion, oxidative stress and Ca^{2+} accumulation as triggers of redistribution of lipids within sub-microdomains containing sphingomyelin, ceramide and cholesterol and the loss of cholesterol was explored over 3 weeks of storage.

The needs for RBC analysis, the new concepts addressing these needs and instrumental diagnostic and monitoring solutions to them are reviewed by Kaestner and Bianchi. More examples of novel approaches to explore RBC include lipidomics (Cloos et al.), metabolomics (San-Millán et al.) and the need to look at single cells and RBC sub-populations (Bogdanova, Kaestner et al.), and use theoretical modeling to amplify the predictive power of experimental data (Svetina).

As expected, participants left the meeting inspired and ready to try new approaches, test new ideas and prepare for the next meeting to come in 2020 (virtually) and in 2022 (in person).

AUTHOR CONTRIBUTIONS

Both authors contributed to compiling, discussing, and editing the editorial.

REFERENCES

Bogdanova, A., Kaestner, L., and the European Red Cell Society (ERCS) (2020). Early Career Scientists' Guide to the Red Blood Cell – Don't Panic! *Front. Physiol.* 11:588. doi: 10.3389/fphys.2020.00588

Bollmann, S. (2019). *Monte Verità. 1900 – der Traum vom alternativen Leben beginnt.* München: Pantheon Verlag.

Conflict of Interest: The authors declare that the research was conducted in the absence of any commercial or financial relationships that could be construed as a potential conflict of interest.

frontiers in Physiology

MINI REVIEW
published: 09 October 2019
doi: 10.3389/fphys.2019.01294

Hepcidin and Anemia: A Tight Relationship

*Alessia Pagani[1], Antonella Nai[1,2], Laura Silvestri[1,2] and Clara Camaschella[1]**

[1]Division of Genetics and Cell Biology, San Raffaele Scientific Institute, Milan, Italy, [2]Vita-Salute San Raffaele University, Milan, Italy

Hepcidin, the master regulator of systemic iron homeostasis, tightly influences erythrocyte production. High hepcidin levels block intestinal iron absorption and macrophage iron recycling, causing iron restricted erythropoiesis and anemia. Low hepcidin levels favor bone marrow iron supply for hemoglobin synthesis and red blood cells production. Expanded erythropoiesis, as after hemorrhage or erythropoietin treatment, blocks hepcidin through an acute reduction of transferrin saturation and the release of the erythroblast hormone and hepcidin inhibitor erythroferrone. Quantitatively reduced erythropoiesis, limiting iron consumption, increases transferrin saturation and stimulates hepcidin transcription. Deregulation of hepcidin synthesis is associated with anemia in three conditions: iron refractory iron deficiency anemia (IRIDA), the common anemia of acute and chronic inflammatory disorders, and the extremely rare hepcidin-producing adenomas that may develop in the liver of children with an inborn error of glucose metabolism. Inappropriately high levels of hepcidin cause iron-restricted or even iron-deficient erythropoiesis in all these conditions. Patients with IRIDA or anemia of inflammation do not respond to oral iron supplementation and show a delayed or partial response to intravenous iron. In hepcidin-producing adenomas, anemia is reverted by surgery. Other hepcidin-related anemias are the "iron loading anemias" characterized by ineffective erythropoiesis and hepcidin suppression. This group of anemias includes thalassemia syndromes, congenital dyserythropoietic anemias, congenital sideroblastic anemias, and some forms of hemolytic anemias as pyruvate kinase deficiency. The paradigm is non-transfusion-dependent thalassemia where the release of erythroferrone from the expanded pool of immature erythroid cells results in hepcidin suppression and secondary iron overload that in turn worsens ineffective erythropoiesis and anemia. In thalassemia murine models, approaches that induce iron restriction ameliorate both anemia and the iron phenotype. Manipulations of hepcidin might benefit all the above-described anemias. Compounds that antagonize hepcidin or its effect may be useful in inflammation and IRIDA, while hepcidin agonists may improve ineffective erythropoiesis. Correcting ineffective erythropoiesis in animal models ameliorates not only anemia but also iron homeostasis by reducing hepcidin inhibition. Some targeted approaches are now in clinical trials: hopefully they will result in novel treatments for a variety of anemias.

Keywords: anemia, iron, hepcidin, erythropoiesis, inflammation

OPEN ACCESS

Edited by:
Anna Bogdanova, University of Zurich, Switzerland

Reviewed by:
Kostas Pantopoulos, McGill University, Canada
Elizabeta Nemeth, David Geffen School of Medicine at UCLA, United States

***Correspondence:**
Clara Camaschella
camaschella.clara@hsr.it

Specialty section:
This article was submitted to Red Blood Cell Physiology, a section of the journal Frontiers in Physiology

Received: *31 August 2019*
Accepted: *25 September 2019*
Published: *09 October 2019*

Citation:
Pagani A, Nai A, Silvestri L and Camaschella C (2019) Hepcidin and Anemia: A Tight Relationship. Front. Physiol. 10:1294. doi: 10.3389/fphys.2019.01294

INTRODUCTION

Anemia is one of the most common disorders worldwide and anemia due to iron deficiency is the prevalent form according to multiple analyses (review in Camaschella, 2019). This type of anemia results from the total body iron deficiency and the inability to supply the large amount of iron that the bone marrow consumes to produce an adequate number of red blood cells in order to maintain tissue oxygenation.

The iron availability is controlled by the liver peptide hormone hepcidin. The body iron increase causes the production of hepcidin, which is released in the circulation and acts on its receptor ferroportin, a transmembrane iron exporter protein highly expressed on enterocyte, macrophages, and hepatocytes. Hepcidin reduces the iron entry to plasma from absorptive duodenal cells and iron recycling macrophages by blocking iron export (Aschemeyer et al., 2018) and by degrading the iron exporter ferroportin (Nemeth et al., 2004). By regulating plasma iron and systemic iron homeostasis, the hepcidin/ferroportin axis strongly affects erythropoiesis, hence the possible development of anemia.

THE IRON-ERYTHROPOIESIS CONNECTION

The process of red blood cells production consumes approximately 80% of circulating iron for hemoglobin synthesis of maturing erythroblasts. Most iron (20–25 mg/daily) is recycled by macrophages, while a limited amount (1–2 mg daily) derives from intestinal absorption. The kidney hormone erythropoietin (EPO) controls the proliferation of erythroid progenitors, especially of CFU-e and at a lower degree of BFU-e, and the early phase of terminal erythropoiesis, while iron needs are increased in the late differentiation stages from proerythroblasts to reticulocyte, for the synthesis of heme incorporated into hemoglobin (Muckenthaler et al., 2017).

Hepcidin regulation requires a crosstalk between liver endothelial sinusoidal cells (LSEC) that produce the bone morphogenetic proteins (BMPs) to activate the BMP-SMAD pathway and hepatocytes that produce and release hepcidin (Babitt et al., 2006; Rausa et al., 2015). BMP6 and BMP2 are the most important BMPs that upregulate hepcidin, while BMP6 expression is iron dependent (Andriopoulos et al., 2009; Meynard et al., 2009) BMP2 appears less iron-responsive (Canali et al., 2017; Koch et al., 2017).

Hepcidin levels are low in absolute iron deficiency and iron deficiency anemia. In these conditions, the iron stores are exhausted and the BMP-SMAD signaling is switched off at multiple levels. First, BMP6 expression is suppressed; next, the activity of TMPRSS6, a protease that cleaves the BMP co-receptor hemojuvelin (Silvestri et al., 2008), is strongly increased (Lakhal et al., 2011); and third, histone deacetylase3 (HDAC3) suppresses the hepcidin locus (Pasricha et al., 2017). In conditions of iron deficiency, the reduction of hepcidin production is an adaptation mechanism that facilitates dietary and pharmacological iron absorption (Camaschella and Pagani, 2018).

When anemia is severe, the coexisting hypoxia stimulates erythropoiesis through increased kidney synthesis and release of EPO. This leads to suppression of hepcidin transcription by erythroferrone (ERFE), an EPO target gene produced by erythroblasts (Kautz et al., 2014), by molecules (e.g., PDGF-BB) released by other tissues (Sonnweber et al., 2014), and likely by soluble components of transferrin receptors (TFR), sTFR1 (Beguin, 2003), and sTFR2 (Pagani et al., 2015). The final aim is to supply enough iron for the needs of an expanded erythropoiesis.

ANEMIAS WITH ABNORMAL HEPCIDIN LEVELS

Anemias may be classified on the basis of hepcidin levels as anemias with high and low hepcidin. It is intuitive that persistently high hepcidin levels, by blocking iron absorption, cause iron deficiency anemia because of decreased iron supply to erythropoiesis. Conversely, ineffective erythropoiesis characterizes the so-called *iron-loading anemias* that have low hepcidin levels and iron overload. These two groups of anemias are the outcome of opposite pathophysiology mechanisms (**Figure 1**). In the first group, anemia is due to the inhibitory effect exerted by hepcidin on iron absorption and recycling that leads to systemic iron deficiency; in the second group, anemia is due to hepcidin suppression by an expanded abnormal erythropoiesis (Camaschella and Nai, 2016).

Anemia Associated With High Hepcidin Levels

This group includes two inherited rare disorders (iron refractory iron deficiency anemia and hepcidin-producing adenomas in an inborn error of glucose metabolism) and an acquired common condition: anemia of inflammation (**Table 1**).

Iron Refractory Iron Deficiency Anemia

Iron refractory iron deficiency anemia (IRIDA) is a rare recessive disorder characterized by hypochromic microcytic anemia, low transferrin saturation, and inappropriately normal/high hepcidin levels. It is caused by mutations of *TMPRSS6* (Finberg et al., 2008), a gene that encodes the type II serine protease, matriptase-2 (Du et al., 2008). Mutations of *TMPRSS6* are spread along the gene and may affect different domains especially the catalytic domain (De Falco et al., 2014). This transmembrane protease, highly expressed in the liver, inhibits hepcidin transcription by cleaving the cell surface BMP co-receptor hemojuvelin, thus attenuating the BMP signaling and hepcidin synthesis (Silvestri et al., 2008). TMPRSS6 function is essential in iron deficiency to allow the compensatory mechanism of increased iron absorption.

IRIDA is present since birth and usually diagnosed in childhood. Compared with classic iron deficiency, iron parameters are atypical and raise the suspicion of the disease. The percent saturation of transferrin is strongly reduced (less than 10%) as in other forms of iron deficiency; however, at variance with iron deficiency, levels of serum ferritin are normal/increased (Camaschella, 2013; De Falco et al., 2013). This reflects an increased ferritin accumulation in macrophages, due to the high hepcidin levels that induce store iron sequestration.

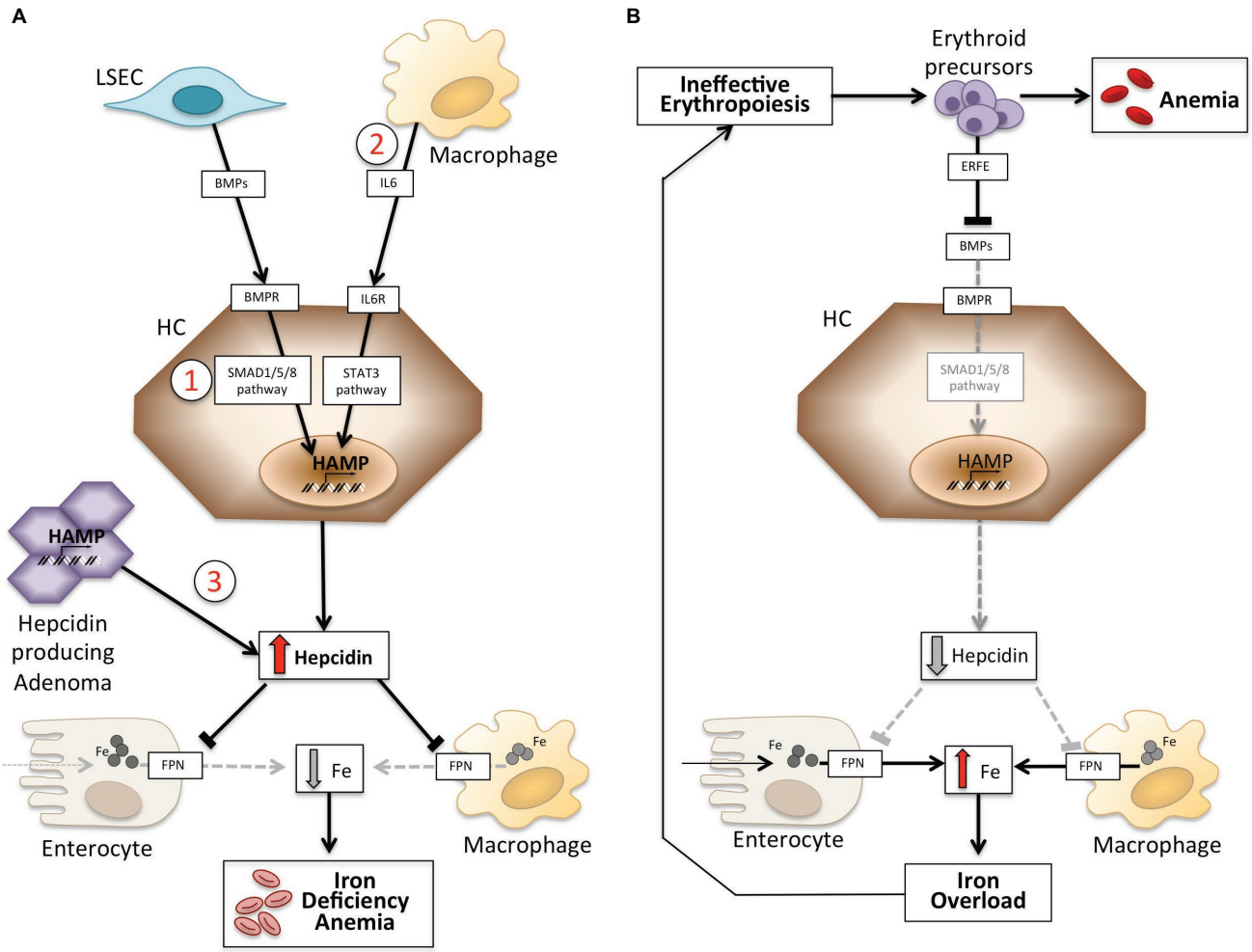

FIGURE 1 | Schematic representation of mechanisms of anemias with high (left panel) and low hepcidin (right panel). Panel **(A)**. Molecular pathogenesis of anemia associated with high hepcidin levels. LSEC, liver sinusoidal endothelial cells producing bone morphogenetic proteins (BMPs); BMPRs, BMP receptors; IL6, interleukin 6; HC, hepatocytes; HAMP, hepcidin gene. Fe, iron; FPN, ferroportin; 1, IRIDA; 2, Anemia of inflammation; 3, hepcidin producing adenoma. Panel **(B)**. Molecular pathogenesis of hepcidin variation in anemias due to ineffective erythropoiesis. ERFE, erythroferrone sequestering BMPs. Other mechanisms inhibiting hepcidin in this type of anemia, as decrease of transferrin saturation and hypoxia, are not shown. See text for details.

None of the tests proposed for IRIDA diagnosis covers 100% of the cases. The genetic test identifies that *TMPRSS6* mutations, that in some cases (non-sense, frame-shift, and splicing mutations), are clearly causal. In other cases, as for previously unreported missense mutations, functional studies are needed to demonstrate causality (Silvestri et al., 2013). However, these tests are scarcely available. Serum hepcidin levels are usually increased/normal, independently of iron deficiency, and consistent with high/normal ferritin. It is important to exclude inflammation by concomitantly dosing C-reactive protein.

Some patients with a phenotype of refractory iron deficiency have been reported to have a single *TMPRSS6* mutated allele; here, the debate is whether they should be considered IRIDA or not. A spectrum of conditions can be envisaged ranging from classic severe IRIDA due to homozygous or compound heterozygous *TMPRSS6* mutations to increased susceptibility to iron deficiency conferred by single mutations/polymorphic changes. One approach proposed to predict classic IRIDA is hepcidin normalization on other iron parameters, as ratios transferrin saturation (Tsat)/log hepcidin or Tsat/log Ferritin (Donker et al., 2016). According to other authors, most patients with a severe IRIDA phenotype have biallelic *TMPRSS6* mutations and, when unidentified, the second allele may be genetically occult (Heeney et al., 2018). In general terms, subjects with a single allele have a milder phenotype than those with two mutations and respond better to iron treatment (Donker et al., 2016). Interestingly, several *TMPRSS6* SNPs have been shown to provide susceptibility to iron deficiency in some populations (An et al., 2012) and in blood donors (Sorensen et al., 2019).

A digenic inheritance has been reported in a 5-year-old female originally found to have an atypical IRIDA genotype with one *TMPRSS6* (I212T) causal and one (R271Q) silent mutation (De Falco et al., 2014). She was later diagnosed *Fibrodysplasia ossificans progressiva* (FOP), a rare dominant

TABLE 1 | Anemias classified according to hepcidin levels.

High-hepcidin anemias		
Hereditary	OMIM n.	Prevalence
Iron refractory iron deficiency anemia (IRIDA)	#206200	Rare
Hepcidin-producing adenomas*	#232200	Rare
Acquired		
Anemia of acute inflammation		Common**
Anemia of chronic inflammation (anemia of chronic disease)		Common
Low-hepcidin anemias		
Hereditary – iron loading anemias	OMIM n.	
β-thalassemia	#613985	Common***
Congenital dyserythropoietic anemia	#224100	Rare
Sideroblastic anemias	#300751	Rare
Acquired		
Low risk MDS with ringed sideroblasts		Rare

*OMIM, online Mendelian Inheritance In Man; MDS, myelodysplastic syndromes.*Described in glycogen-storage-disease 1a.*
***In hospitalized patients and in intensive care units.*
****In people of Mediterranean or southern-east Asian origin.*

disorder with ectopic bone formation in soft tissues due to mutated BMP type I receptor gene *ACVR1*, encoding ALK2 (Shore et al., 2006). The pathological allele $ALK2^{R258S}$ is constitutively active since the mutation affects the glycine-serine-rich domain of the gene and renders the BMP/SMAD pathway overactive being unable to bind its specific inhibitor FKBP12 (Pagani et al., 2017).

This rare case is especially illustrative. First, since the ALK2 glycine-serine-rich domain interacts with FKBP12 and the mutation destabilizes the binding, it has revealed a previously unsuspected role for FKBP12 as a modulator of liver ALK2 and hepcidin (Colucci et al., 2017). Second, it has led to identify a link between activation of bone and liver BMP type I receptors. Third, the case strengthens the relevance of intact TMPRSS6 in controlling the hepatic BMP/SMAD signaling, since no IRIDA was identified among other FOP patients with the same *ACVR1* mutation and presumably normal *TMPRSS6* (Pagani et al., 2017). Finally, this case is consistent with the concept that *TMPRSS6* haploinsufficiency cannot cause classic IRIDA.

The optimal treatment of IRIDA is undefined. Oral iron is ineffective, since it is not absorbed. The addition of vitamin C allows sporadic response. Intravenous iron induces a partial response usually at a slower rate in comparison with patients with acquired iron deficiency. EPO is ineffective in classic cases (De Falco et al., 2013; Heeney and Finberg, 2014).

Anemia of Hepcidin-Producing Adenomas

This is an extremely rare condition in adult patients affected by *glycogen storage disease 1a*, a recessive disorder due to deficiency of glucose-6 phosphatase, which catalyzes a reaction involved in both glycogenolysis and gluconeogenesis. A common dangerous disease symptom is hypoglycemia. The current treatment leads to prolonged survival of affected children up to adult age with the occurrence of several complications, such as anemia and liver adenomas. Anemia is microcytic and hypochromic, iron deficient, and refractory to oral iron treatment. Anemia reverted after surgical adenoma resection. Adenoma tissue was found positive for hepcidin mRNA, while normal surrounding tissue showed hepcidin suppression, as expected because of the ectopic uncontrolled hepcidin production (Weinstein et al., 2002). The hematological features of patients resemble those of IRIDA as they share high hepcidin levels as a common mechanism of anemia.

Anemia of Inflammation

Anemia of inflammation (AI), previously known as anemia of chronic diseases, is a moderate normochromic-normocytic anemia that develops in conditions of systemic inflammation and immune activation. It occurs in several common disorders, including chronic infections, autoimmune diseases, advanced cancer, chronic kidney disease, congestive heart failure, chronic obstructive pulmonary disease, anemia of the elderly (at least partly), and graft versus host disease. AI is one of the most common anemias worldwide and the most frequent anemia in hospitalized patients. Acute inflammation contributes to the severity of anemia in intensive care units. Molecular mechanisms underlying AI are multiple and complex. Overproduction of cytokines such as IL1-β, TNF-α, and IL-6 by macrophages and INF-γ by lymphocytes blunts EPO production, impairs the erythropoiesis response, increases hepcidin levels, and may activate erythrophagocytosis, especially in the acute forms (Weiss and Goodnough, 2005; Ganz, 2019).

Hepcidin is activated by IL-6 through IL-6 receptor (IL-6R) and JAK2-STAT3 signaling. Full hepcidin activation requires an active BMP-SMAD pathway because inactivation of BMP signaling decreases hepcidin in animal models of inflammation (Theurl et al., 2011). The deregulation of systemic iron homeostasis causes macrophage iron sequestration and reduced absorption and recycling that leads to low saturation of transferrin and iron restriction of erythropoiesis and other tissues.

Traditional treatment of AI is based on reversibility/control of the underlying disease, whenever possible. If the disease is untreatable and anemia is mild, a careful evaluation of risks-benefits is needed to avoid side effects of any treatment. Pathophysiology-based treatments are limited to erythropoietin-like compounds and iron. The use of erythropoiesis stimulating agents (ESA) suppresses hepcidin by inducing erythropoiesis expansion. This approach is widely used in patients with chronic kidney disease, low-risk myelodysplastic syndromes, and cancer undergoing chemotherapy. However, a careful clinical control is necessary because high doses have cardiovascular side effects. The administration of intravenous iron may relieve iron restriction, caused by ESA-dependent expansion of erythropoiesis. Oral iron is usually ineffective since the high hepcidin levels counteract its intestinal absorption. Inhibitors of prolyl hydroxylase (hypoxia inducible factor, HIF stabilizers) are experimental in chronic kidney disease, to the aim of increasing endogenous EPO. Chronic treatment with red blood cells transfusions is not recommended because of transient effect and adverse reactions; it is limited to severe refractory anemia (Camaschella, 2019; Weiss et al., 2019).

Anemias Associated With Low Hepcidin Levels

Ineffective erythropoiesis and low or inappropriately normal hepcidin levels, with consequent iron overload, are typical features of the *"iron-loading anemias."* The prototype is β-thalassemia, a genetic recessive disease due to β-globin gene mutations that cause anemia and excess α-globin chain production. The latter precipitates as hemichromes in the bone marrow, damaging maturing erythroid precursors and leading to ineffective erythropoiesis. This occurs in non-transfusion-dependent thalassemia or thalassemia intermedia, whose erythropoiesis is characterized by the prevalence of immature cells that release erythroferrone to inhibit liver hepcidin expression. Hepcidin levels are usually greater in transfusion-dependent thalassemia, where endogenous ineffective erythropoiesis is at least partially suppressed by transfusions (Camaschella and Nai, 2016).

Hepcidin suppression is mediated by the increased cytokine erythroferrone (ERFE), a member of the TNF-α family encoded by *ERFE* gene, synthesized by erythroblasts upon EPO stimulation (Kautz et al., 2014). ERFE is released into the circulation and sequesters BMPs, especially BMP6 (Arezes et al., 2018), attenuating the hepcidin signaling in response to iron. In addition, an epigenetic suppression occurs at the hepcidin locus by histone deacetylase HDAC3 (Pasricha et al., 2017). When anemia causes hypoxia, other mediators such as PDGF-BB (Sonnweber et al., 2014), which is released by different cell types, suppress hepcidin.

Hepcidin levels are decreased by a special mechanism in low-risk myelodysplasia with ringed sideroblasts, a clonal disorder due to mutations of the spliceosome gene *SF3B1*. Iron accumulates in mitochondria, leading to ineffective erythropoiesis and systemic iron overload. An abnormally spliced, elongated ERFE protein is more powerful than wild type ERFE in suppressing hepcidin (Bondu et al., 2019) and causing transfusion-independent iron loading.

TARGETED THERAPIES FOR HEPCIDIN-RELATED ANEMIAS

The identification of molecular mechanisms responsible of the previously discussed anemias has stimulated research in developing targeted therapies to replace current symptomatic treatment (Sebastiani et al., 2016; Crielaard et al., 2017). Approaches differ according to the type of anemia and the aim of decreasing or increasing hepcidin levels or their effects (**Table 2**).

Experimental Therapies to Decrease Hepcidin Levels/Increase Ferroportin Function

Except for hepcidin producing tumors, which have to be surgically removed, compounds that antagonize hepcidin or its effects may be useful in all anemias characterized by high hepcidin levels. Their main application would be in chronic inflammatory diseases in order to reverse hypoferremia and anemia. Several experimental therapies aimed at manipulating the hepcidin pathway and its function have been investigated in preclinical studies. Hepcidin antagonists are inhibitors of hepcidin synthesis/regulators (Ganz, 2019), hepcidin binders that block its function, and compounds that interfere with hepcidin-ferroportin interaction (**Table 2**). Some compounds are in clinical trials especially in chronic kidney disease (Sheetz et al., 2019). In IRIDA, manipulation of the hepcidin pathway has been proposed in preclinical studies with the use of anti-HJV MoAb (Kovac et al., 2016).

TABLE 2 | Experimental therapies targeting the hepcidin-ferroportin axis.

	Mechanism	Compounds
Compounds that decrease hepcidin or increase ferroportin function		
Class I	Reduction of the signaling pathway stimulating hepcidin	Anti IL6-R, anti IL-6
		Anti-BMP6 MoAb*
		BMPR inhibitors
		Anti-HJV MoAb
		Non anticoagulant heparins
Class II	Hepcidin binders	Anti-HAMP MoAb
		Oligonucelotides aptamers
Class III	Interfering with hepcidin-FPN interaction	Anti-FPN MoAb, GDP
Compounds that increase hepcidin or decrease ferroportin function		
Class I	Hepcidin mimics	Hepcidin analogues*
		Minihepcidin
Class II	Activating hepcidin	BMPs (preclinical studies)
	Blocking the hepcidin inhibitor	Anti-*TMPRSS6* (siRNA, ASO*)
	Blocking the hepcidin receptor	FPN Inhibitors*
Class III	Others	Human transferrin infusions
		Protoporphyrin IX (inhibition of HO)
		Bone marrow TFR2 inactivation

*BMPR, BMP receptor; HAMP, hepcidin gene; HJV, hemojuvelin; MoAb, monoclonal antibody; FPN, ferroportin; siRNA, small interfering RNA; ASO, antisense oligonucleotides; GDP, guanosine 5′ diphosphate; HO, heme oxygenase; TFR2, transferrin receptor 2. Compounds indicated by * are in clinical trials.*

Experimental Therapies to Increase Hepcidin Levels/Decrease Ferroportin Function

Increasing hepcidin levels may not only reduce iron overload but also partially control ineffective erythropoiesis in *iron loading anemias.* β-thalassemia is the most studied among these conditions (Casu et al., 2018; Gupta et al., 2018). Proposed drugs are hepcidin analogs (some in clinical trials), hepcidin modulators, especially TMPRSS6 inhibitors, or compounds that interfere with hepcidin-ferroportin interaction decreasing iron export (**Table 2**).

While compounds that increase hepcidin reduce ineffective erythropoiesis due to the vicious cycle between ineffective erythropoiesis and iron loading (Camaschella and Nai, 2016), drugs that favor erythroid precursor maturation, as the activin receptor IIB ligand trap, luspatercept, not only improve anemia but also ameliorate iron homeostasis by reducing hepcidin inhibition (Piga et al., 2019).

Some targeted approaches now in clinical trials will hopefully result in novel treatments for a variety of anemias.

CONCLUSION

The spectacular advances in understanding the regulation of iron metabolism and hepcidin allowed a better understanding of erythropoiesis control, since together with erythropoietin iron is a fundamental factor for erythroid cells maturation. Conditions that lead to anemia can be associated with high and low hepcidin levels. In both instances, contrasting hepcidin deregulation may ameliorate/correct anemia in preclinical models, offering new tools that are already or will be soon clinically explored for the treatment of specific anemias.

AUTHOR CONTRIBUTIONS

AP drafted the paper. CC developed the final version. AN and LS contributed to writing and to critical review the manuscript. All the authors approved the final version.

FUNDING

This paper was supported in part by an EHA Advanced Research Grant in 2018 to AP. Cariplo Foundation Young Investigator Grant n° 2017-0916 to AN.

REFERENCES

An, P., Wu, Q., Wang, H., Guan, Y., Mu, M., Liao, Y., et al. (2012). TMPRSS6, but not TF, TFR2 or BMP2 variants are associated with increased risk of iron-deficiency anemia. *Hum. Mol. Genet.* 21, 2124–2131. doi: 10.1093/hmg/dds028

Andriopoulos, B. Jr., Corradini, E., Xia, Y., Faasse, S. A., Chen, S., Grgurevic, L., et al. (2009). BMP6 is a key endogenous regulator of hepcidin expression and iron metabolism. *Nat. Genet.* 41, 482–487. doi: 10.1038/ng.335

Arezes, J., Foy, N., McHugh, K., Sawant, A., Quinkert, D., Terraube, V., et al. (2018). Erythroferrone inhibits the induction of hepcidin by BMP6. *Blood* 132, 1473–1477. doi: 10.1182/blood-2018-06-857995

Aschemeyer, S., Qiao, B., Stefanova, D., Valore, E. V., Sek, A. C., Ruwe, T. A., et al. (2018). Structure-function analysis of ferroportin defines the binding site and an alternative mechanism of action of hepcidin. *Blood*. 131, 899–910. doi: 10.1182/blood-2017-05-786590

Babitt, J. L., Huang, F. W., Wrighting, D. M., Xia, Y., Sidis, Y., Samad, T. A., et al. (2006). Bone morphogenetic protein signaling by hemojuvelin regulates hepcidin expression. *Nat. Genet.* 38, 531–539. doi: 10.1038/ng1777

Beguin, Y. (2003). Soluble transferrin receptor for the evaluation of erythropoiesis and iron status. *Clin. Chim. Acta* 329, 9–22. doi: 10.1016/S0009-8981(03)00005-6

Bondu, S., Alary, A. S., Lefevre, C., Houy, A., Jung, G., Lefebvre, T., et al. (2019). A variant erythroferrone disrupts iron homeostasis in SF3B1-mutated myelodysplastic syndrome. *Sci. Transl. Med.* 11:pii:eaav5467. doi: 10.1126/scitranslmed.aav5467

Camaschella, C. (2013). How I manage patients with atypical microcytic anaemia. *Br. J. Haematol.* 160, 12–24. doi: 10.1111/bjh.12081

Camaschella, C. (2019). Iron deficiency. *Blood* 133, 30–39. doi: 10.1182/blood-2018-05-815944

Camaschella, C., and Nai, A. (2016). Ineffective erythropoiesis and regulation of iron status in iron loading anaemias. *Br. J. Haematol.* 172, 512–523. doi: 10.1111/bjh.13820

Camaschella, C., and Pagani, A. (2018). Advances in understanding iron metabolism and its crosstalk with erythropoiesis. *Br. J. Haematol.* 182, 481–494. doi: 10.1111/bjh.15403

Canali, S., Wang, C. Y., Zumbrennen-Bullough, K. B., Bayer, A., and Babitt, J. L. (2017). Bone morphogenetic protein 2 controls iron homeostasis in mice independent of Bmp6. *Am. J. Hematol.* 92, 1204–1213. doi: 10.1002/ajh.24888

Casu, C., Nemeth, E., and Rivella, S. (2018). Hepcidin agonists as therapeutic tools. *Blood* 131, 1790–1794. doi: 10.1182/blood-2017-11-737411

Colucci, S., Pagani, A., Pettinato, M., Artuso, I., Nai, A., Camaschella, C., et al. (2017). The immunophilin FKBP12 inhibits hepcidin expression by binding the BMP type I receptor ALK2 in hepatocytes. *Blood* 130, 2111–2120. doi: 10.1182/blood-2017-04-780692

Crielaard, B. J., Lammers, T., and Rivella, S. (2017). Targeting iron metabolism in drug discovery and delivery. *Nat. Rev. Drug Discov.* 16, 400–423. doi: 10.1038/nrd.2016.248

De Falco, L., Sanchez, M., Silvestri, L., Kannengiesser, C., Muckenthaler, M. U., Iolascon, A., et al. (2013). Iron refractory iron deficiency anemia. *Haematologica* 98, 845–853. doi: 10.3324/haematol.2012.075515

De Falco, L., Silvestri, L., Kannengiesser, C., Moran, E., Oudin, C., Rausa, M., et al. (2014). Functional and clinical impact of novel TMPRSS6 variants in iron-refractory iron-deficiency anemia patients and genotype-phenotype studies. *Hum. Mutat.* 35, 1321–1329. doi: 10.1002/humu.22632

Donker, A. E., Schaap, C. C., Novotny, V. M., Smeets, R., Peters, T. M., van den Heuvel, B. L., et al. (2016). Iron refractory iron deficiency anemia: a heterogeneous disease that is not always iron refractory. *Am. J. Hematol.* 91, E482–E490. doi: 10.1002/ajh.24561

Du, X., She, E., Gelbart, T., Truksa, J., Lee, P., Xia, Y., et al. (2008). The serine protease TMPRSS6 is required to sense iron deficiency. *Science* 320, 1088–1092. doi: 10.1126/science.1157121

Finberg, K. E., Heeney, M. M., Campagna, D. R., Aydinok, Y., Pearson, H. A., Hartman, K. R., et al. (2008). Mutations in TMPRSS6 cause iron-refractory iron deficiency anemia (IRIDA). *Nat. Genet.* 40, 569–571. doi: 10.1038/ng.130

Ganz, T. (2019). Anemia of inflammation. *N. Engl. J. Med.* 381, 1148–1157. doi: 10.1056/NEJMra1804281

Gupta, R., Musallam, K. M., Taher, A. T., and Rivella, S. (2018). Ineffective erythropoiesis: anemia and iron overload. *Hematol. Oncol. Clin. North Am.* 32, 213–221. doi: 10.1016/j.hoc.2017.11.009

Heeney, M. M., and Finberg, K. E. (2014). Iron-refractory iron deficiency anemia (IRIDA). *Hematol. Oncol. Clin. North Am.* 28, 637–652. doi: 10.1016/j.hoc.2014.04.009

Heeney, M. M., Guo, D., De Falco, L., Campagna, D. R., Olbina, G., Kao, P. P., et al. (2018). Normalizing hepcidin predicts TMPRSS6 mutation status in patients with chronic iron deficiency. *Blood* 132, 448–452. doi: 10.1182/blood-2017-03-773028

Kautz, L., Jung, G., Valore, E. V., Rivella, S., Nemeth, E., and Ganz, T. (2014). Identification of erythroferrone as an erythroid regulator of iron metabolism. *Nat. Genet.* 46, 678–684. doi: 10.1038/ng.2996

Koch, P. S., Olsavszky, V., Ulbrich, F., Sticht, C., Demory, A., Leibing, T., et al. (2017). Angiocrine Bmp2 signaling in murine liver controls normal iron homeostasis. *Blood* 129, 415–419. doi: 10.1182/blood-2016-07-729822

Kovac, S., Boser, P., Cui, Y., Ferring-Appel, D., Casarrubea, D., Huang, L., et al. (2016). Anti-hemojuvelin antibody corrects anemia caused by inappropriately high hepcidin levels. *Haematologica* 101, e173–e176. doi: 10.3324/haematol.2015.140772

Lakhal, S., Schodel, J., Townsend, A. R., Pugh, C. W., Ratcliffe, P. J., and Mole, D. R. (2011). Regulation of type II transmembrane serine proteinase TMPRSS6 by hypoxia-inducible factors: new link between hypoxia signaling and iron homeostasis. *J. Biol. Chem.* 286, 4090–4097. doi: 10.1074/jbc.M110.173096

Meynard, D., Kautz, L., Darnaud, V., Canonne-Hergaux, F., Coppin, H., and Roth, M. P. (2009). Lack of the bone morphogenetic protein BMP6 induces massive iron overload. *Nat. Genet.* 41, 478–481. doi: 10.1038/ng.320

Muckenthaler, M. U., Rivella, S., Hentze, M. W., and Galy, B. (2017). A red carpet for iron metabolism. *Cell* 168, 344–361. doi: 10.1016/j.cell.2016.12.034

Nemeth, E., Tuttle, M. S., Powelson, J., Vaughn, M. B., Donovan, A., Ward, D. M., et al. (2004). Hepcidin regulates cellular iron efflux by binding to ferroportin and inducing its internalization. *Science* 306, 2090–2093. doi: 10.1126/science.1104742

Pagani, A., Colucci, S., Bocciardi, R., Bertamino, M., Dufour, C., Ravazzolo, R., et al. (2017). A new form of IRIDA due to combined heterozygous mutations of TMPRSS6 and ACVR1A encoding the BMP receptor ALK2. *Blood* 129, 3392–3395. doi: 10.1182/blood-2017-03-773481

Pagani, A., Vieillevoye, M., Nai, A., Rausa, M., Ladli, M., Lacombe, C., et al. (2015). Regulation of cell surface transferrin receptor-2 by iron-dependent cleavage and release of a soluble form. *Haematologica* 100, 458–465. doi: 10.3324/haematol.2014.118521

Pasricha, S. R., Lim, P. J., Duarte, T. L., Casu, C., Oosterhuis, D., Mleczko-Sanecka, K., et al. (2017). Hepcidin is regulated by promoter-associated histone acetylation and HDAC3. *Nat. Commun.* 8:403. doi: 10.1038/s41467-017-00500-z

Piga, A., Perrotta, S., Gamberini, M. R., Voskaridou, E., Melpignano, A., Filosa, A., et al. (2019). Luspatercept improves hemoglobin levels and blood transfusion requirements in a study of patients with beta-thalassemia. *Blood* 133, 1279–1289. doi: 10.1182/blood-2018-10-879247

Rausa, M., Pagani, A., Nai, A., Campanella, A., Gilberti, M. E., Apostoli, P., et al. (2015). Bmp6 expression in murine liver non parenchymal cells: a mechanism to control their high iron exporter activity and protect hepatocytes from iron overload? *PLoS One* 10:e0122696. doi: 10.1371/journal.pone.0122696

Sebastiani, G., Wilkinson, N., and Pantopoulos, K. (2016). Pharmacological targeting of the hepcidin/ferroportin axis. *Front. Pharmacol.* 7:160. doi: 10.3389/fphar.2016.00160

Sheetz, M., Barrington, P., Callies, S., Berg, P. H., McColm, J., Marbury, T., et al. (2019). Targeting the hepcidin-ferroportin pathway in anaemia of chronic kidney disease. *Br. J. Clin. Pharmacol.* 85, 935–948. doi: 10.1111/bcp.13877

Shore, E. M., Xu, M., Feldman, G. J., Fenstermacher, D. A., Cho, T. J., Choi, I. H., et al. (2006). A recurrent mutation in the BMP type I receptor ACVR1 causes inherited and sporadic fibrodysplasia ossificans progressiva. *Nat. Genet.* 38, 525–527. doi: 10.1038/ng1783

Silvestri, L., Pagani, A., Nai, A., De Domenico, I., Kaplan, J., and Camaschella, C. (2008). The serine protease matriptase-2 (TMPRSS6) inhibits hepcidin activation by cleaving membrane hemojuvelin. *Cell Metab.* 8, 502–511. doi: 10.1016/j.cmet.2008.09.012

Silvestri, L., Rausa, M., Pagani, A., Nai, A., and Camaschella, C. (2013). How to assess causality of TMPRSS6 mutations? *Hum. Mutat.* 34, 1043–1045. doi: 10.1002/humu.22321

Sonnweber, T., Nachbaur, D., Schroll, A., Nairz, M., Seifert, M., Demetz, E., et al. (2014). Hypoxia induced downregulation of hepcidin is mediated by platelet derived growth factor BB. *Gut* 63, 1951–1959. doi: 10.1136/gutjnl-2013-305317

Sorensen, E., Rigas, A. S., Didriksen, M., Burgdorf, K. S., Thorner, L. W., Pedersen, O. B., et al. (2019). Genetic factors influencing hemoglobin levels in 15,567 blood donors: results from the Danish blood donor study. *Transfusion* 59, 226–231. doi: 10.1111/trf.15075

Theurl, I., Schroll, A., Sonnweber, T., Nairz, M., Theurl, M., Willenbacher, W., et al. (2011). Pharmacologic inhibition of hepcidin expression reverses anemia of chronic inflammation in rats. *Blood* 118, 4977–4984. doi: 10.1182/blood-2011-03-345066

Weinstein, D. A., Roy, C. N., Fleming, M. D., Loda, M. F., Wolfsdorf, J. I., and Andrews, N. C. (2002). Inappropriate expression of hepcidin is associated with iron refractory anemia: implications for the anemia of chronic disease. *Blood* 100, 3776–3781. doi: 10.1182/blood-2002-04-1260

Weiss, G., Ganz, T., and Goodnough, L. T. (2019). Anemia of inflammation. *Blood* 133, 40–50. doi: 10.1182/blood-2018-06-856500

Weiss, G., and Goodnough, L. T. (2005). Anemia of chronic disease. *N. Engl. J. Med.* 352, 1011–1023. doi: 10.1056/NEJMra041809

Conflict of Interest: CC is a consultant of Vifor Pharma, Celgene, and Novartis.

The remaining authors declare that the research was conducted in the absence of any commercial or financial relationships that could be construed as a potential conflict of interest.

frontiers in Physiology

REVIEW
published: 17 October 2019
doi: 10.3389/fphys.2019.01329

Blood Rheology: Key Parameters, Impact on Blood Flow, Role in Sickle Cell Disease and Effects of Exercise

Elie Nader[1,2†], Sarah Skinner[1,2†], Marc Romana[2,3,4], Romain Fort[1,2,5], Nathalie Lemonne[6], Nicolas Guillot[7], Alexandra Gauthier[1,2,8], Sophie Antoine-Jonville[9], Céline Renoux[1,2,10], Marie-Dominique Hardy-Dessources[2,3,4], Emeric Stauffer[1,2,11], Philippe Joly[1,2,10], Yves Bertrand[8] and Philippe Connes[1,2]*

[1] Laboratory LIBM EA7424, Team "Vascular Biology and Red Blood Cell", University of Lyon 1, Lyon, France, [2] Laboratory of Excellence GR-Ex, Paris, France, [3] Biologie Intégrée du Globule Rouge, Université de Paris, UMR_S1134, BIGR, INSERM, F-75015, Paris, France, [4] Biologie Intégrée du Globule Rouge, The Université des Antilles, UMR_S1134, BIGR, F- 97157, Pointe-a-Pitre, France, [5] Département de Médecine, Hôpital Edouard Herriot, Hospices Civils de Lyon, Lyon, France, [6] Unité Transversale de la Drépanocytose, Hôpital de Pointe-a-Pitre, Hôpital Ricou, Pointe-a-Pitre, France, [7] Laboratoire Carmen INSERM 1060, INSA Lyon, Université Claude Bernard Lyon 1, Université de Lyon, Villeurbanne, France, [8] d'Hématologie et d'Oncologie Pédiatrique, Hospices Civils de Lyon, Lyon, France, [9] Laboratoire ACTES EA 3596, The Université des Antilles, Pointe-a-Pitre, France, [10] Laboratoire de Biochimie et de Biologie Moleiculaire, UF de Biochimie des Pathologies Eirythrocytaires, Centre de Biologie et de Pathologie Est, Hospices Civils de Lyon, Lyon, France, [11] Centre de Médecine du Sommeil et des Maladies Respiratoires, Hospices Civils de Lyon, Hôpital de la Croix Rousse, Lyon, France

OPEN ACCESS

Edited by:
Anna Bogdanova,
University of Zurich, Switzerland

Reviewed by:
Pedro Cabrales,
University of California, San Diego, United States
Ozlem Yalcin,
Koç University, Turkey

***Correspondence:**
Philippe Connes
pconnes@yahoo.fr;
philippe.connes@univ-lyon1.fr

† These authors have contributed equally to this work

Specialty section:
This article was submitted to Red Blood Cell Physiology, a section of the journal Frontiers in Physiology

Received: *25 August 2019*
Accepted: *04 October 2019*
Published: *17 October 2019*

Citation:
Nader E, Skinner S, Romana M, Fort R, Lemonne N, Guillot N, Gauthier A, Antoine-Jonville S, Renoux C, Hardy-Dessources M-D, Stauffer E, Joly P, Bertrand Y and Connes P (2019) Blood Rheology: Key Parameters, Impact on Blood Flow, Role in Sickle Cell Disease and Effects of Exercise. Front. Physiol. 10:1329. doi: 10.3389/fphys.2019.01329

Blood viscosity is an important determinant of local flow characteristics, which exhibits shear thinning behavior: it decreases exponentially with increasing shear rates. Both hematocrit and plasma viscosity influence blood viscosity. The shear thinning property of blood is mainly attributed to red blood cell (RBC) rheological properties. RBC aggregation occurs at low shear rates, and increases blood viscosity and depends on both cellular (RBC aggregability) and plasma factors. Blood flow in the microcirculation is highly dependent on the ability of RBC to deform, but RBC deformability also affects blood flow in the macrocirculation since a loss of deformability causes a rise in blood viscosity. Indeed, any changes in one or several of these parameters may affect blood viscosity differently. Poiseuille's Law predicts that any increase in blood viscosity should cause a rise in vascular resistance. However, blood viscosity, through its effects on wall shear stress, is a key modulator of nitric oxide (NO) production by the endothelial NO-synthase. Indeed, any increase in blood viscosity should promote vasodilation. This is the case in healthy individuals when vascular function is intact and able to adapt to blood rheological strains. However, in sickle cell disease (SCD) vascular function is impaired. In this context, any increase in blood viscosity can promote vaso-occlusive like events. We previously showed that sickle cell patients with high blood viscosity usually have more frequent vaso-occlusive crises than those with low blood viscosity. However, while the deformability of RBC decreases during acute vaso-occlusive events in SCD, patients with the highest RBC deformability at steady-state have a higher risk of developing frequent painful vaso-occlusive crises. This paradox seems to be due to the fact that in SCD RBC with the highest deformability are also the most adherent, which would trigger vaso-occlusion. While acute, intense exercise may increase blood viscosity in

healthy individuals, recent works conducted in sickle cell patients have shown that light cycling exercise did not cause dramatic changes in blood rheology. Moreover, regular physical exercise has been shown to decrease blood viscosity in sickle cell mice, which could be beneficial for adequate blood flow and tissue perfusion.

Keywords: blood rheology, red blood cell deformability, red blood cell aggregation, sickle cell disease, exercise

BLOOD FLOW RESISTANCE AND THE CARDIOVASCULAR SYSTEM

Flow velocity in a given tube depends on pressure and flow resistance. According to Poiseuille's Law (Poiseuille, 1835), flow resistance depends on the geometry of the tube [length (L) and radius of the tube (r)] and the fluid's viscosity (η), and is calculated using the following formula:

$$R = \frac{8\eta L}{\pi r^4}$$

When applying Poiseuille's Law to the cardiovascular system, one must consider the radius and the length of the vessels, and the viscosity of the blood. The dimensions of the vascular system (most notably the radius, which is raised to the fourth power) play a more important role in determining vascular resistance than blood viscosity does. However, several works conducted in the past 10–15 years have shown that, in a physiological context, the parameters of this equation cannot be considered to be truly independent of each other. This is because vessels are not rigid tubes; they can change their diameters in response to various physiological stimuli. One of the most important molecules that promotes an augmentation in vascular diameter (i.e., vasodilation) is nitric oxide (NO). Martini et al. (2005), Tsai et al. (2005), Intaglietta (2009), and Sriram et al. (2012) showed that mild to moderate increases in hematocrit and blood viscosity did not result in a rise in vascular resistance or blood pressure, but actually caused the opposite effect. They also showed that increasing blood viscosity promoted the activation of endothelial NO-synthase through shear stress-dependent mechanisms, resulting in higher NO production, compensatory vasodilation, and decreased arterial pressure. However, evidence shows that these vascular adaptations can only occur in a functioning vascular system with a healthy endothelium. When vascular dysfunction is present, vasodilation is impaired. Therefore, a rise in blood viscosity is not accompanied by an increase in vasodilation. As a result, vascular resistance and arterial pressure increase (Vazquez et al., 2010; Salazar Vazquez et al., 2011). Although the role of blood viscosity in vascular adaptations is often ignored, these studies clearly demonstrate that vascular geometry and blood viscosity should not be considered separately when studying the regulation of vascular resistance in healthy populations or in people with cardiovascular diseases.

BLOOD IS NOT A SIMPLE FLUID

Whole blood is a two-phase liquid, composed of cellular elements suspended in plasma, an aqueous solution containing organic molecules, proteins, and salts (Baskurt and Meiselman, 2003). The cellular phase of blood includes, erythrocytes, leukocytes, and platelets. White blood cells and platelets can affect blood rheology, but under normal conditions, red blood cells (RBCs) have the biggest influence (Pop et al., 2002). Blood rheological properties are determined by the physical properties of these two phases and their relative contribution to total blood volume.

Blood is a non-Newtonian, shear thinning fluid with thixotropic and viscoelastic properties. Many cardiovascular handbooks consider blood viscosity values between 3.5 and 5.5 cP to be normal. However, blood viscosity cannot be summarized by a single value. Due to the shear thinning property of blood, which is dependent on RBC rheological properties, the viscosity of this fluid changes depending on the hemodynamic conditions. The same blood can have a viscosity value of 60 cP at a shear rate of 0.1 s^{-1}, whereas the viscosity would be 5 or 6 cP at a shear rate of 200 s^{-1}. This means that blood viscosity is different in the large arteries, the veins, and the microcirculation, where shear rate can vary from few s^{-1} to more than 1000 s^{-1} (Connes et al., 2016). Blood viscosity depends on several factors: hematocrit, plasma viscosity, the ability of RBCs to deform under flow, and RBC aggregation-disaggregation properties (Baskurt and Meiselman, 2003; Cokelet and Meiselman, 2007).

Effect of Hematocrit

Whole blood viscosity is dependent on the number (and volume) of erythrocytes in the blood, and is thus linearly related to hematocrit (Chien et al., 1975).The impact of hematocrit on blood viscosity is much higher at low shear rates (veins for instance) than at high shear rate (arteries for instance) (Cokelet and Meiselman, 2007). At high shear rate, it is estimated that a rise of hematocrit of one unit would cause an increase of blood viscosity of 4% (if RBC rheological properties remain the same).

Plasma Viscosity

Plasma is a newtonian fluid, which means that its viscosity does not vary with shear rate. The viscosity of plasma is dependent on the concentration of plasma proteins, such as fibrinogen, α1-globulins, α2-globulins, β-globulins, and γ-globulins (Connes et al., 2008). Any elevation in the concentration of these proteins can cause plasma, and thus whole blood, viscosity to increase (Kesmarky et al., 2008). Normal plasma at 37 degrees Celsius

has a viscosity of around 1.2–1.3 cP, but these values may be higher in various inflammatory, metabolic, or cardiovascular diseases (Kesmarky et al., 2008). Furthermore, increased plasma viscosity is associated with higher rates of adverse clinical events in unstable angina pectoris and stroke (Kesmarky et al., 2008).

RBC Deformability

Red blood cell deformability is another important determinant of blood viscosity. RBC deformability depends on several factors, including internal (cytosolic) viscosity (mainly determined by the mean cell hemoglobin concentration), membrane viscoelasticity (which is dependent on cytoskeleton proteins and lipid bilayer properties), and the surface-area-to-volume ratio (also called cell sphericity) (Clark et al., 1983; Renoux et al., 2019). At low shear rates, rigid RBCs are less likely to aggregate than deformable RBCs. Therefore, a loss of RBC deformability at very low shear rates (less than 1 s^{-1}) results in a decrease in blood viscosity (Chien et al., 1970). In contrast, at shear rates above 1 s^{-1}, a decrease in RBC deformability causes blood viscosity to increase (Chien et al., 1970).

Initial experiments done to analyze RBC deformability in blood flow were conducted in the 1970s and 1980s using microtubes (Goldsmith et al., 1972) and rheoscopes (Fischer et al., 1978). These studies demonstrated that, as shear stress increases, normal RBCs align with the direction of flow by deforming into an elliptical shape via a "tank tread-like" motion of the cell membrane around the cytoplasm (Schmid-Schonbein et al., 1969; Goldsmith et al., 1972; Fischer et al., 1978). Rigid RBCs, on the other hand, cannot properly deform into an ellipse and remain perpendicular to blood flow, consequently increasing vascular resistance. In these fundamental experiments, RBCs were suspended in solutions, such as dextrose, with higher viscosities than the internal viscosity of a RBC (Goldsmith et al., 1972; Fischer et al., 1978). However, when a RBC is flowing in plasma *in vivo*, the plasma viscosity is lower than the viscosity of the erythrocyte's cytosol. This is important because recent experiments reveal that the "tank-treading" behavior of erythrocytes does not occur when RBCs are suspended in solutions with lower viscosities that are more similar to plasma viscosity *in vivo* (Dupire et al., 2012). Instead, observations by Lanotte et al. (2016) showed that RBCs display a wide variety of cell shapes for any given flow condition. For example, erythrocytes in dilute suspensions behave like rigid oblate ellipsoids at low shear rates (<1 s^{-1}). Then, as shear rates increase, the erythrocytes successively tumble, roll, and deform into stomatocytes, and eventually adopt highly deformed poly-lobed. The findings of Lanotte et al. (2016) suggest that the pathological alterations of multiple parameters, including plasma composition, erythrocyte cytosol viscosity, and/or membrane mechanical properties could contribute to pathological blood rheology and flow. Further research should be conducted to determine how decreased RBC deformability could affect RBC shape transitions.

Red blood cell deformability is also a key determinant of blood flow in the microcirculation. RBCs are bi-concave disks with an average diameter of around 7–8 μm. Capillaries can have a diameter of less than 5 μm. Therefore, RBC must be highly deformable to pass through the narrowest vessels of the microcirculation. A 15% decrease in RBC deformability has been shown to cause a 75% increase in whole flow resistance in isolated perfused rat hind limbs (Baskurt et al., 2004). Moreover, when dog lungs were perfused with rigid RBC, whole pulmonary arterial pressure increased, and the main increase was localized in the microcirculation (Hakim, 1988; Raj et al., 1991). Indeed, any decrease of RBC deformability may affect flow resistance, tissue perfusion, and oxygenation (Parthasarathi and Lipowsky, 1999).

RBC Aggregation

Red blood cell aggregation is the reversible formation of three-dimensional stacks of RBC, called "rouleaux," which takes place at low shear rates. This unique process requires low energy and is reversible under high shear rate conditions. RBC aggregation depends on both plasma and cellular factors. Initially, most research on RBC aggregation formation was focused on the effects of protein levels, polymer type, and concentration. More recent research has shown that RBC cellular properties can also modulate a cell's intrinsic tendency to aggregate (termed RBC aggregability) (Baskurt and Meiselman, 2009). For example, RBC surface properties, including surface charge and glycocalyx depth, also play an important role in this process. Two models have been proposed to explain RBC aggregation mechanisms (Meiselman et al., 2007), the depletion model and the bridging model. The depletion model suggests that RBC aggregates are formed due to osmotic pressure from surrounding plasma proteins or other macromolecules. The bridging model suggests that aggregates form due to "crossbridges," made of plasma proteins or other macromolecules (Rampling et al., 2004). Fibrinogen is the most physiologically relevant macromolecule that promotes RBC aggregation (Rampling et al., 2004), but other molecules, including thrombospondin and the von-Willebrand factor, also play a role (Nader et al., 2017).

The impact of RBC aggregation on blood flow, tissue perfusion and vascular resistance is complex and depends on the vascular areas where RBC aggregates are flowing. RBC aggregates usually form in low shear rate areas, such as in veins or in bifurcations. Therefore, increased RBC aggregation would cause a dramatic increase of blood viscosity in these zones. RBC aggregates disaggregate in high shear rate areas, such as in arteries and arterioles. However, it has been demonstrated that some RBC aggregates can persist in large arteries and affect flow dynamics. Increased RBC aggregation has been shown to promote RBC axial migration in these vessels, which in turn increases the cell free layer width (Baskurt and Meiselman, 2007). This latter phenomenon has three main consequences: (i) a decrease of apparent dynamic blood viscosity and of flow resistance, (ii) a decrease of wall shear stress, which in turn results in a lower activation of endothelial NO-synthase, lower NO production, and less vasodilation, and (iii) an increase of plasma skimming phenomena at bifurcations, which in turn lowers microcirculatory hematocrit and blood viscosity (Fharaeus and Fahraeaus–Lindqvist effects).

At the microcirculatory level, persisting RBC aggregates may increase pre-capillary resistance. Experiments performed on large glass tubes also shown that the consequences of RBC aggregation

on flow resistance are dependent on the orientation of the tube (vertical vs. horizontal) (Cokelet and Goldsmith, 1991). In horizontal tubes, elevated RBC aggregation increases RBC sedimentation, thereby increasing flow resistance. On the other hand, in vertical tubes RBC aggregation increases RBC axial migration and facilitates blood flow. For this reason, the consequences of increased RBC aggregation on blood flow are difficult to predict. However, experiments done on whole organs, such as guinea pig hearts, reported that gradually increasing RBC aggregation causes a 3-phase evolution of blood flow resistance (Yalcin et al., 2005). First, when RBC aggregation was increased by 50–100%, the authors observed a rise in blood flow resistance. Next, a 100–150% increase in RBC aggregation caused blood flow resistance to decrease. Finally, an increase in RBC aggregation of over 150% caused blood flow resistance to increase once again. Overall, predicting the consequences of increased RBC aggregation *in vivo* appears to be complex. However, clinical works performed to study aggregation in cardiovascular, metabolic, or inflammatory diseases consistently show that people with these diseases generally have higher RBC aggregation levels than healthy individuals, and the elevated aggregation contributes to the development of adverse disease outcomes (Totsimon et al., 2017; Biro et al., 2018; Brun et al., 2018; Ko et al., 2018; Lapoumeroulie et al., 2019; Piecuch et al., 2019; Sheremet'ev et al., 2019).

SICKLE CELL DISEASE, BLOOD RHEOLOGY AND VASCULAR DYSFUNCTION

Sickle cell disease (SCD) is the most prevalent genetic disease in the world. Sickle cell anemia (SCA) is by far the most common form of SCD, followed by hemoglobin SC disease (SC) (Piel et al., 2010).It is estimated that more than 300,000 children are born each year with a severe inherited hemoglobinopathy, over 80% of these infants are born in low-or middle-income countries, and approximately 220,000 are affected by SCA (Piel et al., 2010).

Sickle Cell Anemia as a Hemorheological Disease

Sickle cell anemia is caused by a single nucleotide mutation (adenine → thymine) in exon I of the β-globin gene. This point mutation (rs334 T) leads to the production of sickle hemoglobin (HbS), due to the substitution of valine for glutamic acid at the sixth position of the β-globin chain. The hydrophobic residue of valine associates with other hydrophobic residues, which causes HbS molecules to aggregate, forming fibrous precipitates when hemoglobin is deoxygenated. This phenomenon is called "HbS polymerization," and is responsible for the characteristic shape change, termed "sickling," of RBCs. Sickle RBC are rigid, and therefore do not easily flow through the microcirculation, causing frequent vaso-occlusive episodes in affected patients. In addition, when RBCs lose their deformability, they become more fragile and prone to hemolysis, which is the root cause of chronic hemolytic anemia in SCA (Connes et al., 2014).

Although the loss of RBC deformability is a fundamental characteristic of SCA, patients exhibit varying degrees of RBC rigidity, which can differentially affect SCA disease severity and complications (Renoux et al., 2016). Newborns usually have almost normal RBC deformability because they still have a high percentage of fetal hemoglobin (HbF) (Renoux et al., 2016). However, when patients become older HbF is replaced by HbS, and, as a result, RBC deformability decreases (Renoux et al., 2016). Hydroxyurea (HU) therapy can affect RBC deformability because HU stimulates HbF synthesis, thereby improving RBC deformability, although the deformability values still remain lower than in the healthy population (Lemonne et al., 2015). In individuals who are not under HU therapy, the presence or absence of alpha-thalassemia can also modulate RBC deformability (Renoux et al., 2017), as the inheritance of alpha-thalassemia results in decreased production of HbS (Rees et al., 2010) and thus lower HbS polymerization.

Rigid, sickle deformed RBC can cause pre-capillary obstruction and contribute to vaso-occlusion (Rees et al., 2010). Furthermore, RBC deformability further decreases during acute vaso-occlusive events. However, patients (adults and children over 5 years of age) who have the highest RBC deformability at steady-state, and who are not under HU therapy, actually have a higher risk of developing frequent painful vaso-occlusive crises, as well as osteonecrosis (Lamarre et al., 2012; Lemonne et al., 2013; Renoux et al., 2017). This paradox seems to be due to the fact that in SCA, RBC with the highest deformability are also the most adherent, which would trigger vaso-occlusion (Ballas et al., 1988). On the other hand, individuals who have improved RBC deformability as a result of HU therapy do not have an elevated risk of vaso-occlusive crisis because HU inhibits RBC, platelets and WBC adhesion to the vascular wall via several mechanisms (Bartolucci et al., 2010; Laurance et al., 2011; Chaar et al., 2014; Pallis et al., 2014; Verger et al., 2014). RBC aggregation is usually lower in SCA patients because of low hematocrit and the inability of irreversible sickle cell to form aggregates. However, the formed RBCs aggregates are reported to be much more robust than in healthy population which could further alter blood flow and tissue perfusion at the pre and post capillary levels (Tripette et al., 2009; Connes et al., 2014).

Sickle cell anemia patients with the highest degree of chronic hemolysis (i.e., those with the most severe anemia) are usually characterized by a severe and chronic reduction of RBC deformability as well as the presence of robust RBC aggregates, and seem to be more prone to develop complications such as leg ulcers, priapism and glomerulopathy (Bartolucci et al., 2012; Connes et al., 2013a; Lamarre et al., 2014). In contrast, patients with the highest RBC deformability tend to have less severe anemia and increased blood viscosity, which could increase the risk of developing frequent vaso-occlusive like complications (Nebor et al., 2011; Lamarre et al., 2012; Charlot et al., 2016). Surprisingly, a recent study did not show a further rise of blood viscosity during acute painful vaso-occlusive crisis (Lapoumeroulie et al., 2019). Instead, the authors found a decrease of RBC deformability, as a result of massive RBC sickling (Ballas and Smith, 1992), and a rise in RBC aggregation and RBC

aggregates robustness, which would probably impair blood flow into the microcirculation (Lapoumeroulie et al., 2019).

Vascular Function Cannot Compensate for the Hemorheological Alterations in SCA

As previously discussed, recent works have demonstrated that increased blood viscosity does not systematically cause a rise in vascular resistance in healthy individuals (Vazquez et al., 2010; Salazar Vazquez et al., 2011). Instead, increasing blood viscosity can facilitate vasodilation and decrease vascular resistance through shear stress-dependent mechanisms, which increase NO production. However, when endothelial/vascular dysfunction is present, like in SCA (Kato et al., 2007; Ataga et al., 2016; Charlot et al., 2016), vasodilation is impaired. Therefore, a rise in blood viscosity cannot be fully compensated for, and could increase the risk of frequent vaso-occlusive crises (Lemonne et al., 2012; Charlot et al., 2016).

Chronic hemolysis is highly implicated in the development of vascular dysfunction in SCA. Once hemoglobin is released into the plasma it autoxidizes, forming free heme, iron, and reactive oxygen species, which cause eNOS uncoupling, and decrease NO bioavailability (Kato et al., 2007).These alterations limit the relaxation of vascular smooth muscle, and contribute to the onset of vaso-occlusive crises (Hebbel et al., 2004). In addition, hemolysis releases the arginase contained in erythrocytes into the plasma. The free arginase hydrolyzes arginine, which is the NO precursor, to ornithine and urea, thereby exacerbating the decrease of NO bioavailability (Kato et al., 2007).

Xanthine oxidase (XO) also contributes to vascular dysfunction in SCA. Aslan et al. (2001) demonstrated that episodes of intrahepatic hypoxia-reoxygenation, which can occur in SCA, induce the release of plasma XO. The released XO can impair vascular function by binding to the vessel luminal cells. This creates an oxidative milieu, which results in NO scavenging via an oxygen free radical-dependent mechanism. Furthermore, Mockesch et al. (2017) recently showed that loss of microvascular function in children with SCA was significantly associated with both nitrotyrosine and markers of systemic oxidative stress. These findings confirm the important roles oxidative stress and NO scavenging play in the development of vascular dysfunction in SCA.

Circulating extra-vesicles, such as microparticles (Camus et al., 2012, 2015) and exosomes (Khalyfa et al., 2016), are also thought to play a role in the development of vascular dysfunction in SCA. Indeed, Camus et al. (2012) demonstrated that infusion of *in vitro*-generated RBC microparticles caused kidney vaso-occlusion in sickle cell mice. Additionally, Khalyfa et al. (2016) demonstrated that exosomes isolated from SCA patients with frequent vaso-occlusive crises decreased endothelial permeability and promoted P-selectin expression on cultured endothelial cells. The exosomes isolated from SCA patients with frequent vaso-occlusive crises also significantly increased the adhesion of monocytes to the vascular wall in mice, compared with exosomes isolated from SCA patients with a less severe phenotype. Overall, these works suggest that therapies focusing both on blood rheology and vascular function could be helpful to decrease the clinical severity of SCA patients.

EXERCISE AND BLOOD RHEOLOGY IN HEALTHY INDIVIDUALS AND INDIVIDUALS WITH SCA

Blood rheology plays an important role in the regulation of tissue perfusion at rest and during exercise. For example, RBCs need to be highly deformable to easily flow through small capillaries and transport oxygen to the tissues (Parthasarathi and Lipowsky, 1999). Any changes in RBC rheological properties during exercise may affect blood viscosity (Baskurt and Meiselman, 2003), which in turn may impact blood flow and exercise performance (Connes et al., 2013b; Waltz et al., 2015). Several investigators have reported significant correlations between blood fluidity and indices of physical fitness in sportsmen, such as time of endurance until exhaustion, aerobic working capacity at 170 W (W170), and maximal oxygen consumption (VO_{2max}) (Ernst et al., 1985; Brun et al., 1986, 1989, 1995).

The Effect of Acute Cycling Exercise on Blood Viscosity and Its Determinants in Healthy Individuals

Most of the studies conducted in the eighties and nineties to investigate the acute effects of exercise on blood rheology focused on cycling efforts performed by moderately trained subjects (Brun et al., 1998). These studies reported that acute cycling exercise caused blood viscosity measured at high shear rate (i.e., 100–200 s^{-1}) to increase by more than 15% above pre-exercise values (Brun et al., 1998; Connes et al., 2004a, 2013b; **Figure 1**). This increase in blood viscosity has been attributed to changes in plasma viscosity, hematocrit, and RBC rheological properties (Brun et al., 1998).

Multiple studies have shown that an acute bout of maximal or submaximal cycling exercise may cause plasma viscosity to increase by 10–12%, compared to resting values (Ernst, 1985; Ernst et al., 1991b; Brun et al., 1994b, 1998; Bouix et al., 1998; Connes et al., 2004b). This increase has been attributed to a rise in plasma protein content, such as fibrinogen, α1-globulins, α2-globulins, β-globulins, and γ-globulins during exercise (Nosadova, 1977; Convertino et al., 1981; Vandewalle et al., 1988; Wood et al., 1991).

Several studies have also shown that an acute cycling exercise can result in a 10–12% (i.e., 3–4 units) rise in hematocrit, when compared to pre-exercise values (Brun et al., 1994b; Bouix et al., 1998; Connes et al., 2004a). The effect of elevated hematocrit on blood viscosity at high shear rates has been well described (Cokelet and Meiselman, 2007). A 1-unit increase in hematocrit can cause a 4% increase in blood viscosity. This rise in hematocrit has been attributed to several mechanisms such as fluid shift between intra- and extra-vascular spaces (Sjogaard et al., 1985; Ploutz-Snyder et al., 1995), dehydration (Nosadova, 1977; Stephenson and Kolka, 1988) the release of sequestered

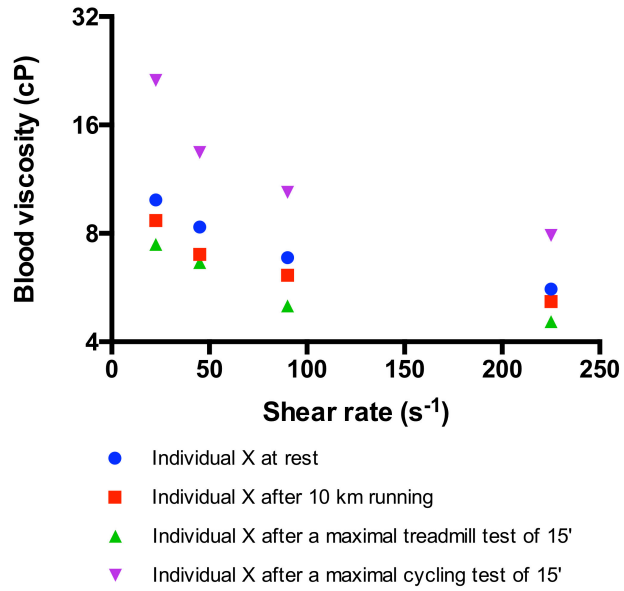

FIGURE 1 | Effects of different kind of exercise on blood viscosity measured at several shear rates in the same trained subject (maximal oxygen consumption, VO_2max = 64 ml/kg/min). The maximal treadmill and cycling tests consisted in a progressive and maximal exercise conducted until VO_2max and performed in laboratory conditions (temperature: 24°C). The 10 km running was performed outdoor (20°C) and at the highest intensity the subject could run. Indeed, the subject ran at 77% of his maximal aerobic velocity determined on the treadmill and reached a heart rate of 92% of his maximal heart rate. The subject did not drink water during each test. For the three tests, blood was sampled immediately at the end of the exercise and blood viscosity was measured with the same cone-plate viscometer within 1 h after sampling.

RBCs from the spleen (Isbister, 1997), and water trapping in muscle (Ploutz-Snyder et al., 1995).

Acute cycling exercise can also modulate RBC deformability. Several authors have reported a decrease in RBC deformability during and immediately after exercise (Reinhart et al., 1983; Galea and Davidson, 1985; Gueguen-Duchesne et al., 1987; Brun et al., 1993, 1994a; Oostenbrug et al., 1997; Yalcin et al., 2000, 2003). This decrease could be a consequence of lactic acid and reactive oxygen species production that occurs during exercise (Connes et al., 2013b). The accumulation of lactate ions and the decrease in pH would promote RBC dehydration through the activation of several RBC cationic channels, leading to RBC shrinkage and decreased RBC deformability (Van Beaumont et al., 1981; Lipovac et al., 1985; Smith et al., 1997; Connes et al., 2004c). Moreover, several groups have suggested that oxidative stress could also play a role in the decreased RBC deformability through the oxidation of membrane lipid and protein components (Senturk et al., 2005a,b; Connes et al., 2013b). However, the magnitude of the change in RBC deformability that occurs during exercise seems to depend on the training status and physical fitness of the subjects. For instance, Senturk et al. (2005a) reported that a short, progressive, maximal cycling exercise test promoted oxidative stress in both sedentary and well-trained subjects, but they only observed a decrease in RBC deformability and an increase of RBC fragility in sedentary individuals.

Very few studies have observed RBC aggregation during cycling exercise, and the results of these studies are very heterogeneous (Connes et al., 2013b). Yalcin et al. (2003) found that RBC aggregation decreased after a Wingate exercise test. In contrast, Ernst et al. (1991b) observed a transient increase in RBC aggregation above pre-exercise values after 1 h of pedaling at a heart rate of 150 beats min^{-1}. RBC aggregation then returned to baseline during the 2 h following the cycling test. Varlet-Marie et al. (2003) and Connes et al. (2007) found no change in RBC aggregation in response to submaximal/maximal cycling exercise. The discrepancies observed are not very well understood and might be related to the (1) kind of exercise performed (short versus prolonged exercise), (2) time of measurement during exercise (i.e., immediately at the end of exercise or few minutes after), (3) time delay for measurement after sampling, and (4) procedure used for RBC aggregation measurement (adequate oxygenation and adjusted hematocrit before measurement or not).

On the whole, these changes lead to a rise in blood viscosity during acute cycling exercise. Large elevations in blood viscosity have generally been considered to be deleterious for the cardiovascular system (Brun et al., 1998; Connes et al., 2013b). However, Connes et al. (2012) reported a positive correlation between the magnitude of change in blood viscosity and the magnitude of change in NO end-stable products, and a negative correlation between the magnitude of change in blood viscosity and the magnitude of change in vascular resistance. These findings suggest that increasing blood viscosity during exercise could be a way to stimulate endothelium-dependent NO production through shear stress-related mechanisms. In healthy individuals, this would result in compensatory vasodilation, thereby preventing any large increases in vascular resistance.

Acute Running Exercise, Blood Viscosity and Its Determinants in Healthy Individuals

Surprisingly, in contrast to cycling exercises, running exercises, such as a marathon or a 10-km race, do not cause a rise in blood viscosity (Neuhaus et al., 1992; Tripette et al., 2011; **Figure 1**). The main reason is that hematocrit and plasma viscosity usually remain very stable during these kinds of efforts, despite dehydration (Galea and Davidson, 1985; Neuhaus et al., 1992; Neuhaus and Gaehtgens, 1994). It has been hypothesized that the lack of change in hematocrit could be explained by repeated RBC foot strike hemolysis during running (Neuhaus et al., 1992; Neuhaus and Gaehtgens, 1994; Tripette et al., 2011; Connes et al., 2013b). However, a recent study in which highly trained subjects performed a progressive and maximal treadmill test did not observe any signs of RBC damage or eryptosis (Nader et al., 2018). However, the picture could be slightly different during ultra-running events. For instance, Robach et al. (2014) reported increased hemolysis and large plasma volume expansion immediately after a 166-km long mountain ultra-endurance marathon with 9500 m of altitude gain/loss. The impact of these changes on blood rheology has not been investigated and further studies are needed to address this question.

Surprisingly, Nader et al. (2018) found a slight but significant increase in RBC deformability in response to a short and maximal exercise test. Indeed, although hematocrit increased, blood viscosity remained unchanged (and tended to decrease), as has been observed in previous studies (Neuhaus and Gaehtgens, 1994; Tripette et al., 2011). The findings suggest that the slight increase in RBC deformability could have compensated for the rise in hematocrit observed during short running events, resulting in a lack of change in blood viscosity. The impact of ultra-run events on RBC deformability is unknown. Several other groups found a slight increase in RBC deformability during running (Suhr et al., 2012) and cycling (Connes et al., 2009) exercises. Although the exact reasons for these findings are unknown, it has been suggested that increased NO production during exercise could increase RBC deformability. One of the first works to suggest that NO could affect RBC deformability was the study of Starzyk et al. (1997), which demonstrated that intravenous infusion of L-NAME (an eNOS inhibitor) in rats caused a reduction of RBC deformability. In addition, Bor-Kucukatay et al. (2003) reported that several eNOS inhibitors also decreased RBC deformability, suggesting that basal release of NO actively maintains RBC deformability. While extracellular sources of NO may impact the deformability of RBC, several works suggest that endogenous RBC NO synthesis may also modulate RBC deformability (Kleinbongard et al., 2006). Suhr et al. (2012) demonstrated that an acute running exercise induced shear stress activation of RBC NOS (increased RBC NOS phosphorylation at Ser1177) via the PI3-kinase/Akt kinase pathway, leading to increased NO production by the RBC, which was critical to maintaining RBC deformability during exercise. Grau et al. (2013) further extended these findings by showing that RBC NOS activation by pharmacological treatment (insulin) increased RBC NO content and improved RBC deformability through direct S-nitrosylation of cytoskeleton proteins, most likely the α- and β-spectrins. In contrast, the use of RBC NOS inhibitors [wortmannin or L-N5-(1-Iminoethyl)-ornithin] resulted in a decrease of RBC NOS Ser1177 phosphorylation, NO content, cytoskeleton protein S-nitrosylation, and RBC deformability.

Impact of Physiological Changes During Acute Exercise on Blood Viscosity

As discussed above, acute cycling exercise would lead to a rise in blood viscosity while running exercise would be characterized by a lack of change in blood viscosity compared to the pre-exercise values. Although methodological aspects could partly explain some of these differences, such as the use of different viscometers (cone-plate viscometer, couette viscometer, capillary viscometer, etc.) or the use of different shear rates (low, moderate, and high shear rate viscosity are affected by different RBC rheological parameters), the picture is probably a little bit more complex. Several physiological changes occur during exercise, which may affect blood viscosity.

To avoid large dehydration during exercise, sportsmen usually drink water or carbohydrate-rich drinks. However, most of the studies performed in the field of blood rheology have been done in laboratory conditions where water is not allowed during the various exercise tests and water loss cannot be compensated by water intake. Tripette et al. (2010) and Diaw et al. (2014) previously tested the impact of add-libitum hydration and water deprivation on blood viscosity during a prolonged submaximal exercise and a soccer game, respectively. Healthy individuals and subjects carrying sickle cell trait were included. While hydration during exercise was able to decrease blood viscosity below the pre-exercise levels in sickle cell trait carriers, blood viscosity increased similarly in healthy individuals in both the "hydration" and "water deprivation" conditions. The rate of dehydration was around 1.5–2% in these studies, which is not very severe. There is a growing interest from the runners community to participate to very prolonged race (>100 kms), sometimes performed at high altitude. The impact of the environment and higher dehydration rate on blood viscosity are unknown and further studies are needed.

Exercise is accompanied by a rise cardiac output and blood flow leading to an increase of shear rate values in the vascular system. For instance, shear rate in the femoral artery has been reported to increase from 60 s^{-1} at rest to 200–250 s^{-1} during exercise (Gonzales et al., 2009). Blood is a shear-thinning fluid, meaning that its viscosity decreases when shear rate increases. Connes et al. (2013b) shown that 15 min of cycling exercise performed at a submaximal intensity increased blood viscosity measured at 90 s^{-1}. However, when the viscosity of the blood sampled at the end of exercise was measured at 225 s^{-1} (which reflects the shear rate reached during exercise), the mean value was almost identical to the viscosity of the blood sampled before exercise and measured at 90 s^{-1}. Indeed, the effects of hemoconcentration, increased plasma viscosity, decreased RBC deformability and increased RBC aggregation on blood viscosity during exercise could be counterbalanced by the effects of increasing shear rate (Connes et al., 2013b). However, the slight remaining changes in blood viscosity observed during exercise were still correlated with the magnitude of changes in NO-end products concentration, suggesting that blood viscosity plays a role in promoting NO production during exercise (Connes et al., 2013b).

Core temperature rises during exercise and it is well known that blood viscosity also depends on temperature (Baskurt et al., 2009). A recent elegant study shown that when the changes in temperature occurring during exercise are took into account in the measurements of blood viscosity, there is no difference between the pre- and post-exercise values (Buono et al., 2016). The slight physiological hyperthermia was shown to increase RBC deformability, which compensated the rise in hematocrit and resulted in a lack of change in blood viscosity. The authors estimated that the combined effects of increasing shear rate and hyperthermia during exercise could decrease blood viscosity by 31% below the pre-exercise levels, in spite of the exercise induced hemoconcentration (Buono et al., 2016). These findings clearly show that studies in the field of exercise hemorheology should consider the effects of various physiological factors for better interpretation about the role of blood viscosity in the cardiovascular adaptations and physical fitness.

Long Term Effects of Exercise on Blood Rheology in Healthy Individuals

Chronic exercise (endurance or resistance exercise) usually decreases blood viscosity (Brun et al., 1998; Romain et al., 2011; Kilic-Toprak et al., 2012). One reason for this change is that plasma volume increases few hours or several days after a single bout of exercise (Fellmann, 1992; Brun et al., 1998), resulting in an "autohemodilution" (Ernst, 1987; Ernst et al., 1991a). Repeated exercise bouts on consecutive days leads to a chronic "autohemodilution" resulting in a low baseline hematocrit – low baseline viscosity pattern (Ernst, 1987; Brun et al., 1998; Kilic-Toprak et al., 2012). The magnitude of plasma volume expansion ranges from 9 to 25%, corresponding to an additional 300 to 700 ml of plasma. It has been shown that the larger the reduction in plasma volume during exercise, the greater the subsequent plasma volume expansion (Fellmann, 1992). The amount of water ingested during and after exercise, as well several fluid-regulating hormones (aldosterone, vasopressin and the atrial natriuretic factor) and the level of plasma proteins, influence the degree of the plasma volume expansion after exercise. Plasma volume expansion is responsible for the decrease in plasma viscosity that contributes to the decrease in blood viscosity (Ernst, 1987).

Exercise training also induces RBC rheological adaptations (Brun et al., 2010; Kilic-Toprak et al., 2012). Ernst (1987) reported increased RBC deformability in athletes compared to sedentary subjects, a finding later confirmed by Smith et al. (1999). A 3-month longitudinal study of initially untrained healthy volunteers who performed regular training also showed a decrease of blood viscosity and a rise of RBC deformability (Ernst, 1987). Few studies have been conducted to determine why RBC deformability improves in healthy individuals after chronic exercise. However, Smith et al. (1999) and Tomschi et al. (2018) found a higher proportion of young deformable RBCs in athletes than in untrained subjects. The hemorheological benefits induced by regular exercise are suspected to contribute to the improvements in cardiovascular health that are induced by training programs in patients with cardiovascular disorders (Sandor et al., 2014).

Acute and Chronic Effects of Exercise in SCA

The metabolic changes occurring during exercise may promote HbS polymerization, RBC sickling, oxidative stress and inflammation. For this reason, physicians have generally been reluctant to promote physical activity for individuals with SCA (Connes, 2010; Waltz and Connes, 2014; Chirico et al., 2016; Martin et al., 2018). However, since regular physical activity has been shown to provide health benefits in various chronic diseases, several groups have begun to study the effects of acute and chronic exercise in individuals and mice with SCA.

Sickle cell anemia patients have decreased aerobic physical fitness compared to the general population (Connes et al., 2011). This is probably due to a combination of several factors, including chronic anemia, reduced muscle mass and strength, abnormal cardiac function, gas exchange abnormalities, mechanical ventilation limitations and peripheral vascular impairment (Callahan et al., 2002; Dougherty et al., 2011; Liem et al., 2015; Badawy et al., 2018; Merlet et al., 2019). A recent study reported negative associations between the oxygen uptake efficiency slope (an index of aerobic physical fitness) and hematocrit, RBC deformability, and RBC aggregate strength in adults with SCA (Charlot et al., 2015). These biological parameters were also associated with the ability of recover from a short submaximal exercise (Charlot et al., 2015). In another study, Waltz et al. (2013) showed that high levels of anemia, low fetal hemoglobin levels, and low RBC deformability were independent predictors of a low 6-min walking test performance.

Blood rheological abnormalities play a key role in the pathophysiology of SCA. For this reason, several works have investigated the effects of acute exercise on various biological parameters to determine what kind of exercise could be considered completely safe for individuals with SCA. In a study performed in Ivory Coast, 17 patients with SCA performed a 20 min moderate exercise (45 Watts) with blood sampling before and at the end of exercise (Balayssac-Siransy et al., 2011; Faes et al., 2014). Despite an increase in the percentages of dense RBC at the end of the effort, blood viscosity and soluble forms of P- and E-selectin remained unchanged compared to the pre-exercise level (Balayssac-Siransy et al., 2011; Faes et al., 2014). Slight increases of the plasma soluble forms of VCAM-1 and ICAM-1 were noted at the end of the exercise in SCA patients, suggesting slight endothelial activation (Faes et al., 2014). On the other hand, another study by Liem et al. (2015) reported higher concentrations of soluble VCAM-1 in the plasma of SCA patients at rest compared to a control group, but progressive and maximal exercise tests did not induce any further rise of VCAM-1. An additional study by Waltz et al. (2012) evaluated blood rheological parameters in subjects with SCA following a short (10–12 min) progressive submaximal cycling exercise, conducted until the first ventilatory threshold was reached. The exercise caused no changes in hematocrit, white blood cell count, blood viscosity, RBC deformability, or RBC aggregation. Furthermore, the strength of RBC aggregates decreased 2 and 3 days after the exercise. This delayed effect of exercise on RBC aggregate strength could be beneficial from a clinical point of view since this parameter is associated with risk of acute chest syndrome (Lamarre et al., 2012), and is increased during vaso-occlusive crises (Lapoumeroulie et al., 2019). Grau et al. (2019) recently confirmed that a short progressive and submaximal cycling exercise had no deleterious effect on RBC deformability and showed that this kind of effort does not exacerbate hemolysis. Finally, Barbeau et al. (2001) previously reported that the repetition of 30 min of moderate exercise for three consecutive days increased plasma NO concentrations in subjects with SCA. This could be viewed as a positive effect since NO bioavailability is reduced in SCA (Kato et al., 2007). It is important to note that none of these studies reported any clinical complications immediately or several days after the exercise (Barbeau et al., 2001; Balayssac-Siransy et al., 2011; Waltz et al., 2012; Faes et al., 2014; Grau et al., 2019). Overall, the results of these studies suggest that mild-to-moderate intensity exercise is probably safe in SCA, but longer or high-intensity

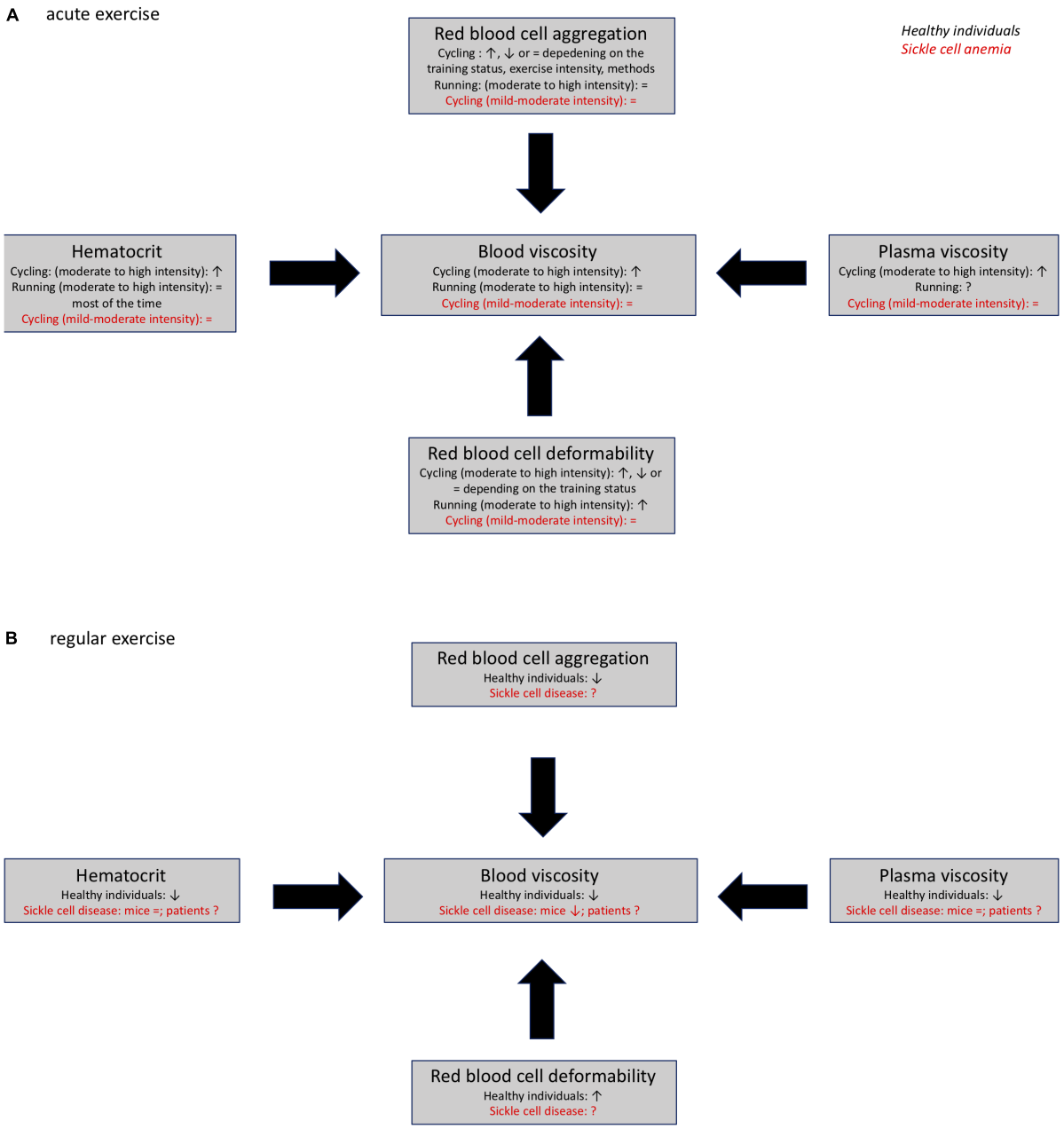

FIGURE 2 | Acute **(A)** and chronic **(B)** effects of exercise on blood rheology (blood viscosity, plasma viscosity, hematocrit, red blood cell deformability, and aggregation) in healthy individuals and patients with sickle cell anemia., ↑, ↓; =, no change; ?, unknown.

exercise should be avoided, or recommended only on a case-by-case basis (Martin et al., 2018). Still, some patients may experience moderate to severe hemoglobin desaturation, even during low-intensity or submaximal exercises, like the 6-min walking test (Waltz et al., 2013). Hemoglobin desaturation can promote RBC sickling in conditions of prolonged hypoxemic stress. Therefore, SCA patients should always be screened for hemoglobin desaturation during exercise tests to identify whether the person is at risk of experiencing exercise-induced hypoxemia during submaximal efforts.

The accumulating evidence showing that acute exercise could be safe for SCA patients prompted several groups to test the effects of regular exercise in mice and humans with SCA. Studies conducted in sickle SAD mice showed that 8 weeks of voluntary wheel running decreased blood viscosity (Faes et al., 2015), limited systemic oxidative stress (Charrin et al., 2015), and decreased pulmonary endothelial activation in response to an hypoxic-reoxygenation stimulus (Aufradet et al., 2014). An additional study conducted by Charrin et al. (2018) evaluated the

effects of 8 weeks of aerobic training (1 h/day, 5 days/week) in a more severe mice model of SCA (Townes mice). The chronic exercise decreased several markers of systemic inflammation, including white blood cell count, plasma Th1/Th2 cytokine ratio, and Interleukin-1β level, and reduced the occurrence of splenomegaly. Furthermore, two other studies have also shown that endurance training improved muscle function in Townes SCA mice (Chatel et al., 2018; Gouraud et al., 2019).

Presently, only a few studies have been conducted to evaluate chronic exercise in people with SCA. Omwanghe et al. (2017) recently reported that 90% of children with SCA participate in physical education and 48% participate in sports. These findings illustrate that children with SCA do moderate to vigorous intensity physical activity for short durations. The same research group also prescribed three home exercise sessions per week, for 12 weeks, to 13 children with SCA. Results showed that 77% of subjects completed 89% of the prescribed sessions without any exercise-related adverse events. These results indicate that regular moderate exercise is safe and feasible in children with SCA. In an additional study by Gellen et al. (2018), adults with SCA performed 45 min of exercise three times a week for 8 weeks. No adverse events were reported in the study period, confirming that regular physical activity can be safe for people with SCA. Moreover, the SCA subjects' power outputs measured at 4 mmol/L blood lactate significantly increased after the 8 weeks training period, indicating improved physical fitness. Currently, no human studies have been conducted to determine whether chronic exercise can modulate the biological parameters (i.e., blood rheology, hematology, inflammation, oxidative stress) that cause the various acute complications experienced by people with SCA. However, the current evidence that exists suggests that moderate-intensity endurance-exercise training could potentially be used as a beneficial therapeutic strategy for patients with SCA (Gellen et al., 2018).

CONCLUSION

In conclusion, whole blood viscosity is a physiological parameter that should be considered when studying vascular resistance in healthy populations or in patients affected by various diseases. Plasma viscosity, hematocrit, RBC deformability, and RBC aggregation are all factors that modulate blood viscosity. Alterations in any of these factors can modify blood flow resistance in the vasculature and alter tissue perfusion. In healthy individuals, the vascular system can adapt to elevations in blood viscosity because increased shear stress results in endothelium-dependent NO production. However, in individuals with vascular dysfunction, the vessels are not able to effectively vasodilate. Therefore, elevated blood viscosity can increase vascular resistance.

Tissue perfusion plays a key role during exercise and exercise can modulate blood viscosity and RBC rheology. The effects of acute exercise in healthy individuals are dependent on exercise modality, intensity, duration and physical fitness of the subjects. Most of the studies have found that acute cycling exercise increases blood viscosity by decreasing RBC deformability and increasing hematocrit and plasma viscosity (**Figure 2**). In contrast, acute running exercise is suggested to not cause any change in blood viscosity because of unaltered hematocrit (**Figure 2**). Furthermore, chronic exercise has been shown to decrease blood viscosity by increasing RBC deformability and decreasing hematocrit because of chronic auto-hemodilution (**Figure 2**).

Sickle cell anemia is a hereditary disease that causes pathological changes in blood rheology that ultimately contribute to the development of vascular dysfunction and disease complications. Several studies have shown that light to moderate intensity acute exercise is well-tolerated in individuals with SCA (**Figure 2**). Additionally, chronic exercise has been shown to cause positive hemorheological adaptations that could play a role in the positive benefits that result from training programs in patients with various cardiovascular disorders (**Figure 2**). Therefore, additional studies should be carried out to determine whether chronic exercise could improve blood rheological profiles in individuals with SCA, and decrease the severity of disease complications.

AUTHOR CONTRIBUTIONS

EN, SS, and PC wrote the first version of the manuscript. All authors read and approved the final version of the manuscript.

REFERENCES

Aslan, M., Ryan, T. M., Adler, B., Townes, T. M., Parks, D. A., Thompson, J. A., et al. (2001). Oxygen radical inhibition of nitric oxide-dependent vascular function in sickle cell disease. *Proc. Natl. Acad. Sci. U.S.A.* 98, 15215–15220. doi: 10.1073/pnas.221292098

Ataga, K. I., Derebail, V. K., Caughey, M., Elsherif, L., Shen, J. H., Jones, S. K., et al. (2016). Albuminuria is associated with endothelial dysfunction and elevated plasma endothelin-1 in sickle cell anemia. *PLoS One* 11:e0162652. doi: 10.1371/journal.pone.0162652

Aufradet, E., Douillard, A., Charrin, E., Romdhani, A., De Souza, G., Bessaad, A., et al. (2014). Physical activity limits pulmonary endothelial activation in sickle cell SAD mice. *Blood* 123, 2745–2747. doi: 10.1182/blood-2013-10-534982

Badawy, S. M., Payne, A. B., Rodeghier, M. J., and Liem, R. I. (2018). Exercise capacity and clinical outcomes in adults followed in the cooperative study of sickle cell disease (CSSCD). *Eur. J. Haematol.* 101, 532–541. doi: 10.1111/ejh.13140

Balayssac-Siransy, E., Connes, P., Tuo, N., Danho, C., Diaw, M., Sanogo, I., et al. (2011). Mild haemorheological changes induced by a moderate endurance exercise in patients with sickle cell anaemia. *Br. J. Haematol.* 154, 398–407. doi: 10.1111/j.1365-2141.2011.08728.x

Ballas, S. K., Larner, J., Smith, E. D., Surrey, S., Schwartz, E., and Rappaport, E. F. (1988). Rheologic predictors of the severity of the painful sickle cell crisis. *Blood* 72, 1216–1223.

Ballas, S. K., and Smith, E. D. (1992). Red blood cell changes during the evolution of the sickle cell painful crisis. *Blood* 79, 2154–2163.

Barbeau, P., Woods, K. F., Ramsey, L. T., Litaker, M. S., Pollock, D. M., Pollock, J. S., et al. (2001). Exercise in sickle cell anemia: effect on inflammatory and vasoactive mediators. *Endothelium* 8, 147–155.

Bartolucci, P., Brugnara, C., Teixeira-Pinto, A., Pissard, S., Moradkhani, K., Jouault, H., et al. (2012). Erythrocyte density in sickle cell syndromes is

associated with specific clinical manifestations and hemolysis. *Blood* 120, 3136–3141. doi: 10.1182/blood-2012-04-424184

Bartolucci, P., Chaar, V., Picot, J., Bachir, D., Habibi, A., Fauroux, C., et al. (2010). Decreased sickle red blood cell adhesion to laminin by hydroxyurea is associated with inhibition of Lu/BCAM protein phosphorylation. *Blood* 116, 2152–2159. doi: 10.1182/blood-2009-12-257444

Baskurt, O., and Meiselman, H. J. (2007). "In vivo hemorheology," in *Handbook of Hemorheology and Hemodynamics*, eds O. K. Baskurt, M. R. Hardeman, M. W. Rampling, and H. J. Meiselman, (Amsterdam: IOS Press), 322–338.

Baskurt, O. K., Boynard, M., Cokelet, G. C., Connes, P., Cooke, B. M., Forconi, S., et al. (2009). New guidelines for hemorheological laboratory techniques. *Clin. Hemorheol. Microcirc* 42, 75–97. doi: 10.3233/CH-2009-1202

Baskurt, O. K., and Meiselman, H. J. (2003). Blood rheology and hemodynamics. *Semin. Thromb. Hemost.* 29, 435–450. doi: 10.1055/s-2003-44551

Baskurt, O. K., and Meiselman, H. J. (2009). Red blood cell "aggregability". *Clin. Hemorheol. Microcirc* 43, 353–354. doi: 10.3233/CH-2009-1255

Baskurt, O. K., Yalcin, O., and Meiselman, H. J. (2004). Hemorheology and vascular control mechanisms. *Clin. Hemorheol. Microcirc* 30, 169–178.

Biro, K., Sandor, B., Kovacs, D., Csiszar, B., Vekasi, J., Totsimon, K., et al. (2018). Lower limb ischemia and microrheological alterations in patients with diabetic retinopathy. *Clin. Hemorheol. Microcirc.* 69, 23–35. doi: 10.3233/CH-189103

Bor-Kucukatay, M., Wenby, R. B., Meiselman, H. J., and Baskurt, O. K. (2003). Effects of nitric oxide on red blood cell deformability. *Am. J. Physiol. Heart Circ. Physiol.* 284, H1577–H1584. doi: 10.1152/ajpheart.00665.2002

Bouix, D., Peyreigne, C., Raynaud, E., Monnier, J. F., Micallef, J. P., and Brun, J. F. (1998). Relationships among body composition, hemorheology and exercise performance in rugbymen. *Clin. Hemorheol. Microcirc* 19, 245–254.

Brun, J. F., Criqui, C., and Orsetti, A. (1986). Paramètres hémorhéologiques et exercice physique. *Sports Med. Acta.* 12, 56–60.

Brun, J. F., Fons, C., Supparo, C., Mallard, C., and Orsetti, A. (1993). Could exercise-induced increase in blood viscosity at high shear rate be entirely explained by hematocrit and plasma viscosity changes? *Clin. Hemorheol.* 13, 187–199.

Brun, J. F., Khaled, S., Raynaud, E., Bouix, D., Micallef, J. P., and Orsetti, A. (1998). The triphasic effects of exercise on blood rheology: which relevance to physiology and pathophysiology? *Clin. Hemorheol. Microcirc.* 19, 89–104.

Brun, J. F., Micallef, J. P., and Orsetti, A. (1994a). Hemorheologic effects of light prolonged exercise. *Clin. Hemorheol.* 14, 807–818.

Brun, J. F., Supparo, C., Mallard, C., and Orsetti, A. (1994b). Low values of resting blood viscosity and erythrocyte aggregation are associated with lower increases in blood lactate during submaximal exercise. *Clin. Hemorheol.* 14, 105–116.

Brun, J. F., Sekkat, M., Lagoueyte, C., Fédou, C., and Orsetti, A. (1989). Relashionships between fitness and blood viscosity in untrained normal short children. *Clin. Hemorheol.* 9, 953–963.

Brun, J. F., Supparo, C., Rama, D., Benezis, C., and Orsetti, A. (1995). Maximal oxygen uptake and lactate thresholds during exercise are related to blood viscosity and erythrocyte aggregation in professional football players. *Clin. Hemorheol.* 15, 201–212.

Brun, J. F., Varlet-Marie, E., Connes, P., and Aloulou, I. (2010). Hemorheological alterations related to training and overtraining. *Biorheology* 47, 95–115. doi: 10.3233/BIR-2010-0563

Brun, J. F., Varlet-Marie, E., Richou, M., Mercier, J., and Raynaud De Mauverger, E. (2018). Blood rheology as a mirror of endocrine and metabolic homeostasis in health and disease1. *Clin. Hemorheol. Microcirc* 69, 239–265. doi: 10.3233/CH-189124

Buono, M. J., Krippes, T., Kolkhorst, F. W., Williams, A. T., and Cabrales, P. (2016). Increases in core temperature counterbalance effects of haemoconcentration on blood viscosity during prolonged exercise in the heat. *Exp. Physiol.* 101, 332–342. doi: 10.1113/EP085504

Callahan, L. A., Woods, K. F., Mensah, G. A., Ramsey, L. T., Barbeau, P., and Gutin, B. (2002). Cardiopulmonary responses to exercise in women with sickle cell anemia. *Am. J. Respir. Crit. Care Med.* 165, 1309–1316. doi: 10.1164/rccm.2002036

Camus, S. M., De Moraes, J. A., Bonnin, P., Abbyad, P., Le Jeune, S., Lionnet, F., et al. (2015). Circulating cell membrane microparticles transfer heme to endothelial cells and trigger vasoocclusions in sickle cell disease. *Blood* 125, 3805–3814. doi: 10.1182/blood-2014-07-589283

Camus, S. M., Gausseres, B., Bonnin, P., Loufrani, L., Grimaud, L., Charue, D., et al. (2012). Erythrocyte microparticles can induce kidney vaso-occlusions in a murine model of sickle cell disease. *Blood* 120, 5050–5058. doi: 10.1182/blood-2012-02-413138

Chaar, V., Laurance, S., Lapoumeroulie, C., Cochet, S., De Grandis, M., Colin, Y., et al. (2014). Hydroxycarbamide decreases sickle reticulocyte adhesion to resting endothelium by inhibiting endothelial lutheran/basal cell adhesion molecule (Lu/BCAM) through phosphodiesterase 4A activation. *J. Biol. Chem.* 289, 11512–11521. doi: 10.1074/jbc.M113.506121

Charlot, K., Romana, M., Moeckesch, B., Jumet, S., Waltz, X., Divialle-Doumdo, L., et al. (2016). Which side of the balance determines the frequency of vaso-occlusive crises in children with sickle cell anemia: Blood viscosity or microvascular dysfunction? *Blood Cells Mol. Dis.* 56, 41–45. doi: 10.1016/j.bcmd.2015.10.005

Charlot, K., Waltz, X., Hedreville, M., Sinnapah, S., Lemonne, N., Etienne-Julan, M., et al. (2015). Impaired oxygen uptake efficiency slope and off-transient kinetics of pulmonary oxygen uptake in sickle cell anemia are associated with hemorheological abnormalities. *Clin. Hemorheol. Microcirc.* 60, 413–421. doi: 10.3233/CH-141891

Charrin, E., Aufradet, E., Douillard, A., Romdhani, A., Souza, G. D., Bessaad, A., et al. (2015). Oxidative stress is decreased in physically active sickle cell SAD mice. *Br. J. Haematol.* 168, 747–756. doi: 10.1111/bjh.13207

Charrin, E., Dube, J. J., Connes, P., Pialoux, V., Ghosh, S., Faes, C., et al. (2018). Moderate exercise training decreases inflammation in transgenic sickle cell mice. *Blood Cells Mol. Dis.* 69, 45–52. doi: 10.1016/j.bcmd.2017.06.002

Chatel, B., Messonnier, L. A., Barge, Q., Vilmen, C., Noirez, P., Bernard, M., et al. (2018). Endurance training reduces exercise-induced acidosis and improves muscle function in a mouse model of sickle cell disease. *Mol. Genet. Metab.* 123, 400–410. doi: 10.1016/j.ymgme.2017.11.010

Chien, S., King, R. G., Skalak, R., Usami, S., and Copley, A. L. (1975). Viscoelastic properties of human blood and red cell suspensions. *Biorheology* 12, 341–346.

Chien, S., Usami, S., Dellenback, R. J., and Gregersen, M. I. (1970). Shear-dependent deformation of erythrocytes in rheology of human blood. *Am. J. Physiol.* 219, 136–142. doi: 10.1152/ajplegacy.1970.219.1.136

Chirico, E. N., Faes, C., Connes, P., Canet-Soulas, E., Martin, C., and Pialoux, V. (2016). Role of exercise-induced oxidative stress in sickle cell trait and disease. *Sports Med.* 46, 629–639. doi: 10.1007/s40279-015-0447-z

Clark, M. R., Mohandas, N., and Shohet, S. B. (1983). Osmotic gradient ektacytometry: comprehensive characterization of red cell volume and surface maintenance. *Blood* 61, 899–910.

Cokelet, G. R., and Goldsmith, H. L. (1991). Decreased hydrodynamic resistance in the two-phase flow of blood through small vertical tubes at low flow rates. *Circ. Res.* 68, 1–17. doi: 10.1161/01.res.68.1.1

Cokelet, G. R., and Meiselman, H. J. (2007). "Macro- and micro-rheological properties of blood," in *Handbook of Hemorheology and Hemodynamics*, eds O. K. Baskurt, M. R. Hardeman, M. W. Rampling, and H. J. Meiselman, (Amsterdam: IOS Press), 45–71.

Connes, P. (2010). Hemorheology and exercise: effects of warm environments and potential consequences for sickle cell trait carriers. *Scand. J. Med. Sci. Sports* 20(Suppl. 3), 48–52. doi: 10.1111/j.1600-0838.2010.01208.x

Connes, P., Alexy, T., Detterich, J., Romana, M., Hardy-Dessources, M. D., and Ballas, S. K. (2016). The role of blood rheology in sickle cell disease. *Blood Rev.* 30, 111–118. doi: 10.1016/j.blre.2015.08.005

Connes, P., Bouix, D., Durand, F., Kippelen, P., Mercier, J., Prefaut, C., et al. (2004a). Is hemoglobin desaturation related to blood viscosity in athletes during exercise? *Int. J. Sports Med.* 25, 569–574.

Connes, P., Bouix, D., Py, G., Caillaud, C., Kippelen, P., Brun, J. F., et al. (2004b). Does exercise-induced hypoxemia modify lactate influx into erythrocytes and hemorheological parameters in athletes? *J. Appl. Physiol.* 97, 1053–1058.

Connes, P., Bouix, D., Py, G., Préfaut, C., Mercier, J., Brun, J. F., et al. (2004c). Opposite effects of in vitro lactate on erythrocyte deformability in athletes and untrained subjects. *Clin. Hemorheol. Microcirc* 31, 311–318.

Connes, P., Caillaud, C., Py, G., Mercier, J., Hue, O., and Brun, J. F. (2007). Maximal exercise and lactate do not change red blood cell aggregation in well trained athletes. *Clin. Hemorheol. Microcirc* 36, 319–326.

Connes, P., Hue, O., Tripette, J., and Hardy-Dessources, M. D. (2008). Blood rheology abnormalities and vascular cell adhesion mechanisms in sickle cell trait carriers during exercise. *Clin. Hemorheol. Microcirc* 39, 179–184.

Connes, P., Lamarre, Y., Hardy-Dessources, M. D., Lemonne, N., Waltz, X., Mougenel, D., et al. (2013a). Decreased hematocrit-to-viscosity ratio and increased lactate dehydrogenase level in patients with sickle cell anemia and recurrent leg ulcers. *PLoS One* 8:e79680. doi: 10.1371/journal.pone.0079680

Connes, P., Simmonds, M. J., Brun, J. F., and Baskurt, O. K. (2013b). Exercise hemorheology: classical data, recent findings and unresolved issues. *Clin. Hemorheol. Microcirc* 53, 187–199. doi: 10.3233/CH-2012-1643

Connes, P., Lamarre, Y., Waltz, X., Ballas, S. K., Lemonne, N., Etienne-Julan, M., et al. (2014). Haemolysis and abnormal haemorheology in sickle cell anaemia. *Br. J. Haematol.* 165, 564–572. doi: 10.1111/bjh.12786

Connes, P., Machado, R., Hue, O., and Reid, H. (2011). Exercise limitation, exercise testing and exercise recommendations in sickle cell anemia. *Clin. Hemorheol. Microcirc.* 49, 151–163. doi: 10.3233/CH-2011-1465

Connes, P., Pichon, A., Hardy-Dessources, M. D., Waltz, X., Lamarre, Y., Simmonds, M. J., et al. (2012). Blood viscosity and hemodynamics during exercise. *Clin. Hemorheol. Microcirc.* 51, 101–109. doi: 10.3233/CH-2011-1515

Connes, P., Tripette, J., Mukisi-Mukaza, M., Baskurt, O. K., Toth, K., Meiselman, H. J., et al. (2009). Relationships between hemodynamic, hemorheological and metabolic responses during exercise. *Biorheology* 46, 133–143. doi: 10.3233/BIR-2009-0529

Convertino, V. A., Keil, L. C., Bernauer, E. M., and Greenleaf, J. E. (1981). Plasma volume, osmolality, vasopressin, and renin activity during graded exercise in man. *J. Appl. Physiol. Respir. Environ. Exerc. Physiol.* 50, 123–128. doi: 10.1152/jappl.1981.50.1.123

Diaw, M., Samb, A., Diop, S., Sall, N. D., Ba, A., Cisse, F., et al. (2014). Effects of hydration and water deprivation on blood viscosity during a soccer game in sickle cell trait carriers. *Br. J. Sports Med.* 48, 326–331. doi: 10.1136/bjsports-2012-091038

Dougherty, K. A., Schall, J. I., Rovner, A. J., Stallings, V. A., and Zemel, B. S. (2011). Attenuated maximal muscle strength and peak power in children with sickle cell disease. *J. Pediatr. Hematol. Oncol.* 33, 93–97. doi: 10.1097/MPH.0b013e318200ef49

Dupire, J., Socol, M., and Viallat, A. (2012). Full dynamics of a red blood cell in shear flow. *Proc. Natl. Acad. Sci. U.S.A.* 109, 20808–20813. doi: 10.1073/pnas.1210236109

Ernst, E. (1985). Changes in blood rheology produced by exercise. *J. Am. Med. Assoc.* 253, 2962–2963.

Ernst, E. (1987). Influence of regular physical activity on blood rheology. *Eur. Heart J.* 8(Suppl. G), 59–62.

Ernst, E., Danburger, L., and Saradeth, T. (1991a). Changes in plasma volume after prolonged endurance exercise. *Med. Sci. Sports Exerc.* 23:884.

Ernst, E., Daburger, L., and Saradeth, T. (1991b). The kinetics of blood rheology during and after prolonged standardized exercise. *Clin Hemorheol.* 11, 429–439.

Ernst, E., Matrai, A., Aschenbrenner, E., Will, V., and Schmidlechner, C. (1985). Relationship between fitness and blood fluidity. *Clin. Hemorheol.* 5, 507–510.

Faes, C., Balayssac-Siransy, E., Connes, P., Hivert, L., Danho, C., Bogui, P., et al. (2014). Moderate endurance exercise in patients with sickle cell anaemia: effects on oxidative stress and endothelial activation. *Br. J. Haematol.* 164, 124–130. doi: 10.1111/bjh.12594

Faes, C., Charrin, E., Connes, P., Pialoux, V., and Martin, C. (2015). Chronic physical activity limits blood rheology alterations in transgenic SAD mice. *Am. J. Hematol.* 90, E32–E33. doi: 10.1002/ajh.23896

Fellmann, N. (1992). Hormonal and plasma volume alterations following endurance exercise. A brief review. *Sports Med.* 13, 37–49. doi: 10.2165/00007256-199213010-00004

Fischer, T. M., Stohr-Lissen, M., and Schmid-Schonbein, H. (1978). The red cell as a fluid droplet: tank tread-like motion of the human erythrocyte membrane in shear flow. *Science* 202, 894–896. doi: 10.1126/science.715448

Galea, G., and Davidson, R. J. (1985). Hemorrheology of marathon running. *Int. J. Sports Med.* 6, 136–138. doi: 10.1055/s-2008-1025826

Gellen, B., Messonnier, L. A., Galacteros, F., Audureau, E., Merlet, A. N., Rupp, T., et al. (2018). Moderate-intensity endurance-exercise training in patients with sickle-cell disease without severe chronic complications (EXDRE): an open-label randomised controlled trial. *Lancet Haematol.* 5, e554–e562. doi: 10.1016/S2352-3026(18)30163-7

Goldsmith, H. L., Frank, J. M., and Maclntosh, C. (1972). Flow behaviour of erythrocytes. Rotation and deformation in dilute suspensions. *Proc. R. Soc. B.* 182, 351–384.

Gonzales, J. U., Parker, B. A., Ridout, S. J., Smithmyer, S. L., and Proctor, D. N. (2009). Femoral shear rate response to knee extensor exercise: an age and sex comparison. *Biorheology* 46, 145–154. doi: 10.3233/BIR-2009-0535

Gouraud, E., Charrin, E., Dube, J. J., Ofori-Acquah, S. F., Martin, C., Skinner, S., et al. (2019). Effects of individualized treadmill endurance training on oxidative stress in skeletal muscles of transgenic sickle mice. *Oxid. Med. Cell Longev.* 2019:3765643. doi: 10.1155/2019/3765643

Grau, M., Jerke, M., Nader, E., Schenk, A., Renoux, C., Collins, B., et al. (2019). Effect of acute exercise on RBC deformability and RBC nitric oxide synthase signalling pathway in young sickle cell anaemia patients. *Sci. Rep.* 9:11813. doi: 10.1038/s41598-019-48364-1

Grau, M., Pauly, S., Ali, J., Walpurgis, K., Thevis, M., Bloch, W., et al. (2013). RBC-NOS-dependent S-nitrosylation of cytoskeletal proteins improves RBC deformability. *PLoS One* 8:e56759. doi: 10.1371/journal.pone.0056759

Gueguen-Duchesne, M., Durand, F., Beillot, J., Dezier, J., Rochcongar, P., Legoff, M., et al. (1987). Could maximal exercise be a hemorheological risk factor? *Clin. Hemorheol.* 7, 418.

Hakim, T. S. (1988). Erythrocyte deformability and segmental pulmonary vascular resistance: osmolarity and heat treatment. *J. Appl. Physiol.* 65, 1634–1641. doi: 10.1152/jappl.1988.65.4.1634

Hebbel, R. P., Osarogiagbon, R., and Kaul, D. (2004). The endothelial biology of sickle cell disease: inflammation and a chronic vasculopathy. *Microcirculation* 11, 129–151.

Intaglietta, M. (2009). Increased blood viscosity: disease, adaptation or treatment? *Clin. Hemorheol. Microcirc.* 42, 305–306. doi: 10.3233/CH-2009-1236

Isbister, J. P. (1997). Physiology and pathophysiology of blood volume regulation. *Transfus. Sci.* 18, 409–423.

Kato, G. J., Gladwin, M. T., and Steinberg, M. H. (2007). Deconstructing sickle cell disease: reappraisal of the role of hemolysis in the development of clinical subphenotypes. *Blood Rev.* 21, 37–47. doi: 10.1016/j.blre.2006.07.001

Kesmarky, G., Kenyeres, P., Rabai, M., and Toth, K. (2008). Plasma viscosity: a forgotten variable. *Clin. Hemorheol. Microcirc.* 39, 243–246.

Khalyfa, A., Khalyfa, A. A., Akbarpour, M., Connes, P., Romana, M., Lapping-Carr, G., et al. (2016). Extracellular microvesicle microRNAs in children with sickle cell anaemia with divergent clinical phenotypes. *Br. J. Haematol.* 174, 786–798. doi: 10.1111/bjh.14104

Kilic-Toprak, E., Ardic, F., Erken, G., Unver-Kocak, F., Kucukatay, V., and Bor-Kucukatay, M. (2012). Hemorheological responses to progressive resistance exercise training in healthy young males. *Med. Sci. Monit.* 18, CR351–CR360. doi: 10.12659/msm.882878

Kleinbongard, P., Schulz, R., Rassaf, T., Lauer, T., Dejam, A., Jax, T., et al. (2006). Red blood cells express a functional endothelial nitric oxide synthase. *Blood* 107, 2943–2951. doi: 10.1182/blood-2005-10-3992

Ko, E., Youn, J. M., Park, H. S., Song, M., Koh, K. H., and Lim, C. H. (2018). Early red blood cell abnormalities as a clinical variable in sepsis diagnosis. *Clin. Hemorheol. Microcirc.* 70, 355–363. doi: 10.3233/CH-180430

Lamarre, Y., Romana, M., Lemonne, N., Hardy-Dessources, M. D., Tarer, V., Mougenel, D., et al. (2014). Alpha thalassemia protects sickle cell anemia patients from macro-albuminuria through its effects on red blood cell rheological properties. *Clin. Hemorheol. Microcirc.* 57, 63–72. doi: 10.3233/CH-131772

Lamarre, Y., Romana, M., Waltz, X., Lalanne-Mistrih, M. L., Tressieres, B., Divialle-Doumdo, L., et al. (2012). Hemorheological risk factors of acute chest syndrome and painful vaso-occlusive crisis in children with sickle cell disease. *Haematologica* 97, 1641–1647. doi: 10.3324/haematol.2012.066670

Lanotte, L., Mauer, J., Mendez, S., Fedosov, D. A., Fromental, J. M., Claveria, V., et al. (2016). Red cells' dynamic morphologies govern blood shear thinning under microcirculatory flow conditions. *Proc. Natl. Acad. Sci. U.S.A.* 113, 13289–13294. doi: 10.1073/pnas.1608074113

Lapoumeroulie, C., Connes, P., El Hoss, S., Hierso, R., Charlot, K., Lemonne, N., et al. (2019). New insights into red cell rheology and adhesion in patients with sickle cell anaemia during vaso-occlusive crises. *Br. J. Haematol.* 185, 991–994. doi: 10.1111/bjh.15686

Laurance, S., Lansiaux, P., Pellay, F. X., Hauchecorne, M., Benecke, A., Elion, J., et al. (2011). Differential modulation of adhesion molecule expression

by hydroxycarbamide in human endothelial cells from the micro- and macrocirculation: potential implications in sickle cell disease vasoocclusive events. *Haematologica* 96, 534–542. doi: 10.3324/haematol.2010.026740

Lemonne, N., Charlot, K., Waltz, X., Ballas, S. K., Lamarre, Y., Lee, K., et al. (2015). Hydroxyurea treatment does not increase blood viscosity and improves red blood cell rheology in sickle cell anemia. *Haematologica* 100, e383–e386. doi: 10.3324/haematol.2015.130435

Lemonne, N., Connes, P., Romana, M., Vent-Schmidt, J., Bourhis, V., Lamarre, Y., et al. (2012). Increased blood viscosity and red blood cell aggregation in a patient with sickle cell anemia and smoldering myeloma. *Am. J. Hematol.* 87:E129. doi: 10.1002/ajh.23312

Lemonne, N., Lamarre, Y., Romana, M., Mukisi-Mukaza, M., Hardy-Dessources, M. D., Tarer, V., et al. (2013). Does increased red blood cell deformability raise the risk for osteonecrosis in sickle cell anemia? *Blood* 121, 3054–3056. doi: 10.1182/blood-2013-01-480277

Liem, R. I., Reddy, M., Pelligra, S. A., Savant, A. P., Fernhall, B., Rodeghier, M., et al. (2015). Reduced fitness and abnormal cardiopulmonary responses to maximal exercise testing in children and young adults with sickle cell anemia. *Physiol. Rep.* 3:e12338. doi: 10.14814/phy2.12338

Lipovac, V., Gavella, M., Turck, Z., and Skrabalo, Z. (1985). Influence of lactate on the insulin action on red blood cell filterability. *Clin. Hemorheol.* 5, 421–428.

Martin, C., Pialoux, V., Faes, C., Charrin, E., Skinner, S., and Connes, P. (2018). Does physical activity increase or decrease the risk of sickle cell disease complications? *Br. J. Sports Med.* 52, 214–218. doi: 10.1136/bjsports-2015-095317

Martini, J., Carpentier, B., Negrete, A. C., Frangos, J. A., and Intaglietta, M. (2005). Paradoxical hypotension following increased hematocrit and blood viscosity. *Am. J. Physiol. Heart Circ. Physiol.* 289, H2136–H2143.

Meiselman, H. J., Neu, B., Rampling, M. W., and Baskurt, O. K. (2007). RBC aggregation: laboratory data and models. *Indian J. Exp. Biol.* 45, 9–17.

Merlet, A. N., Chatel, B., Hourde, C., Ravelojaona, M., Bendahan, D., Feasson, L., et al. (2019). How sickle cell disease impairs skeletal muscle function: implications in daily life. *Med. Sci. Sports Exerc.* 51, 4–11. doi: 10.1249/MSS.0000000000001757

Mockesch, B., Connes, P., Charlot, K., Skinner, S., Hardy-Dessources, M. D., Romana, M., et al. (2017). Association between oxidative stress and vascular reactivity in children with sickle cell anaemia and sickle haemoglobin C disease. *Br. J. Haematol.* 178, 468–475. doi: 10.1111/bjh.14693

Nader, E., Connes, P., Lamarre, Y., Renoux, C., Joly, P., Hardy-Dessources, M. D., et al. (2017). Plasmapheresis may improve clinical condition in sickle cell disease through its effects on red blood cell rheology. *Am. J. Hematol.* 92, E629–E630. doi: 10.1002/ajh.24870

Nader, E., Guillot, N., Lavorel, L., Hancco, I., Fort, R., Stauffer, E., et al. (2018). Eryptosis and hemorheological responses to maximal exercise in athletes: comparison between running and cycling. *Scand. J. Med. Sci. Sports* 28, 1532–1540. doi: 10.1111/sms.13059

Nebor, D., Bowers, A., Hardy-Dessources, M. D., Knight-Madden, J., Romana, M., Reid, H., et al. (2011). Frequency of pain crises in sickle cell anemia and its relationship with the sympatho-vagal balance, blood viscosity and inflammation. *Haematologica* 96, 1589–1594. doi: 10.3324/haematol.2011.047365

Neuhaus, D., Behn, C., and Gaehtgens, P. (1992). Haemorheology and exercise: intrinsic flow properties of blood in marathon running. *Int. J. Sports Med.* 13, 506–511. doi: 10.1055/s-2007-1021307

Neuhaus, D., and Gaehtgens, P. (1994). Haemorrheology and long term exercise. *Sports Med.* 18, 10–21. doi: 10.2165/00007256-199418010-00003

Nosadova, J. (1977). The changes in hematocrit, hemoglobin, plasma volume and proteins during and after different types of exercise. *Eur. J. Appl. Physiol.* 36, 223–230.

Omwanghe, O. A., Muntz, D. S., Kwon, S., Montgomery, S., Kemiki, O., Hsu, L. L., et al. (2017). Self-Reported physical activity and exercise patterns in children with sickle cell disease. *Pediatr. Exerc. Sci.* 29, 388–395. doi: 10.1123/pes.2016-0276

Oostenbrug, G. S., Mensink, R. P., Hardeman, M. R., De Vries, T., Brouns, F., and Hornstra, G. (1997). Exercise performance, red blood cell deformability, and lipid peroxidation: effects of fish oil and vitamin E. *J. Appl. Physiol.* 83, 746–752.

Pallis, F. R., Conran, N., Fertrin, K. Y., Olalla Saad, S. T., Costa, F. F., and Franco-Penteado, C. F. (2014). Hydroxycarbamide reduces eosinophil adhesion and degranulation in sickle cell anaemia patients. *Br. J. Haematol.* 164, 286–295. doi: 10.1111/bjh.12628

Parthasarathi, K., and Lipowsky, H. H. (1999). Capillary recruitment in response to tissue hypoxia and its dependence on red blood cell deformability. *Am. J. Physiol.* 277, H2145–H2157. doi: 10.1152/ajpheart.1999.277.6.H2145

Piecuch, J., Mertas, A., Nowowiejska-Wiewiora, A., Zurawel, R., Gregorczyn, S., Czuba, Z., et al. (2019). The relationship between the rheological behavior of RBCs and angiogenesis in the morbidly obese. *Clin. Hemorheol. Microcirc.* 71, 95–102. doi: 10.3233/CH-180420

Piel, F. B., Patil, A. P., Howes, R. E., Nyangiri, O. A., Gething, P. W., Williams, T. N., et al. (2010). Global distribution of the sickle cell gene and geographical confirmation of the malaria hypothesis. *Nat. Commun.* 1:104. doi: 10.1038/ncomms1104

Ploutz-Snyder, L. L., Convertino, V. A., and Dudley, G. A. (1995). Resistance exercise-induced fluid shifts: change in active muscle size and plasma volume. *Am. J. Physiol.* 269, R536–R543.

Poiseuille, J. L. M. (1835). Recherches sur les causes du mouvement du sang dans les vaisseaux capillaires. *C R Acad. Sci. Paris* 1, 554–560.

Pop, G. A., Duncker, D. J., Gardien, M., Vranckx, P., Versluis, S., Hasan, D., et al. (2002). The clinical significance of whole blood viscosity in (cardio)vascular medicine. *Neth. Heart J.* 10, 512–516.

Raj, J. U., Kaapa, P., Hillyard, R., and Anderson, J. (1991). Pulmonary vascular pressure profile in adult ferrets: measurements in vivo and in isolated lungs. *Acta Physiol. Scand.* 142, 41–48. doi: 10.1111/j.1748-1716.1991.tb09126.x

Rampling, M. W., Meiselman, H. J., Neu, B., and Baskurt, O. K. (2004). Influence of cell-specific factors on red blood cell aggregation. *Biorheology* 41, 91–112.

Rees, D. C., Williams, T. N., and Gladwin, M. T. (2010). Sickle-cell disease. *Lancet* 376, 2018–2031. doi: 10.1016/S0140-6736(10)61029-X

Reinhart, W. H., Staubli, M., and Straub, P. W. (1983). Impaired red cell filterability with elimination of old red blood cells during a 100-km race. *J. Appl. Physiol. Respir. Environ. Exerc. Physiol.* 54, 827–830. doi: 10.1152/jappl.1983.54.3.827

Renoux, C., Connes, P., Nader, E., Skinner, S., Faes, C., Petras, M., et al. (2017). Alpha-thalassaemia promotes frequent vaso-occlusive crises in children with sickle cell anaemia through haemorheological changes. *Pediatr. Blood Cancer* 64:e26455. doi: 10.1002/pbc.26455

Renoux, C., Faivre, M., Bessaa, A., Da Costa, L., Joly, P., Gauthier, A., et al. (2019). Impact of surface-area-to-volume ratio, internal viscosity and membrane viscoelasticity on red blood cell deformability measured in isotonic condition. *Sci. Rep.* 9:6771. doi: 10.1038/s41598-019-43200-y

Renoux, C., Romana, M., Joly, P., Ferdinand, S., Faes, C., Lemonne, N., et al. (2016). Effect of age on blood rheology in sickle cell anaemia and sickle cell haemoglobin C disease: a cross-sectional study. *PLoS One* 11:e0158182. doi: 10.1371/journal.pone.0158182

Robach, P., Boisson, R. C., Vincent, L., Lundby, C., Moutereau, S., Gergele, L., et al. (2014). Hemolysis induced by an extreme mountain ultra-marathon is not associated with a decrease in total red blood cell volume. *Scand. J. Med. Sci. Sports.* 24, 18–27. doi: 10.1111/j.1600-0838.2012.01481.x

Romain, A. J., Brun, J. F., Varlet-Marie, E., and Raynaud De Mauverger, E. (2011). Effects of exercise training on blood rheology: a meta-analysis. *Clin. Hemorheol. Microcirc.* 49, 199–205. doi: 10.3233/CH-2011-1469

Salazar Vazquez, B. Y., Cabrales, P., Tsai, A. G., and Intaglietta, M. (2011). Nonlinear cardiovascular regulation consequent to changes in blood viscosity. *Clin. Hemorheol. Microcirc.* 49, 29–36. doi: 10.3233/CH-2011-1454

Sandor, B., Nagy, A., Toth, A., Rabai, M., Mezey, B., Csatho, A., et al. (2014). Effects of moderate aerobic exercise training on hemorheological and laboratory parameters in ischemic heart disease patients. *PLoS One* 9:e110751. doi: 10.1371/journal.pone.0110751

Schmid-Schonbein, H., Wells, R. E., and Goldstone, J. (1969). [Model experiments on erythrocyte rheology]. *Pflugers. Arch.* 312, R39–R40.

Senturk, U. K., Gunduz, F., Kuru, O., Kocer, G., Ozkaya, Y. G., Yesilkaya, A., et al. (2005a). Exercise-induced oxidative stress leads hemolysis in sedentary but not trained humans. *J. Appl. Physiol.* 99, 1434–1441.

Senturk, U. K., Yalcin, O., Gunduz, F., Kuru, O., Meiselman, H. J., and Baskurt, O. K. (2005b). Effect of antioxidant vitamin treatment on the time course of hematological and hemorheological alterations after an exhausting exercise episode in human subjects. *J. Appl. Physiol.* 98, 1272–1279.

Sheremet'ev, Y. A., Popovicheva, A. N., Rogozin, M. M., and Levin, G. Y. (2019). Red blood cell aggregation, disaggregation and aggregate morphology

in autologous plasma and serum in diabetic foot disease. *Clin. Hemorheol. Microcirc.* 72, 221–227. doi: 10.3233/CH-180405

Sjogaard, G., Adams, R. P., and Saltin, B. (1985). Water and ion shifts in skeletal muscle of humans with intense dynamic knee extension. *Am. J. Physiol.* 248, R190–R196.

Smith, J. A., Martin, D. T., Telford, R. D., and Ballas, S. K. (1999). Greater erythrocyte deformability in world-class endurance athletes. *Am. J. Physiol.* 276, H2188–H2193. doi: 10.1152/ajpheart.1999.276.6.H2188

Smith, J. A., Telford, R. D., Kolbuch-Braddon, M., and Weidemann, M. J. (1997). Lactate/H+ uptake by red blood cells during exercise alters their physical properties. *Eur. J. Appl. Physiol. Occup. Physiol.* 75, 54–61.

Sriram, K., Salazar Vazquez, B. Y., Tsai, A. G., Cabrales, P., Intaglietta, M., and Tartakovsky, D. M. (2012). Autoregulation and mechanotransduction control the arteriolar response to small changes in hematocrit. *Am. J. Physiol. Heart Circ. Physiol.* 303, H1096–H1106. doi: 10.1152/ajpheart.00438.2012

Starzyk, D., Korbut, R., and Gryglewski, R. J. (1997). The role of nitric oxide in regulation of deformability of red blood cells in acute phase of endotoxaemia in rats. *J. Physiol. Pharmacol.* 48, 731–735.

Stephenson, L. A., and Kolka, M. A. (1988). Plasma volume during heat stress and exercise in women. *Eur. J. Appl. Physiol. Occup. Physiol.* 57, 373–381.

Suhr, F., Brenig, J., Muller, R., Behrens, H., Bloch, W., and Grau, M. (2012). Moderate exercise promotes human RBC-NOS activity, NO production and deformability through Akt kinase pathway. *PLoS One* 7:e45982. doi: 10.1371/journal.pone.0045982

Tomschi, F., Bizjak, D., Bloch, W., Latsch, J., Predel, H. G., and Grau, M. (2018). Deformability of different red blood cell populations and viscosity of differently trained young men in response to intensive and moderate running. *Clin. Hemorheol. Microcirc.* 69, 503–514. doi: 10.3233/CH-189202

Totsimon, K., Biro, K., Szabo, Z. E., Toth, K., Kenyeres, P., and Marton, Z. (2017). The relationship between hemorheological parameters and mortality in critically ill patients with and without sepsis. *Clin. Hemorheol. Microcirc.* 65, 119–129. doi: 10.3233/CH-16136

Tripette, J., Alexy, T., Hardy-Dessources, M. D., Mougenel, D., Beltan, E., Chalabi, T., et al. (2009). Red blood cell aggregation, aggregate strength and oxygen transport potential of blood are abnormal in both homozygous sickle cell anemia and sickle-hemoglobin C disease. *Haematologica* 94, 1060–1065. doi: 10.3324/haematol.2008.005371

Tripette, J., Hardy-Dessources, M. D., Beltan, E., Sanouiller, A., Bangou, J., Chalabi, T., et al. (2011). Endurance running trial in tropical environment: a blood rheological study. *Clin. Hemorheol. Microcirc* 47, 261–268. doi: 10.3233/CH-2011-1388

Tripette, J., Loko, G., Samb, A., Gogh, B. D., Sewade, E., Seck, D., et al. (2010). Effects of hydration and dehydration on blood rheology in sickle cell trait carriers during exercise. *Am. J. Physiol. Heart Circ. Physiol.* 299, H908–H914. doi: 10.1152/ajpheart.00298.2010

Tsai, A. G., Acero, C., Nance, P. R., Cabrales, P., Frangos, J. A., Buerk, D. G., et al. (2005). Elevated plasma viscosity in extreme hemodilution increases perivascular nitric oxide concentration and microvascular perfusion. *Am. J. Physiol. Heart Circ. Physiol.* 288, H1730–H1739. doi: 10.1152/ajpheart.00998.2004

Van Beaumont, W., Underkofler, S., and Van Beaumont, S. (1981). Erythrocyte volume, plasma volume, and acid-base changes in exercise and heat dehydration. *J. Appl. Physiol. Respir. Environ. Exerc. Physiol.* 50, 1255–1262. doi: 10.1152/jappl.1981.50.6.1255

Vandewalle, H., Lacombe, C., Lelievre, J. C., and Poirot, C. (1988). Blood viscosity after a 1-h submaximal exercise with and without drinking. *Int. J. Sports Med.* 9, 104–107.

Varlet-Marie, E., Gaudard, A., Monnier, J. F., Micallef, J. P., Mercier, J., Bressolle, F., et al. (2003). Reduction of red blood cell disaggregability during submaximal exercise: relationship with fibrinogen levels. *Clin. Hemorheol. Microcirc* 28, 139–149.

Vazquez, B. Y., Vazquez, M. A., Jaquez, M. G., Huemoeller, A. H., Intaglietta, M., and Cabrales, P. (2010). Blood pressure directly correlates with blood viscosity in diabetes type 1 children but not in normals. *Clin. Hemorheol. Microcirc* 44, 55–61. doi: 10.3233/CH-2010-1252

Verger, E., Schoevaert, D., Carrivain, P., Victor, J. M., Lapoumeroulie, C., and Elion, J. (2014). Prior exposure of endothelial cells to hydroxycarbamide alters the flow dynamics and adhesion of sickle red blood cells. *Clin. Hemorheol. Microcirc* 57, 9–22. doi: 10.3233/CH-131762

Waltz, X., and Connes, P. (2014). Pathophysiology and physical activity in patients with sickle cell anemia. *Mov. Sport Sci. Sci. Motricité* 83, 41–47. doi: 10.1051/sm/2013105

Waltz, X., Hardy-Dessources, M. D., Lemonne, N., Mougenel, D., Lalanne-Mistrih, M. L., Lamarre, Y., et al. (2015). Is there a relationship between the hematocrit-to-viscosity ratio and microvascular oxygenation in brain and muscle? *Clin. Hemorheol. Microcirc.* 59, 37–43. doi: 10.3233/CH-131742

Waltz, X., Hedreville, M., Sinnapah, S., Lamarre, Y., Soter, V., Lemonne, N., et al. (2012). Delayed beneficial effect of acute exercise on red blood cell aggregate strength in patients with sickle cell anemia. *Clin. Hemorheol. Microcirc.* 52, 15–26. doi: 10.3233/CH-2012-1540

Waltz, X., Romana, M., Lalanne-Mistrih, M. L., Machado, R. F., Lamarre, Y., Tarer, V., et al. (2013). Hematologic and hemorheological determinants of resting and exercise-induced hemoglobin oxygen desaturation in children with sickle cell disease. *Haematologica* 98, 1039–1044. doi: 10.3324/haematol.2013.083576

Wood, S. C., Doyle, M. P., and Appenzeller, O. (1991). Effects of endurance training and long distance running on blood viscosity. *Med. Sci. Sports Exerc.* 23, 1265–1269.

Yalcin, O., Bor-Kucukatay, M., Senturk, U. K., and Baskurt, O. K. (2000). Effects of swimming exercise on red blood cell rheology in trained and untrained rats. *J. Appl. Physiol.* 88, 2074–2080.

Yalcin, O., Erman, A., Muratli, S., Bor-Kucukatay, M., and Baskurt, O. K. (2003). Time course of hemorheological alterations after heavy anaerobic exercise in untrained human subjects. *J. Appl. Physiol.* 94, 997–1002.

Yalcin, O., Meiselman, H. J., Armstrong, J. K., and Baskurt, O. K. (2005). Effect of enhanced red blood cell aggregation on blood flow resistance in an isolated-perfused guinea pig heart preparation. *Biorheology* 42, 511–520.

Conflict of Interest: The authors declare that the research was conducted in the absence of any commercial or financial relationships that could be construed as a potential conflict of interest.

frontiers in Physiology

REVIEW
published: 17 January 2020
doi: 10.3389/fphys.2019.01534

The Many Facets of Erythropoietin Physiologic and Metabolic Response

*Sukanya Suresh†, Praveen Kumar Rajvanshi and Constance T. Noguchi**

Molecular Medicine Branch, National Institute of Diabetes and Digestive and Kidney Diseases, National Institutes of Health, Bethesda, MD, United States

In mammals, erythropoietin (EPO), produced in the kidney, is essential for bone marrow erythropoiesis, and hypoxia induction of EPO production provides for the important erythropoietic response to ischemic stress, such as during blood loss and at high altitude. Erythropoietin acts by binding to its cell surface receptor which is expressed at the highest level on erythroid progenitor cells to promote cell survival, proliferation, and differentiation in production of mature red blood cells. In addition to bone marrow erythropoiesis, EPO causes multi-tissue responses associated with erythropoietin receptor (EPOR) expression in non-erythroid cells such neural cells, endothelial cells, and skeletal muscle myoblasts. Animal and cell models of ischemic stress have been useful in elucidating the potential benefit of EPO affecting maintenance and repair of several non-hematopoietic organs including brain, heart and skeletal muscle. Metabolic and glucose homeostasis are affected by endogenous EPO and erythropoietin administration affect, in part via EPOR expression in white adipose tissue. In diet-induced obese mice, EPO is protective for white adipose tissue inflammation and gives rise to a gender specific response in weight control associated with white fat mass accumulation. Erythropoietin regulation of fat mass is masked in female mice due to estrogen production. EPOR is also expressed in bone marrow stromal cells (BMSC) and EPO administration in mice results in reduced bone independent of the increase in hematocrit. Concomitant reduction in bone marrow adipocytes and bone morphogenic protein suggests that high EPO inhibits adipogenesis and osteogenesis. These multi-tissue responses underscore the pleiotropic potential of the EPO response and may contribute to various physiological manifestations accompanying anemia or ischemic response and pharmacological uses of EPO.

Keywords: erythropoietin, erythropoietin receptor, nitric oxide, gender-specific, obesity, inflammation, bone

OPEN ACCESS

Edited by:
Anna Bogdanova, University of Zurich, Switzerland

Reviewed by:
Drorit Neumann, Tel Aviv University, Israel
Angela Risso, University of Udine, Italy
Joachim Fandrey, University of Duisburg-Essen, Germany

***Correspondence:**
Constance T. Noguchi
connien@niddk.nih.gov

†Present address:
Sukanya Suresh, Division of Endocrinology, Department of Medicine, Indiana University School of Medicine, Indianapolis, IN, United States

Specialty section:
This article was submitted to Red Blood Cell Physiology, a section of the journal Frontiers in Physiology

Received: *10 September 2019*
Accepted: *05 December 2019*
Published: *17 January 2020*

Citation:
Suresh S, Rajvanshi PK and Noguchi CT (2020) The Many Facets of Erythropoietin Physiologic and Metabolic Response. Front. Physiol. 10:1534. doi: 10.3389/fphys.2019.01534

Abbreviations: ACTH, Adrenocorticotropic hormone; AKT, Protein kinase B (PKB); ARNT, Aryl hydrocarbon nuclear translocator (HIF-1β); BMP, Bone morphogenetic protein; BMSC, Bone marrow stromal cells; C2C12, Mouse myoblast cell line; EGLN1, Egl-9 Family Hypoxia Inducible Factor 1 (PHD2); eNOS, Endothelial nitric oxide synthase (NOS3); EPAS1, Endothelial PAS Domain Protein 1 (HIF-2α); EPO, Erythropoietin; EPOR, Erythropoietin receptor; ERK, Extracellular signal-regulated kinase; ET-1, Endothelin-1; FGF, Fibroblast growth factor; FIH-1, Factor inhibiting HIF-1; GATA, GATA binding protein; HIF, Hypoxia-inducible factor; JAK, Janus kinase; MDS, Myelodysplastic syndrome; mEPOR−/−, Erythropoietin receptor knockout mouse; Myf-5, Myogenic factor 5; MYF6, Myogenic factor 6; MyoD, Myoblast determination protein 1; NAD, Nicotinamide adenine dinucleotide; NF-κB, Nuclear factor kappa-light-chain-enhancer of activated B cells; NO, Nitric oxide; PAX7, Paired box 7; PGC-1, Peroxisome proliferator-activated receptor gamma coactivator 1-alpha; PHD, Prolyl hydroxylase; PI3K, Phosphoinositide 3-kinase; POMC, Proopiomelanocortin; PPARα, Peroxisome proliferator-activated receptor alpha; PRDM16, PR-domain-containing 16; RAW264.7, Mouse macrophage cell line; Sirt1, Sirtuin 1; STAT, Signal transducers and activators of transcription; TAL1, T-cell acute lymphocytic leukemia protein 1; U/kg, Units per kilogram (EPO dose); UCP1, Uncoupling protein 1; VHL, Von Hippel-Lindau protein; WSXWS, Amino acid motif (tryptophan-serine-X-tryptophan-serine); $\Delta EpoR_E$, Mice with EPOR restricted to erythroid tissue; α-MSH, Alpha-melanocyte stimulating hormone.

INTRODUCTION

Erythropoietin is the hormone that regulates the daily production of 200 billion new red blood cells in the human body. Red blood cells are a renewable resource with a limited lifespan of about 120 days, have an intracellular protein content of about 95% hemoglobin, a tetrameric globular protein that binds oxygen cooperatively, and function primarily to transport oxygen from the lungs to the tissues. EPO binding to erythroid progenitor cells promotes their survival, proliferation, and differentiation to mature erythrocytes. EPO production is hypoxia inducible and is made in the interstitial cells in the adult kidney (Kobayashi et al., 2017; Anusornvongchai et al., 2018). In response to anemia, ischemic stress or high altitude, EPO production is induced (Pugh and Ratcliffe, 2017) and stimulates erythroid progenitor cells in the bone marrow to expand the erythroid lineage thus markedly increasing erythropoiesis and mature red blood cell production. EPO and EPOR on the surface of erythroid progenitor cells are required for red blood cell production and mice with targeted deletion of EPO or EPOR die during embryonic development of severe anemia (Wu et al., 1995; Lin et al., 1996). However, EPOR expression is not restricted to erythroid tissue. This review will address EPO activity in erythroid cells and in select non-hematopoietic tissues expressing EPOR and lessons gleaned from studies in animal models on the protective effects of EPO in ischemic injury and wound healing, regulation of metabolic homeostasis including gender specific EPO response and bone remodeling (**Figure 1**).

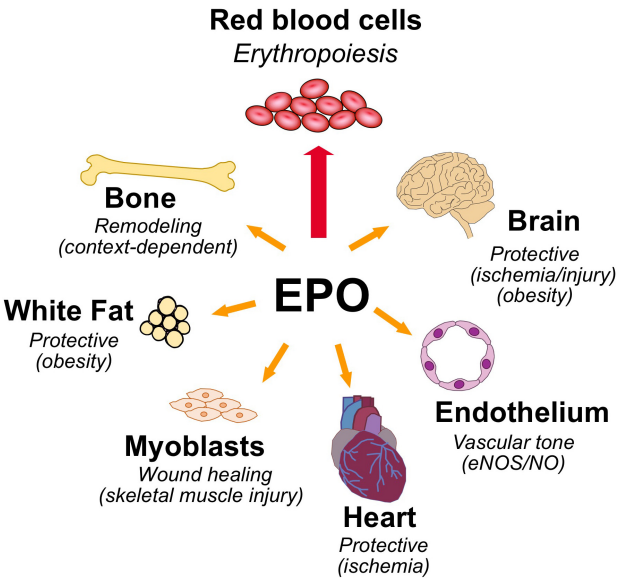

FIGURE 1 | Pleiotropic effects of erythropoietin. High level of EPOR on erythroid progenitor cells accounts for the sensitive erythropoietic response in the bone marrow to hypoxic induction of EPO. EPOR expression determines EPO response and expression beyond erythroid tissue provides for EPO response in non-hematopoietic tissues that include the following: brain for a neuroprotective and metabolic response; cardiovascular system for regulating vascular tone and oxygen delivery in endothelium and protection in heart against ischemic injury; skeletal muscle for muscle maintenance and repair; white adipose tissue for protection for inflammation associated with diet-induced obesity and fat mass accumulation, particularly in males; and bone remodeling.

ERYTHROPOIETIN ACTION IN ERYTHROID CELLS

Erythropoietin is a glycoprotein produced primarily in the fetal liver and adult kidney to regulate red blood cell production. Human EPO is encoded as a 193 amino acid polypeptide with a NH_2-terminal 27 amino acid signal peptide and three potential N-linked glycosylation sites; posttranslational cleavage of the carboxyl terminal arginine gives rise to a 165 amino acid mature polypeptide for human EPO (Jacobs et al., 1985; Lin et al., 1985; Recny et al., 1987). Recombinant EPO produced in Chinese hamster ovary cells yields a glycoprotein with apparent molecular weight about 34,000 that is biologically active (Recny et al., 1987). EPO received approval in 1989 from the U.S. Food and Drug Administration for clinical treatment of anemia associated with chronic renal failure due to insufficient EPO production, which has markedly improved treatment of this disease (Paoletti and Cannella, 2006; Jelkmann, 2013; Wright et al., 2015).

Sites of EPO Production

During mammalian development, observations of EPO production in mice suggest that EPO is first expressed transiently in neural crest cells during mid-gestation to stimulate yolk sac primitive erythropoiesis for oxygen transport in mid-stage embryos (Malik et al., 2013; Suzuki et al., 2013; Hirano and Suzuki, 2019). As development progresses, the liver becomes the site of EPO production and definitive erythropoiesis (Palis, 2014; Palis and Koniski, 2018). EPO is required for definitive erythropoiesis and knockout of EPO or EPOR in mice results in death *in utero* around day 13.5 due to disruption of erythropoiesis in the fetal liver resulting in severe anemia (Wu et al., 1995; Lin et al., 1996). By the last third of gestation in mammalian development, the site of EPO production gradually switches to the kidney which becomes the major site of EPO production in the adult (Zanjani et al., 1981; Dame et al., 1998) and red blood cell production switches from the fetal liver to bone marrow, the site of adult hematopoiesis (Ho et al., 2015). Interstitial peritubular cells of the kidney are the EPO-producing cells and hypoxia induction of EPO production results mainly from the increase in the number of cells producing EPO (Tan et al., 1991; Eckardt et al., 1993; Juul et al., 1998; Obara et al., 2008). EPO expression is detected in tissues beyond liver and kidney including brain and neural cells, spleen, lung, and bone marrow (Fandrey and Bunn, 1993; Masuda et al., 1994; Marti et al., 1996; Dame et al., 1998; Juul et al., 1998), but does not substitute for the required erythropoietic regulation provided by the kidney. Interestingly, genetically over-stabilizing the hypoxic response in osteoblasts in mice resulted in selective expansion of the erythroid lineage leading to development of severe polycythemia due to high level of EPO expression in osteoblasts compared to relatively lower levels of EPO induced by hypoxia in control animals (Rankin et al., 2012).

EPO Is Hypoxia Inducible

Erythropoietin production is hypoxia responsive mediated via binding of HIF to the hypoxic responsive element located downstream of the coding region under hypoxic conditions (Semenza, 2009). HIF is a heterodimer between HIF-α (HIF-1α, HIF-2α or HIF-3α) and HIF-1β (or ARNT), and HIF-2α (or EPAS1) is particularly associated with EPO regulation (Rankin et al., 2007; Suzuki et al., 2017). Oxygen dependent hydroxylases, PHD and FIH-1 down regulate HIF-α stability/activity and provide oxygen sensitivity for HIF regulation of EPO expression (Jaakkola et al., 2001; Mahon et al., 2001; Lando et al., 2002). At normoxia, HIF-α is marked for degradation by proline hydroxylation, primarily by PHD2 (Jaakkola et al., 2001), providing a binding site for VHL which targets HIF-α for ubiquitination and proteasome degradation (Ohh et al., 2000; Ang et al., 2002; Minamishima et al., 2008; Takeda et al., 2008; Kobayashi et al., 2016). With reduced oxygen, HIF-α is stabilized and increased HIF-2α in renal EPO-producing cells up regulates EPO gene expression (Semenza, 2009). The asparaginyl hydroxylase, FIH-1 binds the HIF-α transactivation domain at normoxia and inhibits HIF-α transactivation by hydroxylating asparagine residue in the carboxy-terminal transactivation domain and blocks interactions with coactivator proteins (Mahon et al., 2001; Lando et al., 2002). Mutations in VHL, PHD2, and HIF-2α have been identified in patients with familial erythrocytosis. The Chuvash population of the Russian Federation is associated with a high prevalence of polycythemia due to VHL gene mutation that reduces oxygen dependent HIF-2α degradation and increases EPO production (Ang et al., 2002; Pastore et al., 2003). Mutations in HIF-2α or the EGLN1 gene that encodes PHD2 also give rise to erythrocytosis associated with increased EPO production (Percy et al., 2006, 2008).

EPOR Gene Regulation in the Erythroid Lineage

Erythropoietin receptor is expressed at the highest level on erythroid progenitor cells at the colony forming unit-erythroid (CFU-E) stage that becomes the most responsive to changes in EPO level (Broudy et al., 1991). EPO is required for erythroid progenitor cell survival as cells differentiate from early erythroid progenitors or burst forming unit-erythroid (BFU-E) to CFU-E. Mice that lack EPO or its receptor die *in utero* at day 13.5 due to severe anemia (Wu et al., 1995; Lin et al., 1996). EPO binding to its receptor on erythroid progenitor cells increases expression of erythroid transcription factors, GATA1 and the basic-helix-loop-helix protein, TAL1, that in turn transactivate EPOR expression; hence, EPO regulates expression of its own receptor (Zon et al., 1991; Kassouf et al., 2010; Rogers et al., 2012). The EPOR promoter region contains conserved binding sites for ubiquitous Sp1 transcription factor and GATA1 (AGATAA) and in the 5′ untranslated transcribed region 3 E-box (CAGCTG) TAL1 binding sites (**Figure 2A**). EPO binding at the early erythroid progenitor BFU-E stage with low level EPOR induces GATA1 and TAL1 to activate the erythroid program including EPOR. EPOR is down regulated with progression of erythroid differentiation and is not detected on reticulocytes (Broudy et al., 1991).

EPOR Structure and Signaling

Erythropoietin receptor is a member of the class I cytokine receptor superfamily that contains a WSXWS motif in the extracellular domain, a single transmembrane domain, a cytoplasmic domain that lacks tyrosine kinase activity and associates with JAK kinase, and form complexes that are homodimeric, heterodimeric or heterotrimeric (Bazan, 1990; Liongue et al., 2016). EPO binding to its homodimeric receptor complex brings the cytoplasmic associated JAK2 kinases in close proximity allowing for JAK transphosphorylation, phosphorylation of the receptor, and phosphorylation and activation of STAT and other downstream signaling pathways including AKT and ERK1/2 (Witthuhn et al., 1993; Miura et al., 1994; Watowich, 2011; Kuhrt and Wojchowski, 2015). Phosphorylated STAT5 subunits, STAT5A, and STAT5B, dimerize and translocate to the nucleus to activate select gene expression (Socolovsky et al., 2001).

EPO RESPONSE BEYOND ERYTHROID CELLS

Availability of recombinant human EPO facilitated discovery of EPO response in non-hematopoietic tissue. These include endothelial cells and the cardiovascular system, neural cells and the brain, myoblasts and skeletal muscle, adipocytes and fat depots, and bone (; McGee et al., 2012; Zhang et al., 2014; Hiram-Bab et al., 2017; **Figure 1**).

Endothelial EPO Response

Erythropoietin activity beyond erythropoiesis was first observed in endothelial cells. Cultures of primary endothelial cells from human umbilical vein and bovine adrenal capillary exhibited EPO binding and dose dependent proliferative and chemoattractant response to EPO, and EPOR is expressed in endothelial cells (Anagnostou et al., 1990, 1994). Prior to death *in utero*, mice that lack EPO or EPOR exhibit angiogenic defects including decreased vessel networks (Kertesz et al., 2004).

In endothelial cells, endothelial nitric oxide (NO) synthase (eNOS or NOS3) produces NO to regulate vascular tone and blood pressure. EPO stimulation of endothelial cells activates eNOS and NO production, particularly at reduced oxygen (Beleslin-Cokic et al., 2004, 2011). Transgenic mice expressing high level of human EPO with hematocrit of about 80% also exhibit markedly increased eNOS level and NO production (Ruschitzka et al., 2000). EPO induction by hypoxia or ischemic stress stimulates production of red blood cells to improve oxygen delivery and increase transport of oxygen from the lungs to the tissues. However, increased red blood cell production requires increased proliferation and differentiation of erythroid progenitor cells in bone marrow (and spleen in mice) to expand the erythroid lineage. EPO stimulated induction of NO provides the potential for an acute response regulating vascular tone and improving oxygen delivery.

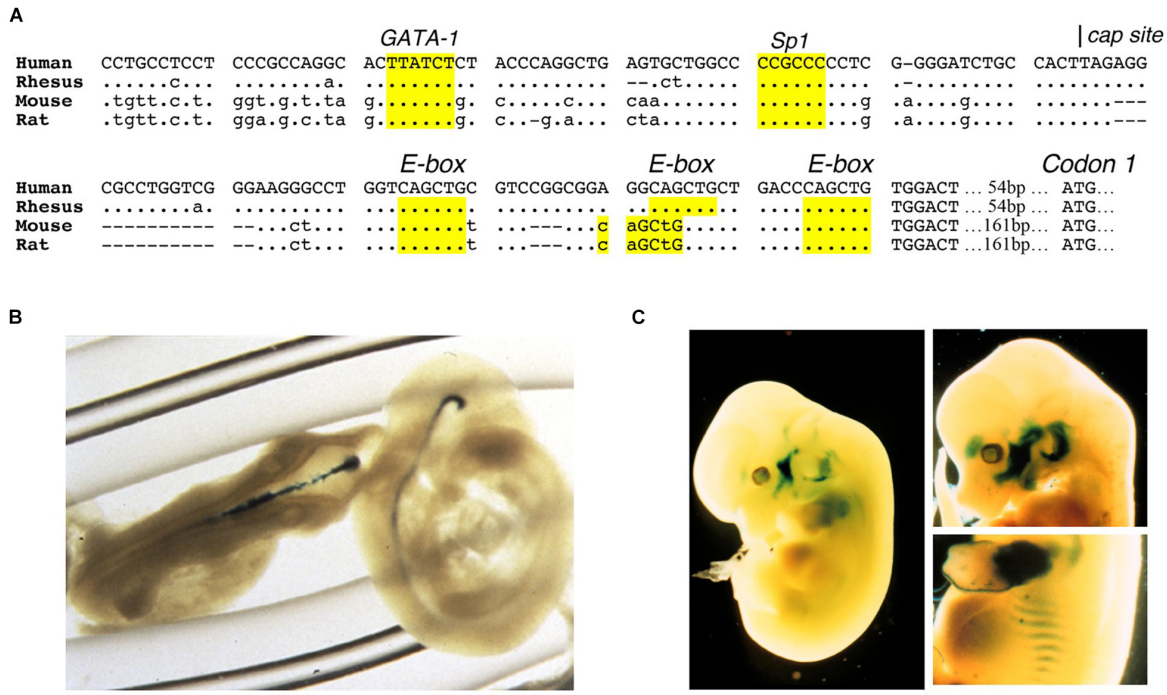

FIGURE 2 | Expression of EPOR reporter gene in transgenic mice. **(A)** The proximal promoter region of the human EPOR gene extending to the translation start site with ATG at +135 in the human EPOR gene, contains conserved regulatory binding sites for GATA proteins (AGATAA) and Sp1 (CCGCCC), and 3-E-boxes (CAGCTG) in the 5′ untranslated transcribed region that can bind basic-helix-loop-helix transcription factors such as erythroid TAL1 and skeletal muscle transcription factors Myf5 and MyoD. **(B)** Transgenic mice containing the human EPOR proximal promoter region extending 1778 bp 5′ of the transcription start site driving the β-galactosidase reporter gene shows EPOR expression in the embryonic brain at embryonic day E9.5 (from Liu et al., 1997, with permission). **(C)** Reporter gene expression at embryonic day 12.5 (left) and embryonic day 13.5 (right) in the visceral arches, base of limbs, intercostal rib regions, and fetal liver (from Ogilvie et al., 2000, with permission).

Erythropoietin stimulation of endothelial cells increases ET-1 secretion that may exacerbate adverse vascular effects (Carlini et al., 1993; Barhoumi et al., 2014). Mice expressing high level of transgenic human EPO with elevated hematocrit and increased NO production also have elevated ET-1 levels, but do not exhibit hypertension (Ruschitzka et al., 2000). Exposure to NO synthase inhibitor (N-nitro-L-arginine methyl ester) decreases eNOS production of NO, increases vasoconstriction and hypertension, and decreases survival of these mice, while pretreatment with ET(A) receptor antagonist (darusentan) improves survival, indicating that increased NO production in these mice suppresses the adverse effects associated with increased ET-1 (Quaschning et al., 2003).

EPO and Cardioprotection

During embryonic development, mice that lack EPO signaling exhibit ventricular hyperplasia indicating defect in proliferation and expansion of the myocardium (Wu et al., 1999; Yu et al., 2001). In studies of isolated adult hearts from rodents, EPO promoted cardioprotection in ischemia reperfusion injury (Cai et al., 2003; Parsa et al., 2003) and EPO administration in rabbits was cardioprotective from myocardial infarction (Cai and Semenza, 2004). In adult rats, EPO administration immediately after myocardial infarction reduced infarct size and improved cardiac function linked to neovascularization (Van Der Meer et al., 2005). Furthermore, EPO treatment in a rat model for chronic heart failure suggested that long term EPO treatment stimulated homing of endothelial progenitor cells to induce neovascularization (Westenbrink et al., 2006). Delayed weekly EPO treatment beginning 7 days after coronary occlusion in rats resulted in reduced injury and improved cardiac function associated with mobilized endothelial progenitor cells (Prunier et al., 2007). Cardioprotective effects of EPO is mediated via induction of coronary endothelial production of NO and require activation of eNOS (Mihov et al., 2009). In genetically modified mice with EPOR restricted to hematopoietic and endothelial cells, EPO cardioprotection was observed in acute ischemia reperfusion injury in heart (Teng et al., 2011a). Cardioprotection was comparable to that observed in wild type mice, but not in eNOS knockout mice, providing evidence that EPOR expression in endothelial cells was sufficient for EPO protection in ischemia reperfusion injury in heart and that activation of eNOS and increased NO production is required (Teng et al., 2011a). In addition, high hematocrit associated with chronic EPO treatment could offset the EPO cardioprotective effect.

EPO and Neuroprotection

Erythropoietin receptor expression in neurons and select locations in brain (Masuda et al., 1993; Digicaylioglu et al., 1995; Morishita et al., 1997) combined with EPO production in

astrocytes and neurons in a hypoxia inducible manner (Masuda et al., 1994; Marti et al., 1996) provide evidence for EPO signaling on the other side of the blood brain barrier. During mouse development, the brain expresses high level of EPOR mid-gestation, localized using reporter gene expression, and mice that lack EPOR exhibit thinning of the neuroepithelium, reduced neural progenitor cells with increased sensitivity to hypoxia, and increased brain apoptosis prior to embryonic death due to severe anemia (Liu et al., 1997; Yu et al., 2002; **Figure 2B**). Mice with EPOR expression restricted to hematopoietic and endothelial tissue and mice with targeted deletion of EPOR in neural cells show no gross morphological defects but do exhibit reduced neural cell proliferation and viability, and increased susceptibility to glutamate damage and stroke (Tsai et al., 2006; Chen et al., 2007). Conversely, EPO infusion into adult rodent brain increases the number of newly generated interneurons (Shingo et al., 2001). In animal models of brain injury, preconditioning with EPO infusion is protective for ischemia or middle cerebral artery occlusion – induced learning disability and neuron death (Sadamoto et al., 1998; Sakanaka et al., 1998; Bernaudin et al., 1999). In a rodent model of neonatal hypoxia/ischemia, EPO protection was associated with brain revascularization and neurogenesis (Iwai et al., 2007).

For clinical application of EPO for ischemic injury, a Phase I clinical trial for EPO treatment of ischemic stroke provided evidence for the safety and potential efficacy showing an association with improvement in clinical outcome at 1 month (Ehrenreich et al., 2002). A following Phase II/III clinical trial of EPO treatment with acute ischemic stroke treated 460 patients with EPO or placebo. Unexpectedly, 63% received recombinant tissue plasminogen activator for treating systemic thrombolysis that was not approved for use in ischemic stroke at the time of the Phase I trial. Favorable effects of EPO were not demonstrated, and overall death rate was 1.8 times higher in the EPO group than in the placebo group (Ehrenreich et al., 2009). Further subgroup analysis including post stroke biomarkers suggested that patients with ischemic stroke not receiving thrombolysis likely benefited from EPO treatment (Ehrenreich et al., 2009, 2011). This negative German Multicenter EPO Stroke Trial underscores the complexity posed by standard of care and difficulties in translating positive results from animal studies to the clinic.

Alternate EPO Receptors and EPO Derivatives

High hematocrit resulting from chronically administered EPO, particularly at high dose, is associated with adverse effects such as hypertension and thromboembolism and could counteract the neuroprotective and cardioprotective effects of EPO. The potential to activate EPO/EPOR protective response in non-hematopoietic tissue via an alternate EPO receptor or an EPO mimetic without increasing erythropoietic activity and hematocrit is of particular interest. An alternate EPO receptor has been proposed for non-hematopoietic tissues such as brain and heart, consisting of a heterodimer between EPOR and the beta common (βc) receptor, also a member of the class I cytokine receptor superfamily and shared by receptors for granulocyte-macrophage colony stimulating factor and interleukins 3 and 5 (Jubinsky et al., 1997; Brines et al., 2004). EPO protection in a model of experimental colitis in mice is proposed to be mediated via activation of the EPOR/βc receptor heterodimer (Nairz et al., 2017). The role of the βc receptor in EPO response is controversial and evidence of direct interaction between EPOR and the βc receptor is lacking. In EPO responsive neural SH-Sy5y and PC12 cells, βc receptor is below the level of detection, and in rat brain, βc receptor does not colocalize with either EPO or EPOR (Nadam et al., 2007; Um et al., 2007). Furthermore, cardioprotection in mice by darbepoetin, a long acting derivative of EPO, did not require the βc receptor (Kanellakis et al., 2010). Biophysical analyses show that the extracellular domains of EPOR and the βc receptor do not directly interact in the presence or absence of EPO (Cheung Tung Shing et al., 2018), and the role of the βc receptor in EPOR response to EPO remains uncertain. Other proposed EPO binding receptors include the Ephrin B4 receptor on cancer cells and the orphan cytokine receptor CRLF3 on insect neural cells (Pradeep et al., 2015; Hahn et al., 2017).

Erythropoietin derivatives that can promote non-hematopoietic tissue protective effects, especially neuroprotection and cardioprotection, without stimulating erythropoiesis, have been proposed to bind alternate EPO receptors such as the EPOR/βc receptor heterodimer. These include asialoerythropoietin, carbamylated EPO, ARA 290 [cibinetide; helix B surface peptide (11 amino acid peptide derived from the EPO sequence)], and recombinant EV-3 (an EPO derived a spliced variant with exon 3 deleted) (Erbayraktar et al., 2003; Brines et al., 2004, 2008; Fiordaliso et al., 2005; Robertson et al., 2013; Bonnas et al., 2017). Clinical studies explored the safety and use of EPO and carbamylated EPO to increase frataxin levels for treatment of Friedreich's Ataxia (Boesch et al., 2014; Egger et al., 2014; Santner et al., 2014). ARA 290 treatment in phase 2 trials for Sarcoidosis-associated small nerve fiber loss showed improved abundance of corneal nerve fiber and neuropathic pain following 28 day treatment (Dahan et al., 2013; Culver et al., 2017). Another phase 2 trial focused on the potential benefit of ARA 290 treatment in subjects with type 2 diabetes for neuropathy as well as metabolic control (Brines et al., 2015). These EPO derivatives suggest the potential to therapeutically activate the tissue-protective activity associated with EPO while minimizing the risk attributed to increases in erythropoiesis and hematocrit.

Skeletal Muscle EPO Response

Reporter gene expression in transgenic mice during development revealed EPOR expression shared resemblance with the expression pattern in developing muscle associated with E-box binding basic-helix-loop-helix muscle transcription factors, MyoD and Myf-5, localizing in the visceral arches, proximal forelimb and intercostal area (Sadamoto et al., 1998; **Figure 2C**). Primary satellite cells isolated from mouse and human skeletal muscle express EPOR (Ogilvie et al., 2000; Rundqvist et al., 2009). Like erythroid progenitor cells, EPO increases proliferation of C2C12 myoblasts and induces EPOR expression that decreases with cell differentiation (Ogilvie et al., 2000). EPOR expression

is regulated by GATA3, GATA4, and TAL1, and can also be transactivated by MyoD and Myf-5 (Ogilvie et al., 2000; Wang et al., 2012). EPO stimulates myoblast proliferation and survival, increases GATA4 and TAL1 that retard myogenic differentiation, mediated in part by Sirt1 activity, and inhibits expression of myogenin associated with differentiating myoblasts and myotube formation (Wang et al., 2012). Improved survival was demonstrated by transplantation of myoblasts over-expressing EPOR into skeletal muscle (Jia et al., 2009). In skeletal muscle, Pax-7^+ satellite cells can self-renew or differentiate to $Myf5^+$ committed muscle progenitor cells that contribute to growth, maintenance and repair of skeletal muscle (Kuang et al., 2007). Mice that express high transgenic human EPO have increased skeletal muscle Pax-7^+ satellite cells and isolated primary myoblasts had enhanced proliferation in culture compared to wild type cultures (Jia et al., 2012). These mice subjected to skeletal muscle injury exhibited improved muscle repair and recovery and increased maximum load tolerated by isolated muscle. In contrast, $\Delta EpoR_E$ have fewer Pax-7^+ satellite cells and isolated primary myoblasts from $\Delta EpoR_E$ mice do not proliferate in culture, and in skeletal muscle injury, these mice show delayed muscle repair and recovery, and reduced maximum load tolerated by isolated muscle (Jia et al., 2012). Furthermore, EPO treatment increases Pax-7^+satellite cells and promotes repair and recovery from skeletal muscle injury (Jia et al., 2012). Skeletal muscle myoblasts produced endogenous EPO that increased at low oxygen, and transgenic mice with high transgenic human EPO exhibit mouse EPO and elevated human EPO expression in primary myoblasts, raising the possibility of an autocrine EPO response in skeletal muscle (Jia et al., 2012). Transgenic knockdown of circulating EPO levels did not show any change in EPOR gene expression in mouse skeletal muscle (Hagström et al., 2010; Mille-Hamard et al., 2012).

In humans, a single injection of EPO increased myogenic regulatory factor *MYF6* mRNA (Lundby et al., 2008) and EPO treatment increased PAX7 and MYOD1 content in human satellite cells (Hoedt et al., 2016), suggesting a role for EPO and its receptor in muscle development or remodeling. EPO administration also enhanced muscle mitochondrial oxidative phosphorylation and electron chain transport capacity following 8 weeks of treatment (Plenge et al., 2012). EPO stimulation in C2C12 myoblasts increased JAK2, STAT5 (Sadamoto et al., 1998) and AKT phosphorylation (Jia et al., 2009), and mice expressing elevated EPO in skeletal muscle by gene transfer also exhibited increased AKT phosphorylation (Hojman et al., 2009). In humans, a single EPO injection followed by exercise was not sufficient to activate the AKT pathway in skeletal muscle (Lamon et al., 2016).

EPO and Skeletal Muscle Fiber Type

Skeletal muscles of vertebrates contain mainly two types of muscle myofibers, type I (slow twitch) and type II (fast twitch) that differ in their function, mitochondrial density, and metabolic properties (Zierath and Hawley, 2004). Type I muscle fibers contain a high concentration of mitochondria and high oxidative capacity, and exhibit fatigue resistance and prolonged duration of muscle activity (Zierath and Hawley, 2004). Endogenous EPO contributes to muscle myofiber type. In ΔEpoRE mice with EPO activity restricted to erythroid tissue, skeletal muscles exhibit fewer type I muscle fibers and reduced mitochondrial activity (Wang et al., 2013a). In contrast, skeletal muscles from transgenic mice with high EPO production with high transgenic EPO production show an increase in the proportion of type I muscle fibers and increased mitochondrial activity (Wang et al., 2013a). Furthermore, mice with high EPO production show prolonged position holding time to an inverted wire grid, suggesting that elevated EPO results in improved muscle response to fatigue (Jia et al., 2012). PGC-1α is expressed mainly and preferentially in type I muscle fibers and activates mitochondrial biogenesis and oxidative metabolism in mice (Lin et al., 2002). EPO treatment of primary skeletal myoblast cultures increases mitochondrial biogenesis gene expression including PGC-1α, increased cytochrome C and oxygen consumption rate that can contribute to skeletal muscle fiber programming and development of type I muscle fibers (Wang et al., 2013a).

EPO PROTECTION IN DIET INDUCED OBESITY

Erythropoietin regulation of metabolism extends beyond oxygen delivery and contributes to maintenance of white adipose tissue and metabolic homeostasis. Diet-induced obesity gives rise to glucose intolerance and insulin resistance, leading to type 2 diabetes. Animal studies suggest that EPO may be protective in diet-induced obesity, improves glucose tolerance, reduces insulin resistance and regulates fat mass accumulation, particularly in male mice (Wang et al., 2014; Zhang et al., 2014; Alnaeeli and Noguchi, 2015).

EPO and Inflammation in Obese White Adipose Tissue

The anti-apoptotic and protective effects of EPO in select tissues such as adult and preterm brain contribute to an anti-inflammatory response, inhibiting expression of proinflammatory cytokines and reducing macrophage infiltration (Villa et al., 2003; Wassink et al., 2017). The immune-modulatory activity of EPO as observed in the gut is mediated by JAK2 activation and inhibition of macrophage NF-kB response (Nairz et al., 2011). In diet-induced obesity, EPO modulates the proinflammatory response of macrophage infiltration in white adipose tissue and promotes an anti-inflammatory phenotype (Alnaeeli et al., 2014).

In white adipose tissue, macrophages are found in the stromal vascular fraction. High fat diet feeding in C57BL/6 mice results in inflammation and macrophage infiltration of white adipose tissue, resulting in crown-like structures of macrophages surrounding necrotic adipocytes. Among non-hematopoietic tissues, EPOR is highly expressed in white adipose tissue and specifically on adipocytes and macrophages in the stromal vascular fraction, and EPO treatment exhibits anti-inflammatory activity in white adipose tissue of obese mice (Alnaeeli and Noguchi, 2015). In obese C57BL/6 male mice, short term EPO treatment (2 weeks) increases hematocrit without

affecting body mass, improves glucose tolerance and insulin resistance, and shifts the inflammation of white adipose tissue associated with high fat diet feeding toward an anti-inflammatory phenotype (Alnaeeli et al., 2014). EPO treatment reduces inflammation and crown-like structures in white adipose tissue, decreases pro-inflammatory cytokine/chemokine expression, and increases anti-inflammatory cytokine interleukin 10 expression. EPO reduces the total number of macrophages and shifts the remaining macrophage population toward the anti-inflammatory macrophage subtype. EPO promotes STAT3 phosphorylation in white adipose tissue macrophages and the EPO stimulated increase in the anti-inflammatory macrophage subtype is dependent on interleukin 4/STAT6 signaling. Furthermore, $\Delta EpoR_E$ lack EPOR expression in white adipose tissue and exhibit higher circulating inflammatory monocytes on high fat diet feeding compared with wild type mice, suggesting a role for immune regulation by endogenous EPO/EPOR signaling (Alnaeeli and Noguchi, 2015). $\Delta EpoR_E$ mice on high fat diet show even greater inflammation and crown-like structures in white adipose tissue, elevated cytokine/chemokine expression in perigonadal white adipose tissue stromal vascular fraction, glucose intolerance and insulin resistance. When treated with EPO, $\Delta EpoR_E$ mice exhibit the expected increase in hematocrit without significant difference in glucose tolerance or inflammation in white adipose tissue (Alnaeeli et al., 2014).

Insulin resistance associated with diet induced obesity has been linked to inflammation of white adipose tissue (Lumeng and Saltiel, 2011; Han and Levings, 2013; Chen et al., 2019). This suggests that the activity of EPO to reduce white adipose tissue inflammation in diet induced obesity may contribute to EPO stimulated improvement in insulin resistance. Other EPO associated metabolic activity can also affect insulin resistance. Adipocyte response to EPO contributes to insulin sensitivity and C57BL/6 mice with adipocyte-specific deletion of EPOR on high fat diet exhibit decreased glucose tolerance and insulin sensitivity, an effect that may depend on mouse background strain (Luk et al., 2013; Wang et al., 2013b). In pancreatic β-cells EPO exerts JAK2 dependent protective effects and induces proliferative, anti-inflammatory and angiogenic activity within the islets in mouse diabetic models (Choi et al., 2010). EPO enhances AKT activation in liver, inhibits gluconeogenesis in high fat diet fed mice and reduces liver inflammation associated with diet induced obesity (Meng et al., 2013). EPO activity in brain, particularly the hypothalamus, also influences metabolic homeostasis (Teng et al., 2011b; Dey et al., 2016).

Endogenous EPO Is Required for Erythropoiesis and Regulates Fat Mass Accumulation

Expression of EPOR beyond erythroid tissue and the protective effects of EPO administration in animal models of ischemia and traumatic injury in non-hematopoietic tissue such as the cardiovascular system, brain and skeletal muscle raise questions about the requisite role of EPO beyond regulation of red blood cell production. $\Delta EpoR_E$ mice with EPOR expression restricted to erythroid tissue were created using an erythroid specific transgene expressing EPOR cDNA driven by the erythroid transcription regulatory regions of the GATA1 erythroid transcription factor to rescue the EPOR knockout mouse (mEPOR-/-) (Suzuki et al., 2002). These mice survive through adulthood, providing evidence that the primary and necessary function of EPO is to regulate red blood cell production, and that the non-hematopoietic EPO activity is dispensable for embryonic development.

While $\Delta EpoR_E$ mice created on a C56BL/6 background exhibit no gross morphologic defects, they exhibit a disproportionate accumulation of fat mass with age (Teng et al., 2011b). By 4 months, the body mass is 60% greater in female $\Delta EpoR_E$ mice than wild type control mice and 25% greater in male $\Delta EpoR_E$ mice than wild type control mice (**Figures 3A,B**). The increase in body mass in $\Delta EpoR_E$ mice is due to an increase in both the visceral and subcutaneous white fat. Fat mass continues to disproportionately increase in $\Delta EpoR_E$ mice and by 8 months, fat mass is more than doubled in female $\Delta EpoR_E$ mice compared to control. $\Delta EpoR_E$ mice are glucose intolerant and with increasing accumulation of fat mass become insulin resistant by 4 months in female and by 6 months in male mice. While there is no difference in food intake by $\Delta EpoR_E$ mice on normal chow, $\Delta EpoR_E$ mice exhibited greater body weight gain normalized to food intake, consistent with decreased energy expenditure. Even before overt obesity, young $\Delta EpoR_E$ mice exhibited decreased locomotor activity and decreased metabolic rate assessed by indirect calorimetry. On high fat diet, $\Delta EpoR_E$ mice behaved similarly with food intake comparable to wild type control mice and had decreased locomotor activity and metabolic rate.

C57BL/6 mice with targeted deletion of EPOR in adipocytes fed normal chow exhibited a modest increase in body weight and fat mass with lower total activity and oxygen consumption (Wang et al., 2013b). High fat diet feeding further accentuated these differences, although food intake was comparable with wild type control mice. Young mice that lack EPOR in adipocytes fed high fat diet for 6 weeks showed a 1.4-fold increase in fat mass compared with control mice and higher blood glucose and serum insulin levels, glucose intolerance and insulin resistance, suggesting that endogenous EPOR expression on adipocytes contributes significantly to metabolic regulation.

EPO Activity in Adipocytes and Regulation of Fat Mass Accumulation

Initial studies in mice suggesting EPO activity in metabolic homeostasis involved skeletal muscle gene transfer to over-express EPO that resulted in weight reduction in obese mice due to reduction in fat mass accompanied by increased muscle oxidation and normalization of glucose sensitivity (Hojman et al., 2009; Teng et al., 2011b). Further studies of exogenous EPO treatment in mice including genetic mouse models of obesity and transgenic mice constitutively overexpressing human EPO showed that elevated serum EPO levels decreased blood glucose and decreased body weight, especially body weight gain in obese mice (Katz et al., 2010). Interestingly, hemodialysis patients on short-term EPO treatment showed improved glucose metabolism

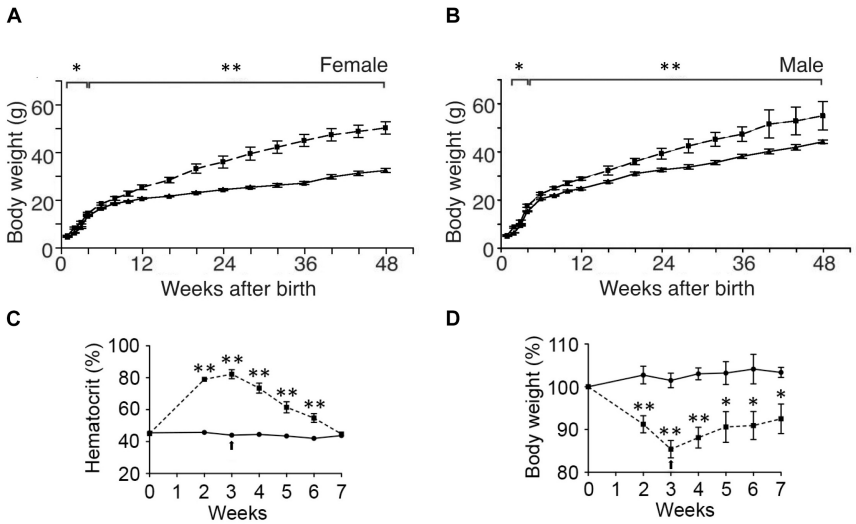

FIGURE 3 | Endogenous and exogenous EPO signaling regulates white fat mass accumulation. **(A,B)** Body weight to 48 weeks of age are indicated for wild type mice (solid line) and mice with EPOR restricted to erythroid tissue (Suzuki et al., 2002) ($\Delta EpoR_E$) (dashed line) for females **(A)** and males **(B)**. **(C,D)** Hematocrit **(C)** and % body weight normalized to starting body weight **(D)** for male wild type mice subjected to 3 weeks of EPO treatment at 3000 U/kg three times weekly (dashed line) or saline (solid line). Arrow indicates end of EPO treatment. *$p < 0.05$; **$p < 0.01$ (from Teng et al., 2011b, with permission).

indicated by a reduction in insulin resistance and decreased glycated hemoglobin and hyperleptinemia (Osman et al., 2017). Accompanying the increase in hematocrit with EPO treatment in C57BL/6 male mice is a decrease of body weight in mice fed normal chow and a reduction in weight gain and fat mass accumulation in mice on high fat diet feeding (Teng et al., 2011b; **Figures 3C,D**). However, $\Delta EpoR_E$ treated with EPO show the expected increase in hematocrit without change in body weight indicating that EPO regulation of fat mass is independent of EPO stimulated red blood cell production (Teng et al., 2011b). Mice with selective deletion of EPOR on adipocytes exhibit increased hematocrit with EPO treatment, but only a non-significant decreasing trend in body weight, exemplifying the direct role of EPO response in adipocytes to EPO regulation of body weight and fat mass accumulation in addition to glucose metabolism and insulin sensitivity (Wang et al., 2013b).

In white adipose tissue, EPOR is expressed at high level (about 60% of spleen, a mouse hematopoietic tissue), and in culture, EPO treatment decreases preadipocyte differentiation and induces ERK activation in primary mouse embryonic fibroblasts but not in embryonic fibroblasts generated from $\Delta EpoR_E$ mice (Teng et al., 2011b). Despite the increase in fat mass in $\Delta EpoR_E$ mice, analysis of adipocyte size distribution in gonadal fat pads showed a shift to smaller cells in $\Delta EpoR_E$ mice indicating a marked increase in adipocyte number with loss of EPOR in non-hematopoietic tissue, providing further evidence that endogenous EPO contributes to regulation of adipocyte number in addition to fat mass accumulation (Teng et al., 2011b).

Insulin stimulates AKT activation and analysis of white adipose tissue from male C57BL/6 mice revealed that EPO treatment also increased AKT phosphorylation in white adipose tissue, but not in mice with targeted deletion of EPOR in adipocytes, suggesting that EPO modulates AKT activation in white adipose tissue and potentially affects insulin signaling (Wang et al., 2013b). Further analysis of white adipose tissue shows that EPO treatment promotes a brown fat-like program, increases mitochondrial biogenesis independent of changes in body weight, and increases cellular respiration rate, and decreases the white fat-like program (Wang et al., 2013b). Conversely, white adipose tissue from mice with targeted deletion of EPOR in adipocytes shows decreased mitochondrial biogenesis, decreased cellular respiration rate and suppression of brown fat-like program and increase in white fat-like program, and no response to EPO stimulation (Wang et al., 2013b). EPO activity in white adipocytes is mediated via increased PPARa that cooperates with increased activity of metabolic sensor Sirt1, an NAD-dependent class III histone deacetylase sirtuin.

In addition to EPO regulation of fat mass accumulation in white adipose tissue, EPO decreased lipid accumulation in the liver while stimulating STAT3/STAT5 activation and promoting lipolysis in white adipose tissue, suggesting benefit in non-alcoholic fatty liver disease (Tsuma et al., 2019). In brown adipose tissue of young C57BL/6 mice, EPO treatment stimulated STAT3 and upregulated transcription factor PRDM16 that controls brown adipocyte differentiation and total UCP1 that is essential for brown adipose tissue thermogenesis (Kodo et al., 2017).

EPO Regulation of Proopiomelanocortin (POMC) and Food Intake

Erythropoietin treatment in male mice fed high fat diet showed both increase in activity and decrease in food intake, pointing to potential EPO regulation in the central nervous system to regulate food intake and energy expenditure (Teng et al., 2011b). The hypothalamus regulates appetite by production in the arcuate nucleus of the orexigenic or appetite-increasing neuropeptide

Y and agouti-related protein, and the anorexigenic or appetite-suppressing precursor protein, POMC. EPOR is expressed in brain, and EPOR expression level in hypothalamus is comparable to white adipose tissue and EPOR in the hypothalamus colocalizes to POMC expressing neurons in the arcuate nucleus (Teng et al., 2011b). EPO treatment in C57BL6 male mice increases hypothalamus expression of POMC and α-MSH, a POMC cleavage product, but not expression of neuropeptide Y or agouti-related protein (Teng et al., 2011b; Dey et al., 2016). Leptin stimulates STAT3 activation in the hypothalamus resulting in production of several neuropeptides including POMC to regulate appetite; hypothalamus neural cultures show that EPO also activates STAT3 (Dey et al., 2016). Conversely, $\Delta EpoR_E$ mice show a decrease in STAT3 activation in hypothalamus and reduced POMC levels with and without EPO treatment, suggesting that EPO regulates appetite, and potentiates leptin response (Dey et al., 2016).

In the pituitary, POMC production gives rise to ACTH. Although EPO treatment in wild type mice increases hypothalamus production of POMC, EPO treatment decreases plasma ACTH level (Dey et al., 2015). On the other hand, plasma concentration of ACTH is high in $\Delta EpoR_E$ mice with reduced POMC production in the hypothalamus, suggesting that both endogenous and exogenous EPO contributes to regulation of plasma ACTH. EPO treatment in cultures of mouse corticotroph pituitary cell line shows decrease in basal intracellular calcium levels, no change in POMC mRNA and increased intracellular ACTH, indicating disruption of post-translational processing of POMC and inhibition of ACTH secretion. EPO regulation of pituitary derived ACTH plasma levels suggests a wider role for EPO regulation of metabolism and obesity via the neuroendocrine hypothalamic-pituitary axis (Dey and Noguchi, 2017).

Gender Specificity of EPO Action and Regulation of Fat Mass

Estrogen can affect EPO action via direct regulation of EPO production or modulation of tissue specific EPO response. For example, in adult female mice, estrogen dependent induction of EPO in the mouse uterus contributes to angiogenic activity and blood vessel formation in the uterine endometrium, contributing to the cyclic remodeling in the estrus cycle transition from diestrus to proestrus (Yasuda et al., 1998). With regards to environmental hypoxia, EPO affects the hypoxic ventilatory response via EPOR expression in brain and carotid body, and this response is increased in women and female mice compared with men and male mice (Soliz et al., 2012). This sexual dimorphism of EPO stimulated hypoxic ventilatory response is attributed, in part, to carotid body sensitivity to sex hormones, particularly estrogen.

Erythropoietin regulation of metabolism also appears to be sex-dependent. In $\Delta EpoR_E$ mice the age dependent accumulation of excess body fat is greater in female that develop obesity and insulin resistance by 4 months of age compared with male mice that exhibit a slower rate of body fat accumulation, becoming obese and insulin resistance at 6 months of age (Teng et al., 2011b; **Figures 3A,B**). In contrast, fat mass is not altered by EPO treatment in female C57BL/6 mice on normal chow or high fat diet, while EPO treatment in male mice on normal chow decreases fat mass and EPO treatment in male mice on high fat diet reduces the accumulation of fat mass (Zhang et al., 2017; **Figures 4A,B**). Gender-specific response was also observed in gene expression in white adipose tissue where EPO treatment in mice increased expression in select oxidative genes in male mice on normal chow and on high fat diet, but not in female mice. The greater increase in fat mass in male mice on high fat diet compared with female mice is evidence of the protective effect of female hormones against diet induced obesity (**Figures 4A,B**) and raises the possibility that female hormones interfere with the anti-obesity effect of EPO observed in male mice. The anti-obesity effect of EPO on mice fed high fat diet was restored in ovariectomized mice. Like male mice, ovariectomized mice on high fat diet treated with EPO showed the decrease in fat mass (**Figure 4C**). The protective effect of estrogen to diet induced obesity was demonstrated in ovariectomized mice supplemented with estradiol which was more effective in reducing fat mass than EPO, and fat mass was not further enhanced with estrogen combined with EPO (**Figure 4C**). EPO stimulated increase in hematocrit was comparable in male in female mice indicating that the sex-dependent regulation of fat mass is independent of EPO regulated response in erythroid tissue.

To further examine the relationship of EPO level with body weight in human, endogenous plasma EPO concentration was assessed in a subset of full-heritage Southwestern Native Americans studied to understand the high prevalence of obesity and type 2 diabetes (Smith et al., 1996; Pavkov et al., 2007). As expected, endogenous plasma EPO level negatively associated with hemoglobin (p = 0.005) and no association was found for EPO and percent weight change per year in the study group of 79 individuals (Reinhardt et al., 2016). However, when segregated by sex, males exhibited an association between higher EPO concentrations and higher 24-h energy expenditure and an inverse association of endogenous EPO level with percent weight change per year (p = 0.02) (**Figure 5A**). In contrast, females exhibited a positive association of EPO plasma level with weight change per year (p = 0.02) (**Figure 5B**). Hence, endogenous EPO association with weight loss in men and with weight gain in women is distinct from EPO regulation of erythropoiesis that is comparable in both men and women and provides additional evidence for non-hematopoietic and gender-specific endogenous EPO action on regulation of body weight.

Elevated EPO in Human and Decreasing Obesity Prevalence at Increasing Altitude

In humans, as one ascends to high altitude increased EPO production via HIF regulation induces an EPO response that increases iron utilization for hemoglobin synthesis with expansion of red blood cell production with elevated blood hemoglobin and hematocrit (Gassmann and Muckenthaler, 1985; Smith et al., 2008). The relationship between elevated EPO and reduction in fat mass suggested by metabolic studies in

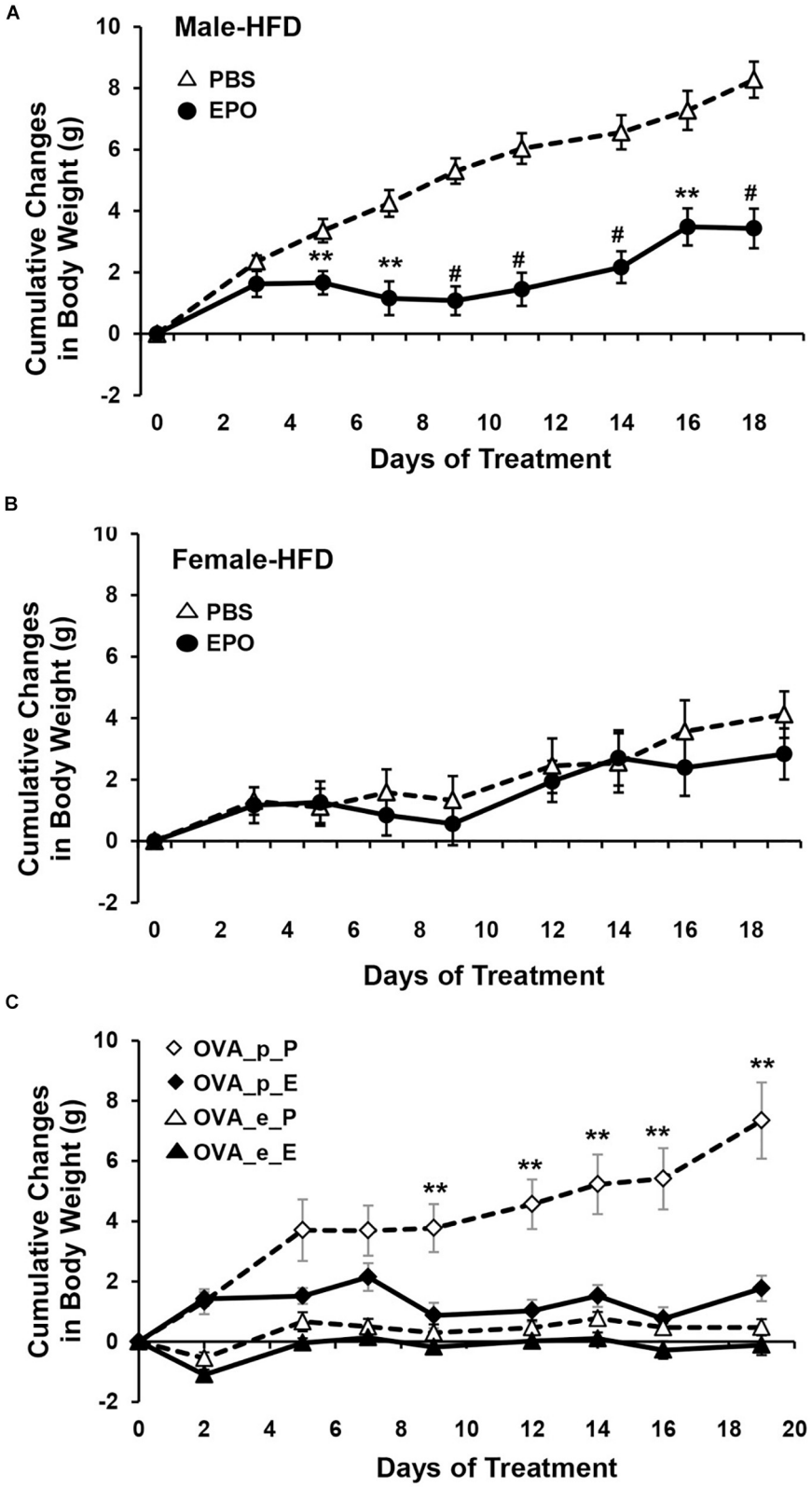

FIGURE 4 | EPO regulation of fat mass is gender specific. **(A,B)** Cumulative body weight change was monitored in male **(A)** and female **(B)** mice (16 weeks) fed high fat diet and treated with EPO at 3000 U/kg three times weekly (solid symbol) or saline (open symbol) for 3 weeks. **(C)** Cumulative body weight change in female ovariectomized (OVA) mice with placebo (p) or estradiol pellet-supplement and treated with EPO (E) or phosphate-buffered saline (P). $^{**}p < 0.01$; $^{\#}p < 0.001$ (from Zhang et al., 2017, with permission).

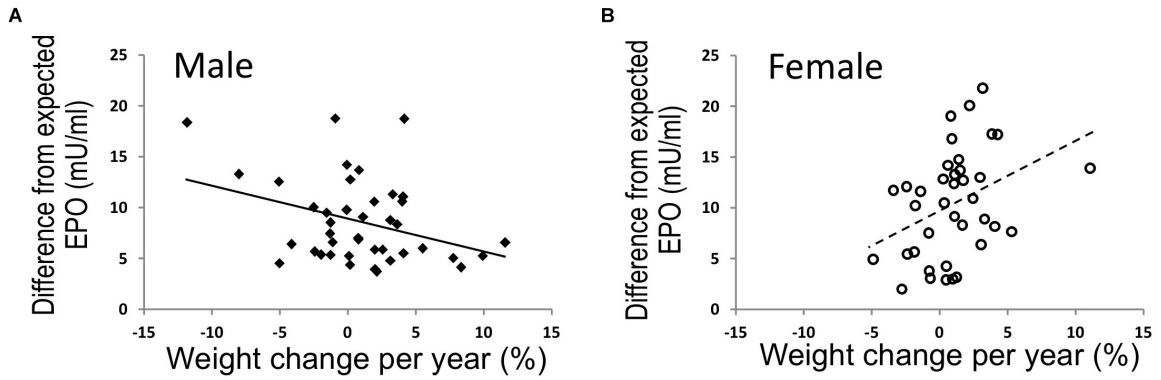

FIGURE 5 | EPO and % weight change per year were associated in opposing directions in males and females. **(A,B)** In full-heritage Southwestern Native Americans, the association of plasma EPO concentrations (adjusted for creatinine, hemoglobin, and storage time) and % weight change per year was negative in men **(A)** (closed squares, $N = 41$; $r = -0.35$, $p = 0.02$). Plasma EPO concentration was positively associated with % weight change per year in females **(B)** (open circles, $N = 38$; $r = 0.37$, $p = 0.02$) (modified from Reinhardt et al., 2016, with permission).

male mice (Teng et al., 2011b; Zhang et al., 2017), raises the possibility that increased EPO levels may explain in part the lower obesity rate reported for humans associated with residence at high altitude (Voss et al., 2013, 2014). In the United States, obesity prevalence is associated inversely with elevation and urbanization after adjusting for diet, ambient temperature, physical activity, smoking and demographic factors, and among overweight service members (proportion male of 93% at low altitude and 94% at high altitude), those stationed at high altitude were associated with lower incidence of obesity (Voss et al., 2013, 2014).

Note that high EPO levels can increase the risks of adverse effects such as cardiovascular complications and thromboembolic events, seizures, pulmonary embolism and death. For individuals in residence above 2500 m above sea level, about 5–10% can develop excessive erythrocytosis and associated Chronic Mountain Sickness (Villafuerte and Corante, 2016). However, Tibetan high-altitude natives are the exception and exhibit a different adaptive response from the hypoxia induction of EPO, allowing more efficient use of oxygen in their tissues (Horscroft et al., 2017). Even without high altitude, increase risk of adverse effects are evident with high endogenous EPO. In the elderly, elevated EPO levels were associated with increased risk of death, and in renal transplant recipients higher endogenous plasma EPO was associated with cardiovascular mortality and all-cause mortality (den Elzen et al., 2010; Sinkeler et al., 2012). Elevated EPO levels may be indicative of EPO resistance resulting from underlying co-morbidities including inflammation, iron status, malnutrition and disrupted NO metabolism (Ganz and Nemeth, 2016; Yokoro et al., 2017). The increase risk of adverse effects with high exogenous EPO administration is exemplified in extreme athletes who use EPO as a performance-enhancing drug. Around the time that EPO received FDA approval in 1989 for treatment of anemia in chronic renal disease, death associated with EPO doping was suspected in eighteen young professional cyclists who died from unknown causes (Noakes, 2004). While patients with renal failure clearly benefit from EPO treatment to correct anemia (Eschbach et al., 1987; Us Renal Data System, 2007; Hasegawa et al., 2018) several clinical trials of EPO treatment to normalize hemoglobin values in kidney disease showed increase cardiovascular morbidity and mortality associated with high dose EPO treatment (Drueke et al., 2006; Singh et al., 2006). With increased concerns about safety of high dose EPO, the FDA issued a "Black Box" warning in 2007 indicating reduced EPO dose to achieve lower target hemoglobin levels. Labeling for erythropoiesis-stimulating agents was further modified by the FDA in 2011 to lower dosing recommendations. Hence, potential benefits and potential risks must be considered with EPO treatment.

EPO PROMOTES CONTEXT-DEPENDENT BONE REMODELING

In bone, functional EPO receptors are expressed by osteoblasts and osteoclasts that remodel the bone and by BMSCs that differentiate into osteoblasts, bone marrow adipocytes and chondrocytes. Studies on the effects of EPO on these specific cell types and overall bone homeostasis have utilized *in vitro* cultures (Kim et al., 2012; Rolfing et al., 2014a; Li et al., 2015), *in vivo* BMSC osteogenic assays using ectopic ossification models (Suresh et al., 2019), bone fracture healing models (Holstein et al., 2007; Mihmanli et al., 2009; Rolfing et al., 2014b; Omlor et al., 2016), transgenic mouse model with high human EPO (model for chronic EPO exposure) (Hiram-Bab et al., 2015; Suresh et al., 2019), administration of exogenous EPO in healthy mice (Shiozawa et al., 2010; Singbrant et al., 2011; Hiram-Bab et al., 2015; Suresh et al., 2019) (model for acute EPO exposure) and, recently, $\Delta EpoR_E$ mice that do not express EPOR in non-erythroid cells (Suresh et al., 2019) (model for endogenous EPO signaling).

Osteoclasts and EPO Response

Several reports including conflicting results suggest EPO regulating osteoblasts, osteoclasts and BMSCs in *in vitro* culture conditions. Osteoclast differentiation assays using marrow

mononuclear cells (Shiozawa et al., 2010), non-adherent bone marrow cells (Hiram-Bab et al., 2015) and RAW264.7 mouse monocyte/macrophage cell line show EPO increasing osteoclast numbers (Li et al., 2015), but not osteoclast activity (Shiozawa et al., 2010; Li et al., 2015). However, increase in osteoclast numbers was not reported in other studies using mouse bone marrow cultures (Suresh et al., 2019) and in osteoblast-osteoclast cocultures treated with EPO (Singbrant et al., 2011). In cultures of preosteoclasts, EPO activates JAK2/PI3K pathways without affecting proliferation and in osteoclasts, EPOR expression decreases with differentiation (Hiram-Bab et al., 2015). Transgenic mice with chronic exposure to high levels of human EPO had more osteoclasts lining the bone surface (Hiram-Bab et al., 2015). Osteoclasts from these mice produced EPO and corresponding BMSC derived cultures from these mice exhibited a greater number of giant multinucleated osteoclasts (Suresh et al., 2019).

Osteoblasts and EPO Response

For osteoblast differentiation assays, studies have utilized mouse primary calvarial osteogenic cells as well as adherent BMSCs. EPO treatment of primary mouse calvarial osteogenic cells did not affect differentiation (Hiram-Bab et al., 2015; Suresh et al., 2019). However, in transgenic mice expressing high human EPO, calvarial osteoblasts produced human EPO and showed increased ALP expression and mineralization (Suresh et al., 2019). Conversely, primary calvarial osteoblasts lacking endogenous EPO signaling had reduced ALP expression and mineralization (Suresh et al., 2019). Other osteoblast assays using human and mouse BMSCs treated with EPO reported increased osteoblast differentiation with the activation of EphrinB2/EphrinB4 (Li et al., 2015), mTOR (Kim et al., 2012), JAK2/PI3K pathways (Rolfing et al., 2014a). BMSC cultures with low EPO doses less than 5 U/mL reduced osteoblast mineralization whereas high EPO doses (50 U/mL–250 U/mL) increased the BMSC proliferation and differentiation into osteoblasts (Rauner et al., 2016). EPO stimulation of HSCs to produce BMP and thereby stimulating osteoblasts are also reported (Shiozawa et al., 2010). In a recent study using mesenchymal stem cells from young and old healthy individuals and patients with MDS, EPO treatment increased mineralization only in cells from young healthy individuals and not in cells from older healthy donors and cells from MDS patients (Balaian et al., 2018), suggesting that EPO bone remodeling activity may be age dependent. EPO treatment of mesenchymal stem cells from MDS patients inhibited Wnt signaling and reactivation of Wnt signaling combined with EPO treatment promoted their differentiation to osteoblasts (Balaian et al., 2018).

EPO and Bone Fracture Repair

A role for EPO in bone regulation was initially reported in mouse models of fracture repair, where 5000 U/kg EPO doses for 6 days stimulated early endochondral ossification and bone mineralization along with reduced EPOR in differentiating chondrocytes (Holstein et al., 2007). A follow up study showed accelerated bone healing with much reduced dose of EPO at 500 U/kg for five-week treatment where EPO promoted endosteal vascularization and reduced NF-KB expression in the fracture callus suggesting anti-inflammatory role for EPO (Garcia et al., 2011). In alveolar bone regeneration studies in rats, EPO administration into the tooth sockets, promoted new bone formation while inhibiting bone resorption (Li et al., 2015). In rabbits with mandibular distraction osteogenesis, 150 IU/kg EPO treatment for 30 days resulted in new bone formation with increased osteoblasts, blood vessels and reduced osteoclasts (Mihmanli et al., 2009). In rabbits, implantation of gelatin sponges soaked with EPO near the bone defects followed by a single high EPO dose of 4900 IU/kg accelerated bone healing and vascularization in the callus (Omlor et al., 2016). In porcine models with calvarial defects, a single EPO dose of 900 IU/ml in collagen carrier moderately increased bone healing without any increase in vasculature (Rolfing et al., 2014b). However, in a separate study in porcine models, EPO enhanced bone healing only in combination with bone marrow concentrate containing mesenchymal stem cells (Betsch et al., 2014).

Studies have also utilized the potential of EPO in recruiting BMSCs to sites of bone healing. In rats with intratibial fracture, tail vein injection of BMSCs along with intramuscular injection of EPO was shown to mobilize BMSCs to bone defects and enhanced bone regeneration while increasing bone strength (Li et al., 2019). EPO loaded scaffolds in BALB/c mice showed increased recruitment of multipotent stem cells, this study also demonstrated that in mouse calvarial defect model, implantation of scaffolds with EPO resulted in accelerated bone healing compared to BMP2 scaffolds (Nair et al., 2013). Two-week EPO treatment of murine cranial defect models with BMP2 scaffolds implanted at the defect site also accelerated healing while promoting stem cell recruitment to the scaffolds (Sun et al., 2012). In patients with tibiofibular fracture, administration of 4000 IU of EPO in the fractures site 2 weeks after surgery had 2 week faster union and fewer non-union rates compared to the placebo group (Bakhshi et al., 2013; Nemati and Fallahi, 2013), suggesting possibility of clinical EPO use in accelerating fracture healing. Thus, using multiple species and various EPO doses and mode of administration, EPO treatment has been demonstrated to exert a beneficial role in bone healing.

Bone Loss Concomitant With EPO Stimulated Erythropoiesis in Mice

In contrast to the bone formation potential of EPO in fracture healing studies, EPO administration in healthy mice results in significant reduction of trabecular bone volume. EPO administration in 9 week old male C57BL/6 mice for 10 days at a physiological dose of 300 U/kg resulted in significant trabecular bone loss in tibia along with increase in the number of osteoclasts and osteoblasts, indicating increased bone turnover induced by EPO treatment (Singbrant et al., 2011). However, dynamic morphometry analysis revealed that EPO administration did not affect mineral apposition rate or double labeled surface, but significantly reduced single labeled surface, suggesting a reduction in osteoblast activity

(Singbrant et al., 2011). Reduction in trabecular bone coupled with increased osteoclast numbers in the femurs of 12-week-old female mouse models was also observed in chronic and acute EPO exposure (Hiram-Bab et al., 2015). Since addition of EPO increased only osteoclast differentiation *in vitro* and did not affect osteoblast differentiation in cultures, the reduced bone formation *in vivo* with EPO treatment was attributed to an indirect effect of EPO (Hiram-Bab et al., 2015). However in subsequent studies, a very low dose of EPO administration in mice was shown to significantly reduce osteoblast activity without affecting bone resorption (Rauner et al., 2016). In contrast, in mice with chronically elevated high EPO, both osteoblast and osteoclast differentiation was increased suggesting increased remodeling contributing to their reduced bone mass (Suresh et al., 2019). Thus, the dose of EPO is important in determining the effect on osteoblasts and subsequently on its impact in bone health.

Studies in transgenic mice with conditional deletion of PHD2 have shown the importance of PHD2-HIF2α-EPO signaling in bone remodeling. Low bone density due to reduced osteoblast activity without affecting osteoclasts was observed in transgenic mice with conditional deletion of PHD2 in hematopoietic lineage, renal and neural cells. In these mice PHD2 deletion resulted in excessive HIF-2α induced EPO production increasing the hematocrit to 86%. Surprisingly, deletion of PHD2 in osteoblastic lineage increased bone density and reduced osteoclast numbers *in vivo* with no change in hematocrits. While deletion of PHD2 in osteoclast lineage did not result in any bone phenotype (Rauner et al., 2016).

Reduced trabecular bone was also observed in the femurs of C57BL/6 mice with 10 day EPO administration at 1200 U/kg (Suresh et al., 2019). In contrast to these studies, increased bone formation with EPO treatment was reported in the vertebrae of young and older mice receiving supraphysiologic doses of EPO up to 6000 U/kg for three times a week for 28 days (Shiozawa et al., 2010). Of note, the reported modest increase in hematocrits with such high doses of EPO treatment has not been explained (Shiozawa et al., 2010). These changes in hematocrit are in marked contrast to the expected increase in hematocrit associated with EPO dose. For example, low dose of 150 U/kg of EPO elevated hematocrits to 60% (Foskett et al., 2011) whilst higher doses of 3000 U/kg of EPO increased hematocrits to 70% in C57BL/6 mice (Zhang et al., 2017).

Osteoblasts exhibit the potential for EPO production. In genetically modified mice, targeted deletion of VHL in osteoblasts over-stabilizes the hypoxic response and gives rise to high EPO production in osteoblasts that leads to severe polycythemia (Rankin et al., 2012). Conversely, inactivation of HIF-2 in osteoblasts resulted in decreased EPO expression in bones of neonatal mice and remained at the limit of detection in adult mice. This novel finding that osteoblasts could produce EPO raises the potential for autocrine regulation of EPO response in osteoblasts. In other studies, EPO stimulated FGF23 production in HSCs was associated with an increase in serum FGF23 and reduced serum phosphate suggesting a possible mechanism of EPO induced bone reduction due to disrupted mineralization (Clinkenbeard et al., 2017).

Endogenous EPO Contributes to Bone Formation and Maintenance

Understanding of the effect of EPO in bone is derived predominantly from animal models with overexpression of EPO or acute EPO administration. Recent studies using $\Delta EpoR_E$ mice demonstrated the importance of endogenous EPO signaling in bone formation and maintenance. These mice had significant reduction in trabecular bone in both male and female mice of mature skeletal age (Suresh et al., 2019; **Figure 6**). Osteoblasts and BMSCs from $\Delta EpoR_E$ mice did not express EPOR, while osteoclasts expressed EPOR because the erythroid transgene in this model was GATA1 dependent and preosteoclasts express GATA1, suggesting that reduction in bone formation in these mice is related to loss of EPO response in osteoblasts rather than osteoclast activity. Administration of EPO in $\Delta EpoR_E$ mice increased hematocrits but did not reduce trabecular bone (**Figure 6**) indicating that EPO induced bone reduction is independent of erythropoiesis.

In addition to reduced trabecular bone, lack of endogenous EPO-EPOR signaling increased bone marrow adipocytes leading to fatty marrow. This raised the possibility of endogenous EPO signaling regulating BMSC differentiation to either osteoblastic or adipogenic lineage.

EPO Regulates Bone Marrow Stromal Cell Differentiation and Bone Formation

The potential for BMSCs to differentiate to osteoblasts or adipocytes can be assessed using transplantation into

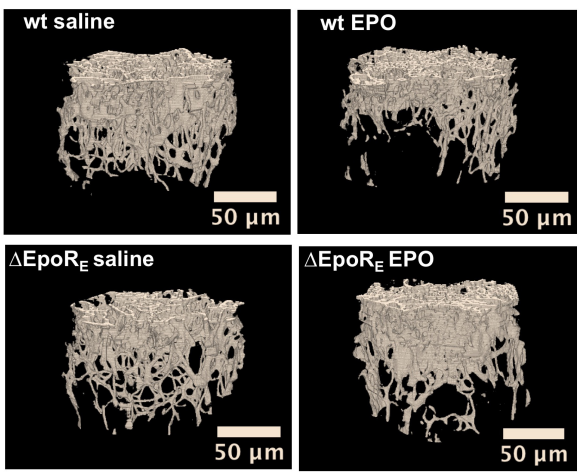

FIGURE 6 | Endogenous and exogenous EPO signaling regulates bone formation. Micro-CT 3D images of trabecular bone from wild type (wt) mice and mice with EPOR restricted to erythroid tissue ($\Delta EpoR_E$) (Suzuki et al., 2002). Mice (age 8 weeks) were treated with EPO at 1200 U/kg for 10 days (EPO) or saline. Images from saline treatment **(left)** show reduction in bone formation in $\Delta EpoR_E$ mice that lack EPOR in non-hematopoietic tissue. Furthermore, the reduction in bone parameters with EPO treatment in wild type mice **(top)** is not seen in $\Delta EpoR_E$ mice **(bottom)**, indicating that bone loss with EPO treatment is mediated by non-erythroid response (from Suresh et al., 2019, with permission).

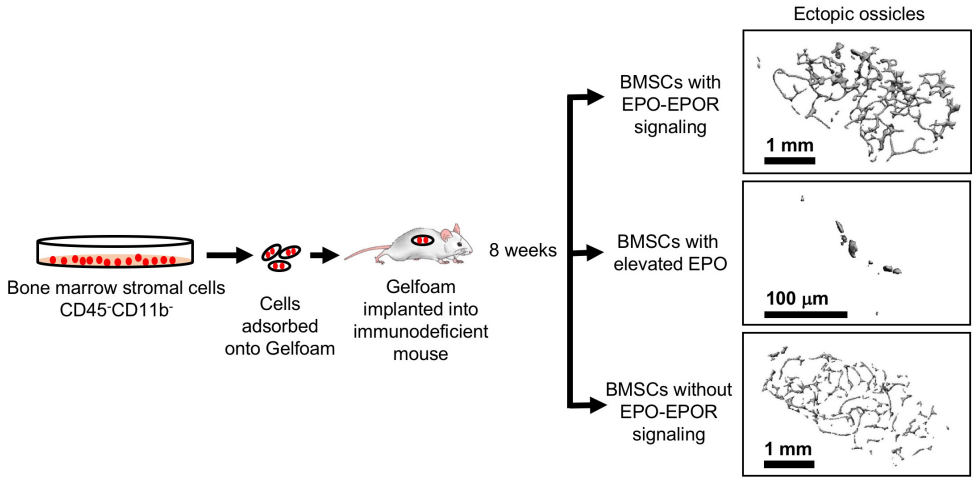

FIGURE 7 | Ectopic bone formation assay with BMSC. Adherent BMSC were selected from cultures of bone marrow cells harvested from wild type and genetically altered mice. Cells were absorbed into Gelfoam and surgically transplanted into immunocompromised NSG mice (Jackson Laboratory). After 8 weeks, ectopic bone ossicles formed and were analyzed by micro-CT. Ossicles formed in transplants from $\Delta EpoR_E$ mice that lack EPOR in non-hematopoietic tissue **(bottom)** showed similar structure to control mice **(top)** with a trend toward fewer trabeculae, consistent with a reduction in endogenous bone formation in $\Delta EpoR_E$ mice. Bone formation was markedly reduced with hardly any trabecular bone in ossicles in transplants from transgenic mice expressing high level of human EPO (Ruschitzka et al., 2000) **(middle)** compared with control mice **(top)**, reflecting the even greater reduction of endogenous bone formation in these transgenic mice compared with $\Delta EpoR_E$ mice and control mice (modified from Suresh et al., 2019, with permissions).

immunodeficient mice and monitoring bone ossicle formation. *In vivo* implantation of gelatin sponge cubes (Gelfoam) carrying BMSCs in immunodeficient mice model showed that BMSCs from $\Delta EpoR_E$ mice that lack of endogenous EPO signaling results in reduced ectopic bone formation and increased marrow adipogenesis (Suresh et al., 2019; **Figure 7**). In contrast, transplanting BMSCs from transgenic mice expressing elevated EPO significantly attenuated both ectopic bone formation and marrow adiposity (**Figure 7**). Furthermore, systemic elevated EPO inhibited BMP2 induced ectopic bone formation without affecting osteoclasts (Suresh et al., 2019). Thus, EPO is a critical regulator of bone. In the absence of endogenous EPO signaling there is reduced bone and increased marrow adiposity. Elevated EPO is also detrimental to bone formation demonstrated by several animal models of EPO administration in healthy animals resulting in significant bone reduction. On the other hand, other animal studies point to EPO potential in accelerating bone healing. Future studies focusing on optimizing the EPO dose and duration of treatment for clinical use along with the observation of any adverse events are warranted.

CONCLUSION

Hypoxia induction of EPO is an important response to ischemic stress resulting in increased red blood cell production to increase tissue oxygen delivery. Animal models have been useful in demonstrating EPOR expression beyond erythroid tissue and EPO response in non-hematopoietic tissue. For example, EPOR expression in vascular endothelium provides the potential for direct response via increase eNOS activation and NO production to regulate vascular tone and oxygen delivery (Beleslin-Cokic et al., 2004, 2011). This acute response is in contrast to the time required to stimulate survival, proliferation and differentiation of erythroid progenitor cells to produce mature red blood cells. Requirement for eNOS for EPO protective activity in heart ischemic reperfusion injury also points to the potential benefit of this acute endothelial response. EPO stimulation of improved oxygen delivery may also contribute to protective action in other non-hematopoietic tissue such as brain ischemia and skeletal muscle injury.

Erythropoietin receptor expression is not for erythroid cells only and expression in non-erythroid tissues provides for tissue specific EPO protective response during ischemic challenge or injury. EPOR expression and EPO activity include the following tissues: endothelium to regulate vascular tone, improve oxygen delivery and provide cardioprotection to ischemic injury; brain (particularly neurons) to provide protection to ischemic stress or injury; skeletal muscle (myoblasts) for tissue maintenance or repair; white adipose tissue (adipocytes and macrophages) to protect from inflammation and from increase in fat mass in male mice during diet-induced obesity; and BMSC and osteoblasts to maintain normal bone development and bone remodeling accompanying exogenous EPO stimulated erythropoiesis (**Figure 1**). Sites of EPO production also extend beyond fetal liver and adult kidney and include the other side of the blood-brain barrier (astrocytes and neurons) (Masuda et al., 1994; Marti et al., 1996), skeletal muscle myoblasts (Kuang et al., 2007), and osteoblasts (Rankin et al., 2012), and estrogen stimulated induction in the uterus contributing to angiogenesis (Yasuda et al., 1998), raising the possibility of EPO/EPOR autocrine response even with low EPOR expression in select non-hematopoietic cells.

In regulation of skeletal bone formation, endogenous EPO contributes to development and maintenance of skeletal bone and bone marrow adipocytes, and loss of non-hematopoietic EPO activity results in decreased bone formation and increased marrow adiposity (Suresh et al., 2019). EPO administration has also demonstrated the capacity to affect bone remodeling, but in two disparate ways: accelerate bone healing in animal models of bone fracture, and cause bone loss in healthy animals responding with increased erythropoiesis. More studies in understanding the role of EPO in bone in specific pathological conditions are warranted as patients with diseases associated with high circulating EPO such as thalassemia (Vichinsky, 1998), sickle cell disease (Sarrai et al., 2007), and polycythemia vera (Farmer et al., 2013) have debilitating bone conditions.

Sex-specific differences in plasma concentration of EPO are not detected (Jelkmann and Wiedemann, 1989). However, estrogen can affect EPO response and confer gender specific EPO action. In ventilatory response in mice, hypoxia induction of EPO modulates ventilatory response, which exhibits a sex-dimorphic behavior mediated via interaction with carotid body cells that is also sensitive to ovarian steroids (Soliz et al., 2012). The sex-dependent EPO regulation of fat mass is demonstrated with EPO treatment during high fat diet feeding that reduces fat mass gain in male mice and in female ovariectomized mice but not in female non-ovariectomized mice and not in ovariectomized mice supplemented with estradiol pellets (Zhang et al., 2017). Endogenous EPO signaling may cooperate with estrogen regulation of fat mass in female mice but mask reduction of fat mass by exogenous EPO treatment. In human, sexual dimorphic response is observed in the association between endogenous plasma EPO concentration and percent weight change per year. A negative relationship is observed in males where the higher EPO level is related to lower percent weight change, while a positive relationship is evident in females (Reinhardt et al., 2016). Elucidation of the potential cross-talk between estrogen and EPO will further the understanding of gender-specific EPO response in non-hematopoietic tissue.

Translation of animal studies that demonstrate protective effects of EPO treatment in non-hematopoietic tissues to human disease manifestations can be problematic. Neuroprotection observed with EPO treatment in animal models of ischemic stroke and brain injury and the encouraging results in the Phase I clinical trial of EPO administration for ischemic stroke (Ehrenreich et al., 2002) did not predict the adverse events associated with the combination of EPO and systemic thrombolysis therapy (Ehrenreich et al., 2009), although some benefit with EPO treatment was suggested in further subgroup analysis of patients not receiving thrombolysis therapy (Ehrenreich et al., 2011). EPO shows promise in treatment of extremely low birth weight premature infants where thrombolysis therapy is not used. EPO treatment in extremely low birth weight infants appears to be well tolerated with no excess morbidity or mortality, and, in addition to improving anemia, is associated with overall benefit in developmental assessment and cognitive development (Fauchere et al., 2008; Juul et al., 2008; Neubauer et al., 2010; Fischer et al., 2017). The potential long-term neurodevelopmental outcomes and whether benefit is a consequence of EPO stimulated erythropoiesis to improved oxygen delivery or a direct consequence of EPO response in the premature brain await further study (Fischer et al., 2017).

AUTHOR CONTRIBUTIONS

All authors listed have made a substantial, direct and intellectual contribution to the work, and approved it for publication.

FUNDING

This work was supported by the Intramural Research Program of the National Institute of Diabetes and Digestive and Kidney Diseases at the National Institutes of Health.

REFERENCES

Alnaeeli, M., and Noguchi, C. T. (2015). Erythropoietin and obesity-induced white adipose tissue inflammation: redefining the boundaries of the immunometabolism territory. *Adipocyte* 4, 153–157. doi: 10.4161/21623945.2014.978654

Alnaeeli, M., Raaka, B. M., Gavrilova, O., Teng, R., Chanturiya, T., and Noguchi, C. T. (2014). Erythropoietin signaling: a novel regulator of white adipose tissue inflammation during diet-induced obesity. *Diabetes Metab. Res. Rev.* 63, 2415–2431. doi: 10.2337/db13-0883

Anagnostou, A., Lee, E. S., Kessimian, N., Levinson, R., and Steiner, M. (1990). Erythropoietin has a mitogenic and positive chemotactic effect on endothelial cells. *Proc. Natl. Acad. Sci. U.S.A.* 87, 5978–5982. doi: 10.1073/pnas.87.15.5978

Anagnostou, A., Liu, Z., Steiner, M., Chin, K., Lee, E. S., Kessimian, N., et al. (1994). Erythropoietin receptor mRNA expression in human endothelial cells. *Proc. Natl. Acad. Sci. U.S.A.* 91, 3974–3978. doi: 10.1073/pnas.91.9.3974

Ang, S. O., Chen, H., Hirota, K., Gordeuk, V. R., Jelinek, J., Guan, Y., et al. (2002). Disruption of oxygen homeostasis underlies congenital Chuvash polycythemia. *Nat. Genet.* 32, 614–621. doi: 10.1038/ng1019

Anusornvongchai, T., Nangaku, M., Jao, T. M., Wu, C. H., Ishimoto, Y., Maekawa, H., et al. (2018). Palmitate deranges erythropoietin production via transcription factor ATF4 activation of unfolded protein response. *Kidney Int.* 94, 536–550. doi: 10.1016/j.kint.2018.03.011

Bakhshi, H., Kazemian, G., Emami, M., Nemati, A., Karimi Yarandi, H., and Safdari, F. (2013). Local erythropoietin injection in tibiofibular fracture healing. *Trauma Mon.* 17, 386–388. doi: 10.5812/traumamon.7099

Balaian, E., Wobus, M., Weidner, H., Baschant, U., Stiehler, M., Ehninger, G., et al. (2018). Erythropoietin inhibits osteoblast function in myelodysplastic syndromes via the canonical Wnt pathway. *Haematologica* 103, 61–68. doi: 10.3324/haematol.2017.172726

Barhoumi, T., Briet, M., Kasal, D. A., Fraulob-Aquino, J. C., Idris-Khodja, N., Laurant, P., et al. (2014). Erythropoietin-induced hypertension and vascular injury in mice overexpressing human endothelin-1: exercise attenuated hypertension, oxidative stress, inflammation and immune response. *J. Hypertens.* 32, 784–794. doi: 10.1097/HJH.0000000000000101

Bazan, J. F. (1990). Structural design and molecular evolution of a cytokine receptor superfamily. *Proc. Natl. Acad. Sci. U.S.A.* 87, 6934–6938. doi: 10.1073/pnas.87.18.6934

Beleslin-Cokic, B. B., Cokic, V. P., Wang, L., Piknova, B., Teng, R., Schechter, A. N., et al. (2011). Erythropoietin and hypoxia increase erythropoietin receptor and nitric oxide levels in lung microvascular endothelial cells. *Cytokine* 54, 129–135. doi: 10.1016/j.cyto.2011.01.015

Beleslin-Cokic, B. B., Cokic, V. P., Yu, X., Weksler, B. B., Schechter, A. N., and Noguchi, C. T. (2004). Erythropoietin and hypoxia stimulate erythropoietin receptor and nitric oxide production by endothelial cells. *Blood* 104, 2073–2080. doi: 10.1182/blood-2004-02-0744

Bernaudin, M., Marti, H. H., Roussel, S., Divoux, D., Nouvelot, A., MacKenzie, E. T., et al. (1999). A potential role for erythropoietin in focal permanent cerebral ischemia in mice. *J. Cereb. Blood Flow Metab.* 19, 643–651. doi: 10.1097/00004647-199906000-00007

Betsch, M., Thelen, S., Santak, L., Herten, M., Jungbluth, P., Miersch, D., et al. (2014). The role of erythropoietin and bone marrow concentrate in the treatment of osteochondral defects in mini-pigs. *PLoS One* 9:e92766. doi: 10.1371/journal.pone.0092766

Boesch, S., Nachbauer, W., Mariotti, C., Sacca, F., Filla, A., Klockgether, T., et al. (2014). Safety and tolerability of carbamylated erythropoietin in Friedreich's ataxia. *Mov. Disord.* 29, 935–939. doi: 10.1002/mds.25836

Bonnas, C., Wustefeld, L., Winkler, D., Kronstein-Wiedemann, R., Dere, E., Specht, K., et al. (2017). EV-3, an endogenous human erythropoietin isoform with distinct functional relevance. *Sci. Rep.* 7:3684. doi: 10.1038/s41598-017-03167-0

Brines, M., Dunne, A. N., van Velzen, M., Proto, P. L., Ostenson, C. G., Kirk, R. I., et al. (2015). ARA 290, a nonerythropoietic peptide engineered from erythropoietin, improves metabolic control and neuropathic symptoms in patients with type 2 diabetes. *Mol. Med.* 20, 658–666. doi: 10.2119/molmed.2014.00215

Brines, M., Grasso, G., Fiordaliso, F., Sfacteria, A., Ghezzi, P., Fratelli, M., et al. (2004). Erythropoietin mediates tissue protection through an erythropoietin and common beta-subunit heteroreceptor. *Proc. Natl. Acad. Sci. U.S.A.* 101, 14907–14912. doi: 10.1073/pnas.0406491101

Brines, M., Patel, N. S., Villa, P., Brines, C., Mennini, T., De Paola, M., et al. (2008). Nonerythropoietic, tissue-protective peptides derived from the tertiary structure of erythropoietin. *Proc. Natl. Acad. Sci. U.S.A.* 105, 10925–10930. doi: 10.1073/pnas.0805594105

Broudy, V. C., Lin, N., Brice, M., Nakamoto, B., and Papayannopoulou, T. (1991). Erythropoietin receptor characteristics on primary human erythroid cells. *Blood* 77, 2583–2590. doi: 10.1182/blood.v77.12.2583.bloodjournal77122583

Cai, Z., Manalo, D. J., Wei, G., Rodriguez, E. R., Fox-Talbot, K., Lu, H., et al. (2003). Hearts from rodents exposed to intermittent hypoxia or erythropoietin are protected against ischemia-reperfusion injury. *Circulation* 108, 79–85. doi: 10.1161/01.cir.0000078635.89229.8a

Cai, Z., and Semenza, G. L. (2004). Phosphatidylinositol-3-kinase signaling is required for erythropoietin-mediated acute protection against myocardial ischemia/reperfusion injury. *Circulation* 109, 2050–2053. doi: 10.1161/01.cir.0000127954.98131.23

Carlini, R. G., Dusso, A. S., Obialo, C. I., Alvarez, U. M., and Rothstein, M. (1993). Recombinant human erythropoietin (rHuEPO). increases endothelin-1 release by endothelial cells. *Kidney Int.* 43, 1010–1014. doi: 10.1038/ki.1993.142

Chen, X., Zhuo, S., Zhu, T., Yao, P., Yang, M., Mei, H., et al. (2019). Fpr2 deficiency alleviates diet-induced insulin resistance through reducing body weight gain and inhibiting inflammation mediated by macrophage chemotaxis and M1 polarization. *Diabetes Metab. Res. Rev.* 68, 1130–1142. doi: 10.2337/db18-0469

Chen, Z. Y., Asavaritikrai, P., Prchal, J. T., and Noguchi, C. T. (2007). Endogenous erythropoietin signaling is required for normal neural progenitor cell proliferation. *J. Biol. Chem.* 282, 25875–25883. doi: 10.1074/jbc.m701988200

Cheung Tung Shing, K. S., Broughton, S. E., Nero, T. L., Gillinder, K., Ilsley, M. D., Ramshaw, H., et al. (2018). EPO does not promote interaction between the erythropoietin and beta-common receptors. *Sci. Rep.* 8:12457.

Choi, D., Schroer, S. A., Lu, S. Y., Wang, L., Wu, X., Liu, Y., et al. (2010). Erythropoietin protects against diabetes through direct effects on pancreatic beta cells. *J. Exp. Med.* 207, 2831–2842. doi: 10.1084/jem.20100665

Clinkenbeard, E. L., Hanudel, M. R., Stayrook, K. R., Appaiah, H. N., Farrow, E. G., Cass, T. A., et al. (2017). Erythropoietin stimulates murine and human fibroblast growth factor-23, revealing novel roles for bone and bone marrow. *Haematologica* 102, e427–e430. doi: 10.3324/haematol.2017.167882

Culver, D. A., Dahan, A., Bajorunas, D., Jeziorska, M., van Velzen, M., Aarts, L., et al. (2017). Cibinetide improves corneal nerve fiber abundance in patients with sarcoidosis-associated small nerve fiber loss and neuropathic pain. *Invest. Ophthalmol. Vis. Sci.* 58, BIO52–BIO60. doi: 10.1167/iovs.16-21291

Dahan, A., Dunne, A., Swartjes, M., Proto, P. L., Heij, L., Vogels, O., et al. (2013). ARA 290 improves symptoms in patients with sarcoidosis-associated small nerve fiber loss and increases corneal nerve fiber density. *Mol. Med.* 19, 334–345. doi: 10.2119/molmed.2013.00122

Dame, C., Fahnenstich, H., Freitag, P., Hofmann, D., Abdul-Nour, T., Bartmann, P., et al. (1998). Erythropoietin mRNA expression in human fetal and neonatal tissue. *Blood* 92, 3218–3225. doi: 10.1182/blood.v92.9.3218.421k11_3218_3225

den Elzen, W. P., Willems, J. M., Westendorp, R. G., de Craen, A. J., Blauw, G. J., Ferrucci, L., et al. (2010). Effect of erythropoietin levels on mortality in old age: the Leiden 85-plus Study. *CMAJ* 182, 1953–1958. doi: 10.1503/cmaj.100374

Dey, S., Li, X., Teng, R., Alnaeeli, M., Chen, Z., Rogers, H., et al. (2016). Erythropoietin regulates POMC expression via STAT3 and potentiates leptin response. *J. Mol. Endocrinol.* 56, 55–67. doi: 10.1530/JME-15-0171

Dey, S., and Noguchi, C. T. (2017). Erythropoietin and hypothalamic-pituitary axis. *Vitam. Horm.* 105, 101–120. doi: 10.1016/bs.vh.2017.02.007

Dey, S., Scullen, T., and Noguchi, C. T. (2015). Erythropoietin negatively regulates pituitary ACTH secretion. *Brain Res.* 1608, 14–20. doi: 10.1016/j.brainres.2015.02.052

Digicaylioglu, M., Bichet, S., Marti, H. H., Wenger, R. H., Rivas, L. A., Bauer, C., et al. (1995). Localization of specific erythropoietin binding sites in defined areas of the mouse brain. *Proc. Natl. Acad. Sci. U.S.A.* 92, 3717–3720. doi: 10.1073/pnas.92.9.3717

Drueke, T. B., Locatelli, F., Clyne, N., Eckardt, K. U., Macdougall, I. C., Tsakiris, D., et al. (2006). Normalization of hemoglobin level in patients with chronic kidney disease and anemia. *N. Engl. J. Med.* 355, 2071–2084. doi: 10.1056/nejmoa062276

Eckardt, K. U., Koury, S. T., Tan, C. C., Schuster, S. J., Kaissling, B., Ratcliffe, P. J., et al. (1993). Distribution of erythropoietin producing cells in rat kidneys during hypoxic hypoxia. *Kidney Int.* 43, 815–823. doi: 10.1038/ki.1993.115

Egger, K., Clemm von Hohenberg, C., Schocke, M. F., Guttmann, C. R., Wassermann, D., Wigand, M. C., et al. (2014). White matter changes in patients with friedreich ataxia after treatment with erythropoietin. *J. Neuroimaging* 24, 504–508. doi: 10.1111/jon.12050

Ehrenreich, H., Hasselblatt, M., Dembowski, C., Cepek, L., Lewczuk, P., Stiefel, M., et al. (2002). Erythropoietin therapy for acute stroke is both safe and beneficial. *Mol. Med.* 8, 495–505. doi: 10.1007/bf03402029

Ehrenreich, H., Kastner, A., Weissenborn, K., Streeter, J., Sperling, S., Wang, K. K., et al. (2011). Circulating damage marker profiles support a neuroprotective effect of erythropoietin in ischemic stroke patients. *Mol. Med.* 17, 1306–1310. doi: 10.2119/molmed.2011.00259

Ehrenreich, H., Weissenborn, K., Prange, H., Schneider, D., Weimar, C., Wartenberg, K., et al. (2009). Recombinant human erythropoietin in the treatment of acute ischemic stroke. *Stroke* 40, e647–e656. doi: 10.1161/STROKEAHA.109.564872

Erbayraktar, S., Grasso, G., Sfacteria, A., Xie, Q. W., Coleman, T., Kreilgaard, M., et al. (2003). Asialoerythropoietin is a nonerythropoietic cytokine with broad neuroprotective activity in vivo. *Proc. Natl. Acad. Sci. U.S.A.* 100, 6741–6746. doi: 10.1073/pnas.1031753100

Eschbach, J. W., Egrie, J. C., Downing, M. R., Browne, J. K., and Adamson, J. W. (1987). Correction of the anemia of end-stage renal disease with recombinant human erythropoietin. Results of a combined phase I and II clinical trial. *N. Engl. J. Med.* 316, 73–78.

Fandrey, J., and Bunn, H. F. (1993). In vivo and in vitro regulation of erythropoietin mRNA: measurement by competitive polymerase chain reaction. *Blood* 81, 617–623. doi: 10.1182/blood.v81.3.617.bloodjournal813617

Farmer, S., Horvath-Puho, E., Vestergaard, H., Hermann, A. P., and Frederiksen, H. (2013). Chronic myeloproliferative neoplasms and risk of osteoporotic fractures; a nationwide population-based cohort study. *Br. J. Haematol.* 163, 603–610. doi: 10.1111/bjh.12581

Fauchere, J. C., Dame, C., Vonthein, R., Koller, B., Arri, S., Wolf, M., et al. (2008). An approach to using recombinant erythropoietin for neuroprotection in very preterm infants. *Pediatrics* 122, 375–382. doi: 10.1542/peds.2007-2591

Fiordaliso, F., Chimenti, S., Staszewsky, L., Bai, A., Carlo, E., Cuccovillo, I., et al. (2005). A nonerythropoietic derivative of erythropoietin protects the myocardium from ischemia-reperfusion injury. *Proc. Natl. Acad. Sci. U.S.A.* 102, 2046–2051. doi: 10.1073/pnas.0409329102

Fischer, H. S., Reibel, N. J., Buhrer, C., and Dame, C. (2017). Prophylactic early erythropoietin for neuroprotection in preterm infants: a meta-analysis. *Pediatrics* 139:e20164317. doi: 10.1542/peds.2016-4317

Foskett, A., Alnaeeli, M., Wang, L., Teng, R., and Noguchi, C. T. (2011). The effects of erythropoietin dose titration during high-fat diet-induced obesity. *J. Biomed. Biotechnol.* 2011, 373781. doi: 10.1155/2011/373781

Ganz, T., and Nemeth, E. (2016). Iron balance and the role of hepcidin in chronic kidney disease. *Semin. Nephrol.* 36, 87–93. doi: 10.1016/j.semnephrol.2016.02.001

Garcia, P., Speidel, V., Scheuer, C., Laschke, M. W., Holstein, J. H., Histing, T., et al. (2011). Low dose erythropoietin stimulates bone healing in mice. *J. Orthopaed. Res.* 29, 165–172. doi: 10.1002/jor.21219

Gassmann, M., and Muckenthaler, M. U. (1985). Adaptation of iron requirement to hypoxic conditions at high altitude. *J. Appl. Physiol.* 119, 1432–1440. doi: 10.1152/japplphysiol.00248.2015

Hagström, L., Agbulut, O., El-Hasnaoui-Saadani, R., Marchant, D., Favret, F., Richalet, J.-P., et al. (2010). Epo is relevant neither for microvascular formation nor for the new formation and maintenance of mice skeletal muscle fibres in both normoxia and hypoxia. *BioMed. Res. Int.* 2010:137817. doi: 10.1155/2010/137817

Hahn, N., Knorr, D. Y., Liebig, J., Wustefeld, L., Peters, K., Buscher, M., et al. (2017). The insect ortholog of the human orphan cytokine receptor CRLF3 is a neuroprotective erythropoietin receptor. *Front. Mol. Neurosci.* 10:223. doi: 10.3389/fnmol.2017.00223

Han, J. M., and Levings, M. K. (2013). Immune regulation in obesity-associated adipose inflammation. *J. Immunol.* 191, 527–532. doi: 10.4049/jimmunol.1301035

Hasegawa, T., Koiwa, F., and Akizawa, T. (2018). Anemia in conventional hemodialysis: finding the optimal treatment balance. *Semin. Dial.* 31, 599–606. doi: 10.1111/sdi.12719

Hiram-Bab, S., Liron, T., Deshet-Unger, N., Mittelman, M., Gassmann, M., Rauner, M., et al. (2015). Erythropoietin directly stimulates osteoclast precursors and induces bone loss. *FASEB J.* 29, 1890–1900. doi: 10.1096/fj.14-259085

Hiram-Bab, S., Neumann, D., and Gabet, Y. (2017). Context-dependent skeletal effects of erythropoietin. *Vitam Horm* 105, 161–179. doi: 10.1016/bs.vh.2017.02.003

Hirano, I., and Suzuki, N. (2019). The neural crest as the first production site of the erythroid growth factor erythropoietin. *Front. Cell Dev. Biol.* 7:105. doi: 10.3389/fcell.2019.00105

Ho, M. S., Medcalf, R. L., Livesey, S. A., and Traianedes, K. (2015). The dynamics of adult haematopoiesis in the bone and bone marrow environment. *Br. J. Haematol.* 170, 472–486. doi: 10.1111/bjh.13445

Hoedt, A., Christensen, B., Nellemann, B., Mikkelsen, U. R., Hansen, M., Schjerling, P., et al. (2016). Satellite cell response to erythropoietin treatment and endurance training in healthy young men. *J. Physiol.* 594, 727–743. doi: 10.1113/JP271333

Hojman, P., Brolin, C., Gissel, H., Brandt, C., Zerahn, B., Pedersen, B. K., et al. (2009). Erythropoietin over-expression protects against diet-induced obesity in mice through increased fat oxidation in muscles. *PLoS One* 4:e5894. doi: 10.1371/journal.pone.0005894

Holstein, J. H., Menger, M. D., Scheuer, C., Meier, C., Culemann, U., Wirbel, R. J., et al. (2007). Erythropoietin (EPO): EPO-receptor signaling improves early endochondral ossification and mechanical strength in fracture healing. *Life Sci.* 80, 893–900. doi: 10.1016/j.lfs.2006.11.023

Horscroft, J. A., Kotwica, A. O., Laner, V., West, J. A., Hennis, P. J., Levett, D. Z. H., et al. (2017). Metabolic basis to Sherpa altitude adaptation. *Proc. Natl. Acad. Sci. U.S.A.* 114, 6382–6387. doi: 10.1073/pnas.1700527114

Iwai, M., Cao, G., Yin, W., Stetler, R. A., Liu, J., and Chen, J. (2007). Erythropoietin promotes neuronal replacement through revascularization and neurogenesis after neonatal hypoxia/ischemia in rats. *Stroke* 38, 2795–2803. doi: 10.1161/strokeaha.107.483008

Jaakkola, P., Mole, D. R., Tian, Y. M., Wilson, M. I., Gielbert, J., Gaskell, S. J., et al. (2001). Targeting of HIF-alpha to the von Hippel-Lindau ubiquitylation complex by O2-regulated prolyl hydroxylation. *Science* 292, 468–472. doi: 10.1126/science.1059796

Jacobs, K., Shoemaker, C., Rudersdorf, R., Neill, S. D., Kaufman, R. J., Mufson, A., et al. (1985). Isolation and characterization of genomic and cDNA clones of human erythropoietin. *Nature* 313, 806–810. doi: 10.1038/313806a0

Jelkmann, W. (2013). Physiology and pharmacology of erythropoietin. *Transfus. Med. Hemother.* 40, 302–309. doi: 10.1159/000356193

Jelkmann, W., and Wiedemann, G. (1989). Lack of sex dependence of the serum level of immunoreactive erythropoietin in chronic anemia. *Klin. Wochenschr.* 67, 1218. doi: 10.1007/bf01716210

Jia, Y., Suzuki, N., Yamamoto, M., Gassmann, M., and Noguchi, C. T. (2012). Endogenous erythropoietin signaling facilitates skeletal muscle repair and recovery following pharmacologically induced damage. *FASEB J.* 26, 2847–2858. doi: 10.1096/fj.11-196618

Jia, Y., Warin, R., Yu, X., Epstein, R., and Noguchi, C. T. (2009). Erythropoietin signaling promotes transplanted progenitor cell survival. *FASEB J.* 23, 3089–3099. doi: 10.1096/fj.09-130237

Jubinsky, P. T., Krijanovski, O. I., Nathan, D. G., Tavernier, J., and Sieff, C. A. (1997). The beta chain of the interleukin-3 receptor functionally associates with the erythropoietin receptor. *Blood* 90, 1867–1873. doi: 10.1182/blood.v90.5.1867

Juul, S. E., McPherson, R. J., Bauer, L. A., Ledbetter, K. J., Gleason, C. A., and Mayock, D. E. (2008). A phase I/II trial of high-dose erythropoietin in extremely low birth weight infants: pharmacokinetics and safety. *Pediatrics* 122, 383–391. doi: 10.1542/peds.2007-2711

Juul, S. E., Yachnis, A. T., and Christensen, R. D. (1998). Tissue distribution of erythropoietin and erythropoietin receptor in the developing human fetus. *Early Hum. Dev.* 52, 235–249. doi: 10.1016/s0378-3782(98)00030-9

Kanellakis, P., Pomilio, G., Agrotis, A., Gao, X., Du, X. J., Curtis, D., et al. (2010). Darbepoetin-mediated cardioprotection after myocardial infarction involves multiple mechanisms independent of erythropoietin receptor-common beta-chain heteroreceptor. *Br. J. Pharmacol.* 160, 2085–2096. doi: 10.1111/j.1476-5381.2010.00876.x

Kassouf, M. T., Hughes, J. R., Taylor, S., McGowan, S. J., Soneji, S., Green, A. L., et al. (2010). Genome-wide identification of TAL1's functional targets: insights into its mechanisms of action in primary erythroid cells. *Genome Res.* 20, 1064–1083. doi: 10.1101/gr.104935.110

Katz, O., Stuible, M., Golishevski, N., Lifshitz, L., Tremblay, M. L., Gassmann, M., et al. (2010). Erythropoietin treatment leads to reduced blood glucose levels and body mass: insights from murine models. *J. Endocrinol.* 205, 87–95. doi: 10.1677/JOE-09-0425

Kertesz, N., Wu, J., Chen, T. H., Sucov, H. M., and Wu, H. (2004). The role of erythropoietin in regulating angiogenesis. *Dev. Biol.* 276, 101–110. doi: 10.1016/j.ydbio.2004.08.025

Kim, J., Jung, Y., Sun, H., Joseph, J., Mishra, A., Shiozawa, Y., et al. (2012). Erythropoietin mediated bone formation is regulated by mTOR signaling. *J. Cell. Biochem.* 113, 220–228. doi: 10.1002/jcb.23347

Kobayashi, H., Liu, J., Urrutia, A. A., Burmakin, M., Ishii, K., Rajan, M., et al. (2017). Hypoxia-inducible factor prolyl-4-hydroxylation in FOXD1 lineage cells is essential for normal kidney development. *Kidney Int.* 92, 1370–1383. doi: 10.1016/j.kint.2017.06.015

Kobayashi, H., Liu, Q., Binns, T. C., Urrutia, A. A., Davidoff, O., Kapitsinou, P. P., et al. (2016). Distinct subpopulations of FOXD1 stroma-derived cells regulate renal erythropoietin. *J. Clin. Invest.* 126, 1926–1938. doi: 10.1172/JCI83551

Kodo, K., Sugimoto, S., Nakajima, H., Mori, J., Itoh, I., Fukuhara, S., et al. (2017). Erythropoietin (EPO). ameliorates obesity and glucose homeostasis by promoting thermogenesis and endocrine function of classical brown adipose tissue (BAT). in diet-induced obese mice. *PLoS One* 12:e0173661. doi: 10.1371/journal.pone.0173661

Kuang, S., Kuroda, K., Le Grand, F., and Rudnicki, M. A. (2007). Asymmetric self-renewal and commitment of satellite stem cells in muscle. *Cell* 129, 999–1010. doi: 10.1016/j.cell.2007.03.044

Kuhrt, D., and Wojchowski, D. M. (2015). Emerging EPO and EPO receptor regulators and signal transducers. *Blood* 125, 3536–3541. doi: 10.1182/blood-2014-11-575357

Lamon, S., Zacharewicz, E., Arentson-Lantz, E., Gatta, P. A. D., Ghobrial, L., Gerlinger-Romero, F., et al. (2016). Erythropoietin does not enhance skeletal muscle protein synthesis following exercise in young and older adults. *Front. Physiol.* 7:292. doi: 10.3389/fphys.2016.00292

Lando, D., Peet, D. J., Gorman, J. J., Whelan, D. A., Whitelaw, M. L., and Bruick, R. K. (2002). FIH-1 is an asparaginyl hydroxylase enzyme that regulates the transcriptional activity of hypoxia-inducible factor. *Genes Dev.* 16, 1466–1471. doi: 10.1101/gad.991402

Li, C., Shi, C., Kim, J., Chen, Y., Ni, S., Jiang, L., et al. (2015). Erythropoietin promotes bone formation through EphrinB2/EphB4 signaling. *J. Dent. Res.* 94, 455–463. doi: 10.1177/0022034514566431

Li, J., Huang, Z., Li, B., Zhang, Z., and Liu, L. (2019). Mobilization of transplanted bone marrow mesenchymal stem cells by erythropoietin facilitates the reconstruction of segmental bone defect. *Stem Cells Int.* 2019:5750967. doi: 10.1155/2019/5750967

Lin, C. S., Lim, S. K., D'Agati, V., and Costantini, F. (1996). Differential effects of an erythropoietin receptor gene disruption on primitive and definitive erythropoiesis. *Genes Dev.* 10, 154–164. doi: 10.1101/gad.10.2.154

Lin, F. K., Suggs, S., Lin, C. H., Browne, J. K., Smalling, R., Egrie, J. C., et al. (1985). Cloning and expression of the human erythropoietin gene. *Proc. Natl. Acad. Sci. U.S.A.* 82, 7580–7584.

Lin, J., Wu, H., Tarr, P. T., Zhang, C. Y., Wu, Z., Boss, O., et al. (2002). Transcriptional co-activator PGC-1 alpha drives the formation of slow-twitch muscle fibres. *Nature* 418, 797–801. doi: 10.1038/nature00904

Liongue, C., Sertori, R., and Ward, A. C. (2016). Evolution of cytokine receptor signaling. *J. Immunol.* 197, 11–18. doi: 10.4049/jimmunol.1600372

Liu, C., Shen, K., Liu, Z., and Noguchi, C. T. (1997). Regulated human erythropoietin receptor expression in mouse brain. *J. Biol. Chem.* 272, 32395–32400. doi: 10.1074/jbc.272.51.32395

Luk, C. T., Shi, S. Y., Choi, D., Cai, E. P., Schroer, S. A., and Woo, M. (2013). In vivo knockdown of adipocyte erythropoietin receptor does not alter glucose or energy homeostasis. *Endocrinology* 154, 3652–3659. doi: 10.1210/en.2013-1113

Lumeng, C. N., and Saltiel, A. R. (2011). Inflammatory links between obesity and metabolic disease. *J. Clin. Invest.* 121, 2111–2117. doi: 10.1172/JCI57132

Lundby, C., Robach, P., Boushel, R., Thomsen, J. J., Rasmussen, P., Koskolou, M., et al. (2008). Does recombinant human Epo increase exercise capacity by means other than augmenting oxygen transport? *J. Appl. Physiol.* 105, 581–587. doi: 10.1152/japplphysiol.90484.2008

Mahon, P. C., Hirota, K., and Semenza, G. L. (2001). FIH-1: a novel protein that interacts with HIF-1alpha and VHL to mediate repression of HIF-1 transcriptional activity. *Genes Dev.* 15, 2675–2686. doi: 10.1101/gad.924501

Malik, J., Kim, A. R., Tyre, K. A., Cherukuri, A. R., and Palis, J. (2013). Erythropoietin critically regulates the terminal maturation of murine and human primitive erythroblasts. *Haematologica* 98, 1778–1787. doi: 10.3324/haematol.2013.087361

Marti, H. H., Wenger, R. H., Rivas, L. A., Straumann, U., Digicaylioglu, M., Henn, V., et al. (1996). Erythropoietin gene expression in human, monkey and murine brain. *Eur. J. Neurosci.* 8, 666–676. doi: 10.1111/j.1460-9568.1996.tb01252.x

Masuda, S., Nagao, M., Takahata, K., Konishi, Y., Gallyas, F. Jr., Tabira, T., et al. (1993). Functional erythropoietin receptor of the cells with neural characteristics. Comparison with receptor properties of erythroid cells. *J. Biol. Chem.* 268, 11208–11216.

Masuda, S., Okano, M., Yamagishi, K., Nagao, M., Ueda, M., and Sasaki, R. (1994). A novel site of erythropoietin production. Oxygen-dependent production in cultured rat astrocytes. *J. Biol. Chem.* 269, 19488–19493.

McGee, S. J., Havens, A. M., Shiozawa, Y., Jung, Y., and Taichman, R. S. (2012). Effects of erythropoietin on the bone microenvironment. *Growth Factors* 30, 22–28. doi: 10.3109/08977194.2011.637034

Meng, R., Zhu, D., Bi, Y., Yang, D., and Wang, Y. (2013). Erythropoietin inhibits gluconeogenesis and inflammation in the liver and improves glucose intolerance in high-fat diet-fed mice. *PLoS One* 8:e53557. doi: 10.1371/journal.pone.0053557

Mihmanli, A., Dolanmaz, D., Avunduk, M. C., and Erdemli, E. (2009). Effects of recombinant human erythropoietin on mandibular distraction osteogenesis. *J. Oral Maxil. Surg.* 67, 2337–2343. doi: 10.1016/j.joms.2008.06.082

Mihov, D., Bogdanov, N., Grenacher, B., Gassmann, M., Zund, G., Bogdanova, A., et al. (2009). Erythropoietin protects from reperfusion-induced myocardial injury by enhancing coronary endothelial nitric oxide production. *Eur. J. Cardiothorac. Surg.* 35, 839–46; discussion 846. doi: 10.1016/j.ejcts.2008.12.049

Mille-Hamard, L., Billat, V. L., Henry, E., Bonnamy, B., Joly, F., Benech, P., et al. (2012). Skeletal muscle alterations and exercise performance decrease in erythropoietin-deficient mice: a comparative study. *BMC Med. Genomics* 5:29. doi: 10.1186/1755-8794-5-29

Minamishima, Y. A., Moslehi, J., Bardeesy, N., Cullen, D., Bronson, R. T., and Kaelin, W. G. Jr. (2008). Somatic inactivation of the PHD2 prolyl hydroxylase causes polycythemia and congestive heart failure. *Blood* 111, 3236–3244. doi: 10.1182/blood-2007-10-117812

Miura, Y., Miura, O., Ihle, J. N., and Aoki, N. (1994). Activation of the mitogen-activated protein kinase pathway by the erythropoietin receptor. *J. Biol. Chem.* 269, 29962–29969.

Morishita, E., Masuda, S., Nagao, M., Yasuda, Y., and Sasaki, R. (1997). Erythropoietin receptor is expressed in rat hippocampal and cerebral cortical neurons, and erythropoietin prevents in vitro glutamate-induced neuronal death. *Neuroscience* 76, 105–116. doi: 10.1016/s0306-4522(96)00306-5

Nadam, J., Navarro, F., Sanchez, P., Moulin, C., Georges, B., Laglaine, A., et al. (2007). Neuroprotective effects of erythropoietin in the rat hippocampus after pilocarpine-induced status epilepticus. *Neurobiol. Dis.* 25, 412–426. doi: 10.1016/j.nbd.2006.10.009

Nair, A. M., Tsai, Y. T., Shah, K. M., Shen, J., Weng, H., Zhou, J., et al. (2013). The effect of erythropoietin on autologous stem cell-mediated bone regeneration. *Biomaterials* 34, 7364–7371. doi: 10.1016/j.biomaterials.2013.06.031

Nairz, M., Haschka, D., Dichtl, S., Sonnweber, T., Schroll, A., Asshoff, M., et al. (2017). Cibinetide dampens innate immune cell functions thus ameliorating the course of experimental colitis. *Sci. Rep.* 7:13012. doi: 10.1038/s41598-017-13046-3

Nairz, M., Schroll, A., Moschen, A. R., Sonnweber, T., Theurl, M., Theurl, I., et al. (2011). Erythropoietin contrastingly affects bacterial infection and experimental colitis by inhibiting nuclear factor-kappaB-inducible immune pathways. *Immunity* 34, 61–74. doi: 10.1016/j.immuni.2011.01.002

Nemati, A., and Fallahi, A. H. (2013). In reply to: queries regarding local erythropoietin injection in tibiofibular fracture healing. *Trauma Mon.* 18, 103–104. doi: 10.5812/traumamon.14208

Neubauer, A. P., Voss, W., Wachtendorf, M., and Jungmann, T. (2010). Erythropoietin improves neurodevelopmental outcome of extremely preterm infants. *Ann. Neurol.* 67, 657–666. doi: 10.1002/ana.21977

Noakes, T. D. (2004). Tainted glory–doping and athletic performance. *N. Engl. J. Med.* 351, 847–849. doi: 10.1056/nejmp048208

Obara, N., Suzuki, N., Kim, K., Nagasawa, T., Imagawa, S., and Yamamoto, M. (2008). Repression via the GATA box is essential for tissue-specific erythropoietin gene expression. *Blood* 111, 5223–5232. doi: 10.1182/blood-2007-10-115857

Ogilvie, M., Yu, X., Nicolas-Metral, V., Pulido, S. M., Liu, C., Ruegg, U. T., et al. (2000). Erythropoietin stimulates proliferation and interferes with differentiation of myoblasts. *J. Biol. Chem.* 275, 39754–39761. doi: 10.1074/jbc.m004999200

Ohh, M., Park, C. W., Ivan, M., Hoffman, M. A., Kim, T. Y., Huang, L. E., et al. (2000). Ubiquitination of hypoxia-inducible factor requires direct binding to the beta-domain of the von Hippel-Lindau protein. *Nat. Cell Biol.* 2, 423–427. doi: 10.1038/35017054

Omlor, G. W., Kleinschmidt, K., Gantz, S., Speicher, A., Guehring, T., and Richter, W. (2016). Increased bone formation in a rabbit long-bone defect model after single local and single systemic application of erythropoietin. *Acta Orthop.* 87, 425–431. doi: 10.1080/17453674.2016.1198200

Osman, H. M., Khamis, O. A., Elfeky, M. S., El Amin Ali, A. M., and Abdelwahed, M. Y. (2017). Effect of short-term erythropoietin therapy on insulin resistance and serum levels of leptin and neuropeptide Y in hemodialysis patients. *Indian J. Endocrinol. Metab.* 21, 724–730. doi: 10.4103/ijem.IJEM_462_16

Palis, J. (2014). Primitive and definitive erythropoiesis in mammals. *Front. Physiol.* 5:3. doi: 10.3389/fphys.2014.00003

Palis, J., and Koniski, A. (2018). Functional analysis of erythroid progenitors by colony-forming assays. *Methods Mol. Biol.* 1698, 117–132. doi: 10.1007/978-1-4939-7428-3_7

Paoletti, E., and Cannella, G. (2006). Update on erythropoietin treatment: should hemoglobin be normalized in patients with chronic kidney disease? *J. Am. Soc. Nephrol.* 17, S74–S77.

Parsa, C. J., Matsumoto, A., Kim, J., Riel, R. U., Pascal, L. S., Walton, G. B., et al. (2003). A novel protective effect of erythropoietin in the infarcted heart. *J. Clin. Invest.* 112, 999–1007. doi: 10.1172/jci200318200

Pastore, Y. D., Jelinek, J., Ang, S., Guan, Y., Liu, E., Jedlickova, K., et al. (2003). Mutations in the VHL gene in sporadic apparently congenital polycythemia. *Blood* 101, 1591–1595. doi: 10.1182/blood-2002-06-1843

Pavkov, M. E., Hanson, R. L., Knowler, W. C., Bennett, P. H., Krakoff, J., and Nelson, R. G. (2007). Changing patterns of type 2 diabetes incidence among Pima Indians. *Diabetes Care* 30, 1758–1763. doi: 10.2337/dc06-2010

Percy, M. J., Furlow, P. W., Lucas, G. S., Li, X., Lappin, T. R., McMullin, M. F., et al. (2008). A gain-of-function mutation in the HIF2A gene in familial erythrocytosis. *N. Engl. J. Med.* 358, 162–168. doi: 10.1056/NEJMoa073123

Percy, M. J., Zhao, Q., Flores, A., Harrison, C., Lappin, T. R., Maxwell, P. H., et al. (2006). A family with erythrocytosis establishes a role for prolyl hydroxylase domain protein 2 in oxygen homeostasis. *Proc. Natl. Acad. Sci. U.S.A.* 103, 654–659. doi: 10.1073/pnas.0508423103

Plenge, U., Belhage, B., Guadalupe-Grau, A., Andersen, P. R., Lundby, C., Dela, F., et al. (2012). Erythropoietin treatment enhances muscle mitochondrial capacity in humans. *Front. Physiol.* 3:50. doi: 10.3389/fphys.2012.00050

Pradeep, S., Huang, J., Mora, E. M., Nick, A. M., Cho, M. S., Wu, S. Y., et al. (2015). Erythropoietin stimulates tumor growth via EphB4. *Cancer Cell* 28, 610–622. doi: 10.1016/j.ccell.2015.09.008

Prunier, F., Pfister, O., Hadri, L., Liang, L., del Monte, F., Liao, R., et al. (2007). Delayed erythropoietin therapy reduces post-MI cardiac remodeling only at a dose that mobilizes endothelial progenitor cells. *Am. J. Physiol. Heart Circ. Physiol.* 292, H522–H529.

Pugh, C. W., and Ratcliffe, P. J. (2017). New horizons in hypoxia signaling pathways. *Exp. Cell Res.* 356, 116–121. doi: 10.1016/j.yexcr.2017.03.008

Quaschning, T., Ruschitzka, F., Stallmach, T., Shaw, S., Morawietz, H., Goettsch, W., et al. (2003). Erythropoietin-induced excessive erythrocytosis activates the tissue endothelin system in mice. *FASEB J.* 17, 259–261. doi: 10.1096/fj.02-0296fje

Rankin, E. B., Biju, M. P., Liu, Q., Unger, T. L., Rha, J., Johnson, R. S., et al. (2007). Hypoxia-inducible factor-2 (HIF-2). regulates hepatic erythropoietin in vivo. *J. Clin. Invest.* 117, 1068–1077. doi: 10.1172/jci30117

Rankin, E. B., Wu, C., Khatri, R., Wilson, T. L., Andersen, R., Araldi, E., et al. (2012). The HIF signaling pathway in osteoblasts directly modulates erythropoiesis through the production of EPO. *Cell* 149, 63–74. doi: 10.1016/j.cell.2012.01.051

Rauner, M., Franke, K., Murray, M., Singh, R. P., Hiram-Bab, S., Platzbecker, U., et al. (2016). Increased EPO levels are associated with bone loss in mice lacking PHD2 in EPO-Producing cells. *J. Bone Miner. Res.* 31, 1877–1887. doi: 10.1002/jbmr.2857

Recny, M. A., Scoble, H. A., and Kim, Y. (1987). Structural characterization of natural human urinary and recombinant DNA-derived erythropoietin. Identification of des-arginine 166 erythropoietin. *J. Biol. Chem.* 262, 17156–17163.

Reinhardt, M., Dey, S., Tom Noguchi, C., Zhang, Y., Krakoff, J., and Thearle, M. S. (2016). Non-hematopoietic effects of endogenous erythropoietin on lean mass and body weight regulation. *Obesity* 24, 1530–1536. doi: 10.1002/oby.21537

Robertson, C. S., Garcia, R., Gaddam, S. S., Grill, R. J., Cerami Hand, C., Tian, T. S., et al. (2013). Treatment of mild traumatic brain injury with an erythropoietin-mimetic peptide. *J. Neurotrauma* 30, 765–774. doi: 10.1089/neu.2012.2431

Rogers, H., Wang, L., Yu, X., Alnaeeli, M., Cui, K., Zhao, K., et al. (2012). T-cell acute leukemia 1 (TAL1). regulation of erythropoietin receptor and association with excessive erythrocytosis. *J. Biol. Chem.* 287, 36720–36731. doi: 10.1074/jbc.M112.378398

Rolfing, J. H., Baatrup, A., Stiehler, M., Jensen, J., Lysdahl, H., and Bunger, C. (2014a). The osteogenic effect of erythropoietin on human mesenchymal stromal cells is dose-dependent and involves non-hematopoietic receptors and multiple intracellular signaling pathways. *Stem Cell Rev.* 10, 69–78. doi: 10.1007/s12015-013-9476-x

Rolfing, J. H., Jensen, J., Jensen, J. N., Greve, A. S., Lysdahl, H., Chen, M., et al. (2014b). A single topical dose of erythropoietin applied on a collagen carrier enhances calvarial bone healing in pigs. *Acta Orthop.* 85, 201–209. doi: 10.3109/17453674.2014.889981

Rundqvist, H., Rullman, E., Sundberg, C. J., Fischer, H., Eisleitner, K., Stahlberg, M., et al. (2009). Activation of the erythropoietin receptor in human skeletal muscle. *Eur. J. Endocrinol.* 161, 427–434. doi: 10.1530/EJE-09-0342

Ruschitzka, F. T., Wenger, R. H., Stallmach, T., Quaschning, T., de Wit, C., Wagner, K., et al. (2000). Nitric oxide prevents cardiovascular disease and determines survival in polyglobulic mice overexpressing erythropoietin. *Proc. Natl. Acad. Sci. U.S.A.* 97, 11609–11613. doi: 10.1073/pnas.97.21.11609

Sadamoto, Y., Igase, K., Sakanaka, M., Sato, K., Otsuka, H., Sakaki, S., et al. (1998). Erythropoietin prevents place navigation disability and cortical infarction in rats with permanent occlusion of the middle cerebral artery. *Biochem. Biophys. Res. Commun.* 253, 26–32. doi: 10.1006/bbrc.1998.9748

Sakanaka, M., Wen, T. C., Matsuda, S., Masuda, S., Morishita, E., Nagao, M., et al. (1998). In vivo evidence that erythropoietin protects neurons from ischemic damage. *Proc. Natl. Acad. Sci. U.S.A.* 95, 4635–4640. doi: 10.1073/pnas.95.8.4635

Santner, W., Schocke, M., Boesch, S., Nachbauer, W., and Egger, K. (2014). A longitudinal VBM study monitoring treatment with erythropoietin in patients with Friedreich ataxia. *Acta Radiol. Short Rep.* 3:2047981614531573. doi: 10.1177/2047981614531573

Sarrai, M., Duroseau, H., D'Augustine, J., Moktan, S., and Bellevue, R. (2007). Bone mass density in adults with sickle cell disease. *Br. J. Haematol.* 136, 666–672. doi: 10.1111/j.1365-2141.2006.06487.x

Semenza, G. L. (2009). Involvement of oxygen-sensing pathways in physiologic and pathologic erythropoiesis. *Blood* 114, 2015–2019. doi: 10.1182/blood-2009-05-189985

Shingo, T., Sorokan, S. T., Shimazaki, T., and Weiss, S. (2001). Erythropoietin regulates the in vitro and in vivo production of neuronal progenitors by mammalian forebrain neural stem cells. *J. Neurosci.* 21, 9733–9743. doi: 10.1523/jneurosci.21-24-09733.2001

Shiozawa, Y., Jung, Y., Ziegler, A. M., Pedersen, E. A., Wang, J., Wang, Z., et al. (2010). Erythropoietin couples hematopoiesis with bone formation. *PLoS One* 5:e10853. doi: 10.1371/journal.pone.0010853

Singbrant, S., Russell, M. R., Jovic, T., Liddicoat, B., Izon, D. J., Purton, L. E., et al. (2011). Erythropoietin couples erythropoiesis, B-lymphopoiesis, and bone homeostasis within the bone marrow microenvironment. *Blood* 117, 5631–5642. doi: 10.1182/blood-2010-11-320564

Singh, A. K., Szczech, L., Tang, K. L., Barnhart, H., Sapp, S., Wolfson, M., et al. (2006). Correction of anemia with epoetin alfa in chronic kidney disease. *N. Engl. J. Med.* 355, 2085–2098.

Sinkeler, S. J., Zelle, D. M., Homan van der Heide, J. J., Gans, R. O., Navis, G., and Bakker, S. J. (2012). Endogenous plasma erythropoietin, cardiovascular mortality and all-cause mortality in renal transplant recipients. *Am. J. Transplant.* 12, 485–491. doi: 10.1111/j.1600-6143.2011.03825.x

Smith, C. J., Nelson, R. G., Hardy, S. A., Manahan, E. M., Bennett, P. H., and Knowler, W. C. (1996). Survey of the diet of Pima Indians using quantitative food frequency assessment and 24-hour recall. Diabetic Renal Disease Study. *J. Am. Diet. Assoc.* 96, 778–784. doi: 10.1016/s0002-8223(96)00216-7

Smith, T. G., Robbins, P. A., and Ratcliffe, P. J. (2008). The human side of hypoxia-inducible factor. *Br. J. Haematol.* 141, 325–334. doi: 10.1111/j.1365-2141.2008.07029.x

Socolovsky, M., Nam, H., Fleming, M. D., Haase, V. H., Brugnara, C., and Lodish, H. F. (2001). Ineffective erythropoiesis in Stat5a(-/-)5b(-/-). mice due to decreased survival of early erythroblasts. *Blood* 98, 3261–3273. doi: 10.1182/blood.v98.12.3261

Soliz, J., Khemiri, H., Caravagna, C., and Seaborn, T. (2012). Erythropoietin and the sex-dimorphic chemoreflex pathway. *Adv. Exp. Med. Biol.* 758, 55–62. doi: 10.1007/978-94-007-4584-1_8

Sun, H., Jung, Y., Shiozawa, Y., Taichman, R. S., and Krebsbach, P. H. (2012). Erythropoietin modulates the structure of bone morphogenetic protein 2-engineered cranial bone. *Tissue Eng. Part A* 18, 2095–2105. doi: 10.1089/ten.TEA.2011.0742

Suresh, S., de Castro, L. F., Dey, S., Robey, P. G., and Noguchi, C. T. (2019). Erythropoietin modulates bone marrow stromal cell differentiation. *Bone Res.* 7, 21. doi: 10.1038/s41413-019-0060-0

Suzuki, N., Gradin, K., Poellinger, L., and Yamamoto, M. (2017). Regulation of hypoxia-inducible gene expression after HIF activation. *Exp. Cell Res.* 356, 182–186. doi: 10.1016/j.yexcr.2017.03.013

Suzuki, N., Hirano, I., Pan, X., Minegishi, N., and Yamamoto, M. (2013). Erythropoietin production in neuroepithelial and neural crest cells during primitive erythropoiesis. *Nat. Commun.* 4:2902. doi: 10.1038/ncomms3902

Suzuki, N., Ohneda, O., Takahashi, S., Higuchi, M., Mukai, H. Y., Nakahata, T., et al. (2002). Erythroid-specific expression of the erythropoietin receptor rescued its null mutant mice from lethality. *Blood* 100, 2279–2288. doi: 10.1182/blood-2002-01-0124

Takeda, K., Aguila, H. L., Parikh, N. S., Li, X., Lamothe, K., Duan, L. J., et al. (2008). Regulation of adult erythropoiesis by prolyl hydroxylase domain proteins. *Blood* 111, 3229–3235. doi: 10.1182/blood-2007-09-114561

Tan, C. C., Eckardt, K. U., and Ratcliffe, P. J. (1991). Organ distribution of erythropoietin messenger RNA in normal and uremic rats. *Kidney Int.* 40, 69–76. doi: 10.1038/ki.1991.181

Teng, R., Calvert, J. W., Sibmooh, N., Piknova, B., Suzuki, N., Sun, J., et al. (2011a). Acute erythropoietin cardioprotection is mediated by endothelial response. *Basic Res. Cardiol.* 106, 343–354. doi: 10.1007/s00395-011-0158-z

Teng, R., Gavrilova, O., Suzuki, N., Chanturiya, T., Schimel, D., Hugendubler, L., et al. (2011b). Disrupted erythropoietin signalling promotes obesity and alters hypothalamus proopiomelanocortin production. *Nat. Commun.* 2:520. doi: 10.1038/ncomms1526

Tsai, P. T., Ohab, J. J., Kertesz, N., Groszer, M., Matter, C., Gao, J., et al. (2006). A critical role of erythropoietin receptor in neurogenesis and post-stroke recovery. *J. Neurosci.* 26, 1269–1274. doi: 10.1523/jneurosci.4480-05.2006

Tsuma, Y., Mori, J., Ota, T., Kawabe, Y., Morimoto, H., Fukuhara, S., et al. (2019). Erythropoietin and long-acting erythropoiesis stimulating agent ameliorate non-alcoholic fatty liver disease by increasing lipolysis and decreasing lipogenesis via EPOR/STAT pathway. *Biochem. Biophys. Res. Commun.* 509, 306–313. doi: 10.1016/j.bbrc.2018.12.131

Um, M., Gross, A. W., and Lodish, H. F. (2007). A "classical" homodimeric erythropoietin receptor is essential for the antiapoptotic effects of erythropoietin on differentiated neuroblastoma SH-SY5Y and pheochromocytoma PC-12 cells. *Cell. Signal.* 19, 634–645. doi: 10.1016/j.cellsig.2006.08.014

Us Renal Data System (2007). *USRDS 2007 Annual Data Report 2007*. Minneapolis, MN: US Renal Data System.

Van Der Meer, P., Lipsic, E., Henning, R. H., Boddeus, K., Van Der Velden, J., Voors, A. A., et al. (2005). Erythropoietin induces neovascularization and improves cardiac function in rats with heart failure after myocardial infarction. *J. Am. Coll. Cardiol.* 46, 125–133. doi: 10.1016/j.jacc.2005.03.044

Vichinsky, E. P. (1998). The morbidity of bone disease in thalassemia. *Ann. N. Y. Acad. Sci.* 850, 344–348. doi: 10.1111/j.1749-6632.1998.tb10491.x

Villa, P., Bigini, P., Mennini, T., Agnello, D., Laragione, T., Cagnotto, A., et al. (2003). Erythropoietin selectively attenuates cytokine production and inflammation in cerebral ischemia by targeting neuronal apoptosis. *J. Exp. Med.* 198, 971–975. doi: 10.1084/jem.20021067

Villafuerte, F. C., and Corante, N. (2016). Chronic mountain sickness: clinical aspects, etiology, management, and treatment. *High Alt. Med. Biol.* 17, 61–69. doi: 10.1089/ham.2016.0031

Voss, J. D., Allison, D. B., Webber, B. J., Otto, J. L., and Clark, L. L. (2014). Lower obesity rate during residence at high altitude among a military population with frequent migration: a quasi experimental model for investigating spatial causation. *PLoS One* 9:e93493. doi: 10.1371/journal.pone.0093493

Voss, J. D., Masuoka, P., Webber, B. J., Scher, A. I., and Atkinson, R. L. (2013). Association of elevation, urbanization and ambient temperature with obesity prevalence in the United States. *Int. J. Obes.* 37, 1407–1412. doi: 10.1038/ijo.2013.5

Wang, L., Di, L., and Noguchi, C. T. (2014). Erythropoietin, a novel versatile player regulating energy metabolism beyond the erythroid system. *Int. J. Biol. Sci.* 10, 921–939. doi: 10.7150/ijbs.9518

Wang, L., Jia, Y., Rogers, H., Suzuki, N., Gassmann, M., Wang, Q., et al. (2013a). Erythropoietin contributes to slow oxidative muscle fiber specification via PGC-1alpha and AMPK activation. *Int. J. Biochem. Cell Biol.* 45, 1155–1164. doi: 10.1016/j.biocel.2013.03.007

Wang, L., Teng, R., Di, L., Rogers, H., Wu, H., Kopp, J. B., et al. (2013b). PPARalpha and Sirt1 mediate erythropoietin action in increasing metabolic activity and browning of white adipocytes to protect against obesity and metabolic disorders. *Diabetes Metab. Res. Rev.* 62, 4122–4131. doi: 10.2337/db13-0518

Wang, L., Jia, Y., Rogers, H., Wu, Y. P., Huang, S., and Noguchi, C. T. (2012). GATA-binding protein 4 (GATA-4). and T-cell acute leukemia 1 (TAL1). regulate myogenic differentiation and erythropoietin response via cross-talk with Sirtuin1 (Sirt1). *J. Biol. Chem.* 287, 30157–30169. doi: 10.1074/jbc.M112.376640

Wassink, G., Davidson, J. O., Dhillon, S. K., Fraser, M., Galinsky, R., Bennet, L., et al. (2017). Partial white and grey matter protection with prolonged infusion of recombinant human erythropoietin after asphyxia in preterm fetal sheep. *J. Cereb. Blood Flow Metab.* 37, 1080–1094. doi: 10.1177/0271678X16650455

Watowich, S. S. (2011). The erythropoietin receptor: molecular structure and hematopoietic signaling pathways. *J. Invest. Med.* 59, 1067–1072. doi: 10.2310/jim.0b013e31820fb28c

Westenbrink, B. D., Visser, F. W., Voors, A. A., Smilde, T. D., Lipsic, E., Navis, G., et al. (2006). Anaemia in chronic heart failure is not only related to impaired renal perfusion and blunted erythropoietin production, but to fluid retention as well. *Eur. Heart J.* 28, 166–171. doi: 10.1093/eurheartj/ehl419

Witthuhn, B. A., Quelle, F. W., Silvennoinen, O., Yi, T., Tang, B., Miura, O., et al. (1993). JAK2 associates with the erythropoietin receptor and is tyrosine phosphorylated and activated following stimulation with erythropoietin. *Cell* 74, 227–236. doi: 10.1016/0092-8674(93)90414-l

Wright, D. G., Wright, E. C., Narva, A. S., Noguchi, C. T., and Eggers, P. W. (2015). Association of erythropoietin dose and route of administration with clinical outcomes for patients on hemodialysis in the United States. *Clin. J. Am. Soc. Nephrol.* 10, 1822–1830. doi: 10.2215/CJN.01590215

Wu, H., Lee, S. H., Gao, J., Liu, X., and Iruela-Arispe, M. L. (1999). Inactivation of erythropoietin leads to defects in cardiac morphogenesis. *Development* 126, 3597–3605.

Wu, H., Liu, X., Jaenisch, R., and Lodish, H. F. (1995). Generation of committed erythroid BFU-E and CFU-E progenitors does not require erythropoietin or the erythropoietin receptor. *Cell* 83, 59–67. doi: 10.1016/0092-8674(95)90234-1

Yasuda, Y., Masuda, S., Chikuma, M., Inoue, K., Nagao, M., and Sasaki, R. (1998). Estrogen-dependent production of erythropoietin in uterus and its implication in uterine angiogenesis. *J. Biol. Chem.* 273, 25381–25387. doi: 10.1074/jbc.273.39.25381

Yokoro, M., Nakayama, Y., Yamagishi, S. I., Ando, R., Sugiyama, M., Ito, S., et al. (2017). Asymmetric dimethylarginine contributes to the impaired response to erythropoietin in CKD-Anemia. *J. Am. Soc. Nephrol.* 28, 2670–2680. doi: 10.1681/ASN.2016111184

Yu, X., Lin, C. S., Costantini, F., and Noguchi, C. T. (2001). The human erythropoietin receptor gene rescues erythropoiesis and developmental defects in the erythropoietin receptor null mouse. *Blood* 98, 475–477. doi: 10.1182/blood.v98.2.475

Yu, X., Shacka, J. J., Eells, J. B., Suarez-Quian, C., Przygodzki, R. M., Beleslin-Cokic, B., et al. (2002). Erythropoietin receptor signalling is required for normal brain development. *Development* 129, 505–516.

Zanjani, E. D., Ascensao, J. L., McGlave, P. B., Banisadre, M., and Ash, R. C. (1981). Studies on the liver to kidney switch of erythropoietin production. *J. Clin. Invest.* 67, 1183–1188. doi: 10.1172/jci110133

Zhang, Y., Rogers, H. M., Zhang, X., and Noguchi, C. T. (2017). Sex difference in mouse metabolic response to erythropoietin. *FASEB J.* 31, 2661–2673. doi: 10.1096/fj.201601223RRR

Zhang, Y., Wang, L., Dey, S., Alnaeeli, M., Suresh, S., Rogers, H., et al. (2014). Erythropoietin action in stress response, tissue maintenance and metabolism. *Int. J. Mol. Sci.* 15, 10296–10333. doi: 10.3390/ijms150610296

Zierath, J. R., and Hawley, J. A. (2004). Skeletal muscle fiber type: influence on contractile and metabolic properties. *PLoS Biol.* 2:e348. doi: 10.1371/journal.pbio.0020348

Zon, L. I., Youssoufian, H., Mather, C., Lodish, H. F., and Orkin, S. H. (1991). Activation of the erythropoietin receptor promoter by transcription factor GATA-1. *Proc. Natl. Acad. Sci. U.S.A.* 88, 10638–10641. doi: 10.1073/pnas.88.23.10638

Conflict of Interest: The authors declare that the research was conducted in the absence of any commercial or financial relationships that could be construed as a potential conflict of interest.

frontiers in Physiology

REVIEW
published: 07 May 2020
doi: 10.3389/fphys.2020.00392

Heterogeneity of Red Blood Cells: Causes and Consequences

Anna Bogdanova[1], Lars Kaestner[2,3], Greta Simionato[2,4], Amittha Wickrema[5] and Asya Makhro[1]*

[1] Red Blood Cell Research Group, Vetsuisse Faculty, The Zurich Center for Integrative Human Physiology (ZHIP), Institute of Veterinary Physiology, University of Zurich, Zurich, Switzerland, [2] Experimental Physics, Dynamics of Fluids, Faculty of Natural Sciences and Technology, Saarland University, Saarbrücken, Germany, [3] Theoretical Medicine and Biosciences, Medical Faculty, Saarland University, Homburg, Germany, [4] Institute for Clinical and Experimental Surgery, Saarland University, Homburg, Germany, [5] Section of Hematology/Oncology, Department of Medicine, University of Chicago, Chicago, IL, United States

Mean values of hematological parameters are currently used in the clinical laboratory settings to characterize red blood cell properties. Those include red blood cell indices, osmotic fragility test, eosin 5-maleimide (EMA) test, and deformability assessment using ektacytometry to name a few. Diagnosis of hereditary red blood cell disorders is complemented by identification of mutations in distinct genes that are recognized "molecular causes of disease." The power of these measurements is clinically well-established. However, the evidence is growing that the available information is not enough to understand the determinants of severity of diseases and heterogeneity in manifestation of pathologies such as hereditary hemolytic anemias. This review focuses on an alternative approach to assess red blood cell properties based on heterogeneity of red blood cells and characterization of fractions of cells with similar properties such as density, hydration, membrane loss, redox state, Ca^{2+} levels, and morphology. Methodological approaches to detect variance of red blood cell properties will be presented. Causes of red blood cell heterogeneity include cell age, environmental stress as well as shear and metabolic stress, and multiple other factors. Heterogeneity of red blood cell properties is also promoted by pathological conditions that are not limited to the red blood cells disorders, but inflammatory state, metabolic diseases and cancer. Therapeutic interventions such as splenectomy and transfusion as well as drug administration also impact the variance in red blood cell properties. Based on the overview of the studies in this area, the possible applications of heterogeneity in red blood cell properties as prognostic and diagnostic marker commenting on the power and selectivity of such markers are discussed.

Keywords: red blood cells, heterogeneity, morphology, erythroid precursor cells, age

OPEN ACCESS

Edited by:
Dmitry A. Fedosov, Helmholtz Association of German Research Centers (HZ), Germany

Reviewed by:
Manouk Abkarian, INSERM U1054 Centre de Biochimie Structurale de Montpellier, France
Roberta Russo, University of Naples Federico II, Italy

****Correspondence:***
Anna Bogdanova
annab@access.uzh.ch

Specialty section:
This article was submitted to Red Blood Cell Physiology, a section of the journal Frontiers in Physiology

Received: *14 January 2020*
Accepted: *02 April 2020*
Published: *07 May 2020*

Citation:
Bogdanova A, Kaestner L, Simionato G, Wickrema A and Makhro A (2020) Heterogeneity of Red Blood Cells: Causes and Consequences. Front. Physiol. 11:392. doi: 10.3389/fphys.2020.00392

INTRODUCTION

Our understanding of red blood cells (RBCs) evolved from acknowledgment of the basic and fundamental role of these cells as key players in gas exchange to the state where we assign multiple complex functions related to sensing and signaling, maintenance of homeostasis of pH and redox state and participation in control of vascular tone, clotting (Andrews and Low, 1999; Bernhardt et al., 2019), and other processes (Helms et al., 2018; Pernow et al., 2019).

Broadening of RBC functions was accompanied with our awareness of complexity of the cellular architecture and biochemistry. Spatial compartmentalization of processes and resources in RBCs was discovered (Hoffman et al., 2009; Chu et al., 2012). Complex dynamics precise orchestration of processes occurring in the circulating RBCs in response to the changes in micro- and macro-environment (hormonal and mechanical stimulation, changes in local or ambient oxygen availability, temperature, circadian rhythm-related processes and others) is becoming evident (e.g., O'Neill and Reddy, 2011; Cahalan et al., 2015; Zhou et al., 2019).

With time it became clear that these changes and responses do not necessarily involve all the circulating cells. As our knowledge of these cells accumulates more and more reports mention the presence of "responding" and "non-responding" cells in the circulation (e.g., Kaestner et al., 2012; Makhro et al., 2013; Wang et al., 2013; Rotordam et al., 2019). As we recognize the existence of multiple fractions of RBCs that are functionally different from each other, we feel a growing need to unravel the nature of these differences, their causes and the potential information hidden in RBC heterogeneity on systemic distress and pathology. In this review we aimed to summarize the current state of knowledge in this rapidly developing research area. We focus on RBCs of healthy humans and give only a few examples of how RBC heterogeneity may be used to predict RBC disease nature and severity. Heterogeneity of stored or transfused RBCs is a broad topic also out of the scope of this review.

INTER-INDIVIDUAL HETEROGENEITY

Inter-individual variation in properties of circulating RBCs of healthy donors reflects genetic and epigenetic variance as well as the state in which the organism resides over the past 3–4 months during which the cells undergo transitions from erythroid progenitors to young, mature, and senescent state. Variance spreads to the number of copies of proteins per cell, activity of enzymes and ion transporters, shapes, differences in density, deformability, membrane stability, redox state, and the collection of Hb variants in a given cell. Most of the studies for healthy humans were performed on stored blood to assess its quality and identify a cohort of best donors (Sparrow, 2017).

The possible causes of this inter-individual variation originate at the level of erythroid precursor cells (as in case of ineffective erythropoiesis (Oikonomidou and Rivella, 2018), for more details see section Cellular Heterogeneity During Erythropoiesis) or emerge later on as the cells enter the circulation and get exposed to a variety of microenvironments (osmolarity gradients in the kidneys, shear in capillaries and spleen, changes in oxygen availability and pH within peripheral tissues, changes in redox state next to the inflammatory side or to the exercising muscle). Development of heterogeneous RBC populations may be an intrinsic property of blood (e.g., RBC aging), or be triggered by the changes in life style or environmental conditions (e.g., hypoxia, microgravity) or state of the organism (e.g., stress, inflammation, changes in dietary preferences and blood metabolites). Finally, it may result from hereditary diseases that destabilize the RBC membrane or perturb its rheological properties, redox or metabolic state. In this review we focus on the possible physiological causes of heterogeneity.

PARAMETERS SHOWING INTER-CELLULAR HETEROGENEITY AND METHODS TO DETECT THEM

Table 1 summarizes the information on the parameters displaying inter-individual and inter-cellular heterogeneity, as well as methodological approaches for detection of heterogeneity.

Shape and Size

First descriptions of RBCs as "red corpuscles" given by Jan Swammerdam and dates back to 1658 (Swammerdam, 1737; Bessis and Delpech, 1981; Hajdu, 2003). Since then, substantial progress was made in imaging equipment as well as in fixation and staining of RBC. Blood smears still remain a part of common diagnostic practice in most of the clinical laboratories (Bain, 2005) despite the fact that smear preparation results in distortions of RBC morphology and lysis of the most fragile of them (Wenk, 1976). This technique allows to discriminate between numerous shapes from discocytes to a broad variety of "static" shapes such as echinocytes and stomatocytes, for healthy humans. The list of shape types will extend manifolds for patients with hereditary or acute disorders.

The biggest drawback of the whole approach with smears is that it provides an immediate snapshot of the shape distribution, whereas living RBCs are very dynamic entities. So are their shapes, and, rather than discussing their "absolute shape," it would be feasible to assign them a probability to be observed in one of the shape types. The first attempts to address RBC shapes in terms of probability density distribution are recently undertaken (Reichel et al., 2019). Each cell has its "static shape" that is preferred over the other ones if no force is applied to it. There are also several preferred shape types caused by shear stress in flow. The probability to observe one of those depends on the shear rates and flow dynamics (Abkarian et al., 2008; Dupire et al., 2015; Lanotte et al., 2016; Kihm et al., 2018; Mauer et al., 2018; Reichel et al., 2019). The restoration of the initial shape of the cells as soon as the flow stops got the name of "shape memory" (Fischer, 2004; Cordasco and Bagchi, 2017). Acute shape changes associated with the ion movements across the cell membrane (dehydration or overhydration) are often reversible (Brugnara, 1997; Cossins and Gibson, 1997; Zhu et al., 2018) whereas shape alterations related to the permanent damage of the cytoskeleton or membrane loss are irreversible (Gallagher, 2005; Perrotta et al., 2008).

Preferred shapes reflect the optimal cytoskeletal conformation, hemoglobin concentration, redox state and metabolic balance and free Ca^{2+} levels that, in turn, define the activity of ion transporters, hydration state and phosphorylation state of proteins. Some of these variables will be addressed below.

Parameters to describe dynamics of RBCs morphology are currently in development. Former classifications of shapes performed by eye (Bessis and Lessin, 1970; Bessis and Delpech,

TABLE 1 | Overview of parameters showing inter-cellular heterogeneity as well as basic principle and methodological approaches of their detection in single cells and sub-populations.

Parameter	Indicator	Method	References
Shape/size	**Direct:** Shape classification Projected area Perimeter/roughness Sphericity/elongation	Microscopy: Blood smears, images of living cells (snapshots, time series in flow, microfluidics), Imaging flow cytometers	Gonzalez-Hidalgo et al., 2015; Quint et al., 2018; Herold-Garcia and Fernandes, 2019
	Volume	Confocal microscopy + 3D deconvolution	Sadafi et al., 2019
		Scanning probe microscopy (semi quantitative)	Kihm et al., 2018
	Indirect: Forward and side light scatter Impedance (coulter principle)	Flow cytometry Coulter counters Multiple Blood analyzers	
Density	**Direct:** Separation according to RBC density	Fractionation in Percoll-, Stractan or similar density gradients	Lutz et al., 1992
		Lab-on-a-chip approaches	Catarino et al., 2019
	Indirect: Swelling- or shrinkage- resistance (e.g., the changes in SS and FS within the swelling test) Single cell rheology	Flow cytometry Cell-flow properties analyzer	Kaul et al., 2008; Barshtein et al., 2016; Fermo et al., 2017
	Membrane surface/EMA test	Flow cytometry	
Free Ca^{2+}/channel activity	Fluorescent dyes for Ca^{2+} Detection of ionic currents across the membranes of single cells	Flow cytometry and fluorescence microscopy Patch-clamp incl. automated planar chips	Kaestner et al., 2006; Makhro et al., 2013; Wang et al., 2013; Fermo et al., 2017; Rotordam et al., 2019
Redox state and metabolism	Fluorescent dyes for reduced thiols (e.g., thiol tracker, monobromobimane), Fluorescent dyes for N_2O_3 (DAF-DA), Dyes for detection of H_2O_2, ONOO, HO* (e.g., H_2DCF-DA) Single cell metabolomics (not yet used for red blood cells)	Flow cytometry Fluorescence microscopy Mass-spectrometry	Jemaa et al., 2017; Gilmore et al., 2019
Hb levels and variance	Antibodies with fluorescent tags Chromicity Sodium metabisulfite (Na_2S_2O5) and similar deoxygenation-based sickling tests Hemoglobin Distribution Width (HDW)	Flow cytometry, Fluorescence microscopy Microscopy	Kunicka et al., 2001; Darrow et al., 2016; Jung et al., 2016
Age	Labeling of cells (biotin conjugated with fluorescent tag or staining with PKH dyes) Reticulocyte count RNA-positive or Transferrin receptor-positive	Flow cytometry, microscopy	Mock et al., 1999; Piva et al., 2010

1982) are non-numerical and cannot be reliably translated into the algorithms for automated segmentation and classification of smears and images of living cells. New approaches are currently developing (Tomari et al., 2014). Roundness, roughness, projected areas are among such numeric descriptors of RBC shapes. 3D volume reconstruction of, e.g., confocal recordings are more informative than 2-dimentional images. High resolution 3D-imaging was performed for fixed RBC (Abay et al., 2019). First attempts to get the 3D imaging working for RBCs in flow are undertaken but is not yet available as a high-throughput mode (Quint et al., 2018). Cell shape recognition and classification involving artificial intelligence (AI) algorithms based on artificial neural networks (Kihm et al., 2018). New optical concepts using optofluidic microlenses-like behavior of RBCs (Mugnano et al., 2018) and indirect adaptive optics as well as label-free quantitative phase imaging (Miccio et al., 2015) enables assessment of cell volume of individual cells, and monitoring of morphometric features (e.g., label-free optical markers) that make high throughput reliable quantification of cell phenotypes possible. It allows to stay unbiased, omit "human factor," and allocate RBC shapes to a continuous scale with high throughput and precision. The challenge is that artificial neural networks need to be set up, customized and most notably trained. This type of analysis will become available routinely in the nearest future.

Hydration State and Density

The best method to visualize the variance in RBC density is fractionation on a Percoll (**Figure 1**), Ficoll, Stractan, or phtalate density gradient (Danon and Marikovsky, 1964; Corry et al., 1982; Salvo et al., 1982; Mosca et al., 1991; Lutz et al., 1992). Upon centrifugation in isotonic solution of any of these materials forming continuous or discontinuous gradients, RBCs

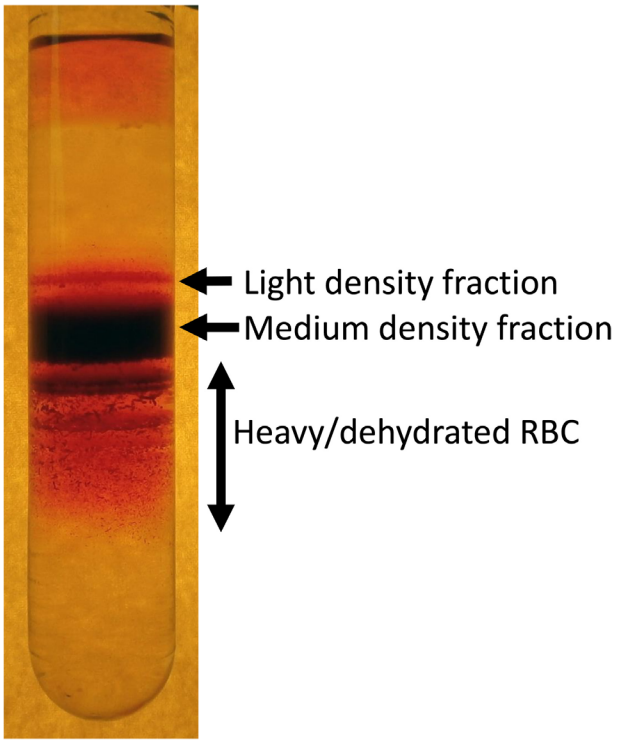

FIGURE 1 | An example of heterogeneity of RBC density revealed by fractionation of RBCs on a self-forming Percoll density gradient. Composition of light, medium and high-density fractions vary depending on human health and environmental stress. About 15–20% of RBCs of healthy human donors forming low density are reticulocytes. However, along with young cells this fraction is "contaminated" with swollen RBCs at the terminal senescence stage (Lew and Tiffert, 2013). Medium fraction is formed by mature RBCs, and heavy dehydrated cells are those with senescent phenotype.

distribute within them according to their densities. As RBCs of healthy human donors are fractionated on a self-forming Percoll gradient, three to five fractions may be collected. A small fraction of cells with lower density bands as the top layer, followed by one or several RBC populations with a medium density and a minor fraction of cells is presented with the highest density (Lutz et al., 1992; Makhro et al., 2013; Makhro et al., 2016b). RBCs of patients with hereditary hemolytic anemias are generally characterized with a broader variance in densities. Often this diversity may contain clinically relevant information on the severity of disease state. For sickle cell disease the abundance of dense cells was suggested to be a predictor of severity of disease manifestation due to the increased probability of irreversible aggregation of HbS (Kaul et al., 1983). For hereditary spherocytosis severity is associated with an increase in abundance of well-hydrated cells that are lost before they have time to mature and lose some of their membrane (Huisjes et al., 2019). Increase in heterogeneity is high in patients with cryohydrocytosis (Bogdanova et al., 2010), Gardos channelopathy (Fermo et al., 2017) beta-thalassemia, G6PD, and pyruvate kinase (PK) deficiency (Mosca et al., 1991).

Factors defining RBC density include changes in water and ion content and membrane loss. During the density fractionation RBCs experience shear stress during centrifugation as they move through the isotonic Percoll solution containing micromolar concentrations of Ca^{2+} in the absence of EGTA. Shear forces may activate mechano-sensitive channels such as PIEZO1 channels (Cahalan et al., 2015) and NMDA receptors (Hanggi et al., 2014) that are permeable for Ca^{2+}. Uptake of Ca^{2+} via these receptors triggers loss of K^+ mediated by opening of Ca^{2+}-dependent Gardos channels. Thus, fractionation of RBCs on Percoll should be viewed as a functional test in which distribution of the cells is not only driven by the steady state density, but also by their mechano-sensitivity.

Indirect methods to assess heterogeneity in RBC density include detection of hypo- and hyperchromic cells in blood smears, HDW as well as the shape of the curve in osmotic fragility test of the right arm of the osmoscan curve obtained by ektacytometry (Clark et al., 1983; Lutz et al., 1992). Hight throughput devices for evaluation of RBC density using functional tests at the single cell level are being developed.

Ca^{2+} Levels (Static and Dynamic Tests) and Electrophysiological Properties

Heterogeneity in basal free Ca^{2+} levels was recorded in RBCs of healthy humans (Kaestner et al., 2006; Makhro et al., 2013; Fermo et al., 2017). Stimulation of Ca^{2+} uptake by treatment of healthy human RBCs with PGE_2 (Danielczok et al., 2017), lysophosphatidic acid (Steffen et al., 2011; Kaestner et al., 2012; Wang et al., 2013; Wesseling et al., 2016) or glutamate (Makhro et al., 2013; Hanggi et al., 2014; Makhro et al., 2016a; Petkova-Kirova et al., 2019) increases variance in the intracellular Ca^{2+}. Not all cells respond to shear stress or pro-oxidative condition with an increase in Ca^{2+}.

Molecular causes for this heterogeneity in responses to various stressors are poorly understood. It is obvious, that they relate to the differences in abundance of either Ca^{2+} channels (Kaestner et al., 1999; Makhro et al., 2013; Kaestner and Egee, 2018; Rotordam et al., 2019) or of the primary receptors responding to the stressor (such as LPA or prostaglandin receptors; Wang et al., 2013; Danielczok et al., 2017). In human RBCs several ion channels are known to mediate Ca^{2+} uptake including PIEZO1, TRPC6, NMDA receptors, $Ca_V2.1$ and several others (for a recent review see Kaestner et al., 2020). As a result of stochastic distribution and opening probability, Ca^{2+} entry into individual RBCs varies in response to stimulation by individual Ca^{2+} channels substantially giving rise to "responders" and "non-responders" cellular sup-populations. This uneven behavior may be further amplified due to the existence of feedback loops supporting Ca^{2+}-dependent Ca^{2+} uptake (Kaestner et al., 2018).

Most documented is inter-cellular variance in distribution of the Ca^{2+}-dependent K^+ (Gardos) channel in RBCs. However, majority of the recordings for this best-studied channel in RBCs were performed as mean values for the unseparated populations, using radioactive tracer kinetics technique or single channel recordings. Reports based on whole-cell recordings for this channel are still sparse (Kucherenko et al., 2005; Kucherenko

et al., 2013; Fermo et al., 2017). A further factor that may amplify heterogeneity of Gardos channel recordings in RBCs is its inactivation upon hypoxic exercises (Mao et al., 2011).

Redox State and Metabolism

Staining of individual cells with fluorescent probes sensitive to pro-oxidative free radicals such as dicarbofluorescein (Amer et al., 2003; Grinberg et al., 2005) and monobromobimane (Kosower and Kosower, 1995) provide a possibility to follow the changes in redox balance in individual cells. One more approach to record redox state in sub-fractions of RBCs is based on pre-fractionation of cells into low, medium and high density fractions before assessment of reduced and oxidized glutathione (GSH and GSSG) and NAD(P)H (Piccinini et al., 1995; D'Alessandro et al., 2013) in these sub-populations. Dense cells were shown to be deprived of GSH and enriched with GSSG compared to the mature RBCs of medium density. Accumulation of GSSG and reduction in GSH was not associated with any substantial changes in the intracellular ATP or NADPH (Sass et al., 1965; D'Alessandro et al., 2013). Finally, redox state of RBCs may be expressed as the ability to tolerate oxidative challenge (Lisovskaya et al., 2008; Sinha et al., 2015) which differs between individual RBCs as well.

Shifts in redox equilibrium in RBCs of healthy donors are associated with age-dependent decrease in pyruvate kinase, hexokinase, glucose-phosphate dehydrogenase, aldolase activities (Salvo et al., 1982; Suzuki and Dale, 1988). Oxidative stress is a hallmark of RBCs of patients with hereditary hemolytic anemias presented with one or two alleles of mutated glucose-6 phosphate dehydrogenase (G6PD). The resulting in acute hemolytic condition known as favism is associated with depletion in NADPH in favor of $NADP^+$ (Mason et al., 2007; Peters and van Noorden, 2017). Furthermore, systemic oxidative stress caused by inflammatory processes, infection and other causes may result in release of reduced glutathione from RBCs and temporary increase in oxidative load and aggravate the differences in redox state between the cells of different ages (Giustarini et al., 2008).

Hb Levels and Variants

Inter-cellular heterogeneity in intracellular hemoglobin content in clinical settings is reflected by the abundance of hypochromic and hyperchromic cells in blood smears. The abundance of hypochrome RBCs for healthy humans should not exceed 2.5% of circulating RBCs (Macdougall et al., 1992; Schaefer and Schaefer, 1995; Braun et al., 1997), dropping below 1% in patients with iron overload, and increasing to 20% and more in patients with iron deficiency. Higher levels of hyperchromic cells was also reported for patients with hereditary spherocytosis (Conway et al., 2002) and sickle cell disease (Ballas and Kocher, 1988).

Even more intercellular heterogeneity is introduced by a pronounced variance in the presence of fetal hemoglobin in a small fraction of cells (F-cells) in healthy humans (Boyer et al., 1975; Thein and Craig, 1998). The abundance of F-cells increases during high altitude exposure (Narayan et al., 2005). Pregnancy has an impact on this parameter (Prus and Fibach, 2013). Moreover, the abundance of F-cells as well as the amount of HbF in them may differ from cell to cell in patients with beta-thalassemia (Narayan et al., 2005). In sickle cell disease, HbF abundance furthermore strongly depends on the haplotype (Menzel and Thein, 2019). Sickle cell trait results in uneven distribution of HbS between the cells, and the pattern for such variance seems to be hereditary (Anyaibe et al., 1985).

CAUSES OF HETEROGENEITY

If we want to make extensive use of RBC heterogeneity as a diagnostic and prognostic marker, we have to understand the origin of the observed variance in RBC properties.

This may stem from the different pools of erythroid precursor cells that equip the resulting reticulocytes with various sets of proteins that may only be produced as long as the synthesis machinery is active before the enucleation.

The other cause of heterogeneity are the age-dependent differences between the young, mature and senescent RBCs. The third cause occurring at the systemic level originates from the alteration in the micro- and macro-environmental conditions (changes in hormonal and metabolic levels, inflammation, shear stress load, hyperthermia and others).

These three sources of heterogeneity will be reviewed below.

Cellular Heterogeneity During Erythropoiesis

Accumulated evidence over the last 25 years has demonstrated the existence of heterogeneity within the erythroid compartment schematically shown in **Figure 2**. Although it is quite expected to have a heterogenic population within the mature RBC population due to the long- life span of mature RBCs (100–120 days in human) representing cells of various ages, it is less clear and more intriguing the reasons for erythroid precursors/progenitors to be heterogeneous in multiple facets of their form and function.

One of the most established and well-explained aspect of erythroid precursor heterogeneity pertains to erythroid precursors possessing differing sensitivities to erythropoietin (EPO). Soon after discovering the precise molecular function of EPO to be a cell survival function (Koury and Bondurant, 1988, 1990), studies revealed that even within a highly homogenous population in terms of the differentiation stage (operationally defined as colony-forming unit-erythroid; CFU-E), erythroid precursors underwent apoptosis following EPO withdrawal in an asynchronous manner (Kelley et al., 1993). These studies demonstrated a dose response effect as reflected by increasing numbers of CFU-Es undergoing apoptosis as EPO concentrations were gradually decreased. These observations clearly highlighted the built-in heterogeneity within the developing erythroid cell compartment with respect to the biochemical nature of each cell within an otherwise "homogenous" precursor pool as defined by morphological characteristics. One of the possible causes supporting heterogeneity are the gradients in various signaling messengers, growth factors, chemokines, oxygen levels and the resulting reactive oxygen species, and other factors (e.g., Thompson et al., 2010; Spencer et al., 2014; Itkin et al., 2016) making conditions in which precursor cells differentiate unique and dependent on their location within the bone marrow

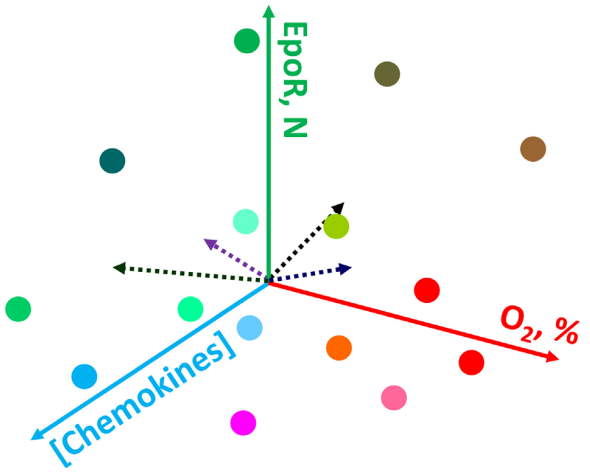

FIGURE 2 | Schematic representation of the possible causes of heterogeneity for erythroid precursor cells within bone marrow. Gradients in oxygen availability, chemokines and other signaling messengers create a plethora of conditions in which cells find themselves during differentiation. For details see the text.

(**Figure 2**). An elegant model proposed by Koury and Bondurant (1992), explained the basis of differing EPO sensitivities as a built-in mechanism to prevent all erythroid precursors undergoing apoptosis during low EPO levels in circulation such as in patients with renal failure. The work by several other groups (Miura et al., 1991; Landschulz et al., 1992; Nakamura et al., 1992; Kelley et al., 1993) had shown that heterogeneic EPO response within the same precursor population cannot be attributed to the numbers of EPO-receptors, affinity or structure, thereby suggesting differences in signal transduction as the likely mechanism for the existence of heterogeneity in EPO response. Based on these findings one can appreciate the existence of signaling heterogeneity within the erythroid precursor compartment as a necessary component during the development process to yield mature red blood cells. Recently developed single-cell intracellular flow cytometry approaches (Liu et al., 2019) are bound to further uncover previously unrecognized levels of regulatory heterogeneity during erythroid cell development.

Besides the existence of biochemical/signaling heterogeneity within the developing erythroid precursors other aspects of erythroid precursor heterogeneity have been observed especially most recently due to the advancement of single-cell technologies at both trascriptomic and phenotypic levels (Woll et al., 2014; La Manno et al., 2018; Brierley and Mead, 2019). Within the erythroid compartment especially during the early stages of erythropoiesis a significant level of transcriptomic variability and heterogeneity seem to exist at least based on mouse bone marrow erythroid precursors (Tusi et al., 2018). The same study also found that cell cycle in erythroid precursors are continuously remodeled during the differentiation program but consistent with very early studies using bulk erythroid precursors (CFU-E), the vast majority of cells were in the S-phase of the cell cycle (Iscove, 1977). These results demonstrate that an individual cell, especially during development, has the ability to program itself to act not in concert each other with respect to signal transduction, gene transcription, cell cycle and many other aspects even though morphologically a cell population may look alike at a particular stage of differentiation.

Overall, accumulated data suggests that heterogeneity during erythroid development may not be evenly spread during the entire development cascade. Most data points to greatest level of inter-cellular heterogeneity during the early phases of development when these cells are responsive to various growth factors. Beyond the late polychromatic stage, when the cells have exited the cell cycle one observes less heterogeneity and most cells undergo dramatic reduction in cell size, chromatin condensation and enucleation. However, it is conceivable even in the bone marrow niche within the blood island not all erythroblasts undergo enucleation adding another layer of heterogeneity. It is also conceivable that due to differing levels of chemokine receptors on these cells the progenitors also exhibit varying degrees of migration within the bone marrow niche. Overall, it may seem the inter-cellular heterogeneity during erythroid precursor development. Each cell is possessing different sensitivity to EPO, and as a result a vast majority of precursors die due to apoptosis, the strategy that seems quite wasteful. However, we speculate that such heterogeneity is critical in order to respond to rapid changes in the micro and macro environment such as changes in oxygen concentration due to changes in altitude, pro-inflammatory and oxidative stress conditions as well as sudden blood loss due to trauma and onset of anemia due to renal failure.

Age of RBCs

Most of the findings for the age-related variance for RBCs of healthy humans were obtained for the fractions of cells of low, medium and high density, that were enriched with young, mature and senescent cells, respectively (Mueller et al., 1985, 1987; Lutz et al., 1992; **Figure 1**). Gradual changes occurring with cell aging were described in several reviews (Lutz and Bogdanova, 2013; Lew and Tiffert, 2017; Badior and Casey, 2018; Minetti et al., 2018) and article collections (Beutler, 1988; Mangani, 1991), and schematically represented in **Figure 3**.

Recent studies of the age-dependent changes in RBCs involve single cell approaches such as flow cytometry and microscopy as well as proteomics (D'Alessandro et al., 2013; Minetti et al., 2013).

Deamidation of asparagine residue 502 of the band 4.1 protein was shown to occur gradually with RBC age as the deamidation rate is an exclusive function of temperature and time (Inaba and Maede, 1988, 1992). Deamidation is manifested as an appearance of a double band on the gels as the native and deamidated form of the protein differ in electrophoretic mobility of the protein. Fractionation of RBCs of healthy humans according to their density has shown that young cells have lower density than mature cells. Senescence is associated with further increase in RBC density and mean corpuscular hemoglobin concentration, and reduction in RBC volume. Using the changes in deamidation of band 4.1 protein or direct labeling of RBCs and monitoring of their aging (Luthra et al., 1979), increase in density were revealed as an intrinsic feature of *in vivo* aging of RBCs of healthy humans. Dense cells obtained by fractionation of leukodepleted RBCs on

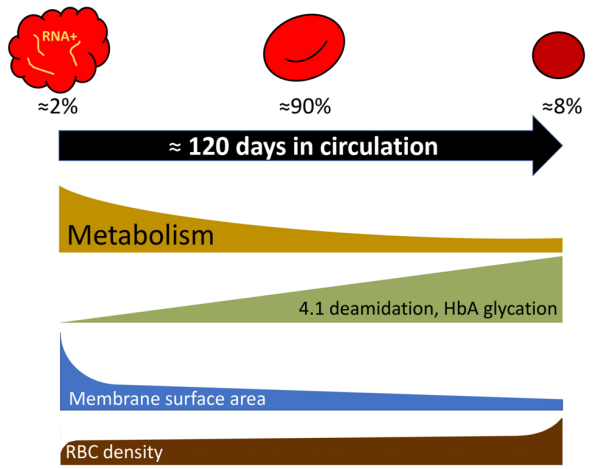

FIGURE 3 | Selected parameters that change during RBC aging following exponential or linear kinetics as cells turn from reticulocytes to mature cells and finally enter the senescent stage. Percentage of reticulocytes, mature cells, and dense senescent cells shown in the scheme correspond to those in adult healthy donors. For more details see Lutz and Bogdanova (2013) and the text.

Percoll density gradient were presented with substantially lower GSH levels and GSSG levels that were doubled compared to the mature RBCs, whereas ATP and NADPH levels were only slightly reduced in the densest cell fractions (Sass et al., 1965; D'Alessandro et al., 2013). These changes were associated with the age-driven decrease in pyruvate kinase, hexokinase, glucose-6-phosphate dehydrogenase, aldolase activities (Salvo et al., 1982; Suzuki and Dale, 1988). Some of the terminally senescent RBCs, that lose control over their Na^+ gradients and volume regulation due to the reduction in Na,K-ATPase activity, were reported to swell and lyse (Lew and Tiffert, 2013, 2017).

Reports on the changes in free Ca^{2+} levels are controversial and depend on the techniques used for assessment of these parameters (Romero and Romero, 1997, 1999; Makhro et al., 2013; Lew and Tiffert, 2017). Both Ca^{2+}-permeable channel activity and that of plasma membrane Ca^{2+} pumps decreases with cellular aging (Romero et al., 2002; Makhro et al., 2013). Despite this inconsistency, changes in the intracellular free Ca^{2+} and the ability to maintain low levels of Ca^{2+} are the factors in control of RBC longevity (Bogdanova et al., 2013; Lew and Tiffert, 2017).

Further hallmarks of RBC aging include the changes in phosphorylation pattern (Fairbanks et al., 1983) and membrane loss (Mohandas and Groner, 1989).

Physical Activity, High Altitude, and Other Stress Conditions

How substantial would the change be at the level of circulating RBCs if the gene expression reprogramming occurs at the level of precursor cells? Simple calculations assuming that the RBC longevity is not affected by these changes and all cells are equally affected by this change, gives a rough estimate of ~0.82% of RBC population changing per day for the "normal" production rate of 2.4×10^6 cells/s. If erythropoiesis is boosted to its maximum (10-fold increase, 8.2% of new cells will appear daily (Elliott and Molineux, 2009). This means that acute reversible changes at the bone marrow level will hardly be noticed if stress conditions persist for just 24 h. On the contrary, when stress conditions boosting erythropoiesis persist for a week, 5.7–57% of cells will get a new feature.

Such kinetics does not favor *de novo* production as an efficient strategy for acute adaptation to hypoxia or single endurance sport exercise bout, dietary changes, or to pathological conditions such as infection or sepsis, cancer, diabetes, or cardiovascular diseases (**Figure 4**). These changes in turn translate into the changes in shear stress, oxygen availability, pH, hormones and proinflammatory cytokines and other microenvironmental factors sensed by RBC directly. Species that undergo such acute changes from hyperoxygenation to severe hypoxia, such as Rainbow trout (*Oncorhynchus mykiss*) (Fago et al., 2001) or Rüppell's griffon vulture (*Gyps rueppelli*). Rüppell's griffon vulture was spotted at 37,000 feet (11277.6 m) when colliding with the plane (Laybourne, 1974) permanently possess several hemoglobin variants. Hemoglobin A and D chains are present in RBC vulture producing high and low affinity hemoglobin variants and allowing these unique birds to fly above 10,000 m with no need to engage any complex adaptive processes as they land (Weber et al., 1988; Hiebl et al., 1989).

Adult humans have by far lower adaptive capacity, possessing generally one Hb variant, HbA with some minor additions of HbF. However, plasticity of O_2 delivery, and its fast on-demand optimization upon the changes in environmental O_2 availability may be associated with other types of heterogeneity in RBC structure and function. Potential adaptive role of variance in RBC properties has to be further explored.

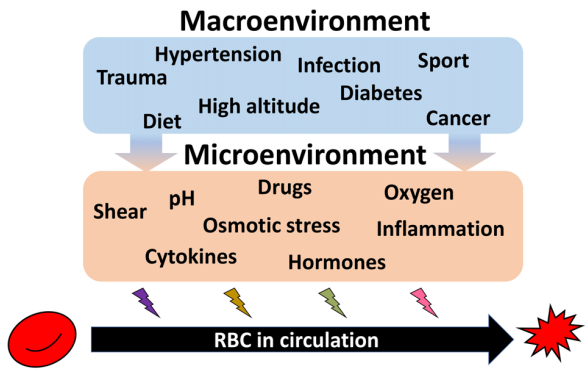

FIGURE 4 | Summary on the environmental causes imposing heterogeneity of circulating RBCs. Exposure of the organism to high altitude or practicing endurance sport as well as dietary preferences cause durable or acute impact on the RBC properties. Along with RBC diseases (anemia, polycythemia), pathologies such as hypertension, diabetes, infection, trauma, cancer, and further systemic diseases are influencing both erythropoietic niche and the circulating cells. All these macroenvironmental stresses translated into the changes in microenvironment for erythroid precursors and circulating RBCs. Shear, alterations in pH and oxygen levels, proinflammatory cytokines, and hormones, as well as drugs work to shape the features of each individual RBC resulting in an increase in the inter-cellular heterogeneity.

It is largely accepted that multiple forms of pathologies, both related to abnormal structure RBC membrane or cytosolic proteins and lipids, as well as systemic disorders such as cancer, diabetes, cardiovascular diseases, sepsis and other diseases of inflammation are associated with anemia, RBC damage and their premature removal from the circulation and increase in their heterogeneity (e.g., Salvagno et al., 2015; Feng et al., 2017; Ahmad et al., 2018; Ko et al., 2018; Yin et al., 2018; Parizadeh et al., 2019; Wang et al., 2019). The causes and consequences as well as predictive power of this increase in variability of RBC properties is out of the scope of this review but deserve special attention.

SUMMARY AND THE STANDING CHALLENGES

The present collection of information on the possible causes and consequences of inter-cellular heterogeneity justifies the increasing attention of researchers to the RBC sub-populations and individual cells. It appears that vast amount of information on the near and distant (within months) past is lost when RBC properties are reduced to a set of single "mean" values. This information appears to be of substantial importance when severity of disease or efficacy of therapy are to be assessed for individual patients. At present we do not have the commercially available and standardized methodologies and machines to be able to compare the data obtained of the single cell features in different labs. These challenges are already addressed by some researchers and will drive the transformation of our understanding of red blood cell biology in the nearest future.

AUTHOR CONTRIBUTIONS

AB and AW have composed the text. All authors contributed to editing and proofreading of the text.

FUNDING

AB and LK received funding from the European Union's Horizon 2020 Research and Innovation Programme under grant agreement number 675115 – RELEVANCE – H2020-MSCA-ITN-2015/H2020-MSCA-ITN-2015 and from the European Union's Horizon 2020 Research and Innovation Programme under the Marie Skłodowska-Curie grant agreement number 860436 – EVIDENCE – H2020-MSCA-ITN-2019.

REFERENCES

Abay, A., Simionato, G., Chachanidze, R., Bogdanova, A., Hertz, L., Bianchi, P., et al. (2019). Glutaraldehyde – a subtle tool in the investigation of healthy and pathologic red blood cells. *Front. Physiol.* 10:514. doi: 10.3389/fphys.2019.00514

Abkarian, M., Faivre, M., Horton, R., Smistrup, K., Best-Popescu, C. A., and Stone, H. A. (2008). Cellular-scale hydrodynamics. *Biomed. Mater.* 3:034011. doi: 10.1088/1748-6041/3/3/034011

Ahmad, H., Khan, M., Laugle, M., Jackson, D. A., Burant, C., Malemud, C. J., et al. (2018). Red cell distribution width is positively correlated with atherosclerotic cardiovascular disease 10-year risk score, age, and CRP in Spondyloarthritis with axial or peripheral disease. *Int. J. Rheumatol.* 2018:2476239. doi: 10.1155/2018/2476239

Amer, J., Goldfarb, A., and Fibach, E. (2003). Flow cytometric measurement of reactive oxygen species production by normal and thalassaemic red blood cells. *Eur. J. Haematol.* 70, 84–90. doi: 10.1034/j.1600-0609.2003.00011.x

Andrews, D. A., and Low, P. S. (1999). Role of red blood cells in thrombosis. *Curr. Opin. Hematol.* 6, 76–82.

Anyaibe, S., Castro, O., and Headings, V. (1985). Distributions of hemoglobins A and S among erythrocytes of heterozygotes. *Hemoglobin* 9, 137–155. doi: 10.3109/03630268508996996

Badior, K. E., and Casey, J. R. (2018). Molecular mechanism for the red blood cell senescence clock. *IUBMB Life* 70, 32–40. doi: 10.1002/iub.1703

Bain, B. J. (2005). Diagnosis from the blood smear. *N. Engl. J. Med.* 353, 498–507. doi: 10.1056/nejmra043442

Ballas, S. K., and Kocher, W. (1988). Erythrocytes in Hb SC disease are microcytic and hyperchromic. *Am. J. Hematol.* 28, 37–39. doi: 10.1002/ajh.2830280108

Barshtein, G., Pries, A. R., Goldschmidt, N., Zukerman, A., Orbach, A., Zelig, O., et al. (2016). Deformability of transfused red blood cells is a potent determinant of transfusion-induced change in recipient's blood flow. *Microcirculation* 23, 479–486. doi: 10.1111/micc.12296

Bernhardt, I., Wesseling, M. C., Nguen, D. B., and Kaestner, L. (2019). "Red blood cells actively contribute to blood coagulation and thrombus formation," in *Erythrocyte*, ed. A. Tombak, (London: IntechOpen).

Bessis, M., and Delpech, G. (1981). Discovery of the red blood cell with notes on priorities and credits of discoveries, past, present and future. *Blood Cells* 7, 447–480.

Bessis, M., and Delpech, G. (1982). Sickle cell shape and structure: images and concepts (1840-1980). *Blood Cells* 8, 359–435.

Bessis, M., and Lessin, L. S. (1970). The discocyte-echinocyte equilibrium of the normal and pathologic red cell. *Blood* 36, 399–403. doi: 10.1182/blood.v36.3.399.399

Beutler, E. (ed.) (1988). *Red Cell Senescence*. Bethesda, MD: American Physiological Society.

Bogdanova, A., Goede, J. S., Weiss, E., Bogdanov, N., Bennekou, P., Bernhardt, I., et al. (2010). Cryohydrocytosis: increased activity of cation carriers in red cells from a patient with a band 3 mutation. *Haematologica* 95, 189–198. doi: 10.3324/haematol.2009.010215

Bogdanova, A., Makhro, A., Wang, J., Lipp, P., and Kaestner, L. (2013). Calcium in red blood cells-a perilous balance. *Int. J. Mol. Sci.* 14, 9848–9872. doi: 10.3390/ijms14059848

Boyer, S. H., Belding, T. K., Margolet, L., and Noyes, A. N. (1975). Fetal hemoglobin restriction to a few erythrocytes (F cells) in normal human adults. *Science* 188, 361–363. doi: 10.1126/science.804182

Braun, J., Lindner, K., Schreiber, M., Heidler, R. A., and Horl, W. H. (1997). Percentage of hypochromic red blood cells as predictor of erythropoietic and iron response after i.v. iron supplementation in maintenance haemodialysis patients. *Nephrol. Dial. Transplant.* 12, 1173–1181. doi: 10.1093/ndt/12.6.1173

Brierley, C. K., and Mead, A. J. (2019). Single-cell sequencing in hematology. *Curr. Opin. Oncol.* 32, 139–145. doi: 10.1097/cco.0000000000000613

Brugnara, C. (1997). Erythrocyte membrane transport physiology. *Curr. Opin. Hematol.* 4, 122–127. doi: 10.1097/00062752-199704020-00008

Cahalan, S. M., Lukacs, V., Ranade, S. S., Chien, S., Bandell, M., and Patapoutian, A. (2015). Piezo1 links mechanical forces to red blood cell volume. *eLife* 4:e07370. doi: 10.7554/eLife.07370

Catarino, S. O., Rodrigues, R. O., Pinho, D., Miranda, J. M., Minas, G., and Lima R. (2019). Blood cells separation and sorting techniques of passive microfluidic devices: from fabrication to applications. *Micromachines (Basel).* 10:593. doi: 10.3390/mi10090593

Chu, H., Puchulu-Campanella, E., Galan, J. A., Tao, W. A., Low, P. S., and Hoffman, J. F. (2012). Identification of cytoskeletal elements enclosing the ATP pools that

fuel human red blood cell membrane cation pumps. *Proc. Natl. Acad. Sci. U.S.A.* 109, 12794–12799. doi: 10.1073/pnas.1209014109

Clark, M. R., Mohandas, N., and Shohet, S. B. (1983). Osmotic gradient ektacytometry: comprehensive characterization of red cell volume and surface maintenance. *Blood* 61, 899–910. doi: 10.1182/blood.v61.5.899.bloodjournal615899

Conway, A. M., Vora, A. J., and Hinchliffe, R. F. (2002). The clinical relevance of an isolated increase in the number of circulating hyperchromic red blood cells. *J. Clin. Pathol.* 55, 841–844. doi: 10.1136/jcp.55.11.841

Cordasco, D., and Bagchi, P. (2017). On the shape memory of red blood cells. *Phys. Fluids* 29:041901. doi: 10.1063/1.4979271

Corry, W. D., Bresnahan, P. A., and Seaman, G. V. (1982). Evaluation of density gradient separation methods. *J. Biochem. Biophys. Methods* 7, 71–82. doi: 10.1016/0165-022x(82)90038-0

Cossins, A. R., and Gibson, J. S. (1997). Volume-sensitive transport systems and volume homeostasis in vertebrate red blood cells. *J. Exp. Biol.* 200, 343–352.

D'Alessandro, A., Blasi, B., D'amici, G. M., Marrocco, C., and Zolla, L. (2013). Red blood cell subpopulations in freshly drawn blood: application of proteomics and metabolomics to a decades-long biological issue. *Blood Transfus.* 11, 75–87. doi: 10.2450/2012.0164-11

Danielczok, J., Hertz, L., Ruppenthal, S., Kaiser, E., Petkova-Kirova, P., Bogdanova, A., et al. (2017). Does erythropoietin regulate TRPC channels in red blood cells? *Cell. Physiol. Biochem.* 41, 1219–1228. doi: 10.1159/000464384

Danon, D., and Marikovsky, V. (1964). Determination of density distribution of red cell population. *J. Lab. Clin. Med.* 64, 668–674.

Darrow, M. C., Zhang, Y., Cinquin, B. P., Smith, E. A., Boudreau, R., Rochat, R. H., et al. (2016). Visualizing red blood cell sickling and the effects of inhibition of sphingosine kinase 1 using soft X-ray tomography. *J. Cell Sci.* 129, 3511–3517. doi: 10.1242/jcs.189225

Dupire, J., Abkarian, M., and Viallat, A. (2015). A simple model to understand the effect of membrane shear elasticity and stress-free shape on the motion of red blood cells in shear flow. *Soft Matter* 11, 8372–8382. doi: 10.1039/c5sm01407g

Elliott, S. M. F., and Molineux, G. (eds.) (2009). *Erythopoietins, Erythropoietic Factors, and Erythropoiesis. Molecular, Cellular, Preclinical, and Clinical Biology*. Boston, MA: Birkenhäuser.

Fago, A., Forest, E., and Weber, R. E. (2001). Hemoglobin and subunit multiplicity in the rainbow trout (*Oncorhynchus mykiss*) hemoglobin system. *Fish Physiol. Biochem.* 24, 335–342.

Fairbanks, G., Palek, J., Dino, J. E., and Liu, P. A. (1983). Protein kinases and membrane protein phosphorylation in normal and abnormal human erythrocytes: variation related to mean cell age. *Blood* 61, 850–857. doi: 10.1182/blood.v61.5.850.850

Feng, G. H., Li, H. P., Li, Q. L., Fu, Y., and Huang, R. B. (2017). Red blood cell distribution width and ischaemic stroke. *Stroke Vasc. Neurol.* 2, 172–175. doi: 10.1136/svn-2017-000071

Fermo, E., Bogdanova, A., Petkova-Kirova, P., Zaninoni, A., Marcello, A. P., Makhro, A., et al. (2017). 'Gardos Channelopathy': a variant of hereditary Stomatocytosis with complex molecular regulation. *Sci. Rep.* 7:1744. doi: 10.1038/s41598-017-01591-w

Fischer, T. M. (2004). Shape memory of human red blood cells. *Biophys. J.* 86, 3304–3313. doi: 10.1016/s0006-3495(04)74378-7

Gallagher, P. G. (2005). Red cell membrane disorders. *Hematol. Am. Soc. Hematol. Educ. Program* 2005, 13–18.

Gilmore, I. S., Heiles, S., and Pieterse, C. L. (2019). Metabolic imaging at the single-cell scale: recent advances in mass spectrometry imaging. *Annu. Rev. Anal. Chem.* 12, 201–224. doi: 10.1146/annurev-anchem-061318-115516

Giustarini, D., Milzani, A., Dalle-Donne, I., and Rossi, R. (2008). Red blood cells as a physiological source of glutathione for extracellular fluids. *Blood Cells Mol. Dis.* 40, 174–179. doi: 10.1016/j.bcmd.2007.09.001

Gonzalez-Hidalgo, M., Guerrero-Pena, F. A., Herold-Garcia, S., Jaume, I. C. A., and Marrero-Fernandez, P. D. (2015). Red blood cell cluster separation from digital images for use in sickle cell disease. *IEEE J. Biomed. Health Inform.* 19, 1514–1525. doi: 10.1109/JBHI.2014.2356402

Grinberg, L., Fibach, E., Amer, J., and Atlas, D. (2005). N-acetylcysteine amide, a novel cell-permeating thiol, restores cellular glutathione and protects human red blood cells from oxidative stress. *Free Radic. Biol. Med.* 38, 136–145. doi: 10.1016/j.freeradbiomed.2004.09.025

Hajdu, S. I. (2003). A note from history: the discovery of blood cells. *Ann. Clin. Lab. Sci.* 33, 237–238.

Hanggi, P., Makhro, A., Gassmann, M., Schmugge, M., Goede, J. S., Speer, O., et al. (2014). Red blood cells of sickle cell disease patients exhibit abnormally high abundance of N-methyl D-aspartate receptors mediating excessive calcium uptake. *Br. J. Haematol.* 167, 252–264. doi: 10.1111/bjh.13028

Helms, C. C., Gladwin, M. T., and Kim-Shapiro, D. B. (2018). Erythrocytes and vascular function: oxygen and nitric oxide. *Front. Physiol.* 9:125. doi: 10.3389/fphys.2018.00125

Herold-Garcia, S., and Fernandes, L. F. (2019). New Methods for Morphological Erythrocytes Classification. *Conf. Proc. IEEE Eng. Med. Biol. Soc.* 2019, 4068–4071.

Hiebl, I., Weber, R. E., Schneeganss, D., and Braunitzer, G. (1989). High-altitude respiration of falconiformes. The primary structures and functional properties of the major and minor hemoglobin components of the adult White-Headed Vulture (*Trigonoceps occipitalis*, Aegypiinae). *Biol. Chem. Hoppe Seyler* 370, 699–706. doi: 10.1515/bchm3.1989.370.2.699

Hoffman, J. F., Dodson, A., and Proverbio, F. (2009). On the functional use of the membrane compartmentalized pool of ATP by the Na+ and Ca++ pumps in human red blood cell ghosts. *J. Gen. Physiol.* 134, 351–361. doi: 10.1085/jgp.200910270

Huisjes, R., Makhro, A., Llaudet-Planas, E., Hertz, L., Petkova-Kirova, P., Verhagen, L. P., et al. (2019). Density, heterogeneity and deformability of red cells as markers of clinical severity in hereditary spherocytosis. *Haematologica* 105, 338–347. doi: 10.3324/haematol.2018.188151

Inaba, M., and Maede, Y. (1988). Correlation between protein 4.1a/4.1b ratio and erythrocyte life span. *Biochim. Biophys. Acta* 944, 256–264. doi: 10.1016/0005-2736(88)90439-7

Inaba, M., and Maede, Y. (1992). The critical role of asparagine 502 in post-translational alteration of protein 4.1. *Comp. Biochem. Physiol. B* 103, 523–526. doi: 10.1016/0305-0491(92)90364-w

Iscove, N. N. (1977). The role of erythropoietin in regulation of population size and cell cycling of early and late erythroid precursors in mouse bone marrow. *Cell Tissue Kinet.* 10, 323–334. doi: 10.1111/j.1365-2184.1977.tb00300.x

Itkin, T., Gur-Cohen, S., Spencer, J. A., Schajnovitz, A., Ramasamy, S. K., Kusumbe, A. P., et al. (2016). Distinct bone marrow blood vessels differentially regulate haematopoiesis. *Nature* 532, 323–328. doi: 10.1038/nature17624

Jemaa, M., Fezai, M., Bissinger, R., and Lang, F. (2017). Methods employed in cytofluorometric assessment of eryptosis, the suicidal erythrocyte death. *Cell Physiol. Biochem.* 43, 431–444. doi: 10.1159/000480469

Jung, J., Matemba, L. E., Lee, K., Kazyoba, P. E., Yoon, J., Massaga, J. J., et al. (2016). Optical characterization of red blood cells from individuals with sickle cell trait and disease in Tanzania using quantitative phase imaging. *Sci. Rep.* 6:31698. doi: 10.1038/srep31698

Kaestner, L., Bogdanova, A., and Egee, S. (2020). "Calcium channels and calcium-regulated channels in human red blood cells," in *Calcium Signalling*, ed. S. Islam, (New York, NY: Springer).

Kaestner, L., Bollensdorff, C., and Bernhardt, I. (1999). Non-selective voltage-activated cation channel in the human red blood cell membrane. *Biochim. Biophys. Acta* 1417, 9–15. doi: 10.1016/s0005-2736(98)00240-5

Kaestner, L., and Egee, S. (2018). Commentary: voltage gating of mechanosensitive PIEZO channels. *Front. Physiol.* 9:1565. doi: 10.3389/fphys.2018.01565

Kaestner, L., Steffen, P., Nguyen, D. B., Wang, J., Wagner-Britz, L., Jung, A., et al. (2012). Lysophosphatidic acid induced red blood cell aggregation in vitro. *Bioelectrochemistry* 87, 89–95. doi: 10.1016/j.bioelechem.2011.08.004

Kaestner, L., Tabellion, W., Weiss, E., Bernhardt, I., and Lipp, P. (2006). Calcium imaging of individual erythrocytes: problems and approaches. *Cell Calcium* 39, 13–19. doi: 10.1016/j.ceca.2005.09.004

Kaestner, L., Wang, X., Hertz, L., and Bernhardt, I. (2018). Voltage-activated ion channels in non-excitable cells-a viewpoint regarding their physiological justification. *Front. Physiol.* 9:450. doi: 10.3389/fphys.2018.00450

Kaul, D. K., Fabry, M. E., Windisch, P., Baez, S., and Nagel, R. L. (1983). Erythrocytes in sickle cell anemia are heterogeneous in their rheological and hemodynamic characteristics. *J. Clin. Invest.* 72, 22–31. doi: 10.1172/jci110960

Kaul, D. K., Koshkaryev, A., Artmann, G., Barshtein, G., and Yedgar, S. (2008). Additive effect of red blood cell rigidity and adherence to endothelial cells in

inducing vascular resistance. *Am. J. Physiol. Heart Circ. Physiol.* 295, H1788–H1793. doi: 10.1152/ajpheart.253.2008

Kelley, L. L., Koury, M. J., Bondurant, M. C., Koury, S. T., Sawyer, S. T., and Wickrema, A. (1993). Survival or death of individual proerythroblasts results from differing erythropoietin sensitivities: a mechanism for controlled rates of erythrocyte production. *Blood* 82, 2340–2352. doi: 10.1182/blood.v82.8.2340.2340

Kihm, A., Kaestner, L., Wagner, C., and Quint, S. (2018). Classification of red blood cell shapes in flow using outlier tolerant machine learning. *PLoS Comput. Biol.* 14:e1006278. doi: 10.1371/journal.pcbi.1006278

Ko, E., Youn, J. M., Park, H. S., Song, M., Koh, K. H., and Lim, C. H. (2018). Early red blood cell abnormalities as a clinical variable in sepsis diagnosis. *Clin. Hemorheol. Microcirc.* 70, 355–363. doi: 10.3233/CH-180430

Kosower, E. M., and Kosower, N. S. (1995). Bromobimane probes for thiols. *Methods Enzymol.* 251, 133–148. doi: 10.1016/0076-6879(95)51117-2

Koury, M. J., and Bondurant, M. C. (1988). Maintenance by erythropoietin of viability and maturation of murine erythroid precursor cells. *J. Cell. Physiol.* 137, 65–74. doi: 10.1002/jcp.1041370108

Koury, M. J., and Bondurant, M. C. (1990). Erythropoietin retards DNA breakdown and prevents programmed death in erythroid progenitor cells. *Science* 248, 378–381. doi: 10.1126/science.2326648

Koury, M. J., and Bondurant, M. C. (1992). The molecular mechanism of erythropoietin action. *Eur. J. Biochem.* 210, 649–663. doi: 10.1111/j.1432-1033.1992.tb17466.x

Kucherenko, Y., Browning, J., Tattersall, A., Ellory, J. C., and Gibson, J. S. (2005). Effect of peroxynitrite on passive K+ transport in human red blood cells. *Cell. Physiol. Biochem.* 15, 271–280. doi: 10.1159/000087237

Kucherenko, Y. V., Wagner-Britz, L., Bernhardt, I., and Lang, F. (2013). Effect of chloride channel inhibitors on cytosolic Ca2+ levels and Ca2+-activated K+ (Gardos) channel activity in human red blood cells. *J. Membr. Biol.* 246, 315–326. doi: 10.1007/s00232-013-9532-0

Kunicka, J., Malin, M., Zelmanovic, D., Katzenberg, M., Canfield, W., Shapiro, P., et al. (2001). Automated quantitation of hemoglobin-based blood substitutes in whole blood samples. *Am. J. Clin. Pathol.* 116, 913–919.

La Manno, G., Soldatov, R., Zeisel, A., Braun, E., Hochgerner, H., Petukhov, V., et al. (2018). RNA velocity of single cells. *Nature* 560, 494–498. doi: 10.1038/s41586-018-0414-6

Landschulz, K. T., Boyer, S. H., Noyes, A. N., Rogers, O. C., and Frelin, L. P. (1992). Onset of erythropoietin response in murine erythroid colony-forming units: assignment to early S-phase in a specific cell generation. *Blood* 79, 2749–2758. doi: 10.1182/blood.v79.10.2749.bloodjournal79102749

Lanotte, L., Mauer, J., Mendez, S., Fedosov, D. A., Fromental, J. M., Claveria, V., et al. (2016). Red cells' dynamic morphologies govern blood shear thinning under microcirculatory flow conditions. *Proc. Natl. Acad. Sci. U.S.A.* 113, 13289–13294. doi: 10.1073/pnas.1608074113

Laybourne, R. C. (1974). Collision between a vulture and an aircraft at an altitude of 37,000 feet. *Wilson Bull.* 86, 461–462.

Lew, V. L., and Tiffert, T. (2013). The terminal density reversal phenomenon of aging human red blood cells. *Front. Physiol.* 4:171. doi: 10.3389/fphys.2013.00171

Lew, V. L., and Tiffert, T. (2017). On the mechanism of human red blood cell longevity: roles of calcium, the sodium pump, PIEZO1, and gardos channels. *Front. Physiol.* 8:977. doi: 10.3389/fphys.2017.00977

Lisovskaya, I. L., Shcherbachenko, I. M., Volkova, R. I., and Tikhonov, V. P. (2008). Modulation of RBC volume distributions by oxidants (phenazine methosulfate and tert-butyl hydroperoxide): role of Gardos channel activation. *Bioelectrochemistry* 73, 49–54. doi: 10.1016/j.bioelechem.2008.04.008

Liu, L., Liu, C., Quintero, A., Wu, L., Yuan, Y., Wang, M., et al. (2019). Deconvolution of single-cell multi-omics layers reveals regulatory heterogeneity. *Nat. Commun.* 10:470. doi: 10.1038/s41467-018-08205-7

Luthra, M. G., Friedman, J. M., and Sears, D. A. (1979). Studies of density fractions of normal human erythrocytes labeled with iron-59 in vivo. *J. Lab. Clin. Med.* 94, 879–896.

Lutz, H. U., and Bogdanova, A. (2013). Mechanisms tagging senescent red blood cells for clearance in healthy humans. *Front. Physiol.* 4:387. doi: 10.3389/fphys.2013.00387

Lutz, H. U., Stammler, P., Fasler, S., Ingold, M., and Fehr, J. (1992). Density separation of human red blood cells on self forming Percoll gradients: correlation with cell age. *Biochim. Biophys. Acta* 1116, 1–10. doi: 10.1016/0304-4165(92)90120-j

Macdougall, I. C., Cavill, I., Hulme, B., Bain, B., Mcgregor, E., Mckay, P., et al. (1992). Detection of functional iron deficiency during erythropoietin treatment: a new approach. *BMJ* 304, 225–226. doi: 10.1136/bmj.304.6821.225

Makhro, A., Haider, T., Wang, J., Bogdanov, N., Steffen, P., Wagner, C., et al. (2016a). Comparing the impact of an acute exercise bout on plasma amino acid composition, intraerythrocytic Ca(2+) handling, and red cell function in athletes and untrained subjects. *Cell Calcium* 60, 235–244. doi: 10.1016/j.ceca.2016.05.005

Makhro, A., Hanggi, P., Goede, J. S., Wang, J., Bruggemann, A., Gassmann, M., et al. (2013). N-methyl-D-aspartate receptors in human erythroid precursor cells and in circulating red blood cells contribute to the intracellular calcium regulation. *Am. J. Physiol. Cell Physiol.* 305, C1123–C1138. doi: 10.1152/ajpcell.00031.2013

Makhro, A., Huisjes, R., Verhagen, L. P., Manu-Pereira Mdel, M., Llaudet-Planas, E., Petkova-Kirova, P., et al. (2016b). Red cell properties after different modes of blood transportation. *Front. Physiol.* 7:288. doi: 10.3389/fphys.2016.00288

Mangani, M. (ed.) (1991). *Red Blood Cell Aging*. New York, NY: Plenum Press.

Mao, T. Y., Fu, L. L., and Wang, J. S. (2011). Hypoxic exercise training causes erythrocyte senescence and rheological dysfunction by depressed Gardos channel activity. *J. Appl. Physiol.* 111, 382–391. doi: 10.1152/japplphysiol.00096.2011

Mason, P. J., Bautista, J. M., and Gilsanz, F. (2007). G6PD deficiency: the genotype-phenotype association. *Blood Rev.* 21, 267–283. doi: 10.1016/j.blre.2007.05.002

Mauer, J., Mendez, S., Lanotte, L., Nicoud, F., Abkarian, M., Gompper, G., et al. (2018). Flow-induced transitions of red blood cell shapes under shear. *Phys. Rev. Lett.* 121:118103. doi: 10.1103/PhysRevLett.121.118103

Menzel, S., and Thein, S. L. (2019). Genetic modifiers of fetal haemoglobin in sickle cell disease. *Mol. Diagn. Ther.* 23, 235–244. doi: 10.1007/s40291-018-0370-8

Miccio, L., Memmolo, P., Merola, F., Netti, P. A., and Ferraro, P. (2015). Red blood cell as an adaptive optofluidic microlens. *Nat. Commun.* 6:6502. doi: 10.1038/ncomms7502

Minetti, G., Achilli, C., Perotti, C., and Ciana, A. (2018). Continuous change in membrane and membrane-skeleton organization during development from proerythroblast to senescent red blood cell. *Front. Physiol.* 9:286. doi: 10.3389/fphys.2018.00286

Minetti, G., Egee, S., Morsdorf, D., Steffen, P., Makhro, A., Achilli, C., et al. (2013). Red cell investigations: art and artefacts. *Blood Rev.* 27, 91–101. doi: 10.1016/j.blre.2013.02.002

Miura, O., D'andrea, A., Kabat, D., and Ihle, J. N. (1991). Induction of tyrosine phosphorylation by the erythropoietin receptor correlates with mitogenesis. *Mol. Cell. Biol.* 11, 4895–4902. doi: 10.1128/mcb.11.10.4895

Mock, D. M., Lankford, G. L., Widness, J. A., Burmeister, L. F., Kahn, D., and Strauss, R. G. (1999). Measurement of red cell survival using biotin-labeled red cells: validation against 51Cr-labeled red cells. *Transfusion* 39, 156–162.

Mohandas, N., and Groner, W. (1989). Cell membrane and volume changes during red cell development and aging. *Ann. N. Y. Acad. Sci.* 554, 217–224. doi: 10.1111/j.1749-6632.1989.tb22423.x

Mosca, A., Paleari, R., Modenese, A., Rossini, S., Parma, R., Rocco, C., et al. (1991). Clinical utility of fractionating erythrocytes into "Percoll" density gradients. *Adv. Exp. Med. Biol.* 307, 227–238. doi: 10.1007/978-1-4684-5985-2_21

Mueller, T. J., Jackson, C. W., Dockter, M. E., and Morrison, M. (1985). Use of an in vivo enrichment procedure to study membrane skeletal protein changes during red cell aging. *Prog. Clin. Biol. Res.* 195, 227–236.

Mueller, T. J., Jackson, C. W., Dockter, M. E., and Morrison, M. (1987). Membrane skeletal alterations during in vivo mouse red cell aging. Increase in the band 4.1a:4.1b ratio. *J. Clin. Invest.* 79, 492–499. doi: 10.1172/jci112839

Mugnano, M., Memmolo, P., Miccio, L., Merola, F., Bianco, V., Bramanti, A., et al. (2018). Label-free optical marker for red-blood-cell phenotyping of inherited anemias. *Anal. Chem.* 90, 7495–7501. doi: 10.1021/acs.analchem.8b01076

Nakamura, Y., Komatsu, N., and Nakauchi, H. (1992). A truncated erythropoietin receptor that fails to prevent programmed cell death of erythroid cells. *Science* 257, 1138–1141. doi: 10.1126/science.257.5073.1138

Narayan, A. D., Ersek, A., Campbell, T. A., Colon, D. M., Pixley, J. S., and Zanjani, E. D. (2005). The effect of hypoxia and stem cell source on haemoglobin

switching. *Br. J. Haematol.* 128, 562–570. doi: 10.1111/j.1365-2141.2004.05336.x

Oikonomidou, P. R., and Rivella, S. (2018). What can we learn from ineffective erythropoiesis in thalassemia? *Blood Rev.* 32, 130–143. doi: 10.1016/j.blre.2017.10.001

O'Neill, J. S., and Reddy, A. B. (2011). Circadian clocks in human red blood cells. *Nature* 469, 498–503. doi: 10.1038/nature09702

Parizadeh, S. M., Jafarzadeh-Esfehani, R., Bahreyni, A., Ghandehari, M., Shafiee, M., Rahmani, F., et al. (2019). The diagnostic and prognostic value of red cell distribution width in cardiovascular disease; current status and prospective. *Biofactors* 45, 507–516. doi: 10.1002/biof.1518

Pernow, J., Mahdi, A., Yang, J., and Zhou, Z. (2019). Red blood cell dysfunction: a new player in cardiovascular disease. *Cardiovasc. Res.* 115, 1596–1605. doi: 10.1093/cvr/cvz156

Perrotta, S., Gallagher, P. G., and Mohandas, N. (2008). Hereditary spherocytosis. *Lancet* 372, 1411–1426. doi: 10.1016/S0140-6736(08)61588-3

Peters, A. L., and van Noorden, C. J. (2017). Single cell cytochemistry illustrated by the demonstration of Glucose-6-phosphate dehydrogenase deficiency in erythrocytes. *Methods Mol. Biol.* 1560, 3–13. doi: 10.1007/978-1-4939-6788-9_1

Petkova-Kirova, P., Hertz, L., Danielczok, J., Huisjes, R., Makhro, A., Bogdanova, A., et al. (2019). Red blood cell membrane conductance in hereditary haemolytic anaemias. *Front. Physiol.* 10:386. doi: 10.3389/fphys.2019.00386

Piccinini, G., Minetti, G., Balduini, C., and Brovelli, A. (1995). Oxidation state of glutathione and membrane proteins in human red cells of different age. *Mech. Ageing Dev.* 78, 15–26. doi: 10.1016/0047-6374(94)01511-j

Piva, E., Brugnara, C., Chiandetti, L., and Plebani, M. (2010). Automated reticulocyte counting: state of the art and clinical applications in the evaluation of erythropoiesis. *Clin. Chem. Lab. Med.* 48, 1369–1380. doi: 10.1515/CCLM.2010.292

Prus, E., and Fibach, E. (2013). Heterogeneity of F cells in beta-thalassemia. *Transfusion* 53, 499–504. doi: 10.1111/j.1537-2995.2012.03769.x

Quint, S., Christ, A. F., Guckenberger, A., Himbert, S., Kaestner, L., Gekle, S., et al. (2018). 3D tomography of cells in micro-channels. *Appl. Phys. Lett.* 111:103701. doi: 10.1063/1.4986392

Reichel, F., Mauer, J., Nawaz, A. A., Gompper, G., Guck, J., and Fedosov, D. A. (2019). High-throughput microfluidic characterization of erythrocyte shape and mechanical variability. *bioRxiv* [Preprint]. doi: 10.1101/488189

Romero, P. J., and Romero, E. A. (1997). Differences in Ca2+ pumping activity between sub-populations of human red cells. *Cell Calcium* 21, 353–358. doi: 10.1016/s0143-4160(97)90028-2

Romero, P. J., and Romero, E. A. (1999). The role of calcium metabolism in human red blood cell ageing: a proposal. *Blood Cells Mol. Dis.* 25, 9–19.

Romero, P. J., Salas, V., and Hernandez, C. (2002). Calcium pump phosphoenzyme from young and old human red cells. *Cell Biol. Int.* 26, 945–949.

Rotordam, M. G., Fermo, E., Becker, N., Barcellini, W., Bruggemann, A., Fertig, N., et al. (2019). A novel gain-of-function mutation of Piezo1 is functionally affirmed in red blood cells by high-throughput patch clamp. *Haematologica* 104, e179–e183.

Sadafi, A., Koehler, N., Makhro, A., Bogdanova, A., Navab, N., Marr, C., et al. (2019). "Multiclass deep active learning for detecting red blood cell subtypes in brightfield microscopy," in *Medical Image Computing and Computer Assisted Intervention – MICCAI 2019 Lecture Notes in Computer Science*, ed. S. D. E. Al (Berlin: Springer).

Salvagno, G. L., Sanchis-Gomar, F., Picanza, A., and Lippi, G. (2015). Red blood cell distribution width: a simple parameter with multiple clinical applications. *Crit. Rev. Clin. Lab. Sci.* 52, 86–105. doi: 10.3109/10408363.2014.992064

Salvo, G., Caprari, P., Samoggia, P., Mariani, G., and Salvati, A. M. (1982). Human erythrocyte separation according to age on a discontinuous "Percoll" density gradient. *Clin. Chim. Acta* 122, 293–300.

Sass, M. D., Caruso, C. J., and O'connell, D. J. (1965). Decreased glutathione in aging red Cells. *Clin. Chim. Acta* 11, 334–340.

Schaefer, R. M., and Schaefer, L. (1995). The hypochromic red cell: a new parameter for monitoring of iron supplementation during rhEPO therapy. *J. Perinat. Med.* 23, 83–88.

Sinha, A., Chu, T. T., Dao, M., and Chandramohanadas, R. (2015). Single-cell evaluation of red blood cell bio-mechanical and nano-structural alterations upon chemically induced oxidative stress. *Sci. Rep.* 5:9768. doi: 10.1038/srep09768

Sparrow, R. L. (2017). Red blood cell components: time to revisit the sources of variability. *Blood Transfus.* 15, 116–125. doi: 10.2450/2017.0326-16

Spencer, J. A., Ferraro, F., Roussakis, E., Klein, A., Wu, J., Runnels, J. M., et al. (2014). Direct measurement of local oxygen concentration in the bone marrow of live animals. *Nature* 508, 269–273. doi: 10.1038/nature13034

Steffen, P., Jung, A., Nguyen, D. B., Muller, T., Bernhardt, I., Kaestner, L., et al. (2011). Stimulation of human red blood cells leads to Ca2+-mediated intercellular adhesion. *Cell Calcium* 50, 54–61. doi: 10.1016/j.ceca.2011.05.002

Suzuki, T., and Dale, G. L. (1988). Senescent erythrocytes: isolation of in vivo aged cells and their biochemical characteristics. *Proc. Natl. Acad. Sci. U.S.A.* 85, 1647–1651.

Swammerdam, J. (1737). *Bybel der Natuure of Historie der Insecten/Biblia Naturae sive Historia Insectorum*. Utrecht: De Banier.

Thein, S. L., and Craig, J. E. (1998). Genetics of Hb F/F cell variance in adults and heterocellular hereditary persistence of fetal hemoglobin. *Hemoglobin* 22, 401–414.

Thompson, C. J., Schilling, T., Howard, M. R., and Genever, P. G. (2010). SNARE-dependent glutamate release in megakaryocytes. *Exp. Hematol.* 38, 504–515. doi: 10.1016/j.exphem.2010.03.011

Tomari, R., Zakaria, W. N. W., Jamil, M. M. A., and Fuad, N. F. N. (2014). Computer aided system for red blood cell classification in blood smear image. *Proc. Comp. Sci.* 42, 206–213.

Tusi, B. K., Wolock, S. L., Weinreb, C., Hwang, Y., Hidalgo, D., Zilionis, R., et al. (2018). Population snapshots predict early haematopoietic and erythroid hierarchies. *Nature* 555, 54–60. doi: 10.1038/nature25741

Wang, J., Wagner-Britz, L., Bogdanova, A., Ruppenthal, S., Wiesen, K., Kaiser, E., et al. (2013). Morphologically homogeneous red blood cells present a heterogeneous response to hormonal stimulation. *PLoS One* 8:e67697. doi: 10.1371/journal.pone.0067697

Wang, P. F., Song, S. Y., Guo, H., Wang, T. J., Liu, N., and Yan, C. X. (2019). Prognostic role of pretreatment red blood cell distribution width in patients with cancer: a meta-analysis of 49 studies. *J. Cancer* 10, 4305–4317. doi: 10.7150/jca.31598

Weber, R. E., Hiebl, I., and Braunitzer, G. (1988). High altitude and hemoglobin function in the vultures *Gyps rueppellii* and *Aegypius monachus*. *Biol. Chem. Hoppe Seyler* 369, 233–240.

Wenk, R. E. (1976). Comparison of five methods for preparing blood smears. *Am. J. Med. Technol.* 42, 71–78.

Wesseling, M. C., Wagner-Britz, L., Boukhdoud, F., Asanidze, S., Nguyen, D. B., Kaestner, L., et al. (2016). Measurements of intracellular Ca2+ content and phosphatidylserine exposure in human red blood cells: methodological issues. *Cell. Physiol. Biochem.* 38, 2414–2425. doi: 10.1159/000445593

Woll, P. S., Kjallquist, U., Chowdhury, O., Doolittle, H., Wedge, D. C., Thongjuea, S., et al. (2014). Myelodysplastic syndromes are propagated by rare and distinct human cancer stem cells in vivo. *Cancer Cell* 25, 794–808. doi: 10.1016/j.ccr.2014.03.036

Yin, Y., Ye, S., Wang, H., Li, B., Wang, A., Yan, W., et al. (2018). Red blood cell distribution width and the risk of being in poor glycemic control among patients with established type 2 diabetes. *Ther. Clin. Risk Manag.* 14, 265–273. doi: 10.2147/TCRM.S155753

Zhou, S., Giannetto, M., Decourcey, J., Kang, H., Kang, N., Li, Y., et al. (2019). Oxygen tension-mediated erythrocyte membrane interactions regulate cerebral capillary hyperemia. *Sci. Adv.* 5:eaaw4466. doi: 10.1126/sciadv.aaw4466

Zhu, C., Shi, W., Daleke, D. L., and Baker, L. A. (2018). Monitoring dynamic spiculation in red blood cells with scanning ion conductance microscopy. *Analyst* 143, 1087–1093. doi: 10.1039/c7an01986f

Conflict of Interest: The authors declare that the research was conducted in the absence of any commercial or financial relationships that could be construed as a potential conflict of interest.

frontiers in Physiology

REVIEW
published: 20 May 2020
doi: 10.3389/fphys.2020.00435

Recent Advances in the Treatment of Sickle Cell Disease

Gabriel Salinas Cisneros[1,2] *and Swee L. Thein*[1]*

[1] Sickle Cell Branch, National Heart Lung and Blood Institute, National Institutes of Health, Bethesda, MD, United States,
[2] Division of Hematology and Oncology, Children's National Medical Center, Washington, DC, United States

Sickle cell anemia (SCA) was first described in the Western literature more than 100 years ago. Elucidation of its molecular basis prompted numerous biochemical and genetic studies that have contributed to a better understanding of its pathophysiology. Unfortunately, the translation of such knowledge into developing treatments has been disproportionately slow and elusive. In the last 10 years, discovery of *BCL11A*, a major γ-globin gene repressor, has led to a better understanding of the switch from fetal to adult hemoglobin and a resurgence of efforts on exploring pharmacological and genetic/genomic approaches for reactivating fetal hemoglobin as possible therapeutic options. Alongside therapeutic reactivation of fetal hemoglobin, further understanding of stem cell transplantation and mixed chimerism as well as gene editing, and genomics have yielded very encouraging outcomes. Other advances have contributed to the FDA approval of three new medications in 2017 and 2019 for management of sickle cell disease, with several other drugs currently under development. In this review, we will focus on the most important advances in the last decade.

Keywords: sickle cell disease, anti-sickling agents, gene editing, gene therapy, hemoglobinopathies

OPEN ACCESS

Edited by:
Lars Kaestner,
Saarland University, Germany

Reviewed by:
Carina Levin,
Ha'Emek Medical Center, Israel
Markus Schmugge,
University Children's Hospital Zurich, Switzerland

***Correspondence:**
Swee L. Thein
sl.thein@nih.gov

Specialty section:
This article was submitted to Red Blood Cell Physiology, a section of the journal Frontiers in Physiology

Received: *30 December 2019*
Accepted: *08 April 2020*
Published: *20 May 2020*

Citation:
Salinas Cisneros G and Thein SL (2020) Recent Advances in the Treatment of Sickle Cell Disease. Front. Physiol. 11:435. doi: 10.3389/fphys.2020.00435

INTRODUCTION

Sickle cell disease (SCD) is an inherited blood disorder that first appeared in the Western literature in 1910 when Dr. James Herrick described a case of severe malaise and anemia in a 20-year-old dental student from Grenada (Herrick, 1910). On examining his blood smear, he noticed many bizarrely shaped red blood cells, leading him to surmise that "…the cause of the disease may be some unrecognized change in the red corpuscle itself" (Herrick, 2014). More than 100 years later we recognize that the change in the red corpuscle is caused by a single base substitution in β-globin, and that the disease is not just present in the United States (US), but prevalent in regions where malaria was historically endemic, including sub-Saharan Africa, India, the Middle East, and the Mediterranean (Williams and Thein, 2018). Presence of SCD in the non-malarial regions is related to the recent migration patterns.

Currently, an estimated 300,000 affected babies are born each year, more than 80% of whom are in Africa. Due to recent population migrations, increasing numbers of individuals affected by SCD are encountered in countries that are not historically endemic for malaria, such as the US. It is estimated that 100,000 Americans are affected with SCD, the majority of whom are of African descent (Hassell, 2010, 2016). The numbers affected with SCD are predicted to increase exponentially; Piel et al. (2013) estimated that between 2010 and 2050, the overall number of births affected by SCD will be 14,242,000; human migration and further globalization will continue to expand SCD throughout the world in the coming decades. While 75% or more of newborns

with SCD in sub-Saharan Africa do not make their fifth birthday (McGann, 2014), in medium- to well-resourced countries almost all of affected babies can now expect to live to adulthood but overall survival still lags behind that of a non-SCD person by 20–30 years (Telfer et al., 2007; Quinn et al., 2010; Elmariah et al., 2014; Gardner et al., 2016; Serjeant et al., 2018). Despite these global prevalence figures, and the fact that SCD is by far the largest public health concern among the hemoglobinopathies, it was not until 2006 when the World Health Organization (WHO) recognized SCD as a global public health problem[1].

In 1949, Linus Pauling showed that an abnormal protein (hemoglobin S, HbS) was the cause of sickle cell anemia (SCA), making SCD the first molecular disease and motivating an enormous amount of scientific and medical research. Because of its genetic simplicity, SCA has been used to illustrate many of the advances in molecular genetics such as detection of a DNA mutation by restriction fragment enzyme analysis, and was used as proof of principle for the polymerase chain reaction (PCR) that we now take for granted (Wilson et al., 1982; Saiki et al., 1985).

In the last 50 years, tremendous progress has been made in understanding the pathophysiology and pathobiological complexities of SCD, but developing treatments has been disproportionately slow and elusive; a history of Perils and Progress, so succinctly summarized by Wailoo (2017). We are confident that in the next 30 years, the therapeutic landscape for SCD will change due to a combination of recent advancements in genetics and genomics, an increase in the number of competing clinical trials, and also an increased awareness from the funding bodies, in particular the NIH, USA.

Here, after a brief review of the pathophysiology, we will focus on the advances in treatment of SCD that have occurred in the last 10 years and that have reached phase 2/3 of clinical trials (**Figure 1**).

PATHOPHYSIOLOGY OF SICKLE CELL DISEASE

Sickle cell disease is caused by an abnormal HbS ($\alpha_2\beta^S{}_2$) in which glutamic acid at position 6 of the β-globin chain of hemoglobin is changed to valine. Goldstein et al. (1963) showed that this amino acid substitution arose from a single base change (A>T) at codon 6 (*rs334*). The genetic causes of SCD include homozygosity for the *rs334* mutation (HbSS, commonly referred as SCA) and compound heterozygosity between *rs334* and mutations that lead to either other structural variants of β-globin (such as HbC, causing HbSC) or reduced levels of β-globin production as in β-thalassemia (causing HbS/β-thalassemia). In patients of African ancestry, HbSS is the most common cause of SCD (65–70%), followed by HbSC (about 30%), with HbS/β-thalassemia being responsible for most of the rest (Steinberg et al., 2001). SCA in which the intracellular concentration of HbS is almost 100%, is by far the most severe and well described (Brittenham et al., 1985). The majority of the therapeutic developments and interventions have focused on this genotype, which is also the focus of this review, although they also impact the other SCD genotypes.

The fundamental event that underlies the complex pathophysiology and multi-systemic consequences of SCD is the polymerization of HbS that occurs under low oxygen tension (**Figure 2**). Polymerization of the de-oxygenated HbS alters the structure and function of the red blood cells (RBCs). These damaged (typically sickled shaped) RBCs are not only less flexible compared to normal RBCs, but also highly adhesive. Repeated cycles of sickling and unsickling shortens the lifespan of the damaged sickle RBCs to about 1/6th that of normal RBCs (Bunn, 1997; Hebbel, 2011). The outcome is the occlusion of blood vessels in almost every organ of the body and chronic hemolytic anemia, the two hallmarks of the disease, that result in recurrent episodic acute clinical events, of which acute pain is the most common, and accumulative organ damage. Acute sickle pain is so severe that it is often referred to as "vaso-occlusive sickle crisis" or VOC.

These events trigger a cascade of pro-inflammatory activity setting off multiple pathophysiological factors that also involve neutrophils, platelets, and vascular endothelium (Sundd et al., 2019). The continual release of cell-free hemoglobin from hemolysis depletes hemopexin and haptoglobin, a consequence of which is the reduced bioavailability of nitric oxide (NO), and vascular endothelial dysfunction that underlies the chronic organ damage in SCD pathology.

The sickle red blood cells do not just interact with the vascular endothelium but trigger activation of neutrophils, monocytes and platelets. During steady-state, patients with SCD have above normal values of neutrophils, monocytes and platelets which further increase during acute events (Villagra et al., 2007). Neutrophilia has been consistently correlated with SCD severity (Ohene-Frempong et al., 1998; Miller et al., 2000); neutrophils play a central role in vaso-occlusion through their interactions with both erythrocytes and endothelium upregulating expression of cytoadhesion molecules such as P- and E-selectins, current therapeutic targets (Zhang et al., 2016).

Platelets, when activated, form aggregates with erythrocytes, monocytes, and neutrophils both in patients and in murine models (Wun et al., 1997; Zhang et al., 2016). As with neutrophils, it appears that platelet aggregation is dependent on P-selectin. As part of this constant inflammatory state, the coagulation cascade is also hyperactivated in SCD. The repeated interaction between RBCs and endothelium promote expression of pro-adhesive and procoagulant proteins evidenced by increased levels of plasma coagulation factors, tissue factor (TF) and interactions between monocyte-endothelium, platelet-neutrophil and platelet-RBC. Patients with SCD have increased rates of venous and arterial thrombotic events (Brunson et al., 2017).

Unraveling these pathophysiological targets has provided insights on clinical trials on anti-platelet and anti-adhesion agents, as well as anti-coagulation factors for the prevention of acute VOC pain in SCD (Telen, 2016; Nasimuzzaman and Malik, 2019; Telen et al., 2019). A case in point is the development of an anti-P-selection molecule (Crizanlizumab) for treatment of sickle VOC, recently approved by the FDA in November 2019 and marketed as Adakveo®.

[1]https://apps.who.int/iris/handle/10665/20890

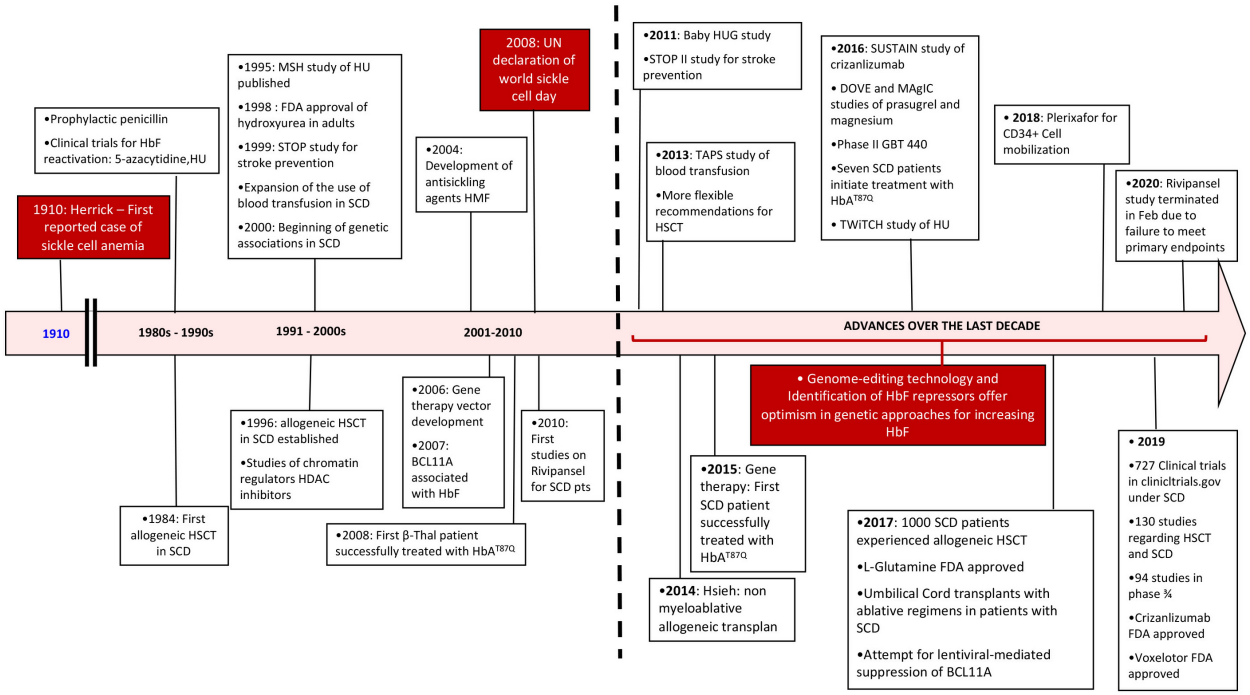

FIGURE 1 | Timeline review of historic events since the diagnosis of sickle cell disease with an emphasis over the last decade. SCD, sickle cell disease; HSCT, hematopoietic stem cell transplant; HU, hydroxyurea.

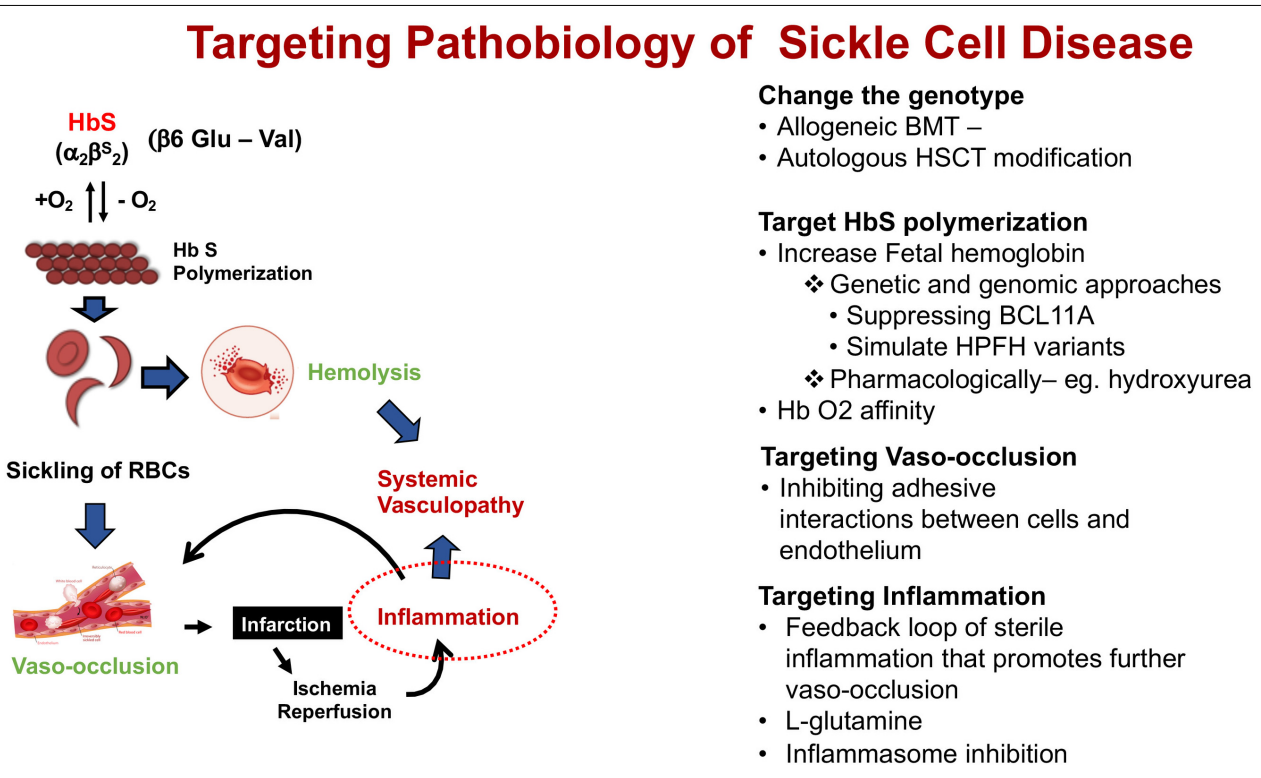

FIGURE 2 | Schematic pathophysiology review of sickle cell disease and its main different targets for intervention. Hb S, hemoglobin S.

New therapeutic approaches that use drugs to ameliorate the downstream sequelae of HbS polymerization have not proved to be as effective as hydroxyurea (HU) which has an "anti-sickling" effect via induction of fetal hemoglobin (HbF, $\alpha 2\gamma 2$) (Ware and Aygun, 2009). Other effects of HU include improvement of RBC hydration, reduction of neutrophil count, reduction of leucocyte adhesion, and reduction of pro-inflammatory markers, all of which add to the clinical efficacy of HU. In addition, HU also acts as NO donor, promoting vasodilation (Cokic et al., 2003). Increasing HbF is highly effective because it dilutes the intracellular HbS concentration, thereby increasing the delay time to HbS polymerization (Eaton and Bunn, 2017); in addition to which, the γ-chains also have an inhibitory effect on the polymerization process. Hydroxyurea, however, is only partially successful because the increase in fetal hemoglobin is uneven and not present in all cells. Nonetheless, the well-established clinical efficacy of HbF increase, substantiated by numerous clinical and epidemiological studies, has motivated both pharmacological and genetic approaches to induce HbF (Nevitt et al., 2017).

A more detailed understanding of the switch from fetal to adult hemoglobin, and identification of transcriptional regulators such as BCL11A, aided by the developments in genetic and genomic platforms, provide hope that genomic-based approaches for therapeutic reactivation of HbF may soon be possible (Vinjamur et al., 2018). In the meanwhile, a gene addition approach that infects the patient's stem cells with a virus expressing an anti-sickling β-globin variant, T87Q, shows great promise (Negre et al., 2016; Ribeil et al., 2017). The most successful "curative" approach so far, is transplantation with stem cells from an immunologically matched sibling but this is severely limited by the lack of availability of matched donors (Walters et al., 1996a; Gluckman et al., 2017).

Parallel to the new medications being developed blood transfusions with normal red blood cells, remain an effective and increasing therapeutic option for managing and preventing SCD complications, but this strategy has limitations (not uniformly accessible, accompanied by risks of alloimmunization, hemolytic transfusion reactions and transfusional iron overload). Blood transfusion improves the oxygen-carrying capacity and improves microvascular perfusion by decreasing the HbS percentage. A major complication of blood transfusion is hemolytic transfusion reactions that occur primarily in RBC alloimmunized patients and SCD patients, in particular, are at high risk because of the mismatch in donor pool (predominantly Northern European descent) while SCD patients are predominantly of African descent (Vichinsky et al., 1990; Thein et al., 2020). Limiting blood from ethnic-matched donors has reduced but did not eliminate alloimmunization (Chou et al., 2013), and a major cause is the mismatch between serologic Rh phenotype and *RHD* or *RHCE* genotype due to variant *RH* alleles in a large proportion of the individuals (Chou et al., 2013). *RH* genotyping in addition to serologic typing may be required to identify the most compatible RBCs and recent studies have shown that a prospective rather than reactive (after appearance of allo-antibodies) genotyping approach may be feasible (Chou et al., 2018, 2020; Hendrickson and Tormey, 2018). Until prospective genotyping of RBC antigens become a practical feasibility, as a prevention, many blood transfusion centers have adopted extended red cell phenotyping, including ABO, Rh, Kell, Kidd, Duffy, and S and s antigens, and some centers have also adopted molecular genotyping for red blood cell phenotype prediction using microarray chips (e.g., the PreciseType HEA BeadChip assay). It should be noted that, while blood transfusion remains an important therapeutic option in SCD, evidence for its role in management of acute or chronic complications is lacking except for prevention of primary and secondary strokes (Howard, 2016). Supportive evidence for the role of preoperative transfusion in patients with HbSS or HbS/β^0-thalassemia was demonstrated in the Transfusion Alternatives Preoperatively in Sickle Cell disease (TAPS) study (Howard et al., 2013).

Insight on the pathophysiology of SCD (**Figure 2**) has allowed different targets for interventions in patients with SCD summarized under four categories of its pathobiology – (1). Modifying the genotype, (2). Targeting HbS polymerization, (3). Targeting vasocclusion, and (4). Targeting inflammation.

Understanding of the kinetics of HbS polymerization suggest that there are many ways to inhibit HbS polymerization (Eaton and Bunn, 2017) other than induction of HbF (**Table 1**). One approach is to increase oxygen affinity of the hemoglobin molecule, an example is Oxbryta^{TM} (Voxelotor/GBT440) (Vichinsky et al., 2019) that was recently approved by the FDA in November 2019, making this the second anti-sickling agent.

One of the biggest challenges in managing SCD is the clinical complexity and extreme variable clinical course that cannot be explained by the specific disease genotype. Patients with identical sickle genotype still display extreme clinical course; both acquired and inherited factors contribute to this clinical complexity of SCD (Gardner and Thein, 2016). Although laboratory prognostic factors (HbF, hemoglobin, reticulocyte count, leukocytosis) and clinical phenotypes (such as stroke/TIA, acute chest syndrome/pulmonary hypertension, avascular necrosis, kidney injury, or skin ulcers) have been described and analyzed, classifying disease severity remains complex and should be assessed individually. Prediction of disease severity and clinical course of SCD has been the topic of many reviews and, to date there is no clear algorithm using genetic and/or imaging, and/or laboratory markers that can reliably predict mortality risk in SCD (Quinn, 2016).

CURRENT ADVANCES IN THERAPY

(1) Modifying the Patient's Genotype

Modifying the patient's genotype via hemopoietic stem cell transplantation (HSCT) was first reported to be performed over 30 years ago in an 8-year-old child who had SCD (HbSS) with frequent VOCs; she subsequently developed acute myeloid leukemia. The patient received HSCT for the acute myeloid leukemia from an HLA-matched sister who was a carrier for HbS (HbAS). She was cured of her leukemia and at the same time, her sickle cell complications also resolved (Johnson et al., 1984; Johnson, 1985). Until then, HSCT had not been considered as a therapeutic option for SCD. This successful HSCT demonstrated

TABLE 1 | Current advances on therapy for sickle cell disease.

Changing the genotype		
(1) Allogeneic stem cell transplant	Myeloablative regimens (MAC), reduced intensity regimens (RIC), and non-myeloablative regimens (NMA)	50 clinical trials listed in ClinicalTrials.gov
(2) Autologous transplant		10 clinical trials listed in ClinicalTrials.gov
	a) Gene therapy	
	Lentiviral strategies (NCT02247843, NCT02140554, NCT02186418)	
	Inducing fetal hemoglobin	Downregulation of *BCL11*A (NCT03282656) Globin chromatin structure manipulation Downregulating beta^S globin expression
	b) Gene editing	
	Using zinc finger nucleosomes (ZFN), transcription activator-like effector nucleases (TALENs), CRISPR/Cas9 techniques (NCT03745287)	Downregulation of *BCL11*A Reactivation of HbF by HPFH mutations Globin gene repair
Hemoglobin S polymerization	Hydroxyurea (FDA approved)	Ribonucleotide diphosphate reductase inhibitor
	LBH589/Panobinostat (NCT01245179)	Pan histone deacetylase inhibitor
	Voxelotor/GBT440 (NCT03036813) (FDA approved)	α-Globin reversible binding
	Decitabine/THU (NCT01685515)	DNMT1 inhibition
	Sanguinate (NCT02411708)	Targeting carbon monoxide delivery
	IMR-687 (NCT04053803)	Phosphodiesterase 9 inhibitor
Vasocclusion	L-Glutamine (FDA approved)	Increase NADH and NAD redox potential
	Crizanlizumab (NCT03264989) (FDA approved)	P-selectin inhibitor
	Heparinoids: Sevuparin (NCT02515838)	P-selectin and L-selectin inhibitor
	Poloxamer and Vepoloxamer	Nonionic block copolymer surfactant
Inflammation	Prasugrel, ticagrelor (NCT02482298)	P2Y2 inhibitors
	Intravenous immunoglobulin (NCT01783691)	Effects on neutrophils and monocytes activation
	Simvastatin (NCT03599609)	Vascular endothelium
	Rivaroxaban (NCT02072668)	Anti factor Xa
	N-Acetylcysteine (NCT01800526)	Oxidative stress reduction

HbF, hemoglobin F; HPFH, hereditary persistence of fetal hemoglobin; THU, tetrahydrouridine; DNMT1, DNA methyltransferase type 1.

that reversal of SCD could be achieved without complete reversal of the hematological phenotype to HbAA, and paved the way for bone marrow transplant (BMT) as a curative option for children with severe SCD (Walters et al., 1996b).

The conclusion was that, as long as stable mixed hemopoietic chimerism after BMT can be achieved, patients can be cured of their SCD without complete replacement of their bone marrow (Walters et al., 2001).

Allogeneic Bone Marrow Transplant

Hematopoietic stem cell transplant (HSCT) has now become an important therapeutic option for patients with SCD. Currently there are about 35 clinical trials at ClinicalTrials.gov studying allogeneic BMT in patients with SCD. As described by Walters et al. (2010), HSCT can establish donor-derived erythropoiesis, but even more importantly, can stabilize or even restore function in affected organs of patients with SCD when performed in time.

Between 1986 and 2013, 1,000 patients received HLA-identical matched sibling donor (MSD) HSCTs (Gluckman et al., 2017). The outcomes for both children and adults were excellent, demonstrating 93% overall survival. Eighty seven percent of the patients received myeloablative chemotherapy (MAC) and the rest (13%) received reduced intensity chemotherapy (RIC). It is important to note that patients 16 years or older had worse overall survival (95% vs. 81% $p = 0.001$) and a higher probability of graft versus host disease (GVHD)-free survival (77% vs. 86% $p = 0.001$). These results should encourage physicians to provide early referrals to SCD patients for transplant evaluation so that the donor search can be started in a timely matter (Gluckman et al., 2017).

Although myeloablative conditioning has achieved high rates of overall and event free survival, the conditioning is too toxic for adult patients with pre-existing organ dysfunction. Reversal of the sickle hematology without complete replacement of the patient's bone marrow led to the development of less intense conditioning regimens expanding allogeneic transplantation in adult patients, who otherwise would not be able to tolerate the intense myeloablative conditioning. Donors could be HbAA or HbAS, and in order to reverse the sickle hematological genotype, the myeloid donor chimerism has to be >20% (Fitzhugh et al., 2017).

In an international, multicenter study, 59 patients had MSD HSCT, of which 50 survived and were cured of SCD. Of the nine patients that had a negative outcome, five had graft rejection and four intracranial hemorrhage. Thirteen patients developed

mixed chimerism. Of those patients that developed mixed chimerism, there was no GVHD or disease recurrence/graft rejection. Patients with stable mixed chimerism did not have worse outcomes related to complications of SCD. Hsieh et al. (2009) developed a protocol for non-myeloablative HSCT with low dose total body radiation, alemtuzumab, and sirolimus. In the initial 10 patients with SCD, nine had long-term, stable, mixed donor chimerism and reversal of their sickle cell phenotype (Hsieh et al., 2009). An updated report showed that 87% of the 30 patients had long-term stable donor engraftment without acute or chronic graft-versus-host disease (Clinical trials [NCT00061568]) (Walters et al., 2001; Hsieh et al., 2014). More recent data reported at least 95% cure rate in 234 children and young adults (<30 years) with SCA after MSD with no increased mortality compared to SCA itself and better quality of life. The data also showed that myeloablative HSCT can be a safe option for patients <15 years old if a MSD is available unless there is a clear and strong recommendation not to undergo transplant (Bernaudin et al., 2020).

However, in the US, less than 15% of patients with SCD have HLA- matched siblings as donors, but a promising alternative donor source is haplo-identical family members. Studies are now underway in several centers to find a balance of conditioning regime that provides adequate immunosuppression without rejection and minimal GVHD (Joseph et al., 2018). Matched unrelated donors (MUD) have shown promising results in patients with thalassemia major and are currently being evaluated in patients with SCD (Fitzhugh et al., 2014). One of the main limitations, unfortunately, is the low probability of finding suitable donors for African and African American populations as per the National Marrow Donor Program and so, not sufficient MUD transplants have been completed in patients with SCD. HLA-haploidentical HSCT following RIC has been reported to show promising results with prolonged and stable engraftment, but for both unrelated umbilical cord blood (UCB) and haploidentical HSCT, rejection remains a major obstacle in the context of RIC (Bolanos-Meade et al., 2012; Angelucci et al., 2014; Fitzhugh et al., 2014; Saraf et al., 2018; Bolanos-Meade et al., 2019).

Although encouraging options with promising results in clinical trials, acute and chronic GVHD remain major complications which can be life threatening and have severe effects on quality of life. Multiple factors affect the development of GVHD in patients undergoing transplant, including the source of the stem cells, the intensity of immunosuppression in the conditioning regime (dose of anti-thymoglobulin) and the mismatch status of the donor to the recipient (Shenoy, 2013; Inamoto et al., 2016; Bernaudin et al., 2020).

Acute GVHD remains a concern in patients receiving mismatched donor transplants but UCB continues to show reduced rates of chronic GVHD (Kamani et al., 2012). Reduced-intensity conditioning regimens have also been studied in related and unrelated HSCT, and while a suitable option for patients with a matched sibling, patients with unrelated donor should be made aware of the not-so-favorable short and long-term outcomes (Guilcher et al., 2018).

As new transplant modalities emerge with less transplant related mortality, better immunomodulators to prevent GVHD are being developed and graft rejection has become less frequent and accepted indications for HSCT have become less restrictive (**Table 2**). Nonetheless, clinicians continue to have reservation toward transplant and tend to delay the referral to a HSCT specialist because of concerns for GVHD, mortality/morbidity related to transplant itself and the risk of graft rejection, which has not been eliminated completely (Leonard and Tisdale, 2018). An ongoing clinical trial will compare 2-year overall survival and outcomes related to SCD in patients that undergo transplant compared with current standard of care (ClinicalTrail.gov Identifier: NCT02766465).

In allogeneic transplant, the source of hematopoietic stem cells (HSCs) is from a donor (matched sibling, haplo-identical family members, UCB or MUD). Allogeneic BMT using HSCs from the latter 3 donor sources are still risky; and donor availability presents a huge limitation. These limitations can be overcome by autologous transplant, in which the patient receives his own cells after being modified by gene therapy.

TABLE 2 | Indications for HSCT balanced with donor availability: Risk/benefit ratio considerations.

Matched sibling donor	Matched unrelated donor or minimally mismatched good quality cord product	Mismatched marrow donor, haploidentical donor
• Stroke • Elevated TCD velocity • Acute chest syndrome • VOC • Pulmonary Hypertension/tricuspid regurgitation jet velocity.2.5 m/s • Osteonecrosis/AVN • Red cell alloimmunization • Silent stroke specially with cognitive impairment • Recurrent priapism • Sickle nephropathy	• Stroke • Elevated TCD velocity • Recurrent acute chest syndrome despite supportive care • Recurrent severe VOC despite supportive care • Red cell alloimmunization despite intervention plus established indication for chronic transfusion therapy • Pulmonary hypertension	• Recurrent stroke despite adequate chronic transfusion therapy • Inability to tolerate supportive care though strongly indicated, e.g., red cell alloimmunization, severe VOC and inability to take hydroxyurea

HSCT, hematopoietic stem cell transplantation; AVN, avascular necrosis; TCD, transcranial doppler; VOC, vaso-occlusive crisis.

Autologous Hematopoietic Stem Cell Transplant Modification: Gene Editing or Gene Therapy

Genetically engineered autologous cells eliminate the need to find a HSCT donor, and thus available to all patients. Since these are the patient's own stem cells, there is no need for immunosuppression, thus eliminating the risks of GVHD and immune-mediated graft rejection (Esrick and Bauer, 2018; Orkin and Bauer, 2019).

Sickle cell disease patients represent a special and complicated population for this therapy for two major reasons. First, patients that undergo autologous stem cell transplant require collection of hematopoietic stem cells (CD34+) and the traditional method of collection is a bone marrow harvest done by a specialist but in patients with SCD this process yields CD34+ cells with suboptimal quantity and quality requiring multiple harvests, each harvesting procedure increasing the risk of triggering acute pain crisis. Second, the current gold standard procedure for cell mobilization is with granulocyte-colony stimulating factor (G-CSF) but this is contraindicated in patients with SCD due to risk of causing complications such as pain crisis, acute chest syndrome, and even death, from the increased white cell counts.

Recently, great advances have been made in using an alternative approach for harvesting CD34+ cells using Plerixafor. Plerixafor acts by reversibly blocking the binding between chemokine CXC-receptor 4 (CXCR4) and the stromal cell derived factor-1α triggering the mobilization of progenitor cells into the peripheral blood. It allows peripheral mobilization of stem cells by releasing CD34+ cells from the bone marrow niches, without the massive increase in white blood cells. Its development has been crucial in optimization of CD34+ collection in patients with SCD. Results have shown appropriate mobilization of CD34+ cells 6 h after a single dose of Plerixafor and are of higher quality and purity, decreasing the need for multiple bone marrow harvests and the associated stress/pain. Associated with hyper-transfusion therapy, it has become the preferred way of marrow stimulation to yield appropriate hematopoietic stem/progenitor cells in patients with SCD (Boulad et al., 2018; Esrick et al., 2018; Hsieh and Tisdale, 2018; Lagresle-Peyrou et al., 2018).

The genetic defect in the sickle HSPCs can be corrected via several approaches.

(A) Gene addition using lentiviral vector-based strategies

(a) Anti- or non-sickling strategies: Several gene therapies based on gene addition using viral vectors to carry therapeutic genes in HSCs are being actively developed with curative purposes. Gene addition strategies that have reached clinical trials include a promising one where the patient's stem cells are infected with a lentivirus expressing an anti-sickling β-globin variant, T87Q. The unique feature of this vector is that the amino acid substitution (β^{A-T87Q}) allows for high performance liquid chromatography (HPLC) monitoring of the transgene globin levels in the patient's cells (Cavazzana-Calvo et al., 2010). The first SCD patient who received this Bluebird vector (protocol HGB-205) was reported in 2017; engraftment was stable with no sickle cell crises reported at 15 months of follow up (Ribeil et al., 2017), with further undergoing studies (ClinicalTrials.gov Identifier: NCT02140554, NCT03282656). Other approaches to anti-sickling gene therapy in erythroid-specific lentiviral vectors include utilizing a β-globin gene with three specific point mutations that confer anti-sickling properties (ClinicalTrials.gov Identifier: NCT02247843) or the introduction of a γ-globin coding sequence in a β-globin gene to increase HbF levels and decrease HbS (ClinicalTrials.gov Identifier: NCT02186418) (Cavazzana et al., 2017). Thus far, the most promising of these LV vectors is the one utilizing anti-sickling β-globin variant, T87Q.

(b) Hb F induction: The well-established efficacy of increasing HbF has motivated both pharmacological and genetic approaches to HbF induction.

A gene addition approach that is already in clinical trials (ClinicalTrials.gov Identifier: NCT03282656) utilizes a lentiviral mediated erythroid specific short hairpin RNA (shRNA) for BCL11A. This shRNA is modified to target the specific gene and downregulate its expression (Brendel et al., 2016). As of December 2018, three adults have been enrolled, utilizing plerixafor mobilized HSC, all three patients showed prompt neutrophil engraftment, and at 2 months follow up, the average HbF was 30% (ASH abstract #1023 – 2018 ASH conference). Other lentiviral therapies using zinc-finger nucleases (ZFN) directed against the γ-globin promoter have been proposed. This would force an interacting loop between the LCR and γ-globin which would reactivate γ-globin production, increasing HbF and decreasing HbS production at the same time. These lentiviral-based approaches still need preclinical *in vivo* studies to address safety and specificity before they can be considered in human patients (Breda et al., 2016; Orkin and Bauer, 2019).

Viral vectors, such as lentivirus, are a great tool for gene therapy but these results underscore the need to develop gene transfer protocols that ensure efficient and consistent delivery of the therapeutic globin gene cargo to HSC. Their major limitations include:

(1) Their immunogenicity which can create an inflammatory response in the donor which can lead to degeneration of the transducted tissue, (2) they can produce non-specific toxins, (3) due to the semi-random integration to the genome, there is a theoretical risk of insertional mutagenesis, (4) they have limitations of transgenic capacity size. An additional challenge in SCD is the ability to maintain a persistent myeloid donor chimerism of >20% to prevent return of SCD symptoms (Fitzhugh et al., 2017). Due to these limitations, long-term monitoring of patients to evaluate both safety and efficacy is necessary. Until now, over the last decade of clinical trials, no genotoxicity secondary to LV vectors has been reported but the main challenge has been to keep the myeloid donor chimerism above the 20% threshold (Nayerossadat et al., 2012).

(B) Gene editing

Gene-editing corrects a specific defective DNA in its native location. SCD with its simple single base change presents a very attractive prototype. Over the last couple of decades, there has been a spectacular growth of such strategies, setting the scene for developing therapies that could precisely genetically

correct a single base mutation in patient with SCD. These strategies include ZFNs, transcription activator-like effector nucleases (TALENs) and the clustered regularly interspaced short palindromic repeat (CRISPR)-associated nuclease Cas9 approach which is the most advanced of the three. The CRISPR-Cas9 technology typically make a double-stranded break (DSB) in a particular genomic sequence directed to that site by a guide RNA. The most common method of DSB repair is non-homologous end joining, often resulting in gene disruption or knockout. This strategy is currently being tested in a clinical trial (ClinicalTrials.gov Identifier: NCT03745287) in which the patient's own *BCL11A* gene (a major inhibitor of γ-globin gene expression) is disrupted to induce HbF expression. BCL11A also has roles in lymphoid and neurological development but gene-editing for SCD exploits the erythroid-specific enhancers in intron 2 of the gene (Bauer et al., 2013; Brendel et al., 2016). CRISPR-Cas9 technology is also being explored to mimic the rare, genetic variants that promote expression of the γ-globin genes as in hereditary persistence of fetal hemoglobin (Traxler et al., 2016; Wienert et al., 2018). Disrupting the putative binding sites for γ-globin repressors like BCL11A to induce HbF production will be an attractive therapeutic strategy for both β-thalassemic and SCD patients (Masuda et al., 2016; Liu et al., 2018; Martyn et al., 2018). The ultimate challenge, however, is to genetically correct the mutation, a single nucleotide change in the codon of the globin gene from GAG to GTG, by providing a homology template with the correct sequence at the sixth codon. Although this has been completed in preclinical studies, current techniques do not allow for specific transversion mutations like those required to cure SCD in humans (Dever et al., 2016; Orkin and Bauer, 2019). The enormous selective advantage of red blood cells with normal hemoglobin or anti-sickling hemoglobin predicts that genetic modification of a proportion of HSCs (estimated 10–20%) may suffice as a one-off treatment (Fitzhugh et al., 2017). Before gene therapy can become a reality, however, many hurdles need to be overcome; genetically manipulated HSCs need to be able to retain long-term repopulating potential; pre-transplant conditioning is toxic and needs to be modified to reduce the morbidity. A clinical trial exploring antibody-mediated non-chemotherapy conditioning is being evaluated in patients with severe combined immunodeficiency, in an attempt to reduce the exposure to chemotherapy and its toxicities is currently recruiting patients (ClincialTrials.gov Identifier: NCT02963064). Further understanding of this technology could represent a new option for patients with SCD.

Although different gene strategies have reached clinical trials showing promising results they remain in early phases of development and allogeneic HSCT remain the only curative treatment modality for SCD. For the majority of patients without a MSD, haploidentical HSCT with recent promising data of improved overall survival presents an alternative for curative therapy. Multiple gene therapy strategies utilizing patient's own stem cells, are also being pursued, but this has the disadvantage of myeloablative conditioning (Leonard et al., 2020).

In addition to great advances in HSCT and gene therapy, new pharmacological anti-sickling approaches have developed.

(2) Targeting Hemoglobin S Polymerization

Approaches targeting HbS polymerization presents a very attractive strategy as this "puts out the fire" rather than dealing with the sequelae of the sickling event (Eaton and Bunn, 2017). HbF has long been known to have a major beneficial effect in SCD – increased intracellular HbF not only dilutes the intracellular HbS concentration but inhibits sickling as the mixed hybrid tetramers do not partake in HbS polymerization. Hydroxyurea (HU) works via induction of fetal hemoglobin (HbF, $\alpha 2\gamma 2$) synthesis, but hydroxyurea is only partially successful as the increase in HbF is uneven and not equally present in all the red blood cells (Ware, 2015). Nonetheless, use of HU therapy in SCD has expanded substantially in recent years. Follow on studies include demontration of its efficacy and safety in the pediatric population (BABY HUG) (Wang et al., 2011), the Transcranial doppler with Transfusion Changing to Hydroxyurea Study (TWiTCH) that showed HU was comparable to blood transfusions for primary stroke prevention (Ware et al., 2016) although the Stroke with Transfusion Changing to Hydroxyurea study (SWiTCH) concluded that HU is not comparable to blood transfusion in secondary stroke prevention (Ware et al., 2011).

More recently, two clinical studies have shown that HU is relatively safe in Sub Saharan Africa, a setting with high infectious disease and SCD burden. Hydroxyurea has been shown to not only decrease complications from SCD such as VOC, acute chest syndrome, frequency of transfusions, death and infections – including malaria but also to be a feasible approach in these under-resourced countries (Opoka et al., 2017; Tshilolo et al., 2019).

Despite having a significant impact in patients with SCD, there are still multiple unanswered questions regarding HU. Its mechanism of action has not been fully understood and its impact on HbF will decrease over time. Older patients become more sensitive to the dosage and they require frequent blood tests and readjustment of their dose. Regardless of the advances, there is no clear evidence of the long-term effect of hydroxyurea in preventing end organ damage (Nevitt et al., 2017; Luzzatto and Makani, 2019). There is also conflicting evidence of the effects of HU on male fertility (DeBaun, 2014). Chronic complications of SCD such as recurrent episodes of priapism, asymptomatic testicular infarctions and primary hypogonadism have been described as potential etiologies of low fertility in male SCD patients. Studies in transgenic SCD mice showed that SCD itself was associated with inhibition of spermatogenesis and primary hypogonadism but when compared to HU (25 mg/kg/day), testicular volume was lower in those mice with SCD exposed to HU, inferring lower spermatogenesis. Berthaut et al. (2008) measured the semen quality of 4 patients with SCA at baseline and 4 years after starting hydroxyurea. In three of four patients the spermatozoan concentration continued to drop while patients were taking the medication and did not return to baseline after discontinuing HU (Berthaut et al., 2008). Although the evidence is limited, full disclosure regarding implications on male fertility should be given to patients and families in order to make an informed decision before starting HU (Jones et al., 2009).

Other than HU, other pharmacological options to increase HbF are still experimental undergoing clinical trials. Molecular studies on γ-globin identified regulatory elements in the gene expression and subsequent HbF production. Such molecules; histone deacetylase (HDAC), DNA methyltransferase 1 (DNMT1), BCL11A and SOX6 modifying HbF expression have been explored as possible therapeutic options.

One of the proposed mechanisms for HU effect on HbF is stimulation of cyclic guanosine monophosphate (cGMP). Phosphodiesterase 9 (PDE9) is a specific enzyme in charge of degrading cGMP and is highly present in neutrophils and RBCs of patients with SCD. A novel, potent and selective PDE9 inhibitor (IMR-687) has been shown to increase levels of cGMP and HbF without signs of myelosuppression in cell lines of patients with SCD. An open-label extension to a previous phase 2a study is ongoing in adults with SCD (ClinicalTrials.gov Identifier: NCT04053803) (McArthur et al., 2019).

Panobinostat is a pan HDAC inhibitor currently being studied in adult patients with SCD as a phase 1 study (ClinicalTrials.gov Identifier: NCT01245179). *In vitro* analysis of human erythroid progenitor cells that underwent shRNA knockdown of HDAC1 or HDAC2 genes resulted in increased levels of γ-globin but without altering cellular proliferation of the cell cycle phase.

Associated with HU, HDAC gene inhibition produced a more pronounced increase of γ-globin and HbF (Esrick et al., 2015).

DNA Methyltransferase 1 is involved in the shutting down of γ-globin gene after birth and its subsequent production. DNA methylransferase inhibitor 5-azacytidine was one of the chemotherapeutic agents used to reactivate HbF but it was quickly abandoned due to its toxicity and carcinogenicity. Decitabine, an analog of 5-azacytidine, is also a potent DNMT1 inhibitor with a more favorable safety profile but decitabine is rapidly deaminated and inactivated by cytosine deaminase, if taken orally. To overcome this limitation, a clinical study combines decitabine and tetrahydrouridine (THU), a cytosine deaminase inhibitor, as a therapeutic strategy for inducing HbF (ClinicalTrials.gov Identifier: NCT01685515). In a phase 1 study, Molokie et al. (2017) showed that the inhibition of DNMT1 led to appropriate blood levels of decitabine that were safe and induced a large increase in fetal hemoglobin in healthy red blood cells. These agents did not induce cytoreduction, but increased platelets count that can potentially trigger vaso-occlusion in SCD patients (Molokie et al., 2017).

Voxelotor (Oxbryta/GBT440) binds specifically to the N-terminus of the alpha subunit of HbS to stabilize the oxygenated hemoglobin state (Strader et al., 2019), thus reducing the predisposition to sickling. Voxelotor (Oxbryta/GBT440) was approved by the FDA in November 2019 for the treatment of SCD in adults and pediatric patients 12 years of age and older. The HOPE study showed an increase in hemoglobin levels and reduced markers of hemolysis in 274 patients with HbS that were randomly assigned to receive the study drug versus placebo. These findings have not correlated with reduced episodes of pain crisis and/or end organ damage. Agents that shift Hb oxygen affinity present some concerns of potential negative effects as the bound oxygen cannot be off loaded in tissues with high oxygen requirements, particularly concerning in a disease characterized by decreased oxygen delivery (Hebbel and Hedlund, 2018; Thompson, 2019). These concerns are being addressed in a current phase 3, double-blind, randomized, placebo-controlled, multicenter study of Voxelotor (ClinicalTrials.gov Identifier: NCT03036813) (Vichinsky et al., 2019).

Dehydration of the RBC appears to be closely controlled by the efflux of potassium through 2 specific pathways; one is the potassium chloride cotransport and the other, calcium-activated potassium efflux (Gardos channel). Senicapoc blocks the Gardos channels, thus preventing dehydration of the red cells. Preclinical and phase 1/2 showed that inhibition of potassium flow through the Gardos channel increased Hb levels and decreased hemolysis (ClinicalTrials.gov Identifier: NCT00040677). A phase 3 study was terminated for lack of efficacy (ClinicalTrials.gov Identifier: NCT00294541) (Ataga et al., 2008; Ataga and Stocker, 2009).

N-Methyl D-aspartate receptors (NMDARs) are non-selective calcium channels present in erythroid precursors and circulating RBCs and have been shown to be abnormally increased in RBCs of patients with SCD (Hanggi et al., 2014). These channels are closely related with RBC hydration that affects the intracellular HbS concentration and thereby HbS polymerization and sickling of RBCs. Memantine is a NMDAR inhibitor which has shown to improve hydration of RBCs of patients with SCD *in vitro* and to reduce sickling in the setting of deoxygenation. It is being explored in an ongoing phase 2 clinical trial (ClinicalTrials.gov Identifier: NCT03247218).

Sanguinate which is a bovine PEGylated hemoglobin product attempts to block polymerization by targeting carbon monoxide (CO) delivery. By binding to HbS polymers, CO enhances their melting and minimize their persistence in peripheral blood. However, this equilibrium is based on high concentrations of CO. A phase 1/2 single-blind, randomized, placebo-controlled study of this agent in the management of pain crisis has been carried out but no results have yet been posted (ClinicalTrials.gov Identifier: NCT02411708).

(3) Targeting Vasocclusion

Increased expression and activation of normally inactive erythroid adhesion molecules promote cytoadherence of sickle RBCs to the endothelium accompanied by platelets and leukocytes. Activated leukocytes and platelets further increase the risk to develop VOC (Nasimuzzaman and Malik, 2019; Sundd et al., 2019; Telen et al., 2019).

Previous *in vitro* studies had demonstrated that glutamine depletion contributed to red blood cell membrane damage and adhesion. Uptake of L-glutamine uptake is markedly increased in patients with SCD, primarily to increase the total intracellular NAD level (Morris et al., 2008). In a phase 3 study, L-glutamine demonstrated a 25% reduction in the median number of pain crisis, 30% less hospitalizations and reduced acute chest episodes in children and adults with SCD with or without HU over a 48-week period. There were 36% drop-out rate in the glutamine arm and 24% in the placebo control arm from unknown reasons. L-Glutamine appears to significantly increase NADH and NAD redox potential and decrease endothelial adhesion, but its mechanism remains still unknown and there are concerns regarding its use in patients with renal impairment, a common

sickle-related complication (Quinn, 2018). In July 2017, the pharmacological grade of L-glutamine (Endari) was approved by the FDA for use in patients with SCD, 5 years or older (Niihara et al., 2018). Of note, L-glutamine has not been approved by the European Medicines Agency for treating SCD.

In the future it could be a useful combination therapy with HU (Minniti, 2018) but uptake among patients is still low, one of the reasons is the unpleasant taste. There are potentially less expensive pharmaceutical formulations of L-glutamine available off the counter, but purity of the effective agents in these compounds have not been validated.

As the endothelium emerge as a key factor in the constant activation of adhesion molecules in sickle RBCs, these adhesion molecules present a very attractive therapeutic target. Selectins, which are present in endothelial cells and are the initial step toward a firm adhesion between RBCs and the endothelium, have been further studied and targeted as possible therapeutic approaches.

Crizanlizumab is a monoclonal antibody to P-selectin and its mechanism of action is to block the adhesion of activated erythrocytes, neutrophils and platelets. In a phase 2, multicenter, randomized, placebo controlled double blind study, crizanlizumab with or without hydroxyurea (SUSTAIN study) (ClinicalTrails.gov Identifier: NCT01895361) showed that patients on the treatment arm had significantly lower rate of sickle-related pain crises compared to placebo with a lower incidence of adverse events - 10% of patients suffered from moderate side effects while one patient suffered from an intracranial bleed during treatment with this drug that could also interfere with platelet function via its effects on selectins (Ataga et al., 2017). *Post hoc* analyses showed that more patients were VOC event-free in the crizanlizumab arm than in the placebo arm, and that crizanlizumab also significantly increased time-to-first VOC compared to the placebo (Kutlar et al., 2019). A phase 3 interventional, multicenter, randomized, double-blind clinical trial is ongoing to assess safety and efficacy of crinalizumab with or without hydroxyurea in patients with SCD and history of VOC (ClinicalTrials.gov Identifier: NCT03814716). In November 2019, the US Food and Drug Administration approved crizanlizumab-tmca (ADAKVEO, Novartis) to reduce the frequency of VOC in adults and pediatric patients aged 16 years and older with SCD.

Rivipansel is a pan-selectin inhibitor with its strongest activity against E-selectin. In a multicenter, randomized, double−blind, placebo−controlled phase 2 study (ClinicalTrails.gov Identifier: NCT01119833), Rivipansel showed clinical and meaningful reductions in multiple measures of VOC compared with those receiving standard of care treatment (Telen et al., 2015). A phase 3 study (Identifier: NCT02187003) to evaluate the efficacy and safety of rivipansel in the treatment of VOC in hospitalized patients with SCD was terminated (posted on ClinicalTrials.gov February 20, 2020) based on failure of the primary study (NCT02433158) to meet the study efficacy endpoints of time to readiness-for-discharge.

In a phase 1, dose-escalation study propranolol showed it significantly reduced epinephrine-stimulated sickle RBCs adhesion. A phase 2 study (NCT01077921) showed decrease in adhesion molecules such as E-selectin and P-selectin but results were not statistically significant and no clinical endpoints were discussed (De Castro et al., 2012).

Due to their P-selectin mediated adhesion inhibition properties, heparinoids have been additionally investigated with interesting results. Sevuparin, a heparin derivate polysaccharide that has shown to bind to P− and L−selectins, thrombospondin, fibronectin and von Willebrand factor, all of which are thought to contribute to vasocclusion in SCD. It has been reported to inhibit sickle RBC adhesion to the endothelial cells and to reduce tumor necrosis factor-induced vasocclusion. It is currently being tested in a phase 2 clinical trial, placebo controlled, to study its efficacy and safety in patients with SCD during VOC (ClinicalTrials.gov Identifier: NCT02515838) (Telen et al., 2016). Other heparinoids such as Dalteparin showed incomplete evidence to support or refute its effectiveness in the management of patients with SCD. There are ongoing trials (ClinicalTrials.gov Identifier: NCT02098993) to assess the feasibility of unfractionated heparin in patients with SCD admitted with pain crisis. Well-designed studies are still needed to clarify its role in the management of patients with SCD and to assess the safety of this approach (van Zuuren and Fedorowicz, 2015).

Poloxamer 188 is a non-ionic block copolymer surfactant thought to seal stable defects in the microvasculature leading to an improvement in blood flow and decreasing blood viscosity. Although its mechanism is not well understood, a randomized, double-blind, placebo-controlled trial showed that it decreased the duration of sickle crisis by 8 h compared to placebo (133 h vs. 141 h, $p = 0.04$) and more patients receiving the medication reported crisis resolution (52% vs. 37%, $p = 0.02$) (Orringer et al., 2001). In an early phase 2 study, one patient receiving the medication developed renal dysfunction due to presence of low molecular weight substances and a purified version was designed (Adams-Graves et al., 1997). Vepoloxamer, a purified form of Poloxamer 188 with multi mechanistic properties, was believed to improve RBC adhesion, membrane fragility and organ damage. Unfortunately, a phase 3 study failed to reduce the mean duration of VOC in patients with SCD compared to placebo (Adams-Graves et al., 1997).

(4) Targeting Inflammation

Continual background inflammation contributes to organ damage in patients with SCD. Persistent activation of platelets, neutrophils, monocytes, endothelium, and coagulation factors are key participants in this vicious cycle. Different therapeutic approaches have been proposed to assess the impact in patients with SCD (Nasimuzzaman and Malik, 2019; Sundd et al., 2019; Telen et al., 2019).

Intravenous immunoglobulin (IVIG) and statins have been studied for their anti-inflammatory effects on neutrophils and monocyte adhesion. Patients on statin demonstrated a decrease in C-reactive protein, soluble ICAM1, soluble E-selectin and vascular endothelial growth. Simvastatin was found to reduce adhesion of white blood cells and in combination with hydroxyurea, was found to decrease the number of pain crisis and markers of inflammation (Hoppe et al., 2017). Currently,

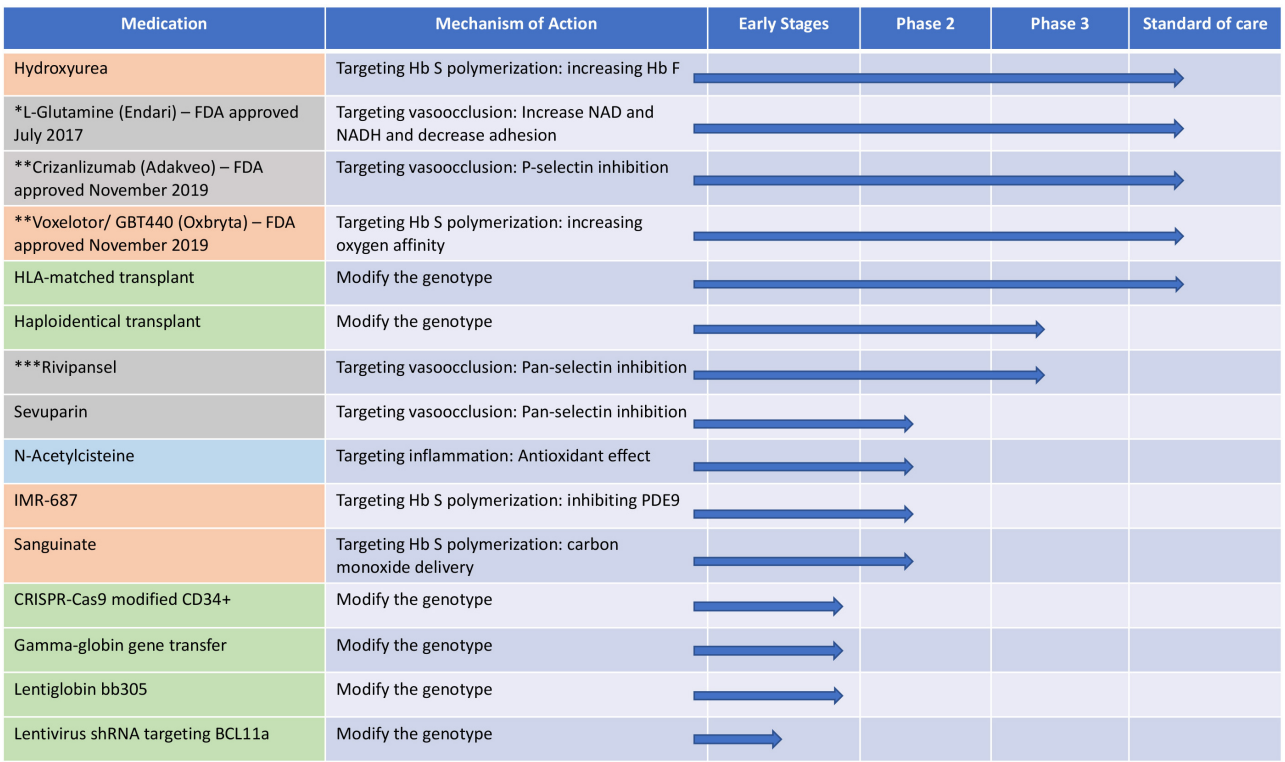

FIGURE 3 | The different therapeutic approaches for sickle cell disease and their mechanisms and current status in clinical trials. Orange: targeting hemoglobin S polymerization; gray: targeting vasocclusion; light blue: targeting inflammation and green: modification of the genotype. shRNA, short hairpin RNA; Hb S, hemoglobin S; Hb F, hemoglobin F; PDE9, phosphodiesterase 9. *FDA approved July 2017; **FDA approved November 2019; ***Terminated in February 20, 2020 due to failure to meet primary endpoints.

there is an active clinical trial to assess the effect of simvastatin on central nervous system vasculature in patients with SCD (ClinicalTrials.gov Identifier: NCT03599609).

N-Acetylcysteine (NAC) commonly used in respiratory conditions has also been tested for patients with SCD. In a phase 2 study, NAC proved to inhibit dense cell formation and restored glutathione levels toward normal. The decrease in irreversible sickling of RBCs was not statistically significant but a downward trend was observed (Pace et al., 2003; Nur et al., 2012). Further studies have shown decreased red cell membrane expression of phosphatidylserine which seems to reflect overall reduced oxidative stress. To better assess its clinical effect in patients with SCD, a pilot study, currently enrolling with invitation is studying its effect in redox and RBC function during VOC (ClinicalTrials.gov Identifier: NCT01800526).

Aberrant activation of the coagulation cascade, abnormal excess of TF on the endothelial wall and high plasma levels of different coagulation factors drive increased thrombin and fibrin production leading to further inflammation and risk of VOC (Sundd et al., 2019). In a SCD mouse model, factor Xa, TF, and thrombin differentially contributed to vascular inflammation (Sparkenbaugh and Pawlinski, 2013). Factor Xa inhibition demonstrated a decrease in vascular inflammation as assessed by the lower interleukin 6 levels. Although thrombin had no effect on interleukin 6, it was a significant factor for neutrophil infiltration and further inflammation (Sparkenbaugh et al., 2014). A retrospective analysis of rivaroxaban, a factor Xa inhibitor, demonstrated non-inferiority with regard to thrombosis compared to warfarin with the advantage of less outpatient visits and monitoring (Bhat and Han, 2017). Currently, a two-treatment phase clinical trial with rivaroxaban on the pathology of SCD has been completed but results are pending (ClinicalTrials.gov Identifier: NCT02072668). Patients with SCD have increased platelet levels at baseline that are further increased during acute VOC. Platelet activation triggers further leukocyte activation and promote RBC adhesion to an exposed endothelium (Conran and Belcher, 2018) setting off a vicious cycle of adhesion events. Antiplatelet therapy with Clopidogrel in patients with SCD, unfortunately, were disappointing. New, third generation P2Y12 inhibitors such as ticagrelor and prasugrel have also been studied in patients with SCD. Prasugrel showed appropriate levels of anti-platelet aggregation compared to healthy patients in *ex vivo* studies, and was well tolerated by patients, but on a 24-month follow up, patients on the treatment arm failed to show reduction in the frequency of VOC (Heeney et al., 2016; Conran and Rees, 2017). Ticagrelor, in a phase 2b study, was well tolerated, but failed to show effect in the frequency of VOC (Kanter et al., 2019) (ClinicalTrials.gov identifier: NCT02482298). Previous studies have also showed that aspirin as an anticoagulant therapy did not

provide benefit over placebo, although it is used as an analgesic in many parts of Africa (Sins et al., 2017).

In patients with SCD, continual lysis of RBCs activates the inflammasome triggering the release of multiple cytokines, including IL-1β (Awojoodu et al., 2014). Canakinumab is a humanized monoclonal antibody that targets interleukin 1-β (IL-1β), and thus potentially could be useful in mitigating some of the inflammation in SCD. Canakinumab was shown to be well tolerated and not associated with major side effects in pediatric and young adult patients (Rees, 2019). A clinical trial to assess its efficacy, safety and tolerability is ongoing in the pediatric population (ClinicalTrials.gov Identifier: NCT02961218).

CONCLUSION

In the last 30 years, there has been a revolution in the medical sciences, and SCD because of its genetic simplicity, has been at the forefront of the numerous scientific discoveries. Tremendous progress has been made in understanding its pathophysiology and pathobiological complexities, but developing treatments, has been disproportionately slow and elusive. However, after a century of neglect, going back to basics offers hope for translating these insights into better therapeutic options – pharmacological and genetic – and for finding curative genetic options for SCD (**Figure 3**). Although frequent in the US, SCD is far more prevalent in Africa where patients have less access to resources, medical treatment and facilities and the consequences of the disease are devastating. As we move forward, we have to continue focus our therapeutic approaches so that they can be accessed by those that suffer the most.

AUTHOR CONTRIBUTIONS

GSC and ST wrote and revised the manuscript.

FUNDING

This work was supported by the Intramural Research Program of the National Heart, Lungs, and Blood Institute, NIH (ST).

REFERENCES

Adams-Graves, P., Kedar, A., Koshy, M., Steinberg, M., Veith, R., Ward, D., et al. (1997). RheothRx (poloxamer 188) injection for the acute painful episode of sickle cell disease: a pilot study. *Blood* 90, 2041–2046.

Angelucci, E., Matthes-Martin, S., Baronciani, D., Bernaudin, F., Bonanomi, S., Cappellini, M. D., et al. (2014). Hematopoietic stem cell transplantation in thalassemia major and sickle cell disease: indications and management recommendations from an international expert panel. *Haematologica* 99, 811–820. doi: 10.3324/haematol.2013.099747

Ataga, K. I., Kutlar, A., Kanter, J., Liles, D., Cancado, R., Friedrisch, J., et al. (2017). Crizanlizumab for the prevention of pain crises in sickle cell disease. *N. Engl. J. Med.* 376, 429–439. doi: 10.1056/NEJMoa1611770

Ataga, K. I., Smith, W. R., De Castro, L. M., Swerdlow, P., Saunthararajah, Y., Castro, O., et al. (2008). Efficacy and safety of the Gardos channel blocker, senicapoc (ICA-17043), in patients with sickle cell anemia. *Blood* 111, 3991–3997. doi: 10.1182/blood-2007-08-110098

Ataga, K. I., and Stocker, J. (2009). Senicapoc (ICA-17043): a potential therapy for the prevention and treatment of hemolysis-associated complications in sickle cell anemia. *Expert Opin. Investig. Drugs* 18, 231–239. doi: 10.1517/13543780802708011

Awojoodu, A. O., Keegan, P. M., Lane, A. R., Zhang, Y., Lynch, K. R., Platt, M. O., et al. (2014). Acid sphingomyelinase is activated in sickle cell erythrocytes and contributes to inflammatory microparticle generation in SCD. *Blood* 124, 1941–1950. doi: 10.1182/blood-2014-01-543652

Bauer, D. E., Kamran, S. C., Lessard, S., Xu, J., Fujiwara, Y., Lin, C., et al. (2013). An erythroid enhancer of BCL11A subject to genetic variation determines fetal hemoglobin level. *Science* 342, 253–257. doi: 10.1126/science.1242088

Bernaudin, F., Dalle, J. H., Bories, D., de Latour, R. P., Robin, M., Bertrand, Y., et al. (2020). Long-term event-free survival, chimerism and fertility outcomes in 234 patients with sickle-cell anemia younger than 30 years after myeloablative conditioning and matched-sibling transplantation in France. *Haematologica* 105, 91–101. doi: 10.3324/haematol.2018.213207

Berthaut, I., Guignedoux, G., Kirsch-Noir, F., de Larouziere, V., Ravel, C., Bachir, D., et al. (2008). Influence of sickle cell disease and treatment with hydroxyurea on sperm parameters and fertility of human males. *Haematologica* 93, 988–993. doi: 10.3324/haematol.11515

Bhat, S., and Han, J. (2017). Outcomes of rivaroxaban use in patients with sickle cell disease. *Ann. Pharmacother.* 51, 357–358. doi: 10.1177/1060028016681129

Bolanos-Meade, J., Cooke, K. R., Gamper, C. J., Ali, S. A., Ambinder, R. F., Borrello, I. M., et al. (2019). *Lancet Haematol.* 6, e183–e193.

Bolanos-Meade, J., Fuchs, E. J., Luznik, L., Lanzkron, S. M., Gamper, C. J., Jones, R. J., et al. (2012). HLA-haploidentical bone marrow transplantation with post-transplant cyclophosphamide expands the donor pool for patients with sickle cell disease. *Blood* 120, 4285–4291. doi: 10.1182/blood-2012-07-438408

Boulad, F., Shore, T., van Besien, K., Minniti, C., Barbu-Stevanovic, M., Fedus, S. W., et al. (2018). Safety and efficacy of plerixafor dose escalation for the mobilization of CD34(+) hematopoietic progenitor cells in patients with sickle cell disease: interim results. *Haematologica* 103, 770–777. doi: 10.3324/haematol.2017.187047

Breda, L., Motta, I., Lourenco, S., Gemmo, C., Deng, W., Rupon, J. W., et al. (2016). Forced chromatin looping raises fetal hemoglobin in adult sickle cells to higher levels than pharmacologic inducers. *Blood* 128, 1139–1143. doi: 10.1182/blood-2016-01-691089

Brendel, C., Guda, S., Renella, R., Bauer, D. E., Canver, M. C., Kim, Y. J., et al. (2016). Lineage-specific BCL11A knockdown circumvents toxicities and reverses sickle phenotype. *J. Clin. Invest.* 126, 3868–3878. doi: 10.1172/JCI87885

Brittenham, G. M., Schechter, A. N., and Noguchi, C. T. (1985). Hemoglobin S polymerization: primary determinant of the hemolytic and clinical severity of the sickling syndromes. *Blood* 65, 183–189.

Brunson, A., Lei, A., Rosenberg, A. S., White, R. H., Keegan, T., and Wun, T. (2017). Increased incidence of VTE in sickle cell disease patients: risk factors, recurrence and impact on mortality. *Br. J. Haematol.* 178, 319–326. doi: 10.1111/bjh.14655

Bunn, H. F. (1997). Pathogenesis and treatment of sickle cell disease. *N. Engl. J. Med.* 337, 762–769.

Cavazzana, M., Antoniani, C., and Miccio, A. (2017). Gene therapy for beta-hemoglobinopathies. *Mol. Ther.* 25, 1142–1154. doi: 10.1016/j.ymthe.2017.03.024

Cavazzana-Calvo, M., Payen, E., Negre, O., Wang, G., Hehir, K., Fusil, F., et al. (2010). Transfusion independence and HMGA2 activation after gene therapy of human beta-thalassaemia. *Nature* 467, 318–322. doi: 10.1038/nature09328

Chou, S. T., Alsawas, M., Fasano, R. M., Field, J. J., Hendrickson, J. E., Howard, J., et al. (2020). American society of hematology 2020 guidelines for sickle cell disease: transfusion support. *Blood Adv.* 4, 327–355. doi: 10.1182/bloodadvances.2019001143

Chou, S. T., Evans, P., Vege, S., Coleman, S. L., Friedman, D. F., Keller, M., et al. (2018). RH genotype matching for transfusion support in sickle cell disease. *Blood* 132, 1198–1207. doi: 10.1182/blood-2018-05-851360

Chou, S. T., Jackson, T., Vege, S., Smith-Whitley, K., Friedman, D. F., and Westhoff, C. M. (2013). High prevalence of red blood cell alloimmunization in sickle

cell disease despite transfusion from RH-matched minority donors. *Blood* 122, 1062–1071. doi: 10.1182/blood-2013-03-490623

Cokic, V. P., Smith, R. D., Beleslin-Cokic, B. B., Njoroge, J. M., Miller, J. L., Gladwin, M. T., et al. (2003). Hydroxyurea induces fetal hemoglobin by the nitric oxide-dependent activation of soluble guanylyl cyclase. *J. Clin. Invest.* 111, 231–239. doi: 10.1172/JCI16672

Conran, N., and Belcher, J. D. (2018). Inflammation in sickle cell disease. *Clin. Hemorheol. Microcirc.* 68, 263–299. doi: 10.3233/CH-189012

Conran, N., and Rees, D. C. (2017). Prasugrel hydrochloride for the treatment of sickle cell disease. *Expert Opin. Investig. Drugs* 26, 865–872. doi: 10.1080/13543784.2017.1335710

De Castro, L. M., Zennadi, R., Jonassaint, J. C., Batchvarova, M., and Telen, M. J. (2012). Effect of propranolol as antiadhesive therapy in sickle cell disease. *Clin. Transl. Sci.* 5, 437–444. doi: 10.1111/cts.12005

DeBaun, M. R. (2014). Hydroxyurea therapy contributes to infertility in adult men with sickle cell disease: a review. *Expert Rev. Hematol.* 7, 767–773. doi: 10.1586/17474086.2014.959922

Dever, D. P., Bak, R. O., Reinisch, A., Camarena, J., Washington, G., Nicolas, C. E., et al. (2016). CRISPR/Cas9 beta-globin gene targeting in human haematopoietic stem cells. *Nature* 539, 384–389. doi: 10.1038/nature20134

Eaton, W. A., and Bunn, H. F. (2017). Treating sickle cell disease by targeting HbS polymerization. *Blood* 129, 2719–2726. doi: 10.1182/blood-2017-02-765891

Elmariah, H., Garrett, M. E., De Castro, L. M., Jonassaint, J. C., Ataga, K. I., Eckman, J. R., et al. (2014). Factors associated with survival in a contemporary adult sickle cell disease cohort. *Am. J. Hematol.* 89, 530–535. doi: 10.1002/ajh.23683

Esrick, E. B., and Bauer, D. E. (2018). Genetic therapies for sickle cell disease. *Semin. Hematol.* 55, 76–86. doi: 10.1053/j.seminhematol.2018.04.014

Esrick, E. B., Manis, J. P., Daley, H., Baricordi, C., Trebeden-Negre, H., Pierciey, F. J., et al. (2018). Successful hematopoietic stem cell mobilization and apheresis collection using plerixafor alone in sickle cell patients. *Blood Adv.* 2, 2505–2512. doi: 10.1182/bloodadvances.2018016725

Esrick, E. B., McConkey, M., Lin, K., Frisbee, A., and Ebert, B. L. (2015). Inactivation of HDAC1 or HDAC2 induces gamma globin expression without altering cell cycle or proliferation. *Am. J. Hematol.* 90, 624–628. doi: 10.1002/ajh.24019

Fitzhugh, C. D., Abraham, A. A., Tisdale, J. F., and Hsieh, M. M. (2014). Hematopoietic stem cell transplantation for patients with sickle cell disease: progress and future directions. *Hematol. Oncol. Clin. N. Am.* 28, 1171–1185. doi: 10.1016/j.hoc.2014.08.014

Fitzhugh, C. D., Cordes, S., Taylor, T., Coles, W., Roskom, K., Link, M., et al. (2017). At least 20% donor myeloid chimerism is necessary to reverse the sickle phenotype after allogeneic HSCT. *Blood* 130, 1946–1948. doi: 10.1182/blood-2017-03-772392

Gardner, K., Douiri, A., Drasar, E., Allman, M., Mwirigi, A., Awogbade, M., et al. (2016). Survival in adults with sickle cell disease in a high-income setting. *Blood* 128, 1436–1438. doi: 10.1182/blood-2016-05-716910

Gardner, K., and Thein, S. L. (2016). "Genetic factors modifying sickle cell disease severity," in *Sickle Cell Anemia - From Basic Science to Clinical Practice*, eds F. F. Costa and N. Conran (Cham: Springer International), 371–397.

Gluckman, E., Cappelli, B., Bernaudin, F., Labopin, M., Volt, F., Carreras, J., et al. (2017). Sickle cell disease: an international survey of results of HLA-identical sibling hematopoietic stem cell transplantation. *Blood* 129, 1548–1556. doi: 10.1182/blood-2016-10-745711

Goldstein, J., Konigsberg, W., and Hill, R. J. (1963). The structure of human hemoglobin: VI. The sequence of amino acids in the tryptic peptides of the β chain. *J. Biol. Chem.* 238, 2016–2027.

Guilcher, G. M. T., Truong, T. H., Saraf, S. L., Joseph, J. J., Rondelli, D., and Hsieh, M. M. (2018). Curative therapies: allogeneic hematopoietic cell transplantation from matched related donors using myeloablative, reduced intensity, and nonmyeloablative conditioning in sickle cell disease. *Semin. Hematol.* 55, 87–93. doi: 10.1053/j.seminhematol.2018.04.011

Hanggi, P., Makhro, A., Gassmann, M., Schmugge, M., Goede, J. S., Speer, O., et al. (2014). Red blood cells of sickle cell disease patients exhibit abnormally high abundance of N-methyl D-aspartate receptors mediating excessive calcium uptake. *Br. J. Haematol.* 167, 252–264. doi: 10.1111/bjh.13028

Hassell, K. L. (2010). Population estimates of sickle cell disease in the U.S. *Am. J. Prev. Med.* 38, S512–S521. doi: 10.1016/j.amepre.2009.12.022

Hassell, K. L. (2016). Sickle cell disease: a continued call to action. *Am. J. Prev. Med.* 51, S1–S2. doi: 10.1016/j.amepre.2015.11.002

Hebbel, R. P. (2011). Reconstructing sickle cell disease: a data-based analysis of the "hyperhemolysis paradigm" for pulmonary hypertension from the perspective of evidence-based medicine. *Am. J. Hematol.* 86, 123–154. doi: 10.1002/ajh.21952

Hebbel, R. P., and Hedlund, B. E. (2018). Sickle hemoglobin oxygen affinity-shifting strategies have unequal cerebrovascular risks. *Am. J. Hematol.* 93, 321–325. doi: 10.1002/ajh.24975

Heeney, M. M., Hoppe, C. C., Abboud, M. R., Inusa, B., Kanter, J., Ogutu, B., et al. (2016). A multinational trial of prasugrel for sickle cell vaso-occlusive events. *N. Engl. J. Med.* 374, 625–635. doi: 10.1056/NEJMoa1512021

Hendrickson, J. E., and Tormey, C. A. (2018). Rhesus pieces: genotype matching of RBCs. *Blood* 132, 1091–1093. doi: 10.1182/blood-2018-07-865634

Herrick, J. B. (1910). Peculiar elongated and sickle-shaped red blood corpuscles in a case of severe anemia. *Arch. Intern. Med.* 6, 517–521. doi: 10.1001/jama.2014.11011

Herrick, J. B. (2014). Peculiar elongated and sickle-shaped red blood corpuscles in a case of severe anemia. *JAMA* 312:1063. doi: 10.1001/jama.2014.11011

Hoppe, C., Jacob, E., Styles, L., Kuypers, F., Larkin, S., and Vichinsky, E. (2017). Simvastatin reduces vaso-occlusive pain in sickle cell anaemia: a pilot efficacy trial. *Br. J. Haematol.* 177, 620–629. doi: 10.1111/bjh.14580

Howard, J. (2016). Sickle cell disease: when and how to transfuse. *Hematol. Am. Soc. Hematol. Educ. Program* 2016, 625–631. doi: 10.1182/asheducation-2016.1.625

Howard, J., Malfroy, M., Llewelyn, C., Choo, L., Hodge, R., Johnson, T., et al. (2013). The transfusion alternatives preoperatively in sickle cell disease (TAPS) study: a randomised, controlled, multicentre clinical trial. *Lancet* 381, 930–938. doi: 10.1016/S0140-6736(12)61726-7

Hsieh, M. M., Fitzhugh, C. D., Weitzel, R. P., Link, M. E., Coles, W. A., Zhao, X., et al. (2014). Nonmyeloablative HLA-matched sibling allogeneic hematopoietic stem cell transplantation for severe sickle cell phenotype. *JAMA* 312, 48–56. doi: 10.1001/jama.2014.7192

Hsieh, M. M., Kang, E. M., Fitzhugh, C. D., Link, M. B., Bolan, C. D., Kurlander, R., et al. (2009). Allogeneic hematopoietic stem-cell transplantation for sickle cell disease. *N. Engl. J. Med.* 361, 2309–2317. doi: 10.1056/NEJMoa0904971

Hsieh, M. M., and Tisdale, J. F. (2018). Hematopoietic stem cell mobilization with plerixafor in sickle cell disease. *Haematologica* 103, 749–750. doi: 10.3324/haematol.2018.190876

Inamoto, Y., Kimura, F., Kanda, J., Sugita, J., Ikegame, K., Nakasone, H., et al. (2016). Comparison of graft-versus-host disease-free, relapse-free survival according to a variety of graft sources: antithymocyte globulin and single cord blood provide favorable outcomes in some subgroups. *Haematologica* 101, 1592–1602. doi: 10.3324/haematol.2016.149427

Johnson, F. L. (1985). Bone marrow transplantation in the treatment of sickle cell anemia. *Am. J. Pediatr. Hematol. Oncol.* 7, 254–257.

Johnson, F. L., Look, A. T., Gockerman, J., Ruggiero, M. R., Dalla-Pozza, L., and Billings, F. T. (1984). Bone-marrow transplantation in a patient with sickle-cell anemia. *N. Engl. J. Med.* 311, 780–783. doi: 10.1056/NEJM198409203111207

Jones, K. M., Niaz, M. S., Brooks, C. M., Roberson, S. I., Aguinaga, M. P., Hills, E. R., et al. (2009). Adverse effects of a clinically relevant dose of hydroxyurea used for the treatment of sickle cell disease on male fertility endpoints. *Int. J. Environ. Res. Public Health* 6, 1124–1144. doi: 10.3390/ijerph6031124

Joseph, J. J., Abraham, A. A., and Fitzhugh, C. D. (2018). When there is no match, the game is not over: alternative donor options for hematopoietic stem cell transplantation in sickle cell disease. *Semin. Hematol.* 55, 94–101. doi: 10.1053/j.seminhematol.2018.04.013

Kamani, N. R., Walters, M. C., Carter, S., Aquino, V., Brochstein, J. A., Chaudhury, S., et al. (2012). Unrelated donor cord blood transplantation for children with severe sickle cell disease: results of one cohort from the phase II study from the blood and marrow transplant clinical trials network (BMT CTN). *Biol. Blood Marrow Transplant.* 18, 1265–1272. doi: 10.1016/j.bbmt.2012.01.019

Kanter, J., Abboud, M. R., Kaya, B., Nduba, V., Amilon, C., Gottfridsson, C., et al. (2019). Ticagrelor does not impact patient-reported pain in young adults with sickle cell disease: a multicentre, randomised phase IIB study. *Br. J. Haematol.* 184, 269–278. doi: 10.1111/bjh.15646

Kutlar, A., Kanter, J., Liles, D. K., Alvarez, O. A., Cancado, R. D., Friedrisch, J. R., et al. (2019). Effect of crizanlizumab on pain crises in subgroups of patients

with sickle cell disease: a SUSTAIN study analysis. *Am. J. Hematol.* 94, 55–61. doi: 10.1002/ajh.25308

Lagresle-Peyrou, C., Lefrere, F., Magrin, E., Ribeil, J. A., Romano, O., Weber, L., et al. (2018). Plerixafor enables safe, rapid, efficient mobilization of hematopoietic stem cells in sickle cell disease patients after exchange transfusion. *Haematologica* 103, 778–786. doi: 10.3324/haematol.2017.184788

Leonard, A., Tisdale, J., and Abraham, A. (2020). Curative options for sickle cell disease: haploidentical stem cell transplantation or gene therapy? *Br. J. Haematol.* doi: 10.1111/bjh.16437 [Epub ahead of print].

Leonard, A., and Tisdale, J. F. (2018). Stem cell transplantation in sickle cell disease: therapeutic potential and challenges faced. *Expert Rev. Hematol.* 11, 547–565. doi: 10.1080/17474086.2018.1486703

Liu, N., Hargreaves, V. V., Zhu, Q., Kurland, J. V., Hong, J., Kim, W., et al. (2018). Direct promoter repression by BCL11A controls the fetal to adult hemoglobin switch. *Cell* 173, 430–42.e17. doi: 10.1016/j.cell.2018.03.016

Luzzatto, L., and Makani, J. (2019). Hydroxyurea - an essential medicine for sickle cell disease in Africa. *N. Engl. J. Med.* 380, 187–189. doi: 10.1056/NEJMe1814706

Martyn, G. E., Wienert, B., Yang, L., Shah, M., Norton, L. J., Burdach, J., et al. (2018). Natural regulatory mutations elevate the fetal globin gene via disruption of BCL11A or ZBTB7A binding. *Nat. Genet.* 50, 498–503. doi: 10.1038/s41588-018-0085-0

Masuda, T., Wang, X., Maeda, M., Canver, M. C., Sher, F., Funnell, A. P., et al. (2016). Transcription factors LRF and BCL11A independently repress expression of fetal hemoglobin. *Science* 351, 285–289. doi: 10.1126/science.aad3312

McArthur, J. G., Svenstrup, N., Chen, C., Fricot, A., Carvalho, C., Nguyen, J., et al. (2019). A novel, highly potent and selective phosphodiesterase-9 inhibitor for the treatment of sickle cell disease. *Haematologica* 105, 623–631. doi: 10.3324/haematol.2018.213462

McGann, P. T. (2014). Sickle cell anemia: an underappreciated and unaddressed contributor to global childhood mortality. *J. Pediatr.* 165, 18–22. doi: 10.1016/j.jpeds.2014.01.070

Miller, S. T., Sleeper, L. A., Pegelow, C. H., Enos, L. E., Wang, W. C., Weiner, S. J., et al. (2000). Prediction of adverse outcomes in children with sickle cell disease. *N. Engl. J. Med.* 342, 83–89. doi: 10.1056/NEJM200005253422114

Minniti, C. P. (2018). l-glutamine and the dawn of combination therapy for sickle cell disease. *N. Engl. J. Med.* 379, 292–294. doi: 10.1056/NEJMe1800976

Molokie, R., Lavelle, D., Gowhari, M., Pacini, M., Krauz, L., Hassan, J., et al. (2017). Oral tetrahydrouridine and decitabine for non-cytotoxic epigenetic gene regulation in sickle cell disease: a randomized phase 1 study. *PLoS Med.* 14:e1002382. doi: 10.1371/journal.pmed.1002382

Morris, C. R., Suh, J. H., Hagar, W., Larkin, S., Bland, D. A., Steinberg, M. H., et al. (2008). Erythrocyte glutamine depletion, altered redox environment, and pulmonary hypertension in sickle cell disease. *Blood* 111, 402–410. doi: 10.1182/blood-2007-04-081703

Nasimuzzaman, M., and Malik, P. (2019). Role of the coagulation system in the pathogenesis of sickle cell disease. *Blood Adv.* 3, 3170–3180. doi: 10.1182/bloodadvances.2019000193

Nayerossadat, N., Maedeh, T., and Ali, P. A. (2012). Viral and nonviral delivery systems for gene delivery. *Adv. Biomed. Res.* 1:27. doi: 10.4103/2277-9175.98152

Negre, O., Eggimann, A. V., Beuzard, Y., Ribeil, J. A., Bourget, P., Borwornpinyo, S., et al. (2016). Gene therapy of the beta-hemoglobinopathies by lentiviral transfer of the beta(A(T87Q))-globin gene. *Hum. Gene Ther.* 27, 148–165. doi: 10.1089/hum.2016.007

Nevitt, S. J., Jones, A. P., and Howard, J. (2017). Hydroxyurea (hydroxycarbamide) for sickle cell disease. *Cochrane Database. Syst. Rev.* 4:CD002202. doi: 10.1002/14651858.CD002202.pub2

Niihara, Y., Miller, S. T., Kanter, J., Lanzkron, S., Smith, W. R., Hsu, L. L., et al. (2018). A phase 3 trial of l-glutamine in sickle cell disease. *N. Engl. J. Med.* 379, 226–235. doi: 10.1056/NEJMoa1715971

Nur, E., Brandjes, D. P., Teerlink, T., Otten, H. M., Oude Elferink, R. P., Muskiet, F., et al. (2012). N-acetylcysteine reduces oxidative stress in sickle cell patients. *Ann. Hematol.* 91, 1097–1105. doi: 10.1007/s00277-011-1404-z

Ohene-Frempong, K., Weiner, S. J., Sleeper, L. A., Miller, S. T., Embury, S., Moohr, J. W., et al. (1998). Cerebrovascular accidents in sickle cell disease: rates and risk factors. *Blood* 91, 288–294.

Opoka, R. O., Ndugwa, C. M., Latham, T. S., Lane, A., Hume, H. A., Kasirye, P., et al. (2017). Novel use of hydroxyurea in an African region with malaria (NOHARM): a trial for children with sickle cell anemia. *Blood* 130, 2585–2593. doi: 10.1182/blood-2017-06-788935

Orkin, S. H., and Bauer, D. E. (2019). Emerging genetic therapy for sickle cell disease. *Annu. Rev. Med.* 70, 257–271. doi: 10.1146/annurev-med-041817-125507

Orringer, E. P., Casella, J. F., Ataga, K., Koshy, M., Adams-Graves, P., Luchtman-Jones, L., et al. (2001). Purified poloxamer 188 for treatment of acute vaso-occlusive crisis of sickle cell disease: a randomized controlled trial. *JAMA* 286, 2099–2106. doi: 10.1001/jama.286.17.2099

Pace, B. S., Shartava, A., Pack-Mabien, A., Mulekar, M., Ardia, A., and Goodman, S. R. (2003). Effects of N-acetylcysteine on dense cell formation in sickle cell disease. *Am. J. Hematol.* 73, 26–32. doi: 10.1002/ajh.10321

Piel, F. B., Hay, S. I., Gupta, S., Weatherall, D. J., and Williams, T. N. (2013). Global burden of sickle cell anaemia in children under five, 2010-2050: modelling based on demographics, excess mortality, and interventions. *PLoS Med.* 10:e1001484. doi: 10.1371/journal.pmed.1001484

Quinn, C. T. (2016). Minireview: clinical severity in sickle cell disease: the challenges of definition and prognostication. *Exp. Biol. Med.* 241, 679–688. doi: 10.1177/1535370216640385

Quinn, C. T. (2018). l-Glutamine for sickle cell anemia: more questions than answers. *Blood* 132, 689–693. doi: 10.1182/blood-2018-03-834440

Quinn, C. T., Rogers, Z. R., McCavit, T. L., and Buchanan, G. R. (2010). Improved survival of children and adolescents with sickle cell disease. *Blood* 115, 3447–3452. doi: 10.1182/blood-2009-07-233700

Rees, D. C. (2019). Double-blind, randomized study of canakinumab treatment in pediatric and young adult patients with sickle cell anemia. *Blood* 134(Suppl._1):615.

Ribeil, J. A., Hacein-Bey-Abina, S., Payen, E., Magnani, A., Semeraro, M., Magrin, E., et al. (2017). Gene therapy in a patient with sickle cell disease. *N. Engl. J. Med.* 376, 848–855.

Saiki, R. K., Scharf, S., Faloona, F., Mullis, K. B., Horn, G. T., Erlich, H. A., et al. (1985). Enzymatic amplification of b-globin genomic sequences and restriction site analysis for diagnosis of sickle cell anaemia. *Science* 230, 1350–1354.

Saraf, S. L., Oh, A. L., Patel, P. R., Sweiss, K., Koshy, M., Campbell-Lee, S., et al. (2018). Haploidentical peripheral blood stem cell transplantation demonstrates stable engraftment in adults with sickle cell disease. *Biol. Blood Marrow Transplant.* 24, 1759–1765. doi: 10.1016/j.bbmt.2018.03.031

Serjeant, G. R., Chin, N., Asnani, M. R., Serjeant, B. E., Mason, K. P., Hambleton, I. R., et al. (2018). Causes of death and early life determinants of survival in homozygous sickle cell disease: the Jamaican cohort study from birth. *PLoS One* 13:e0192710. doi: 10.1371/journal.pone.0192710

Shenoy, S. (2013). Hematopoietic stem-cell transplantation for sickle cell disease: current evidence and opinions. *Ther. Adv. Hematol.* 4, 335–344. doi: 10.1177/2040620713483063

Sins, J. W. R., Mager, D. J., Davis, S., Biemond, B. J., and Fijnvandraat, K. (2017). Pharmacotherapeutical strategies in the prevention of acute, vaso-occlusive pain in sickle cell disease: a systematic review. *Blood Adv.* 1, 1598–1616. doi: 10.1182/bloodadvances.2017007211

Sparkenbaugh, E., Chantrathammachart, P., Mickelson, J., van Ryn, J., Hebbel, R. P., Monroe, D. M., et al. (2014). Differential contribution of FXa and thrombin to vascular inflammation in a mouse model of sickle cell disease. *Blood* 123, 1747–1756. doi: 10.1182/blood-2013-08-523936

Sparkenbaugh, E., and Pawlinski, R. (2013). Interplay between coagulation and vascular inflammation in sickle cell disease. *Br. J. Haematol.* 162, 3–14. doi: 10.1111/bjh.12336

Steinberg, M. H., Forget, B. G., Higgs, D. R., and Nagel, R. L. (2001). *Disorders of Hemoglobin: Genetics, Pathophysiology, and Clinical Management*, 1st Edn. Cambridge: Cambridge University Press.

Strader, M. B., Liang, H., Meng, F., Harper, J., Ostrowski, D. A., Henry, E. R., et al. (2019). Interactions of an anti-sickling drug with hemoglobin in red blood cells from a patient with sickle cell anemia. *Bioconjug. Chem.* 30, 568–571. doi: 10.1021/acs.bioconjchem.9b00130

Sundd, P., Gladwin, M. T., and Novelli, E. M. (2019). Pathophysiology of sickle cell disease. *Annu. Rev. Pathol.* 14, 263–292.

Telen, M. J. (2016). Beyond hydroxyurea: new and old drugs in the pipeline for sickle cell disease. *Blood* 127, 810–819. doi: 10.1182/blood-2015-09-618553

Telen, M. J., Batchvarova, M., Shan, S., Bovee-Geurts, P. H., Zennadi, R., Leitgeb, A., et al. (2016). Sevuparin binds to multiple adhesive ligands and reduces sickle red blood cell-induced vaso-occlusion. *Br. J. Haematol.* 175, 935–948. doi: 10.1111/bjh.14303

Telen, M. J., Malik, P., and Vercellotti, G. M. (2019). Therapeutic strategies for sickle cell disease: towards a multi-agent approach. *Nat. Rev. Drug Discov.* 18, 139–158. doi: 10.1038/s41573-018-0003-2

Telen, M. J., Wun, T., McCavit, T. L., De Castro, L. M., Krishnamurti, L., Lanzkron, S., et al. (2015). Randomized phase 2 study of GMI-1070 in SCD: reduction in time to resolution of vaso-occlusive events and decreased opioid use. *Blood* 125, 2656–2664. doi: 10.1182/blood-2014-06-583351

Telfer, P., Coen, P., Chakravorty, S., Wilkey, O., Evans, J., Newell, H., et al. (2007). Clinical outcomes in children with sickle cell disease living in England: a neonatal cohort in East London. *Haematologica* 92, 905–912. doi: 10.3324/haematol.10937

Thein, S. L., Pirenne, F., Fasano, R. M., Habibi, A., Bartolucci, P., Chonat, S., et al. (2020). Hemolytic transfusion reactions in sickle cell disease: underappreciated and potentially fatal. *Haematologica* 105, 539–544. doi: 10.3324/haematol.2019.224709

Thompson, A. A. (2019). Targeted agent for sickle cell disease - changing the protein but not the gene. *N. Engl. J. Med.* 381, 579–580. doi: 10.1056/NEJMe1906771

Traxler, E. A., Yao, Y., Wang, Y. D., Woodard, K. J., Kurita, R., Nakamura, Y., et al. (2016). A genome-editing strategy to treat beta-hemoglobinopathies that recapitulates a mutation associated with a benign genetic condition. *Nat. Med.* 22, 987–990. doi: 10.1038/nm.4170

Tshilolo, L., Tomlinson, G., Williams, T. N., Santos, B., Olupot-Olupot, P., Lane, A., et al. (2019). Hydroxyurea for children with sickle cell anemia in sub-saharan Africa. *N. Engl. J. Med.* 380, 121–131. doi: 10.1056/NEJMoa1813598

van Zuuren, E. J., and Fedorowicz, Z. (2015). Low-molecular-weight heparins for managing vaso-occlusive crises in people with sickle cell disease. *Cochrane Database Syst. Rev.* 6:CD010155. doi: 10.1002/14651858.CD010155.pub3

Vichinsky, E., Hoppe, C. C., Ataga, K. I., Ware, R. E., Nduba, V., El-Beshlawy, A., et al. (2019). A phase 3 randomized trial of voxelotor in sickle cell disease. *N. Engl. J. Med.* 381, 509–519. doi: 10.1056/NEJMoa1903212

Vichinsky, E. P., Earles, A., Johnson, R. A., Hoag, M. S., Williams, A., and Lubin, B. (1990). Alloimmunization in sickle cell anemia and transfusion of racially unmatched blood. *N. Engl. J. Med.* 322, 1617–1621. doi: 10.1056/NEJM199006073222301

Villagra, J., Shiva, S., Hunter, L. A., Machado, R. F., Gladwin, M. T., and Kato, G. J. (2007). Platelet activation in patients with sickle disease, hemolysis-associated pulmonary hypertension, and nitric oxide scavenging by cell-free hemoglobin. *Blood* 110, 2166–2172. doi: 10.1182/blood-2006-12-061697

Vinjamur, D. S., Bauer, D. E., and Orkin, S. H. (2018). Recent progress in understanding and manipulating haemoglobin switching for the haemoglobinopathies. *Br. J. Haematol.* 180, 630–643. doi: 10.1111/bjh.15038

Wailoo, K. (2017). Sickle cell disease - a history of progress and peril. *N. Engl. J. Med.* 376, 805–807. doi: 10.1056/NEJMp1700101

Walters, M. C., Hardy, K., Edwards, S., Adamkiewicz, T., Barkovich, J., Bernaudin, F., et al. (2010). Pulmonary, gonadal, and central nervous system status after bone marrow transplantation for sickle cell disease. *Biol. Blood Marrow Transplant.* 16, 263–272. doi: 10.1016/j.bbmt.2009.10.005

Walters, M. C., Patience, M., Leisenring, W., Eckman, J. R., Buchanan, G. R., Rogers, Z. R., et al. (1996a). Barriers to bone marrow transplantation for sickle cell anemia. *Biol. Blood Marrow Transplant.* 2, 100–104.

Walters, M. C., Patience, M., Leisenring, W., Eckman, J. R., Scott, J. P., Mentzer, W. C., et al. (1996b). Bone marrow transplantation for sickle cell disease. *N. Engl. J. Med.* 335, 369–376. doi: 10.1002/ajh.24995

Walters, M. C., Patience, M., Leisenring, W., Rogers, Z. R., Aquino, V. M., Buchanan, G. R., et al. (2001). Stable mixed hematopoietic chimerism after bone marrow transplantation for sickle cell anemia. *Biol. Blood Marrow Transplant.* 7, 665–673. doi: 10.1053/bbmt.2001.v7.pm11787529

Wang, W. C., Ware, R. E., Miller, S. T., Iyer, R. V., Casella, J. F., Minniti, C. P., et al. (2011). Hydroxycarbamide in very young children with sickle-cell anaemia: a multicentre, randomised, controlled trial (BABY HUG). *Lancet* 377, 1663–1672. doi: 10.1016/S0140-6736(11)60355-3

Ware, R. E. (2015). Optimizing hydroxyurea therapy for sickle cell anemia. *Hematol. Am. Soc. Hematol. Educ. Program* 2015, 436–443. doi: 10.1182/asheducation-2015.1.436

Ware, R. E., and Aygun, B. (2009). Advances in the use of hydroxyurea. *Hematol. Am. Soc. Hematol. Educ. Program* 2009, 62–69.

Ware, R. E., Davis, B. R., Schultz, W. H., Brown, R. C., Aygun, B., Sarnaik, S., et al. (2016). Hydroxycarbamide versus chronic transfusion for maintenance of transcranial doppler flow velocities in children with sickle cell anaemia-TCD with transfusions changing to hydroxyurea (TWiTCH): a multicentre, open-label, phase 3, non-inferiority trial. *Lancet* 387, 661–670. doi: 10.1016/S0140-6736(15)01041-7

Ware, R. E., Schultz, W. H., Yovetich, N., Mortier, N. A., Alvarez, O., Hilliard, L., et al. (2011). Stroke with transfusions changing to hydroxyurea (SWiTCH): a phase III randomized clinical trial for treatment of children with sickle cell anemia, stroke, and iron overload. *Pediatr. Blood Cancer* 57, 1011–1017. doi: 10.1002/pbc.23145

Wienert, B., Martyn, G. E., Funnell, A. P. W., Quinlan, K. G. R., and Crossley, M. (2018). Wake-up sleepy gene: reactivating fetal globin for beta-hemoglobinopathies. *Trends Genet.* 34, 927–940. doi: 10.1016/j.tig.2018.09.004

Williams, T. N., and Thein, S. L. (2018). Sickle cell anemia and its phenotypes. *Annu. Rev. Genomics Hum. Genet.* 19, 113–147. doi: 10.1146/annurev-genom-083117-021320

Wilson, J. T., Milner, P. F., Summer, M. E., Nallaseth, F. S., Fadel, H. E., Reindollar, R. H., et al. (1982). Use of restriction endonucleases for mapping the allele for beta s-globin. *Proc. Natl. Acad. Sci. U.S.A.* 79, 3628–3631. doi: 10.1073/pnas.79.11.3628

Wun, T., Paglieroni, T., Tablin, F., Welborn, J., Nelson, K., and Cheung, A. (1997). Platelet activation and platelet-erythrocyte aggregates in patients with sickle cell anemia. *J. Lab. Clin. Med.* 129, 507–516. doi: 10.1016/s0022-2143(97)90005-6

Zhang, D., Xu, C., Manwani, D., and Frenette, P. S. (2016). Neutrophils, platelets, and inflammatory pathways at the nexus of sickle cell disease pathophysiology. *Blood* 127, 801–809. doi: 10.1182/blood-2015-09-618538

Conflict of Interest: The authors declare that the research was conducted in the absence of any commercial or financial relationships that could be construed as a potential conflict of interest.

frontiers in Physiology

MINI REVIEW
published: 26 May 2020
doi: 10.3389/fphys.2020.00387

Trends in the Development of Diagnostic Tools for Red Blood Cell-Related Diseases and Anemias

Lars Kaestner[1,2]* *and Paola Bianchi*[3]

[1] Theoretical Medicine and Biosciences, Medical Faculty, Saarland University, Homburg, Germany, [2] Experimental Physics, Faculty of Natural Science and Technology, Saarland University, Saarbrücken, Germany, [3] Fondazione IRCCS Ca' Granda Ospedale Maggiore Policlinico Milano, UOC Ematologia, UOS Fisiopatologia delle Anemie, Milan, Italy

In the recent years, the progress in genetic analysis and next-generation sequencing technologies have opened up exciting landscapes for diagnosis and study of molecular mechanisms, allowing the determination of a particular mutation for individual patients suffering from hereditary red blood cell-related diseases or anemia. However, the huge amount of data obtained makes the interpretation of the results and the identification of the pathogenetic variant responsible for the diseases sometime difficult. Moreover, there is increasing evidence that the same mutation can result in varying cellular properties and different symptoms of the disease. Even for the same patient, the phenotypic expression of the disorder can change over time. Therefore, on top of genetic analysis, there is a further request for functional tests that allow to confirm the pathogenicity of a molecular variant, possibly to predict prognosis and complications (e.g., vaso-occlusive pain crises or other thrombotic events) and, in the best case, to enable personalized theranostics (drug and/or dose) according to the disease state and progression. The mini-review will reflect recent and future directions in the development of diagnostic tools for red blood cell-related diseases and anemias. This includes point of care devices, new incarnations of well-known principles addressing physico-chemical properties, and interactions of red blood cells as well as high-tech screening equipment and mobile laboratories.

Keywords: point of care, functional screening, physico-chemical properties, mobile laboratory, sickle cell disease, personalized medication, artificial intelligence

OPEN ACCESS

Edited by:
Philippe Connes, Université Claude Bernard Lyon 1, France

Reviewed by:
Egee Stéphane, UMR 8227 Laboratoire de Biologie Intégrative des Modèles Marins, France
Yves Colin, INSERM U1134 Biologie Intégrée du Globule Rouge, France

***Correspondence:**
Lars Kaestner
lars_kaestner@me.com

Specialty section:
This article was submitted to Red Blood Cell Physiology, a section of the journal Frontiers in Physiology

Received: *15 January 2020*
Accepted: *01 April 2020*
Published: *26 May 2020*

Citation:
Kaestner L and Bianchi P (2020) Trends in the Development of Diagnostic Tools for Red Blood Cell-Related Diseases and Anemias. Front. Physiol. 11:387. doi: 10.3389/fphys.2020.00387

DO WE NEED NOVEL DIAGNOSTIC TOOLS?

There is a demand for novel diagnostic assays and devices from several perspectives. (i) Since we are still facing huge economic differences across our planet, there is a need (and a market) for low-cost diagnosis of common and rare red blood cell-related diseases. This includes sickle cell disease, thalassemia, malaria, and other less common hereditary and acquired hemolytic anemias. (ii) Scientific progress and the omics era allowed to unravel new diseases. This covers so far undiagnosed red blood cell diseases as well as identifying new pathogenetic variants in previously phenomenologically defined diseases. However, the huge amount of data obtained need to be

interpreted, and often variants predicted at *in silico* analysis as possibly pathogenic—the so-called variants of unknown significance (VUS)—may have no or very little impact on protein function and obviously require further diagnostic tests to assess their functional involvement in the disease. (iii) Even knowing the molecular defect in diseases does not tell us much about the severity and the current state of the disease (e.g., severity of anemia, vaso-occlusive crisis in sickle cell disease). Thus, there is a need to establish the prognosis and possible complications of particular disease states and to determine an appropriate treatment. This is not restricted to the selection or combination of particular drugs but also the dose of these drugs. The concept of personalized theranostics addresses this issue but requires new approaches to become effective.

Given the rarity and the heterogeneity of this group of disorders, the interest of pharmaceutical companies and device maufacturers in developing drugs and technological devices, respectively was limited in the past. The strong possibility not to reach a sufficient volume of requests, the approach to rare disorders, in particular the congenital ones, was scanty up to some years ago. Funding initiatives for rare diseases, especially by the European Commission (within the 7th Framework Program and Horizon 2020) boosted research in the field of rare anemias, and this will continue within the coming years (Horizon Europe). A consensus document highlighting major achievements in diagnosis and treatment of blood disorders, including rare red blood cell disorders, and identifying the greatest unmet clinical and scientific needs has been recently prepared by more than 300 experts belonging to the European Hematology Association (EHA) (Engert et al., 2016).

POINT OF CARE DIAGNOSTIC DEVICES

There are many requirements that should be taken into consideration in the development of a point of care device. It is important that the test performed will be rapid, user-friendly, easily interpretable, sensitive and specific (to avoid false negative and positive results). Another aspect that should always be considered in the development of point of care diagnostic devices is their size. They need to be transportable and in the best case being pocket size. Furthermore, such devices need to be affordable, although the threshold for the market price is different depending on the socio-economic environment of the patient(s). In particular, one of the technical developments of the past decade is in favor of such developments: the smartphones (and tablets) are ever improving mini-computers with innovative interaction interfaces that often "only" require particular sensors and the complementary software to turn into a diagnostic device. Even smartwatches (or fitness watches) already measure routinely heart rate and other health-related parameters start to become routine read-outs such as oxygen saturation (see, e.g., Garmin watch portfolio) or blood pressure. It is worthwhile to mention that most point of care devices work completely non-invasive or at least only require such small amounts of blood that can be taken by finger prick avoiding venous puncture (e.g., Pandey et al., 2018). Examples of early developments of smartphone-based diagnostic devices in conjunction with an "App" and appropriate sensors have been described for the detection of sickle cell disease (Knowlton et al., 2015; Ung et al., 2015), although not all point of care diagnostic devices are smartphone based. Promising recent developments are the HemoTypeSC to determine the hemoglobin types by Silver Lake Research (Azusa, CA, United States) (e.g., Nankanja et al., 2019; Steele et al., 2019; Mukherjee et al., 2020) or Sickle SCAN with a similar application by BioMedomics (Morrisville, NC, United States) (Nguyen-Khoa et al., 2018). Also, a recent enrichment on the market was Q-POC by QuantuMDx (Newcastle, United Kingdom). Although initially developed to diagnose infectious diseases, it is also tested to diagnose all the different β-thalassemia mutations (Elion, 2019).

A very special test for sickle cell disease was recently developed. The test is utilizing filter paper and, thus, costs less than 0.05€ per test (Delobel et al., 2018).

A NEW GENERATION OF DEVICES PROBING FOR PHYSICO-CHEMICAL PROPERTIES OF RED BLOOD CELLS

As outlined in the introduction, although the identification of a molecular lesion is mandatory in genetic disorders to confirm the diagnosis, clinical observations reveal that the genotype/phenotype correlation is not always possible and that other genetic/epigenetic factors (other than the molecular defect) may contribute to the clinical phenotype. This is particularly evident in case of intrafamily clinical variability in presence of the same mutation, or in clinical variability in the same patient during his life (Grace et al., 2018; Bianchi et al., 2020). Therefore, diagnostic devices that address physico-chemical properties such as cellular deformability, hemolysis, and red blood cell interaction properties entered the market or are under development.

An example addressing cell deformability is the LoRRca (RR Mechatronics, Hoorn, Netherlands) (**Figure 1**). The instrument was developed and commercialized only some years ago. Initially, it was used in a few highly specialized centers, but now, it is increasingly used to routinely diagnose rare red cell disorders (Da Costa et al., 2016; Zaninoni et al., 2018). Moreover, its new oxygen scan application, measuring the relative oxygen pressure at the critical point the red blood cells start to sickle, might offer in the future new opportunities for monitoring sickling during new treatment strategies, personalized medicine, and prediction of complication in sickle cell disease (Rab et al., 2020).

A neat concept to test red blood cell stability based on a bead mill and spectral measurement of hemoglobins was developed by Blaze Medical Devices (Ann Arbor, MI, United States). Although the concept was convincing (Tarasev et al., 2016), the device never entered the market. However, measurements as a service are offered by Functional Fluidics (Detroit, MI, United States).

Yet another example is a table top device called MeCheM (mechanical and chemical modulator) that was developed by Epigem Ltd. (Redcar, United Kingdom) within the project CoMMiTMenT (Combined Molecular Microscopy for Therapy

A

B

KEY PARAMETERS

- Deformability
- Osmoscan
- Aggregation & dis-aggregation
- Oxygenscan
- **Time of analysis:** 6 min for an osmoscan
- **Consumables:** Polyvinylpyrrolidone (PVP) buffer to resuspend RBC
  High /Low osmolality medium
- **Blood sample size:** 200µl

C

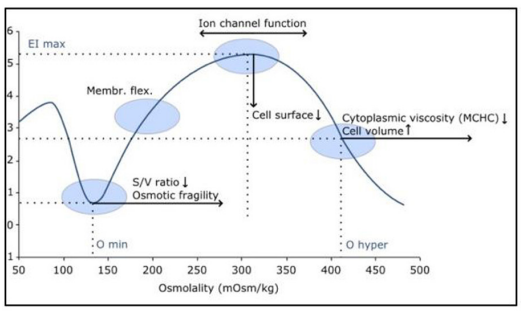

OSMOSCAN ANALYSIS
Parameters analysed
Omin = Osmolality at minimum deformability
El Max = Elongation index max corresponding to the maximal deformability
Ohyper = Osmolality in the hypertonic region corresponding to 50% of the Elmax
AUC = Area under the curve

D

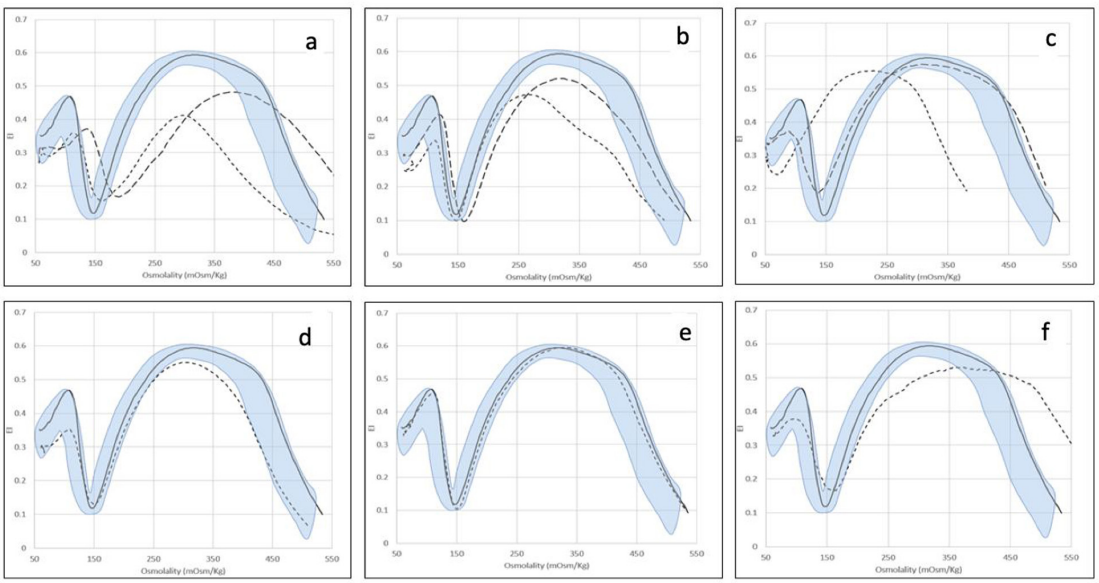

FIGURE 1 | Analysis of RBC membrane disorders and other rare haemolytic anaemias by ektacytometry analysis. **(A)** Image of the Laser Optical Rotational Red Cell Analyzer (LoRRca Maxsis RR Mechatronics, Netherlands). **(B)** List of key parameters analyzed by the instruments. **(C)** Osmoscan profile in normal subjects and parameters analyzed: the Omin value represents the 50% of the RBCs hemolysis in conventional osmotic fragility assays, reflecting mean cellular surface-to volume ratio; the Elongation Index (EI) max corresponds to the maximal deformability obtained near the isotonic osmolality and is an expression of the membrane surface; the Ohyper reflects mean cellular hydration status; the AUC correspond to the area under the curve beginning from a starting point in the hypo-osmolar region and an ending point in the hyper-osmolar region. **(D)** Examples of typical osmoscan profiles in hemolytic anemias resulting from the analysis of 202 patients affected by congenital hemolytic anemia of different etiology. Continuous line represents a daily control and shaded area the control range curve. **(a)** HS = hereditary spherocytosis, **(b)** HE = hereditary elliptocytosis, **(c)** HSt = hereditary stomatocytosis: HSt-PIEZO1 (hereditary xerocytosis) (dotted line), HSt-KCNN4 (Gardos channelopathy) (dashed line), **(d)** CDAII = congenital diserythropoietic anemia type II, **(e)** RBC enzymopathies (pyruvate kinase deficiency), **(f)** other rarer RBC enzymopathies (glucosephosphate isomerase deficiency). Panels **(A)** and **(C)** are reproduced with permission from RR Mechatronics. Panels **(D)** is reproduced from Zaninoni et al. (2018).

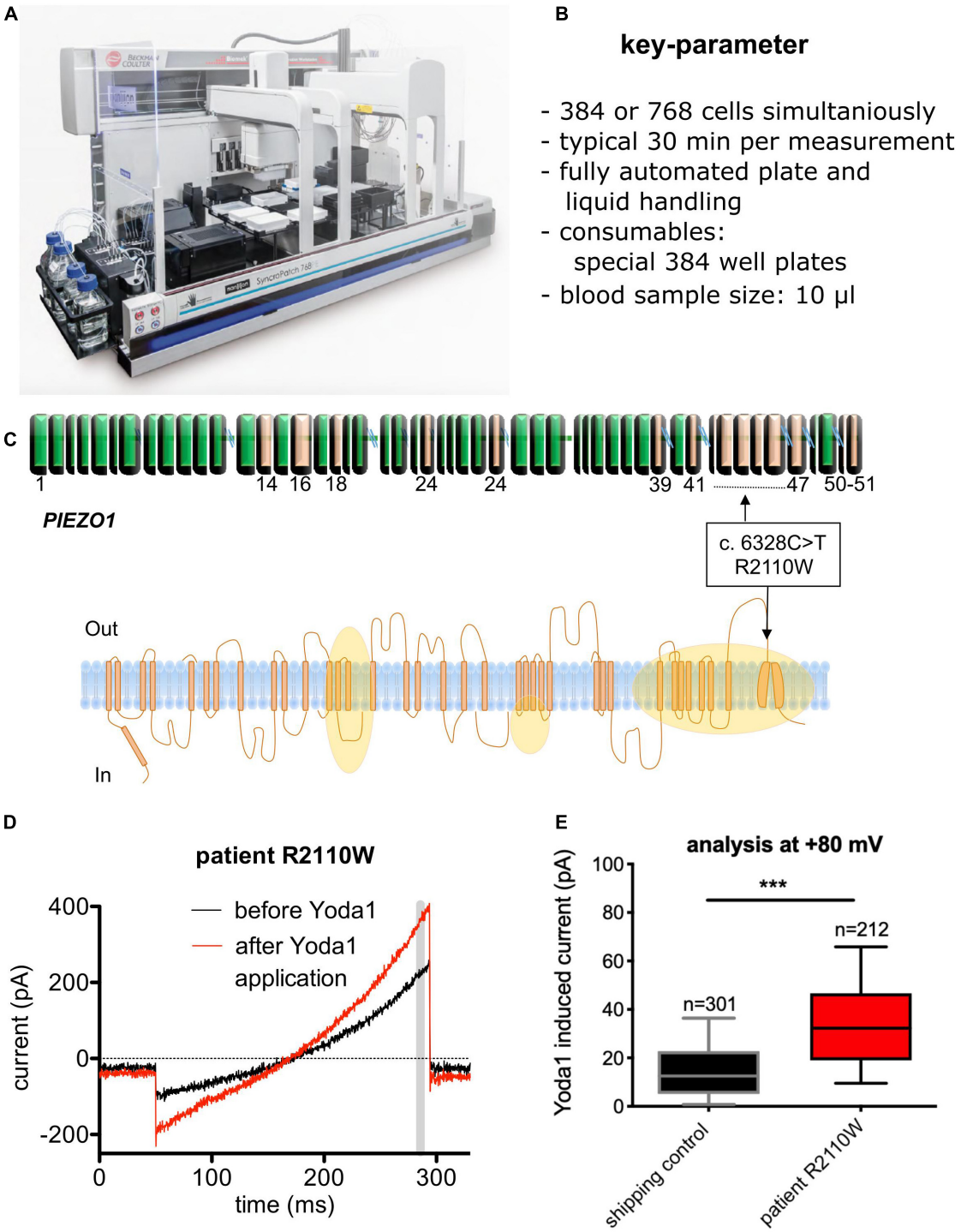

FIGURE 2 | Diagnosis of a novel *PIEZO* mutation with automated patch-clamp technology. **(A)** Image of the SyncroPatch device (Nanion Technologies, Munich, Germany). **(B)** List of key parameters of the SyncroPatch. **(C)** Illustration of a novel mutation (R2110W) of the Piezo 1 ion channel. Although detected *per se*, it was unknown if the mutation has a functional effect on the red blood cells. Orange areas represent regions affected by previously reported mutations. **(D)** Raw data traces of a red blood cell recording for illustration. Yoda1 is a specific activator of Piezo 1. The gray bar depicts the time point (= membrane potential), which was used for the statistical analysis. **(E)** Statistical analysis of all measured cells (R2110W mutation vs. control) to exemplify the functional impact of the mutation. n gives the number of successful measured and analyzed cells. **(A)** Reproduced with permission from Nanion Technologies. **(C–E)** Reproduced from Rotordam et al. (2019) with permission of the Ferrata Storti Foundation.

and Personalized Medication in Rare Anemias Treatments, funded in the European Community 7th Framework Program). It is a microfluidic device that can challenge red blood cells chemically or with functional surfaces, while red blood cells are microscopically observed. Although it is not yet on the market, it is under investigation in several hematologic laboratories within Europe and in a clinical trial testing the efficiency of Memantine for the treatment of sickle cell disease (Makhro et al., 2020).

NOVEL SCREENS BASED ON HIGH-TECH, ROBOTICS, AND ARTIFICIAL INTELLIGENCE

The opposite of point of care devices are machines or procedures that are so complicated and/or expensive that they are exclusively established in expert centers or even in specialized research laboratories. For these devices/procedures, it is sometimes hard to distinguish between the generation of new knowledge and diagnosis—at least this borderline is fuzzy. An example of such a device is an automated patch-clamp robot that in the past proofed to be useful for the investigation of red blood cells (Makhro et al., 2013; Minetti et al., 2013). An image of the device and the joint test is given in **Figure 2**. This patch-clamp robot, originally developed for pharmacological compound screening, was used for a functional diagnosis of a new variant of a mutation of the mechanosensitive ion-channel Piezo1, which is associated with hereditary xerocytosis (Rotordam et al., 2019).

Another procedure used to understand/diagnose diseases is the *in vitro* erythropoiesis, which was refined and optimized considerably also in the past decade. Although bioreactors for an automated and controlled differentiation from peripheral stem cells to erythrocytes are under development (Heshusius et al., 2020), up to date, *in vitro* erythropoiesis still requires the human resource of a scientist or technician to be performed. However, we like to emphasize that recent results showed the importance of erythropoiesis for determination of the severity of the disease (Moura et al., 2019; Caulier et al., 2020).

Artificial intelligence based on artificial neuronal networks is a concept that will enter all incarnations of diagnostic devices as long as they involve computational power. A very old and established diagnostic tool, the analysis of blood smears, is currently reinvented based on the recordings of confocal stacks, three-dimensional rendering of the cells, and classification of the cell shapes by artificial neural networks (compare Bogdanova et al., 2020 within this research topic). Whether it will indeed be possible to link the occurrence of particular cell shapes with concrete mutations still needs to be explored.

LOGISTIC CONCEPTS FOR HIGH-TECH DIAGNOSIS AND RESEARCH

Given the rarity and the heterogeneity of this group of disorders, the confinement between research and diagnostics is sometimes faint, especially for the rare or undiagnosed diseases. In the presence of very rare disorders (e.g., some rare red blood cell enzyme defects or in defects of cell volume regulation), each case seems unique and worth to be described and deeply characterized. Networking activities to recruit similar cases and to joint expertise and collaborations is utmost important in this field (e.g., Vives Corrons et al., 2014; Fermo et al., 2017; Petkova-Kirova et al., 2019). However, this requires a logistic organization of collaboration, in particular for sharing the blood samples. The most common mode is the shipment of samples. This is easy and straightforward when cells or cell extracts can be preserved, like for blood smears, chemically fixed cells for morphological investigations (Abay et al., 2019), isolated RNA for genetic investigations, frozen cells, e.g., for protein analysis, etc. However, it is much more complicated when assays are based on living cells. Some years ago, we performed a dedicated study on healthy red blood cells to mimic transportation conditions (Makhro et al., 2016). The outcome was surprising in the respect that different red blood cell parameters require different conditions in terms of anticoagulant and temperature to resemble the results of fresh red blood cells. With cells of patients, the situation can be even worse. In a recent study on cellular intracellular Ca^{2+} (Hertz et al., 2017), the effect of the transportation was bigger than the effect of the disease. In this particular study, the data could be "rescued" by normalizing to healthy transportation controls. However, we also found that in certain conditions, differences between patients and control can easily be lost during some hours *in vitro* (Rotordam et al., 2019). Taking all these indications and although shipment of blood samples is the most common and popular method of interlaboratory collaboration, it is by far not an ideal configuration. However, a much better option would be if the patients travel to the specialized laboratories. Although we recently introduced this practice in our laboratory, it does work only for a minority of patients (due to the state of the patients, their compliance, or other restrictions) and is only a kind of control that hardly can reach statistical power, especially for rare and very rare diseases. The third option would be mobile specialized laboratories. Surprisingly, this idea, so far, got stuck within discussion among researchers, presumably because appropriate funding programs are the restriction. From the technical point of view, (i) we are, in principle, able to catapult even confocal microscopes with biological samples into space (Thiel et al., 2019) and (ii) an increasing number of devices are designed for transportation. This is not restricted to the classical point of care devices mentioned above but also applies for fairly complicated machines such as flow cytometers (e.g., CyFlow Cube6, Sysmex, Germany). Therefore, a mobile laboratory down on earth for red blood cell-related diseases should be a challenging project but with high chances of success and only limited risks as it was realized for other purposes before (e.g., Weidmann et al., 2018). However, the intended project/use should define whether such a laboratory should be on wheels, on a boat, or on board an aircraft.

CONCLUSION AND OUTLOOK

Point of care, artificial intelligence, and personalized theranostocs are probably the major keywords that

characterize current and future developments in diagnostic devices for red blood cell-related diseases, in general, and for rare anemias, in particular. From a conceptual point of view, genetic analysis is well established, and decrease in the size of devices and significant cost drops will increase the spread and the regular use of this diagnostic tool. In line with this, a targeted analysis of a defined (group of) protein(s) will be replaced by a full genome analysis. However, functional analysis (more and more based on individual cells) on top of gene characterization will become increasingly important. This may go far beyond the samples given above and is likely to include further miniaturized assays of well-known tests such as the investigation of cell density distributions or measurements considering filterability properties.

AUTHOR CONTRIBUTIONS

Both authors wrote and approved the manuscript.

FUNDING

This work received funding from the European Union's Horizon 2020 Research and Innovation Programme under Grant Agreement No. 860436 – EViDENCE.

ACKNOWLEDGMENTS

We would like to thank Prof. Jacques Elion for valuable information exchange.

REFERENCES

Abay, A., Simionato, G., Chachanidze, R., Bogdanova, A., Hertz, L., Bianchi, P., et al. (2019). Glutaraldehyde – a subtle tool in the investigation of healthy and pathologic red blood cells. *Front. Physiol.* 10:514. doi: 10.3389/fphys.2019.00514

Bianchi, P., Fermo, E., Lezon-Geyda, K., van Beers, E., Morton, D. H., Barcellini, W., et al. (2020). Genotype-phenotype correlation and molecular heterogeneity in pyruvate kinase deficiency. *Am. J. Hemtol.* 95, 472–482. doi: 10.1002/ajh.25753

Bogdanova, A., Kaestner, L., Simionato, G., Wickrema, A., and Makhro, A. (2020). Heterogeneity of red blood cells: causes and consequences. *Front. Physiol.* 11:392. doi: 10.3389/fphys.2020.00392

Caulier, A., Jankovsky, N., Demont, Y., Ouled-Haddou, H., Demagny, J., Guitton, C., et al. (2020). PIEZO1 activation delays erythroid differentiation of normal and hereditary xerocytosis-derived human progenitor cells. *Haematologica* 105, 610–622. doi: 10.3324/haematol.2019.218503

Da Costa, L., Suner, L., Galimand, J., Bonnel, A., Pascreau, T., Couque, N., et al. (2016). Diagnostic tool for red blood cell membrane disorders: assessment of a new generation ektacytometer. *Blood Cells Mol. Dis.* 56, 9–22. doi: 10.1016/j.bcmd.2015.09.001

Delobel, J., Keitel, K., Balmas-Bourloud, K., and Mlaganile, T. (2018). Harnessing the power of global health studies for sickle cell disease: validation of a rapid, open-source, paper- based screening assay in a cohort of 1103 Tanzanian children. *Blood* 132:150.

Elion, J. (2019). personal communication. UMR Inserm U1134 - Université Paris Diderot/USCP Institut National de la Transfusion Sanguine.

Engert, A., Balduini, C., Brand, A., Coiffier, B., Cordonnier, C., Döhner, H., et al. (2016). The European hematology association roadmap for european hematology research: a consensus document. *Haematologica* 101, 115–208. doi: 10.3324/haematol.2015.136739

Fermo, E., Petkova-Kirova, P., Zaninoni, A., Marcello, A. P., Makhro, A., et al. (2017). 'Gardos Channelopathy': a variant of hereditary Stomatocytosis with complex molecular regulation. *Sci. Rep.* 7:1744. doi: 10.1038/s41598-017-01591-w

Grace, R. F., Bianchi, P., van Beers, E. J., Eber, S. W., Glader, B., Yaish, H. M., et al. (2018). Clinical spectrum of pyruvate kinase deficiency: data from the pyruvate kinase deficiency natural history study. *Blood* 131, 2183–2192. doi: 10.1182/blood-2017-10-810796

Hertz, L., Huisjes, R., Llaudet-Planas, E., Petkova-Kirova, P., Makhro, A., Danielczok, J., et al. (2017). Is increased intracellular calcium in red blood cells a common component in the molecular mechanism causing anemia? *Front. Physiol.* 8:673. doi: 10.3389/fphys.2017.00673

Heshusius, S., Heideveld, E., Burger, P., Thiel-Valkhof, M., Sellink, E., Varga, E., et al. (2020). Large-scale in vitro production of red blood cells from human peripheral blood mononuclear cells. *Blood Adv.* 3, 3337–3350. doi: 10.1182/bloodadvances.2019000689

Knowlton, S. M., Sencan, I., Aytar, Y., Khoory, J., and Heeney, M. M. (2015). Sickle cell detection using a smartphone. *Sci. Rep.* 5:15022.

Makhro, A., Hanggi, P., Goede, J., Wang, J., Bruggemann, A., Gassmann, M., et al. (2013). N-methyl D-aspartate (n.d.) receptors in human erythroid precursor cells and in circulating red blood cells contribute to the intracellular calcium regulation. *Am. J. Physiol. Cell Physiol.* 305, C1123–C1138. doi: 10.1152/ajpcell.00031.2013

Makhro, A., Hegemann, I., Seiler, E., Simionato, G., Claveria, V., Bogdanov, N., et al. (2020). MemSID clinical trial: acute and long-term changes of red blood cells of sickle cell disease patients on memantine treatment. *eJHaem* doi: 10.1002/jha2.11

Makhro, A., Huisjes, R., Verhagen, L. P., Mañú-Pereira, M. M., Llaudet-Planas, E., Petkova-Kirova, P., et al. (2016). Red cell properties after different modes of blood transportation. *Front. Physiol.* 7:288. doi: 10.3389/fphys.2016.00288

Minetti, G., Egée, S., Mörsdorf, D., Steffen, P., Makhro, A., Achilli, C., et al. (2013). Red cell investigations: art and artefacts. *Blood Rev.* 27, 91–101. doi: 10.1016/j.blre.2013.02.002

Moura, P. L., Hawley, B. R., Dobbe, J. G. G., Streekstra, G. J., Rab, M. A. E., Bianchi, P., et al. (2019). PIEZO1 gain-of-function mutations delay reticulocyte maturation in hereditary xerocytosis. *Haematologica* [Epub ahead of print]. doi: 10.3324/haematol.2019.231159

Mukherjee, M. B., Colah, R. B., Mehta, P. R., Shinde, N., Jain, D., Desai, S., et al. (2020). Multicenter Evaluation of HemoTypeSC as a point-of-care sickle cell disease rapid diagnostic test for newborns and adults across India. *Am. J. Clin. Pathol.* 153, 82–87. doi: 10.1093/ajcp/aqz108

Nankanja, R., Kadhumbula, S., Tagoola, A., Geisberg, M., Serrao, E., and Balyegyusa, S. (2019). HemoTypeSC Demonstrates >99% field accuracy in a sickle cell disease screening initiative in children of Southeastern Uganda. *Am. J. Hematol.* 94, E164–E166. doi: 10.1002/ajh.25458

Nguyen-Khoa, T., Mine, L., Allaf, B., Ribeil, J. A., Remus, C., Stanislas, A., et al. (2018). Sickle SCAN^{TM} (BioMedomics) fulfills analytical conditions for neonatal screening of sickle .cell disease. *Ann. Biol. Clin.* 76, 416–420. doi: 10.1684/abc.2018.1354

Pandey, C. M., Augustine, S., Kumar, S., Kumar, S., Nara, S., Srivastava, S., et al. (2018). Microfluidics based point-of-care diagnostics. *Biotechnol. J.* 13:1700047.

Petkova-Kirova, P., Hertz, L., Danielczok, J., Huisjes, R., Makhro, A., Bogdanova, A., et al. (2019). Red blood cell membrane conductance in hereditary haemolytic anaemias. *Front. Physiol.* 10:386. doi: 10.3389/fphys.2019.00386

Rab, M. A. E., Kanne, C. K., Bos, J., Boisson, C., van Oirschot, B. A., Nader, E., et al. (2020). Methodological aspects of the oxygenscan in sickle cell disease: a need for standardization. *Am. J. Hematol.* 95, E5–E8. doi: 10.1002/ajh.25655

Rotordam, G. M., Fermo, E., Becker, N., Barcellini, W., Brüggemann, A., Fertig, N., et al. (2019). A novel gain-of-function mutation of Piezo1 is functionally

affirmed in red blood cells by high-throughput patch clamp. *Haematologica* 104:e181. doi: 10.3324/haematol.2018.201160

Steele, C., Sinski, A., Asibey, J., Hardy-Dessources, M. D., Elana, G., Brennan, C., et al. (2019). Point-of-care screening for sickle cell disease in low-resource settings: a multi-center evaluation of HemoTypeSC, a novel rapid test. *Am. J. Hematol.* 94, 39–45. doi: 10.1002/ajh.25305

Tarasev, M., Muchnik, M., Light, L., Alfano, K., and Chakraborty, S. (2016). Individual variability in response to a single sickling event for normal, sickle cell, and sickle trait erythrocytes. *Transl. Res.* 181, 96–107. doi: 10.1016/j.trsl.2016.09.005

Thiel, C. S., Tauber, S., Lauber, B., Polzer, J., Seebacher, C., Uhl, R., et al. (2019). Rapid morphological and cytoskeletal response to microgravity in human primary macrophages. *Int. J. Mol. Sci.* 20:E2402. doi: 10.3390/ijms20102402

Ung, R., Alapan, Y., Hasan, M. N., Romelfanger, M., He, P., Tam, A., et al. (2015). Point-of-care screening for sickle cell disease by a mobile micro-electrophoresis platform. *Blood* 126:3379.

Vives Corrons, J. L., Manu Pereira, M. D. M., Casabona, C. R., Nicolas, P., Gulbis, B., Eleftheriou, A., et al. (2014). The ENERCA white book - recommendations for centres of expertise in rare anaemias. *Thalassemia Rep.* 4, 86–90. doi: 10.4081/thal.2014.4878

Weidmann, M., Faye, O., Faye, O., Abd El Wahed, A., Patel, P., Batejat, C., et al. (2018). Development of mobile laboratory for viral hemorrhagic fever detection in Africa. *J. Infect. Dis.* 218, 1622–1630. doi: 10.1093/infdis/jiy362

Zaninoni, A., Fermo, E., Vercellati, C., Consonni, D., Marcello, A. P., Zanella, A., et al. (2018). Use of laser assisted optical rotational cell analyzer (LoRRca MaxSis) in the diagnosis of RBC membrane disorders, enzyme defects, and congenital dyserythropoietic anemias: a monocentric study on 202 patients. *Front. Physiol.* 9:451. doi: 10.3389/fphys.2018.00451

Conflict of Interest: The authors declare that the research was conducted in the absence of any commercial or financial relationships that could be construed as a potential conflict of interest.

frontiers in Physiology

ORIGINAL RESEARCH
published: 05 June 2020
doi: 10.3389/fphys.2020.00578

Metabolomics of Endurance Capacity in World Tour Professional Cyclists

Iñigo San-Millán[1,2,3], Davide Stefanoni[4], Janel L. Martinez[2], Kirk C. Hansen[4], Angelo D'Alessandro[4] and Travis Nemkov[4]**

[1] Department of Human Physiology and Nutrition, University of Colorado Colorado Springs, Colorado Springs, CO, United States, [2] Division of Endocrinology, Metabolism and Diabetes, Department of Medicine, University of Colorado Anschutz Medical Campus, Aurora, CO, United States, [3] Department of Research and Development, UAE Team Emirates, Abu Dhabi, United Arab Emirates, [4] Department of Biochemistry and Molecular Genetics, University of Colorado Anschutz Medical Campus, Aurora, CO, United States

The study of elite athletes provides a unique opportunity to define the upper limits of human physiology and performance. Across a variety of sports, these individuals have trained to optimize the physiological parameters of their bodies in order to compete on the world stage. To characterize endurance capacity, techniques such as heart rate monitoring, indirect calorimetry, and whole blood lactate measurement have provided insight into oxygen utilization, and substrate utilization and preference, as well as total metabolic capacity. However, while these techniques enable the measurement of individual, representative variables critical for sports performance, they lack the molecular resolution that is needed to understand which metabolic adaptations are necessary to influence these metrics. Recent advancements in mass spectrometry-based analytical approaches have enabled the measurement of hundreds to thousands of metabolites in a single analysis. Here we employed targeted and untargeted metabolomics approaches to investigate whole blood responses to exercise in elite World Tour (including Tour de France) professional cyclists before and after a graded maximal physiological test. As cyclists within this group demonstrated varying blood lactate accumulation as a function of power output, which is an indicator of performance, we compared metabolic profiles with respect to lactate production to identify adaptations associated with physiological performance. We report that numerous metabolic adaptations occur within this physically elite population (n = 21 males, 28.2 ± 4.7 years old) in association with the rate of lactate accumulation during cycling. Correlation of metabolite values with lactate accumulation has revealed metabolic adaptations that occur in conjunction with improved endurance capacity. In this population, cycling induced increases in tricarboxylic acid (TCA) cycle metabolites and Coenzyme A precursors. These responses occurred proportionally to lactate accumulation, suggesting a link between enhanced mitochondrial networks and the ability to sustain higher workloads. In association with lactate accumulation, altered levels of amino acids before and after exercise point to adaptations that confer

OPEN ACCESS

Edited by:
Lars Kaestner, Saarland University, Germany

Reviewed by:
Giel Bosman, Radboud University Nijmegen, Netherlands
Lello Zolla, University of Tuscia, Italy

***Correspondence:**
Iñigo San-Millán
inigo.sanmillan@cuanschutz.edu
Travis Nemkov
travis.nemkov@cuanschutz.edu

Specialty section:
This article was submitted to Red Blood Cell Physiology, a section of the journal Frontiers in Physiology

Received: *28 February 2020*
Accepted: *08 May 2020*
Published: *05 June 2020*

Citation:
San-Millán I, Stefanoni D, Martinez JL, Hansen KC, D'Alessandro A and Nemkov T (2020) Metabolomics of Endurance Capacity in World Tour Professional Cyclists. Front. Physiol. 11:578. doi: 10.3389/fphys.2020.00578

unique substrate preference for energy production or to promote more rapid recovery. Cyclists with slower lactate accumulation also have higher levels of basal oxidative stress markers, suggesting long term physiological adaptations in these individuals that support their premier competitive status in worldwide competitions.

Keywords: metabolomics, elite athletes, endurance, exercise, lactate, oxidative stress, amino acid metabolism, mitochondrial metabolism

INTRODUCTION

The physiological and metabolic response to exercise has fascinated scientists for centuries. In 1784, Antoine Lavoisier and Pierre-Simon Laplace designed an ice-calorimeter to measure the amount of heat emitted during combustion and respiration, which enabled the measurement of oxygen (O_2) consumption during exercise (Underwood, 1944; Karamanou and Androutsos, 2013). Since then, maximal oxygen consumption (VO_2max) has been considered the gold standard to measure cardiorespiratory fitness (Shephard, 1984). In the last two decades, the monitoring of physiological and metabolic response to exercise using this technique has become increasingly popular in the area of sports medicine and performance, fostered in part by studies involving elite professional athletes. These studies have shaped programs for individualized training, recovery and nutritional regimes and have been based traditionally on VO_2max as the representative parameter due to its relatively easy measurement by indirect calorimetry using commercially available metabolic carts (Jensen et al., 2002).

Despite widespread use, laboratory physiological testing is not ubiquitous as not all athletes have access to advanced exercise laboratory facilities. In addition, respiration-based measurements are not always reproducible in monitoring performance, due to the multiple unmeasured variables that influence this the measured output. As such, additional markers of training status that are more acutely tied to cellular and tissue metabolism have been proposed. Lactate is one such metabolic biomarker that enables measurement of metabolic responses to exercise and serves as a surrogate for muscle stress. Although it had been considered a waste product of anaerobic metabolism, foundational studies by Brooks and colleagues began to shift this decades-old paradigm by demonstrating a higher degree of lactate consumption under fully aerobic conditions than previously thought using isotope tracing studies in rats (Brooks, 1986). Since then, lactate has been shown to be a major fuel source for the body, and even possesses hormone-like properties (Brooks, 2018).

Whole blood lactate measurement has been widely accepted as a valid method to evaluate the metabolic responses to exercise (Jacobs, 1986; Billat, 1996). This measurement also serves as a monitor of training status, since well-trained athletes have a higher lactate clearance capacity and decreased blood lactate levels (Donovan and Brooks, 1983; Bergman et al., 1999) likely due to enhanced mitochondrial function resulting from training (McDermott and Bonen, 1993; Dubouchaud et al., 2000). In addition to ease of measurement using portable equipment, these findings have promoted lactate monitoring as a viable readout for personalized athletic training programs.

To expand upon metabolic programs that may elicit lactate production, studies into substrate utilization (such as fat and carbohydrate oxidation) during exercise using indirect calorimetry have provided improved resolution of exercise physiology (Frayn, 1983). The subsequent combination of blood lactate measurement and substrate utilization during exercise has thus offered novel approaches to measure metabolic function and, indirectly, mitochondrial function and metabolic flexibility (San-Millán and Brooks, 2018). However, despite growing interest into the cellular responses to exercise, these techniques only enable the monitoring of a limited number of parameters thereby hampering our full understanding of metabolic responses in exercise physiology.

The field of metabolomics has emerged strongly in the last decade in many areas of scientific research as a powerful tool to precisely measure metabolic pathways at the cellular and systematic level (D'Alessandro, 2019). Chromatography-based separation of metabolites combined with improved scanning speeds and accuracy of mass detectors has greatly enhanced the breadth and depth of metabolite coverage monitored in a single experiment. These techniques are amenable to measuring metabolites within any biological matrix (Nemkov et al., 2017) and have been applied to multiple exercise-focused studies into metabolic response to exercise that varies by type, intensity, and duration (reviewed in Sakaguchi et al., 2019).

Given the predictive importance of lactate measurement in sports physiology and the robustness of mass spectrometry-based metabolomics, we hypothesized that identification of metabolic pathways altered in conjunction with lactate production will reveal molecular mechanisms of enhanced physical performance. To test this hypothesis, we measured metabolite levels in whole blood samples isolated from a team of elite professional cyclists before and after a graded maximal physiological test and compared metabolic profiles with respect to a lactate-dependent performance cutoff (PC). Expansion of knowledge around lactate-associated metabolic traits could serve to improve multiple aspects of individualized training, nutrition, overtraining, injury prevention and rehabilitation.

MATERIALS AND METHODS

Twenty-one international-level World Tour professional male cyclists (Tour de France Level) performed a graded exercise test to exhaustion on an electrically controlled resistance leg cycle

TABLE 1 | Physiological parameters of male cyclists used in this study.

Age (year)	28.2 ± 4.7
Height (cm)	179.2 ± 7.6
Weight (kg)	70.7 ± 6.7
Body fat (%)	10.4 ± 0.7

ergometer (Elite, Suito, Italy). Physical parameters are included in **Table 1**. After a 15 min warm-up, participants started leg cycling at a low intensity of 2.0 W kg^{-1} of body weight. Exercise intensity was increased 0.5 W kg^{-1} every 10 min as previously described (San-Millán et al., 2009). Power output, heart rate and lactate were measured throughout the entire test and recorded every 10 min including at the end of the test. All study procedures were conducted in accordance with the Declaration of Helsinki and in accordance with a predefined protocol that was approved by all researchers and the Colorado Multiple Institutional Review Board (COMIRB 17-1281). Written informed consent was obtained from all subjects.

Blood Lactate Concentration Measurement

At the end of every intensity stage throughout the graded training period, a sample of capillary blood was collected to analyze both intra- and extra-cellular levels of L-lactate (Lactate Plus, Nova Biomedical, Waltham, MA, United States). Heart rate was monitored during the whole test with a heart monitor (Polar S725x, Polar Electro, Kempele, Finland).

Subjects Group Classification – Performance Cutoff

Cyclists were separated into two groups based on the blood lactate concentration at an exercise intensity of 5.0 W kg^{-1}, designated as the PC. Cyclists with PC lactate levels below the group average of 5 mmol L^{-1} were classified as the Gold group, while cyclists above the average were classified in the Silver group (**Figure 2A**).

Metabolomics Assessment

Sample Collection

Whole blood samples were collected using the Touch-Activated Phlebotomy (TAP) device (Seventh Sense Biosystems, Medford, MA) as previously described (Catala et al., 2018). Due to a limited 100 μL sample volume collected with the TAP device, and to assess the utility of whole blood analyses with the goal of simplifying sample isolation by circumventing the need for centrifugation, whole blood samples were frozen in dry ice within 15 min of isolation and stored at -80°C until analysis. Prior to LC-MS analysis, samples were placed on ice and re-suspended with nine volumes of ice cold methanol:acetonitrile:water (5:3:2, v:v). Suspensions were vortexed continuously for 30 min at 4°C. Insoluble material was removed by centrifugation at 18,000 *g* for 10 min at 4°C and supernatants were isolated for metabolomics analysis by UHPLC-MS. The extract was then dried down under speed vacuum and re-suspended in an equal volume of 0.1% formic acid for analysis.

UHPLC-MS Analysis

Analyses were performed as previously published (Nemkov et al., 2017; Reisz et al., 2019). Briefly, the analytical platform employs a Vanquish UHPLC system (Thermo Fisher Scientific, San Jose, CA, United States) coupled online to a Q Exactive mass spectrometer (Thermo Fisher Scientific, San Jose, CA, United States). The (semi)polar extracts were resolved over a Kinetex C18 column, 2.1 mm× 150 mm, 1.7 μm particle size (Phenomenex, Torrance, CA, United States) equipped with a guard column (SecurityGuard^{TM} Ultracartridge – UHPLC C18 for 2.1 mm ID Columns – AJO-8782 – Phenomenex, Torrance, CA, United States) using an aqueous phase (A) of water and 0.1% formic acid and a mobile phase (B) of acetonitrile and 0.1% formic acid for positive ion polarity mode, and an aqueous phase (A) of water:acetonitrile (95:5) with 1 mM ammonium acetate and a mobile phase (B) of acetonitrile:water (95:5) with 1 mM ammonium acetate for negative ion polarity mode. The Q Exactive mass spectrometer (Thermo Fisher Scientific, San Jose, CA, United States) was operated independently in positive or negative ion mode, scanning in Full MS mode (2 μscans) from 60 to 900 *m/z* at 70,000 resolution, with 4 kV spray voltage, 45 sheath gas, 15 auxiliary gas. Calibration was performed prior to analysis using the Pierce^{TM} Positive and Negative Ion Calibration Solutions (Thermo Fisher Scientific). Acquired data was then converted from.raw to.mzXML file format using Mass Matrix (Cleveland, OH, United States). Samples were analyzed in randomized order with a technical mixture injected after every 15 samples to qualify instrument performance. Metabolite assignments, isotopologue distributions, and correction for expected natural abundances of deuterium, ^{13}C, and ^{15}N isotopes were performed using MAVEN (Princeton, NJ, United States) (Melamud et al., 2010). Discovery mode alignment, feature identification, and data filtering was performed using Compound Discoverer 2.0 (Thermo Fisher Scientific).

Graphs, heat maps and statistical analyses (either *T*-Test or ANOVA), metabolic pathway analysis, partial least squares discriminant analysis (PLS-DA) and hierarchical clustering was performed using the MetaboAnalyst 4.0 package (Chong et al., 2018). *XY* graphs were plotted through GraphPad Prism 8 (GraphPad Software Inc., La Jolla, CA, United States).

RESULTS

The Whole Blood Metabolome Changes Significantly in Response to Exercise

In order to determine systemic metabolic changes during intense cycling, untargeted metabolomics analyses using LC-MS/MS were performed on whole blood samples isolated from cyclists before (Pre) and after (Post) a graded exercise test with cycling intensity normalized to individual cyclist body mass (**Figure 1A**). Of the 2,790 putative compounds detected in discovery mode analysis (ranging from Level 1 to Level 4 confidence, Schrimpe-Rutledge et al., 2016) 355 metabolites were manually identified using accurate intact mass, isotopic pattern, fragmentation and an in-house standard library. These

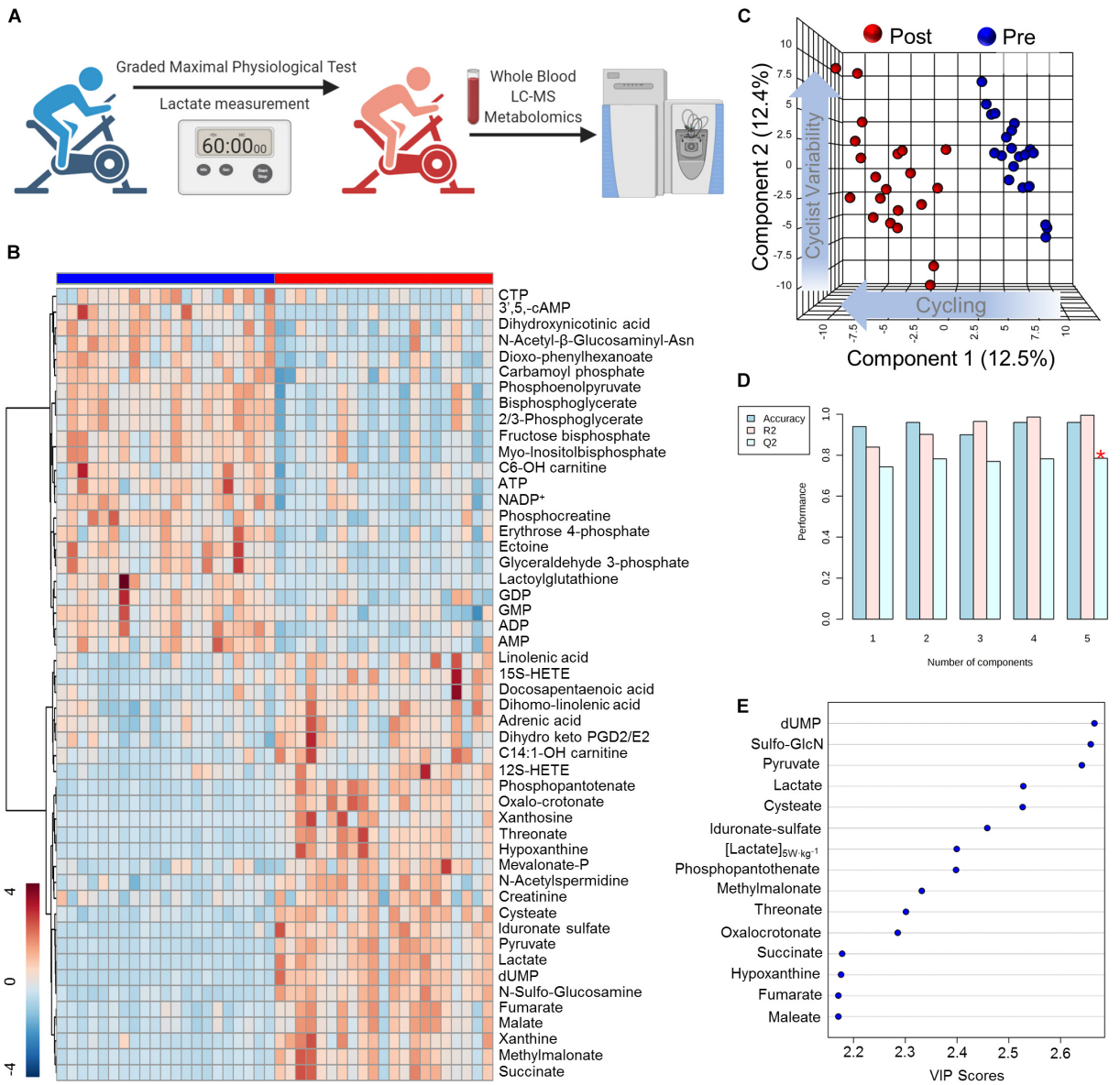

FIGURE 1 | High-Throughput Metabolomics of Endurance Training in Elite Professional Cyclists. **(A)** Blood samples were drawn from subjects using a TAP™ push-button blood collection device before and after 1 h of a graded exercise test. Samples were extracted for hydrophilic or non-polar metabolites and analyzed using a high-throughput LC-MS based metabolomics platform. **(B)** Hierarchical Clustering Analysis of the top 50 T-Test significant metabolites is shown as a heat map and are Z-score normalized, with the color-coded gradient depicted in the lower left corner. **(C)** Partial Least Squares Discriminant Analysis (PLS-DA) shows a distinct clustering pattern of baseline (Pre, blue) and post-test (Post, blue) samples along Component 1 axis (12.5% variance explained), while inter-individual variability is described by the Component 2 axis (12.4% variance explained). **(D)** PLS-DA cross validation details are shown for the first 5 components. **(E)** Parameter with the top 15 variable importance in projection (VIP) scores are shown.

metabolites were systematically analyzed by multivariate analyses such as Principal Component Analysis (PCA; **Figure 1B**) and Hierarchical Clustering Analysis (HCA, **Figure 1C**). A table including the molecular weight, retention time, polarity of detection, and raw peak area top values is provided in **Supplementary Table 1**. The top 50 significant metabolites by a two-tailed Student's *T*-Test were hierarchically clustered to illustrate acute metabolic responses to cycling, showing significant changes for metabolites involved in central energy metabolism (glycolysis, TCA cycle), nucleotide homeostasis, and lipid metabolism (**Figure 1B**). Partially supervised PLS-DA distinguished samples by time point across Component 1 (12.5% of metabolic difference described) and demonstrated variability of metabolic responses amongst cyclists along the Component 2 axis (12.4% of the total metabolic difference described) (**Figure 1C**). The PLS-DA model demonstrated a high degree of accuracy using just the first component ($R2$ = 0.84, $Q2$ = 0.74, Accuracy = 0.92, **Figure 1D**). A larger degree of biological

variability was noted in the Post time point cluster relative to the Pre time point, indicating that the cyclists' responses to strenuous exercise varied within this group. The top 15 metabolites contributing to the clustering pattern include mitochondrial and glycolytic metabolites, indicating importance of these pathways (**Figure 1E**). A heatmap of metabolite values for the entire manually curated dataset is provided in **Supplementary Figure 1**.

Metabolite Abundance Before and After Exercise Associates With Lactate Production in Response to Workload

Interval measurements of whole blood lactate levels in response to workload serves as a personalized metric for cycling performance (Jacobs, 1986). The training status of an individual cyclist can be determined in large part based on the power output (measured in watts per kilogram, W kg^{-1}) at which lactate is produced more rapidly than it is consumed and begins to accumulate, also referred to as the lactate threshold (Brooks, 1985). As training status improves, the lactate threshold increases allowing the cyclist to exert a higher workload for longer periods of time prior to the onset of fatigue. Lactate levels in response to power output varied significantly amongst this group of cyclists. While all but 1 of the 21 cyclists monitored in this study were able to maintain a power output of 5 W kg^{-1}, 14 cyclists reached 5.5 W kg^{-1}, and only three cyclists were able to maintain 6 W kg^{-1} for 10 min (**Figure 2A**). To understand how the network between metabolic pathways differs in these cyclists (a concept we have previously referred to as metabolic linkage (D'Alessandro et al., 2017) we first classified the cyclists into two groups based on whether blood lactate concentration was higher (Gold) or lower (Silver) than the overall average at the designated PC of 5 W kg^{-1} (**Figure 2A**). Using the metabolomics dataset from the Gold group, a Spearman's correlation matrix was prepared and hierarchically clustered to identify regions of the metabolome that are positively and negatively correlated (**Figure 2B**, left panel). A Spearman's correlation matrix of metabolite levels in the Silver group was then prepared and plotted according to the same hierarchical order of the Gold group, and the difference in Spearman's correlation coefficients for each relationship was calculated to highlight changes in metabolic networks between the two groups (**Figure 2B**, central and right panel, respectively). The Spearman's correlation matrix values are provided in **Supplementary Table 2**. This metabolic network analysis revealed numerous significant associations between blood lactate concentration measured at 5 W kg^{-1} and metabolite levels before and after the fitness test (**Figure 2C**). Most of the significant correlations observed in this analysis are metabolites central to energy homeostasis and involved in glycolysis, the TCA cycle, purine homeostasis, and oxidative stress. While the top two negative correlates with lactate at 5 W kg^{-1} were the tyrosine catabolite 4-hydroxyphenylacetylglycine (R = -0.58, $p = 5.92 \times 10^{-5}$) and the late glycolysis intermediate phosphoenolpyruvate (R = -0.58, $p = 6.55 \times 10^{-5}$), the top two positive correlates with peri-test lactate production were the polyamine intermediate N-acetylspermidine (R = 0.62, $p = 1.06 \times 10^{-5}$) and post-test lactate (R = 0.59, $p = 3.26 \times 10^{-5}$) (**Figure 2D**). Furthermore, these two groups appeared to be distinguishable before the initiation of the graded-exercise test, suggesting that the metabolic status prior to exercise could theoretically predict performance (**Supplementary Figure 2**).

Performance Cutoff Is Associated With Basal Oxidative Stress

Lactate production is principally fueled by the metabolic routing of glucose through Embden–Meyerhof–Parnas glycolysis and the pentose phosphate pathway (PPP). In both the Gold and Silver groups, while whole blood glucose increased during exercise due to ongoing glycogenolysis for energy generation, all measured glycolytic intermediates significantly decreased in conjunction with accumulation of end-stage products pyruvate and lactate (**Figure 3A**). Although insignificant by T-test, glucose levels trend higher both before and after exercise, along with higher post-pyruvate and post-lactate levels in the Gold group, indicating an increased glycolytic capacity in these cyclists.

The PPP serves as a primary source of NADPH, which helps manage oxidative stress by functioning as a co-factor for glutathione reductase to convert oxidized glutathione (GSSG) to its reduced state reduced glutathione (GSH). Cycling resulted in overall decreases in PPP intermediates, indicating a preference of glucose metabolism through glycolysis for energy generation (**Figure 3B**). However, PPP intermediates 6-phosphogluconolactone, 6-phosphogluconate, and erythrose 4-phosphate were observed at higher levels overall in the Silver cycling group. This trend suggests increased activation of NADPH generating pathways to cope with the oxidative stress that arises during exercise. Interestingly, oxidative stress markers including oxidized glutathione (GSSG) and methionine sulfoxide (Met-O) were both significantly higher in the Gold group both pre- and post-test, suggesting alterations to oxidative stress and signaling pathways in these individuals (**Figure 3C**). Since handling of these samples was performed *in situ* in the exercise facility, a potential role of iatrogenic intervention on these measurements cannot be ruled out. As such, increased basal levels of these metabolites can be alternatively interpreted as a larger redox reservoir for the athletes in the Gold group at baseline and post-exercise.

Lactate to Pyruvate Ratio Is Associated With Endurance Capacity

Through the activity of GADPH, NAD^+ is reduced to NADH during the conversion of glyceraldehyde 3-phosphate into 1,3-bisphosphoglycerate. Under normal homeostasis in general, and especially in cases of high glycolytic flux that is required during high intensity exercise, lactate dehydrogenase oxidizes NADH back to NAD^+ in the conversion of pyruvate to lactate, thereby maintaining necessary levels of the cofactor for the continuation of glycolysis. Cyclists in the Gold group had a higher post-test lactate-to-pyruvate ratio, which is proportional to $NADH/NAD^+$ and a marker of glycolytic capacity. Interestingly, this ratio was lower at before the test, suggesting increased basal pyruvate oxidation capacity in Gold group cyclists due to larger mitochondrial networks (**Figure 3A**, lower right corner).

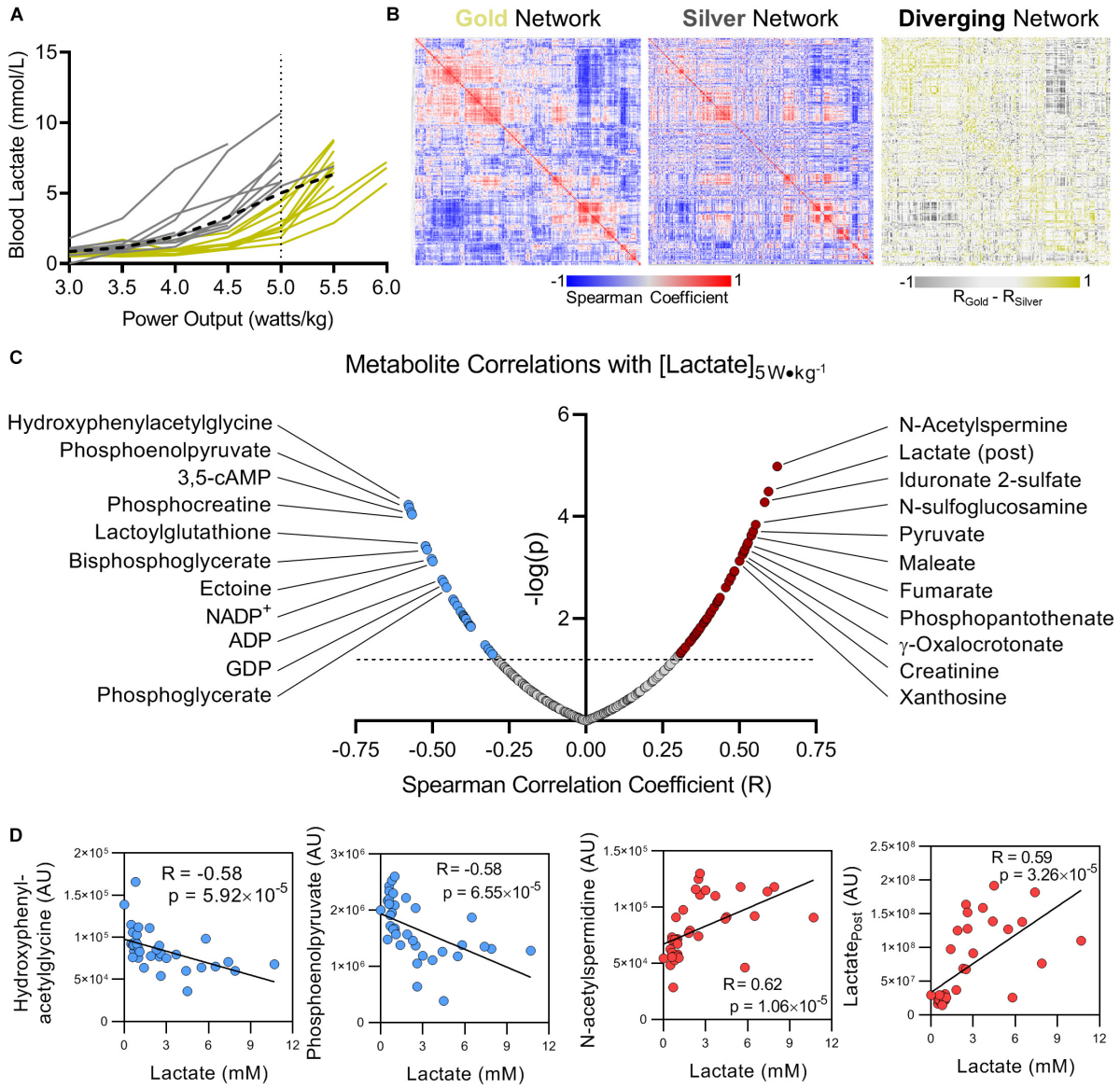

FIGURE 2 | Blood lactate levels as a function of power output can metabolically distinguish cyclists. **(A)** Using blood lactate levels (in mM) at a power output of 5 W kg^{-1} (the maximum output of which most riders achieved, referred to as the performance cutoff, or PC), cyclists were assigned to the Gold or Silver performance groups for having blood lactate levels below or above the group average, respectively (group average indicated with a black dashed line). **(B)** A Spearman Rank Correlation matrix of metabolites measured in the Gold group was Hierarchically clustered and plotted as a heat map **(left)**. A Spearman Rank Correlation matrix of metabolites measured in the Silver group was then plotted according to the same hierarchical order determined for the Gold group **(center)**. The difference of Spearman correlation coefficients between the Gold and Silver group (Gold minus Silver) was then plotted as a heat map according to the same hierarchical order determined for the Gold group. Positive Spearman differences are colored gold, and negative Spearman differences are colored silver. **(C)** The top significant positive (red) and negative (blue) metabolite correlates with blood lactate concentration measured at 5 W kg^{-1} are shown, with the Spearman Correlation Coefficient (*R*) on the *x*-axis, and -log(*p*) on the *y*-axis. **(D)** Individual plots are shown for the top 2 metabolites with negative (blue, Hydroxyphenylacetylglycine and Phosphoenolpyruvate) and positive (red, N-acetylspermidine and Lactate post) Spearman correlations with blood lactate concentration measured at 5 W kg^{-1}. Associated Spearman Correlation Coefficients and *p*-values are provided for each. Statistically significant correlations with log(*p*) > 1.3 ($p < 0.05$) are indicated above the dashed line.

Coenzyme A Synthesis Distinguishes Lactate Production Capacity

In addition to its dehydrogenation into lactate for the regeneration of NAD^+, pyruvate can also enter the mitochondria where it undergoes oxidative decarboxylation to form acetyl coenzyme A (acetyl-CoA). Exercise stimulated significant increases in many TCA cycle intermediates including α-ketoglutarate, succinate, fumarate, and malate (**Figure 4A**). The magnitude of increased TCA cycle intermediates in blood was larger in the Gold group, suggesting that these cyclists have a

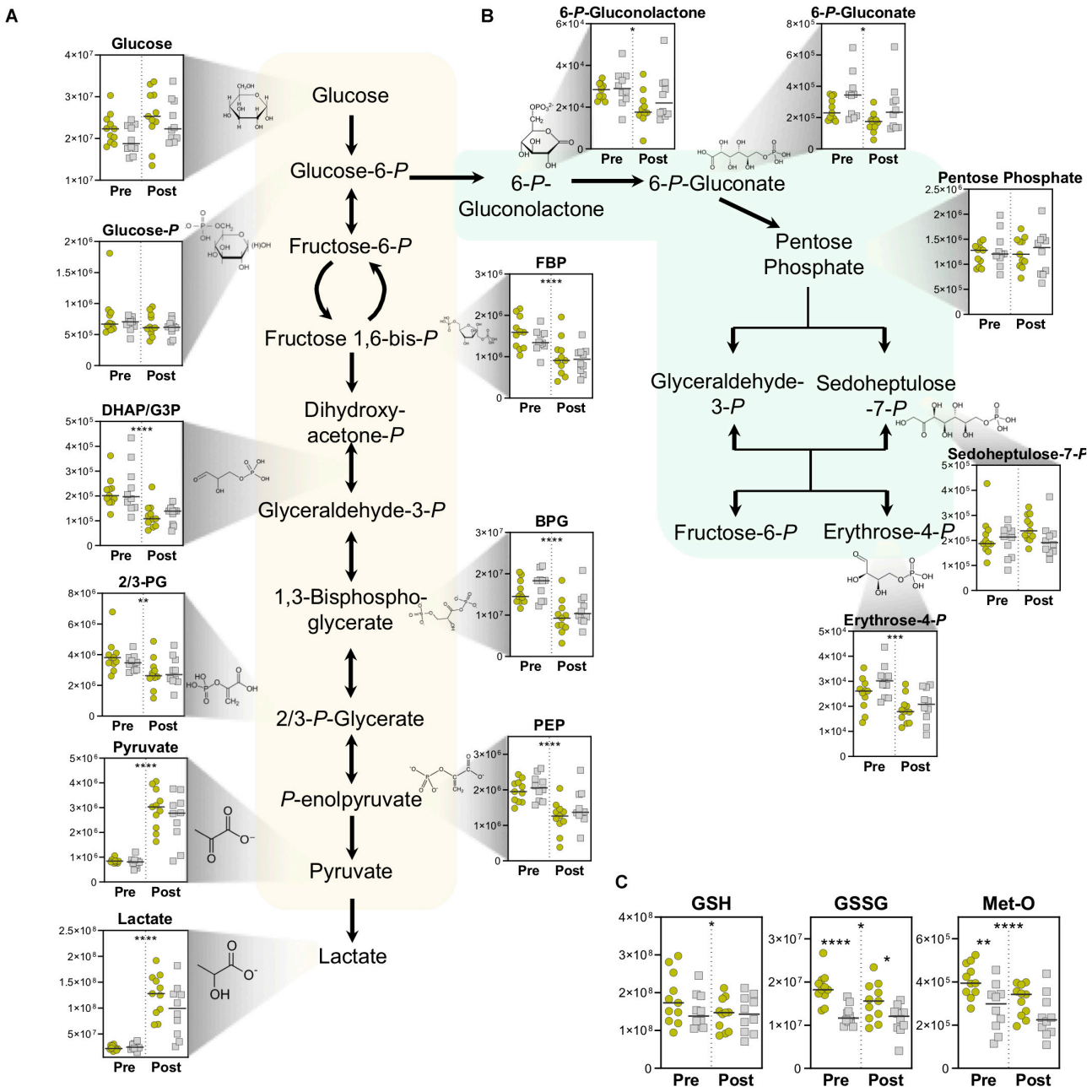

FIGURE 3 | Energy and Redox Metabolism. Metabolite abundances (*y*-axis, Peak Area (AU)) are plotted for **(A)** Glycolysis, **(B)** pentose phosphate pathway, and **(C)** Reduced (GSH) and oxidized (GSSG) glutathione, as well as oxidative-stress derived methionine sulfoxide (Met-O). Samples from the Gold (○) and Silver (□) groups are shown Pre and Post exercise test (divided by a dotted line). *p*-values from a two-tailed paired *T*-test of comparisons between the Pre and Post time points using combined Gold/Silver group values are shown above the dashed line. p-values from a two-tailed unpaired homoscedastic *T*-test comparing the Gold and Silver groups at each time point are shown on the respective side of the dashed line. $^{*}p < 0.05$; $^{**}p < 0.01$; $^{***}p < 0.001$; $^{****}p < 0.0001$.

larger mitochondrial capacity to generate energy during exertion, possibly due to increased mitochondrial content in tissues such as skeletal muscle. In addition, this group demonstrated significantly higher levels of the coenzyme A (CoA) precursor 4'-phospho-pantetheine at baseline, and significantly higher levels of the upstream precursor, 4'-phospho-pantothenate after exercise. These trends point to enhancements in CoA synthesis as a metabolic adaptation that occurs in association with lower PC lactate levels.

In addition to its conjugation to carbohydrate-derived acetate, CoA also plays a critical role in mobilizing fatty acids for oxidation into acetyl-CoA. During aerobic periods of exercise, catecholamine and endocrine signaling results in the lipase-mediated liberation of fatty acids from di- and triacylglycerides

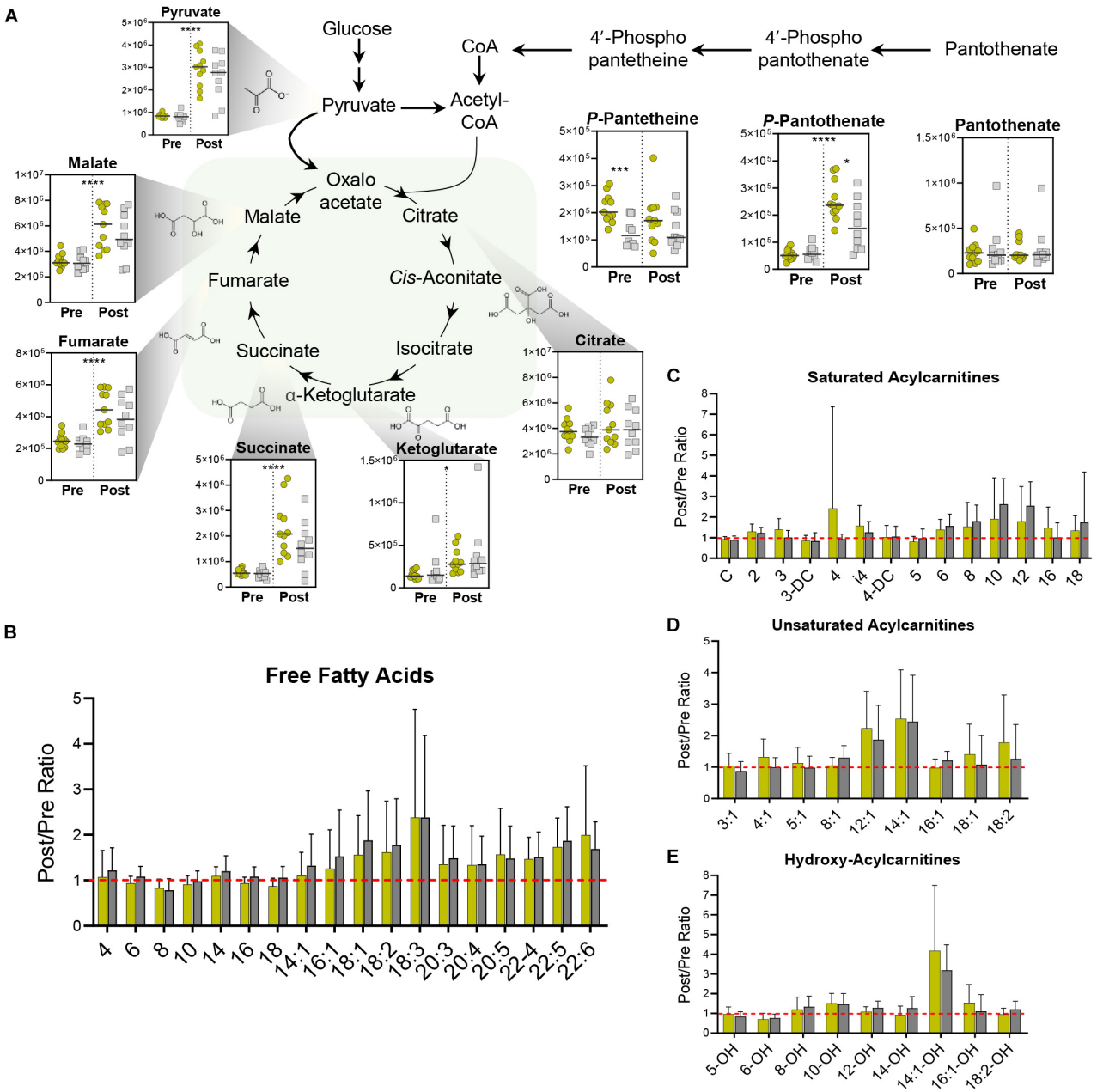

FIGURE 4 | Mitochondrial Metabolism. **(A)** TCA Cycle metabolite abundances [*y*-axis, Peak Area (AU)] are plotted. Samples from the Gold (○) and Silver (□) groups are shown Pre and Post exercise test (divided by a dotted line). *p*-values from a two-tailed paired *T*-test of comparisons between the Pre and Post time points using combined Gold/Silver group values are shown above the dashed line. *p*-values from a two-tailed unpaired homoscedastic *T*-test comparing the Gold and Silver groups at each time point are shown on the respective side of the dashed line. Intra-subject ratios between the Post and Pre timepoints for both Gold and Silver groups are shown for **(B)** free fatty acids, **(C)** saturated acylcarnitines, **(D)** unsaturated acylcarnitines, and **(E)** hydroxy acylcarnitines. $^{*}p < 0.05$; $^{**}p < 0.01$; $^{***}p < 0.001$; $^{****}p < 0.0001$.

stored in lipid droplets of muscle tissue and adipocytes. These fatty acids are chaperoned through circulation by albumin and transferred to tissues, where they are reversibly conjugated to carnitine and CoA for oxidation in the mitochondria. During the graded exercise test, all cyclists mobilized similar levels of free fatty acids (**Figure 4B**) and produced similar amounts of acylcarnitines (**Figures 4C–E**).

Strenuous Exercise Depletes Energy-Rich Nucleoside Phosphates and Leads to Accumulation of Purine Degradation Products

As expected, high energy phosphate compounds are depleted during exercise. Utilization of phosphocreatine pools maintains

a steady state of creatine, and fuels the significantly increased pools of creatinine (**Figure 5B**). The conversion of creatine to creatinine is an irreversible, non-enzymatic process that is favored in low-pH and high-temperature environments (Lempert, 1959) both of which onset during exercise. As creatinine levels serve as a rough measure of muscle mass (Virgili et al., 1994) higher basal levels in the Gold group indicate increased muscle mass that is associated with lower PC lactate (**Figure 5B**). In addition to dietary sources, creatine can also be synthesized from arginine by Arginine:Glycine amidinotransferase (AGAT), producing ornithine in the process. While arginine levels decrease overall during exercise, ornithine

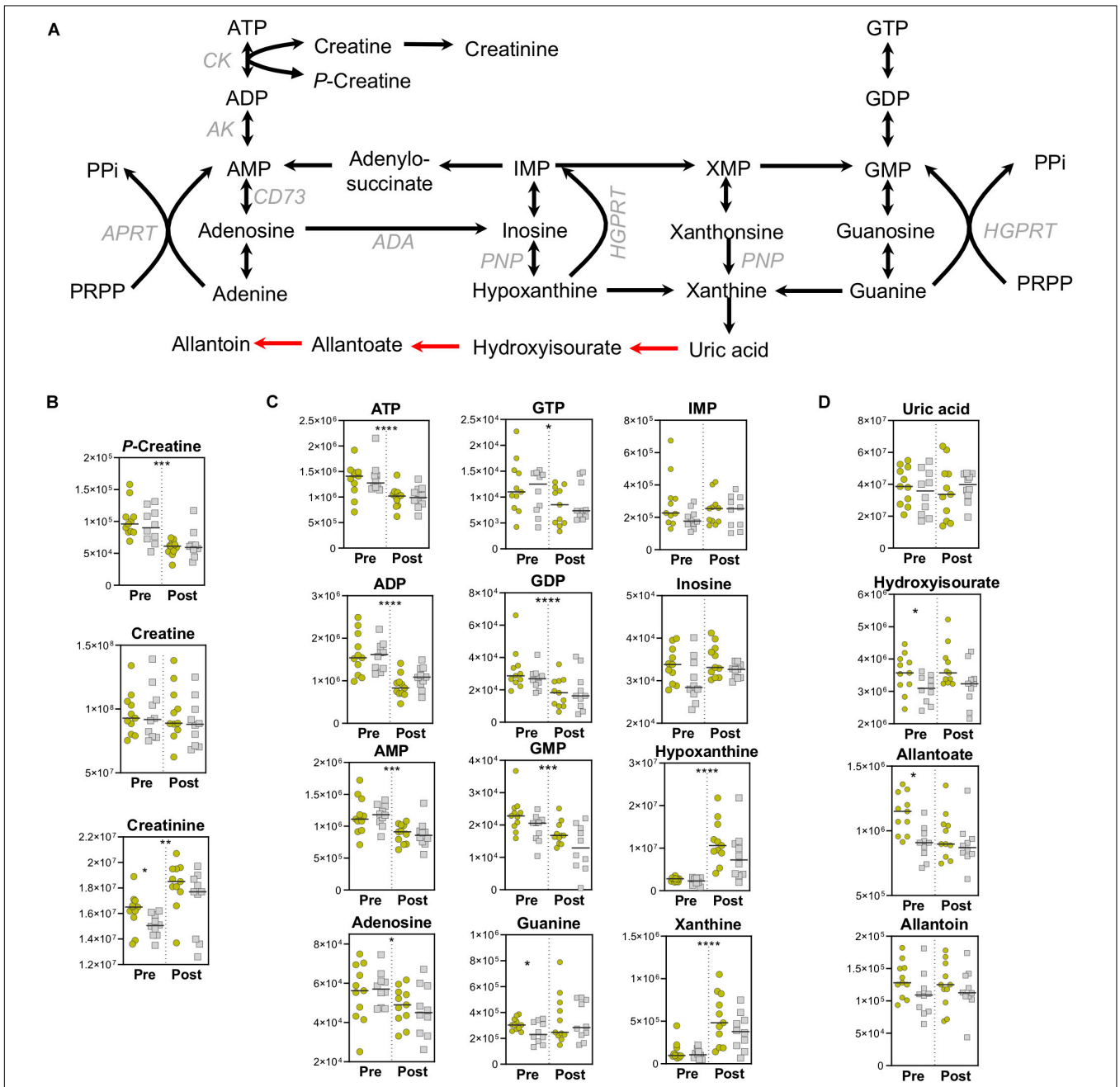

FIGURE 5 | High-Energy Phosphates and Purine Metabolism. **(A)** A pathway map for high-energy phosphate and purine homeostasis is shown. Spontaneous, non-enzymatic reactions are shown in red arrows. Metabolite abundances [*y*-axis, Peak Area (AU)] are plotted for **(B)** Creatine homeostasis, **(C)** Purine salvage, and **(D)** Purine catabolism. Samples from the Gold (○) and Silver (□) groups are shown Pre and Post exercise test (divided by a dotted line). *p*-values from a two-tailed paired *T*-test of comparisons between the Pre and Post time points using combined Gold/Silver group values are shown above the dashed line. *p*-values from a two-tailed unpaired homoscedastic *T*-test comparing the Gold and Silver groups at each time point are shown on the respective side of the dashed line. $^{*}p < 0.05$; $^{**}p < 0.01$; $^{***}p < 0.001$; $^{****}p < 0.0001$.

levels are higher at baseline in the Gold group, suggesting alterations to nitrogen metabolism that may serve to differentially fuel creatine pools (**Supplementary Figure 2**).

In like fashion to the depletion of phosphocreatine, high-energy pools of ATP and GTP are also utilized, resulting in increased levels of purine catabolites and intermediates of the salvage and deamination pathways, including hypoxanthine (**Figure 5C**). Despite increased levels of the purine catabolite xanthine, the end stage metabolite of enzymatic purine catabolism, uric acid, did not increase (**Figure 5D**). Although humans do not contain uricase, which converts uric acid into 5-hydroxyisourate and allantoin, this process can proceed spontaneously through the mediation of reactive oxygen species (ROS). As such, ROS-driven production of allantoin is a marker of oxidative stress in red blood cells (Kanďár and Záková, 2008). Higher baseline levels of 5-hydroxyisourate and allantoate were observed in the Gold cyclists, suggesting higher levels of oxidative stress in these individuals that could be due to adapted metabolic pathways that result in lower PC lactate levels (**Figure 5D**).

Amino Acid Utilization, in Addition to Performance Cutoff Can Distinguish Cyclists

In addition to energy and redox metabolites involved in glycolysis, the PPP, and the TCA cycle, amino acid levels at both baseline and after exercise differ based on PC lactate. At baseline, circulating levels of phenylalanine, lysine, asparagine, serine, threonine, valine, tryptophan, and tyrosine were significantly higher in Gold group cyclists (**Figure 6A**). In addition, the post-exercise levels of most amino acids were lower only in the Gold group, especially for isoleucine, leucine, and asparagine (**Figure 6B**). Given that elevated protein synthesis during this exercise period is unlikely to explain these changes due to both time- and energetic-constraints, it is possible that these amino acids are catabolized preferentially in the Gold group for ATP production (**Figure 6C**). In support, acylcarnitines involved in amino acid catabolism including C3-carnitine and C4-carnitine appear to increase more in this group (**Figure 4C**).

Untargeted Metabolomics Identifies Distinct Tyrosine Metabolic Profiles in Relation to Performance Cutoff

In an attempt to improve and streamline the analysis of complex biological systems, models have been developed to catalog the system of metabolic reactions (Thiele et al., 2013). Using large unannotated metabolomic datasets, these models hold the potential to efficiently identify networks of metabolic pathways that may be up or downregulated in response to a biological stimulus or setting. In order to gain better insight into basal metabolic differences in cyclists with varying PC levels, we applied an unbiased network analysis using the Recon2 model to the 2,790 putative compounds identified in this study. With a specific focus on compounds that showed distinct levels in the Gold versus Silver groups at baseline (**Figure 7A**), pathway analysis revealed the significant enrichment of multiple regions of metabolism including tyrosine, biopterin, ascorbate, nicotinate, and glycine/serine/alanine/threonine metabolism (**Figure 7B**). The most significantly enriched pathway, tyrosine metabolism, is interesting given that it is responsible for catecholamine synthesis, as well as the production of metabolites that can fuel the TCA cycle directly, such as fumarate, or indirectly, such as the ketone body, acetoacetate, and maleate. Subsequent manual interrogation of this pathway highlighted that many of the contained metabolites are elevated prior to exercise in the Gold group, and many are depleted more so in this group than in the Silver group (**Figure 7C**).

DISCUSSION

Studies on metabolic adaptations to exercise training in humans have been ongoing for decades. While early studies observed elevated activities and levels of glycolytic and electron transport chain proteins in response to endurance training (Gollnick et al., 1973; Holloszy et al., 1977) more recent work has elucidated the molecular mechanisms of such adaptations [reviewed in Hawley et al. (2018), Hackney (2019)]. Endurance training increases the capacity for lactate consumption in the mitochondria, thus increasing the lactate threshold and athletic output (Brooks, 2018). Lactate clearance capacity is enhanced through increased mitochondrial biogenesis (Little et al., 2010) which is upregulated at the transcriptional level in response to endurance training (Mahoney et al., 2005; Perry et al., 2010) and is controlled in large part by the key mediator, PGC-1α (Kim et al., 2015; Stepto et al., 2012). Increased mitochondrial networks driven by biogenesis, promotion of mitochondrial-rich Type I skeletal muscle fibers (Joyner and Coyle, 2008) and overall upregulations of muscle tissue synthesis, subsequently drive demand for substrates in addition to glucose and lactate including fatty acids and, to a lesser extent, amino acids. Lactate itself may regulate transcriptional activity (San-Millán et al., 2020) possibly through post-translation modifications of histones that alter the epigenomic landscape (Zhang et al., 2019). Future studies in sports and exercise science should focus on the extent of which these latter mechanisms apply to endurance training-mediated physiological adaptations.

The application of metabolomics to understand physiological responses to exercise has led to great advancements in the field of sports physiology over the past decade (Sakaguchi et al., 2019). These investigations have explored the effects of exercise intensity and workout duration on metabolism, as well as metabolic adaptations to chronic training in male and female populations over a range of training status (though female populations have been underrepresented in studies up to the present day). While the vast majority of studies involved amateur subjects with various levels of training, few have included elite or professional athletes assessed either at baseline (single sample) (Al-Khelaifi et al., 2018) or over a 10-day period (Knab et al., 2013). In this study, we analyzed the metabolome of whole blood in 21 international-level World Tour professional male cyclists using samples taken before and after a graded exercise test to exhaustion on a leg cycle ergometer. By normalizing

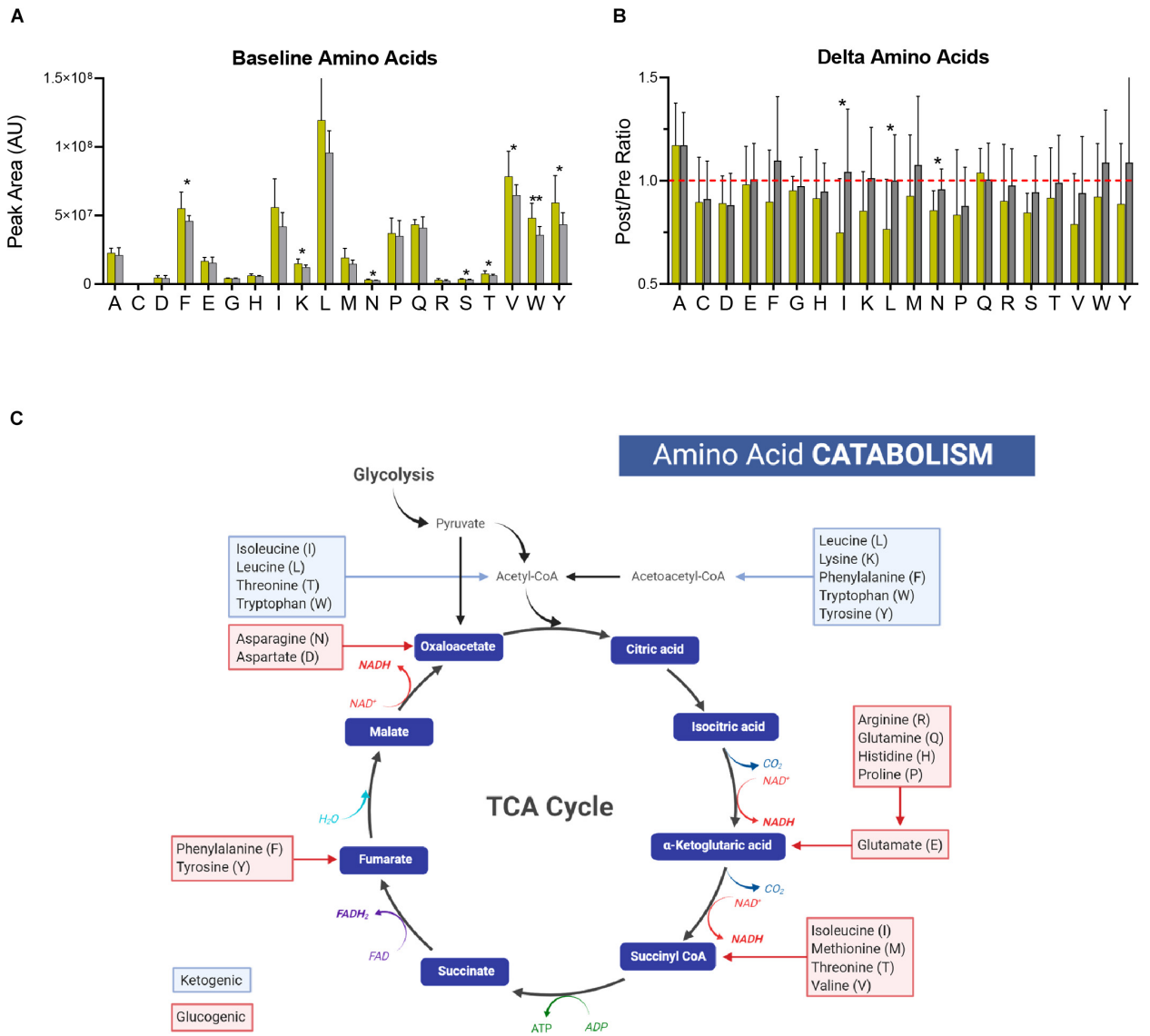

FIGURE 6 | Amino Acid Catabolism. **(A)** The baseline (pre-training) levels of amino acids (labeled with single letter code) are shown for the Gold and Silver performance groups. **(B)** Fold changes of amino acid levels (Post/Pre) for both performance groups are shown. A ratio of 1 is indicated by a dashed red line. **(C)** A generalized schematic of amino acid catabolism through the TCA cycle is shown. Glucogenic amino acids, which have the capacity to fuel gluconeogenesis, are listed in red boxes. Ketogenic amino acids, which contribute to acetoacetate and acetyl-CoA pools, are listed in blue boxes. *p*-values from a two-tailed Student's *T*-test are shown as $^{*}p < 0.05$; $^{**}p < 0.01$; $^{***}p < 0.001$; $^{****}p < 0.0001$.

power output to body mass, all cyclists exerted similar effort relative to their body type. Furthermore, the use of identical leg cycle ergometers in an indoor, climate-controlled environment, enabled a controlled monitoring of metabolic responses to exertion in this elite population.

Previously published metabolomics studies have analyzed other biological matrices including serum, plasma, saliva, and urine. While these matrices possess unique advantages in their own right, such as the ability to measure freely circulating metabolites between tissues as is the case with plasma, they disregard the metabolism of circulating blood cells by nature of their collection methods. As appreciation is growing with respect to blood cell adaptations to exercise (Bizjak et al., 2019; de Oliveira Ottone et al., 2019; Estruel-Amades et al., 2019; Shi et al., 2019; Uchida et al., 2019), whole blood analysis enables a more complete representation of physiology. Furthermore, this sample collection is less labor intensive than serum or plasma isolation. The introduction of TAP capillary blood collection devices have enabled field blood collection that does not necessitate traditional venipuncture blood draw (Blicharz et al., 2018) yet does provide comparable quantitative metabolomics data (Catala et al., 2018). Thus, TAP use makes possible rapid sample collection from large subject cohorts, such as participants in cycling races or marathons, thereby fostering metabolomics

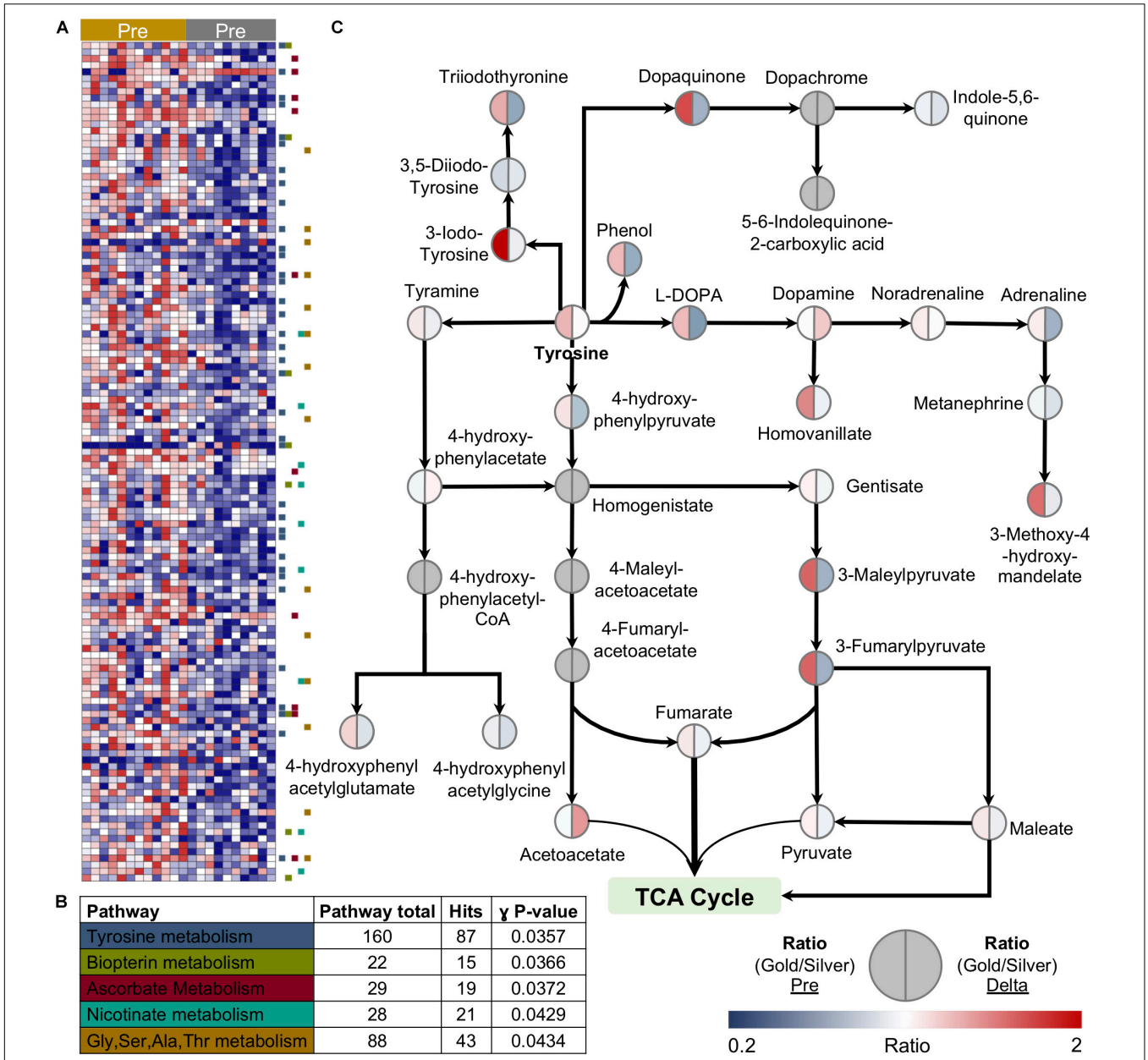

B

Pathway	Pathway total	Hits	ɣ P-value
Tyrosine metabolism	160	87	0.0357
Biopterin metabolism	22	15	0.0366
Ascorbate Metabolism	29	19	0.0372
Nicotinate metabolism	28	21	0.0429
Gly,Ser,Ala,Thr metabolism	88	43	0.0434

FIGURE 7 | Unbiased metabolomic pathway analysis reveals a link between tyrosine metabolism and lactate levels at performance cutoff. **(A)** A heatmap of features significantly different between the Gold and Silver groups at baseline is shown. **(B)** Pathway analysis using the Recon2 model identified the top five pathways enriched in this discovery dataset. **(C)** Manually validated features within Tyrosine metabolism are shown. The ratio of median values between Gold and Silver groups at baseline is shown on the left side of the circle, while the ratio of the median Delta values (calculated as the Post/Pre fold change) between Gold and Silver groups is shown on the right side of the circle. Values are plotted according to the color scale shown in the lower right.

analyses of active exercise in substantially larger populations than has been previously performed.

Use of whole blood lactate measurements taken during the graded exercise test allowed us to analyze metabolic states of individuals respective to lactate levels at the PC. One advantage of this approach is that it highlighted unique metabolic characteristics between two distinct groups classified based on the amount of lactate produced at a specific power output. This point should be acknowledged when comparing the best performing athletes (Gold group) in this study to the rest of the cohort (Silver group) at the post-exercise time point. However, it is interesting to appreciate that this classification also revealed significant differences at baseline, even prior to the graded exercise test. As the measurements of blood lactate accumulation during a short, graded exercise test can discriminate performance in different groups of cyclists (San-Millán et al., 2009) these results indicate that metabolomic measurements at baseline and during graded exercise testing may serve to expand the predictive qualities of

lactate measurement alone. In support, it is noteworthy that the World-Tour cycling season started two weeks after our testing was performed. Many cyclists in the Gold group ended up winning or reaching the podium in the first few races of the season, while riders in the Silver group did not show a great level of performance at the beginning of the year. These results highlight the use of our metabolomics platform as a powerful tool to monitor training status and predict athletic performance.

In agreement with many metabolomics studies, we observed increases in TCA cycle intermediates immediately following exercise. These increases may result from mild ischemia that occurs once oxygen demand exceeds the rate in which it can be supplied by erythrocytes (Zhang et al., 2018). Notably, cyclists with lower PC lactate levels tended to have higher levels of circulating TCA cycle metabolites following exercise. As lactate consumption rate is a marker of mitochondrial content in skeletal muscle (owing in most part to slow-twitch, Type I fibers), TCA cycle metabolite concentrations may also serve as a measure of muscle composition. Surprisingly, cyclists with lower PC lactate had significantly higher levels of the CoA precursor 4'-phospho-pantetheine at baseline, and 4'-phospho-pantothenate after exercise, suggesting upregulation of CoA biosynthesis in these athletes. Notably, these metabolites are intracellular and not readily measurable in plasma. This upregulation may represent a natural adaptation of which previously proposed supplementation strategies have attempted to achieve (Williams, 1989). However, pantothenic acid supplementation alone was shown to have no effect on cycling performance (Webster, 1998) indicating that improved bioavailability, in addition to other adaptations, may be required for the body to upregulate this system.

The preference for carbon sources to fuel the TCA cycle may also depend on lactate threshold. All cyclists exhibited similar mobilization of fatty acids and corresponding acylcarnitines for beta oxidation, of which the medium and long-chain forms tend to be released into circulation predominantly from skeletal muscle during exercise (Makrecka-Kuka et al., 2017). However, cyclists with lower PC lactate in the Gold group demonstrated slightly higher levels of short chain acylcarnitines such as propionylcarnitine and butyrlcarnitine. Propionylcarnitine in particular is released into circulation from the hepato-splanchnic bed after exercise (Xu et al., 2016) pointing to potential liver-mediated adaptations to training that support improved endurance capacity. While short- and odd-chain acylcarnitines can be formed be formed as end products of even- and odd-chain fatty acid oxidation, they are also abundantly produced during the catabolism of certain amino acids, such as branched-chain amino acids (BCAA). Indeed, Gold group cyclists had higher levels of multiple amino acids at baseline, and lower levels of BCAAs leucine, isoleucine, as well as asparagine, after exercise. Amino acids provide small stores of ATP during prolonged exercise (Phillips et al., 1993) and may be dependent on glycogen dynamics (Jackman et al., 1997), which are lactate-dependent (Brooks, 1986). Higher amino acid utilization may also reflect orthogonal mechanisms responsible for protein synthesis (Rundqvist et al., 2013), exercise recovery (Saunders et al., 2007), and overall exercise performance (Kephart et al., 2016). Indeed, skeletal muscle transport of amino acids has been shown to increase in response to training (Roberson et al., 2018).

Amino acid catabolism may serve additional endocrine purposes as well. The upregulation of tyrosine metabolism that is associated with lower PC lactate levels was a particularly interesting finding. Tyrosine is utilized in multiple pathways including protein synthesis, anaplerosis of the TCA cycle, and as a precursor for catecholamine biosynthesis. Catecholamines, including dopamine, norepinephrine, and epinephrine, serve an important role during exercise by mediating sypathoadrenal system function. In addition to cardiovascular and respiratory responses (Zouhal et al., 2008) they modulate hepatic glucose production (Sigal et al., 1996) release of fatty acids from triglycerides (Wahrenberg et al., 1991) and fatigue (Foley and Fleshner, 2008). Indeed, the ratio of dopamine to serotonin decreases with fatigue (Bailey et al., 1993). A study of human metabolic responses to starvation, which offers insight into the physiology of extreme nutrient depletion, observed increased tryptophan consumption (the precursor to serotonin), as well as increased levels of circulating tyrosine, possibly due to decreased utilization (Steinhauser et al., 2018). Meanwhile, pharmacological modulation of serotonin receptors appears to affect time to exhaustion (Meeusen and De Meirleir, 1995). Conversely, aerobic exercise training in animal studies has been show to increase dopamine levels in various brain regions (Foley and Fleshner, 2008). Neuroendocrine control mechanisms of fatigue may have evolved to prevent overexertion (Cordeiro et al., 2017) and as such, these mechanisms should be linked to other mechanisms of endurance capacity in the body. Of note, tyrosine metabolism by monoamine oxidase enzymes is regulated by oxidant stress and glutathione levels (Maker et al., 1981) further suggesting a link between dopamine metabolism, lactate metabolism, and oxidative stress observed in the present study. In this view, it is interesting to note that dopamine (and catecholamines in general) is a direct ROS scavenger (Zhong et al., 2019) and a vasomodulator (Murphy, 2000). As such, dopamine may represent an underappreciated contributor to exercise performance.

In addition to catecholamine biosynthesis, tyrosine could be re-routed for ketogenic roles to provide energy in high endurance trained states. Indeed, levels of tyrosine metabolites were basally higher in the Gold cyclists, and consumed to a larger extent during exertion in conjunction with accumulated levels of acetoacetate. Considering that past reports on tyrosine supplementation have provided mixed results (Chinevere et al., 2002; Tumilty et al., 2011; Watson et al., 2012) future studies using isotopically-labeled tyrosine will help to disentangle its possible catabolic routes with regards to fatigue, lactate clearance capacity, and overall training status.

Glycolysis has long been known as a principal energy generating pathway in tissues due to its high rates of ATP generation under anaerobic conditions. Increased glycolytic markers have also been identified in plasma during exercise (Jacobs et al., 2014). While lactate production as a function of output has been shown to discriminate cyclists of differing training status (San-Millán et al., 2009) all cyclists reached a point of exhaustion just prior to whole blood sampling for

metabolomics. As such, only a few glycolytic intermediates trended with rates of lactate accumulation, but none significantly differed between the two groups. Of note, the intra-subject lactate-to-pyruvate ratio is potentially illustrative of performance capacity. Given that this ratio represents an indirect measure of the NAD^+/NADH ratio, inverse trends between the two groups at baseline and post-test time points is suggestive of specific glycolytic capacity that can drive performance during bouts of high-intensity cycling. Indeed, training strategies centered on high-altitude simulation have shown to be beneficial in promoting glycolysis and work capacity in cyclists (Terrados et al., 1988).

Unlike glycolytic comparisons, the observations of lower PPP intermediates in conjunction with significantly higher levels of oxidant-associated metabolites including oxidized glutathione (GSSG), Met-O, 5-hydroxyisourate and allantoate in the Gold group point to an increased level of basal oxidative stress. Considering that glutathione and PPP intermediates are intracellular metabolites, it is likely that the major contributors to these pools in whole blood are red blood cells (RBCs), by far the most abundant cell in both circulation and the human body (Sender et al., 2016). While exercise promotes erythropoiesis due to increased oxygen demand and need to replenish RBC populations in response to elevated hemolysis (reviewed in Mairbäurl, 2013) effects on RBC circulatory lifespan have only recently been appreciated (Bizjak et al., 2019). One of the hallmarks of RBC aging both in circulation (Lutz and Bogdanova, 2013) and in the blood bank (Nemkov et al., 2015; Yoshida et al., 2019) an environment that accelerates RBC aging (D'Alessandro et al., 2015) is the accumulation of oxidative stress markers including oxidized glutathione and allantoate. Thus, while exercise is known to cause localized inflammation and oxidative stress, systemic markers of such may indeed be indicative of altered hemostasis. In addition to gas exchange, RBC play a multitude of roles in human physiology including regulation of vascular tone, circulatory glucose, lactate, and amino acid content, and catecholamine transport (Nemkov et al., 2018). While it is likely that these characteristics are also important factors in exercise, future work is needed to elucidate the mechanisms RBC use to control physical performance and responses to exercise.

CONCLUSION

Here, we report a metabolomics-based investigation of elite, world-competing professional cyclists. Although this group represents a relatively distinct population from the perspective of physical fitness, the robustness and breadth of coverage provided by high-throughput metabolomics highlighted differences with regards to energy and amino acid metabolism, and oxidative stress. These measurements complemented and expanded upon the utility of lactate clearance capacity, which has served as a gold standard to monitor athletic training status. While this study design focused on differences in cyclist oxidative capacity, additional studies can be designed to emphasize the contribution of alternative purely anaerobic energy systems that are needed for very high intensity cycling and sprinting. Future studies using metabolomics-based methodologies should expand steady state measurements by increasing time points, applied to additional forms of exercise that include varying intensity levels and longer endurance periods, and in additional populations with a wider range of physical fitness that are gender- and age-balanced. Despite temporal sampling, steady state measurements lack the molecular resolution necessary to determine metabolic flux. The use of stable isotope tracing with various substrates in the future will allow for a better understanding of the preference for and rates of utilization. Finally, we observed responses in the levels of intracellular metabolites, which in part arise from erythrocytes as these are substantially the most abundant cell population in whole blood. However, while whole blood analysis offers a comprehensive view of physiology, future studies should focus on understanding contribution of different blood components to overall metabolic response to exercise.

DATA AVAILABILITY STATEMENT

All relevant data is contained within the article.

ETHICS STATEMENT

The studies involving human participants were reviewed and approved by Colorado Multiple Institutional Review Board Protocol ID 17-1281. The patients/participants provided their written informed consent to participate in this study.

AUTHOR CONTRIBUTIONS

IS-M, TN, and AD'A designed the experiments. IS-M and TN collected samples. TN, AD'A, and DS acquired and processed the data. TN prepared the figures. TN and IS-M wrote the first draft of the manuscript. All authors commented on the final preparation of the manuscript.

FUNDING

This article was supported by funds from the Boettcher Webb-Waring Investigator Award (AD'A), RM1GM131968 (AD'A and KH) from the National Institute of General and Medical Sciences, and R01HL146442 (AD'A), R01HL149714 (AD'A), R01HL148151 (AD'A), R21HL150032 (AD'A), and T32 HL007171 (TN) from the National Heart, Lung, and Blood Institute.

SUPPLEMENTARY MATERIAL

The Supplementary Material for this article can be found online at: https://www.frontiersin.org/articles/10.3389/fphys.2020.00578/full#supplementary-material

FIGURE S1 | Partial Least Squares Discriminant Analysis (PLS-DA) to determine metabolic co-variance between the Gold and Silver cycling groups is shown, along with the metabolites that most strongly contribute to the clustering pattern based on variable importance in projection (VIP) scores.

FIGURE S2 | Urea Cycle metabolism. Samples from the Gold (○) and Silver (□) groups are shown Pre and Post exercise test (divided by a dotted line). *p*-values from a two-tailed paired *T*-test of comparisons between the Pre and Post time points using combined Gold/Silver group values are shown above the dashed line. *p*-values from a two-tailed unpaired homoscedastic *T*-test comparing the Gold and Silver groups at each time point are shown on the respective side of the dashed line. $^{*}p < 0.05$; $^{**}p < 0.01$; $^{***}p < 0.001$; $^{****}p < 0.0001$.

TABLE S1 | A table of the physiological and raw metabolomics data is provided. For the metabolomics data, information is included for the compound name, Compound ID in either KEGG or HMDB, the observed parent mass, median retention time, polarity of detection, and peak area top values in arbitrary units.

TABLE S2 | A table of Spearman Correlation Coefficients for the Gold Network, Silver Network, and the Diverging Network (i.e., the difference between the Gold and Silver Networks) is provided.

DATA SHEET S1 | A heat map of metabolite hierarchical clustering analysis is shown. Rows and columns were hierarchically clustered according to 1 minus the Spearman rank correlation. Metabolite values are depicted as Z-scores, with the values color coded from row minimum to maximum on a gradient from blue to red, respectively.

REFERENCES

Al-Khelaifi, F., Diboun, I., Donati, F., Botrè, F., Alsayrafi, M., Georgakopoulos, C., et al. (2018). A pilot study comparing the metabolic profiles of elite-level athletes from different sporting disciplines. *Sports Med. Open* 4:2. doi: 10.1186/s40798-017-0114-z

Bailey, S. P., Davis, J. M., and Ahlborn, E. N. (1993). Neuroendocrine and substrate responses to altered brain 5-HT activity during prolonged exercise to fatigue. *J. Appl. Physiol.* 74, 3006–3012. doi: 10.1152/jappl.1993.74.6.3006

Bergman, B. C., Wolfel, E. E., Butterfield, G. E., Lopaschuk, G. D., Casazza, G. A., Horning, M. A., et al. (1999). Active muscle and whole body lactate kinetics after endurance training in men. *J. Appl. Physiol.* 87, 1684–1696. doi: 10.1152/jappl.1999.87.5.1684

Billat, L. V. (1996). Use of blood lactate measurements for prediction of exercise performance and for control of training. Recommendations for long-distance running. *Sports Med. Auckl.* 22, 157–175. doi: 10.2165/00007256-199622030-00003

Bizjak, D. A., Tomschi, F., Bales, G., Nader, E., Romana, M., Connes, P., et al. (2019). Does endurance training improve red blood cell aging and hemorheology in moderate-trained healthy individuals?. *J. Sport Health Sci.* 10:S2095254619300225. doi: 10.1016/j.jshs.2019.02.002

Blicharz, T. M., Gong, P., Bunner, B. M., Chu, L. L., Leonard, K. M., Wakefield, J. A., et al. (2018). Microneedle-based device for the one-step painless collection of capillary blood samples. *Nat. Biomed. Eng.* 2, 151–157. doi: 10.1038/s41551-018-0194-1

Brooks, G. A. (1985). Anaerobic threshold: review of the concept and directions for future research. *Med. Sci. Sports Exerc.* 17, 22–34.

Brooks, G. A. (1986). The lactate shuttle during exercise and recovery. *Med. Sci. Sports Exerc.* 18, 360–368. doi: 10.1249/00005768-198606000-00019

Brooks, G. A. (2018). The science and translation of lactate shuttle theory. *Cell Metab.* 27, 757–785. doi: 10.1016/j.cmet.2018.03.008

Catala, A., Culp-Hill, R., Nemkov, T., and D'Alessandro, A. (2018). Quantitative metabolomics comparison of traditional blood draws and TAP capillary blood collection. *Metab. Off. J. Metab. Soc.* 14:100. doi: 10.1007/s11306-018-1395-z

Chinevere, T. D., Sawyer, R. D., Creer, A. R., Conlee, R. K., and Parcell, A. C. (2002). Effects of l -tyrosine and carbohydrate ingestion on endurance exercise performance. *J. Appl. Physiol.* 93, 1590–1597. doi: 10.1152/japplphysiol.00625.2001

Chong, J., Soufan, O., Li, C., Caraus, I., Li, S., Bourque, G., et al. (2018). MetaboAnalyst 4.0: towards more transparent and integrative metabolomics analysis. *Nucleic Acids Res.* 46, W486–W494. doi: 10.1093/nar/gky310

Cordeiro, L. M. S., Rabelo, P. C. R., Moraes, M. M., Teixeira-Coelho, F., Coimbra, C. C., Wanner, S. P., et al. (2017). Physical exercise-induced fatigue: the role of serotonergic and dopaminergic systems. *Braz. J. Med. Biol. Res. Rev. Bras. Pesqui. Medicas E Biol.* 50:e6432. doi: 10.1590/1414-431X20176432

D'Alessandro, A. (2019). *High-Throughput Metabolomics: Methods and Protocols*. New York, NY: Springer.

D'Alessandro, A., Nemkov, T., Kelher, M., West, F. B., Schwindt, R. K., Banerjee, A., et al. (2015). Routine storage of red blood cell (RBC) units in additive solution-3: a comprehensive investigation of the RBC metabolome: metabolomics of AS-3 RBCs. *Transfusion* 55, 1155–1168. doi: 10.1111/trf.12975

D'Alessandro, A., Nemkov, T., Reisz, J., Dzieciatkowska, M., Wither, M. J., and Hansen, K. C. (2017). Omics markers of the red cell storage lesion and metabolic linkage. *Blood Transfus. Trasfus.* 15, 137–144. doi: 10.2450/2017.0341-16

de Oliveira Ottone, V., Costa, K., Tossige-Gomes, R., de Matos, M., Brito-Melo, G., Magalhaes, F., et al. (2019). Late neutrophil priming following a single session of high-intensity interval exercise. *Int. J. Sports Med.* 40, 171–179. doi: 10.1055/a-0810-8533

Donovan, C. M., and Brooks, G. A. (1983). Endurance training affects lactate clearance, not lactate production. *Am. J. Physiol.* 244, E83–E92. doi: 10.1152/ajpendo.1983.244.1.E83

Dubouchaud, H., Butterfield, G. E., Wolfel, E. E., Bergman, B. C., and Brooks, G. A. (2000). Endurance training, expression, and physiology of LDH, MCT1, and MCT4 in human skeletal muscle. *Am. J. Physiol. Endocrinol. Metab.* 278, E571–E579. doi: 10.1152/ajpendo.2000.278.4.E571

Estruel-Amades, S., Ruiz-Iglesias, P., Périz, M., Franch, À, Pérez-Cano, F. J., Camps-Bossacoma, M., et al. (2019). Changes in lymphocyte composition and functionality after intensive training and exhausting exercise in rats. *Front. Physiol.* 10:1491. doi: 10.3389/fphys.2019.01491

Foley, T. E., and Fleshner, M. (2008). Neuroplasticity of dopamine circuits after exercise: implications for central fatigue. *Neuromolecular Med.* 10, 67–80. doi: 10.1007/s12017-008-8032-3

Frayn, K. N. (1983). Calculation of substrate oxidation rates *in vivo* from gaseous exchange. *J. Appl. Physiol.* 55, 628–634. doi: 10.1152/jappl.1983.55.2.628

Gollnick, P. D., Armstrong, R. B., Saltin, B., Saubert, C. W., Sembrowich, W. L., and Shepherd, R. E. (1973). Effect of training on enzyme activity and fiber composition of human skeletal muscle. *J. Appl. Physiol.* 34, 107–111. doi: 10.1152/jappl.1973.34.1.107

Hackney, A. C. (2019). "Molecular and physiological adaptations to endurance training," in *Concurrent Aerobic and Strength Training*, eds M. Schumann and B. R. Rønnestad (Cham: Springer International Publishing), 19–34. doi: 10.1007/978-3-319-75547-2_3

Hawley, J. A., Lundby, C., Cotter, J. D., and Burke, L. M. (2018). Maximizing cellular adaptation to endurance exercise in skeletal muscle. *Cell Metab.* 27, 962–976. doi: 10.1016/j.cmet.2018.04.014

Holloszy, J. O., Rennie, M. J., Hickson, R. C., Conlee, R. K., and Hagberg, J. M. (1977). Physiological consequences of the biochemical adaptations to endurance exercise. *Ann. N. Y. Acad. Sci.* 301, 440–450. doi: 10.1111/j.1749-6632.1977.tb38220.x

Jackman, M. L., Gibala, M. J., Hultman, E., and Graham, T. E. (1997). Nutritional status affects branched-chain oxoacid dehydrogenase activity during exercise in humans. *Am. J. Physiol.* 272, E233–E238. doi: 10.1152/ajpendo.1997.272.2.E233

Jacobs, D. M., Hodgson, A. B., Randell, R. K., Mahabir-Jagessar-T, K., Garczarek, U., Jeukendrup, A. E., et al. (2014). Metabolic response to decaffeinated green tea extract during rest and moderate-intensity exercise. *J. Agric. Food Chem.* 62, 9936–9943. doi: 10.1021/jf502764r

Jacobs, I. (1986). Blood lactate. Implications for training and sports performance. *Sports Med. Auckl.* 3, 10–25. doi: 10.2165/00007256-198603010-00003

Jensen, K., Jørgensen, S., and Johansen, L. (2002). A metabolic cart for measurement of oxygen uptake during human exercise using inspiratory flow rate. *Eur. J. Appl. Physiol.* 87, 202–206. doi: 10.1007/s00421-002-0616-2

Joyner, M. J., and Coyle, E. F. (2008). Endurance exercise performance: the physiology of champions. *J. Physiol.* 586, 35–44. doi: 10.1113/jphysiol.2007.143834

Kand'ár, R., and Záková, P. (2008). Allantoin as a marker of oxidative stress in human erythrocytes. *Clin. Chem. Lab. Med.* 46, 1270–1274. doi: 10.1515/CCLM.2008.244

Karamanou, M., and Androutsos, G. (2013). Antoine-Laurent de Lavoisier (1743-1794) and the birth of respiratory physiology. *Thorax* 68, 978–979. doi: 10.1136/thoraxjnl-2013-203840

Kephart, W. C., Wachs, T. D., Thompson, R. M., Brooks Mobley, C., Fox, C. D., McDonald, J. R., et al. (2016). Ten weeks of branched-chain amino acid supplementation improves select performance and immunological variables in trained cyclists. *Amino Acids* 48, 779–789. doi: 10.1007/s00726-015-2125-8

Kim, S. H., Koh, J. H., Higashida, K., Jung, S. R., Holloszy, J. O., and Han, D.-H. (2015). PGC-1α mediates a rapid, exercise-induced downregulation of glycogenolysis in rat skeletal muscle. *J. Physiol.* 593, 635–643. doi: 10.1113/jphysiol.2014.283820

Knab, A. M., Nieman, D. C., Gillitt, N. D., Shanely, R. A., Cialdella-Kam, L., Henson, D. A., et al. (2013). Effects of a flavonoid-rich juice on inflammation, oxidative stress, and immunity in elite swimmers: a metabolomics-based approach. *Int. J. Sport Nutr. Exerc. Metab.* 23, 150–160. doi: 10.1123/ijsnem.23.2.150

Lempert, C. (1959). The chemistry of the glycocyamidines. *Chem. Rev.* 59, 667–736. doi: 10.1021/cr50028a005

Little, J. P., Safdar, A., Wilkin, G. P., Tarnopolsky, M. A., and Gibala, M. J. (2010). A practical model of low-volume high-intensity interval training induces mitochondrial biogenesis in human skeletal muscle: potential mechanisms. *J. Physiol.* 588, 1011–1022. doi: 10.1113/jphysiol.2009.181743

Lutz, H. U., and Bogdanova, A. (2013). Mechanisms tagging senescent red blood cells for clearance in healthy humans. *Front. Physiol.* 4:387. doi: 10.3389/fphys.2013.00387

Mahoney, D. J., Parise, G., Melov, S., Safdar, A., and Tarnopolsky, M. A. (2005). Analysis of global mRNA expression in human skeletal muscle during recovery from endurance exercise. *FASEB J. Off. Publ. Fed. Am. Soc. Exp. Biol.* 19, 1498–1500. doi: 10.1096/fj.04-3149fje

Mairbäurl, H. (2013). Red blood cells in sports: effects of exercise and training on oxygen supply by red blood cells. *Front. Physiol.* 4:332. doi: 10.3389/fphys.2013.00332

Maker, H. S., Weiss, C., Silides, D. J., and Cohen, G. (1981). Coupling of dopamine oxidation (Monoamine Oxidase Activity) to glutathione oxidation via the generation of hydrogen peroxide in rat brain homogenates. *J. Neurochem.* 36, 589–593. doi: 10.1111/j.1471-4159.1981.tb01631.x

Makrecka-Kuka, M., Sevostjanovs, E., Vilks, K., Volska, K., Antone, U., Kuka, J., et al. (2017). Plasma acylcarnitine concentrations reflect the acylcarnitine profile in cardiac tissues. *Sci. Rep.* 7:17528. doi: 10.1038/s41598-017-17797-x

McDermott, J. C., and Bonen, A. (1993). Endurance training increases skeletal muscle lactate transport. *Acta Physiol. Scand.* 147, 323–327. doi: 10.1111/j.1748-1716.1993.tb09505.x

Meeusen, R., and De Meirleir, K. (1995). Exercise and brain neurotransmission. *Sports Med. Auckl.* 20, 160–188. doi: 10.2165/00007256-199520030-00004

Melamud, E., Vastag, L., and Rabinowitz, J. D. (2010). Metabolomic analysis and visualization engine for LC-MS data. *Anal. Chem.* 82, 9818–9826. doi: 10.1021/ac1021166

Murphy, M. B. (2000). Dopamine: a role in the pathogenesis and treatment of hypertension. *J. Hum. Hypertens.* 14(Suppl. 1), S47–S50. doi: 10.1038/sj.jhh.1000987

Nemkov, T., Hansen, K. C., and D'Alessandro, A. (2017). A three-minute method for high-throughput quantitative metabolomics and quantitative tracing experiments of central carbon and nitrogen pathways. *Rapid Commun. Mass Spectrom.* 31, 663–673. doi: 10.1002/rcm.7834

Nemkov, T., Hansen, K. C., Dumont, L. J., and D'Alessandro, A. (2015). Metabolomics in transfusion medicine. *Transfusion* 56, 980–993. doi: 10.1111/trf.13442

Nemkov, T., Reisz, J. A., Xia, Y., Zimring, J. C., and D'Alessandro, A. (2018). Red blood cells as an organ? How deep omics characterization of the most abundant cell in the human body highlights other systemic metabolic functions beyond oxygen transport. *Expert Rev. Proteomics* 15, 855–864. doi: 10.1080/14789450.2018.1531710

Perry, C. G. R., Lally, J., Holloway, G. P., Heigenhauser, G. J. F., Bonen, A., and Spriet, L. L. (2010). Repeated transient mRNA bursts precede increases in transcriptional and mitochondrial proteins during training in human skeletal muscle. *J. Physiol.* 588, 4795–4810. doi: 10.1113/jphysiol.2010.199448

Phillips, S. M., Atkinson, S. A., Tarnopolsky, M. A., and MacDougall, J. D. (1993). Gender differences in leucine kinetics and nitrogen balance in endurance athletes. *J. Appl. Physiol.* 75, 2134–2141. doi: 10.1152/jappl.1993.75.5.2134

Reisz, J. A., Zheng, C., D'Alessandro, A., and Nemkov, T. (2019). Untargeted and semi-targeted lipid analysis of biological samples using mass spectrometry-based metabolomics. *Methods Mol. Biol.* 1978, 121–135. doi: 10.1007/978-1-4939-9236-2_8

Roberson, P. A., Haun, C. T., Mobley, C. B., Romero, M. A., Mumford, P. W., Martin, J. S., et al. (2018). Skeletal muscle amino acid transporter and BCAT2 expression prior to and following interval running or resistance exercise in mode-specific trained males. *Amino Acids* 50, 961–965. doi: 10.1007/s00726-018-2570-2

Rundqvist, H. C., Lilja, M. R., Rooyackers, O., Odrzywol, K., Murray, J. T., Esbjörnsson, M., et al. (2013). Nutrient ingestion increased mTOR signaling, but not hVps34 activity in human skeletal muscle after sprint exercise. *Physiol. Rep.* 1:e00076. doi: 10.1002/phy2.76

Sakaguchi, C. A., Nieman, D. C., Signini, E. F., Abreu, R. M., and Catai, A. M. (2019). Metabolomics-based studies assessing exercise-induced alterations of the human metabolome: a systematic review. *Metabolites* 9:E164. doi: 10.3390/metabo9080164

San-Millán, I., and Brooks, G. A. (2018). Assessment of metabolic flexibility by means of measuring blood lactate, fat, and carbohydrate oxidation responses to exercise in professional endurance athletes and less-fit individuals. *Sports Med. Auckl.* 48, 467–479. doi: 10.1007/s40279-017-0751-x

San-Millán, I., González-Haro, C., and Sagasti, M. (2009). Physiological differences between road cyclists of different categories. a new approach.: 733. *Med. Sci. Sports Exerc.* 41, 64–65. doi: 10.1249/01.mss.0000353467.61975.ae

San-Millán, I., Julian, C. G., Matarazzo, C., Martinez, J., and Brooks, G. A. (2020). Is lactate an oncometabolite? Evidence supporting a role for lactate in the regulation of transcriptional activity of cancer-related genes in mcf7 breast cancer cells. *Front. Oncol.* 9:1536. doi: 10.3389/fonc.2019.01536

Saunders, M. J., Luden, N. D., and Herrick, J. E. (2007). Consumption of an oral carbohydrate-protein gel improves cycling endurance and prevents postexercise muscle damage. *J. Strength Cond. Res.* 21, 678–684. doi: 10.1519/R-20506.1

Schrimpe-Rutledge, A. C., Codreanu, S. G., Sherrod, S. D., and McLean, J. A. (2016). Untargeted metabolomics strategies—challenges and emerging directions. *J. Am. Soc. Mass Spectrom.* 27, 1897–1905. doi: 10.1007/s13361-016-1469-y

Sender, R., Fuchs, S., and Milo, R. (2016). Revised estimates for the number of human and bacteria cells in the body. *PLoS Biol.* 14:e1002533. doi: 10.1371/journal.pbio.1002533

Shephard, R. J. (1984). Tests of maximum oxygen intake a critical review. *Sports Med.* 1, 99–124. doi: 10.2165/00007256-198401020-00002

Shi, Y., Shi, H., Nieman, D. C., Hu, Q., Yang, L., Liu, T., et al. (2019). Lactic acid accumulation during exhaustive exercise impairs release of neutrophil extracellular traps in mice. *Front. Physiol.* 10:709. doi: 10.3389/fphys.2019.00709

Sigal, R. J., Fisher, S., Halter, J. B., Vranic, M., and Marliss, E. B. (1996). The roles of catecholamines in glucoregulation in intense exercise as defined by the islet cell clamp technique. *Diabetes Metab. Res. Rev.* 45, 148–156. doi: 10.2337/diab.45.2.148

Steinhauser, M. L., Olenchock, B. A., O'Keefe, J., Lun, M., Pierce, K. A., Lee, H., et al. (2018). The circulating metabolome of human starvation. *JCI Insight* 3:e121434. doi: 10.1172/jci.insight.121434

Stepto, N. K., Benziane, B., Wadley, G. D., Chibalin, A. V., Canny, B. J., Eynon, N., et al. (2012). Short-term intensified cycle training alters acute and chronic responses of PGC1α and Cytochrome C oxidase IV to exercise in human skeletal muscle. *PLoS One* 7:e53080. doi: 10.1371/journal.pone.0053080

Terrados, N., Melichna, J., Sylvn, C., Jansson, E., and Kaijser, L. (1988). Effects of training at simulated altitude on performance and muscle metabolic capacity in competitive road cyclists. *Eur. J. Appl. Physiol.* 57, 203–209. doi: 10.1007/BF00640664

Thiele, I., Swainston, N., Fleming, R. M. T., Hoppe, A., Sahoo, S., Aurich, M. K., et al. (2013). A community-driven global reconstruction of human metabolism. *Nat. Biotechnol.* 31, 419–425. doi: 10.1038/nbt.2488

Tumilty, L., Davison, G., Beckmann, M., and Thatcher, R. (2011). Oral tyrosine supplementation improves exercise capacity in the heat. *Eur. J. Appl. Physiol.* 111, 2941–2950. doi: 10.1007/s00421-011-1921-4

Uchida, M., Horii, N., Hasegawa, N., Fujie, S., Oyanagi, E., Yano, H., et al. (2019). Gene expression profiles for macrophage in tissues in response to different exercise training protocols in senescence mice. *Front. Sports Act. Living* 1:50. doi: 10.3389/fspor.2019.00050

Underwood, E. A. (1944). Lavoisier and the history of respiration. *Proc. R. Soc. Med.* 37, 247–262. doi: 10.1177/003591574403700603

Virgili, F., Maiani, G., Zahoor, Z. H., Ciarapica, D., Raguzzini, A., and Ferro-Luzzi, A. (1994). Relationship between fat-free mass and urinary excretion of creatinine and 3-methylhistidine in adult humans. *J. Appl. Physiol.* 76, 1946–1950. doi: 10.1152/jappl.1994.76.5.1946

Wahrenberg, H., Bolinder, J., and Arner, P. (1991). Adrenergic regulation of lipolysis in human fat cells during exercise. *Eur. J. Clin. Invest.* 21, 534–541. doi: 10.1111/j.1365-2362.1991.tb01406.x

Watson, P., Enever, S., Page, A., Stockwell, J., and Maughan, R. J. (2012). Tyrosine supplementation does not influence the capacity to perform prolonged exercise in a warm environment. *Int. J. Sport Nutr. Exerc. Metab.* 22, 363–373. doi: 10.1123/ijsnem.22.5.363

Webster, M. J. (1998). Physiological and performance responses to supplementation with thiamin and pantothenic acid derivatives. *Eur. J. Appl. Physiol.* 77, 486–491. doi: 10.1007/s004210050364

Williams, M. H. (1989). Vitamin supplementation and athletic performance. *Int. J. Vitam. Nutr. Res. Suppl. Int. Z. Vitam. Ernahrungsforschung Suppl.* 30, 163–191.

Xu, G., Hansen, J. S., Zhao, X. J., Chen, S., Hoene, M., Wang, X. L., et al. (2016). Liver and muscle contribute differently to the plasma acylcarnitine pool during fasting and exercise in humans. *J. Clin. Endocrinol. Metab.* 101, 5044–5052. doi: 10.1210/jc.2016-1859

Yoshida, T., Prudent, M., and D'Alessandro, A. (2019). Red blood cell storage lesion: causes and potential clinical consequences. *Blood Transfus.* 17, 27–52. doi: 10.2450/2019.0217-18

Zhang, D., Tang, Z., Huang, H., Zhou, G., Cui, C., Weng, Y., et al. (2019). Metabolic regulation of gene expression by histone lactylation. *Nature* 574, 575–580. doi: 10.1038/s41586-019-1678-1

Zhang, J., Wang, Y. T., Miller, J. H., Day, M. M., Munger, J. C., and Brookes, P. S. (2018). Accumulation of succinate in cardiac ischemia primarily occurs via canonical krebs cycle activity. *Cell Rep.* 23, 2617–2628. doi: 10.1016/j.celrep.2018.04.104

Zhong, G., Yang, X., Jiang, X., Kumar, A., Long, H., Xie, J., et al. (2019). Dopamine-melanin nanoparticles scavenge reactive oxygen and nitrogen species and activate autophagy for osteoarthritis therapy. *Nanoscale* 11, 11605–11616. doi: 10.1039/C9NR03060C

Zouhal, H., Jacob, C., Delamarche, P., and Gratas-Delamarche, A. (2008). Catecholamines and the effects of exercise, training and gender. *Sports Med.* 38, 401–423. doi: 10.2165/00007256-200838050-00004

Conflict of Interest: The authors declare that IS-M, AD'A, and TN are founders of Altis Biosciences LLC and KCH. AD'A and TN are founders of Omix Technologies, Inc. AD'A is a consultant for Hemanext Inc.

The remaining authors declare that the research was conducted in the absence of any commercial or financial relationships that could be construed as a potential conflict of interest.

frontiers in Physiology

REVIEW
published: 09 June 2020
doi: 10.3389/fphys.2020.00544

Theoretical Bases for the Role of Red Blood Cell Shape in the Regulation of Its Volume

Saša Svetina[1,2]*

[1] Institute of Biophysics, Faculty of Medicine, University of Ljubljana, Ljubljana, Slovenia, [2] Jožef Stefan Institute, Ljubljana, Slovenia

The red blood cell (RBC) membrane contains a mechanosensitive cation channel Piezo1 that is involved in RBC volume homeostasis. In a recent model of the mechanism of its action it was proposed that Piezo1 cation permeability responds to changes of the RBC shape. The aim here is to review in a descriptive manner different previous studies of RBC behavior that formed the basis for this proposal. These studies include the interpretation of RBC and vesicle shapes based on the minimization of membrane bending energy, the analyses of various consequences of compositional and structural features of RBC membrane, in particular of its membrane skeleton and its integral membrane proteins, and the modeling of the establishment of RBC volume. The proposed model of Piezo1 action is critically evaluated, and a perspective presented for solving some remaining experimental and theoretical problems. Part of the discussion is devoted to the usefulness of theoretical modeling in studies of the behavior of cell systems in general.

Keywords: Piezo1, Gárdos channel, mechanosensitivity, spectrin skeleton, curvature dependent protein–membrane interaction, cell to cell variability, osmotic fragility, negative feedback loop

OPEN ACCESS

Edited by:
Lars Kaestner,
Saarland University, Germany

Reviewed by:
Chaouqi Misbah,
UMR 5588 Laboratoire Interdisciplinaire de Physique (LIPhy), France
Dmitry A. Fedosov,
Helmholtz-Verband Deutscher Forschungszentren (HZ), Germany

***Correspondence:**
Saša Svetina
sasa.svetina@mf.uni-lj.si

Specialty section:
This article was submitted to Red Blood Cell Physiology, a section of the journal Frontiers in Physiology

Received: *15 January 2020*
Accepted: *30 April 2020*
Published: *09 June 2020*

Citation:
Svetina S (2020) Theoretical Bases for the Role of Red Blood Cell Shape in the Regulation of Its Volume. Front. Physiol. 11:544. doi: 10.3389/fphys.2020.00544

INTRODUCTION

The red blood cell (RBC) shape is, basically, assumed to depend on the cohesion and mechanical stability of its membrane (Mohandas and Chasis, 1993) and its volume to depend on the harmonized action of several different membrane pumps and channels that define the content of cytoplasm cations (Hoffmann et al., 2009). It is therefore considered that RBC shape and volume attain their physiological states independently of each other. The discovery that the RBC membrane includes a mechanosensitive channel, Piezo1, that has an effect on RBC dehydration (Murthy et al., 2017), indicated that RBC volume may also depend on membrane mechanics. Piezo1 acts through the activation of Gárdos channels by Ca^{++} ions that enter the cell when it is open (Cahalan et al., 2015). Recently we proposed a theoretical model in which it was postulated that Piezo1 cation permeability depends on an RBC discoid shape (Svetina et al., 2019). The model revealed the existence of a negative feedback loop that interrelates this shape with the RBC content of potassium ions and, thus, also with its volume. At the Monte Verita RBC meeting I reported about how predictions of the model were verified by utilizing the concepts developed in studies on RBC cell to cell variability (Svetina, 1982, 2017; Svetina et al., 2003). However, the model is

a combination of these and several other concepts, together with views expressed previously in different theoretical studies on RBC shape and volume behavior. The present review will include the topics of these studies. This review is also motivated by the fact that the organizers of the Monte Verita meeting asked some senior participants to disseminate to newcomers to the field their research experiences. In this sense it will be rather subjective and thus largely concentrated on the work of our research group. The model discussed here is an example of the research approach by which, on the basis of theoretical analyses and exploitation of existing experimental data, it is possible to make predictions about the behavior of a treated system, thus providing new ideas as to how to advance the corresponding inquiries (Goldstein, 2018). We shall therefore discuss also some general capabilities of theoretical approaches in studies of cell processes.

To understand a given cell process it is necessary to identify the structural elements responsible and to provide a description of the mode of their operation. The corresponding theoretical studies are aimed at obtaining their structure–function relationship in a quantitative manner. This task is, in general, difficult, since cells are complex. The only way to make progress is frequently by analyses of mathematical models. In modeling it is usually necessary first to identify the structural level that is proper for the description of different aspects and for the function of a treated physiological process, and then to reveal its essential features on the basis of the simplest possible system. Models are, as a rule, built on the basis of a set of assumptions that can then be tested experimentally. When these assumptions are found to be correct, and it is thus possible to obtain model predictions by exact either analytical or numerical calculations, a model becomes a theory. The modeling approach should be distinguished from the use of mathematics in the analysis of experimental results and from simulations where, on the basis of the already established theory, the system's behavior can be described mathematically in an exact manner. When modeling the behavior of whole cells it is advantageous to study those that are simple. RBCs, although composed of several thousand different molecules and ions, are, in some aspects, extremely simple. Basically, they are constituted by a concentrated hemoglobin solution enclosed by an essentially smooth membrane. Moreover, they also have a well-defined main function of carrying respiratory gasses. Therefore, and because of its availability, the RBC served, and still serves, as an ideal system for developing the principles of modeling structure–function relationships in cell systems in general (Lux, 2016).

This review will be focused on the bases on which we recently developed a model of the role of Piezo1 in the regulation of the RBC volume (Svetina et al., 2019). The aim is to help build a more thorough critical view on this model. The model was formed on the basis of several RBC and other research directions. It illustrates a circuitous nature of modeling approaches: the past theoretical studies on RBC shape have opened up some other research topics which have turned out to be relevant to studies of the regulation of RBC volume after the identification of the mechanosensitive protein Piezo1 (Coste et al., 2010) and the elucidation of its role in hereditary xerocytosis (Zarychanski et al., 2012). Briefly, some years ago we examined the possible osmotic states of RBC in dependence on the permeability state of its membrane (Brumen et al., 1979, 1981). In another study we presented (Svetina et al., 1982) a theoretical counterpart of the earlier proposed bilayer couple hypothesis of RBC shape transformation (Sheetz and Singer, 1974). This led us to formulate a general theory of shapes of vesicular objects with flexible membranes (Svetina and Žekš, 1989). This theory predicted that, among the possible stable shapes, some exhibit polar symmetry. We proposed that such shapes could serve as a mechanical origin of cell polarity, and also speculated that this could have been realized through curvature dependent interaction between membrane inclusions such as channels and pumps and the surrounding membrane (Svetina and Žekš, 1990; Svetina et al., 1990). We later derived a general phenomenological interaction term for the curvature dependent inclusion–lipid matrix interaction (Kralj-Iglič et al., 1999), and formulated the procedure for treating the mutual effects of the shape of a vesicular object and the lateral distribution of membrane inclusions on each other (Kralj-Iglič et al., 1996; Božič et al., 2006). These results gained significance because, in the meantime, several membrane proteins had been disclosed that were characterized by their membrane sensing and curvature forming capabilities (McMahon and Gallop, 2005; Zimmerberg and Kozlov, 2006). The curved Piezo1 structure (Ge et al., 2015; Guo and MacKinnon, 2017; Saotome et al., 2018; Zhao et al., 2018) indicates that it affects the shape of the surrounding membrane. A possible role of curvature dependent protein–membrane interaction in the process of mechanosensitivity has also been indicated (Svetina, 2015). The described broad modeling background thus seemed to be well suited also for analyzing different possible modes of Piezo1 operation in the regulation of RBC volume.

The review is organized as follows. The treated model (Svetina et al., 2019) will be described and commented in the last section (see section "Model of the Effect of RBC Discocyte Shape on RBC Volume and its Outlook"). The two intermediate sections will describe the model background. Section "The Mechanical and Thermodynamic Bases of RBC Shape and Deformability" deals with the RBC shape and deformability. In its first subsection it will be described how the initial theoretical studies of RBC shapes in which it was assumed that its membrane is laterally homogeneous led to a general theory of vesicular objects with flexible membranes. In the second subsection it will be shown how the difference between the predictions of this theory and the behavior of RBCs helps to understand the role of RBC membrane skeleton. Section "RBC Volume and Related Aspects of the Variability of RBC Population" will deal with the models of the regulation of RBC volume. Special attention will be devoted to the aspects of RBC population variability. It will then be shown how the results described in two previous sections can be combined in the model of the effect of Piezo1 on RBC volume. A critical review of this model will be given and some suggestions presented for the necessary future work. Throughout the review, the emphasis will be on the development of concepts, therefore it will be mostly presented in a descriptive manner. The

corresponding equations and their derivation can be found in the cited literature.

THE MECHANICAL AND THERMODYNAMIC BASES OF RBC SHAPE AND DEFORMABILITY

The function of RBC as the carrier of respiratory gasses led to its adoption throughout evolution of numerous specific mechanical and thermodynamic properties. In the absence of external forces, the normal RBCs of most vertebrates assume the shape of a disk that involves, at its poles, the presence of symmetrically indented dimples. RBCs are deformable, e.g., under microcirculatory flow conditions, at sufficiently high shear stress, deform into rolling stomatocytes and, finally, adopt polylobed shapes (Lanotte et al., 2016). An important factor that allows for these shape transformations is that RBC occupies only about 60% of the volume that a cell could at a given area of its membrane. This property of RBCs is conveniently quantified in terms of the reduced volume (v) defined as the ratio between the RBC volume (V) and the volume of the sphere with the same membrane area (A):

$$v = 3V/4\pi R_s{}^3 \quad (1)$$

where $R_s = (A/4\pi)^{1/2}$. The mechanism for the establishment of RBC volume will be dealt with in section "RBC Volume and Related Aspects of the Variability of RBC Population." Here our focus is on how, at a given value of v, RBC shape and its deformation depend on the mechanical properties of its membrane. RBC membrane is composed of a lipid bilayer occupied densely by membrane integral proteins, and the underlying membrane skeleton, a two-dimensional pseudo-hexagonal network with actin based protein complexes as nodes and spectrin tetramers as bonds. The bilayer and the skeleton are linked by chemical bonds between spectrin and integral membrane proteins band3 and glycophorin C, via ankirin and actin complexes, respectively (Mohandas and Gallagher, 2008; Lux, 2016). The RBC membrane differs from those of most other eukaryotic cells in that it has no cytoplasm reservoirs and has therefore a smooth appearance. Because of a relatively large value of the compressibility modulus of the bilayer it is, laterally, practically incompressible. RBC mechanical behavior depends crucially on the characteristic of its membrane that its three layers, the two leaflets of the bilayer and the underlying skeleton, can slide, one over the other. The bilayer resists bending of the membrane and the skeleton to exhibit shear deformation. The first reasonable models of RBC shape behavior were based on the assumption that their shapes correspond to the minimum of membrane bending energy. In the subsequent subsection it will be revealed how, out of these models, a theory of shapes of simple vesicular objects such as phospholipid vesicles developed, and how the stability of shapes depends on the elastic properties of multilayered membranes. In the second subsection it will be shown how the comparison between the predictions of this theory and the behavior of RBC helps the different roles of its membrane skeleton to be understood.

Interpretation of RBC and Vesicle Shapes on the Basis of Membrane Bending

Red blood cell shape has been treated by assuming its membrane to be a single, thin, laterally homogeneous mechanical entity. RBC membrane can, at its reduced volume v of about 0.6, take up an infinite number of shapes, exhibiting different values of the total membrane bending energy (W_b) that can be for symmetrical bilayer obtained by the integral of the square of the mean membrane curvature ($H = (C_1 + C_2)/2$ where C_1 and C_2 are the principal membrane curvatures) over the whole membrane area expressed as

$$W_b = 2k_c \int H^2 dA \quad (2)$$

with k_c membrane bending constant. In general membrane bending energy involves also a contribution due to Gaussian curvature ($K = C_1C_2$) (Helfrich, 1973). However, because the integral of K over the membrane area is for a given membrane topology constant this term will be in further discussions here ignored. Canham (1970) looked for the minimum of W_b (Eq. 2) and found that, at $v = 0.6$, the shape is a discoid. He assumed that the membrane has zero energy when it is flat and took into consideration that the membrane has no lateral shear, i.e., that it behaves laterally as a two-dimensional liquid. Helfrich (1973) generalized the expression for membrane bending energy by assuming that the membrane may have, due to transmembrane asymmetry, zero energy when it is bent to its spontaneous curvature (C_0). Deuling and Helfrich (1976), by applying their "spontaneous curvature model," obtained by minimizing the Helfrich's (1973) expression of membrane bending energy at given reduced volumes and reduced values of the spontaneous curvature (R_sC_0) beside the discocyte also several other shapes including cup shaped stomatocytes. At about the same time Sheetz and Singer (1974) introduced the "bilayer couple hypothesis" based on the evidence that RBCs change shape under conditions of asymmetric changes of the areas of the outer and inner leaflets of the membrane bilayer. They showed that, by adding a drug (chlorpromazine) that intercalates into the inner monolayer of the RBC bilayer, the discocyte transforms into a cup shape (stomatocyte) whereas drugs intercalating into the outer layer cause shape transformation into a spiculated echinocyte. In a theoretical treatment of the bilayer couple hypothesis, RBC shapes (which were defined in terms of the finite number of geometrical parameters) were obtained by minimization of the membrane bending energy at a fixed difference between the areas of the outer and inner leaflets of the bilayer (Svetina et al., 1982). It was implied that this area difference (ΔA) constitutes a convenient single parameter whose continuous decrease causes the shape to be transformed from discocyte to stomatocyte in a continuous manner. This result was confirmed and, also, further explored by an exact variational procedure for minimizing membrane bending energy under the constraints of constant membrane area, cell volume, and area difference (Svetina and Žekš, 1989). While bilayer couple hypothesis represents for

some aspects of RBC shape transformations a useful workable model, it also turned out to be a strict theory for shapes of simple vesicular objects defined as a liquid interior enclosed by a flexible membrane. For students of RBC shape behavior and deformability it is useful to be familiar with the basic results of this theory because knowledge of its predictions may help to distinguish which aspects of RBC behavior depend on properties of its bilayer and which on its other structural features.

The bilayer couple theory (Svetina and Žekš, 1989) predicts that vesicle shapes depend on only two geometrical parameters, the reduced volume v and the reduced area difference Δa (defined as the ratio between ΔA and its value for the sphere which is $8\pi h R_s$ with h the distance between the neutral surfaces of the bilayer leaflets and R_s, as already defined, the radius of the sphere). The geometrical meaning of Δa is that it is also equal to the integral of the reduced mean membrane curvature ($R_s H$) over the membrane surface. Vesicle shapes can be grouped into classes that occupy different parts of the v – Δa (or Δa – v as used in Seifert et al., 1991) shape phase diagram. The shapes belong to a given class if they have the same symmetry and if, by continuously changing Δa and/or v, they are changing continuously. The sense of such shape classification is illustrated in **Figures 1A–C**. There are two types of shape class boundaries. One type comprises shapes obtained by variational search of the extreme values of the reduced volume v at a fixed value of the reduced area difference Δa (**Figure 1A**). They are composed of spheres or spherical parts with only two possible values of their radius (Svetina and Žekš, 1983, 1989). For example, lines 1 and 6 are boundaries of shape class to which belongs the discocyte (located in the minimum of the bending energy curve "S" in **Figure 1C**). All these shapes are axisymmetric and involve equatorial mirror symmetry. The second type of shape class boundaries are symmetry breaking lines (lines 9 to 12 in **Figure 1B**). For example, the class of cup (stomatocyte) shapes is, on one side, bounded by the limiting shape (line 5 in **Figure 1A**) and, on the other side, by the symmetry breaking line (line 9 in **Figure 1B**) that connects the points at which the equatorial mirror symmetry of disk shapes breaks down (shown by an arrow in **Figure 1C**) at all reduced volumes. Notably, the class of non-axisymmetric (ellipsoidal) shapes is bounded by symmetry breaking lines on both of its sides (lines 10 and 11 in **Figure 1B**) at which disk and cigar shapes, respectively, break down their axial symmetry (Heinrich et al., 1993). As demonstrated by curves A and S in **Figure 1C**, classes overlap. Only the shape with the lowest bending energy is stable. **Figure 1B** shows which shapes are stable within the presented central part of the v – Δa shape phase diagram. Red point and triangle in **Figures 1A–C** indicate where in the v – Δa shape phase diagram are located the discocyte and typical stomatocyte, respectively. The significance of the bilayer couple theory is that it predicts all possible shapes of vesicular objects with laterally homogeneous membranes. If a vesicle shape differs from any of these shapes it means that there are external forces acting on it (Svetina and Žekš, 1996) or that its membrane is laterally inhomogeneous (Božič et al., 2006).

The described predictions of the bilayer couple model are strictly only valid if the two equally composed leaflets of a bilayer are incompressible. In reality they are compressible and therefore it has to be taken into account that, in general, in a given shape, they might be deformed differently, for example in that the area of one is extended and of the other compressed. In such cases the reduced area difference (Δa) differs from analogously defined equilibrium (preferred) area difference (Δa_0) which corresponds to the situation where leaflets are neither extended nor compressed. The bilayer thus exhibits, in addition to the already defined bending energy (Eq. 2), also the non-local bending energy (W_k) (Evans, 1980), termed also as area difference elastic term (Miao et al., 1994), expressed in its reduced form ($w_k = W_k/8\pi k_c$) as

$$w_k = k_r(\Delta a - \Delta a_0)^2/2 \quad (3)$$

where k_r is the non-local bending constant. The derivation and consequences of non-local bending energy were comprehensively reviewed in Svetina and Žekš (2014). Briefly, in the generalized bilayer couple model, vesicle shapes correspond to the minimum of the sum of the bending (Helfrich, 1973) and non-local bending energies. The shape equation to be solved is the same as in the limit of the strict bilayer couple model so the shapes obtained are the same. However, not all of them are necessarily stable. Why it is so is demonstrated by **Figure 1D**. The minimization of the sum of the two bending energies with respect to Δa gives rise to the requirement

$$\partial w_b/\partial \Delta a = -(k_r/k_c)(\Delta a - \Delta a_0) \quad (4)$$

The solution of Eq. 4 for its unknown Δa can, for a given value of Δa_0, be obtained graphically as a point on the graph of **Figure 1D** where a dashed curve (right hand side of Eq. 4) crosses one (either S or A) of the $\partial w_b/\partial \Delta a$ curves (left hand side of Eq. 4). The number of solutions of Eq. 4 at given Δa_0 depends on the slope of dashed curves that is proportional to the ratio k_r/k_c. There is only one solution if this slope is steeper than that of the largest derivative by Δa of the function $\partial w_b/\partial \Delta a$ of asymmetrical shapes (A) which is at the symmetry breaking point (**Figure 1C**). A vesicle can thus attain all possible shapes predicted by the strict bilayer couple model. At values of k_r/k_c that are smaller than above defined critical value of $\partial w_b/\partial \Delta a$ there are, for some values of Δa_0 (e.g., 0.82 in **Figure 1D**), three solutions of Eq. 4. The shape at the middle value of Δa is not stable. Consequently there is, e.g., at continuously decreasing value of Δa_0, a discontinuous shape transformation from the Δa at a cross-section of a dotted line with the curve S to the smaller Δa at which this line crosses the curve A. The shapes of the strict bilayer couple model that correspond to the intermediate Δa values are not stable. Possible stable shapes of the generalized bilayer couple model are thus defined by the 3-dimensional v – Δa – k_r/k_c shape phase diagram. The example of the cross-section of this diagram is for $v = 0.85$ shown in Figure 12 of Svetina and Žekš (1996). The slope of the $\partial w_b/\partial \Delta a$ curve at the symmetry breaking point is at $v = 0.6$ close to – 3. The estimated ratio k_r/k_c for RBC membrane is about 2 (Hwang and Waugh, 1997) which indicates that the discocyte–stomatocyte transition is discontinuous. The described reasoning can be generalized straightforwardly to cover also the effects of transmembrane asymmetry characterized by membrane spontaneous curvature

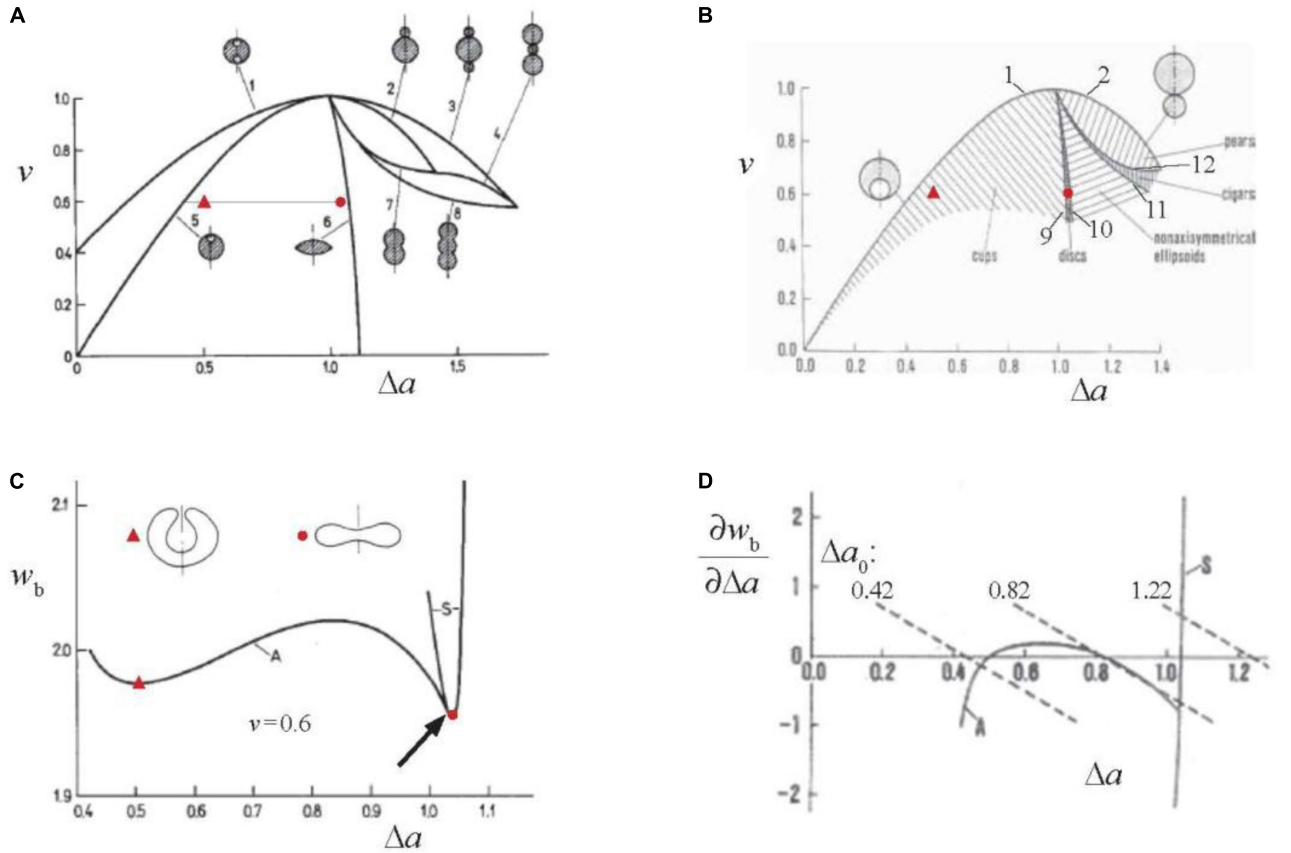

FIGURE 1 | Demonstration of basic features of the bilayer couple theories of vesicle shapes [**(A–C)** of "strict" and **(D)** of "generalized"]. **(A)** $v(\Delta a)$ dependences of limiting shapes which correspond to the extreme values of v at a given value of Δa (lines 1 to 8) plotted in the $v - \Delta a$ shape phase diagram (Svetina and Žekš, 1989). Examples of corresponding shape cross-section are also shown. The dotted horizontal line at $v = 0.6$ indicates the range of Δa values for which minimal membrane bending energy is presented in **(C)**. Red point indicates the phase diagram location of a discocyte and red triangle of a characteristic stomatocyte. **(B)** Stable vesicle shapes in the central part of the $v - \Delta a$ shape phase diagram. Lines 9–12 are symmetry breaking lines. Marked areas represent the parts of the shape phase diagram where there are no contacts between different regions of the membrane. The meaning of red points is the same as in **(A)**. **(C)** Membrane bending energy w_b (defined relative to the bending energy of the sphere which is $8\pi k_c$) calculated at $v = 0.6$ for the Δa values indicated by the dotted line in **(A)**. Line S shows bending energy of disk shapes and line A of the cup shapes. The arrow indicates the point of the symmetry breaking of the disk shape as predicted by Svetina and Žekš (1989). Shown are also contours of cross-sections of a discocyte (red point) and a stomatocyte (red triangle) and it is indicated which are their Δa values. **(D)** The dependence of the partial derivatives of the bending energies S and A presented in **(C)** by the area difference Δa. The dotted lines present the right hand side of Eq. 4 for the indicated values of Δa_0 and $k_r/k_c = 3$ (reprinted with permission from Svetina, 1998).

C_0. C_0 and ΔA_0, in spite of having different physical background affect the shapes of vesicular objects with bilayer membranes in a similar manner. The stationary shapes obtained by solving the shape equation are the same as in the strict bilayer couple model if for the reduced equilibrium area difference is taken an effective one defined as

$$\Delta a_{0,eff} = \Delta a_0 + c_0 k_c / 2k_r \quad (5)$$

It has to be noted that in this case the region of stable shapes in the generalized shape phase diagram $v - \Delta a_{0,eff} - k_r/k_c$ depends on the relative contribution to $\Delta a_{0,eff}$ of Δa_0 and c_0. It is because the energy term due to Δa_0 (Eq. 3) involves Δa^2 whereas the energy term due to c_0 is a linear function of Δa. Therefore the discontinuous transition indicated in **Figure 1D** occurs at shifted Δa values, such that at increasing the relative contribution of c_0, the region of stable shapes is diminishing. The limit $k_r/k_c = 0$ represents the spontaneous curvature model of Deuling and Helfrich (1976). A full description of which shapes are stable in this limit was presented by Seifert et al. (1991) (reviewed in Seifert, 1997). The spontaneous curvature model also applies in the case that due to transmembrane lipid transport the bilayer relaxes into the state with $\Delta a_0 = \Delta a$. The relaxation time for this process was estimated to be 8 min (Raphael and Waugh, 1996) or even much less (Svetina et al., 1998).

Effects of Compositional and Structural Features of the RBC Membrane

Red blood cell membrane is, compared to phospholipid membranes, complex. Its bilayer part is crowded with integral membrane proteins such as band3 that is involved in RBC's function of carrying carbon dioxide, different pumps and

channels that take care of the establishment of RBC volume, and many other proteins serving in its protection (Mohandas and Gallagher, 2008). As already noted, it contains, on its cytoplasmic side, a spectrin based membrane skeleton which is the main element that accounts for how RBC shape behavior differs from that of simple phospholipid vesicles. In this respect we here discuss skeleton shear elasticity, its role in the formation of RBC shape, and its possible effects on the lateral distribution of integral membrane proteins and their lateral diffusion.

Red blood cell membrane exhibits shear elasticity. Because its bilayer part can be considered as two-dimensional liquid, the shear elasticity can be ascribed solely to its membrane skeleton which is a two-dimensional pseudo-hexagonal network of spectrin tetramers as bonds and acting filaments as nodes. To understand the skeleton behavior it is crucial to realize that RBC membrane deformation may cause an alteration of local skeleton densities while the density of the lipids remains the same, as was observed by measuring skeleton lateral distribution in RBC partially aspirated into the micropipette (Discher et al., 1994; Discher and Mohandas, 1996; **Figure 2A**). These results imply that skeleton nodes shift their position relative to the bilayer and that the bonds deform elastically. This is possible because the bilayer integral proteins to which the skeleton is anchored can move laterally in the plane of the bilayer. The observed changes of skeleton density indicate that the extension ratios (λ_i, the ratio between the final length and the initial length of the deformed skeleton material in the i-th direction) may reach a value of about 3, which corresponds to a fully extended spectrin tetramer of length $\sim$ 200 nm. Skeleton deformation may be described by shear and area compressibility deformational modes (Mohandas and Evans, 1994). The area compressibility elastic modulus of the RBC skeleton is estimated at 26 μN/m (Svetina et al., 2016), which is about four orders of magnitude less than that of the whole RBC membrane determined to be 0.29 N/m (Evans et al., 1976). Consequently, the deformed skeleton redistributes over the RBC membrane at its practically constant total area A. Different parts of RBC skeleton are kept together by non-covalent bonds which can break and reform, indicating the possibility that it is plastic. The undeformed state of the skeleton may thus depend on the RBC's history and is in general not well defined.

Theoretical modeling of the RBC skeleton is developing in several different directions (e.g., Discher et al., 1998; Fedosov et al., 2010; Peng et al., 2010; Svetina et al., 2016). The present discussion will focus on the type of models aimed at making a distinction between skeleton deformation due to the change of the shape of the cell membrane and that due to its mechanical properties. In this respect Mukhopadhyay et al. (2002) applied in their model of the RBC membrane the concept of a mapping function defined in terms of the dependence of the original position of a skeleton element on its position in the deformed state. They used this concept in their studies of the effect of the skeleton on RBC shapes (see below). For axisymmetric shapes it is possible to express the mapping function as $s_0(s)$ where s_0 is the arc-length distance from the cell pole to a given contour point of the original skeleton state and s the corresponding distance of the deformed state. Mathematically, the dependence $s_0(s)$ is sought at which the sum of the skeleton energy and the membrane bending energy is minimal. We treated a simplified version of this problem by studying cases in which the deformed shape is defined by rigid walls and therefore there is no need to consider the bending energy (Svetina et al., 2016). Examples of such deformations are RBC aspiration into medium sized (with respect to the RBC size) (**Figure 2A**) and narrow ($\sim$ 1 μm) pipettes. Following Discher et al. (1998) we also assumed that the main contribution to the skeleton energy is the energy of spectrin bonds. Instead of using for bond energy a more realistic flexible chain model (Discher et al., 1998), we described this energy by a harmonic potential which is a good approximation at sufficiently small deformations (Figure 8 in Svetina et al., 2016). The energy of the deformed skeleton was determined in the mean field approximation. In this simple model the skeleton deformation is the same for any value of the bond strength. This means that the most important factor for the observed change in skeleton lateral distribution is the changed cell geometry. For axisymmetric shapes it is, to some extent, possible to reason about the effect of changed geometry in qualitative terms. When a patch of the skeleton that is at a distance r_0 from the axis moves in the deformed state to the distance r from the axis, its extension along the parallels is $\lambda_p = r/r_0$. The corresponding compression (in case that $r < r_0$) exerts a tendency to make λ_m larger than 1. The local magnitudes of the extensions along meridians are restricted by the requirement that the total skeleton area is constant. The effect of this requirement cannot be visualized so clearly; however, it can still be concluded that the skeleton prevents shape changes with significant changes of the distances of the membrane from the axis. In **Figure 2B**, as an example, is shown by this model predicted deformation of RBC discocyte aspirated into a medium sized pipette.

Red blood cell shape behavior differs qualitatively from that of phospholipid vesicles in the region of the $v - \Delta a$ shape phase diagram, where prolates are the typical equilibrium shapes of vesicles with simple membranes (e.g., dumb-bells and pears) with their limiting shapes involving external buds (**Figures 1A,B**). In contrast, RBC shapes are, in the respective Δa region, echinocytic (reviewed in Svetina et al., 2004). Mukhopadhyay et al. (2002) studied the formation of echinocytes on the basis of continuum mechanics by searching for the minimum of the sum of the local and non-local bending energies of the bilayer, and the stretching and shear elastic energies of the membrane skeleton. The bending energy of the spiculated membrane is larger than that of the dumb-bell shape. However, the echinocyte can be understood to be more stable since the deformation of the skeleton into the geometry of a dumb-bell would, because of large changes of the distances from the axis, require a much larger increase of the skeleton energy than that for its transformation into a quasi-spherical echinocyte (neglecting that some skeleton albeit with decreased density is also present in its spicules). The formation of echinocytes has a physiological advantage by preventing the occurrence of shapes with large external buds that form in simple vesicles at increased values of Δa (c.f. line 3 in **Figure 1A**). The probable pinching off of such buds in

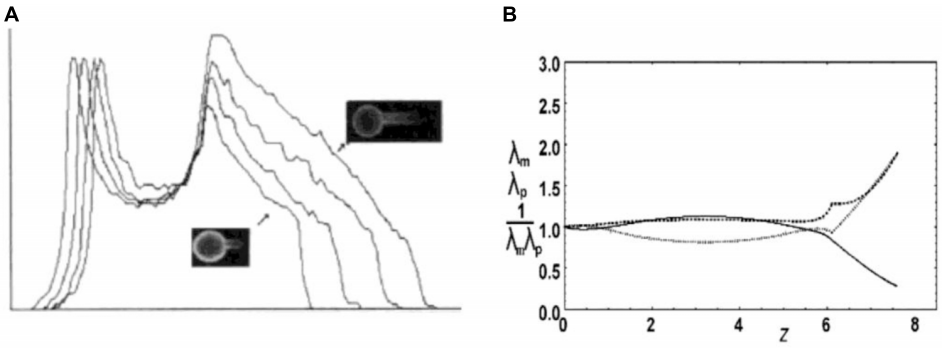

FIGURE 2 | Deformation of RBC skeleton. **(A)** Experimental evidence for the deformation of the membrane skeleton when RBC ghost is aspirated into a medium size pipette ($R_p \approx 2$ μm) (from Discher et al., 1994; reprinted with permission from AAAS). The skeleton density profiles along the projection of four aspirated RBC ghosts are shown, obtained by measuring fluorescein-phalloidin-labeled actin. Relevant for the present discussion is the decrease of the intensity along the aspirated part of the ghosts (arrows). **(B)** Skeleton extension ratios along parallels λ_p (dashed) and along meridians λ_m (dots) and the density $1/\lambda_p\lambda_m$ (relative to its mean value; full line) calculated according to the described model (Svetina et al., 2016) for the RBC aspirated into medium size pipette **(A)** (reprinted with permission from Švelc and Svetina, 2012). The pipette is on the right. The initial shape with, presumably, homogeneous skeleton distribution is a discocyte.

the turbulent blood flow would increase RBC reduced volume considerably, thus diminishing its deformability. It should be noted that when RBC changes its shape from discocyte to stomatocyte, e.g., due to possible decrease of membrane Δa_0, the skeleton is not deformed so much because these two shapes are both oblate and the distances of skeleton elements from the axis in them do not differ appreciably. Therefore, the behavior of RBC shape in the "oblate" region of the $v - \Delta a$ shape phase diagram does not differ essentially from the behavior of simple phospholipid vesicles. In cases where the buds are internal (c.f. lines 1 and 5 in **Figure 1A**) there is also no danger that they would be pinched off.

Another physiological role of the RBC membrane skeleton is that of the prevention of formation of risky budded shapes due to lateral segregation of its integral proteins. Membrane embedded proteins interact with the surrounding membrane when their intrinsic principal curvatures differ from those of the membrane at their location. For example, when the drastically curved protein Piezo1 (Guo and MacKinnon, 2017) is embedded in a flat phospholipid membrane it is predicted that it will cause the membrane in its surroundings to form a kind of dome-shaped invagination (**Figure 3A**, from Haselwandter and MacKinnon, 2018). It is possible to treat such a protein–membrane interaction in terms of a phenomenological expression that takes into account the fact that there is a mismatch between the intrinsic principal curvatures of membrane inclusion (e.g., a protein) and those of the membrane. The general expression for the corresponding energy term, in the limit of a rigid inclusion surface, is conveniently written as (Kralj-Iglič et al., 1999)

$$W_{curv,j} = \frac{\kappa_j}{2}\left(H - H_{P,j}\right)^2 + \frac{\kappa_j^*}{2}\left[\Delta H^2 - 2\Delta H \Delta H_{P,j}\cos\left(2\omega_j\right) + \Delta H_{P,j}^2\right] \quad (6)$$

where $H_{P,j} = (C_{1,P,j} + C_{2,P,j})/2$ is the mean principal intrinsic curvature of the transmembrane part of the inclusion and $\Delta H_{P,j} = (C_{1,P,j} - C_{2,P,j})/2$ is a measure of the difference between its two principal curvatures. κ_j and κ_j^* are independent interaction constants. The angle ω_j defines the mutual orientation of the coordinate systems of the intrinsic principal curvatures of the inclusion and the principal curvatures of the membrane. One consequence of such interaction term is curvature sensing, meaning that mobile membrane proteins, due to curvature dependent interaction energy term, accumulate in membrane regions where this mismatch is small and are depleted from regions where it is large. For example, it is reasonable to expect that it is more probable for the Piezo1, due to its curved structure, to reside in regions of RBC discocyte poles (dimples) than on its equator. The second possible consequence of the curvature dependent protein–membrane interaction is its effect on shape which, for a membrane with mobile proteins, corresponds to the minimum of the sum of their distributional free energy and the bending energy of the membrane (Božič et al., 2006). The effect of inclusions on RBC shape depends on their number. Using a model study (Svetina et al., 1996), it was shown that, for the discocyte, the minimum system's free energy depends on the number of inclusions in a much stronger manner than in that for a budded shape (**Figure 3B**). If this number is sufficiently small the bending energy prevails and the stable shape remains to be the disk. However, above a certain critical value, the budded shape has a lower free energy. RBC membrane contains about 10^6 band3 proteins which could constitute a potential danger for the stability of the RBC if most of them were not linked to the skeleton.

Red blood cell membrane proteins that are not linked to the skeleton can, upon the deformation, redistribute over the membrane with a time constant that depends on their diffusion coefficient. The latter can be smaller than in a vesicle because of the corralling effect of the spectrin skeleton (Tomishige et al., 1998). A drastic reduction of the diffusion constant can be expected for Piezo1 because the membrane indentation that it causes (**Figure 3A**). It just about fits into the triangle formed

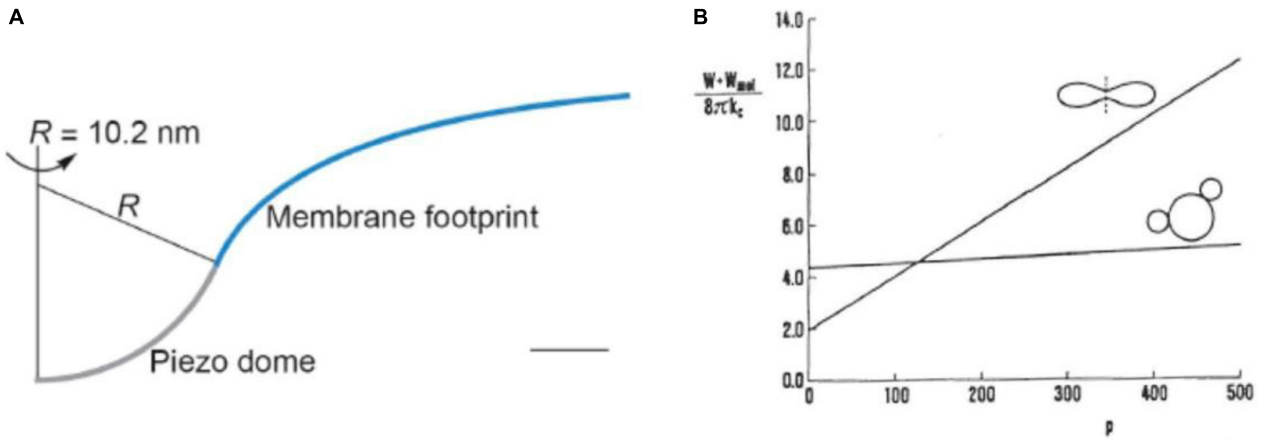

FIGURE 3 | Illustrations of effects of protein–membrane interaction. **(A)** The shape of the Piezo1 membrane footprint shown as the cross-section of the mid-bilayer surface and its intersection with the Piezo1 dome; scale bar: 4 nm (reprinted from Haselwandter and MacKinnon, 2018, held under CC-BY 4.0 license). **(B)** The sum of the membrane bending energy and the distributional free energy of mobile membrane inclusions calculated for the disk shape and for the shape that involves two buds for a cell with the reduced volume 0.6 in the dependence of the number of inclusions *p* (in some reduced units) (reprinted with permission from Svetina et al., 1996).

by the three spectrin tetramers, with each of them having in the RBC's resting state the length of about 70 nm.

RBC VOLUME AND RELATED ASPECTS OF THE VARIABILITY OF RBC POPULATION

Red blood cell membrane is, as those of most mammalian cells, well permeable for water. Therefore the RBC's water content, and thus also its volume, depend on its content of osmotically active substances and on the external tonicity (Hoffmann et al., 2009). Hemoglobin, the main protein constituent of the RBC cytoplasm, cannot cross its membrane, so therefore the RBC is under osmotic stress. In RBCs of many species, their reduced volume is, by virtue of the active pump-leak system for monovalent cations K^+ and Na^+, nevertheless kept at about 0.6. These cations are pumped by Na^+/K^+- ATPase which actively expels three sodium ions and takes in two potassium ions (Tosteson and Hoffman, 1960; Kay and Blaustein, 2019). The consequent higher cell concentration of K^+ and lower concentration of Na^+, both relative to their concentration in the environment, cause fluxes of these two cations in the direction of their concentration gradients. The pumping and leaking of K^+ and Na^+ eventually leads to the stationary volume level. There are several channels/transporters involved in the passive leakage of these two cations. The results of many studies of their action and of the data on cation pumping made it possible to formulate realistic mathematical modeling of RBC volume regulation (Lew and Bookchin, 1986; Armstrong, 2003; Ataullakhanov et al., 2009). K^+ and Na^+ attain their stationary value in a time scale which is several orders of magnitude larger than that of water and also of univalent anions Cl^- and HCO_3^- which can thus be treated at correspondingly short time scales as being in quasi-equilibrium between the inside and outside solutions. Because hemoglobin is charged, this equilibrium can be described by models that involve a version of the Donnan equilibrium in which cations do not exchange (Brumen et al., 1979; Freedman and Hoffman, 1979).

The issue here is the extension of already established models of RBC volume regulation that take into consideration the role of Piezo1 and Gárdos channels (Svetina et al., 2019). The predictions of the proposed model were supported by studies on properties of RBC population cell to cell variability. RBCs, in otherwise homogeneous RBC population, are known to be variable with respect to many of their measurable parameters such as cell volume, membrane area, hemoglobin content, density, etc. RBCs vary because of the variable properties of their precursors and because, throughout their lifespan, they are releasing nanovesicles (Westerman and Porter, 2016). In general, cells of the same kind are presumably organized in an identical manner, meaning that their state is defined by the same physical-chemical processes. On the basis of this assumption it can be deduced that, if there are some strict algebraic relations between the parameters that define the state of a single cell, there are also relationships between the parameters that measure the variability of these parameters, e.g., coefficients of variation and correlation coefficients. This notion has been confirmed by analysis of relations between standard deviations and correlation coefficients extracted from different single cell measurements of RBC volume, membrane area, density, and hemoglobin and cation contents (Svetina, 1982). Moreover, this analysis also revealed the possibility that an RBC involves a strict relationship, of at that time unknown origin, between membrane area and hemoglobin and cation contents. The analogous conclusion was later, by a different approach, obtained by Lew et al. (1995). The basic source for such relation was realized to be the strong correlation between RBC volume and membrane area. Simultaneous single cell determinations of these two cell

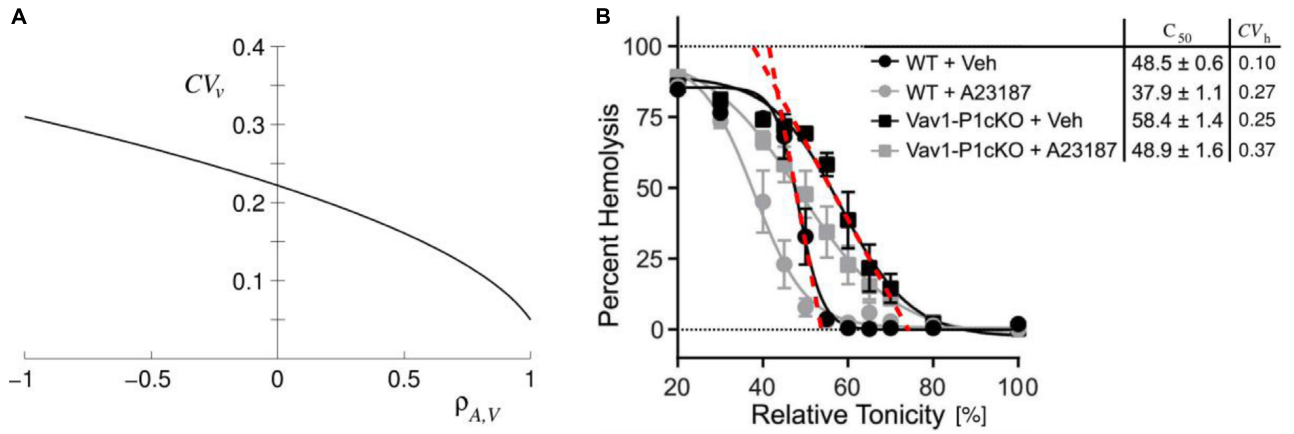

FIGURE 4 | Illustrations of consequences of the correlation between RBC area (*A*) and volume (*V*). **(A)** Coefficient of variation of RBC reduced volume (CV_v) in dependence on the correlation coefficient $\rho_{A,V}$ obtained for the values of coefficients of variations of RBC volume and membrane area to be 0.12 and 0.13, respectively (reprinted with permission from Svetina et al., 2019). CV_v at $\rho_{A,V}$ = 0.96 is about 0.06. **(B)** Evidence for the role of Piezo1 based regulation of RBC volume on the mouse RBC *V* – *A* correlation. Cahalan et al. (2015) measured osmotic fragility of normal (WT) and of Piezo1 knocked out (Vav1-PicKO) mouse RBC in the absence (+Veh) and presence (+A23187) of Ca^{2+} ionophore A23187 (reprinted with permission from Svetina et al., 2019). In Figure 5 of Svetina et al. (2019) we added to Figure 3D of Cahalan et al. (2015) the column of the corresponding coefficients of variation (CV_h) obtained from steepness of osmotic fragility curves as indicated by red dashed lines.

parameters yielded for the corresponding correlation coefficient a value of $\rho_{A,V} \sim 0.97$ (Canham and Burton, 1968) and of $\sim$ 0.96 (Gifford et al., 2003). The strong correlation between *V* and *A* is reflected in the fact that the coefficient of variation of the reduced volume is only about one half of the coefficients of variation of *V* and *A* (**Figure 4A**). It also explains the narrowness of the coefficient of variation for the hemolytic osmotic pressure presented in Figure 2 of Lew et al. (1995). With respect to the modeling of the regulation of the RBC volume it can be concluded that one of the model parameters should be membrane area. Recent evidence indicates that the process responsible for *V* – *A* correlation involves Piezo1 (Cahalan et al., 2015). Namely, in Piezo1 knockout mice, and in the case where Piezo1 action of opening Gárdos channels was overruled by the Ca^{2+} ionophore A23187, this correlation was lost (**Figure 4B**).

MODEL OF THE EFFECT OF RBC DISCOCYTE SHAPE ON RBC VOLUME AND ITS OUTLOOK

The fact that RBC dehydration in hereditary xerocytosis can be caused by malfunctioning of a mechanosensitive protein Piezo1 indicates that RBC volume may also depend on mechanical properties of RBC membrane. Piezo1 system appeared to represent a relatively independent module of the otherwise complex regulation of RBC volume, and could thus be considered as an ideal candidate for application of the modeling approach. In the model under consideration (Svetina et al., 2019) we chose, for its elements that are crucial for the action of Piezo1, the sensing of the membrane curvature through curvature dependent inclusion–membrane interaction (Svetina et al., 1990; Kralj-Iglič et al., 1996, 1999), and the assumption that the mechanical properties of an RBC membrane affect its volume through the dependence of Piezo1 Ca^{++} permeability on RBC discocyte shape. These ideas were supported by curved structure of the Piezo1 trimer, evidenced by its structural studies (Ge et al., 2015; Guo and MacKinnon, 2017; Saotome et al., 2018; Zhao et al., 2018) and, indirectly, also by the altered RBC membrane cation permeability when stressing the cells by a distorting device (Kuchel and Shishmarev, 2017) or by a flow through a capillary constriction (Cinar et al., 2015; Danielczok et al., 2017). Here we shall first outline which of the topics presented in the previous two sections formed the basis of this model. Then we shall evaluate its outcome, define its deficiencies and indicate some model implications to improve the understanding of RBC Piezo1 action by further experimental and theoretical studies.

The essential ingredients of the proposed mechanism of the effect of Piezo1 on RBC volume are schematically represented by the cause-effect links shown in **Figure 5**. These links represent either experimental evidence or the results of theory or modeling. The upper dashed link indicates that RBC discocyte shape, according to theories described in the subsection "Interpretation of RBC and Vesicle Shapes on the Basis of Membrane Bending," depends on RBC reduced volume. The lower dashed line link represents Eq.1. The link between RBC content of K^+ and RBC volume is in a broad sense the consequence of the fact that RBC volume is established through osmotic equilibrium with the surrounding solution and that thus depends on the level of its cytoplasm cations. As discussed in section "RBC Volume and Related Aspects of the Variability of RBC Population" the regulation of cell cation content operates on the basis of active and passive membrane cation permeabilities (Hoffmann et al., 2009). The model concentrates on the homeostasis of K^+. The preceding two links are thus based on the experiments of Cahalan et al. (2015) who have shown that Piezo1 channels act by the

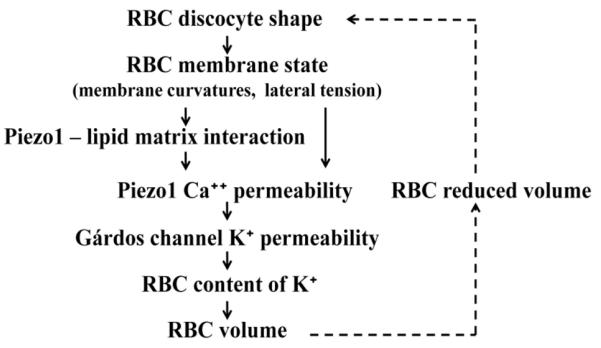

FIGURE 5 | Schematic presentation of processes involved in the effect of RBC discocyte shape on RBC volume. The meanings of the links are described in the text. Because the volume affects the shape (dashed links) the described system as a whole represents a closed regulatory loop. It is indicated that Piezo1 Ca^{++} permeability can be affected either by membrane curvature or membrane lateral tension.

way that, when they are temporarily transformed into their open conformation, allow the influx calcium ions which activate the potassium specific Gárdos channels. The enhanced leakage of potassium ions then causes a decrease of their cell content and consequent loss of water. The Piezo1–Gárdos channel system is thus considered as a complement to the mechanism of RBC volume regulation based on the balance between influx and efflux of cations K^+ and Na^+. In the model it is assumed that, due to active Ca^{++} efflux, the Gárdos channels are on the average open only part of the time and that it is therefore reasonable to express membrane permeability coefficient for K^+ (P_K) as the sum two contributions

$$P_K = P_{K,0} + f_G P_{K,G} \tag{7}$$

where $P_{K,G}$ is RBC K^+ permeability of its Gárdos channels, f_G the average fraction of them that are open, and $P_{K,0}$ the potassium permeability of its other K^+ channels. Due to osmotic equilibrium between its interior and exterior (see section "RBC Volume and Related Aspects of the Variability of RBC Population"), RBC volume is at larger values of f_G smaller. In the treated model we derived a relationship between f_G and the reduced volume v in which appeared as model parameters the ratio $P_{K,G}/P_{K,0}$, the relative amount of other RBC cytoplasm ingredients that cannot penetrate the membrane, and the reduced volume at $f_G = 0$. The crucial task of the model was to reveal a plausible mechanism for the effect of RBC shape on the fraction of time that Piezo1 channels are open. In the model it was proposed that there is another relationship between f_G and v based on the dependence of Piezo1 cation permeability on RBC shape. This relationship is represented in **Figure 5** by the links that relate RBC discocyte shape and Piezo1 Ca^{++} permeability. The theory described in sub-section "Interpretation of RBC and Vesicle Shapes on the Basis of Membrane Bending" makes it possible to determine reduced mean membrane curvature (h) at each point on the membrane and its dependence on the reduced volume v. In the model (Svetina et al., 2019) it was shown that its value in RBC poles can be well represented by a linear function

$$h_{pole} = h_{pole,r} + \beta_{pole}(v - v_r) \tag{8}$$

where $h_{pole,r}$ is the reduced mean curvature at an arbitrarily chosen reference reduced volume v_r. The value of the coefficient β_{pole} is 4.0. It was then taken into account that due to Piezo1 intrinsic curvature and its interaction with the membrane (Eq. 6), its molecules would tend to concentrate in the regions of RBC poles. On the basis of the assumption of that open Piezo1 conformation is less curved than its closed conformation it follows that, at the decrease of v, the probability that Piezo1 is closed increases. The parameters that defined thus obtained increasing function $f_G(v)$ are a combination of parameters that appear in Eqs. 6 and 8. Due to thus obtained relationships between f_G and v it is possible to express these two parameters in terms of other RBC structural parameters. On the basis of assuming the curvature dependent Piezo1–lipid matrix interaction it has been thus established that the system operates as a negative feedback regulatory loop between the average of the fraction of open Gárdos channels (f_G) and the RBC reduced volume (v).

The described model was meant primarily to serve as the proof of principle for Piezo1 based regulation of RBC volume. Therefore it involves many simplifications of the real system. For example, it was restricted to K^+ homeostasis and did not take into consideration possible concomitant changes of RBC Na^+ content; the fraction of open Piezo1 channels was calculated as if they would all be located at the RBC poles; it was assumed that there are only two relevant Piezo1 conformations, etc. However, some of the model predictions are general in that they do not depend on its specific features. The main outcome of the effect of the RBC discoid shape on its volume is that it implies the existence of a closed regulatory loop for RBC volume regulation. The Piezo1–Gárdos channel system can be considered as a complement to the mechanism for the regulation of cell volume that operates on the basis of active and passive membrane cation permeabilities (Hoffmann et al., 2009). Within the mechanism of RBC volume regulation based on the balance between influx and efflux of cations K^+ and Na^+, Piezo1 acts at the level of K^+ efflux. The membrane permeability coefficient for K^+ involves a contribution that depends on the RBC reduced volume v and thus also on the membrane area A. The consequence of the regulation of v is the strong V–A correlation. Such correlation has been observed by simultaneous measurements of V and A in the RBC population (Canham and Burton, 1968; Gifford et al., 2003) and is evidenced by the steepness of the osmotic fragility curve (**Figure 4B**). Confirmation of this prediction of the model lies in the fact that the V–A correlation is lost, either in the absence of Piezo1 or by the application of the Ca^{2+} ionophore A23187 which overrules its action (Cahalan et al., 2015). The regulation of the RBC reduced volume is physiologically important because RBC, during the process of its aging, constantly releases nanovesicles (Westerman and Porter, 2016).

In this type of vesiculation the loss of area is more significant than the loss of volume and, therefore, without this regulation the cells would lose their deformability because of the consequent increase of their reduced volume.

The model presented here points to the involvement of the RBC discoid shape in the fine regulation of its volume in a rather consistent manner. However, there are still many unanswered questions that require further experimentation. One such concern is whether the response of Piezo1 to change of RBC shape is due to change of membrane curvature or to the change of membrane lateral tension (**Figure 5**). For example, the theory of vesicle shapes predicts that the lateral tension is negative and that its absolute value at lowering the v increases (Svetina and Žekš, 1989). Changes of the lateral tension thus act in the appropriate direction but their effect was estimated to be small (Svetina et al., 2019). It could, however, be enhanced by the action of myosin motors (Smith et al., 2018). The dilemma about possible role of lateral tension could be resolved by experimental determination of the distribution of Piezo1 channels over the RBC membrane. Because mean principal membrane curvature is most negative in the RBC dimples, the analogously curved Piezo1 (Guo and MacKinnon, 2017) would preferentially reside in this region. With regard to the question as to whether the described mechanism of fine regulation of RBC volume also functions *in vivo* it should be realized that RBCs spend only about 50% of their time in veins, in which hydrodynamic conditions allow them to establish their discocyte shape. Namely, freely movable, membrane embedded proteins have diffusion coefficients that would cause them to equilibrate along the whole RBC surface in about 1 min. It would thus be important to determine whether the Piezo1 lateral diffusion coefficient is, for one reason or another, sufficiently smaller. It could be smaller because the RBC membrane is crowded (with more than 10^4 proteins per 1 μm^2) or because the Piezo1 molecule modifies the shape of the surrounding membrane to the size (Haselwandter and MacKinnon, 2018) that fits well into the area of the triangle of the structural unit of the hexagonal network of the spectrin skeleton. With regard to the Piezo1 oligomeric homo-trimer structure it can be noted that, in the case where its subunits can, independently, have two different conformation, it may attain at least four different structures, of which two have axial symmetry and two not. It still has to be established which of these structures corresponds to the Piezo1 open state. In the analyses of the variations within RBC population it has been assumed that there is no variation in membrane areal density of different RBC membrane proteins. In the context of the presented model it would be of particular interest to determine whether there are differences in the variability parameters of pumps and channels that are involved in the regulation of RBC volume.

There are also many aspects of the proposed model that require further theoretical modeling. For example, there is the question as to what is causing, in the A–V scatter plot, the remaining cell to cell variability. It could be ascribed to RBC variability with respect to its hemoglobin content (Svetina, 1982), but also to cell to cell variability of the ratio between the permeabilities of Gárdos channel and other potassium channels. In the model presented here it was taken that, for a given fixed membrane shape, the inclusions redistribute due to their interaction with the surrounding membrane. However, in general the effect is mutual: due to the curvature dependent interaction of Piezo1 molecules with the surrounding membrane, the RBC shape may also change (Božič et al., 2006). The consequent coupling between the RBC shape and the conformational state of Piezo1 molecules could cause oscillatory non-stationary behavior of the treated system. One has to be aware also of possible second order factors such as membrane lateral inhomogeneity (Hoffman, 2019). It still needs to be established as to the nature of the physical basis for the Piezo1–lipid matrix interaction. It could be based on the perturbed energy of the lipid bilayer (Haselwandter and MacKinnon, 2018) but may also involve specific interactions between a protein and its surrounding molecules, e.g., the curvature dependence of the number of hydrogen bonds that Piezo1 forms with surrounding lipids. Curvature dependent Piezo1–lipid matrix interaction may also involve energy terms due to Piezo1 intrinsic elasticity (Lin et al., 2019).

AUTHOR CONTRIBUTIONS

The author confirms being the sole contributor of this work and has approved it for publication.

FUNDING

The study was partly supported by the Slovenian Research Agency through grant P1-0055.

ACKNOWLEDGMENTS

The author thanks Prof. Roger H. Pain for critical reading of the manuscript.

REFERENCES

Armstrong, C. M. (2003). The Na/K pump, Cl ion, and osmotic stabilization of cells. *Proc. Natl. Acad. Sci. U.S.A.* 100, 6257–6262. doi: 10.1073/pnas.0931278100

Ataullakhanov, F. I., Korunova, N. O., Spiridonov, I. S., Pivovarov, I. O., Kalyagina, N. V., and Martinov, M. V. (2009). How erythrocyte volume is regulated, or what mathematical models can and cannot do for biology. *Biochem. Mosc. Suppl. Ser. A Membr. Cell Biol.* 3, 101–115. doi: 10.1134/s1990747809020019

Božič, B., Kralj-Iglič, V., and Svetina, S. (2006). Coupling between vesicle shape and lateral distribution of mobile membrane inclusions. *Phys. Rev. E* 73:041915.

Brumen, M., Glaser, R., and Svetina, S. (1979). Osmotic states of red blood cells. *Bioelectrochem. Bioenerget.* 6, 227–241. doi: 10.1016/0302-4598(79)87010-5

Brumen, M., Glaser, R., and Svetina, S. (1981). Study of the red blood cell osmotic behaviour in the "pump-leak" model. *Period. Biol.* 83, 151–153.

Cahalan, S. M., Lukacs, V., Ranade, S. S., Chien, S., Bandell, M., and Patapoutian, A. (2015). Piezo1 links mechanical forces to red blood cell volume. *eLife* 4:e07370. doi: 10.7554/eLife.07370

Canham, P. B. (1970). Minimum energy of bending as a possible explanation of biconcave shape of human red blood cell. *J. Theor. Biol.* 26, 61–81. doi: 10.1016/s0022-5193(70)80032-7

Canham, P. B., and Burton, A. C. (1968). Distribution of size and shape in populations of normal human red cells. *Circ. Res.* 22, 405–422. doi: 10.1161/01.res.22.3.405

Cinar, E., Zhou, S., DeCourcey, J., Wang, Y., Waugh, R. E., and Wan, J. (2015). Piezo1 regulates mechanotransductive release of ATP from human RBCs. *Proc. Natl. Acad. Sci. U.S.A.* 112, 11783–11788. doi: 10.1073/pnas.1507309112

Coste, B., Mathur, J., Schmidt, M., Earley, T. J., Ranade, S., Petrus, M. J., et al. (2010). Piezo1 and Piezo2 are essential components of distinct mechanically activated cation channels. *Science* 330, 55–60. doi: 10.1126/science.1193270

Danielczok, J. G., Terriac, E., Hertz, L., Petkova-Kirova, P., Lautenschläger, F., Laschke, M. W., et al. (2017). Red blood cell passage of small capillaries is associated with transient Ca2+-mediated adaptations. *Front. Physiol.* 8:979. doi: 10.3389/fphys.2017.00979

Deuling, H. J., and Helfrich, W. (1976). Red blood cell shapes as explained on the basis of curvature elasticity. *Biophys. J.* 71, 861–868. doi: 10.1016/s0006-3495(76)85736-0

Discher, D. E., Boal, D. H., and Boey, S. K. (1998). Simulations of the erythrocyte skeleton at large deformation. II. Micropipette aspiration. *Biophys. J.* 75, 1584–1597. doi: 10.1016/s0006-3495(98)74076-7

Discher, D. E., and Mohandas, N. (1996). Kinematics of red cell aspiration by fluorescence-imaged microdeformation. *Biophys. J.* 71, 1680–1694. doi: 10.1016/s0006-3495(96)79424-9

Discher, D. E., Mohandas, N., and Evans, E. A. (1994). Molecular maps of red cell deformation: hidden elasticity and in situ connectivity. *Science* 266, 1032–1035. doi: 10.1126/science.7973655

Evans, E. A. (1980). Minimum energy analysis of membrane deformation applied to pipet aspiration and surface adhesion of red blood cells. *Biophys. J.* 30, 265–284. doi: 10.1016/s0006-3495(80)85093-4

Evans, E. A., Waugh, R., and Melnik, L. (1976). Elastic area compressibility modulus of red cell membrane. *Biophys. J.* 16, 585–595. doi: 10.1016/s0006-3495(76)85713-x

Fedosov, D. A., Caswell, B., and Karniadakis, G. E. (2010). Systematic coarse-graining of spectrin-level red blood cell models. *Comput. Methods Appl. Mech. Eng.* 199, 1937–1948. doi: 10.1016/j.cma.2010.02.001

Freedman, J. C., and Hoffman, J. F. (1979). Ionic and osmotic equilibria of human red blood cells treated by nystatin. *J. Gen. Physiol.* 74, 157–185. doi: 10.1085/jgp.74.2.157

Ge, J., Li, W., Zhao, Q., Chen, M., Zhi, P., Li, R., et al. (2015). Architecture of the mammalian mechanosensitive Piezo1 channel. *Nature* 527, 64–69. doi: 10.1038/nature15247

Gifford, S. C., Frank, M. G., Derganc, J., Gabel, C., Austin, R. H., Yoshida, T., et al. (2003). Parallel microchannel-based measurements of individual erythrocyte areas and volumes. *Biophys. J.* 84, 623–633. doi: 10.1016/s0006-3495(03)74882-6

Goldstein, R. E. (2018). Are theoretical results 'results'? *eLife* 7:e40018.

Guo, Y. R., and MacKinnon, R. (2017). Structure-based membrane dome mechanism for Piezo mechanosensitivity. *eLife* 6:e33660. doi: 10.7554/eLife.33660

Haselwandter, C. A., and MacKinnon, R. (2018). Piezo's membrane footprint and its contribution to mechanosensitivity. *eLife* 7:e41968. doi: 10.7554/eLife.41968

Heinrich, V., Svetina, S., and Žekš, B. (1993). Nonaxisymmetric vesicle shapes in a generalized bilayer-couple model and the transition between oblate and prolate axisymmetric shapes. *Phys. Rev. E* 48, 3112–3123. doi: 10.1103/physreve.48.3112

Helfrich, W. (1973). Elastic properties of lipid bilayers: theory and possible experiments. *Z. Naturforsch.* 28c, 693–703. doi: 10.1515/znc-1973-11-1209

Hoffman, J. F. (2019). Reflections on the crooked timber of red blood cell physiology. *Blood Cells Mol. Dis.* 79:102354. doi: 10.1016/j.bcmd.2019.102354

Hoffmann, E. K., Lambert, I. H., and Pedersen, S. F. (2009). Physiology of cell volume regulation in vertebrates. *Physiol. Rev.* 89, 193–277. doi: 10.1152/physrev.00037.2007

Hwang, W. C., and Waugh, R. E. (1997). Energy of dissociation of lipid bilayer from the membrane skeleton of red blood cells. *Biophys. J.* 72, 2669–2678. doi: 10.1016/s0006-3495(97)78910-0

Kay, A. R., and Blaustein, M. P. (2019). Evolution of our understanding of cell volume regulation by the pump-leak mechanism. *J. Gen. Physiol.* 151, 407–416. doi: 10.1085/jgp.201812274

Kralj-Iglič, V., Heinrich, V., Svetina, S., and Žekš, B. (1999). Free energy of closed membrane with anisotropic inclusions. *Eur. Phys. J. B* 10, 5–8. doi: 10.1007/s100510050822

Kralj-Iglič, V., Svetina, S., and Žekš, B. (1996). Shapes of bilayer vesicles with membrane embedded molecules. *Eur. Biophys. J.* 24, 311–321. doi: 10.1007/bf00180372

Kuchel, P. W., and Shishmarev, D. (2017). Accelerating metabolism and transmembrane cation flux by distorting red blood cells. *Sci. Adv.* 3:eaao1016. doi: 10.1126/sciadv.aao1016

Lanotte, L., Mauer, J., Mendez, S., Fedosov, D. A., Fromental, J.-M., Claveria, V., et al. (2016). Red cells' dynamic morphologies govern blood shear thinning under microcirculatory flow conditions. *Proc. Natl. Acad. Sci. U.S.A.* 113, 13289–13294. doi: 10.1073/pnas.1608074113

Lew, V. L., and Bookchin, R. M. (1986). Volume, pH, and ion-content regulation in human red cells: analysis of transient behavior with an integrated model. *J. Membr. Biol.* 92, 57–74. doi: 10.1007/bf01869016

Lew, V. L., Raftos, J. E., Sorette, M., Bookchin, R. M., and Mohandas, N. (1995). Generation of normal human red cell volume, hemoglobin content, and membrane area distributions by "birth" or regulation? *Blood* 86, 334–341. doi: 10.1182/blood.v86.1.334.bloodjournal861334

Lin, Y. C., Guo, R., Miyagi, A., Levring, J., MacKinnon, R., and Scheuring, S. (2019). Force-induced conformational changes in PIEZO1. *Nature* 92, 57–74.

Lux, S. E. (2016). Anatomy of the red cell membrane skeleton: unanswered questions. *Blood* 127, 187–199. doi: 10.1182/blood-2014-12-512772

McMahon, H. T., and Gallop, J. L. (2005). Membrane curvature and mechanisms of dynamic cell membrane remodelling. *Nature* 438, 590–596. doi: 10.1038/nature04396

Miao, L., Seifert, U., Wortis, M., and Döbereiner, H.-G. (1994). Budding transitions of fluid-bilayer vesicles: the effect of area-difference elasticity. *Phys. Rev. E* 49, 5389–5407. doi: 10.1103/physreve.49.5389

Mohandas, N., and Chasis, J. A. (1993). Red blood cell deformability, membrane material properties and shape: regulation by transmembrane, skeletal and cytosolic proteins and lipids. *Semin. Hematol.* 30, 171–192.

Mohandas, N., and Evans, E. (1994). Mechanical properties of the red cell membrane in relation to molecular structure and genetic effects. *Ann. Rev. Biophys. Biomol. Struct.* 23, 787–818. doi: 10.1146/annurev.bb.23.060194.004035

Mohandas, N., and Gallagher, P. G. (2008). Red cell membrane: past, present, and future. *Blood* 112, 3939–3947. doi: 10.1182/blood-2008-07-161166

Mukhopadhyay, R., Lim, G. H. W., and Wortis, M. (2002). Echinocyte shapes: bending, stretching, and shear determine spicule shape and spacing. *Biophys. J.* 82, 1756–1772. doi: 10.1016/s0006-3495(02)75527-6

Murthy, S. E., Dubin, A. E., and Patapoutian, A. (2017). Piezos thrive under pressure: mechanically activated ion channels in health and disease. *Nat. Rev. Mol. Cell Biol.* 18, 771–783. doi: 10.1038/nrm.2017.92

Peng, Z., Asaro, R. J., and Zhu, Q. (2010). Multiscale simulation of erythrocyte membranes. *Phys. Rev. E* 81:031904.

Raphael, R. M., and Waugh, R. E. (1996). Accelerated interleaflet transport of phosphatidylcholine molecules in membranes under deformation. *Biophys. J.* 82, 1756–1772.

Saotome, K., Murthy, S. E., Kefauver, J. M., Whitwam, T., Patapoutian, A., and Ward, A. B. (2018). Structure of the mechanically activated ion channel Piezo1. *Nature* 554, 481–486. doi: 10.1038/nature25453

Seifert, U. (1997). Configurations of fluid membranes and vesicles. *Adv. Phys.* 46, 13–137. doi: 10.1080/00018739700101488

Seifert, U., Berndl, K., and Lipowsky, R. (1991). Shape transformations of vesicles - phase-diagram for spontaneous-curvature and bilayer-coupling models. *Phys. Rev. A* 44, 1182–1202. doi: 10.1103/physreva.44.1182

Sheetz, M. P., and Singer, S. J. (1974). Biological-membranes as bilayer couples - molecular mechanism of drug-erythrocyte interactions. *Proc. Natl. Acad. Sci. U.S.A.* 71, 4457–4461. doi: 10.1073/pnas.71.11.4457

Smith, A. S., Nowak, R. B., Zhou, S., Giannetto, M., Gokhin, D. S., Papoin, J., et al. (2018). Myosin IIA interacts with the spectrin-actin membrane skeleton to control red blood cell membrane curvature and deformability. *Proc. Natl. Acad. Sci. U.S.A.* 115, E4377–E4385.

Švelc, T., and Svetina, S. (2012). Stress-free state of the red blood cell membrane and the deformation of its skeleton. *Cell. Mol. Biol. Lett.* 17, 217–227. doi: 10.2478/s11658-012-0005-8

Svetina, S. (1982). Relations among variations in human red cell volume, density, membrane area, hemoglobin content and cation content. *J. Theor. Biol.* 95, 123–134. doi: 10.1016/0022-5193(82)90291-0

Svetina, S. (1998). Skeleton –bilayer interaction and the shape of red blood cells. *Cell. Mol. Biol. Lett.* 3, 449–463.

Svetina, S. (2015). Curvature–dependent protein–lipid bilayer interaction and cell mechanosensitivity. *Eur. Biophys. J.* 44, 513–519. doi: 10.1007/s00249-015-1046-5

Svetina, S. (2017). Investigating cell functioning by theoretical analysis of cell-to-cell variability. *Eur. Biophys. J.* 46, 739–748. doi: 10.1007/s00249-017-1258-y

Svetina, S., Brumen, M., Gros, M., Vrhovec, S., and Žnidarčič, T. (2003). "On the variation of parameters that characterize the state of a physiological system. Red blood cells as an example," in *Simulations in Biomedicine V*, eds Z. M. Arnež, C. A. Brebbia, F. Solina, and V. Stankovski (Southampton: WITT Press), 3–14.

Svetina, S., Iglič, A., Kralj-Iglič, V., and Žekš, B. (1996). Cytoskeleton and red cell shape. *Cell. Mol. Biol. Lett.* 1, 67–78.

Svetina, S., Kokot, G., Švelc Kebe, T., Žekš, B., and Waugh, R. E. (2016). A novel strain energy relationship for red blood cell membrane skeleton based on spectrin stiffness and its application to micropipette deformation. *Biomech. Model. Mechanobiol.* 15, 745–758. doi: 10.1007/s10237-015-0721-x

Svetina, S., Kralj-Iglič, V., and Žekš, B. (1990). "Cell shape and lateral distribution of mobile membrane constituents," in *Biophysics of Membrane Transport: Tenth School on Biophysics of Membrane Transport, Part II*, eds J. Kuczera and S. Przestalski (Wrocław: Agricultural University of Wrocław), 139–155.

Svetina, S., Kuzman, D., Waugh, R. E., Ziherl, P., and Žekš, B. (2004). The cooperative role of membrane skeleton and bilayer in the mechanical behaviour of red blood cells. *Bioelectrochemistry* 62, 107–113. doi: 10.1016/j.bioelechem.2003.08.002

Svetina, S., Ottova-Leitmannová, A., and Glaser, R. (1982). Membrane bending energy relation to bilayer couples concept of red blood cell shape transformations. *J. Theor. Biol.* 94, 13–23. doi: 10.1016/0022-5193(82)90327-7

Svetina, S., Švelc Kebe, T., and Božič, B. (2019). A model of Piezo1 based regulation of red blood cell volume. *Biophys. J.* 116, 151–164. doi: 10.1016/j.bpj.2018.11.3130

Svetina, S., and Žekš, B. (1983). Bilayer couple hypothesis of red-cell shape transformations and osmotic hemolysis. *Biomed. Biochim. Acta* 42, S86–S90.

Svetina, S., and Žekš, B. (1989). Membrane bending energy and shape determination of phospholipid vesicles and red blood cells. *Eur. Biophys. J.* 17, 101–111. doi: 10.1007/bf00257107

Svetina, S., and Žekš, B. (1990). The mechanical behavior of cell membranes as a possible physical origin of cell polarity. *J. Theor. Biol.* 146, 115–122. doi: 10.1016/s0022-5193(05)80047-5

Svetina, S., and Žekš, B. (1996). "Elastic properties of closed bilayer membranes and the shapes of giant phospholipid vesicles," in *Handbook of Nonmedical Applications of Liposomes*, Vol. I, eds D. D. Lasic and Y. Barenholz (Boca Raton, FL: CRC), 13–42.

Svetina, S., and Žekš, B. (2014). Nonlocal membrane bending: a reflection, the facts and its relevance. *Adv. Coll. Interface Sci.* 208, 189–196. doi: 10.1016/j.cis.2014.01.010

Svetina, S., Žekš, B., Waugh, R. E., and Raphael, R. M. (1998). Theoretical analysis of the effect of the transbilayer movement of phospholipid molecules on the dynamic behavior of a microtube pulled out of an aspirated vesicle. *Eur. Biophys. J.* 27, 197–209. doi: 10.1007/s002490050126

Tomishige, M., Sako, Y., and Kusumi, A. (1998). Regulation mechanism of the lateral diffusion of band 3 in erythrocyte membranes by the membrane skeleton. *J. Cell Biol.* 142, 989–1000. doi: 10.1083/jcb.142.4.989

Tosteson, D. C., and Hoffman, J. F. (1960). Regulation of cell volume by active cation transport in high and low potassium sheep red cells. *J. Gen. Physiol.* 44, 169–196.

Westerman, M., and Porter, J. B. (2016). Red blood cell-derived microparticles: an overview. *Blood Cells Mol. Dis.* 59, 134–139. doi: 10.1016/j.bcmd.2016.04.003

Zarychanski, R., Schulz, V. P., Brett, L. H., Maksimova, Y., Houston, D. S., Smith, J., et al. (2012). Mutations in the mechanotransduction protein PIEZO1 are associated with hereditary xerocytosis. *Blood* 120, 1908–1915. doi: 10.1182/blood-2012-04-422253

Zhao, Q., Zhou, H., Chi, S., Wang, Y., Wang, J., Geng, J., et al. (2018). Structure and mechanogating mechanism of the Piezo1 channel. *Nature* 554, 487–492. doi: 10.1038/nature25743

Zimmerberg, J., and Kozlov, M. M. (2006). How proteins produce cellular membrane curvature. *Nat. Rev. Mol. Cell Biol.* 7, 9–19.

Conflict of Interest: The author declares that the research was conducted in the absence of any commercial or financial relationships that could be construed as a potential conflict of interest.

frontiers in Physiology

REVIEW
published: 17 June 2020
doi: 10.3389/fphys.2020.00577

N-Methyl-D-Aspartate Receptors in Hematopoietic Cells: What Have We Learned?

Maggie L. Kalev-Zylinska[1,2], James I. Hearn[1], Asya Makhro[3,4] and Anna Bogdanova[3,4]*

[1]Blood and Cancer Biology Laboratory, Department of Molecular Medicine and Pathology, University of Auckland, Auckland, New Zealand, [2]Department of Pathology and Laboratory Medicine, LabPlus Haematology, Auckland City Hospital, Auckland, New Zealand, [3]Red Blood Cell Research Group, Institute of Veterinary Physiology, Vetsuisse Faculty, University of Zurich, Zürich, Switzerland, [4]Zurich Center for Integrative Human Physiology, University of Zurich, Zürich, Switzerland

The *N*-methyl-D-aspartate receptor (NMDAR) provides a pathway for glutamate-mediated inter-cellular communication, best known for its role in the brain but with multiple examples of functionality in non-neuronal cells. Data previously published by others and us provided *ex vivo* evidence that NMDARs regulate platelet and red blood cell (RBC) production. Here, we summarize what is known about these hematopoietic roles of the NMDAR. Types of NMDAR subunits expressed in megakaryocytes (platelet precursors) and erythroid cells are more commonly found in the developing rather than adult brain, suggesting trophic functions. Nevertheless, similar to their neuronal counterparts, hematopoietic NMDARs function as ion channels, and are permeable to calcium ions (Ca^{2+}). Inhibitors that block open NMDAR (memantine and MK-801) interfere with megakaryocytic maturation and proplatelet formation in primary culture. The effect on proplatelet formation appears to involve Ca^{2+} influx-dependent regulation of the cytoskeletal remodeling. In contrast to normal megakaryocytes, NMDAR effects in leukemic Meg-01 cells are diverted away from differentiation to increase proliferation. NMDAR hypofunction triggers differentiation of Meg-01 cells with the bias toward erythropoiesis. The underlying mechanism involves changes in the intracellular Ca^{2+} homeostasis, cell stress pathways, and hematopoietic transcription factors that upon NMDAR inhibition shift from the predominance of megakaryocytic toward erythroid regulators. This ability of NMDAR to balance both megakaryocytic and erythroid cell fates suggests receptor involvement at the level of a bipotential megakaryocyte-erythroid progenitor. In human erythroid precursors and circulating RBCs, NMDAR regulates intracellular Ca^{2+} homeostasis. NMDAR activity supports survival of early proerythroblasts, and in mature RBCs NMDARs impact cellular hydration state, hemoglobin oxygen affinity, and nitric oxide synthase activity. Overexcitation of NMDAR in mature RBCs leads to Ca^{2+} overload, K^+ loss, RBC dehydration, and oxidative stress, which may contribute to the pathogenesis of sickle cell disease. In summary, there is growing evidence that glutamate-NMDAR signaling regulates megakaryocytic and erythroid cells at different stages of maturation, with some intriguing differences emerging in NMDAR expression and function between normal and diseased cells. NMDAR signaling may provide new therapeutic opportunities in hematological disease, but *in vivo* applicability needs to be confirmed.

Keywords: glutamate, intracellular calcium signaling, megakaryocyte, erythropoiesis, red cells, platelets

OPEN ACCESS

Edited by:
Alan N. Schechter, National Institutes of Health (NIH), United States

Reviewed by:
Kate Hsu, Mackay Memorial Hospital, Taiwan
John Strouboulis, King's College London, United Kingdom

****Correspondence:***
Maggie L. Kalev-Zylinska
m.kalev@auckland.ac.nz

Dr. Heimo Mairbäurl, Heidelberg University Hospital, also contributed to the review process for this manuscript.

Specialty section:
This article was submitted to Red Blood Cell Physiology, a section of the journal Frontiers in Physiology

Received: *29 October 2019*
Accepted: *08 May 2020*
Published: *17 June 2020*

Citation:
Kalev-Zylinska ML, Hearn JI, Makhro A and Bogdanova A (2020) N-Methyl-D-Aspartate Receptors in Hematopoietic Cells: What Have We Learned? Front. Physiol. 11:577. doi: 10.3389/fphys.2020.00577

INTRODUCTION

This review summarizes what has been learned about the roles of *N*-methyl-D-aspartate receptor (NMDAR) in megakaryocytic and erythroid cells. NMDARs are best known for their functions as glutamate-gated cation channels in the central nervous system (Traynelis et al., 2010). It appears that the NMDAR ion channel functionality is maintained in blood progenitors but NMDAR channel properties and its downstream pathways await further characterization in these cells. This paper starts with a brief overview of glutamate signaling in the brain. On this background, we highlight distinctive features of NMDAR in hematopoietic cells. Other glutamate receptors and mature blood cells are not discussed in detail but the appropriate background is provided to place this emerging field of research in a meaningful context. We describe NMDAR effects on hematopoietic differentiation, including some of our recent observations that suggest a novel role for the receptor in balancing megakaryocytic and erythroid cell fates (Hearn et al., 2020).

CLASSICAL GLUTAMATE-NMDAR AXIS IN THE BRAIN

Glutamate is synthesized from glutamine as a part of normal cellular metabolism in all cells (Yelamanchi et al., 2016). In neurons, vesicular glutamate transporters (VGLUT) pump glutamate into pre-synaptic vesicles (Daikhin and Yudkoff, 2000; Zhou and Danbolt, 2014). Upon membrane depolarization, vesicles fuse with the pre-synaptic plasma membrane and glutamate is released into the synaptic cleft. This process engages soluble *N*-ethyl-maleimide-sensitive factor attachment protein receptor (SNARE) proteins that are activated by Ca^{2+} entry through voltage-gated Ca^{2+} channels. Following release, glutamate concentrations in the synaptic cleft increase markedly, from 2–5 μM to approximately 1.1 mM. While in the synaptic cleft, glutamate activates ionotropic and metabotropic receptors located on the post-synaptic plasma membrane (Reiner and Levitz, 2018). Ionotropic receptors function as ion channels (for Na^+, K^+, and Ca^{2+}), and metabotropic receptors activate G-proteins that modulate ion channels directly and indirectly. The main purpose of the ionic flux is to generate and propagate action potentials characteristic of excitable tissues. The synaptic glutamate signal is terminated by the excitatory amino acid transporters (EAAT) present on astrocytes that remove glutamate from the synaptic cleft (Featherstone, 2010).

Abbreviations: ADP, adenosine diphosphate; AMPA, α-amino-3-hydroxy-5-methyl-4-isoxazolepropionic acid; AP5, D-2-amino-5-phosphonopentanoate; CaMK, Ca^{2+}/calmodulin-dependent kinase; CREB, cAMP response element binding protein; EAAT, excitatory amino acid transporters; EC_{50}, the concentration of an agonist that gives half-maximal response; EPO, erythropoietin; ER, endoplasmic reticulum; ErbB4, epidermal growth factor receptor Erb-B2 receptor tyrosine kinase 4; ERK, extracellular signal-regulated kinase; IC_{50}, the concentration of an inhibitor where the response (or binding) is reduced by half; MAPK, mitogen-activated protein kinase; MEP, megakaryocyte-erythroid progenitor; MK, megakaryocyte; NMDAR, *N*-methyl-D-aspartate receptor; PI3-K, phosphoinositide 3-kinase; PMA, phorbol 12-myristate 13-acetate; PSD, post-synaptic density; RBC, red blood cell; SNARE, soluble *N*-ethyl maleimide-sensitive factor attachment protein receptor; TPO, thrombopoietin; VGLUT, vesicular glutamate transporter.

The family of ionotropic glutamate receptors includes NMDA, α-amino-3-hydroxy-5-methyl-4-isoxazolepropionic acid (AMPA), and kainate receptors, each named after a distinct, synthetic agonist that activates them (Traynelis et al., 2010). AMPA and kainate receptors respond to glutamate first. They mediate intracellular influx of mostly Na^+, which leads to membrane depolarization and if large enough, triggers action potential. Membrane depolarization releases a Mg^{2+} ion blocking the pore of NMDAR, enabling receptor function. This order of events highlights that neuronal NMDAR can activate only when glutamate binding and membrane depolarization coincide (which is named "coincidence detection"). NMDAR-mediated Ca^{2+} influx contributes little to membrane depolarization but modifies synaptic strength through molecular events related to the Ca^{2+} role as "second messenger" (Traynelis et al., 2010; Hansen et al., 2018).

Typical NMDARs are built as tetramers that combine two obligate GluN1 subunits with another two GluN2 (A–D) or GluN3 (A or B) subunits, in various combinations. It is believed that GluN1 subunit is an essential component of all NMDARs, and variable GluN2 and GluN3 subunits are modulatory. NMDAR activation requires binding of L-glutamate on each of the GluN2 subunits, as well as glycine (co-agonist) on the GluN1 and GluN3 subunits. The alternative NMDAR ligands include D- and L- aspartate, homocysteine, homocysteic acid, and D-serine. NMDAR subunit composition varies substantially in different areas of the brain, and changes during development (Monyer et al., 1994; Wenzel et al., 1997). NMDAR subunits define the current amplitude and inactivation time, as well as cation selectivity and the regulation patterns, such as agonist affinity, mechano-sensitivity, Mg^{2+}-sensitivity, and responsiveness to polyamines. GluN2A and GluN2B subunits contribute high channel conductance and relatively fast de-activation kinetics compared to GluN2C- and GluN2D- containing NMDAR (Traynelis et al., 2010). In addition, NMDARs containing GluN2C, GluN2D, and GluN3 subunits display low affinity for Mg^{2+} blocking the pore, making activation of such receptors independent of membrane depolarization (Monyer et al., 1994; Chatterton et al., 2002; Wrighton et al., 2008).

NMDAR sensitivity (EC_{50}) to agonists is high, ranging from 0.4 to 1.7 μM for glutamate (in GluN1–GluN2D and GluN1–GluN2A receptors, respectively), and 0.1 to 2.1 μM for glycine (in GluN1–GluN2D and GluN1–GluN2A receptors, respectively) (Yamakura and Shimoji, 1999). These concentrations lie within the range that is normal in an inactive synaptic cleft. However, all types of NMDAR are extremely sensitive to the inhibition by protons (IC_{50} around 7.4 μM for most of the subunits) (Yamakura and Shimoji, 1999; Low et al., 2003; Cavara et al., 2009), and Zn^{2+} [IC_{50} of 10 nM, 1 μM, and 10 μM for the NMDAR containing GluN2A, GluN2B, and GluN2D, respectively (Gielen et al., 2009)].

NMDAR-mediated Ca^{2+} entry activates a number of intracellular signaling pathways, including Ca^{2+}/calmodulin-dependent kinase (CaMK), mitogen-activated protein kinase (MAPK) [including extracellular signal-regulated kinase (ERK), Jun kinase, and p38 MAPK], and phosphoinositide 3-kinase (PI3K) (Hardingham, 2006). NMDARs regulate activity-dependent gene expression

through cAMP response element binding protein (CREB) transcription factor (Hardingham et al., 2001). Other mediators downstream of NMDAR include Ras, Fyn, striatal-enriched protein tyrosine phosphatase, and nitric oxide synthase. Highly coordinated (albeit incompletely elucidated) NMDAR signaling plays critical roles in embryonic brain development and later, in neuronal plasticity, which allows the brain to respond to new experiences and changing environment (Traynelis et al., 2010).

Unexpected Discoveries Outside of the Brain

During the past 10–20 years, NMDARs have been reported in multiple non-neuronal cell types, including hematopoietic (Bozic and Valdivielso, 2015; Hogan-Cann and Anderson, 2016), which raised a principal question of why non-excitable cells need these receptors. We admit this area of research is not very clear, sometimes even controversial, mainly due to the very low abundance of NMDAR in non-neuronal cells. Nevertheless, some progress has been achieved in the characterization of the subunit composition and currents mediated by non-neuronal NMDAR, in particular in red blood cells (RBC) (Makhro et al., 2010), platelets (Kalev-Zylinska et al., 2014), lymphocytes (Fenninger and Jefferies, 2019), and hematopoietic precursors, erythroblasts (Makhro et al., 2013; Hanggi et al., 2014, 2015) and megakaryocytes (Genever et al., 1999; Kamal et al., 2015). Information on the potential physiological role of these receptors is accumulating as well, including in erythroid cells (Makhro et al., 2013, 2016), and megakaryocytes (Hitchcock et al., 2003; Green et al., 2017; Kamal et al., 2018; Hearn et al., 2020). The subsequent sections will focus on the subunit composition, properties and the roles of NMDAR in megakaryocytic and erythroid precursors, and their mature progeny, platelets and RBCs.

PLATELET RESPONSIVENESS TO GLUTAMATE

Peripheral blood platelets store and respond to a number of regulatory molecules best known for their roles in neurotransmission, including serotonin, epinephrine, dopamine, histamine, γ-aminobutyric acid, and glutamate (Todrick et al., 1960; Ponomarev, 2018; Canobbio, 2019). In psychiatric patients, there is evidence of a crosstalk between abnormal NMDAR function in the brain and platelet responsiveness to glutamate (Berk et al., 1999). Platelets bind glutamate with similar kinetics to neurons (Almazov et al., 1988), store it in dense granules, and express AMPA, kainate, and NMDA receptors (Franconi et al., 1996, 1998; Morrell et al., 2008; Sun et al., 2009; Kalev-Zylinska et al., 2014; Green et al., 2017). Although there are variations between studies, all main types of ionotropic glutamate receptors have now been shown to be functional in platelets. Morrell et al. demonstrated that AMPA and kainate (but not NMDA) receptors amplify platelet activation by contributing Na^+ influx to membrane depolarization, but not Ca^{2+} influx (Morrell et al., 2008; Sun et al., 2009). Franconi et al. provided the first evidence of NMDAR functionality in platelets, demonstrating that NMDARs induce Ca^{2+} influx into platelets but inhibit platelet function in the presence of adenosine diphosphate (ADP) and arachidonic acid (Franconi et al., 1996, 1998). Our own work demonstrated that NMDAR inhibitors (memantine, MK-801, and anti-GluN1 antibodies) interfere with platelet activation, aggregation and thrombus formation *ex vivo* (Kalev-Zylinska et al., 2014; Green et al., 2017). It is likely that methodological differences contributed to variable NMDAR effects between studies.

Intriguingly, in schizophrenia and bipolar disorders that are driven by deregulated NMDAR signaling, platelet Ca^{2+} levels are elevated, including in response to glutamate (Berk et al., 2000; Ruljancic et al., 2013; Harrison et al., 2019). Schizophrenia is characterized by NMDAR hypofunction in the limbic system (Coyle, 2012; Nakazawa et al., 2017), compensated by high glutamate levels and NMDAR hypersensitivity in other areas of the brain (Merritt et al., 2016). The fact that platelets from patients with schizophrenia also show glutamate hypersensitivity further argues that NMDAR functioning in platelets is similar to that in neurons (Berk et al., 2000).

Because platelets have limited protein synthesis, one would expect a similar range of glutamate receptors to be present in megakaryocytes. However, most data thus far indicate regulation of megakaryocytic differentiation by NMDAR, with little or no data on AMPA and kainate receptors (Genever et al., 1999; Hitchcock et al., 2003; Kamal et al., 2018). Nevertheless, electrophysiological recordings from freshly isolated mouse megakaryocytes support expression of functional AMPA receptors in megakaryocytes, most likely GluR2-containing and Ca^{2+}-impermeable (Morrell et al., 2008).

GLUTAMATE AND NMDAR IN MEGAKARYOCYTIC CELLS

Evidence for NMDAR Functionality in Megakaryocytic Cells

The first evidence that NMDARs operate as ion channels in megakaryocytes was obtained by demonstrating that [^{3}H]MK-801 binds to native mouse megakaryocytes *in vivo*. Mice were injected with [^{3}H]MK-801 intracardially, followed by bone marrow examination 15 min later (Genever et al., 1999). Because MK-801 is a non-competitive, use-dependent NMDAR inhibitor that can only bind within an open NMDAR pore (Traynelis et al., 2010), its labeling of megakaryocytes was consistent with the NMDAR function as an ion channel in megakaryocytic cells. Later, we showed that glutamate, NMDA, and glycine induce Ca^{2+} fluxes in Meg-01 cells, and NMDAR antagonists (MK-801, memantine, and AP5 [D-2-amino-5-phosphonopentanoate]) counteract this effect, indicating that NMDARs operate as Ca^{2+} channels in these cells (Kamal et al., 2015, 2018).

Table 1 provides a summary of the NMDAR subunit expression in megakaryocytic and erythroid cells, reported at either protein or transcript level. Unfortunately, testing for GluN proteins in hematopoietic cells has been difficult due to (a) very low abundance, (b) various protein isoforms and post-translational

modifications, and (c) the lack of antibodies optimized for use in non-neuronal cells. Human megakaryocytes were first shown to express GluN1 using immunocytochemistry and Western blotting, the latter indicated that GluN1 was non-glycosylated, which may affect NMDAR distribution in the plasma membrane (Genever et al., 1999). Our group demonstrated expression of GluN1, GluN2A, and GluN2D in Meg-01, K-562, and Set-2 cells using flow cytometry and a modified Western blotting procedure that employed membrane enrichment and high-sensitivity peroxidase substrates (Kamal et al., 2015).

The composition of NMDAR in megakaryocytes differs from that in neurons. In the brain, NMDARs are built mostly from GluN1, GluN2A, and/or GluN2B subunits, but human, native and culture-derived megakaryocytes express predominantly GluN2D, with some GluN2A and GluN1 (**Table 1**; Genever et al., 1999; Hitchcock et al., 2003; Kamal et al., 2015, 2018). The dominant expression of GluN2D in normal megakaryocytes will affect NMDAR functioning, however no electrophysiological recordings are available from these cells to document the effect. In other systems, GluN2D-containing NMDAR displays the following differences compared with GluN2A and GluN2B containing receptors: approximately 5-fold higher sensitivity to glutamate, 10-fold higher sensitivity to glycine, 100-fold longer deactivation time, lower conductance, lower Ca^{2+} permeability and weaker Mg^{2+} block (Paoletti et al., 2013; Wyllie et al., 2013; Hansen et al., 2018). The weak Mg^{2+} block suggests that NMDAR in megakaryocytes may not require membrane depolarization to become active; meaning the principle of "coincidence detection" may not apply. The unique functionality of the GluN2D subunit is underscored by its dominant expression in the embryonic and postnatal brain; however, the mechanism through which GluN2D subunits provide trophic effects remains incompletely understood (Watanabe et al., 1992; Akazawa et al., 1994).

For those of us working with mouse models, it is relevant to note that there are differences in the NMDAR expression patterns between human and mouse cells. In contrast to human megakaryocytes (that express only GluN1, GluN2A, and GluN2D), mouse megakaryocytes also express GluN2C and GluN3B (**Table 1**; Kamal et al., 2018). Small numbers of other, yet un-identified mononuclear cells in the mouse bone marrow also express NMDAR, but there is no documented expression in mouse erythroid precursors or mature RBCs (Genever et al., 1999), which differs from human cells (**Table 1**; Makhro et al., 2013; Hanggi et al., 2014, 2015).

In contrast to normal megakaryocytes, patient-derived leukemic megakaryoblasts and megakaryocyte leukemia cell lines (Meg-01, K-562, and Set-2) carry all possible NMDAR subunits, including GluN2B, GluN3A, and GluN3B (**Table 1**; Kamal et al., 2015). Meg-01 and K-562 cell lines are derived from patients with chronic myeloid leukemia in megakaryocytic and myeloid blast crisis respectively, and carry oncogenic *BCR-ABL1* gene fusion (Lozzio and Lozzio, 1975; Ogura et al., 1985). Both Meg-01 and K-562 cell lines express thrombopoietin (TPO) and erythropoietin (EPO) receptors and can be induced to differentiate into megakaryocytic (Ogura et al., 1988, Herrera et al., 1998) and erythroid cells (Andersson et al., 1979; Morle et al., 1992), thus providing experimental models of bipotential megakaryocyte-erythroid progenitors. Set-2 cell line is derived from a leukemic transformation of essential thrombocythemia and carries *JAK2* V617F mutation, an established driver in myeloproliferative neoplasms. Set-2 differentiates spontaneously into megakaryocyte-like cells (Uozumi et al., 2000). Biological characteristics of leukemic cell lines are obviously very different from normal progenitors, which we should keep in mind while interpreting cell line data.

We found that Meg-01 cells are better suited for studies of NMDAR function than K-562 and Set-2 cells, mostly because of their higher levels of NMDAR expression. Upon differentiation with phorbol-12-myristate-13-acetate (PMA), Meg-01 cells up-regulate NMDAR expression further,

TABLE 1 | Expression of NMDAR subunits documented in megakaryocytic and erythroid cells.

	Megakaryocytic cells[1]						**Erythroid cells[2]**			**Mature brain cortex[3]**
	Human				Mouse		Human			Mouse and human
	Normal		Leukemic		Normal		Normal – cultured			Normal
GluN subunit	Whole bone marrow	Isolated mature MKs	Cell lines	Patient-derived	Isolated mature MKs	Early cultured MKs	Proerythroblasts	Orthochromatic	Retics /RBC	Neurons
1	+; P	–	+/++; P	+	+	++; P	+	+	+; P	+++; P
2A	+	+	++; P	+	+	++	++; P	+	+; P	++; P
2B	–	–	–/+	+	–	–	–	–	–	++; P
2C	–	–	–/+	++	+	–	+; P	+++; P	++; P	+; P
2D	+	+	+++; P	+++	++	–	++; P	++; P	++; P	+; P
3A	–	–	+	++	–	–	+; P	+; P	+; P	–
3B	–	–	+++	++	++	–	+; P	++; P	++; P	–

[1]Data generated mostly by RT-PCR, conventional and real-time (Genever et al., 1999; Hitchcock et al., 2003; Kamal et al., 2015, 2018).

[2]Data generated by TaqMan quantitative RT-PCR, flow cytometry and immunoblotting (Makhro et al., 2013; Hanggi et al., 2014, 2015).

[3]Shown by multiple techniques. The "+" symbol means expression was demonstrated; the number of "+" signs reflects the level of expression; "–" means expression was not detected. The letter "P" indicates protein expression was documented using flow cytometry or immunostaining in addition to transcript data, on which the semi-quantitative assessment was based. MK, megakaryocyte; Retics, reticulocytes; RBC, red blood cells.

providing a model in which to examine NMDAR involvement in megakaryocytic differentiation (Genever et al., 1999; Kamal et al., 2018).

The role of GluN3 subunits (highly expressed in leukemic cells; **Table 1**) is poorly understood, including in the brain, but its functions have already been described as exquisite, peculiar, unconventional, and transformative (Kehoe et al., 2013; Perez-Otano et al., 2016; Grand et al., 2018). This is because GluN3 subunits do not require glutamate for activation (Nilsson et al., 2007). In GluN1-GluN3 receptors, glycine acts both as the sole agonist binding on GluN3, and provides feedback inhibition through GluN1. In GluN1-GluN2-GluN3 receptors, the presence of GluN3 reduces Mg^{2+} block and Ca^{2+} entry (Matsuda et al., 2002; Cavara and Hollmann, 2008).

Overall, the presence of nonconventional GluN subunits (in particular GluN2D and GluN3) in megakaryocytic cells, normal and leukemic, suggests that NMDAR generates weaker but more sustained Ca^{2+} influx, and may allow stronger modulation by glycine than glutamate, in particular in leukemic cells. There is also a possibility of regulation by metabolic factors through GluN1. This is because megakaryocytic cells express h1-1 to h1-4 GluN1 isoforms, all of type "a" (Kamal et al., 2015). GluN1a isoforms lack the N1-cassette from the N-terminal domain (encoded by exon 5) that if present, reduces inhibition by protons and zinc, and potentiation by polyamines (Traynelis et al., 1995; Yi et al., 2018). Because the bone marrow environment is intrinsically hypoxic (Spencer et al., 2014), this form of metabolic regulation warrants testing in blood progenitors.

Evidence for Regulation of Glutamate Levels

Mouse and human megakaryocytes express a range of molecules for glutamate re-uptake, storage, and release, including VGLUT1, VGLUT2, SNARE, and the high-affinity glutamate re-uptake system, EAAT1, shown at both transcript and protein levels (Genever et al., 1999; Thompson et al., 2010). Fluorimetric measurements of glutamate concentrations in culture media suggest that human and mouse megakaryocytes, and Meg-01 cells release glutamate in a constitutive manner (Thompson et al., 2010); congruently, similar has been shown for ADP packaged together with glutamate in dense granules (Balduini et al., 2012). We do not know why megakaryocytes need glutamate sensitivity but it is a critical question to seek answers to in the future. A possible auto-regulatory loop (autocrine or paracrine) is suggested by the observation that Meg-01 cells release more glutamate upon differentiation with PMA (Thompson et al., 2010). Glutamate regulation may be independent of TPO, as NMDAR expression is maintained in megakaryocytes from c-Mpl-(TPO receptor) knockout mice (Hitchcock et al., 2003).

Unfortunately, there is no information on glutamate concentrations in the interstitial fluid of the bone marrow. In peripheral blood plasma, physiological glutamate levels are usually maintained between 20 and 100 μM (Kiessling et al., 2000), but vary widely depending on the diet (Stegink et al., 1983) and exercise (Makhro et al., 2016). In the interstitial fluids, concentrations of glutamate have been observed to be as low as 0.5 μM in the masseter muscle of myofascial temporomandibular joint (Castrillon et al., 2010), to as high as blood plasma levels in the vastus lateralis muscle of the lower limb (Gerdle et al., 2016). There is no experimental data on how plasma/interstitial glutamate levels impact endogenous NMDAR in blood/progenitor cells. Paracrine NMDAR activation in neuron-like fashion appears more likely in tissues with low, steady state glutamate concentrations. On the other hand, conditional NMDAR activation *via* local pH changes would be more likely in tissues with higher, plasma-like glutamate concentrations. Different types of NMDAR subunits will also affect cellular sensitivity to glutamate, and modulate the receptor response (as described in section Evidence for NMDAR Functionality in Megakaryocytic Cells).

NMDAR Effects on Megakaryocytic Differentiation

NMDAR channel blockers (memantine and MK-801) induce two types of apparently opposing effects in cultured megakaryocytic cells: inhibition of differentiation in normal megakaryocytes, but induction of differentiation in megakaryocytic leukemia cell lines (**Figure 1Ai–ii**).

When human megakaryocytes are grown from CD34-positive umbilical cord stem cells, the addition of MK-801 inhibits acquisition of megakaryocytic markers (CD61, CD41a, and CD42a), nuclear ploidy and proplatelet formation; however, progenitor proliferation is unaffected (Hitchcock et al., 2003). Similar effects are seen in cultures of mouse hematopoietic progenitors, and in the native bone marrow milieu of mouse bone marrow explants. MK-801 inhibits actin reorganization in mature mouse megakaryocytes, suggesting that NMDAR-mediated Ca^{2+} influx is required for the cytoskeletal remodeling that underlies proplatelet formation (Kamal et al., 2018). This process may be similar to dendritic spine formation arising in response to neuronal NMDAR firing (Furuyashiki et al., 2002). NMDAR links with cytoskeletal elements through post-synaptic density (PSD) proteins such as PSD-95 and Yotiao; both of which are expressed in megakaryocytes, suggesting similar interactions may be possible in hematopoietic cells (Hitchcock et al., 2003).

In contrast to normal megakaryocytes that utilize NMDAR function to assist differentiation, leukemic cell lines (Meg-01, K-562, and Set-2) appear to divert NMDAR activity to increase proliferation (**Figure 1Ai–ii**). In the presence of NMDAR blockers (memantine and MK-801) Meg-01 cells undergo atypical differentiation and accumulate prominent cytoplasmic vacuoles (**Figure 1Aiii**; Kamal et al., 2015, 2018). The opposing NMDAR effects on cellular phenotype between normal and leukemic cells suggest divergence of NMDAR pathways during leukemogenesis to increase cell proliferation.

To get more insights into the mechanism of this divergence, we recently created a model of NMDAR hypofunction in Meg-01 cells using CRISPR-Cas9 mediated knockout of the *GRIN1* gene that encodes the obligate, GluN1 subunit of the NMDAR (Hearn et al., 2020). We found that *GRIN1* deletion caused marked changes in the intracellular Ca^{2+} homeostasis, including higher cytosolic Ca^{2+} levels at baseline but lower

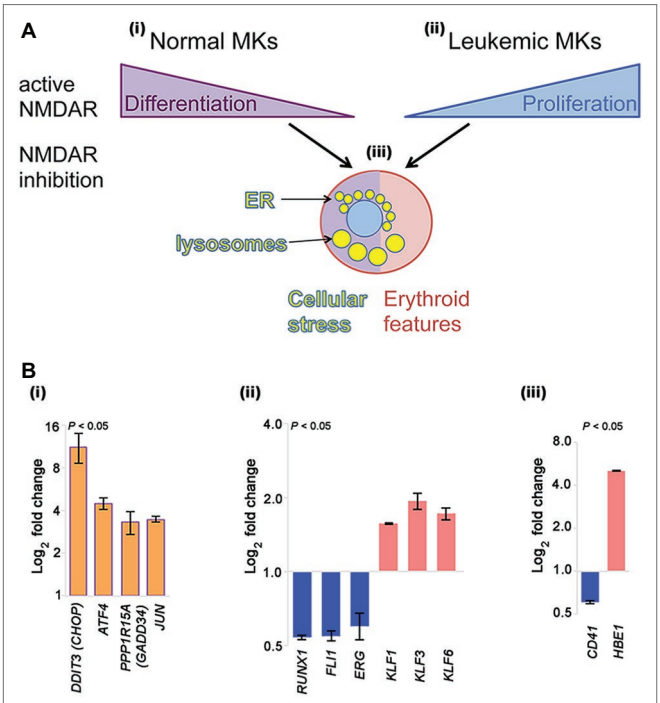

FIGURE 1 | NMDAR effects in normal megakaryocytes and leukemic Meg-01 cells. **(A)** Schematic indicating that in normal megakaryocytes NMDAR activity supports differentiation, in particular proplatelet formation **(i)**. In contrast, in leukemic cell lines NMDARs increase cell proliferation **(ii)**. In both normal and leukemic cells, NMDAR inhibition induces cellular stress response associated with endoplasmic reticulum (ER) dilatation and accumulation of lysosomes **(iii)**. Red shade in a cell reflects features of erythroid differentiation. **(B)** Experimental data showing that CRISPR-Cas9-mediated deletion of *GRIN1* in Meg-01 cells increased expression of ER stress markers (*DDIT3/CHOP*, *ATF4*, *PPP1R15A/GADD34*, and *JUN*; **Bi**; orange bars), associated with decreased expression of megakaryocytic transcription factors (*RUNX1*, *FLI1*, *ERG*; **Bii**) and megakaryocytic maturation marker, CD41 **(Biii)** (blue bars). Instead, expression of erythroid transcription factors (*KLF1*, *KLF3*, *KLF6*; **Bii**) and embryonic hemoglobin (*HBE1*; **Biii**) was increased (red bars). Transcript levels were determined by real-time RT-PCR **(Bi)** and Clariom S microarrays **(Bii–iii)**, as described (Hearn et al., 2020). Statistical significance is shown ($p < 0.05$ for all markers versus unmodified Meg-01 cells set at 1.0, tested by one-way ANOVA with Dunnett post-hoc. MK, megakaryocyte.

ER Ca^{2+} release after activation. Deregulated Ca^{2+} handling led to endoplasmic reticulum (ER) stress and induced autophagy. Prominent cytoplasmic vacuoles accumulated in Meg-01-*GRIN1*$^{-/-}$ cells and were found to represent dilated ER and lysosomal organelles (**Figure 1Aiii**). Microarray analysis revealed that Meg-01-*GRIN1*$^{-/-}$ cells had deregulated expression of transcripts involved in Ca^{2+} metabolism, together with a shift in the pattern of hematopoietic transcription factors toward erythropoiesis (**Figure 1Bi–ii**). In keeping with the pro-erythroid pattern of transcription factors, Meg-01-*GRIN1*$^{-/-}$ cells displayed features of erythroid differentiation (**Figure 1Biii**). Our data provide the first evidence that NMDARs comprise an integral component of the Ca^{2+} toolkit in megakaryocytic cells, and argue that intracellular Ca^{2+} homeostasis may be more important than currently recognized for balancing megakaryocytic with erythroid differentiation at the level of a common progenitor (Hearn et al., 2020).

In support of our findings, Kinney et al. provided computational evidence of NMDAR involvement in erythropoiesis (Kinney et al., 2019). The authors analyzed 164 publicly available erythroid microarray datasets using an enhanced CellNet bioinformatics algorithm to delineate key transitional states of erythroid differentiation at high resolution. This approach identified a role for signaling through epidermal growth factor receptor Erb-B2 receptor tyrosine kinase 4 (ErbB4) in erythroid differentiation, which was further validated experimentally in zebrafish, mouse and human models. The authors linked ErbB4 with NMDAR signaling by finding increased levels of *GRIN3B* transcripts, coding for GluN3B, in the reticulocyte gene cluster. A similar link between ErbB4 and NMDAR is well-documented in neurons, where ErbB4 and its neuregulin ligands stabilize synaptic NMDAR (Li et al., 2007). In fact, altered neuregulin 1–ErbB4 signaling is a well-established mechanism of NMDAR hypofunction in schizophrenia (Hahn et al., 2006). Encouragingly, we also found that in Meg-01-*GRIN1*$^{-/-}$ cells, transcripts for neuregulin 1 and ErbB receptor feedback inhibitor 1 were up-regulated (1.98- and 2.05-fold, respectively), implying the ErbB4-NMDAR link is maintained during megakaryocytic-erythroid differentiation (Hearn et al., 2020).

The interrogation of publicly available transcriptomic data obtained from human megakaryocyte-erythroid progenitors at a single cell level demonstrated the presence of *GRINA* transcripts (encoding NMDAR-associated protein 1, known to be expressed at relatively high levels) and a scatter of low signals for *GRIN1*, *GRIN2A*, *GRIN2C*, and *GRIN2D* (Lu et al., 2018). Deep sequencing in that study was performed with approximately 3 million reads per cell, which captured approximately 6,000 of the most highly expressed transcripts in a cell, which may explain why *GRIN* transcripts were detected at very low levels.

NMDAR FUNCTIONALITY IN ERYTHROID CELLS AND IN THE CIRCULATING RBCs

RBCs sense plasma glutamate levels through the NMDAR. Using radiolabeled antagonist ([^{3}H]MK-801) binding assay, basal activity of NMDARs in RBCs suspended in plasma was shown (Makhro et al., 2013). Supplementation of glutamate to plasma caused further activation of the receptors (Hanggi et al., 2014). Other findings suggest that the shear of flowing blood may also activate NMDAR in RBCs of patients with sickle cell disease (Hanggi et al., 2014, 2015).

NMDAR in Erythroid Precursor Cells

The abundance of NMDARs is particularly high in erythroid precursors and the UT-7/EPO cell line (Makhro et al., 2013; Hanggi et al., 2015). The receptor density decreases from hundreds of thousands per cell in proerythroblasts and erythroblasts cultured from peripheral blood-derived CD34-positive progenitors, to 35 in young human RBCs, and five in mature and senescent RBCs from healthy people (Makhro et al., 2013; Hanggi et al., 2014).

In UT-7/EPO cell line 350,000 NMDARs were detected per cell (Makhro et al., 2010). UT-7/EPO is a subclone of a UT-7 megakaryoblastic leukemia cell line that was maintained in the presence of EPO for more than 6 months to increase erythroid differentiation (Komatsu et al., 1993). In keeping with the NMDAR expression data, the density of currents produced by the NMDAR decreased during differentiation from proerythroblastic to the orthochromatic stage of erythroid progenitors (Hanggi et al., 2015).

Similar to megakaryocytes, the pattern of GluN subunits evolves during erythroid differentiation. Except for GluN2B, all other types of NMDAR subunits have been detected in erythroid cells at either mRNA or protein levels, or both (**Table 1**). During early stages, (proerythroblasts and basophilic erythroblasts) higher levels of GluN2A and GluN2D were shown along with lower levels of GluN3A, GluN3B, and GluN1 (Makhro et al., 2013; Hanggi et al., 2014, 2015). Orthochromatic erythroblasts switched from GluN2A-containing receptors to those predominantly containing GluN2C (Hanggi et al., 2015). As a result, high amplitude, fast, inactivating currents, mediated by the receptor at early stages of erythroid differentiation were replaced by currents of lesser amplitude but longer duration (Hanggi et al., 2015). This change in receptor subunit composition and its function gave rise to a switch in signal transmitted by the NMDAR, and probably, to the alteration in sensitivity to the physiological stimuli. Whereas GluN2A-containing receptors contributed to the modulation of the transmembrane potential, GluN2C/GluN2D-NMDAR mediated Ca^{2+} entry through the channels that remained open for a longer time (Hanggi et al., 2015). Mg^{2+} block is not supposed to control the NMDAR activity in RBCs due to the low transmembrane potential (about −10 mV) and the presence of GluN2C, GluN2D, and GluN3 subunits (Monyer et al., 1994; Wrighton et al., 2008).

Hyperactivation of the NMDAR by repeated stimulation resulted in the channel inactivation and did not affect viability of erythroid precursor cells. However, exposure of erythroid progenitors to the NMDAR channel blockers (MK-801 and memantine) triggered vacuolization and apoptosis, with maximal cell death observed at the early differentiation stages (Hanggi et al., 2014, 2015). This observation is in line with the earlier findings by Miller and Cheung on the importance of Ca^{2+} signaling for EPO-driven effects in precursor cells (Miller and Cheung, 1994; Tong et al., 2008).

NMDAR Function and Physiological Significance in the Circulating RBCs

Relatively low numbers of active NMDAR copies are retained by the circulating RBCs. Young RBCs of healthy humans carry 35 NMDARs per cell on average, whereas mature and senescent cells contain about five receptor copies per cell (Makhro et al., 2013; Hanggi et al., 2014). The NMDAR abundance is 3–4-fold higher in RBCs from patients with sickle cell disease (Hanggi et al., 2014). Activation of NMDAR by exposing the cells to the saturating concentrations of agonists (NMDA and glycine, 300 μM each) results in an acute, transient increase in the intracellular free Ca^{2+} (Makhro et al., 2013). There is striking inter-cellular heterogeneity in responses of the cells to the NMDAR agonists, including changes in transmembrane currents and Ca^{2+} uptake shown with a fluorescent dye, as well as the level of dehydration and echinocyte formation. These differences cannot be explained solely by the differences in RBC age. Whereas some cells are insensitive to the stimulation, others show a clear response to the NMDAR agonists suggesting inter-cellular heterogeneity in NMDAR numbers/distribution. Along with the changes in RBC volume and density of Ca^{2+} uptake following the NMDAR stimulation, we observed regulation of nitric oxide production in RBCs by the nitric oxide synthase and modulation of the redox state (Makhro et al., 2010).

Physiological responses to the changes in NMDAR activity in the circulating RBCs include regulation of hemoglobin oxygen affinity, cell rheology, and most likely, longevity. Pathophysiological downstream effects associated with NMDAR hyperactivation were revealed *ex vivo* for RBCs of patients with sickle cell disease. These included Ca^{2+} overload, dehydration, and increase in cell density, and oxidative stress (Hanggi et al., 2014). There are no reports of abnormal RBC counts in patients with Alzheimer's disease taking memantine to protect the brain from glutamatergic excitotoxicity (Kavirajan, 2009). One pilot clinical trial was performed at the University Hospital Zurich, in which patients with sickle cell disease received memantine over a year (Makhro et al., 2020; trial identifier NCT02615847), and the other is currently ongoing (trial identifier NCT03247218). These trials provide an opportunity to explore long-term effects of NMDAR inhibition on RBC and platelet production, and cell properties in humans.

CONCLUSIONS AND FUTURE DIRECTIONS

In summary, megakaryocytic and erythroid precursors carry nonconventional NMDAR subunits, therefore NMDAR activity during hematopoiesis may be unique and should be tested. NMDARs regulate megakaryocytic and erythroid differentiation *ex vivo*, and balance both fates during differentiation of Meg-01 cells, suggesting NMDAR role at the level of a bipotential megakaryocyte-erythroid progenitor. NMDAR effects in hematopoietic cells are mediated by Ca^{2+} influx, which in early megakaryoblasts affects transcriptional program of differentiation, and in mature megakaryocytes induces cytoskeletal rearrangements required for proplatelet formation. In contrast to normal progenitors, leukemic cell lines re-direct NMDAR signaling to increase proliferation. The shift in the dominant NMDAR effect in leukemic cells may be at least partially related to different GluN subunits these cells express, which may offer therapeutic opportunities.

In keeping with the proliferative NMDAR effects in leukemic cells, other prominent groups found that GluN2B-containing NMDAR promotes growth of pancreatic tumors (Li and Hanahan, 2013; Li et al., 2018), and enable brain metastases by breast cancer (Zeng et al., 2019). The following molecules acting downstream of NMDAR were shown to assist cancer spread in these studies: CaMKII, MAPK, guanylate-kinase-associated protein, heat shock factor 1, and fragile X mental retardation protein (Li and Hanahan, 2013; Li et al., 2018);

we should examine similar pathways in leukemic cells as they may provide novel therapeutic targets.

In cultured human proerythroblasts, GluN2A-containing NMDAR provides depolarization, and inward Ca^{2+} current of high amplitude and fast inactivation kinetics. The presence of active NMDAR supports survival of early erythroid progenitors, which likely contributes to the EPO-driven signaling; however, this link is still to be demonstrated. Expression of GluN2C and GluN2D in the late erythroid precursors coincides with the onset of hemoglobinization. Thus, the NMDAR role in iron uptake warrants investigation. In mature RBCs, NMDAR regulates basal intracellular Ca^{2+} levels, contributing toward the regulation of cell volume, density, redox balance, and nitric oxide production by RBCs, which most likely contributes to the regulation of RBC longevity and oxygen carrying capacity.

NMDAR signaling can be modulated using small molecules. Memantine is an approved drug for neurological patients and could be repurposed against certain hematological disorders, such as sickle cell disease, megakaryocytic cancers and thrombosis. Preclinical studies have already advanced to stage I clinical trials in sickle cell disease, but a lot more needs to be done to determine if NMDAR modulation could be useful in patients with certain myeloid blood cancers or thrombotic disease. Neurological side effects may limit the use of memantine in hematological patients; therefore, alternative strategies may need to be considered. These include subunit-specific NMDAR inhibitors, compounds that do not cross the blood-brain-barrier, and drugs that target pathways downstream, or glutamate release upstream of NMDAR.

Considering that the NMDAR role in megakaryocytic cells was first reported in Genever et al. (1999), the progress in this field may be viewed as relatively modest. However, we have reached a state of acceptance that NMDARs provide meaningful biological effects in hematopoietic cells. The field is attracting renewed attention. We await results from the first, stage I clinical trial in patients with sickle cell disease, primarily to establish safety of memantine outside of neurological indications. Further progress into NMDAR role in human leukemia and thrombosis will require studies in more advanced *ex vivo* and *in vivo* models. In addition, the overall principle and purpose of peripheral glutamate signaling needs to be determined. We, thus, invite collaborative approaches engaging experts from multiple disciplines to join us forming an interest group focusing on peripheral glutamate signaling.

AUTHOR CONTRIBUTIONS

MK-Z, AM and AB wrote the paper. JH contributed research data. All authors approved the final version for submission.

FUNDING

Auckland Medical Research Foundation (grant reference 1115012) provided working expenses for megakaryocytic studies conducted in the laboratory of MK-Z. JH received a scholarship funded by Anne and Victoria Norman.

REFERENCES

Akazawa, C., Shigemoto, R., Bessho, Y., Nakanishi, S., and Mizuno, N. (1994). Differential expression of five *N*-methyl-D-aspartate receptor subunit mRNAs in the cerebellum of developing and adult rats. *J. Comp. Neurol.* 347, 150–160. doi: 10.1002/cne.903470112

Almazov, V. A., Popov Iu, G., Gorodinskii, A. I., Mikhailova, I. A., and Dambinova, S. A. (1988). The sites of high affinity binding of *L*-[3H]glutamic acid in human platelets. A new type of platelet receptor? *Biokhimiia* 53, 848–852.

Andersson, L. C., Jokinen, M., and Gahmberg, C. G. (1979). Induction of erythroid differentiation in the human leukaemia cell line K562. *Nature* 278, 364–365. doi: 10.1038/278364a0

Balduini, A., Di Buduo, C. A., Malara, A., Lecchi, A., Rebuzzini, P., Currao, M., et al. (2012). Constitutively released adenosine diphosphate regulates proplatelet formation by human megakaryocytes. *Haematologica* 97, 1657–1665. doi: 10.3324/haematol.2011.059212

Berk, M., Plein, H., and Belsham, B. (2000). The specificity of platelet glutamate receptor supersensitivity in psychotic disorders. *Life Sci.* 66, 2427–2432. doi: 10.1016/S0024-3205(00)00573-7

Berk, M., Plein, H., and Csizmadia, T. (1999). Supersensitive platelet glutamate receptors as a possible peripheral marker in schizophrenia. *Int. Clin. Psychopharmacol.* 14, 119–122. doi: 10.1097/00004850-199903000-00009

Bozic, M., and Valdivielso, J. M. (2015). The potential of targeting NMDA receptors outside the CNS. *Expert Opin. Ther. Targets* 19, 399–413. doi: 10.1517/14728222.2014.983900

Canobbio, I. (2019). Blood platelets: circulating mirrors of neurons? *Res. Pract. Thromb. Haemost.* 3, 564–565. doi: 10.1002/rth2.12254

Castrillon, E. E., Ernberg, M., Cairns, B. E., Wang, K., Sessle, B. J., Arendt-Nielsen, L., et al. (2010). Interstitial glutamate concentration is elevated in the masseter muscle of myofascial temporomandibular disorder patients. *J. Orofac. Pain* 24, 350–360.

Cavara, N. A., and Hollmann, M. (2008). Shuffling the deck anew: how NR3 tweaks NMDA receptor function. *Mol. Neurobiol.* 38, 16–26. doi: 10.1007/s12035-008-8029-9

Cavara, N. A., Orth, A., and Hollmann, M. (2009). Effects of NR1 splicing on NR1/NR3B-type excitatory glycine receptors. *BMC Neurosci.* 10:32. doi: 10.1186/1471-2202-10-32

Chatterton, J. E., Awobuluyi, M., Premkumar, L. S., Takahashi, H., Talantova, M., Shin, Y., et al. (2002). Excitatory glycine receptors containing the NR3 family of NMDA receptor subunits. *Nature* 415, 793–798. doi: 10.1038/nature715

Coyle, J. T. (2012). NMDA receptor and schizophrenia: a brief history. *Schizophr. Bull.* 38, 920–926. doi: 10.1093/schbul/sbs076

Daikhin, Y., and Yudkoff, M. (2000). Compartmentation of brain glutamate metabolism in neurons and glia. *J. Nutr.* 130, 1026S–1031S. doi: 10.1093/jn/130.4.1026S

Featherstone, D. E. (2010). Intercellular glutamate signaling in the nervous system and beyond. *ACS Chem. Neurosci.* 1, 4–12. doi: 10.1021/cn900006n

Fenninger, F., and Jefferies, W. A. (2019). What's bred in the bone: calcium channels in lymphocytes. *J. Immunol.* 202, 1021–1030. doi: 10.4049/jimmunol.1800837

Franconi, F., Miceli, M., Alberti, L., Seghieri, G., De Montis, M. G., and Tagliamonte, A. (1998). Further insights into the anti-aggregating activity of NMDA in human platelets. *Br. J. Pharmacol.* 124, 35–40. doi: 10.1038/sj.bjp.0701790

Franconi, F., Miceli, M., De Montis, M. G., Crisafi, E. L., Bennardini, F., and Tagliamonte, A. (1996). NMDA receptors play an anti-aggregating role in human platelets. *Thromb. Haemost.* 76, 84–87.

Furuyashiki, T., Arakawa, Y., Takemoto-Kimura, S., Bito, H., and Narumiya, S. (2002). Multiple spatiotemporal modes of actin reorganization by NMDA receptors and voltage-gated Ca^{2+} channels. *Proc. Natl. Acad. Sci. U. S. A.* 99, 14458–14463. doi: 10.1073/pnas.212148999

Genever, P. G., Wilkinson, D. J., Patton, A. J., Peet, N. M., Hong, Y., Mathur, A., et al. (1999). Expression of a functional *N*-methyl-D-aspartate-type glutamate receptor by bone marrow megakaryocytes. *Blood* 93, 2876–2883. doi: 10.1182/blood.V93.9.2876

Gerdle, B., Ernberg, M., Mannerkorpi, K., Larsson, B., Kosek, E., Christidis, N., et al. (2016). Increased interstitial concentrations of glutamate and pyruvate in vastus lateralis of women with fibromyalgia syndrome are normalized after an exercise intervention—a case-control study. *PLoS One* 11:e0162010. doi: 10.1371/journal.pone.0162010

Gielen, M., Siegler Retchless, B., Mony, L., Johnson, J. W., and Paoletti, P. (2009). Mechanism of differential control of NMDA receptor activity by NR2 subunits. *Nature* 459, 703–707. doi: 10.1038/nature07993

Grand, T., Abi Gerges, S., David, M., Diana, M. A., and Paoletti, P. (2018). Unmasking GluN1/GluN3A excitatory glycine NMDA receptors. *Nat. Commun.* 9:4769. doi: 10.1038/s41467-018-07236-4

Green, T. N., Hamilton, J. R., Morel-Kopp, M. C., Zheng, Z., Chen, T. T., Hearn, J. I., et al. (2017). Inhibition of NMDA receptor function with an anti-GluN1-S2 antibody impairs human platelet function and thrombosis. *Platelets* 28, 799–811. doi: 10.1080/09537104.2017.1280149

Hahn, C. G., Wang, H. Y., Cho, D. S., Talbot, K., Gur, R. E., Berrettini, W. H., et al. (2006). Altered neuregulin 1-erbB4 signaling contributes to NMDA receptor hypofunction in schizophrenia. *Nat. Med.* 12, 824–828. doi: 10.1038/nm1418

Hanggi, P., Makhro, A., Gassmann, M., Schmugge, M., Goede, J. S., Speer, O., et al. (2014). Red blood cells of sickle cell disease patients exhibit abnormally high abundance of *N*-methyl D-aspartate receptors mediating excessive calcium uptake. *Br. J. Haematol.* 167, 252–264. doi: 10.1111/bjh.13028

Hanggi, P., Telezhkin, V., Kemp, P. J., Schmugge, M., Gassmann, M., Goede, J. S., et al. (2015). Functional plasticity of the *N*-methyl-D-aspartate receptor in differentiating human erythroid precursor cells. *Am. J. Physiol. Cell Physiol.* 308, C993–C1007. doi: 10.1152/ajpcell.00395.2014

Hansen, K. B., Yi, F., Perszyk, R. E., Furukawa, H., Wollmuth, L. P., Gibb, A. J., et al. (2018). Structure, function, and allosteric modulation of NMDA receptors. *J. Gen. Physiol.* 150, 1081–1105. doi: 10.1085/jgp.201812032

Hardingham, G. E. (2006). Pro-survival signalling from the NMDA receptor. *Biochem. Soc. Trans.* 34, 936–938. doi: 10.1042/BST0340936

Hardingham, G. E., Arnold, F. J., and Bading, H. (2001). Nuclear calcium signaling controls CREB-mediated gene expression triggered by synaptic activity. *Nat. Neurosci.* 4, 261–267. doi: 10.1038/85109

Harrison, P. J., Hall, N., Mould, A., Al-Juffali, N., and Tunbridge, E. M. (2019). Cellular calcium in bipolar disorder: systematic review and meta-analysis. *Mol. Psychiatry*. doi: 10.1038/s41380-019-0622-y

Hearn, J. I., Green, T. N., Chopra, M., Nursalim, Y. N. S., Ladvanszky, L., Knowlton, N., et al. (2020). NMDA receptor hypofunction in Meg-01 cells reveals a role for intracellular calcium homeostasis in balancing megakaryocytic-erythroid differentiation. *Thromb. Haemost.* 120, 671–686. doi: 10.1055/s-0040-1708483

Herrera, R., Hubbell, S., Decker, S., and Petruzzelli, L. (1998). A role for the MEK/MAPK pathway in PMA-induced cell cycle arrest: modulation of megakaryocytic differentiation of K562 cells. *Exp. Cell Res.* 238, 407–414. doi: 10.1006/excr.1997.3847

Hitchcock, I. S., Skerry, T. M., Howard, M. R., and Genever, P. G. (2003). NMDA receptor-mediated regulation of human megakaryocytopoiesis. *Blood* 102, 1254–1259. doi: 10.1182/blood-2002-11-3553

Hogan-Cann, A. D., and Anderson, C. M. (2016). Physiological roles of non-neuronal NMDA receptors. *Trends Pharmacol. Sci.* 37, 750–767. doi: 10.1016/j.tips.2016.05.012

Kalev-Zylinska, M. L., Green, T. N., Morel-Kopp, M. C., Sun, P. P., Park, Y. E., Lasham, A., et al. (2014). *N*-methyl-D-aspartate receptors amplify activation and aggregation of human platelets. *Thromb. Res.* 133, 837–847. doi: 10.1016/j.thromres.2014.02.011

Kamal, T., Green, T. N., Hearn, J. I., Josefsson, E. C., Morel-Kopp, M. C., Ward, C. M., et al. (2018). *N*-methyl-D-aspartate receptor mediated calcium influx supports in vitro differentiation of normal mouse megakaryocytes but proliferation of leukemic cell lines. *Res. Pract. Thromb. Haemost.* 2, 125–138. doi: 10.1002/rth2.12068

Kamal, T., Green, T. N., Morel-Kopp, M. C., Ward, C. M., McGregor, A. L., McGlashan, S. R., et al. (2015). Inhibition of glutamate regulated calcium entry into leukemic megakaryoblasts reduces cell proliferation and supports differentiation. *Cell. Signal.* 27, 1860–1872. doi: 10.1016/j.cellsig.2015.05.004

Kavirajan, H. (2009). Memantine: a comprehensive review of safety and efficacy. *Expert Opin. Drug Saf.* 8, 89–109. doi: 10.1517/14740330802528420

Kehoe, L. A., Bernardinelli, Y., and Muller, D. (2013). GluN3A: an NMDA receptor subunit with exquisite properties and functions. *Neural Plast.* 2013:145387. doi: 10.1155/2013/145387

Kiessling, K., Roberts, N., Gibson, J. S., and Ellory, J. C. (2000). A comparison in normal individuals and sickle cell patients of reduced glutathione precursors and their transport between plasma and red cells. *Hematol. J.* 1, 243–249. doi: 10.1038/sj.thj.6200033

Kinney, M. A., Vo, L. T., Frame, J. M., Barragan, J., Conway, A. J., Li, S., et al. (2019). A systems biology pipeline identifies regulatory networks for stem cell engineering. *Nat. Biotechnol.* 37, 810–818. doi: 10.1038/s41587-019-0159-2

Komatsu, N., Yamamoto, M., Fujita, H., Miwa, A., Hatake, K., Endo, T., et al. (1993). Establishment and characterization of an erythropoietin-dependent subline, UT-7/Epo, derived from human leukemia cell line, UT-7. *Blood* 82, 456–464. doi: 10.1182/blood.V82.2.456.456

Li, B., Woo, R. S., Mei, L., and Malinow, R. (2007). The neuregulin-1 receptor erbB4 controls glutamatergic synapse maturation and plasticity. *Neuron* 54, 583–597. doi: 10.1016/j.neuron.2007.03.028

Li, L., and Hanahan, D. (2013). Hijacking the neuronal NMDAR signaling circuit to promote tumor growth and invasion. *Cell* 153, 86–100. doi: 10.1016/j.cell.2013.02.051

Li, L., Zeng, Q., Bhutkar, A., Galvan, J. A., Karamitopoulou, E., Noordermeer, D., et al. (2018). GKAP acts as a genetic modulator of NMDAR signaling to govern invasive tumor growth. *Cancer Cell* 33, 736.e5–751.e5. doi: 10.1016/j.ccell.2018.02.011

Low, C. M., Lyuboslavsky, P., French, A., Le, P., Wyatte, K., Thiel, W. H., et al. (2003). Molecular determinants of proton-sensitive *N*-methyl-D-aspartate receptor gating. *Mol. Pharmacol.* 63, 1212–1222. doi: 10.1124/mol.63.6.1212

Lozzio, C. B., and Lozzio, B. B. (1975). Human chronic myelogenous leukemia cell-line with positive Philadelphia chromosome. *Blood* 45, 321–334. doi: 10.1182/blood.V45.3.321.321

Lu, Y. C., Sanada, C., Xavier-Ferrucio, J., Wang, L., Zhang, P. X., Grimes, H. L., et al. (2018). The molecular signature of megakaryocyte-erythroid progenitors reveals a role for the cell cycle in fate specification. *Cell Rep.* 25, 2083.e4–2093.e4. doi: 10.1016/j.celrep.2018.10.084

Makhro, A., Hanggi, P., Goede, J. S., Wang, J., Bruggemann, A., Gassmann, M., et al. (2013). *N*-methyl-D-aspartate receptors in human erythroid precursor cells and in circulating red blood cells contribute to the intracellular calcium regulation. *Am. J. Physiol. Cell Physiol.* 305, C1123–C1138. doi: 10.1152/ajpcell.00031.2013

Makhro, A., Haider, T., Wang, J., Bogdanov, N., Steffen, P., Wagner, C., et al. (2016). Comparing the impact of an acute exercise bout on plasma amino acid composition, intraerythrocytic $Ca^{(2+)}$ handling, and red cell function in athletes and untrained subjects. *Cell Calcium* 60, 235–244. doi: 10.1016/j.ceca.2016.05.005

Makhro, A., Hegemann, I., Seiler, E., Simionato, G., Claveria, V., Bogdanov, N., et al. (2020). A pilot clinical phase II trialMemSID: Acute and durable changes of red blood cells of sickle cell disease patients on memantine treatment. eJHaem. 2020, 1–12. doi: 10.1002/jha2.11

Makhro, A., Wang, J., Vogel, J., Boldyrev, A. A., Gassmann, M., Kaestner, L., et al. (2010). Functional NMDA receptors in rat erythrocytes. *Am. J. Physiol. Cell Physiol.* 298, C1315–C1325. doi: 10.1152/ajpcell.00407.2009

Matsuda, K., Kamiya, Y., Matsuda, S., and Yuzaki, M. (2002). Cloning and characterization of a novel NMDA receptor subunit NR3B: a dominant subunit that reduces calcium permeability. *Brain Res. Mol. Brain Res.* 100, 43–52. doi: 10.1016/S0169-328X(02)00173-0

Merritt, K., Egerton, A., Kempton, M. J., Taylor, M. J., and McGuire, P. K. (2016). Nature of glutamate alterations in schizophrenia: a meta-analysis of proton magnetic resonance spectroscopy studies. *JAMA Psychiat.* 73, 665–674. doi: 10.1001/jamapsychiatry.2016.0442

Miller, B. A., and Cheung, J. Y. (1994). Mechanisms of erythropoietin signal transduction: involvement of calcium channels. *Proc. Soc. Exp. Biol. Med.* 206, 263–267. doi: 10.3181/00379727-206-43756

Monyer, H., Burnashev, N., Laurie, D. J., Sakmann, B., and Seeburg, P. H. (1994). Developmental and regional expression in the rat brain and functional properties of four NMDA receptors. *Neuron* 12, 529–540. doi: 10.1016/0896-6273(94)90210-0

Morle, F., Laverriere, A. C., and Godet, J. (1992). Globin genes are actively transcribed in the human megakaryoblastic leukemia cell line MEG-01. *Blood* 79, 3094–3096. doi: 10.1182/blood.V79.11.3094.3094

Morrell, C. N., Sun, H., Ikeda, M., Beique, J. C., Swaim, A. M., Mason, E., et al. (2008). Glutamate mediates platelet activation through the AMPA receptor. *J. Exp. Med.* 205, 575–584. doi: 10.1084/jem.20071474

Nakazawa, K., Jeevakumar, V., and Nakao, K. (2017). Spatial and temporal boundaries of NMDA receptor hypofunction leading to schizophrenia. *NPJ Schizophr.* 3:7. doi: 10.1038/s41537-016-0003-3

Nilsson, A., Duan, J., Mo-Boquist, L. L., Benedikz, E., and Sundstrom, E. (2007). Characterisation of the human NMDA receptor subunit NR3A glycine binding site. *Neuropharmacology* 52, 1151–1159. doi: 10.1016/j.neuropharm.2006.12.002

Ogura, M., Morishima, Y., Ohno, R., Kato, Y., Hirabayashi, N., Nagura, H., et al. (1985). Establishment of a novel human megakaryoblastic leukemia cell line, MEG-01, with positive Philadelphia chromosome. *Blood* 66, 1384–1392. doi: 10.1182/blood.V66.6.1384.1384

Ogura, M., Morishima, Y., Okumura, M., Hotta, T., Takamoto, S., Ohno, R., et al. (1988). Functional and morphological differentiation induction of a human megakaryoblastic leukemia cell line (MEG-01s) by phorbol diesters. *Blood* 72, 49–60. doi: 10.1182/blood.V72.1.49.49

Paoletti, P., Bellone, C., and Zhou, Q. (2013). NMDA receptor subunit diversity: impact on receptor properties, synaptic plasticity and disease. *Nat. Rev. Neurosci.* 14, 383–400. doi: 10.1038/nrn3504

Perez-Otano, I., Larsen, R. S., and Wesseling, J. F. (2016). Emerging roles of GluN3-containing NMDA receptors in the CNS. *Nat. Rev. Neurosci.* 17, 623–635. doi: 10.1038/nrn.2016.92

Ponomarev, E. D. (2018). Fresh evidence for platelets as neuronal and innate immune cells: their role in the activation, differentiation, and deactivation of Th1, Th17, and Tregs during tissue inflammation. *Front. Immunol.* 9:406. doi: 10.3389/fimmu.2018.00406

Reiner, A., and Levitz, J. (2018). Glutamatergic signaling in the central nervous system: ionotropic and metabotropic receptors in concert. *Neuron* 98, 1080–1098. doi: 10.1016/j.neuron.2018.05.018

Ruljancic, N., Mihanovic, M., Cepelak, I., and Bakliza, A. (2013). Platelet and serum calcium and magnesium concentration in suicidal and non-suicidal schizophrenic patients. *Psychiatry Clin. Neurosci.* 67, 154–159. doi: 10.1111/pcn.12038

Spencer, J. A., Ferraro, F., Roussakis, E., Klein, A., Wu, J., Runnels, J. M., et al. (2014). Direct measurement of local oxygen concentration in the bone marrow of live animals. *Nature* 508, 269–273. doi: 10.1038/nature13034

Stegink, L. D., Baker, G. L., and Filer, L. J. Jr. (1983). Modulating effect of Sustagen on plasma glutamate concentration in humans ingesting monosodium L-glutamate. *Am. J. Clin. Nutr.* 37, 194–200. doi: 10.1093/ajcn/37.2.194

Sun, H., Swaim, A., Herrera, J. E., Becker, D., Becker, L., Srivastava, K., et al. (2009). Platelet kainate receptor signaling promotes thrombosis by stimulating cyclooxygenase activation. *Circ. Res.* 105, 595–603. doi: 10.1161/CIRCRESAHA.109.198861

Thompson, C. J., Schilling, T., Howard, M. R., and Genever, P. G. (2010). SNARE-dependent glutamate release in megakaryocytes. *Exp. Hematol.* 38, 504–515. doi: 10.1016/j.exphem.2010.03.011

Todrick, A., Tait, A. C., and Marshall, E. F. (1960). Blood platelet 5-hydroxytryptamine levels in psychiatric patients. *J. Ment. Sci.* 106, 884–890. doi: 10.1192/bjp.106.444.884

Tong, Q., Hirschler-Laszkiewicz, I., Zhang, W., Conrad, K., Neagley, D. W., Barber, D. L., et al. (2008). TRPC3 is the erythropoietin-regulated calcium channel in human erythroid cells. *J. Biol. Chem.* 283, 10385–10395. doi: 10.1074/jbc.M710231200

Traynelis, S. F., Hartley, M., and Heinemann, S. F. (1995). Control of proton sensitivity of the NMDA receptor by RNA splicing and polyamines. *Science* 268, 873–876. doi: 10.1126/science.7754371

Traynelis, S. F., Wollmuth, L. P., McBain, C. J., Menniti, F. S., Vance, K. M., Ogden, K. K., et al. (2010). Glutamate receptor ion channels: structure, regulation, and function. *Pharmacol. Rev.* 62, 405–496. doi: 10.1124/pr.109.002451

Uozumi, K., Otsuka, M., Ohno, N., Moriyama, T., Suzuki, S., Shimotakahara, S., et al. (2000). Establishment and characterization of a new human megakaryoblastic cell line (SET-2) that spontaneously matures to megakaryocytes and produces platelet-like particles. *Leukemia* 14, 142–152. doi: 10.1038/sj.leu.2401608

Watanabe, M., Inoue, Y., Sakimura, K., and Mishina, M. (1992). Developmental changes in distribution of NMDA receptor channel subunit mRNAs. *Neuroreport* 3, 1138–1140. doi: 10.1097/00001756-199212000-00027

Wenzel, A., Fritschy, J. M., Mohler, H., and Benke, D. (1997). NMDA receptor heterogeneity during postnatal development of the rat brain: differential expression of the NR2A, NR2B, and NR2C subunit proteins. *J. Neurochem.* 68, 469–478. doi: 10.1046/j.1471-4159.1997.68020469.x

Wrighton, D. C., Baker, E. J., Chen, P. E., and Wyllie, D. J. (2008). Mg^{2+} and memantine block of rat recombinant NMDA receptors containing chimeric NR2A/2D subunits expressed in *Xenopus laevis* oocytes. *J. Physiol.* 586, 211–225. doi: 10.1113/jphysiol.2007.143164

Wyllie, D. J., Livesey, M. R., and Hardingham, G. E. (2013). Influence of GluN2 subunit identity on NMDA receptor function. *Neuropharmacology* 74, 4–17. doi: 10.1016/j.neuropharm.2013.01.016

Yamakura, T., and Shimoji, K. (1999). Subunit- and site-specific pharmacology of the NMDA receptor channel. *Prog. Neurobiol.* 59, 279–298. doi: 10.1016/S0301-0082(99)00007-6

Yelamanchi, S. D., Jayaram, S., Thomas, J. K., Gundimeda, S., Khan, A. A., Singhal, A., et al. (2016). A pathway map of glutamate metabolism. *J. Cell Commun. Signal.* 10, 69–75. doi: 10.1007/s12079-015-0315-5

Yi, F., Zachariassen, L. G., Dorsett, K. N., and Hansen, K. B. (2018). Properties of triheteromeric *N*-methyl-D-aspartate receptors containing two distinct GluN1 isoforms. *Mol. Pharmacol.* 93, 453–467. doi: 10.1124/mol.117.111427

Zeng, Q., Michael, I. P., Zhang, P., Saghafinia, S., Knott, G., Jiao, W., et al. (2019). Synaptic proximity enables NMDAR signalling to promote brain metastasis. *Nature* 573, 526–531. doi: 10.1038/s41586-019-1576-6

Zhou, Y., and Danbolt, N. C. (2014). Glutamate as a neurotransmitter in the healthy brain. *J. Neural Transm.* 121, 799–817. doi: 10.1007/s00702-014-1180-8

Conflict of Interest: The authors declare that the research was conducted in the absence of any commercial or financial relationships that could be construed as a potential conflict of interest.

frontiers in Physiology

ORIGINAL RESEARCH
published: 03 July 2020
doi: 10.3389/fphys.2020.00712

Interplay Between Plasma Membrane Lipid Alteration, Oxidative Stress and Calcium-Based Mechanism for Extracellular Vesicle Biogenesis From Erythrocytes During Blood Storage

*Anne-Sophie Cloos[1], Marine Ghodsi[1], Amaury Stommen[1], Juliette Vanderroost[1], Nicolas Dauguet[2], Hélène Pollet[1], Ludovic D'Auria[3], Eric Mignolet[4], Yvan Larondelle[4], Romano Terrasi[5], Giulio G. Muccioli[5], Patrick Van Der Smissen[1] and Donatienne Tyteca[1]**

[1] CELL Unit and PICT Platform, de Duve Institute, Université catholique de Louvain, Brussels, Belgium, [2] GECE Unit and CYTF Platform, de Duve Institute, Université catholique de Louvain, Brussels, Belgium, [3] NCHM Unit, Institute of Neuroscience, Université catholique de Louvain, Brussels, Belgium, [4] Louvain Institute of Biomolecular Science and Technology, Université catholique de Louvain, Louvain-la-Neuve, Belgium, [5] Bioanalysis and Pharmacology of Bioactive Lipids Research Group, Louvain Drug Research Institute, Université catholique de Louvain, Brussels, Belgium

OPEN ACCESS

Edited by:
Lars Kaestner,
Saarland University, Germany

Reviewed by:
Eitan Fibach,
Hadassah Medical Center, Israel
Giampaolo Minetti,
University of Pavia, Italy

***Correspondence:**
Donatienne Tyteca
donatienne.tyteca@uclouvain.be

Specialty section:
This article was submitted to Red Blood Cell Physiology, a section of the journal Frontiers in Physiology

Received: 15 January 2020
Accepted: 29 May 2020
Published: 03 July 2020

Citation:
Cloos A-S, Ghodsi M, Stommen A, Vanderroost J, Dauguet N, Pollet H, D'Auria L, Mignolet E, Larondelle Y, Terrasi R, Muccioli GG, Van Der Smissen P and Tyteca D (2020) Interplay Between Plasma Membrane Lipid Alteration, Oxidative Stress and Calcium-Based Mechanism for Extracellular Vesicle Biogenesis From Erythrocytes During Blood Storage. Front. Physiol. 11:712. doi: 10.3389/fphys.2020.00712

The shedding of extracellular vesicles (EVs) from the red blood cell (RBC) surface is observed during senescence *in vivo* and RBC storage *in vitro*. Two main models for EV shedding, respectively based on calcium rise and oxidative stress, have been proposed in the literature but the role of the plasma membrane lipid composition and properties is not understood. Using blood in K^+/EDTA tubes stored for up to 4 weeks at 4°C as a relevant RBC vesiculation model, we showed here that the RBC plasma membrane lipid composition, organization in domains and biophysical properties were progressively modified during storage and contributed to the RBC vesiculation. First, the membrane content in cholesterol and linoleic acid decreased whereas lipid peroxidation and spectrin:membrane occupancy increased, all compatible with higher membrane rigidity. Second, phosphatidylserine surface exposure showed a first rapid rise due to membrane cholesterol decrease, followed by a second calcium-dependent increase. Third, lipid domains mainly enriched in GM1 or sphingomyelin strongly increased from the 1st week while those mainly enriched in cholesterol or ceramide decreased during the 1st and 4th week, respectively. Fourth, the plasmatic acid sphingomyelinase activity considerably increased upon storage following the sphingomyelin-enriched domain rise and potentially inducing the loss of ceramide-enriched domains. Fifth, in support of the shedding of cholesterol- and ceramide-enriched domains from the RBC surface, the number of cholesterol-enriched domains lost and the abundance of EVs released during the 1st week perfectly matched. Moreover, RBC-derived EVs were enriched in ceramide at the 4th week but depleted in sphingomyelin. Then, using K^+/EDTA tubes supplemented with glucose to longer preserve the ATP content, we better defined the sequence of events. Altogether, we showed that EV shedding from

lipid domains only represents part of the global vesiculation mechanistics, for which we propose four successive events (cholesterol domain decrease, oxidative stress, sphingomyelin/sphingomyelinase/ceramide/calcium alteration and phosphatidylserine exposure).

Keywords: lipid domains, membrane transversal asymmetry, reactive oxygen species, lipidomics, cell vesiculation, cholesterol, plasmatic acid sphingomyelinase, ceramide

INTRODUCTION

Continuous change in membrane and membrane skeleton organization takes place during development from proerythroblasts to senescent red blood cells (RBCs). For instance, R1 reticulocytes undergo significant rearrangements in their membrane and intracellular components via several mechanisms including exosome release. Circulating R2 reticulocytes complete this maturational process, which involves additional loss of significant amounts of membrane and selected membrane proteins (Minetti et al., 2018, 2020). Membrane remodelling and vesicle formation also occur during RBC ageing (Ciana et al., 2017b). Bosman and coll. have proposed that generation of extracellular vesicles (EVs) constitutes a mechanism for the elimination of RBC membrane patches containing removal molecules, thereby postponing the untimely elimination of otherwise healthy RBCs (Willekens et al., 2008). Mechanistically, current knowledge indicates that part of the membrane skeleton is probably lost together with part of the lipid bilayer in a balanced way (Ciana et al., 2017a).

Those EVs are also released from RBCs *in vitro* upon storage partially expose phosphatidylserine (PS) at their outer membrane leaflet (Almizraq et al., 2018) leading to blood coagulation through thrombin generation (Rubin et al., 2013). RBC-derived EVs also promote excessive production of reactive oxygen species (ROS) and thereby exhortation of the "respiratory burst" in neutrophils (Jank and Salzer, 2011), which could be part of post-transfusional acute lung inflammation. Due to higher accessibility as compared to hemoglobin (Hb) entrapped in RBCs, Hb enclosed in RBC-derived EVs acts as a efficient nitric oxide scavenger, thereby reducing bioavailability of the latter as vasoregulator (Donadee et al., 2011; Said and Doctor, 2017).

Two main models for EV shedding from RBCs upon storage have been proposed. They are based on calcium rise and oxidative stress and lead to the destabilization of membrane:cytoskeleton anchorage followed by membrane loss through vesiculation (Alaarg et al., 2013; Tissot, 2013; Pollet et al., 2018). While the oxidative stress-based model is widely documented in the literature, the calcium-based model is still highly controversed for three main reasons (i) the origin of calcium accumulation is not elucidated; (ii) the contribution of this model to the EV release has been shown mainly through the use of calcium ionophores (Allan et al., 1980; Salzer et al., 2002; Nguyen et al., 2016); and (iii) the accumulation of calcium and the PS externalization, which were for a long time directly associated, are nowadays rather viewed as independent processes (Arashiki and Takakuwa, 2017). Discrepancies between studies could be reconciled if there are different types of EVs that are simultaneously or sequentially released by RBCs.

Surprisingly, the contribution of plasma membrane lipids in the vesiculation process is not understood. For instance, it is not known whether the budding of EVs could occur from specific regions of the plasma membrane and if some specific lipid domains could represent the starting point of the vesiculation process. Three types of submicrometric lipid domains have been identified at the outer plasma membrane leaflet of resting RBCs (i.e., RBCs that are not in the deformation process): (i) those mainly enriched in cholesterol (hereafter referred as cholesterol-enriched domains), (ii) those co-enriched in the ganglioside GM1, phosphatidylcholine and cholesterol (hereafter referred as GM1-enriched domains), and (iii) those co-enriched in sphingomyelin, phosphatidylcholine and cholesterol (hereafter referred as sphingomyelin-enriched domains) (Carquin et al., 2014, 2015, 2016; Conrard et al., 2018). During RBC deformation, cholesterol-enriched domains gather in high curvature areas, forming or stabilizing highly curved membrane regions. GM1- and sphingomyelin-enriched domains increase in abundance upon calcium influx and efflux respectively, thereby potentially participating to calcium exchanges, also essential for RBC deformation (Leonard et al., 2017, 2018; Conrard et al., 2018). Although those domains appeared to contribute to the RBC deformation process, their contribution to RBC vesiculation is not known. In support of the potential EV budding from specific regions of the RBC plasma membrane, the activity of the plasmatic acid sphingomyelinase (aSMase) has been proposed to be implicated in the biogenesis of EVs from RBCs during storage (Hoehn et al., 2017) but this is not proved and the link between ceramide production and membrane blebbing is still unclear.

The main goal of the present study was to evaluate whether the RBC plasma membrane lipid composition and organization could contribute to the RBC vesiculation process. To this aim, we used as main model RBCs stored in K^+/EDTA tubes for two reasons. First, tubes are readily available by simple venipuncture and are less precious than RBC concentrates used for medical applications. Second, they allow to explore a significant amount of parameters upon a limited storage period of only 4 weeks, which is not possible on RBC concentrates that can be stored for up to 42 days before transfusion with limited storage lesions and vesiculation. We found that RBC vesiculation in K^+/EDTA tubes was clearly accelerated as compared to RBC concentrates, mainly due to the rapid intracellular ATP drop. Nevertheless, the progressive rise of calcium and oxidative stress, as in RBCs upon senescence *in vivo* or upon storage in RBC concentrates (Pollet et al., 2018; Yoshida et al., 2019), supported the relevance of K^+/EDTA tubes to explore the RBC vesiculation

mechanisms. Thus, using this model, we determined the RBC membrane lipid composition, organization in lipid domains and biophysical properties during storage. To evaluate if lipid domains were lost by vesiculation, EVs isolated from RBCs were measured for their lipid content. Then, using K^+/EDTA tubes supplemented with glucose, we could better define the sequence of events.

MATERIALS AND METHODS

Blood Collection and Preparation

The study was approved by the Medical Ethics Committee of the University of Louvain, Brussels, Belgium. Blood from 13 adult healthy volunteers (11 women and 2 men), who gave written informed consent, was collected by venipuncture into K^+/EDTA-coated tubes (except otherwise stated). Blood tubes were stored at 4°C for 0–30 days. From those storage days, storage time intervals covering a period of 4 days (except the first one which covered 3 days) were defined and were referenced in the whole manuscript as 0, 0.6, 1.2, 1.8, 2.4, 3.0, 3.6, and 4.2 storage weeks. To supplement blood with an additional energy source, 0.5 ml of Dulbecco's Modified Eagle Medium (DMEM; LifeTechnologies) containing 4.5 g/l of glucose was added per 1 ml of blood in K^+/EDTA-coated tubes directly after collection. Before experiments (except for EV isolation and measurement of aSMase activity), RBCs were isolated from other blood components by a 10-fold dilution in the adapted experimental medium (i.e., DMEM with or without glucose for RBC hemoglobin release, calcium, ATP and PS exposure measurements or Krebs-Ringer-Hepes (KRH) solution for ROS content determination; see below), washed twice by centrifugation at 200 *g* for 2 min and resuspended. This procedure allowed us to efficiently separate RBCs, as revealed by the absence of contamination of RBC preparations by platelets and white blood cells in our routine fluorescence imaging experiments.

Chemical Treatments

All treatments were performed on washed isolated RBCs, except amitriptyline (AMI) which was applied on whole blood at 5 μM for 60 min at 37°C to inhibit the aSMase. To induce acute ATP depletion, RBCs were preincubated for 2 h in glucose-free DMEM (Life Technologies). ATP repletion was performed after RBC washing and resuspension in 4.5 g/l glucose-containing DMEM. To modulate the intracellular calcium content, RBCs were preincubated with 20 μM BAPTA-AM (Abcam): (i) for 15 min at 37°C, followed by a 60 min-reincubation at 37°C in the presence of Fluo-4 AM (see below), to measure its effect on the intracellular calcium content; or (ii) for 60 min at 37°C to determine EV abundance and PS exposure. To deplete membrane cholesterol, RBCs were preincubated with 0.9 mM methyl-β-cyclodextrin (mβCD; Sigma-Aldrich) for 30 min at 37°C. Cholesterol repletion was achieved with 7.5 and 15 μg/ml water-soluble cholesterol (Sigma-Aldrich) for 60 min at 37°C.

RBC Scanning Electron Microscopy on Filters

Washed RBCs were pelleted, resuspended and fixed in 0.1M cacodylate buffer containing graded concentrations (0.1, 0.5, and 1.5%) of glutaraldehyde for 5 min each. Fixed RBCs were then filtered on 0.4 μm polycarbonate (it4ip) filters using a syringe and washed by cacodylate buffer pushed gently through the syringe. Post-fixation was performed directly on the filters in the syringe in 1% OsO_4 in 0.1M cacodylate for 2 h followed by extensive washing in 0.1M cacodylate and six times for 10 min in water. Samples were dissociated from the filter capsule and covered by a second filter in order to protect the sample during further processing, i.e., the dehydration and the critical point drying. Dehydration was performed in graded baths of ethanol (50, 60, 70, 80, 90, 95% for 10 min each, followed by 100% three times for 10 min) and critical point dried. Finally, samples were mounted on scanning electron microscopy stubs and sputtered with 10 nm gold. All samples were observed in the CM12 electron microscope with the SED detector at 80 kV.

RBC Hemoglobin Release Measurement

Isolated RBCs were incubated at RT for 10 min into gradually hypotonic media prepared by dilution of DMEM with water. RBCs were then pelleted by centrifugation at 200 g for 2 min. RBC pellets were lysed in 0.2% Triton-X-100 and both supernatants and pellet lysates were assessed for Hb content by spectrophotometry (Packard SpectraCount Absorbance Microplate Reader) at 450 nm as oxy and deoxy forms of hemoglobin show main peaks of light absorption around 450 nm (Ratanasopa et al., 2015; Chung et al., 2020). For each medium, Hb in the supernatant was then expressed as ratio of the sum of Hb in the supernatant and the pellet. The osmolarity leading to 50% hemolysis (half-maximal effective hemolysis, EC50) was finally extrapolated using GraphPad Prism.

RBC Calcium, ATP, ROS and Outer Plasma Membrane PS Measurements

All determinations were performed on isolated washed RBCs. Intracellular calcium was measured by fluorimetry using the Fluo-4 AM probe and normalized to the corresponding intracellular Hb content (detected by spectrophotometry as described above) as previously (Conrard et al., 2018). Such method generated only qualitative measurements as the Fluo-4 fluorescence signal is not a linear function of the calcium concentration (Kaestner et al., 2006). Alternatively, RBCs were labeled for 30 min at 37°C with Fluo-4 AM, washed and analyzed by flow cytometry (FACSVerse, BD Biosciences). Calcium exchanges upon RBC deformation were evaluated on RBCs spread onto a poly-L-Lysine (PLL)-precoated polydimethylsiloxane stretchable chamber (PDMS; Strex Inc) as in Conrard et al. (2018). Intracellular ATP content was measured using a chemiluminescence assay kit (Abcam). Luminescence produced during the reaction of the luciferase with luciferine in the presence of ATP was detected with a luminometer (GloMax Explorer Multimode Microplate Reader, Promega) and normalized to the Hb

content. Intracellular ROS content and PS externalization were determined by flow cytometry. For ROS measurement, RBCs were labeled with 7.5 μM 2′,7′-dichlorodihydrofluorescein diacetate (H_2DCFDA; Invitrogen) at 37°C for 20 min in KRH, washed and resuspended. For PS externalization, RBCs were incubated with Annexin-V FITC (Invitrogen; 25 μl for $5*10^5$ RBCs) in DMEM at RT for 20 min. For all flow cytometry experiments, acquisition was performed at the FacsVerse with a medium flow rate and a total analysis of 10.000 events. The software FlowJo was used to determine upon storage (i) the Median Fluorescence Intensity (MFI) of whole RBC populations for ROS and calcium contents and PS exposure; and (ii) the percentage of PS-exposing RBCs by positioning the cursor at the edge of the labeled cell population at 0 week of storage.

RBC Calpain Activity Measurement

RBCs were lysed in the buffer provided in the Calpain activity assay kit (Abcam). Twenty five μg proteins of the RBC lysates were then mixed with the "reaction buffer" and the calpain substrate, incubated for 1 h at 37°C and measured by fluorimetry (GloMax, Promega) at $\lambda_{exc}/\lambda_{em}$ of 400/505 nm.

RBC Methemoglobin Determination

RBC lysates obtained through repeated freeze-thaw cycles were analyzed for methemoglobin (metHb) content following indications of a sandwich Elisa assay kit (LifeSpan Biosciences). Briefly, samples were added to the plate, incubated with a biotinylated detection antibody, washed and incubated with an avidin-conjugated Horseradish peroxidase, which in presence of a tetramethylbenzidine substrate induces blue color development. Addition of the stop solution induced color change into yellow and allowed metHb detection by spectrophotometry (SpectraCount, Packard) at 450 nm.

RBC Spectrin Immunofluorescence

Isolated RBCs were immobilized onto PLL-precoated coverslips, permeabilized with 0.5% Triton X-100 for 3 min (to open the RBC and have access to the cytoskeleton overhanging the PLL-coated RBC membrane), fixed with 4% paraformaldehyde for 10 min and blocked with 1% bovine serum albumin (BSA) in phosphate buffer saline (PBS) for 30 min. RBCs were then labeled for 60 min at RT with an antibody against α/β-spectrin (Sigma; 1:100), washed and incubated for 2 h with the secondary antibody coupled to AlexaFluor488. All coverslips were finally mounted in Mowiol in the dark for 24 h and examined with a Zeiss LSM510 confocal microscope using a plan-Apochromat 63x NA 1.4 oil immersion objective. Spectrin membrane occupancy was quantified on confocal images using the Fiji software.

RBC Membrane Cholesterol Content and Lipid Peroxidation Measurements

Cholesterol content was assessed using the Amplex Red cholesterol assay kit (Invitrogen) in the absence of cholesterol esterase (Grimm et al., 2005; Tyteca et al., 2010). Lipid peroxidation was determined with the Lipid Peroxidation (malondialdehyde, MDA) Assay kit (Abcam) applying the high sensitivity protocol (Tsikas, 2017). Both the cholesterol and the MDA levels were reported to the corresponding Hb content.

RBC Membrane Fatty Acid Determination

RBC total lipids were extracted with chloroform/methanol/water (2:2:1.8; v:v:v) according to the Bligh and Dyer method. Nonadecanoic acid (C19:0; Sigma-Aldrich) was used as internal standard. Each sample was then dried under nitrogen and methylated at 70°C through a 1 h-incubation with 0.5 ml of 0.1 mol/l KOH in methanol, followed by a 15 min-incubation in 0.2 ml of 1.2 mol/l HCl in methanol. The fatty acid methyl esters (FAME) were then extracted by 1 ml hexane and separated by gaz chromatography (Schneider et al., 2012). The chromatograph (GC Trace-1310, Thermo Quest, Italy) was equipped with a RT2560 capillary column (100 m × 0.25 mm internal diameter, 0.2 μm film thickness; Restek) and a flame ionization detector (FID, Thermo Quest). The carrier gas used was H_2 at constant pressure (200 kPa). The FID was continuously flowed by H_2 (35 ml/min) and air (350 ml/min) and kept at a constant temperature of 255°C. The temperature program was as follows: an initial temperature of 80°C, which increased at 25°C/min up to 175°C, a holding temperature of 175°C during 25 min, a new increase at 10°C/min up to 205°C, a holding temperature of 205°C during 4 min, a new increase at 10°C/min up to 215°C, a holding temperature of 215°C during 25 min, a last increase at 10°C/min up to 235°C and a final holding temperature of 235°C during 10 min (Ferain et al., 2016).

RBC Membrane Lipid Vital Imaging

To decorate endogenous membrane cholesterol, RBCs were labeled at RT with the mCherry-Theta toxin fragment at 0.6–0.7 μM and then spread onto PLL-coated coverslips, as in Conrard et al. (2018). Sphingomyelin, ceramide and GM1 ganglioside were analyzed through fluorescent BODIPY-sphingomyelin, -ceramide or -GM1 analogs inserted at the plasma membrane of RBCs spread onto PLL-coated coverslips, also as in Conrard et al. (2018). All samples were then placed upside down in Lab-Tek chambers (Fisher Scientific) filled with medium and observed with a Zeiss wide-field fluorescence microscope (Observer.Z1; plan-Apochromat 100X 1.4 oil Ph3 objective). For quantification, the number of lipid domains was assessed by manual counting on fluorescence images and reported to the hemi-RBC projected area determined with the Fiji software.

Plasmatic aSMase Activity and pH Measurements

Whole blood diluted with PBS was laid down on Ficoll Paque Plus (GE Healthcare; 4:3 v/v) and centrifuged for 30 min at 400 *g* at RT to collect cell-free plasma. Plasma samples were increasingly diluted according to storage time

to prevent interference with Hb released into plasma during hemolysis. Thereafter samples were processed according to indications of the Amplex Red Sphingomyelinase Assay Kit (Invitrogen). The plasmatic pH was determined using the GEM PREMIER 3500 (Instrumentation Laboratory; Croix-Rouge de Belgique).

Blood EV Isolation and Analysis

Whole blood maintained at 4°C was centrifuged at 2000 *g* for 15 min. The plasma was recovered and centrifuged again at 2000 *g* for 15 min to pellet eventually remaining blood cells. The obtained plasma was diluted in sterile filtered PBS and centrifugated one additional time at 2000 *g* before ultracentrifugation at 20.000 *g* for 20 min at 4°C. The resulting EV pellet was resuspended in sterile PBS and the centrifugation step at 20.000 g was repeated. The final pellet was resuspended in 1 ml sterile PBS and used for electron microscopy, Nanoparticle tracking and/or flow cytometry analyses. For electron microscopy, isolated EVs were allowed to attach for 8 min onto PLL-coated coverslips. Coverslips were then washed with 0.1M cacodylate, fixed with 1% glutaraldehyde in 0.1M cacodylate and processed by scanning electron microscopy as for RBCs on filters (see above). Nanoparticle tracking analysis was realized with the Zetaview (Particle Metrix) by diluting the samples 5–5000-fold in sterile filtered PBS. For flow cytometry analysis, isolated EVs were successively labeled with 4 μM Carboxyfluorescein succinimidyl ester (CFSE, Invitrogen), 1 μg/ml anti-glycophorin A (GPA)-AlexaFluor647 antibodies (Bio-Rad) and 1 μg/ml anti-CD41-Phycoerythrin (PE) antibodies (BioLegend), each for 20 min at RT. Labeled EVs were analyzed with a FACSVerse (BD Biosciences) with a threshold set on CFSE fluorescence. If needed, samples were diluted for appropriate data acquirement.

RBC-Released EV Purification and Analysis

EVs specifically released by RBCs were purified from other blood EVs by addition to 10^{11} EVs of 100 μl EasySep RBC Depletion Reagent magnetic beads coupled to anti-GPA antibodies (EasyPlate EasySep Magnet, StemCell). After 3 min, samples were split and charged on a 96-well plate which was then laid down on a magnetic plate (StemCell) for 3 min. Supernatants were discarded, the 96-well plate was separated from the magnet and the attached material was resuspended in sterile PBS. The deposit of the plate on the magnet and the resuspension of attached material were repeted and the purified material was finally collected into Eppendorfs. Purity of preparations was then analyzed by western blotting using 4–15% sodium dodecylsufalte-polyacrylamide gel electrophoresis (SDS-PAGE; Bio-Rad) and antibodies against CD41 (Abcam, 1:2000) and GPA (Abcam, 1:500), followed by incubation with HRP-conjugated secondary antibodies and revelation by chemiluminescence (SuperSignal west pico/femto chemiluminescent substrate, Thermo Fisher Scientific) with the Fusion Solo S from Vilber.

RBC-Released EV Lipid Quantification

Lipid content of sorted EVs was characterized by liquid chromatography–mass spectrometry (LC-MS). Lipid species were analyzed after liquid/liquid extraction and solid phase extraction purification in the presence of internal standards. Lysophospholipids and phospholipids were analyzed on a LC-coupled tandem quadrupole (Xevo-TQS from Waters). A Kinetex LC-18 (150 × 4.6 mm, 5.0 μm) column (Phenomenex) and a gradient between phase A [MeOH-ACN (9:1, v/v) 75%, H_2O 25% containing 5 mM ammonium acetate], phase B [MeOH-ACN (9:1, v/v) containing 5 mM ammonium acetate] and phase C (IpOH containing 5 mM ammonium acetate) were used. The gradient (400 μl/min) increased linearly from 100% A to 100% B in 15 min, and after 10 min from 100% B to 70% B – 30% C over 5 min. This was maintained over 30 min before requilibrating the system. The lipids were analyzed in negative mode using an ESI probe. Sphingomyelin species were analyzed using a LTQ-Orbitrap mass spectrometer coupled to an Accela LC system (from Thermo Fischer Scientific) using the same chromatographic system as described above. Those species were analyzed in negative mode using an ESI probe (Guillemot-Legris et al., 2016). Ceramides and dihydroceramides were analyzed using a LTQ-Orbitrap mass spectrometer coupled to an Accela LC system (from Thermo Fischer Scientific) as in Mutemberezi et al. (2016). A Poroshell 120 LC-18 (150 × 4.6 mm, 4.0 μm) column (Agilent) and a gradient between phase A (MeOH-H_2O (75:25, v/v) containing 0.1% of acetic acid) and phase B (MeOH containing 0.1% acetic acid) were used. The gradient (400 μl/min) increased linearly from 100% A to 100% B over 15 min and was held at 100% for an additional 75 min before requilibrating the system. These lipids were analyzed in positive mode using an APCI probe. For all lipid species, the relative quantification was based on the ratio of area under the curve (AUC) of the lipid of interest and the AUC of the respective internal standard.

Data Presentation and Statistical Analyses

Data are expressed as means ± SEM when the number of independent experiments was ≥3 or as means ± SD if $n \leq 2$. For kinetics, the storage time needed to induce half-effect was determined with GraphPad Prism (EC50). Statistical analyses were applied only if three independent experiments were available. For kinetics, the statistical signification of the differences between data before and after the EC50 was determined with the Mann–Whitney *U* test (only when $n \geq 3$). For the effect of pharmacological agents, the Wilcoxon signed rank test or Friedman test followed by Dunn's multiple comparisons test were used for paired data whereas the Kruskal–Wallis test followed by Dunn's multiple comparisons test was used for unpaired data. ns, not significant; $^{*}p < 0.05$; $^{**}p < 0.01$; $^{***}p < 0.001$; $^{****}p < 0.0001$.

RESULTS

Upon Storage in K^+/EDTA Tubes for Up to 4 Weeks at 4°C, RBCs Rapidly Lose Biconcavity and Energy and Become More Fragile

RBCs stored for up to 4 weeks at 4°C sustained morphological transformation from biconcave discocytes to smaller and rounded spherocytes, as revealed by scanning electron microscopy (**Figure 1A**). The abundance of discocytes *vs.* spherocytes was in favor of the latter from 1.4 weeks of storage (**Figure 1B**) and was accompanied by membrane area loss (**Figure 1C**). The high proportion of spherocytes at the beginning of the storage period (**Figure 1B**) probably mainly resulted from RBC swelling. Moreover, transition to spherocytes was accompanied by the budding of EVs, mostly visible at 2–3 weeks of storage (**Figure 1A**), and by increased RBC fragility, fresh and 4.2 weeks-stored RBCs exhibiting 50% hemolysis in 120 and 260 mOsm media respectively (**Figure 1D**). The intracellular ATP decreased by ∼50% after 0.6 weeks and was totally depleted from 1.8 weeks (**Figure 1E**). Of note, ATP levels in fresh RBCs were similar whatever the anticoagulant used for the venipuncture (**Supplementary Figure S1A**) and the ATP drop was not biased by normalization with the global Hb content which was largely preserved during the storage period (**Supplementary Figure S2A**). Altogether those data indicated that RBC storage in K^+/EDTA tubes induced morphological and biochemical storage lesions, including RBC vesiculation.

Upon Storage in K^+/EDTA Tubes for Up to 4 Weeks at 4°C, RBCs Release a High Amount of Extracellular Vesicles

As RBCs stored for up to 4 weeks exhibited vesicles at their surface (**Figure 1A**), we next isolated those vesicles from the plasma by ultracentrifugation and analyzed them for morphology, size, abundance and cell origin. Blood EVs were characterized by a round to slightly elongated morphology (**Figure 2A**) and a relatively homogenous size ranging from 160 to 180 nm (**Figure 2B**). Their abundance strongly rised during storage, showing a half-maximal increase at 1.7 weeks and a 600-fold increase after 4 weeks (**Figure 2C**). Since platelets and megakaryocytes are generally considered as main EV source (at least in fresh blood; Italiano et al., 2010) we next determined the relative proportion of EVs released by platelets and RBCs upon labeling with CFSE (a general EV marker) and fluorescent antibodies directed against GPA and CD41 (to decorate respectively RBC- and platelet-released EVs) and flow cytometry analysis. At time 0, RBC- and platelet-produced EVs were detected in equivalent proportions (**Supplementary Figure S3** and **Figure 2D**). The half-maximal increase of EVs produced by RBCs was seen at 1.7 weeks, i.e., exactly at the same time than the half-maximal increase of blood EVs (**Figure 2C**). Based on the number of EVs per µl of blood and the proportion of EVs produced by RBCs *vs.* platelets, we next calculated the number of EVs produced per RBC during storage (**Figure 2E**). While only five EVs were released per RBC after 1 week of storage, this number rised up to 50, 70, and 100 at 2, 3, and 4 weeks.

The RBC Methemoglobin Content and the Calpain Activity Increase Faster Than Calcium and ROS Intracellular Contents Upon Storage

The next step was to determine whether the calcium rise and the oxidative stress could contribute to the RBC vesiculation in K^+/EDTA tubes as in RBCs upon senescence or upon storage in RBC concentrates. The RBC calcium content increased by half after 2.1 weeks and showed a ∼2.5-fold increase after 4 weeks of storage (**Figure 3A**). Of note, neither the EDTA present in the tubes nor data normalization by the global Hb content appeared to affect the intracellular calcium content (**Supplementary Figures S1B,C, S2B**). The activity of the calcium-dependent calpain was only slightly but significantly increased with a half-maximal effect at 1.4 weeks of storage (**Figure 3B**). In contrast, the RBC content in free ROS highly increased during the storage period, as reflected by the strong rise of the median fluorescence intensity of the RBC population labeled with H_2DCFDA. The half-maximal effect was detected at 2.2 weeks (**Figure 3C** and **Supplementary Figure S4A**). Accordingly, metHb (the oxidized form of Hb) also increased, exhibiting a very rapid half-maximal effect at 0.4 weeks and a maximal increase from 1.2 weeks of storage (**Figure 3D**). Those data indicated that the calcium- and the oxidative-based models were both relevant to RBC storage in K^+/EDTA tubes.

Spectrin:Membrane Occupancy and Membrane Rigidity Increase Upon Storage

To then analyze the RBC cytoskeleton:membrane interaction, the α- and β-spectrin tetramers were immunolabeled and vizualized by confocal microscopy. A significant increase of the spectrin occupancy per RBC area was already visible after the first week of storage and maintained thereafter (**Figures 3E,F**). To decipher whether membrane:cytoskeleton alteration could in turn modify membrane rigidity, confocal imaging with Laurdan, a fluorescent tracer of membrane lipid order (Golfetto et al., 2013), was performed. This analysis revealed an increased membrane rigidity of discocytes, but not of spherocytes after 2 weeks of storage (**Supplementary Figure S5**), suggesting that the loss of EVs allowed to partially restore membrane lipid order. The increased membrane rigidity, which was confirmed by atomic force microscopy (data not shown), did not appear to result from changes of the plasmatic pH which only slightly decreased during the 4-week storage period (**Supplementary Figure S6**).

Membrane Cholesterol and Linoleic Acid Decrease During Storage While Lipid Peroxidation Slightly Increases

We then determined whether the increased membrane rigidity resulted exclusively from the stronger membrane:spectrin occupancy or also from alterations of membrane lipid

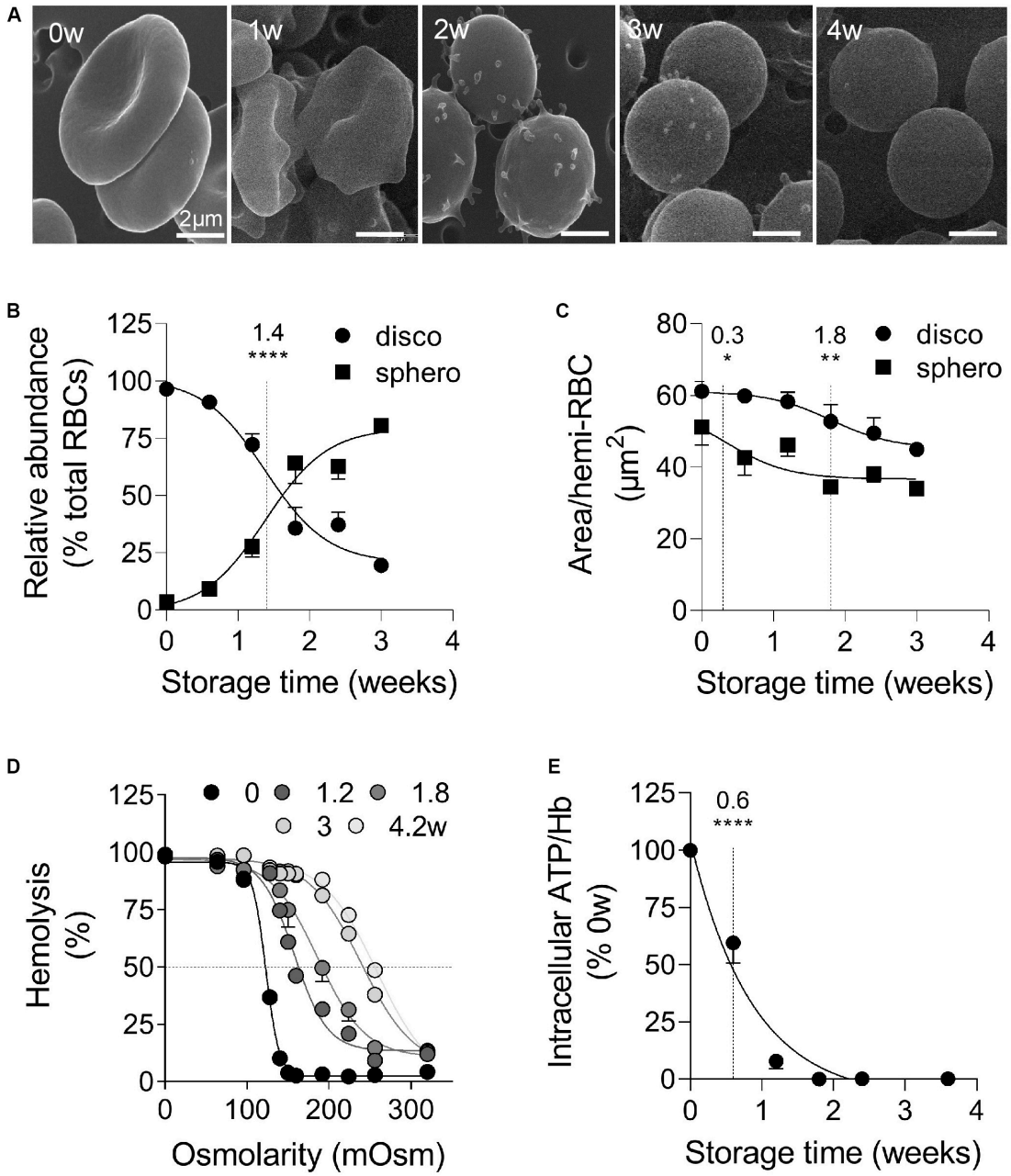

FIGURE 1 | During storage in K^+/EDTA tubes at 4°C, RBCs rapidly lose biconcavity and energy, become more fragile and form surface vesicles. RBCs stored for 0 to 4 weeks (w) in K^+/EDTA tubes at 4°C were isolated and analyzed for morphology **(A,B)**, size **(C)**, fragility **(D)**, and intracellular ATP content **(E)**. The time needed to reach 50% effect and the corresponding statistical analysis (Mann–Whitney *U* test) are indicated above the vertical dotted line. **(A)** Scanning electron microscopy images of RBCs on filters. RBCs were fixed in increasingly concentrated glutaraldehyde solutions, deposited on filters, post-fixed with osmium tetroxide, covered with gold and observed by electron microscopy. Representative images of 1 experiment including 3 preparations per storage time. **(B,C)** Abundance and surface area of spherocytes *vs.* discocytes. RBCs were immobilized on poly-L-lysine (PLL)-coated coverslips, imaged and classified into two categories, the discocytes (disco; circles) and the spherocytes (sphero; squares), which are smaller and possess higher circularity. In **(B)**, data are means ± SEM of 7 independent experiments where at least 100 RBCs were analyzed. In **(C)**, data are means ± SEM of 4 independent experiments where at least 150 RBCs were analyzed. **(D)** RBC osmotic fragility. RBCs were incubated at RT in media of decreasing osmolarity. After centrifugation, the hemoglobin (Hb) content in the supernatant and in the pellet were measured by spectrophotometry at 450 nm. The horizontal dotted line indicates the medium osmolarity at which 50% of the RBCs were lysed. Data are means ± SD of 1 experiment representative of 2. **(E)** Intracellular ATP content. RBCs were lysed and incubated with firefly luciferase and luciferin. The intensity of the light emitted following the oxidation of luciferin to oxyluciferin by luciferase in the presence of ATP was then measured by luminescence. The intracellular ATP concentration was normalized on the Hb content and then expressed in % of fresh RBCs (i.e., 0 weeks of storage). Data are means ± SEM of 4 independent experiments. *$p < 0.05$; **$p < 0.01$; ****$p < 0.0001$.

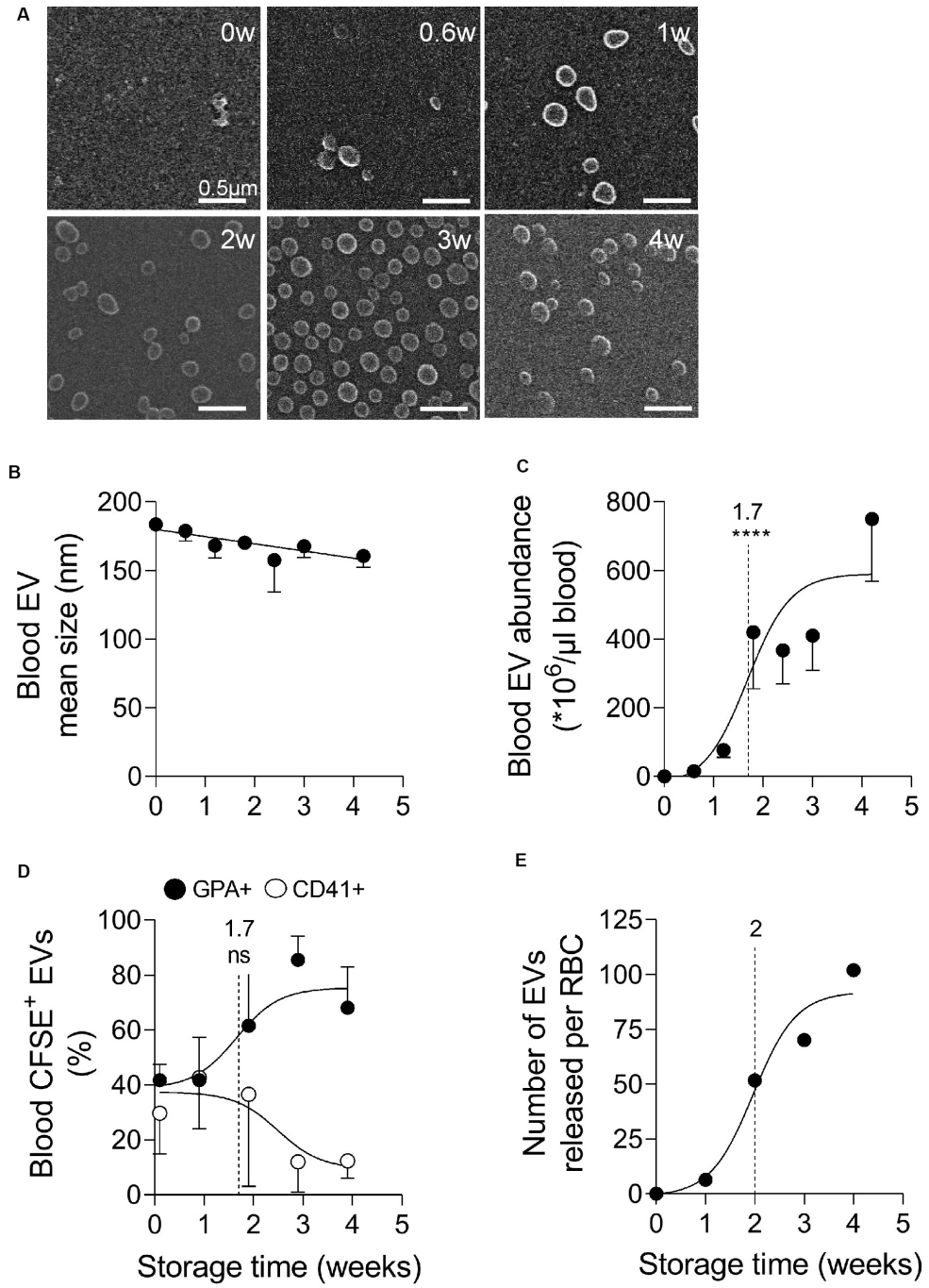

FIGURE 2 | Blood extracellular vesicles increase in abundance upon storage and originate from both platelets and RBCs in the first 2 weeks of storage, then mainly from RBCs. Extracellular vesicles (EVs), isolated by ultracentrifugation from plasmas obtained from K^+/EDTA tubes stored at 4°C for the indicated times, were analyzed for morphology **(A)**, size **(B)**, abundance **(C)**, and cellular origin **(D,E)**. The time needed to reach 50% effect and the corresponding statistical analysis (Mann–Whitney *U* test) are indicated above the vertical dotted line. **(A)** EV morphology evidenced by electron microscopy. Isolated EVs were immobilized on PLL-coated coverslips, fixed with glutaraldehyde, post-fixed with osmium tetroxide, gold-labeled and observed by electron microscopy. Representative images from 1 experiment. **(B,C)** EV size and concentration determined by nanoparticle tracking analysis using the ZetaView. In **(B)**, EV size expressed in nm. In **(C)**, number of EVs/µl of blood determined as follows. The number of EVs/µl of liquid in which EVs were suspended was determined by the Zetaview and then normalized by the factor between the volume of plasma used for EV isolation and the volume of plasma contained in 1 µl of blood (i.e., 0.6 µl). Data are means ± SEM of 5 independent experiments. **(D)** Proportion of blood EVs produced by RBCs and platelets determined by flow cytometry. Isolated EVs were labeled with fluorescent carboxyfluorescein succinimidyl ester (CFSE) and anti-glycophrorin A (anti-GPA-AlexaFluor647; black circles) and -CD41 (anti-CD41-PE; white circles) antibodies to respectively label EVs originating from RBCs and platelets and then analyzed by flow cytometry. Results are expressed as % of GPA (RBCs) or CD41 (platelets) positive CFSE-labeled EVs. Mean ± SEM of 4 independent experiments. **(E)** Estimation of the abundance of EVs released per RBC based on the number of EVs per µl of blood **(C)** and the proportion of EVs produced by RBCs **(D)**. ns, not significant; ****$p < 0.0001$.

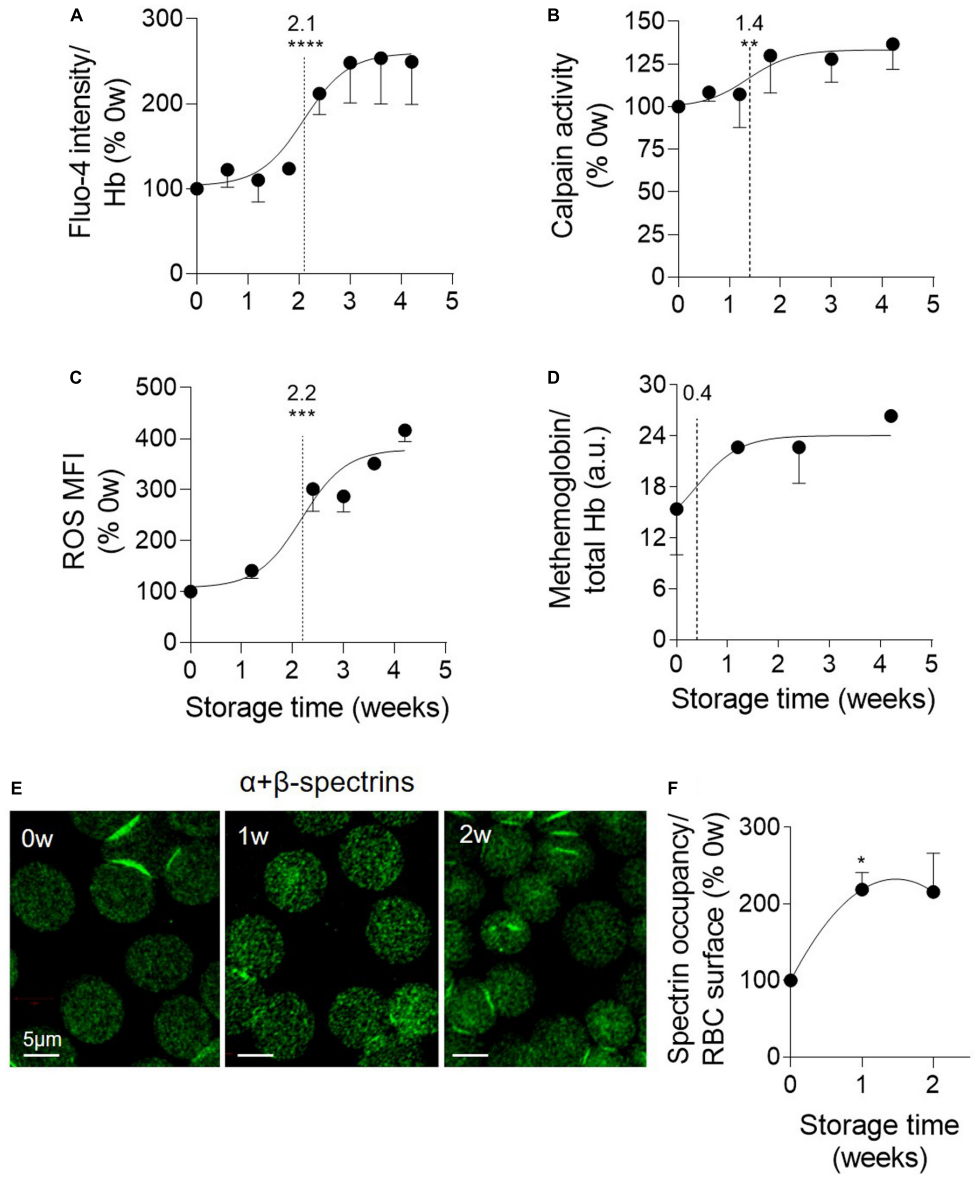

FIGURE 3 | Oxidized hemoglobin and spectrin density rapidly increase upon storage while calpain activity increase and accumulation of calcium and reactive oxygen species take place later. RBCs stored for the indicated times at 4°C in K^+/EDTA tubes were isolated and analyzed for intracellular calcium **(A)**, active calpain **(B)**, reactive oxygen species (ROS; **C**), methemoglobin (metHb) content **(D)** and spectrin occupancy at the RBC surface **(E,F)**. The time needed to reach 50% effect and the statistical analysis (Mann–Whitney *U* test) are indicated above the vertical dotted line [except in **(F)** in which the comparison was done *vs.* the 0 week]. **(A)** RBC calcium content. RBCs were incubated with the non-fluorescent Fluo-4 AM and then in Fluo-4 AM-free medium to allow for probe de-esterification and calcium binding, generating fluorescent Fluo-4 measured at 494 nm. Data were normalized on the Hb content and expressed in % of 0 weeks of storage. Means ± SEM of 7 independent experiments. **(B)** µ-calpain activity. Lysates of isolated RBCs were incubated with the substrate of calpain which emits fluorescence at 505 nm upon cleavage. Data are expressed as % of 0 weeks of storage and are means ± SEM of 6 independent experiments. **(C)** RBC ROS content. RBCs were labeled with H_2DCFDA, which is transformed into fluorescent 2,7-dichlorofluorescein (DCF) after de-esterification and interaction with intracellular ROS, and then analyzed by flow cytometry. Median fluorescence intensity (MFI) as % of 0 weeks of storage. Means ± SEM of 3 independent experiments. **(D)** MetHb determination. RBCs were assessed for metHb concentration by a sandwich ELISA. Data were then normalized to the total Hb content. Means ± SD of 2 independent experiments. **(E,F)** Membrane:spectrin occupancy. RBCs were immunolabeled for pan-spectrin, analyzed by confocal microscopy **(E)** and quantified for spectrin occupancy per RBC surface **(F)**. Data were expressed as % of 0 weeks of storage and are means ± SEM of 3 independent experiments. $^*p < 0.05$; $^{**}p < 0.01$; $^{***}p < 0.001$; $^{****}p < 0.0001$.

composition and organization. We started by analyzing the RBC membrane lipid composition, giving a particular attention to cholesterol and fatty acid (FA) unsaturation, both involved in the regulation of membrane fluidity (Arisawa et al., 2016; Subczynski et al., 2017), and to peroxidized lipids, since ROS were strongly increased upon storage. The membrane

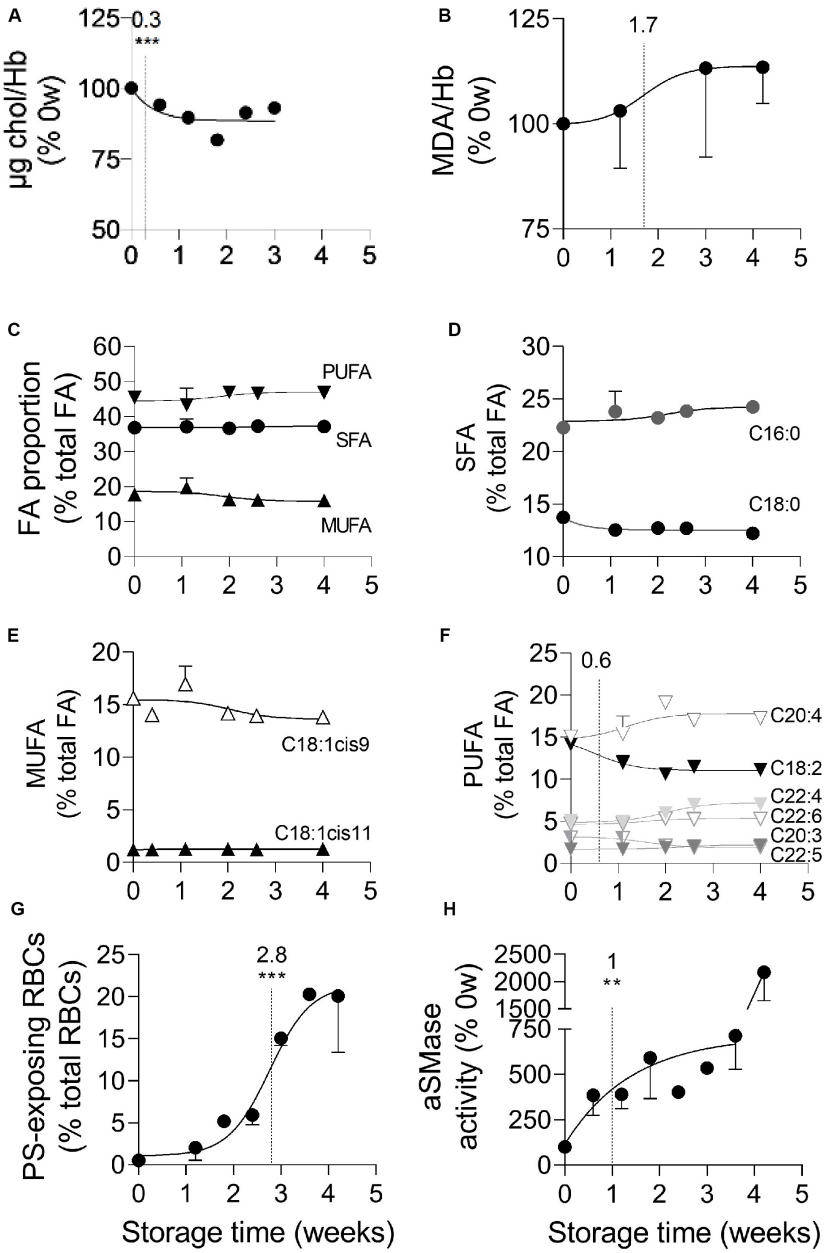

FIGURE 4 | Cholesterol and linoleic acid (C18:2) decreases, plasmatic acid sphingomyelinase activation, lipid peroxidation and PS surface exposure successively take place at the RBC membrane during storage. RBCs isolated from K^+/EDTA tubes stored at 4°C were analyzed for their membrane content in cholesterol (chol, **A**), peroxidized lipids **(B)**, fatty acids (FA; **C–F**) and external phosphatidylserine (PS; **G**) while isolated plasmas were assessed for the plasmatic acid sphingomyelinase (aSMase) activity **(H)**. The time needed to reach 50% effect and the corresponding statistical analysis (Mann–Whitney *U* test) are indicated above the vertical dotted line. **(A)** Chol content. Chol was quantified based on successive enzymatic reactions leading to the production of H_2O_2 which allows the transformation of non–fluorescent Amplex Red into fluorescent resofurin measured at 585 nm. Data were normalized to the Hb content and expressed in % of 0 week of storage. Means ± SEM of 4 independent experiments. Error bars were included in the symbols. **(B)** Malondialdehyde (MDA) content. Lysates of isolated RBCs were incubated with thiobarbituric acid (TBA) which reacts with free MDA, one of the end products of lipid peroxidation, to form a fluorescent adduct measured at 553 nm. Data were normalized to the Hb content and expressed in % of 0 weeks of storage. Means ± SD of 2 independent experiments. **(C–F)** FA composition. Total lipid extraction from isolated RBCs was followed by methylation and extraction of FA methyl esters and analysis by gas chromatography. All data are means ± SD of triplicates from 1 representative experiment out of 2 and are expressed as % of total FAs. **(C)** Proportion of saturated fatty acids (SFA), mono- (MUFA) and poly-unsaturated fatty acids (PUFA). **(D)** Relative proportion of the two major SFAs (C16:0 and C18:0). **(E)** Relative proportion of the two major MUFAs (i.e., C18 with one double bond either on position 9 or 11). **(F)** Relative proportion of the major PUFAs (chains of 18–22C and 2–6 double bonds). **(G)** Exposure of PS at the RBC surface. RBCs were labeled with Annexin-V coupled to FITC and then analyzed in flow cytometry. The % of Annexin V-FITC positive RBCs was determined by positioning the cursor at the edge of the labeled cell population at 0 weeks of storage. Data are means ± SEM of 3 independent experiments. **(H)** aSMase activity. The activity of aSMase in isolated plasmas was measured thanks to successive enzymatic reactions leading to the formation of a fluorescent product, the resorufin, measured at 585 nm. Means ± SEM of 5 independent experiments. $^{**}p < 0.01$; $^{***}p < 0.001$.

cholesterol content decreased slightly but very rapidly, with a half-maximal effect at 0.3 weeks of storage (**Figure 4A**). A slight rise of lipid peroxidation was also detected, with a half-maximal increase at 1.7 weeks (**Figure 4B**). None of those modifications was influenced by data normalization by global Hb content (**Supplementary Figures S2C,D**). To then evaluate the relative proportion of saturated *vs.* (poly)unsaturated FA, gas chromatography was used. A total of 42 FA belonging to phospholipids, sphingolipids and neutral lipids or consisting in free FA were detected and thereafter classified into three groups, saturated (SFA), monounsaturated (MUFA) and polyunsaturated FA (PUFA). The relative abundance of FA on fresh RBCs was in good agreement with (Rise et al., 2007). No major changes in the proportion of those three groups was observed during the storage (**Figure 4C**). The proportion of the two major SFA (C16:0 and C18:0) and MUFA (C18:1cis9 and C18:1cis11) was also largely maintained (**Figures 4D,E**). Among PUFA, the C18:2c9c12 (or linoleic acid) decreased at the benefit of long chain PUFA (such as C20:4 and C22:4), with a half-time effect at 0.6 weeks (**Figure 4F**). In conclusion, the RBC membrane lipid composition was altered upon blood storage, exhibiting decreased cholesterol and linoleic acid contents and increased lipid peroxidation.

PS Surface Exposure Rapidly Increases Upon Storage

To next evaluate the membrane transversal asymmetry, PS surface exposure was determined by flow cytometry upon RBC labeling with fluorescent Annexin V. Whereas the mean fluorescence intensity did not increase upon storage (**Supplementary Figure S4B**), the proportion of PS-exposing RBCs already increased by ∼5-fold during the first 2 weeks of storage, showed a half-maximal significant effect at 2.8 weeks and then continued to increase throughout the entire storage period (**Supplementary Figure S4C** and **Figure 4G**). Thus, as compared to calcium rise (see **Figure 3A**), the increase of abundance of PS-exposing RBCs showed a delayed half-maximal effect but started more rapidly.

The Plasmatic aSMase Activity Increases in Two Stages Upon Storage

To assess whether membrane lateral asymmetry could also be affected upon storage, we evaluated the activity of the aSMase, which is responsible for the transformation of sphingomyelin into ceramide and was proposed to induce RBC vesiculation (Dinkla et al., 2012; Pollet et al., 2018). The aSMase activity increased in a strong and fast manner, with a half-maximal effect at 1 week of storage, followed by a second increase after 4 weeks of storage (**Figure 4H**).

Sphingomyelin- and GM1-Enriched Domains Increase in Abundance Upon Storage Whereas Cholesterol- and Ceramide-Enriched Domains Decline

The above observation prompted us to evaluate by fluorescence microscopy the lateral distribution of sphingomyelin and ceramide at the RBC surface. This analysis was limited to the three first weeks of storage because the loss of membrane area per hemi-RBC above this period becomes significant (see **Figure 1C**) and would therefore have required careful adaptation of the labeling procedure to avoid toxicity. As expected from our previous data (Conrard et al., 2018), sphingomyelin clustered into well-defined submicrometric domains associated with the center of the fresh RBCs, which correspond to the RBC low curvature areas (Leonard et al., 2017, **Figure 5A**, 0w). Quite surprisingly, the abundance of those domains increased strongly (by six fold) and rapidly upon storage (**Figure 5B**, EC50, 0.6w; **Figure 5A**, SM, 2w), in a kinetics similar to that observed for the aSMase activity (see **Figure 4H**). Ceramide also clustered into domains well-visible on fresh RBCs, but in contrast to the sphingomyelin-enriched domains, they decreased upon storage (**Figures 5A,C**). We then analyzed the two other submicrometric domains present at the RBC surface, i.e., those mainly enriched in GM1 and those mainly enriched in cholesterol (Conrard et al., 2018). Like sphingomyelin-enriched domains, GM1-enriched domains increased in abundance upon storage, with a similar half-time effect (**Figures 5A,D**). In contrast, cholesterol-enriched domains very rapidly (EC50, 0.2) but slightly decreased (**Figures 5A,E**). In conclusion, whereas sphingomyelin- and GM1-enriched domains increased in abundance upon storage, those enriched in ceramide and cholesterol instead decreased. The next question was whether those modifications resulted from domain loss by vesiculation, which was investigated through the determination of the lipid content of RBC-derived EVs.

RBC-Derived EVs Are Enriched in Ceramide, Lysophosphatidylinositol and Lysophosphatidylglycerol Species at the End of the Storage but Are Nearly Depleted in Their Precursors

To analyze the lipid content of EVs originating from RBCs without contamination by those produced by platelets (see **Figure 2D**), the former were isolated by immunopurification. Purity of preparations was confirmed by Western Blotting for GPA and CD41 (**Supplementary Figure S7**). Purified EVs were then analyzed by LC-MS for their content in (i) ceramide, sphingomyelin and phosphatidylcholine, as major lipids enriched in lipid domains and mainly present in the outer leaflet or generated there; (ii) phosphatidylinositol, phosphatidylglycerol and phosphatidylethanolamine, as inner leaflet lipids; and (iii) lysophospholipids, which promote the formation of curved membrane due to their inverted cone-shape (Sobko et al., 2004; Lahdesmaki et al., 2010). In agreement with the decrease of ceramide-enriched domain abundance at the RBC membrane upon storage (see **Figures 5A,C**), ceramide and dihydroceramide species were enriched in RBC-derived EVs at the end of the storage period (**Figures 6A,B**). In contrast and in agreement with the increased abundance of sphingomyelin-enriched domains at the RBC surface upon storage, the main lipid species of those domains, i.e., sphingomyelin and phosphatidylcholine, were already at the detection limit at 1 week and further decreased upon storage (**Figures 6C–E**). The EV content in

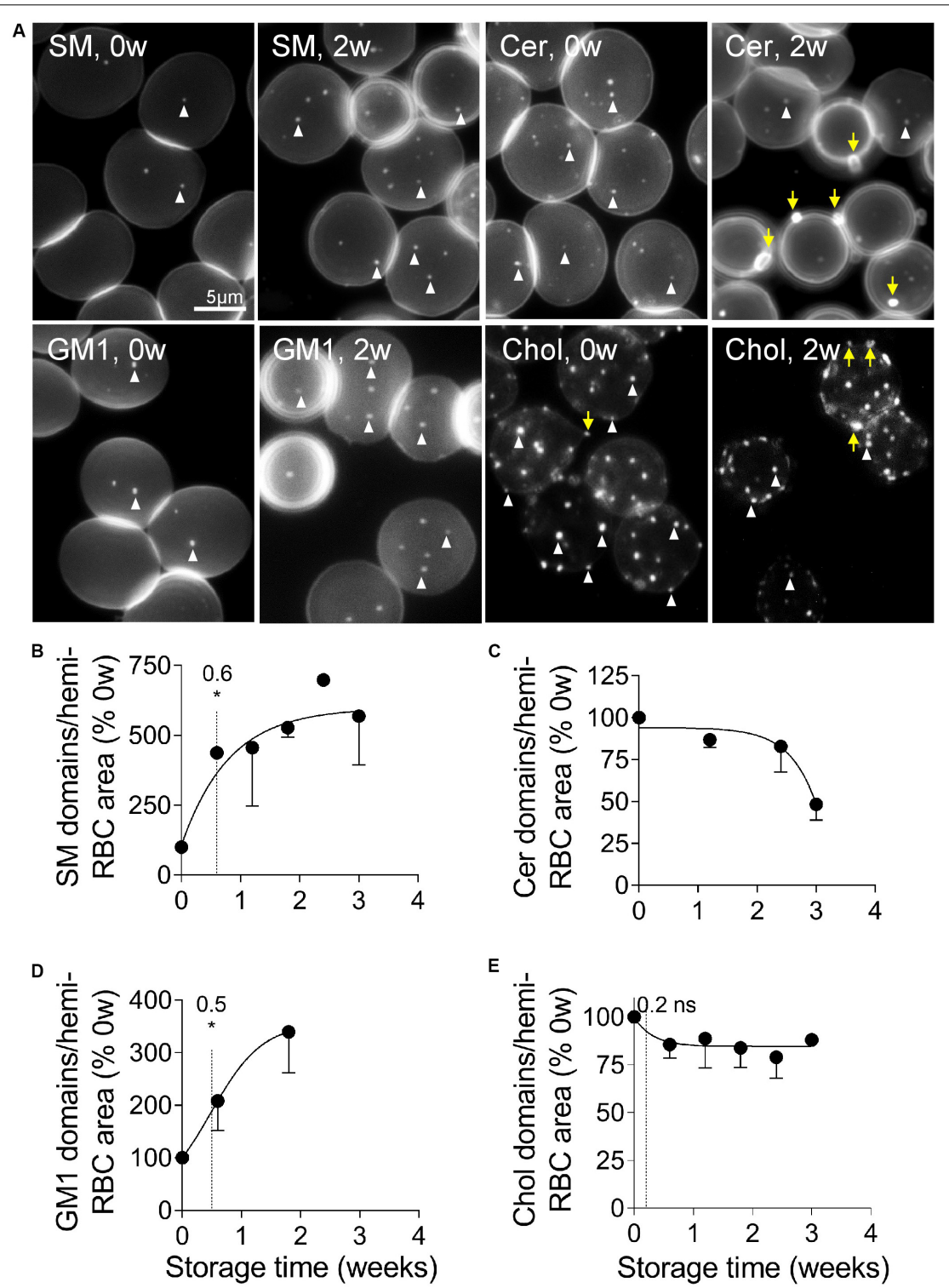

FIGURE 5 | Sphingomyelin- and GM1-enriched domains increase in abundance upon storage whereas those enriched in ceramide and cholesterol decrease. RBCs isolated from K^+/EDTA tubes stored at 4°C for the indicated times were either immobilized on PLL-coated coverslips and then labeled with fluorescent analogs of sphingomyelin (SM; **A,B**), ceramide (cer; **A,C**) or ganglioside GM1 (GM1; **A,D**); or first labeled with the fluorescent Theta toxin specific to endogenous cholesterol and then immobilized on PLL-coated coverslips (chol; **A,E**). All coverslips were then directly observed by fluorescence microscopy. **(A)** Representative images of lipid domains on RBCs stored for 0 and 2 weeks. White arrowheads, lipid domains; yellow arrows, lipid-enriched EVs. **(B–E)** Quantification. 150–300 RBCs per storage time and per lipid were counted for the number of domains. This number was then divided by the average RBC surface area and expressed as % of 0 weeks of storage. Data are means ± SD of 2 experiments in **(C)** and means ± SEM of at least 3 independent experiments in **(B,D,E)**. The time needed to reach 50% effect and the corresponding statistical analysis (Mann–Whitney *U* test) are indicated above the vertical dotted line. ns, not significant; *$p < 0.05$.

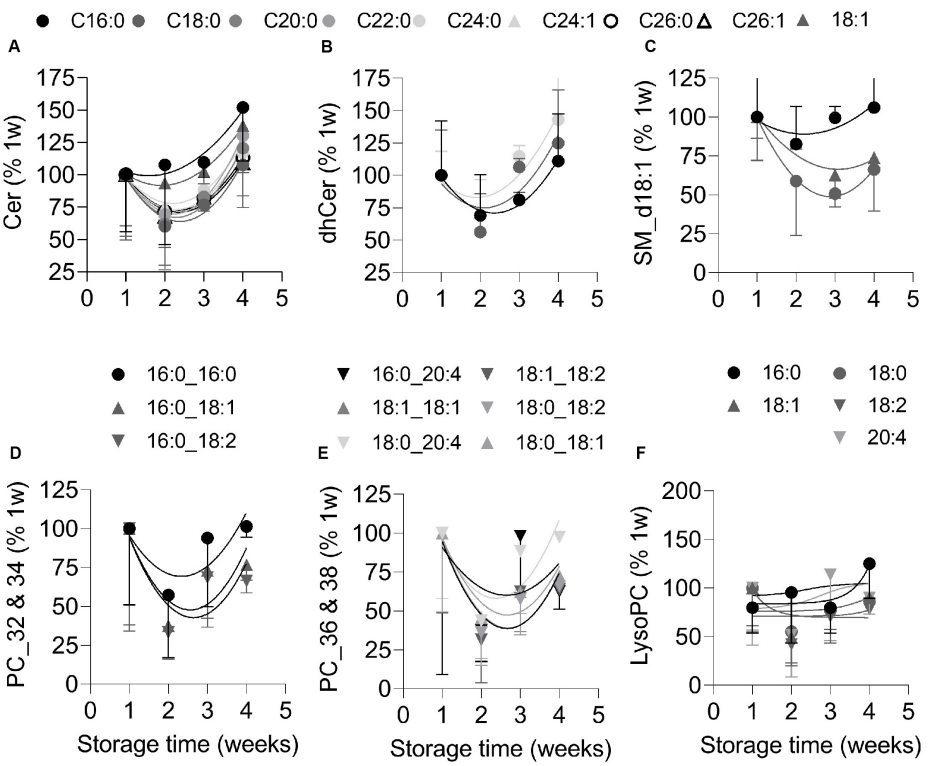

FIGURE 6 | RBC-derived EVs are enriched in ceramide and dihydroceramide species at the end of storage but nearly depleted in sphingomyelin and phosphatidylcholine species. RBC-released EVs were isolated from total blood EVs by immunopurification and analyzed by LC-MS for their content in: **(A,B)** ceramide (cer) and dihydroceramide (dhcer) species; **(C)** SM d18:1 species; and **(D–F)** phosphatidylcholine (PC; presented in two graphs according to the length of their carbon chains) and lysoPC species. Each curve depicts one lipid species; circle, saturated lipid; triangle, lipid containing at least one MUFA; inverted triangle, lipid containing at least one PUFA; black to light gray and white colors, short to long carbon chains. Notice that most of the SM species (e.g., 16:1) and some PC species (e.g., 16:0_18:0) were at the limit of detection. Representative experiment out of 2. All data were expressed as % of the EVs stored for 1 week and are means ± SD of 4 replicates.

inner leaflet phosphatidylinositol and phosphatidylglycerol was globally decreased over the storage period, except for two species, whereas phosphatidylethanolamine species remained stable (**Supplementary Figures S8A,C,D,F,G**). In contrast to their precursors lysophosphatidylinositol and lysophosphatidylglycerol increased in RBC-derived EVs between the 3th and 4th weeks (**Supplementary Figures S8B,E**) whereas lysophosphatidylcholine and lysophosphatidylethanolamine species remained almost stable (**Figure 6F** and **Supplementary Figure S8H**).

Longer ATP Preservation Does Not Restore Cholesterol-Enriched Domains, Delays ROS Accumulation and EV Release, Decreases the PS Exposure and SM- and GM1-Enriched Domain Rise and Abrogates the Increase of aSMase Activity and Calcium

The above data indicated that the RBC intracellular calcium and ROS contents, the membrane content in cholesterol, polyunsaturated FA and lipid peroxidation as well as the lipid transversal and lateral asymmetry were altered during storage of RBCs in K^+/EDTA tubes. To next define the succession of events, the K^+/EDTA tubes were supplemented directly after collection with an energy source, as in RBC concentrates (D'alessandro et al., 2010). As expected, such glucose addition delayed by 1.1 weeks the half-maximal decrease of intracellular ATP content and the complete loss of ATP to 3.6 weeks instead of 1.8 weeks (**Figure 7A**). In this condition, the aSMase activity, the intracellular RBC calcium content and the membrane cholesterol level were not modified at all upon storage (**Figures 7B,C,F**). In contrast, the intracellular ROS content, the PS surface exposure and the blood EV abundance were longer preserved upon energy supply but started to be modified from 1.8 weeks of storage, i.e., as soon as the RBC intracellular ATP content droped to ∼30% (**Figures 7D,E,H**). Finally lipid domains were differentially affected by the longer ATP preservation. For instance, sphingomyelin- and GM1-enriched domains were largely but not fully restored whereas cholesterol-enriched domains were not restored at all (**Figure 7G**). Three main observations were derived from those data. First, the oxidative stress appeared highly dependent to the intracellular ATP content

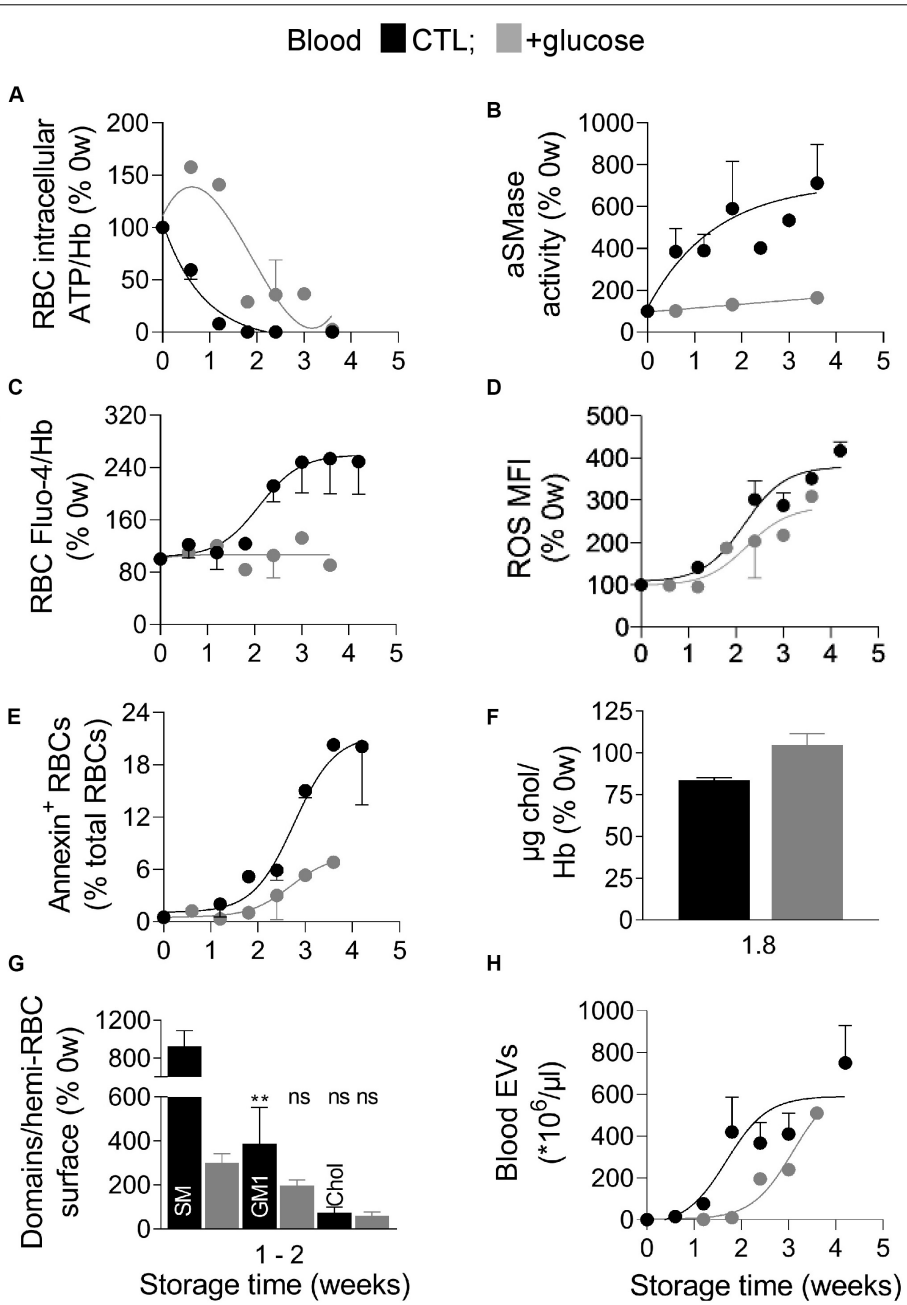

FIGURE 7 | Blood glucose supplementation delays ATP drop, ROS accumulation and EV release, decreases the extent of PS exposure and of SM- and GM1-enriched domain increase and abrogates the increase of aSMase activity and calcium content. Blood samples were stored for the indicated times at 4°C in K^+/EDTA tubes supplemented or not (black symbols) with a glucose-enriched solution (gray symbols) and measured for the intracellular ATP **(A)**, aSMase activity **(B)**, intracellular calcium and ROS contents **(C,D)**, PS surface exposure **(E)**, membrane cholesterol (chol) content **(F)**, lipid domain abundance **(G)**, and blood EVs **(H)**. **(A)** RBC ATP content determined as in **Figure 1E**. **(B)** aSMase activity evaluated as in **Figure 4H**. **(C)** RBC calcium content measured as in **Figure 3A**. **(D)** RBC ROS content assessed as in **Figure 3C**. **(E)** Proportion of PS-exposing RBCs determined as in **Figure 4G**. **(F)** RBC membrane cholesterol (chol) content, measured as in **Figure 4A**. **(G)** Sphingomyelin (SM), GM1- and cholesterol-enriched domain abundance, counted as in **Figure 5**. **(H)** Blood EV abundance, evaluated as in **Figure 2C**. Data are means ± SD of 1 **(A,C–E,H)** or 2 independent experiments [**B,F,G** (SM domains)] or means ± SEM of 3–4 independent experiments [**G** (GM1 and chol domains)]. Kruskal–Wallis test followed by Dunn's multiple comparisons test to compare GM1- and chol -enriched domains at 0 weeks, 1–2 weeks – glucose and 1–2 weeks + glucose. ns, not significant; $^{**}p < 0.01$.

and could represent the main contributor to the release of EVs. Second, the ATP level differentially influenced the abundance of lipid domains. Third, PS surface exposure during storage can be observed despite stable intracellular calcium content. These two last observations were further investigated by complementary pharmacological approaches.

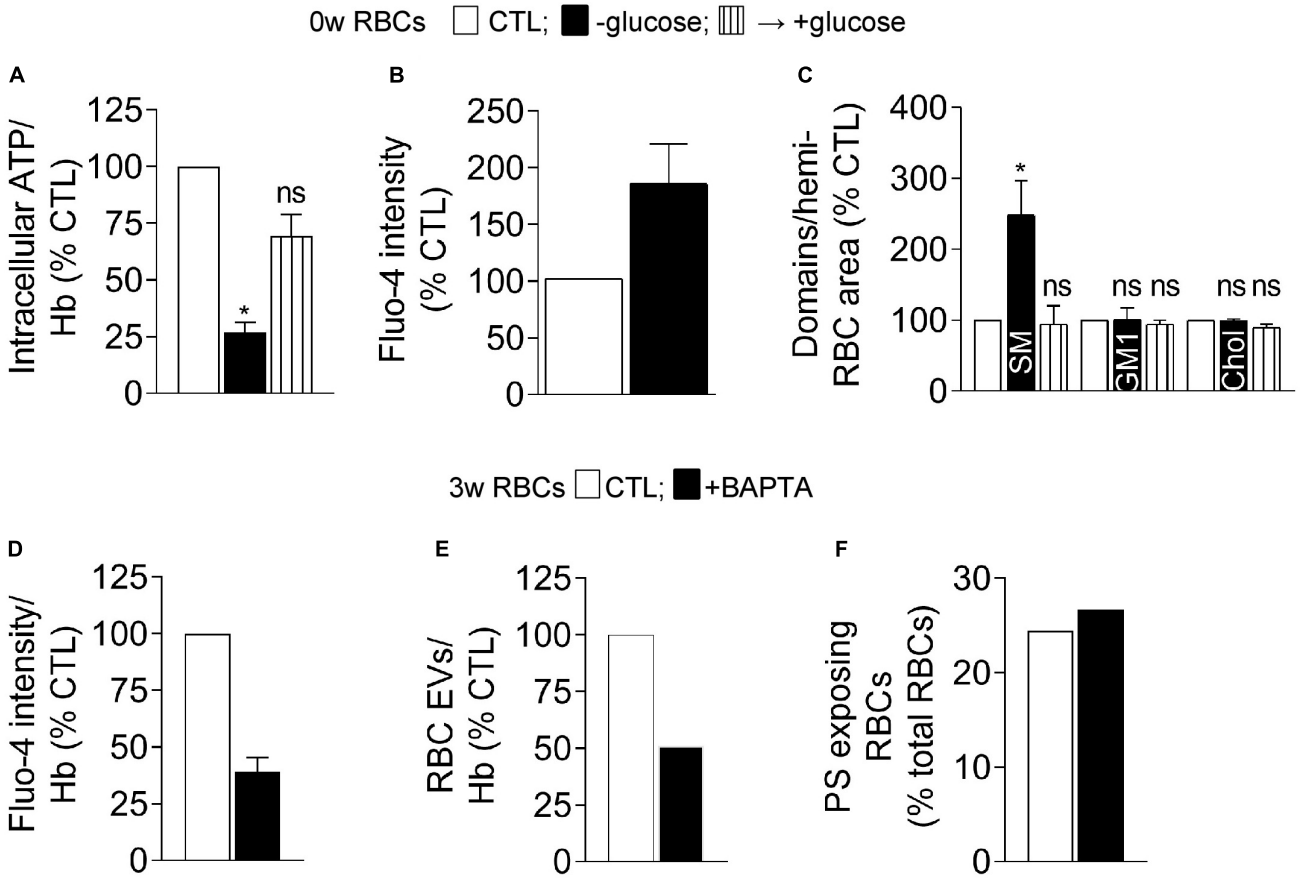

FIGURE 8 | Acute ATP depletion in fresh RBCs increases the calcium content and the abundance of sphingomyelin-enriched domains whereas calcium chelation in 3 week-stored RBCs decreases the extent of vesiculation but not PS externalization. **(A–C)** Isolated fresh RBCs were incubated or not (open columns) in a medium devoid of glucose for 2 h to induce acute ATP depletion, followed or not (-glucose, black columns) by reincubation in a glucose-rich medium for 1 h for ATP repletion (+glucose, stripped black columns). RBCs were then analyzed for ATP content **(A)**, calcium content **(B)**, and abundance of lipid domains **(C)**. **(A)** RBC ATP content determined as in **Figure 1E**. Data were expressed in % of the CTL condition and are means ± SEM of 3 independent experiments (Friedman test followed by Dunn's multiple comparisons test). **(B)** RBC calcium content. RBCs were labeled with Fluo-4-AM as in **Figure 3A**, immobilized on a silicon chamber and observed by fluorescence microscopy under destretching of the chamber for 7 min. Data were expressed in % of the CTL condition and are means ± SD of triplicates from 1 representative experiment out of two. **(C)** RBC lipid domain abundance counted as in **Figure 5**. Means ± SEM of 4–6 experiments (Wilcoxon signed rank test). **(D–F)** RBCs stored for 3 weeks at 4°C were isolated, incubated or not (CTL, open columns) with the intracellular calcium chelator BAPTA-AM (black columns) and analyzed for their calcium content **(D)**, EV production **(E)**, and PS surface exposure **(F)**. **(D)** RBC calcium content determined with Fluo-4-AM as in **Figure 3A**. Data were expressed in % of the CTL condition and are means ± SD from 2 independent experiments. **(E)** Abundance of EVs produced by RBCs. After incubation or not with BAPTA-AM, RBCs were pelleted to collect EV-containing supernatants which were submitted to ultracentrifugation to isolate EVs. EV abundance was then determined by Nanoparticle tracking analysis and normalized to the Hb content (as an estimation of the RBC abundance). Data were expressed in % of the CTL condition. **(F)** Proportion of PS-exposing RBCs determined as in **Figure 4G**. Data were expressed in % of total RBCs. ns, not significant; *$p < 0.05$.

The Abundance of Sphingomyelin-Enriched Domains Is Specifically Increased Both Upon Acute ATP Depletion and aSMase Inhibition

To further test the dependency on ATP of the intracellular calcium content and the sphingomyelin-enriched domain abundance, fresh RBCs were acutely depleted in their ATP content. Upon ∼75% depletion by a 2 h-incubation in glucose-free medium, the intracellular calcium content was almost doubled (**Figures 8A,B**). Sphingomyelin-enriched domain abundance was significantly increased in contrast to GM1- and cholesterol-enriched domains whose abundance remained stable (**Figure 8C**). ATP repletion through addition of glucose-rich medium completely restored the number of sphingomyelin-enriched domains indicating non-toxicity of the treatment (**Figures 8A,C**). These results indicated that sphingomyelin-enriched domains can be modified by the intracellular ATP level, in agreement with observations in stored RBCs upon long term ATP decrease.

To then test the possible link between the aSMase activity and the abundance of sphingomyelin-enriched domains, RBCs were treated with amitriptyline (a functional inhibitor of this enzyme, Dinkla et al., 2012) and evaluated for sphingomyelin-enriched domains. Full aSMase activity inhibition specifically increased the abundance of sphingomyelin- but not GM1-enriched domains

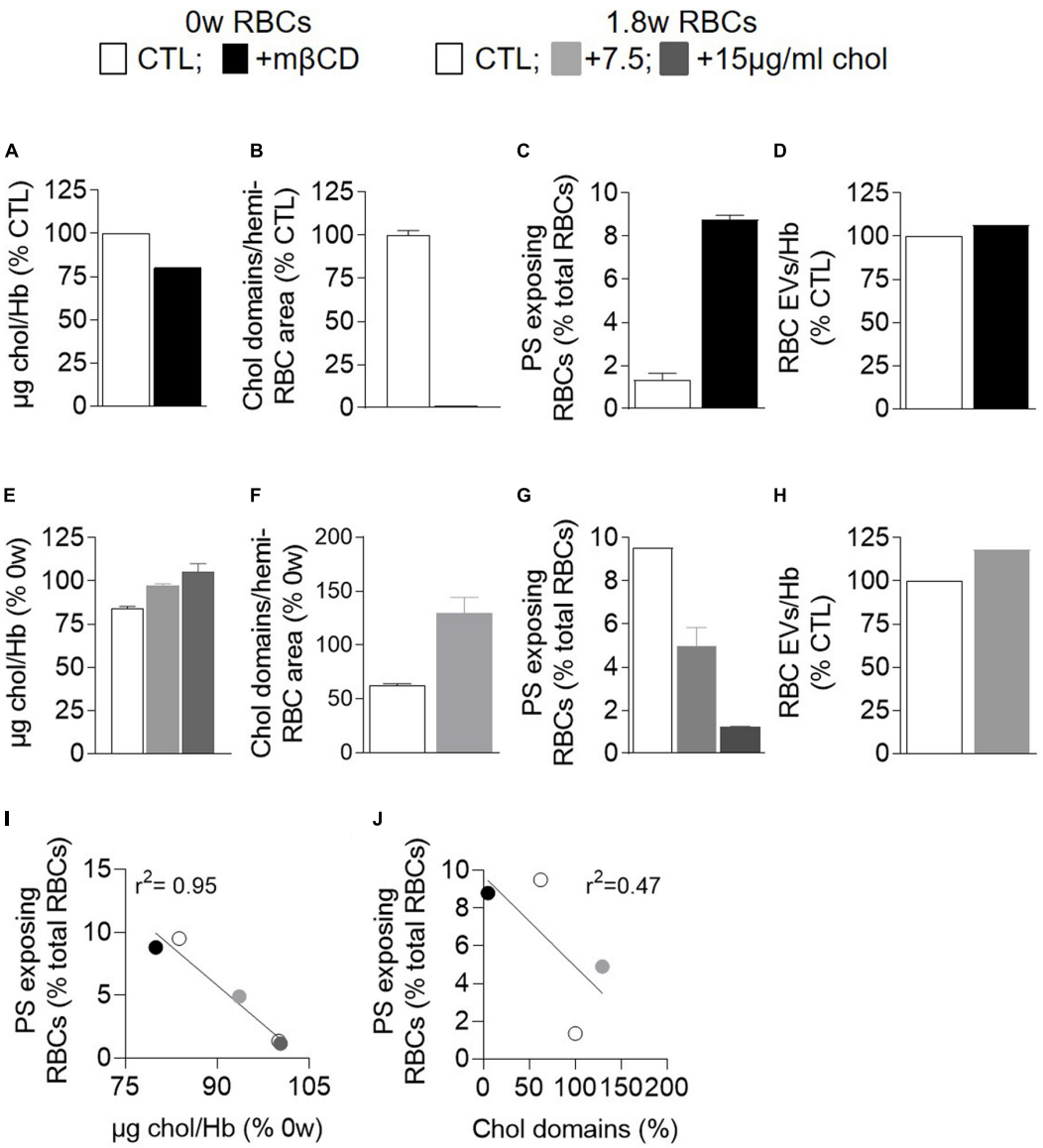

FIGURE 9 | Modulation of the membrane cholesterol content correlates with the extent of PS surface exposure but not with the abundance of RBC EVs. Fresh RBCs were depleted in membrane chol with methyl-β-cyclodextrin (mβCD; **A–D,I,J**; black) whereas 1.8 week-stored RBCs were repleted with water-soluble chol at 7.5 or 15 µg/ml (**E–J**; light and dark gray). All RBCs were then analyzed for their chol content **(A,E)**, chol-enriched domain abundance **(B,F)**, PS surface exposure **(C,G),** and EV release **(D,H)**. **(A,E)** Chol content determined as in **Figure 4A**. Data are from Carquin et al. (2015) in **(A)** and are expressed as % of fresh untreated RBCs in **(E)** (means ± SD of 2 independent experiments). **(B,F)** Abundance of chol-enriched domains. Data were determined at in **Figure 5** and are expressed in % of fresh untreated RBCs (means ± SD of 2 experiments). **(C,G)** PS exposure determined as in **Figure 4G**. Data are means ± SD of 2 independent experiments in **(C)** and of 1 experiment in duplicates in **(G)**. **(D,H)** EV released by RBCs determined as in **Figure 8E**. Data are expressed in % of untreated RBCs. **(I,J)** Correlation between PS surface exposure and the chol content **(I)** or the abundance of chol-enriched domains **(J)**.

(**Supplementary Figure S9**), suggesting that sphingomyelin-enriched domains could be the target of aSMase upon storage.

PS Surface Exposure Is Restored by Cholesterol Supplementation but Not by Calcium Chelation

To finally explore the apparent discrepancy between PS surface exposure and EV release during storage upon additional energy supply despite stable intracellular calcium content (see **Figure 7C**), 3 week-stored RBCs were treated with the intracellular calcium chelator BAPTA-AM. This treatment, which allowed to decrease the free calcium content by ∼65% (**Figure 8D**), declined by half the number of EVs produced by RBCs but did not affect the proportion of PS-exposing cells (**Figures 8E,F**). Those data again supported the absence of direct correlation between PS surface exposure, calcium increase and EV release by RBCs.

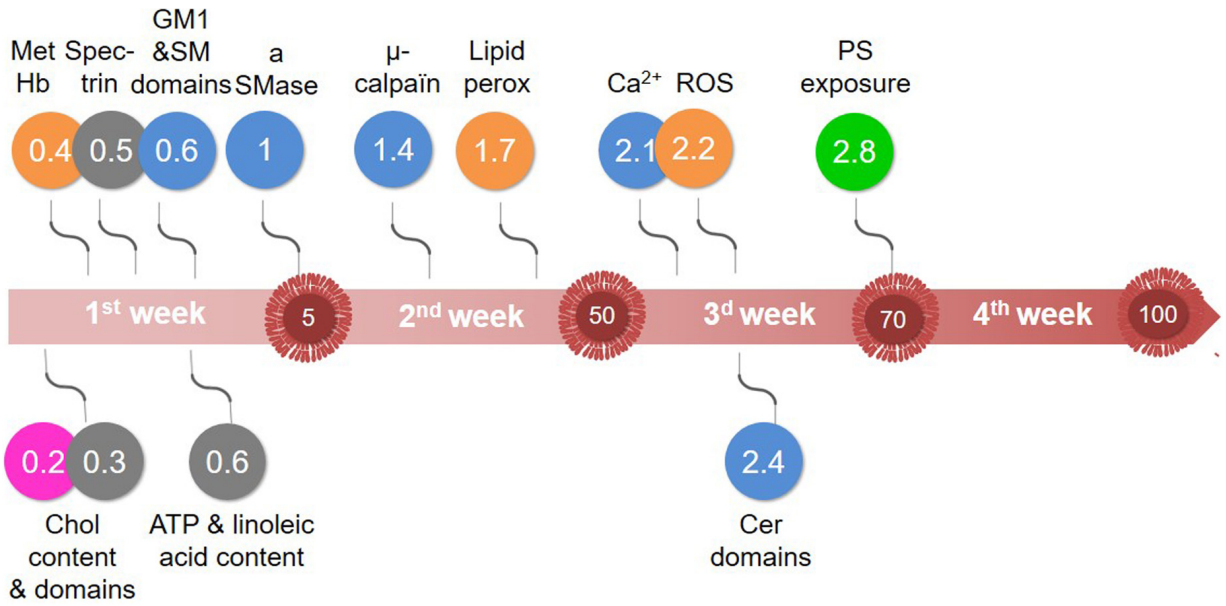

FIGURE 10 | Major vesiculation-related events that take place during RBC storage in K^+/EDTA tubes. Although the sequence of events may depend on the sensitivity of assays used, our data indicate alterations of: (pink) chol-enriched domain abundance; (orange) oxidative stress; (blue) calcium content and aSMase activity, with the increase of sphingomyelin-enriched domains and the decrease of cer-enriched domains; and (green) membrane transversal asymmetry, with the increase of PS surface exposure. Those events are initiated by the rapid decrease of the intracellular ATP content and modifications of the membrane lipid content and the spectrin membrane occupancy (gray). The large red arrow depicts the storage period analyzed in this study. The numbers highlighted inside red EVs indicate the number of EVs released by RBC at the end of each week, as estimated in **Figure 2E**. Events depicted above the arrow are increased by half of their maximal increase at the time indicated in the colored circles. Events depicted below the arrow are decreased by half of their maximal decrease at the time indicated in the circles. For additional explanations, see discussion.

We then tested whether cholesterol-related alterations could increase PS surface exposure. Indeed, cholesterol has been shown to inhibit the RBC scramblase activity at low intracellular calcium concentration (Arashiki and Takakuwa, 2017) and the cholesterol content and cholesterol-enriched domains were decreased upon storage before the free intracellular calcium started to increase (see above). To do so, fresh RBCs were incubated with mβCD to deplete ∼25% cholesterol (**Figure 9A**) and abolish cholesterol-enriched domains (**Figure 9B**). Whereas RBC vesiculation was not modified by this treatment, the proportion of PS-exposing RBCs was increased by ∼5-fold (**Figures 9C,D**), indicating that the alteration of cholesterol content and/or organization into domains could induce PS surface exposure in fresh RBCs and suggesting the implication of cholesterol in PS exposition upon storage.

To test the latter hypothesis, 1.8 week-stored RBCs were repleted with cholesterol through incubation with water soluble cholesterol at two different concentrations (**Figure 9E**). Such cholesterol repletion allowed to recover cholesterol-enriched domains to an even higher extent than on fresh RBCs (**Figure 9F**). The proportion of PS-exposing RBCs declined in a concentration-dependent manner, reaching at the highest concentration the level observed in fresh RBCs (**Figure 9G**), whereas the extent of RBC vesiculation was not modified (**Figure 9H**). Altogether, those data indicated that, as long as the intracellular calcium was low, surface PS exposure depended on the cholesterol content/organization into domains, as revealed by the correlation between those parameters (**Figures 9I,J**). However, as soon as the intracellular calcium increased, this correlation was no longer valid (data not shown), suggesting that other parameters such as calcium increase and ATP depletion also contributed to PS exposure.

DISCUSSION

Evidence for the Modification of the RBC Plasma Membrane Lateral and Transversal Heterogeneity During Storage in K^+/EDTA Tubes and Consequences for the RBC Physiology

Several lines of evidence provided in this study indicated that the RBC plasma membrane was strongly altered during storage in K^+/EDTA tubes. First, the membrane lipid components were not randomly modified during storage, exhibiting a decrease of membrane cholesterol and linoleic acid at the benefit of long chain PUFA and a slight increase of lipid peroxidation. All those lipid modifications should contribute to affect the RBC morphology and functionality since (i) cholesterol and linoleic acid have all a rather fluidizing effect (Heron et al., 1980; Hochgraf et al., 1997), their decline being thus compatible with the increased membrane rigidity revealed by Laurdan and AFM; (ii) long chain PUFA are able to modulate Piezo1 channel

(a mechano-activated ion channel) inactivation by decreasing membrane bending stiffness (Romero et al., 2019); (iii) the increased lipid peroxidation at the inner leaflet alters membrane packing and thickness (Wong-Ekkabut et al., 2007); and (iv) linoleic acid is known for its proinflammatory properties (Pereira et al., 2008; Innes and Calder, 2018). Second, all lipid domains were modified in abundance but not simultaneously neither at the same level nor by the same mechanism, as discussed below. For instance, cholesterol-enriched domains and cholesterol content were decreased very rapidly and simultaneously, which could be highly detrimental for RBCs through: (i) lower RBC deformability and increased elimination in the spleen, since cholesterol deficiency causes impaired RBC osmotic stability during *ex vivo* erythropoiesis (Bernecker et al., 2019) and cholesterol-enriched domains are necessary for the formation of high curvature areas during RBC deformation (Leonard et al., 2017); (ii) PS exposure and subsequent RBC elimination by macrophages, as revealed by the direct correlation between cholesterol content and the extent of PS exposure; and (iii) the increase of membrane rigidity, as revealed by Laurdan and AFM. Those modifications could in turn affect the dynamics of the low RBC curvature-associated domains enriched in GM1 or sphingomyelin, precluding calcium exchanges at the RBC surface (Conrard et al., 2018; Conrard and Tyteca, 2019). Hence, ceramide-enriched domains were lost upon storage, which could be favorable for the RBC as ceramide is known to be involved in several signaling pathways including cell death (Dinkla et al., 2012). Third, lipidomic analysis of EVs indicated their differential lipid enrichment/depletion upon storage, suggesting their shedding from lipid domains at the RBC surface. For instance, ceramide was enriched in EVs after 4 weeks but rather depleted before, in agreement with the late decrease of those domains from the cell surface. In contrast, sphingomyelin and phosphatidylcholine species, which were not expected to be lost from the cell surface based on the increased abundance of corresponding domains, were accordingly depleted in EVs upon storage. Fourth, the increased PS exposure during the first 2 weeks correlated with the level of membrane cholesterol while the later PS exposure correlated with the increased calcium concentration.

Implication of the Modification of the Plasma Membrane Lateral Heterogeneity for RBC Vesiculation During Storage in K^+/EDTA Tubes

We have previously proposed that lipid domains could represent platforms for vesicle biogenesis and shedding (Pollet et al., 2018). This hypothesis was based on the fact that domains are less ordered than the rest of the membrane, which causes a line tension and in turn induces vesiculation (Leonard et al., 2018). However, although all the types of domains are less ordered than the rest of the membrane (Conrard et al., 2018; Leonard et al., 2018), only those enriched in cholesterol and ceramide were able to vesiculate, suggesting a fine tuning of lipid domain dynamics at the RBC surface and specific triggering events for their vesiculation.

For cholesterol-enriched domains (**Figure 10**, pink), this triggering event could be the increased membrane rigidity resulting from the alteration of both membrane lipid FA composition and membrane:cytoskeleton anchorage. Since cholesterol-enriched domains are particularly abundant in high curvature areas of resting RBCs where they exhibit the highest lipid order that can be found in lipid domains (Conrard et al., 2018) they represent the best target for EV release. This increased rigidity upon storage will create a line tension between the bulk membrane and cholesterol-enriched domains, which is then abrogated by vesiculation (Vind-Kezunovic et al., 2008). Those data indicate that EV shedding depends on cholesterol, in agreement with the hypothesis that the RBC membrane cholesterol content is declined by the release of cholesterol-enriched EVs (Santos et al., 2005) and with the increased number of EVs released upon low concentrations of mβCD to remove part of the membrane cholesterol (Gonzalez et al., 2009).

For sphingomyelin-enriched domains, the starting point could be the aSMase activation. Indeed, RBC exposure to the enzyme appeared to correlate with the release of EVs (Dinkla et al., 2012) and treatment with AMI (a functional enzyme inhibitor) is known to reduce vesiculation during storage (Hoehn et al., 2017). We showed here that the activity of aSMase increased in two stages during storage; first gradually, reaching at 4 weeks an activity six times higher than its initial activity; and then still three times more. This second peak of activity could be explained by the increased acidification of the plasma (Salzer et al., 2008) but this remains to be tested. Regarding the first increase, it correlated with the increased abundance of sphingomyelin-enriched domains and was followed by the decreased abundance of ceramide-enriched domains from the 3rd week of storage, suggesting that sphingomyelin clustering at the RBC surface represented a preferential target for aSMase activity (**Figure 10**, blue). However, the link between ceramide production and membrane blebbing is still unclear. Alterations of the membrane biophysical properties due to ceramide generation could partly provide this link, based on the following features. First, in agreement with (Fanani et al., 2009; Henry et al., 2013), we reported the ability of ceramide to form domains. Second, ceramide has a cone-shaped structure that can give a spontaneous curvature to the membrane. This property, combined with the fact that ceramide generated in the external leaflet may be redistributed to the inner one, could lead to membrane evagination (Lopez-Montero et al., 2005; Verderio et al., 2018).

The key question was whether the number of cholesterol- and ceramide-enriched domains lost could correspond to the number of EVs released per RBC each week. The abundance of EVs released per RBC rose from 5 after 1 week to ∼100 EVs after 4 weeks of storage (**Figure 10**, timeline), which is faster than in RBCs *in vivo* [up to 230 EVs during their 120 day-lifetime; Said and Doctor, 2017) and in RBC concentrates (Almizraq et al., 2013), mainly due to the absence of an energy source. Such fast RBC membrane area loss by vesiculation was supported by the increase of the spectrin occupancy per RBC area already after the 1st week of storage, which suggested spectrin-depleted EV release. Cholesterol-enriched domains decreased by ∼25%

during the 1st week, which represented a loss of ∼4 domains per RBC, close to the 5 EVs measured at the end of the 1st week. Ceramide-enriched domains decreased in abundance during the 3rd week of storage, period during which ∼20 EVs were released by one RBC. Since those domains appeared to partially originate from the sphingomyelin-enriched domains which increased in abundance upon time, it is difficult to estimate the extent of their decrease. Thus, although lipid domain loss was compatible with a vesiculation-related process, they only represented a part of EVs released from RBCs, suggesting additional events, as discussed in the next two sections.

Interplay With the Calcium-Based Model

We showed that calcium accumulated in RBCs upon storage in K^+/EDTA tubes. As EDTA did not appear to completely chelate calcium in the extracellular medium, calcium accumulation in RBCs could result from calcium entry from the plasma. Furthermore, the plasma calcium concentration could be modified upon storage through calcium release by platelets and leukocytes upon death, eventually leading to calcium capture by RBCs. In terms of succession of events (**Figure 10**, blue), two events started to increase before calcium accumulates, i.e., the μ-calpain activity, which is not surprising based on its strong affinity for calcium (Bogdanova et al., 2013), and the PS surface exposure. Thus, PS exposure did not only depend on the calcium-dependent scramblase activation, as further supported by two other lines of evidence: (i) upon glucose addition to the blood tubes before storage, PS exposure was clearly visible despite normal intracellular calcium level; and (ii) PS exposure directly correlated with the membrane cholesterol content, as revealed by cholesterol depletion of fresh RBCs and cholesterol repletion of 1.8 week-old RBCs, in agreement with (Arashiki and Takakuwa, 2017). According to this model, cholesterol could act as a scramblase inhibitor, as a first indication of the interplay between the calcium-based model and membrane lipid alteration during storage.

The accumulation of the calcium itself occurred later, when ATP was no more detectable. Such accumulation therefore probably resulted from the shutdown of the plasma membrane calcium ATPase (PMCA) (Bogdanova et al., 2013). Moreover, several lines of evidence suggested that calcium accumulation also resulted from modifications of the biophysical properties of sphingomyelin-enriched domains during storage. We indeed previously showed the increased abundance of sphingomyelin-enriched domains during calcium efflux after RBC deformation. Since PMCA is the only calcium efflux pump in RBCs, we suggested at that time the implication of the sphingomyelin-enriched domains in the recruitment of PMCA and/or regulation of its activity. Since the aSMase activity increased during storage exactly after the increase of the abundance of sphingomyelin-enriched domains and because the inhibition of this enzyme by AMI also increased the abundance of these domains while decreasing the level of intracellular calcium (data not shown), we suggest that the modification of sphingomyelin-enriched domain biophysical properties (such as fluidity and curvature) through aSMase attack could alter the PMCA activity which requires an optimal environment in terms of fluidity (Tang et al., 2006). According to this model, the aSMase acts as a triggering event leading to sphingomyelin domain biophysical properties alteration, as a second indication of the interplay between the calcium-based model and membrane alteration during storage.

Interplay With the Oxidative Stress-Based Model

We also confirmed the implication of the oxidative stress during storage. The first event detected was the oxidation of Hb into metHb followed by the oxidation of membrane lipids and ROS accumulation (**Figure 10**, orange). The fact that metHb accumulated before free ROS could result from the fact that under the storage conditions of tubes, the external O_2 can diffuse. As a result, Hb is likely to be subject to a constant risk of auto-oxidation and as the antioxidant system becomes ineffective more quickly, metHb could accumulate without ROS at the beginning. In addition, Hb is both the source and the major target of these species. It could therefore serve as a buffer preventing their accumulation for a time. After 1 week of storage, the metHb did not increase anymore in contrast to free ROS, which could be due to the fact that metHb can be irreversibly transformed into hemichrome (Pauling and Coryell, 1936). While we did not measure the interaction between oxidized Hb and the membrane, such interaction could be reflected in the increase of the membrane stiffness during storage (Leonard et al., 2018). A long time after metHb production started the accumulation of ROS and the increase in lipid peroxidation which was surprisingly very low as compared to RBC concentrates (D'alessandro et al., 2012) a discrepancy that could result from the fact that we only measured malondialdehyde, one of the three products of lipid peroxidation besides isoprostanes and 4-hydroxynonenal (Janero, 1990).

The mechanism of oxidative stress appeared to act independently of the calcium accumulation and aSMase activity, as shown after supplementing the tubes with glucose. Nevertheless, since metHb increased before the first calcium-dependent event (i.e., the boost of calpain activity) and since acute ATP depletion (a condition not expected to lead to metHb accumulation) increased the abundance of sphingomyelin-enriched domains to a lower extent than upon similar ATP depletion obtained during storage, it is most than likely that the oxidative stress will influence the calcium- and aSMase-based models. This could occur through the accumulation of oxidized forms of Hb at the membrane (Kriebardis et al., 2007), and the resulting membrane cytoskeleton interaction alteration which could in turn increase the abundance of sphingomyelin-enriched domains, as previously shown (D'auria et al., 2013). Alternatively, oxidative stress could decrease the PMCA activity, as already shown in neurodegenerative diseases (Gorlach et al., 2015).

Hypothetical Model for the Succession of Events Leading to RBC Vesiculation in K^+/EDTA Tubes

Based on data in tubes supplemented or not with glucose, we propose the following model. The first event was the decrease of cholesterol-enriched domain abundance whatever glucose

supplementation or not, suggesting an ATP-independent process (**Figure 10**, pink). The second event, which started to increase when the ATP was ∼30% and represented the main contributor to blood EV release, was the oxidative stress (**Figure 10**, orange). The third event was the calcium/aSMase. This model was less ATP-dependent but appeared related to the increase of sphingomyelin-enriched domains, the increased activity of aSMase and the alteration of sphingomyelin domain biophysical properties, leading to calcium accumulation and ceramide-enriched domain formation and vesiculation (**Figure 10**, blue). The fourth ultimate event occurred during the 4th week and was marked by PS externalization (**Figure 10**, green). In conclusion, we have shown that the modulation of lipid domains plays a significant role in the RBC vesiculation, releasing EVs of various lipid composition upon storage in tubes, but oxidative stress and PS exposure are also major events. The next step will be to test the relevance of those mechanisms to RBC vesiculation in blood bags before transfusion.

DATA AVAILABILITY STATEMENT

All datasets generated for this study are included in the article/**Supplementary Material**.

ETHICS STATEMENT

The study was approved by the Medical Ethics Committee of the University of Louvain, Brussels, Belgium. The participants gave written informed consent.

AUTHOR CONTRIBUTIONS

A-SC and DT designed the experiments, analyzed and interpreted the data, and wrote the manuscript. MG and HP collected and analyzed the data. AS and JV were in charge of lipid imaging and quantification. ND assisted to flow cytometry experiments. LD'A assisted to nanoparticle tracking analysis. RT and GM were responsible for lipidomics on sorted EVs. EM and YL were responsible for fatty acid analysis on RBCs. PVDS did all the electron microscopy experiments. All the authors reviewed the final version of the manuscript.

FUNDING

This work was supported by grants from the UCLouvain (FSR and Actions de Recherche Concertées, ARC), the F.R.S-FNRS, and the Salus Sanguinis Foundation.

ACKNOWLEDGMENTS

We thank Drs. A. Miyawaki, M. Abe, and T. Kobayashi (Riken Brain Science Institute, Saitama, Japan and University of Strasbourg, France) as well as H. Mizuno (KU Leuven, Belgium) for generously supplying the Dronpa-theta-D4 plasmid. We also thank Dr. L. Gatto (de Duve Institute, UCLouvain) for supporting us with statistical analyses, and Dr. S. Horman (IREC Institute, UCLouvain) for providing us platelet lysates to confirm purity of sorted EVs. The MASSMET platform (UCLouvain) is acknowledged for the access to the LC-MS equipment. We also thank Drs. A. Rapaille and T. Najdovski (Croix-Rouge de Belgique) for providing us access to the equipment for plasmatic pH measurements.

SUPPLEMENTARY MATERIAL

The Supplementary Material for this article can be found online at: https://www.frontiersin.org/articles/10.3389/fphys.2020.00712/full#supplementary-material

FIGURE S1 | Fresh RBCs in K^+/EDTA, heparin or citrate tubes exhibit similar intracellular ATP and calcium contents. Fresh isolated RBCs from K^+/EDTA, heparin or citrate tubes were analyzed for their intracellular ATP **(A)** and calcium contents **(B,C)**. Data are expressed as % of K^+/EDTA tubes. **(A)** Intracellular ATP content, determined as in **Figure 1E**. Means ± SEM of 4 independent experiments for heparin tubes (Mann–Whitney *U* test) and means ± SD of 2 independent experiments for citrate tubes. **(B)** Calcium content in heparin *vs.* K^+/EDTA tubes, assessed as in **Figure 3A**. Means ± SD of triplicates. **(C)** Calcium content in citrate *vs.* K^+/EDTA tubes. RBCs were labeled with Fluo-4 AM and analyzed by flow cytometry. The MFI of the RBC population was then determined. Data are means ± SEM of 4 independent experiments.

FIGURE S2 | The global RBC intracellular hemoglobin content starts to decrease from 3 weeks of storage in K^+/EDTA tubes. Global Hb content was determined by spectrophotometry at 450 nm upon storage to normalize contents in intracellular ATP **(A)**, intracellular calcium **(B)**, membrane chol **(C)** and membrane lipid peroxidation **(D)**. Data represented Hb absorbance values based on the quantity of RBCs engaged in each type of test (means ± SEM of 1–3 independent experiments).

FIGURE S3 | Flow cytometry allows to distinguish EVs released by RBCs *vs.* those released by platelets. EVs were isolated from plasma by ultracentrifugation and labeled with CFSE, a general EV marker, and with fluorescent anti-GPA and anti-CD41 antibodies to identify EVs released by RBCs and platelets, respectively. EVs were increasingly diluted according to the storage time of the blood sample to avoid overcharge of the cytometer. The side scatter (SSC) *vs.* CFSE profiles and the anti-CD41-PE *vs.* anti-GPA-AlexaFluor647 profiles were gathered. Representative plots are shown.

FIGURE S4 | Flow cytometry analysis upon storage reveals a single population of H_2DCFDA-labeled RBCs with higher median fluorescence intensity which contrasts with distinct populations of Annexin V-labeled RBCs without fluorescence increase. RBCs were labeled with H_2DCFDA to determine the intracellular ROS content **(A)** or with Annexin V-FITC to evaluate PS surface exposure **(B,C)** and analyzed by flow cytometry. **(A)** Representative plots of RBCs labeled with H_2DCFDA upon storage. **(B)** MFI values determined with FlowJo of the global RBC population labeled with Annexin V-FITC (means ± SEM of 3 independent experiments). **(C)** Representative plots of RBCs labeled with Annexin V.

FIGURE S5 | Membrane lipid order increases upon storage. Fresh (0w) or 2 week-stored RBCs (2w) were labeled with Laurdan, spread on PLL-coated coverslips and observed by vital multiphoton microscopy. Discocytes (disco) were distinguished from spherocytes (sphero) based on size and circularity. **(A)** Representative vital imaging. **(B)** Quantification of hemi-RBC area after 2 weeks of storage. **(C)** Quantification of membrane generalized polarization (GP) values for discocytes and spherocytes after 2 weeks of storage. Images are representative from 2 independent experiments and results are means ± SEM of 37–231 RBCs (one-way ANOVA followed by Tukey's *post hoc* test). Adapted from Leonard et al. (2018).

FIGURE S6 | Plasmatic pH levels are only very slightly decreased upon storage. Plasmatic pH levels were determined in 0–4 week-stored blood samples with the GEM PREMIER 3500.

FIGURE S7 | RBC- and platelet-derived EVs are successfully sorted by magnetic force. EVs were isolated by ultracentrifugation from plasmas of K^+/EDTA tubes stored for 0.9 and 1.3 weeks at 4°C. EVs released from RBCs were then sorted through incubation with magnetic beads coupled to anti-GPA antibodies by magnetic force. The sorted EVs were then analyzed by Western Blot for the presence of GPA to confirm successful sorting **(A)** and CD41 to exclude contamination **(B)**. A platelet lysate and EVs isolated from 1.3 weeks-stored tubes but not sorted were used as internal controls.

FIGURE S8 | RBC-derived EVs are enriched in lysophosphatidylinositol and lysophosphatidylglycerol species but depleted in their precursors at the end of storage. RBC-released EVs were isolated from total blood EVs by immunopurification and analyzed by LC-MS for their content in: **(A,B)** phosphatidylinositol (PI) and lysoPI species; **(C–E)** phosphatidylglycerol (PG, further classified according to the length of their carbon chains) and lysoPG species; and **(F–H)** phosphatidylethanolamine (PE, further classified according to the length of their carbon chains) and lysoPE species. Each curve depicts one lipid species; circle, saturated lipid; triangle, lipid containing at least one MUFA; inverted triangle, lipid containing at least one PUFA; black to light gray colors, short to long carbon chains. All data are expressed as % of the EVs stored for 1 week and are means ± SD of 4 replicates from 1 experiment representative of 2.

FIGURE S9 | Inhibition of the aSMase activity by amitriptyline specifically increases the abundance of sphingomyelin-enriched domains. Whole blood was incubated or not (CTL, open columns) with amitriptyline (+AMI, black columns) for 1h. Isolated plasmas were then tested for aSMase activity **(A)** while isolated RBCs were analyzed for the abundance of lipid domains **(B)**. **(A)** aSMase activity determined as in **Figure 4H**. Data are expressed in % of CTL. **(B)** Sphingomyelin (SM)- and GM1-enriched domain abundance determined as in **Figure 5**. Data are expressed in % of CTL (means ± SEM of 3–4 independent experiments; Wilcoxon signed rank test).

REFERENCES

Alaarg, A., Schiffelers, R. M., Van Solinge, W. W., and Van Wijk, R. (2013). Red blood cell vesiculation in hereditary hemolytic anemia. *Front. Physiol.* 4:365. doi: 10.3389/fphys.2013.00365

Allan, D., Thomas, P., and Limbrick, A. R. (1980). The isolation and characterization of 60 nm vesicles ('nanovesicles') produced during ionophore A23187-induced budding of human erythrocytes. *Biochem. J.* 188, 881–887. doi: 10.1042/bj1880881

Almizraq, R., Tchir, J. D., Holovati, J. L., and Acker, J. P. (2013). Storage of red blood cells affects membrane composition, microvesiculation, and in vitro quality. *Transfusion* 53, 2258–2267.

Almizraq, R. J., Holovati, J. L., and Acker, J. P. (2018). Characteristics of extracellular vesicles in red blood concentrates change with storage time and blood manufacturing method. *Transfus. Med. Hemother.* 45, 185–193. doi: 10.1159/000486137

Antonelou, M. H., and Seghatchian, J. (2016). Update on extracellular vesicles inside red blood cell storage units: adjust the sails closer to the new wind. *Transfus. Apher. Sci.* 55, 92–104. doi: 10.1016/j.transci.2016.07.016

Arashiki, N., and Takakuwa, Y. (2017). Maintenance and regulation of asymmetric phospholipid distribution in human erythrocyte membranes: implications for erythrocyte functions. *Curr. Opin. Hematol.* 24, 167–172. doi: 10.1097/moh.0000000000000326

Arisawa, K., Mitsudome, H., Yoshida, K., Sugimoto, S., Ishikawa, T., Fujiwara, Y., et al. (2016). Saturated fatty acid in the phospholipid monolayer contributes to the formation of large lipid droplets. *Biochem. Biophys. Res. Commun.* 480, 641–647. doi: 10.1016/j.bbrc.2016.10.109

Bernecker, C., Kofeler, H., Pabst, G., Trotzmuller, M., Kolb, D., Strohmayer, K., et al. (2019). Cholesterol deficiency causes impaired osmotic stability of cultured red blood cells. *Front. Physiol.* 10:1529. doi: 10.3389/fphys.2013.001529

Bogdanova, A., Makhro, A., Wang, J., Lipp, P., and Kaestner, L. (2013). Calcium in red blood cells-a perilous balance. *Int. J. Mol. Sci.* 14, 9848–9872. doi: 10.3390/ijms14059848

Carquin, M., Conrard, L., Pollet, H., Van Der Smissen, P., Cominelli, A., Veiga-Da-Cunha, M., et al. (2015). Cholesterol segregates into submicrometric domains at the living erythrocyte membrane: evidence and regulation. *Cell. Mol. Life Sci.* 72, 4633–4651. doi: 10.1007/s00018-015-1951-x

Carquin, M., D'auria, L., Pollet, H., Bongarzone, E. R., and Tyteca, D. (2016). Recent progress on lipid lateral heterogeneity in plasma membranes: From rafts to submicrometric domains. *Prog. Lipid Res.* 62, 1–24. doi: 10.1016/j.plipres.2015.12.004

Carquin, M., Pollet, H., Veiga-Da-Cunha, M., Cominelli, A., Van Der Smissen, P., N'kuli, F., et al. (2014). Endogenous sphingomyelin segregates into submicrometric domains in the living erythrocyte membrane. *J. Lipid Res.* 55, 1331–1342. doi: 10.1194/jlr.m048538

Chung, H. J., Chung, J. W., Yi, J., Hur, M., Lee, T. H., Hwang, S. H., et al. (2020). Automation of Harboe method for the measurement of plasma free hemoglobin. *J. Clin. Lab. Anal.* 2020:e23242.

Ciana, A., Achilli, C., Gaur, A., and Minetti, G. (2017a). Membrane remodelling and vesicle formation during ageing of human red blood cells. *Cell. Physiol. Biochem.* 42, 1127–1138. doi: 10.1159/000478768

Ciana, A., Achilli, C., and Minetti, G. (2017b). Spectrin and other membrane-skeletal components in human red blood cells of different age. *Cell. Physiol. Biochem.* 42, 1139–1152. doi: 10.1159/000478769

Conrard, L., Stommen, A., Cloos, A. S., Steinkuhler, J., Dimova, R., Pollet, H., et al. (2018). Spatial relationship and functional relevance of three lipid domain populations at the erythrocyte surface. *Cell Physiol. Biochem.* 51, 1544–1565. doi: 10.1159/000495645

Conrard, L., and Tyteca, D. (2019). Regulation of membrane calcium transport proteins by the surrounding lipid environment. *Biomolecules* 9:513. doi: 10.3390/biom9100513

D'alessandro, A., D'amici, G. M., Vaglio, S., and Zolla, L. (2012). Time-course investigation of SAGM-stored leukocyte-filtered red bood cell concentrates: from metabolism to proteomics. *Haematologica* 97, 107–115. doi: 10.3324/haematol.2011.051789

D'alessandro, A., Liumbruno, G., Grazzini, G., and Zolla, L. (2010). Red blood cell storage: the story so far. *Blood Transfus.* 8, 82–88.

D'auria, L., Fenaux, M., Aleksandrowicz, P., Van Der Smissen, P., Chantrain, C., Vermylen, C., et al. (2013). Micrometric segregation of fluorescent membrane lipids: relevance for endogenous lipids and biogenesis in erythrocytes. *J. Lipid Res.* 54, 1066–1076. doi: 10.1194/jlr.m034314

Dinkla, S., Wessels, K., Verdurmen, W. P., Tomelleri, C., Cluitmans, J. C., Fransen, J., et al. (2012). Functional consequences of sphingomyelinase-induced changes in erythrocyte membrane structure. *Cell Death Dis.* 3:e410. doi: 10.1038/cddis.2012.143

Donadee, C., Raat, N. J., Kanias, T., Tejero, J., Lee, J. S., Kelley, E. E., et al. (2011). Nitric oxide scavenging by red blood cell microparticles and cell-free hemoglobin as a mechanism for the red cell storage lesion. *Circulation* 124, 465–476. doi: 10.1161/circulationaha.110.008698

Fanani, M. L., De Tullio, L., Hartel, S., Jara, J., and Maggio, B. (2009). Sphingomyelinase-induced domain shape relaxation driven by out-of-equilibrium changes of composition. *Biophys. J.* 96, 67–76. doi: 10.1529/biophysj.108.141499

Ferain, A., Bonnineau, C., Neefs, I., Rees, J. F., Larondelle, Y., Schamphelaere, K. A., et al. (2016). The fatty acid profile of rainbow trout liver cells modulates their tolerance to methylmercury and cadmium. *Aquat. Toxicol.* 177, 171–181. doi: 10.1016/j.aquatox.2016.05.023

Golfetto, O., Hinde, E., and Gratton, E. (2013). Laurdan fluorescence lifetime discriminates cholesterol content from changes in fluidity in living cell membranes. *Biophys. J.* 104, 1238–1247. doi: 10.1016/j.bpj.2012.12.057

Gonzalez, L. J., Gibbons, E., Bailey, R. W., Fairbourn, J., Nguyen, T., Smith, S. K., et al. (2009). The influence of membrane physical properties on microvesicle release in human erythrocytes. *PMC Biophys.* 2:7. doi: 10.1186/1757-5036-2-7

Gorlach, A., Bertram, K., Hudecova, S., and Krizanova, O. (2015). Calcium and ROS: A mutual interplay. *Redox Biol.* 6, 260–271. doi: 10.1016/j.redox.2015.08.010

Grimm, M. O., Grimm, H. S., Patzold, A. J., Zinser, E. G., Halonen, R., Duering, M., et al. (2005). Regulation of cholesterol and sphingomyelin metabolism by amyloid-beta and presenilin. *Nat. Cell Biol.* 7, 1118–1123. doi: 10.1038/ncb1313

Guillemot-Legris, O., Masquelier, J., Everard, A., Cani, P. D., Alhouayek, M., and Muccioli, G. G. (2016). High-fat diet feeding differentially affects the development of inflammation in the central nervous system. *J. Neuroinflamm.* 13:206.

Henry, B., Ziobro, R., Becker, K. A., Kolesnick, R., and Gulbins, E. (2013). Acid sphingomyelinase. *Handb. Exp. Pharmacol.* 215, 77–88.

Heron, D. S., Shinitzky, M., Hershkowitz, M., and Samuel, D. (1980). Lipid fluidity markedly modulates the binding of serotonin to mouse brain membranes. *Proc. Natl. Acad. Sci. U.S.A.* 77, 7463–7467. doi: 10.1073/pnas.77.12.7463

Hochgraf, E., Mokady, S., and Cogan, U. (1997). Dietary oxidized linoleic acid modifies lipid composition of rat liver microsomes and increases their fluidity. *J. Nutr.* 127, 681–686. doi: 10.1093/jn/127.5.681

Hoehn, R. S., Jernigan, P. L., Japtok, L., Chang, A. L., Midura, E. F., Caldwell, C. C., et al. (2017). Acid sphingomyelinase inhibition in stored erythrocytes reduces transfusion-associated lung inflammation. *Ann. Surg.* 265, 218–226. doi: 10.1097/sla.0000000000001648

Innes, J. K., and Calder, P. C. (2018). Omega-6 fatty acids and inflammation. *Prostagland. Leukot Essent. Fatty Acids* 132, 41–48. doi: 10.1016/j.plefa.2018.03.004

Italiano, J. E. Jr., Mairuhu, A. T., and Flaumenhaft, R. (2010). Clinical relevance of microparticles from platelets and megakaryocytes. *Curr. Opin. Hematol.* 17, 578–584. doi: 10.1097/moh.0b013e32833e77ee

Janero, D. R. (1990). Malondialdehyde and thiobarbituric acid-reactivity as diagnostic indices of lipid peroxidation and peroxidative tissue injury. *Free Radic. Biol. Med.* 9, 515–540. doi: 10.1016/0891-5849(90)90131-2

Jank, H., and Salzer, U. (2011). Vesicles generated during storage of red blood cells enhance the generation of radical oxygen species in activated neutrophils. *Sci. World J.* 11, 173–185. doi: 10.1100/tsw.2011.25

Kaestner, L., Tabellion, W., Weiss, E., Bernhardt, I., and Lipp, P. (2006). Calcium imaging of individual erythrocytes: problems and approaches. *Cell Calcium* 39, 13–19. doi: 10.1016/j.ceca.2005.09.004

Kriebardis, A. G., Antonelou, M. H., Stamoulis, K. E., Economou-Petersen, E., Margaritis, L. H., and Papassideri, I. S. (2007). Progressive oxidation of cytoskeletal proteins and accumulation of denatured hemoglobin in stored red cells. *J. Cell Mol. Med.* 11, 148–155. doi: 10.1111/j.1582-4934.2007.00008.x

Lahdesmaki, K., Ollila, O. H., Koivuniemi, A., Kovanen, P. T., and Hyvonen, M. T. (2010). Membrane simulations mimicking acidic pH reveal increased thickness and negative curvature in a bilayer consisting of lysophosphatidylcholines and free fatty acids. *Biochim. Biophys. Acta* 1798, 938–946. doi: 10.1016/j.bbamem.2010.01.020

Leonard, C., Conrard, L., Guthmann, M., Pollet, H., Carquin, M., Vermylen, C., et al. (2017). Contribution of plasma membrane lipid domains to red blood cell (re)shaping. *Sci. Rep.* 7:4264.

Leonard, C., Pollet, H., Vermylen, C., Gov, N., Tyteca, D., and Mingeot-Leclercq, M. P. (2018). Tuning of differential lipid order between submicrometric domains and surrounding membrane upon erythrocyte reshaping. *Cell Physiol. Biochem.* 48, 2563–2582. doi: 10.1159/000492700

Lopez-Montero, I., Rodriguez, N., Cribier, S., Pohl, A., Velez, M., and Devaux, P. F. (2005). Rapid transbilayer movement of ceramides in phospholipid vesicles and in human erythrocytes. *J. Biol. Chem.* 280, 25811–25819. doi: 10.1074/jbc.m412052200

Minetti, G., Achilli, C., Perotti, C., and Ciana, A. (2018). Continuous change in membrane and membrane-skeleton organization during development from proerythroblast to senescent red blood cell. *Front. Physiol.* 9:286. doi: 10.3389/fphys.2018.00286

Minetti, G., Bernecker, C., Dorn, I., Achilli, C., Bernuzzi, S., Perotti, C., et al. (2020). Membrane rearrangements in the maturation of circulating human reticulocytes. *Front. Physiol.* 11:215. doi: 10.3389/fphys.2020.00215

Mutemberezi, V., Masquelier, J., Guillemot-Legris, O., and Muccioli, G. G. (2016). Development and validation of an HPLC-MS method for the simultaneous quantification of key oxysterols, endocannabinoids, and ceramides: variations in metabolic syndrome. *Anal. Bioanal. Chem.* 408, 733–745. doi: 10.1007/s00216-015-9150-z

Nguyen, D. B., Ly, T. B., Wesseling, M. C., Hittinger, M., Torge, A., Devitt, A., et al. (2016). Characterization of microvesicles released from human red blood cells. *Cell Physiol. Biochem.* 38, 1085–1099. doi: 10.1159/000443059

Pauling, L., and Coryell, C. D. (1936). The magnetic properties and structure of the hemochromogens and related substances. *Proc. Natl. Acad. Sci. U.S.A.* 22, 159–163. doi: 10.1073/pnas.22.3.159

Pereira, L. M., Hatanaka, E., Martins, E. F., Oliveira, F., Liberti, E. A., Farsky, S. H., et al. (2008). Effect of oleic and linoleic acids on the inflammatory phase of wound healing in rats. *Cell Biochem. Funct.* 26, 197–204. doi: 10.1002/cbf.1432

Pollet, H., Conrard, L., Cloos, A. S., and Tyteca, D. (2018). Plasma membrane lipid domains as platforms for vesicle biogenesis and shedding? *Biomolecules* 8:94. doi: 10.3390/biom8030094

Ratanasopa, K., Strader, M. B., Alayash, A. I., and Bulow, L. (2015). Dissection of the radical reactions linked to fetal hemoglobin reveals enhanced pseudoperoxidase activity. *Front. Physiol.* 6:39. doi: 10.3389/fphys.2013.0039

Rise, P., Eligini, S., Ghezzi, S., Colli, S., and Galli, C. (2007). Fatty acid composition of plasma, blood cells and whole blood: relevance for the assessment of the fatty acid status in humans. *Prostagland. Leukot Essent. Fatty Acids* 76, 363–369. doi: 10.1016/j.plefa.2007.05.003

Romero, L. O., Massey, A. E., Mata-Daboin, A. D., Sierra-Valdez, F. J., Chauhan, S. C., Cordero-Morales, J. F., et al. (2019). Dietary fatty acids fine-tune Piezo1 mechanical response. *Nat. Commun.* 10:1200.

Rubin, O., Delobel, J., Prudent, M., Lion, N., Kohl, K., Tucker, E. I., et al. (2013). Red blood cell-derived microparticles isolated from blood units initiate and propagate thrombin generation. *Transfusion* 53, 1744–1754. doi: 10.1111/trf.12008

Said, A. S., and Doctor, A. (2017). Influence of red blood cell-derived microparticles upon vasoregulation. *Blood Transfus.* 15, 522–534.

Salzer, U., Hinterdorfer, P., Hunger, U., Borken, C., and Prohaska, R. (2002). Ca(++)-dependent vesicle release from erythrocytes involves stomatin-specific lipid rafts, synexin (annexin VII), and sorcin. *Blood* 99, 2569–2577. doi: 10.1182/blood.v99.7.2569

Salzer, U., Zhu, R., Luten, M., Isobe, H., Pastushenko, V., Perkmann, T., et al. (2008). Vesicles generated during storage of red cells are rich in the lipid raft marker stomatin. *Transfusion* 48, 451–462. doi: 10.1111/j.1537-2995.2007.01549.x

Santos, N. C., Martins-Silva, J., and Saldanha, C. (2005). Gramicidin D and dithiothreitol effects on erythrocyte exovesiculation. *Cell Biochem. Biophys.* 43, 419–430. doi: 10.1385/cbb:43:3:419

Schneider, A. C., Beguin, P., Bourez, S., Perfield, J. W. II, Mignolet, E., Debier, C., et al. (2012). Conversion of t11t13 CLA into c9t11 CLA in Caco-2 cells and inhibition by sterculic oil. *PLoS One* 7:e32824. doi: 10.1371/journal.pone.0032824

Sobko, A. A., Kotova, E. A., Antonenko, Y. N., Zakharov, S. D., and Cramer, W. A. (2004). Effect of lipids with different spontaneous curvature on the channel activity of colicin E1: evidence in favor of a toroidal pore. *FEBS Lett.* 576, 205–210. doi: 10.1016/j.febslet.2004.09.016

Subczynski, W. K., Pasenkiewicz-Gierula, M., Widomska, J., Mainali, L., and Raguz, M. (2017). High cholesterol/low cholesterol: effects in biological membranes: a review. *Cell Biochem. Biophys.* 75, 369–385. doi: 10.1007/s12013-017-0792-7

Tang, D., Dean, W. L., Borchman, D., and Paterson, C. A. (2006). The influence of membrane lipid structure on plasma membrane Ca2+ -ATPase activity. *Cell Calcium* 39, 209–216. doi: 10.1016/j.ceca.2005.10.010

Tissot, J. D. (2013). Blood microvesicles: From proteomics to physiology. *Transl. Proteom.* 1, 38–52. doi: 10.1016/j.trprot.2013.04.004

Tsikas, D. (2017). Assessment of lipid peroxidation by measuring malondialdehyde (MDA) and relatives in biological samples: analytical and biological challenges. *Anal. Biochem.* 524, 13–30. doi: 10.1016/j.ab.2016.10.021

Tyteca, D., D'auria, L., Van Der Smissen, P., Medts, T., Carpentier, S., Monbaliu, J. C., et al. (2010). Three unrelated sphingomyelin analogs spontaneously cluster into plasma membrane micrometric domains. *Biochim. Biophys. Acta* 1798, 909–927. doi: 10.1016/j.bbamem.2010.01.021

Verderio, C., Gabrielli, M., and Giussani, P. (2018). Role of sphingolipids in the biogenesis and biological activity of extracellular vesicles. *J Lipid Res.* 59, 1325–1340. doi: 10.1194/jlr.r083915

Vind-Kezunovic, D., Nielsen, C. H., Wojewodzka, U., and Gniadecki, R. (2008). Line tension at lipid phase boundaries regulates formation of membrane vesicles in living cells. *Biochim. Biophys. Acta Biomemb.* 1778, 2480–2486. doi: 10.1016/j.bbamem.2008.05.015

Willekens, F. L., Werre, J. M., Groenen-Dopp, Y. A., Roerdinkholder-Stoelwinder, B., De Pauw, B., and Bosman, G. J. (2008). Erythrocyte vesiculation: a self-protective mechanism? *Br. J. Haematol.* 141, 549–556. doi: 10.1111/j.1365-2141.2008.07055.x

Wong-Ekkabut, J., Xu, Z., Triampo, W., Tang, I. M., Tieleman, D. P., and Monticelli, L. (2007). Effect of lipid peroxidation on the properties of lipid bilayers: a molecular dynamics study. *Biophys. J.* 93, 4225–4236. doi: 10.1529/biophysj.107.112565

Yoshida, T., Prudent, M., and D'alessandro, A. (2019). Red blood cell storage lesion: causes and potential clinical consequences. *Blood Transfus.* 17, 27–52.

Conflict of Interest: The authors declare that the research was conducted in the absence of any commercial or financial relationships that could be construed as a potential conflict of interest.

Advantages of publishing in Frontiers

OPEN ACCESS
Articles are free to read for greatest visibility and readership

FAST PUBLICATION
Around 90 days from submission to decision

HIGH QUALITY PEER-REVIEW
Rigorous, collaborative, and constructive peer-review

TRANSPARENT PEER-REVIEW
Editors and reviewers acknowledged by name on published articles

Frontiers
Avenue du Tribunal-Fédéral 34
1005 Lausanne | Switzerland

Visit us: www.frontiersin.org
Contact us: info@frontiersin.org | +41 21 510 17 00

REPRODUCIBILITY OF RESEARCH
Support open data and methods to enhance research reproducibility

DIGITAL PUBLISHING
Articles designed for optimal readership across devices

FOLLOW US
@frontiersin

IMPACT METRICS
Advanced article metrics track visibility across digital media

EXTENSIVE PROMOTION
Marketing and promotion of impactful research

LOOP RESEARCH NETWORK
Our network increases your article's readership